frontiers | Research Topics

Underlying mechanisms transitioning seeds to seedlings

Edited by
Muhammad Awais Farooq, Ewa M. Kalemba and Alma Balestrazzi

Published in
Frontiers in Plant Science

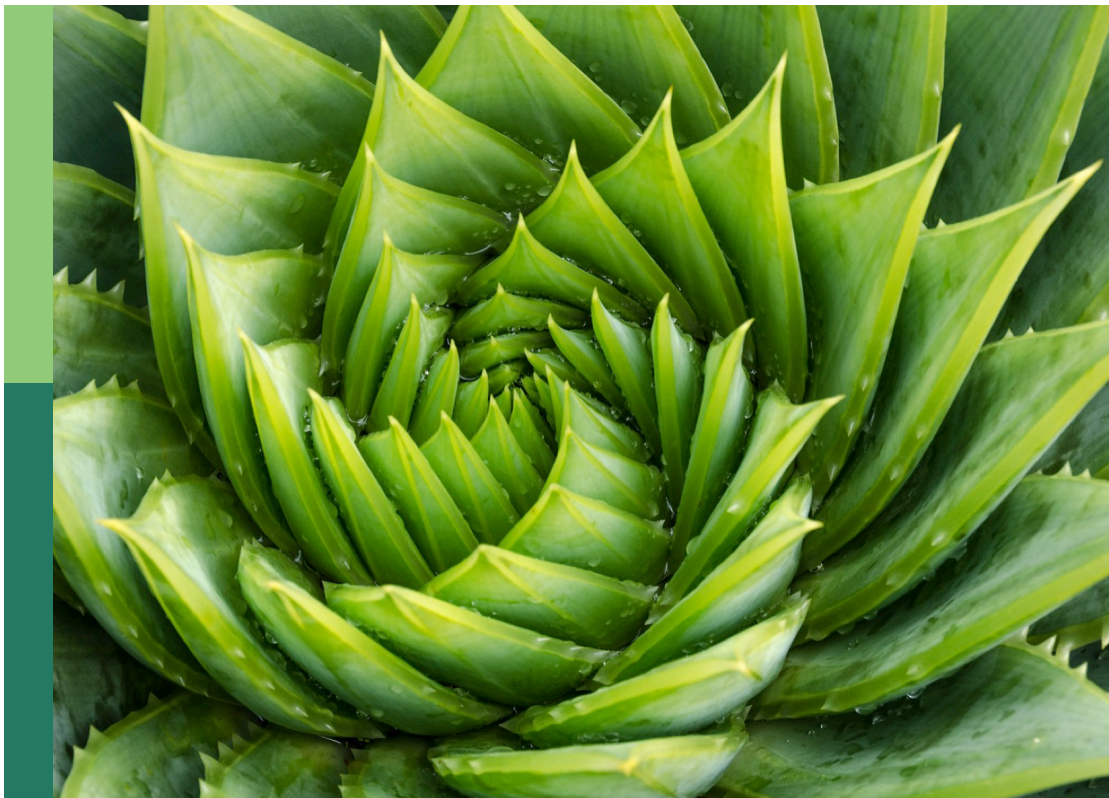

ISSN 1664-8714
ISBN 978-2-8325-6853-8
DOI 10.3389/978-2-8325-6853-8

Generative AI statement
Any alternative text (Alt text) provided alongside figures in the articles in this ebook has been generated by Frontiers with the support of artificial intelligence and reasonable efforts have been made to ensure accuracy, including review by the authors wherever possible. If you identify any issues, please contact us.

About Frontiers

Frontiers is more than just an open access publisher of scholarly articles: it is a pioneering approach to the world of academia, radically improving the way scholarly research is managed. The grand vision of Frontiers is a world where all people have an equal opportunity to seek, share and generate knowledge. Frontiers provides immediate and permanent online open access to all its publications, but this alone is not enough to realize our grand goals.

Frontiers journal series

The Frontiers journal series is a multi-tier and interdisciplinary set of open-access, online journals, promising a paradigm shift from the current review, selection and dissemination processes in academic publishing. All Frontiers journals are driven by researchers for researchers; therefore, they constitute a service to the scholarly community. At the same time, the *Frontiers journal series* operates on a revolutionary invention, the tiered publishing system, initially addressing specific communities of scholars, and gradually climbing up to broader public understanding, thus serving the interests of the lay society, too.

Dedication to quality

Each Frontiers article is a landmark of the highest quality, thanks to genuinely collaborative interactions between authors and review editors, who include some of the world's best academicians. Research must be certified by peers before entering a stream of knowledge that may eventually reach the public - and shape society; therefore, Frontiers only applies the most rigorous and unbiased reviews. Frontiers revolutionizes research publishing by freely delivering the most outstanding research, evaluated with no bias from both the academic and social point of view. By applying the most advanced information technologies, Frontiers is catapulting scholarly publishing into a new generation.

What are Frontiers Research Topics?

Frontiers Research Topics are very popular trademarks of the *Frontiers journals series*: they are collections of at least ten articles, all centered on a particular subject. With their unique mix of varied contributions from Original Research to Review Articles, Frontiers Research Topics unify the most influential researchers, the latest key findings and historical advances in a hot research area.

Find out more on how to host your own Frontiers Research Topic or contribute to one as an author by contacting the Frontiers editorial office: frontiersin.org/about/contact

Underlying mechanisms transitioning seeds to seedlings

Topic editors
Muhammad Awais Farooq — University of Bologna, Italy
Ewa M. Kalemba — Institute of Dendrology, Polish Academy of Sciences, Poland
Alma Balestrazzi — University of Pavia, Italy

Citation
Farooq, M. A., Kalemba, E. M., Balestrazzi, A., eds. (2025). *Underlying mechanisms transitioning seeds to seedlings*. Lausanne: Frontiers Media SA.
doi: 10.3389/978-2-8325-6853-8

Table of contents

frontiers | Frontiers in Plant Science

TYPE Editorial
PUBLISHED 30 October 2024
DOI 10.3389/fpls.2024.1503165

OPEN ACCESS

Edited and reviewed by: M. Naeem, Aligarh Muslim University, India

*CORRESPONDENCE
Muhammad Awais Farooq
awaisfarooq724@gmail.com
Ewa Marzena Kalemba
kalemba@man.poznan.pl
Alma Balestrazzi
alma.balestrazzi@unipv.it

RECEIVED 28 September 2024
ACCEPTED 11 October 2024
PUBLISHED 30 October 2024

CITATION
Farooq MA, Kalemba EM and Balestrazzi A (2024) Editorial: Underlying mechanisms transitioning seeds to seedlings.
Front. Plant Sci. 15:1503165.
doi: 10.3389/fpls.2024.1503165

Editorial: Underlying mechanisms transitioning seeds to seedlings

Muhammad Awais Farooq[1]*, Ewa Marzena Kalemba[2]* and Alma Balestrazzi[3]*

[1]Department of Agricultural and Food Sciences (DISTAL), Alma Mater Studiorum, University of Bologna, Bologna, Italy, [2]Institute of Dendrology, Polish Academy of Sciences, Kórnik, Poland, [3]Department of Biology and Biotechnology 'L. Spallanzani', University of Pavia, Pavia, Italy

KEYWORDS

seed germination, seedling development, seed priming, omics in seed development, seed dormancy

Editorial on the Research Topic
Underlying mechanisms transitioning seeds to seedlings

Successful seed germination marks a critical phase in the life cycle of a plant where the dormant seed transitions into a seedling capable of independent growth. The ability of the seed to transform into a seedling and eventually develop into a mature plant determines the reproductive and ecological success of the plant in the environment and, from a human perspective, economic profit. This transition is a highly coordinated process governed by an intricate interplay of omics networks that ensure the proper utilization of stored resources and the activation of developmental programs. Omics networks involving phytohormones, proteins, metabolites, specific transcription factors, epigenetic remodeling of chromatin, and small RNAs constitute the molecular control of the seed germination process which is modulated by the mechanical forces between seed tissues and external factors such as light, water, and oxygen (Carrera-Castaño et al., 2020; Baud et al., 2023). A complete understanding of the mechanisms underlying the transition from seeds to seedlings is crucial to managing the genetic resources via *in situ* and *ex situ* conservation programs and for sustainable agriculture because seedling emergence and establishment are considered to be the most vulnerable stages of plant growth and development in global warming scenarios (Badano and Sánchez-Montes de Oca, 2022). In this Research Topic "*Underlying mechanisms transitioning seeds to seedlings*" eight articles have been published that cover the main themes of the Research Topic: gene regulatory network, physiological processes regulating seed germination under stress conditions, and interaction between the internal and external environment driving the seed germination.

Selection of specific genotypes and sustainable seed priming techniques in response to water shortage stress leads to the cultivation of efficient, environmentally friendly crops. Dueñas et al. demonstrated that poly-gamma-glutamic acid (γ-PGA), denatured γ-PGA (dPGA) and iron pulses are able to enhance the resilience to drought stress in four Italian rice varieties and indicated one rice variety as highly stress sensitive. The enhancement was manifested by altered expression of genes involved in DNA damage response, antioxidant defense mechanism, drought stress response, amino acid transport, and iron homeostasis. In another study, a novel seed treatment using 2-(N-methyl benzyl aminoethyl)-3-methyl butanoate (BMVE) was reported by Dharni et al. to consistently improve seed development

subsequent seed germination, seedling vigor, and stress tolerance in the case of rice and wheat. Transcriptomic analysis revealed that changes in reactive oxygen species (ROS) scavenging, hormone signaling and stress response pathways are the molecular mechanisms determining enhanced seedling growth and productivity of rice and wheat. Both articles suggested that priming methods could be a practical seed treatment to mitigate the impact of climate change on enhancing crop growth. In the third study related to seed priming, the effect of melatonin (MT), pollen polysaccharide (SF), and 14-hydroxyed brassinosteroid (14-HBR) on the growth of kiwifruit seedlings was investigated by Zhang et al. MT, SF, and 14-HBR were found to increase leaf chlorophyll content, photosynthetic capacity, and antioxidant enzyme activities, to enhance dry shoot biomass and modify the soil parameters, as reflected in the activities of soil enzymes, the abundance of bacteria and the content of available K and organic matter. In conclusion, 14-HBR combined with MT was the most efficient in promoting rhizosphere bacterial distribution, nutrient absorption and plant growth.

Transcriptome study approaches enable the complex mapping of a genome to various phenotypes, developmental stages, and environmental factors. Since literature data present little information regarding seedling establishment in heteromorphic species, the work of Arshad et al. on the dimorphic diaspore model *Aethionema arabicum* is particularly valuable. Transcriptomics of the natural dimorphic diaspores, the mucilaginous seeds and the dispersed indehiscent fruits during late germination revealed morph-specific differential expression of hormone regulators, water and ion transporters, nitrate transporters and assimilation enzymes, and cell wall remodeling protein genes. In another article, Slocum et al. analyzed the expression of genes encoding enzymes and transporters of nucleotide metabolism in pyrimidine-starved Arabidopsis seedlings after uridine supplementation. Genome-wide transcriptional profiling revealed that stress responses, cellular responses to hypoxia or pathogens, auxin, and calcium (Ca^{2+}) homeostasis and signaling, root development, cell wall loosening during growth, plastid development, and photosynthesis are the main processes impacted by changes in pyrimidine availability. Additionally, transcription factors involved in the abiotic and biotic stress responses appeared to be important agents controlling key steps in pyrimidine and purine synthesis and salvage. Although the mechanisms of ABA-mediated seed germination inhibition have been previously investigated, Xiang et al. demonstrated that the gene encoding pectin methylesterase 31 (*PME31*) is transcriptionally inhibited by ABI5, the transcription factor involved in abscisic acid (ABA) signaling, and therefore negatively regulates ABA-mediated seed germination inhibition. The authors suggested that tissue-specific pectin methylesterification may play a role in the regulation of seed germination because *PME31* was expressed in the embryo, leaf vasculature, and primary root of Arabidopsis.

Studies of mutants of *Arabidopsis thaliana* are providing crucial findings in seed science. The role of arogenate dehydratase (ADT), which is involved in phenylalanine synthesis, in the switch from heterotrophic growth to light-driven autotrophy is addressed in an article by Muhammad et al. who investigated the impact of light conditions and specific hormone responses in *A. thaliana* seedlings using six *adt* mutants. The authors demonstrated that phenylalanine pools are specific to tissues with respect to age and level of development and are implicated in the regulation of seed germination, hypocotyl elongation, root development, and plastid development.

Huang et al. investigated the hydroponic-based cultivation of two lettuce varieties. The authors demonstrated that pH, nutrient concentration (Hoagland solution), light intensity, cultivation substrate hardness, and porosity affect the lettuce germination time and success rate. Their research contributed to a better understanding of the hydrogel-aided lettuce germination and may help to optimize its use in agricultural production.

The collection of eight articles included in this Research Topic demonstrates the complexity of the seed-to-seedling transition and highlights the significance of investigating the mechanisms that regulate this process. These studies have contributed to a better understanding of the factors that determine seedling emergence and performance, which can facilitate successful and sustainable agriculture, horticulture and forest practices. This Research Topic delivers a key message: expanding current seed treatments to include novel approaches and tools is a sustainable strategy to reinforce crop resilience to climate change whereas exhaustive omics profiles can disclose the molecular basis of specific seed features, useful to improve germination performance in response to stress.

Author contributions

MF: Conceptualization, Writing – original draft, Writing – review & editing. EK: Conceptualization, Writing – original draft, Writing – review & editing. AB: Conceptualization, Writing – original draft, Writing – review & editing.

Conflict of interest

The authors declare that the research was conducted in the absence of any commercial or financial relationships that could be construed as a potential conflict of interest.

The author(s) declared that they were an editorial board member of Frontiers, at the time of submission. This had no impact on the peer review process and the final decision.

Publisher's note

References

Badano, E. I., and Sánchez-Montes de Oca, E. J. (2022). Seed fate, seedling establishment and the role of propagule size in forest regeneration under climate change conditions. *For. Ecol. Manag* 503, 119776. doi: 10.1016/j.foreco.2021.119776

Baud, S., Corso, M., Debeaujon, I., Dubreucq, B., Job, D., Marion-Poll, A., et al. (2023). Recent progress in molecular genetics and omics-driven research in seed biology. *C R Biol.* 345, 61–110. doi: 10.5802/crbiol.104

Carrera-Castaño, G., Calleja-Cabrera, J., Pernas, M., Gómez, L., and Oñate-Sánchez, L. (2020). An updated overview on the regulation of seed germination. *Plants* 9, 703. doi: 10.3390/plants9060703

frontiers | Frontiers in Plant Science

TYPE Original Research
PUBLISHED 02 August 2023
DOI 10.3389/fpls.2023.1220732

OPEN ACCESS

EDITED BY
Muhammad Awais Farooq,
Hebei Agricultural University, China

REVIEWED BY
Saurabh Gupta,
Curtin University, Australia
Shinji Masuda,
Tokyo Institute of Technology, Japan

*CORRESPONDENCE
Beronda L. Montgomery
montgomb@grinnell.edu
Katherine M. Warpeha
kwarpeha@uic.edu

†These authors have contributed equally to this work

RECEIVED 11 May 2023
ACCEPTED 11 July 2023
PUBLISHED 02 August 2023

CITATION
Muhammad D, Alameldin HF, Oh S, Montgomery BL and Warpeha KM (2023) Arogenate dehydratases: unique roles in light-directed development during the seed-to-seedling transition in *Arabidopsis thaliana*. *Front. Plant Sci.* 14:1220732. doi: 10.3389/fpls.2023.1220732

Arogenate dehydratases: unique roles in light-directed development during the seed-to-seedling transition in *Arabidopsis thaliana*

DurreShahwar Muhammad[1†], Hussien F. Alameldin[2,3†], Sookyung Oh[2], Beronda L. Montgomery[2,4,5,6,7†*] and Katherine M. Warpeha[1†*]

[1]Department of Biological Science, University of Illinois at Chicago, Chicago, IL, United States, [2]MSU-DOE Plant Research Lab, Plant Biology Laboratories, East Lansing, MI, United States, [3]Agricultural Genetic Engineering Research Institute (AGERI), Agriculture Research Center (ARC), Giza, Egypt, [4]Cell and Molecular Biology Program, Michigan State University, East Lansing, MI, United States, [5]Department of Biochemistry and Molecular Biology, Michigan State University, East Lansing, MI, United States, [6]Department of Microbiology and Molecular Genetics, Michigan State University, East Lansing, MI, United States, [7]Department of Biology, Grinnell College, Grinnell, IA, United States

The seed-to-seedling transition is impacted by changes in nutrient availability and light profiles, but is still poorly understood. Phenylalanine affects early seedling development; thus, the roles of arogenate dehydratases (ADTs), which catalyze phenylalanine formation, were studied in germination and during the seed-to-seedling transition by exploring the impact of light conditions and specific hormone responses in *adt* mutants of *Arabidopsis thaliana*. *ADT* gene expression was assessed in distinct tissues and for light-quality dependence in seedlings for each of the six-member *ADT* gene family. Mutant *adt* seedlings were evaluated relative to wild type for germination, photomorphogenesis (blue, red, far red, white light, and dark conditions), anthocyanin accumulation, and plastid development-related phenotypes. ADT proteins are expressed in a light- and tissue-specific manner in transgenic seedlings. Among the analyzed *adt* mutants, *adt3*, *adt5*, and *adt6* exhibit significant defects in germination, hypocotyl elongation, and root development responses during the seed-to-seedling transition. Interestingly, *adt5* exhibits a light-dependent disruption in plastid development, similar to a *phyA* mutant. These data indicate interactions between photoreceptors, hormones, and regulation of phenylalanine pools in the process of seedling establishment. ADT5 and ADT6 may play important roles in coordinating hormone and light signals for normal early seedling development.

KEYWORDS

photomorphogenesis, hypocotyl, phytochrome, phenylalanine, seedling, hormone, seed-to-seedling transition

1 Introduction

Higher plant development from seed to seedling is an intricate multi-component process. This transition involves a switch from heterotrophic growth to light-driven autotrophy. Biologically active wavelengths of light, hormones, and nutrients act through an unknown number of signal transduction mechanisms to initiate autotrophic growth and coordinate many aspects of higher plant development (Borevitz et al., 2002; Sullivan and Deng, 2003; Warpeha and Montgomery, 2016). Light and hormones affect gene expression, where ~20% or more of the plant genome is regulated by white light (Jiao et al., 2005) and nearly 15% of the genome may respond to hormones (Nemhauser et al., 2006). Partitioning, regulation, and use of metabolic resources are still poorly understood, but postulated to be under the control of light and circadian regulators (Farré and Weise, 2012). What is known about photoreceptor-, hormone-, and metabolite-dependent regulation, and interactions among these factors during development from seed to seedling have been recently reviewed (Warpeha and Montgomery, 2016).

Among metabolites critical to the seed-to-seedling transition process is phenylalanine (Phe), which was recently reviewed (Perkowski and Warpeha, 2019). Phe is an amino acid utilized both in protein synthesis and as the precursor to thousands of compounds used by the plant (Hahlbrock and Scheel, 1989; Kliebenstein, 2004; Tzin and Galili, 2010; Maeda and Dudareva, 2012), including protectants against environmental signals, and that are directly upregulated by blue light (BL) and ultraviolet light (UV) (Bruns et al., 1986; Ohl et al., 1989). Phe can account for up to a third of the total organic carbon in a plant (Van Heerden et al., 1996), is the first committed precursor of the phenylpropanoid pathway, and is a concentration-limiting substrate for phenolics, phenylpropanoids, and other key compounds (Margna, 1977; Margna et al., 1989b; Maranville and Zhu, 2000; Rohde et al., 2004; Voll et al., 2004; Warpeha et al., 2008; Para et al., 2016). Arogenate dehydratase (ADT) enzyme isoforms are regulators of Phe in plants as they are involved in the final step of Phe biosynthesis (Fischer and Jensen, 1987). Cho et al. (2007) described six members of the *ADT* gene family, namely, *ADT1* (*At1g11790*), *ADT2* (*At3g07630*), *ADT3* (*At2g27820*), *ADT4* (*At3g44720*), *ADT5* (*At5g22630*), and *ADT6* (*At1g08250*), encoding proteins identified primarily in chloroplasts of light-grown plant material. *ADT3* (then called *prephenate dehydratase1* (*PD1*) (Warpeha et al., 2006) before the preferred substrate arogenate was indicated in detailed studies (Cho et al., 2007; Yamada et al., 2008) is expressed in young etiolated seedlings (Para et al., 2016), unlike other ADTs studied in more mature tissues. However, a recent study indicated that sequence conservation of amino acid residues conferring prephenate dehydratase activity is retained in plants throughout evolution (El-Azaz et al., 2016), and in vascular plants, relaxed feedback inhibition by Phe may have a profound impact on the induction and biosynthesis of phenylpropanoids (El-Azaz et al., 2022), raising many interesting possibilities for regulation of Phe.

Recent studies have revealed activities of ADT proteins that could impact seedling establishment. In 3- to 5-week-old *Nicotiana benthamiana* leaves with transiently expressed *A. thaliana ADT* genes, ADT2 localized to a chloroplast pole and at the chloroplast equatorial plane in a ring indicating involvement with chloroplast division machinery (Bross et al., 2017). ADT5 was identified in the nucleus, but the functional reason is unknown (Bross et al., 2017). In addition, Chen et al. reported that ADT proteins, and ADT2 the most, also contribute to anthocyanin accumulation (Chen et al., 2016). Recently, ADT2 was also shown to be vital for seed development (El-Azaz et al., 2018). *ADT3* is expressed at high levels in seed development (Rippert et al., 2009), and in young seedlings (Warpeha et al., 2006; Warpeha et al., 2008; Para et al., 2016). Phe supplied by ADT3 indicated roles in carbon storage, chloroplast development, cell division, and cell lineage commitment and cell morphology in the epidermis, and coordinates reactive oxygen species (ROS) homeostasis in young seedlings (Para et al., 2016).

It is not known how *ADT* expression affects germination processes or the transition to a photosynthetically competent seedling. Gene expression profiles at specific times have indicated that transcripts of *ADT2* and *ADT3* are expressed in seeds (Rippert et al., 2009), only *ADT3* in young (~4 days old) etiolated seedlings (Warpeha et al., 2006; Para et al., 2016), and in young seedlings in general (*ADT2* was only expressed in prolonged white light at 6 days) (Warpeha et al., 2006); other *ADT* genes are reported to be primarily expressed in older tissues (Rippert et al., 2009). Utilizing a number of genetic mutants, Corea et al. (2012) showed that some *ADT* genes regulate the carbon flux and then later lignin biosynthesis in maturing (3-week-old and older) plants.

The seed-to-seedling transition is a simple system with which to study abiotic signal responses, prior to full maturation of the photosynthetic apparatus. Light perceived by photoreceptors is central to germination, the transition from heterotrophy to autotrophy, hypocotyl elongation, and cotyledon and leaf development during seedling establishment (Franklin and Quail, 2010; Kami et al., 2010). Hormones also contribute to the seed-to-seedling progression. Abscisic acid (ABA), gibberellins (GAs), auxins (e.g., indole-3-acetic acid [IAA]), and ethylene are among the hormones that all contribute to this process (reviewed in Warpeha and Montgomery, 2016). ABA and, to a lesser degree, auxins prevent early germination, whereas GA and ethylene promote germination. GA and auxins promote hypocotyl elongation. Light and hormone signaling pathways interface during the seed-to-seedling transition, and this is still not well understood (Warpeha and Montgomery, 2016).

The seed-to-seedling transition is a rapid process where a program of embryonic dormancy is phased out in favor of an independent vegetative organism, which includes the transition of the cotyledons from storage to photosynthesizing organs in Arabidopsis that includes chloroplast development. Some nutrients and other compounds are stored in the seed, but the network of metabolic induction and control in seedling development is still a complicated puzzle. To better understand potential Phe dynamics, we explored potential roles of individual ADT family members during the seed-to-seedling transition.

2 Materials and methods

2.1 Plant materials

Columbia WT and T-DNA insertions originally obtained from ABRC/TAIR were utilized (Alonso et al., 2003). Null mutant insertions for *Pirin1* (*PRN1*; At3g59220; SALK_006939) were utilized as controls in some experiments, and T-DNA insertion mutant line *sig6-1* (AT2G36990; SAIL_893_C09) was used in the RNA-seq experiment. Null ADT mutants were tested in genetic and developmental assays, including *ADT1* (At1g11790; SALK_138343; SALK_124232), *ADT3* (At2g027820; SALK_029949; SALK_071907), *ADT4* (At3g44720; SALK_065483; SALK_123367), *ADT5* (At5g22630; SALK_088171; SALK_028611), and *ADT6* (At1g08250; SALK_030329; SALK_109552). All mutant phenotype responses were confirmed in two accessions; the more common null mutant utilized in research (accession listed first) was featured in the data shown. Bulk seed stocks were grown as previously reported (Orozco-Nunnelly et al., 2014). T-DNA insertion *phyA* and *phyB* mutants used in these studies were previously isolated and described (Mayfield et al., 2007; Ruckle et al., 2007). The *phyAphyB* mutant was obtained from a genetic cross of the single mutants as described (Oh and Montgomery, 2013). Seed lines completely null for *ADT2* (At3g07630) have not been available. Recently, it has been proven that ADT2 null mutation is lethal because ADT2 is essential for proper seed development (El-Azaz et al., 2018), and hence, *ADT2* is not studied herein.

2.2 Light-dependent hypocotyl and root elongation phenotyping assays

Seeds were surface sterilized and plated on 1X MS containing 1% sucrose and 0.7% Phytoblend (Caisson Laboratories, UT) essentially as previously described (Warnasooriya and Montgomery, 2009). Plated, sterilized seeds were cold stratified during imbibition in darkness at 4°C for 4 days. All experiments were conducted at constant temperature and humidity under continuous light in controlled-environment chambers. Light sources were those previously described (Warnasooriya and Montgomery, 2009) with continuous red, R (Rc; λ_{max} ~ 670 nm), continuous far-red, FR (FRc; λ_{max} ~ 735 nm), and continuous blue, B (Bc; λ_{max} ~ 470 nm) at the indicated fluences in μmol m^{-2} s^{-1}. Continuous darkness is signified by Dc or 7D0L.

For light-dependent hypocotyl elongation experiments, hypocotyl lengths of seedlings grown under defined light conditions were measured by scanning the seedling images and quantifying lengths using ImageJ software (Plug-in used to stitch pictures that required two images to get whole seedling). We measured 25 seedlings in each of three independent biological replicates, resulting in 75 measured seedlings per line. For vertical plate assays, hypocotyl and root lengths were compared to a scanned ruler image taken at the same time by scanning and photography on day 7, post-stratification. After hypocotyl and root lengths were measured, the mean ratio of hypocotyl length:root length was determined.

2.3 Vertical growth phenotyping and germination assays

Seeds were surface sterilized and plated on 0.5X MS (pH 5.8) with no sucrose and no added vitamins as described (Voll et al., 2004) on square (positioned vertically) petri plates or phytatrays, as detailed herein. For germination assays on phytatrays, sterilized seeds were mixed with 0.8% low melt agarose (0.5X MS; top agarose) with the addition of 1 μM ACC or 500 nM ABA or 1 μM IAA or 1 μM GA or 0.5X MS (control); then, a 100-μl aliquot of seed and top agarose was spotted onto a 0.5X MS phytatray base plate, where germination assays were performed similarly to Kim et al. (2019). Plated, sterilized phytatrays were placed into light-tight black Plexiglas boxes, sealed with aluminum foil, and then were cold stratified in a dark cold room at 4°C for 48 h (Kim et al., 2019). After 48 h, the plates were moved to one of several locations: to a 24-h, 20°C dark environmental room, or a white light environmental room (Orozco-Nunnelly et al., 2014) for varying numbers of days, ranging from 0 to 7 days, depending on the experiment. White light sources, as well as dim green light for handling dark-grown seedlings, have been described (Voll et al., 2004); red and blue Plexiglas and filters used for supporting (low fluence) work have been described (Warpeha et al., 1989), where the fluence rate received by the vertical plates determined by a LiCor meter was 3 (Rc) and 7 (Bc) μmol m^{-2} s^{-1}, respectively. All accessions of mutants were tested in these experiments; one representative accession is featured in the figures.

2.4 Constructs and transformation of *adt* mutants

ADT construct development and subsequent plant transformation occurred as has been described (Orozco-Nunnelly et al., 2014). Standard molecular biology techniques and the Gateway system (Invitrogen) were used in the cloning procedures of the *ADT* family members described herein. Purified WT Arabidopsis cDNA was used to generate the *ADT* full ORF fragments for each *ADT* member (except *ADT2* as aforementioned), where each ORF was represented by *ADT1* [1,179 bp], *ADT4* [1,275 bp], *ADT5* [1,278 bp], and *ADT6* [1,242 bp], and where *ADT3* cloning of the ORF was described previously (Para et al., 2016). Each *ADT* ORF fragment was cloned into the Invitrogen pENTR/D-TOPO vector. LR reactions (Invitrogen) were then performed with verified (i.e., by sequencing in both directions) entry clones to obtain expression clones. The *35S* promoter was cloned as described (Orozco-Nunnelly et al., 2014), and the dpGreen binary vector derivative containing a NOS terminator with a C-terminal GFP fusion and spectinomycin and BASTA resistance genes was used, resulting in each *ADT* construct (*35S::ADTX-GFP*), except for *ADT3*, which was cloned for an earlier study as described with the native promoter (Para et al., 2016), and separate construct utilizing the 35S promoter. All constructs were confirmed via restriction enzyme digest, PCR, and sequencing. Verified expression clones were transformed in *adt* mutant backgrounds via floral dip as described (Para et al., 2016). *35S::ADTX-GFP* was introduced into null mutants (*ADT1* [At1g11790; SALK_138343]; *ADT3* [At2g27820; SALK_029949]; *ADT4* [At3g44720;

SALK_065483]; *ADT5* [At5g22630; SALK_088171]; and *ADT6* (At1g08250; SALK_030329]) via the floral dip method as described, and screened by BASTA resistance in each generation until homozygous (T3) for experimentation (Orozco-Nunnelly et al., 2014). For each *ADT*, the four most vigorous T3 lines were selected for experiments. Living seedlings were mounted in sterile water on slides at the same time (~9 a.m.) in the day cycle, then viewed on a Zeiss Observer.Z1 deconvoluting microscope fitted with a high-resolution camera (Axiovision 503; Zeiss, Oberkochen, Germany), using the 20× objective to view expression fluorescence, sectioned by optical apotome (1-µm optical slices, no bleed through) illuminated by XCite 120 LED (Lumen Dynamics, Waltham, MA USA) DAPI, FITC, and Texas Red LEDs. Images were managed by Zeiss Zen pro software (2012). At least 30 seedlings were viewed per experimental replicate, with three biological replicates performed. Merged images of DAPI, FITC, and Texas Red LEDs are shown.

2.5 Germination and phenotyping

Germination was scored as complete emergence of the radicle as described (Kim et al., 2019). Phenotypic responses on untreated (control) and experimental hormone plates were determined by comparison of mutants to Columbia WT on a Zeiss Stereo Discovery V.8 microscope at 1× using Axiovision with images recorded, and entire plates were photographed on day 4 after stratification using Nikon Coolpix on a white light box or black background. At least three sets of 30 seeds were scored for germination on phytatrays at 0 to 72 h every 4 h, post-stratification.

2.6 Anthocyanin extraction and quantification

Anthocyanins were extracted and quantified from 5-day-old seedlings as previously detailed (Montgomery et al., 1999; Warnasooriya and Montgomery, 2009). At least 100 seedlings per line from four biological replicates were used.

2.7 Heat map analysis

Heat maps were constructed using AtGenExpress public Arabidopsis microarray datasets with mean-normalized values (www.weigelworld.org) and visualization tools from BAR Heatmapper Plus (http://bar.utoronto.ca). For tissue-specific data, seedlings were 7 days old grown in continuous white light (Wc). Light-pulsed seedlings were 4 days old.

2.8 Far-red block of greening treatment

The far-red block of greening (FR-BOG) experiment was performed according to Alameldin et al. (2020); Arabidopsis seeds were surface sterilized with 35% (v/v) commercial bleach containing 0.025% (v/v) SDS for 15 min. Seeds were rinsed five times with sterile distilled water and planted on growth medium containing 0.5X MS salts (Caisson Laboratories, Smithfield, Utah, USA) and 0.7% (w/v) Phytoblend (Caisson Laboratories). Seeds on solid medium were stratified for 4 days at 4°C in the dark and were then divided into two groups. One group was incubated in a Percival LED (light-emitting diode)-equipped growth chamber (model E-30LED; Percival, Perry, IA, USA) at 22°C under constant far-red LED (FRc; λ_{max} ~ 735 nm) light at 5 µmol m^{-2} s^{-1} for 5 days, then in a Percival environmental chamber model no. CU36LA under Wc at 100 µmol m^{-2} s^{-1} for 5 days. The second group was kept in the dark (D) for 5 days at 22°C as the control treatment, then grown under 100 µmol m^{-2} s^{-1} Wc for 5 days.

2.9 Chlorophyll assay

Ten-day-old seedlings were soaked in 200 µl of N,N-dimethylformamide per milligram fresh mass and kept in the dark for 24 h at 4°C (Moran, 1982). The absorbance of samples was then measured at 647 nm, 664 nm, and 900 nm (baseline control) using an Agilent 8453E UV-visible spectrophotometer (Santa Clara, CA, USA). Chlorophyll content was calculated based on previously described equations (Inskeep and Bloom, 1985). All assays were done with at least three biological replicates.

2.10 RNA library preparation and sequencing

Total RNA was extracted from whole seedlings (FR BOG-treated and controls) grown at 22°C using the OMEGA E.Z.N.A Plant RNA kit (catalog no. R6827). cDNA was synthesized using a Reverse Transcription System (Quanta bio) qScript cDNA SuperMix (Omega Bio-tek, Norcross, GA, USA) and the instructions of the manufacturer. Libraries were prepared using the Illumina Stranded mRNA Library Kit and Ligation with IDT for Illumina RNA UD Indexes following the manufacturer's recommendations except that half volume reactions were used. Completed libraries were quality checked and quantified using a combination of Qubit dsDNA HS and Agilent 4200 TapeStation HS DNA1000 assays. All libraries were normalized down to the lowest concentration and equal volumes of these normalized libraries were pooled. The pool was quantified using the Invitrogen Collibri Quantification qPCR kit. The library pool was loaded onto one lane of an Illumina NovaSeq 6000 S4 flow cell and sequencing was performed in a 2 × 150-bp paired-end format using a NovaSeq v1.5 300 cycle reagent cartridge. Base calling was done by Illumina Real Time Analysis (RTA) v3.4.4, and output of RTA was demultiplexed and converted to FastQ format with Illumina Bcl2fastq v2.20.0.

2.11 RNA-Seq data analyses

An initial quality check of the RNA reads was performed using FastQC (https://www.bioinformatics.babraham.ac.uk/projects/

fastqc/). Trimmomatic v0.32 (Bolger et al., 2014) was used to filter the RNA reads to remove adaptors and low-quality reads. A sliding window method was used to scan the reads with 4-base wide and cut when the base quality was below a threshold of 2. The minimum read length cutoff was 100 bp. Data quality was explored after filtering with FastQC. STAR/2.6.0c (Spliced Transcripts Alignment to a Reference; Dobin et al., 2013) was used to map the RNAseq reads to the TAIR10.1 *Arabidopsis thaliana* genome (RefSeq assembly accession: GCF_000001735.4) with the default settings of the twopassMode Basic option with intron size 21–6,000 nt. In all samples, >90% of the RNAseq reads were mapped to the reference genome. RNA-Seq data have been deposited to the NCBI Gene Expression Omnibus database (BioProject accession number: PRJNA991474).

2.12 Differential expression and clustering analyses

The HTseq-count function in HTseq (High-Throughput sequencing) v0.6.1 (Anders et al., 2015) was used in the default mode and stranded=yes for generating read counts. HTseq-count output was fed into DESeq2 (Love et al., 2017) for differential expression analysis using the standard steps represented in the DESeq function (Love et al., 2014). A gene was considered differentially expressed if the adjusted p-value <0.05 and the |log fold change| > 1 and had a Transcript Per Million (TPM) > 1 in at least one condition. The p-value was adjusted with a q-value false discovery rate (Benjamini and Hochberg, 1995).

2.13 Statistical analyses

There were different kinds of data collected, including hypocotyl measurements, numbers of germinated seeds, pigment content, and expression data. Appropriate statistical tests were selected based on the experiment. Germination data were plotted in GraphPad Prism showing mean and error based on SD with error bars indicated. Data were considered significant when p was <0.05. For chlorophyll content and light-dependent hypocotyl elongation experiments in R, FR, and B light, data were analyzed using one-way ANOVA, with the *post-hoc* Tukey HSD test applied where relevant (https://astatsa.com/OneWay_Anova_with_TukeyHSD/). For anthocyanin content, two-tailed, unpaired Mann–Whitney U-test analyses were performed to compare the means of anthocyanin contents per milligram of fresh weight for a particular mutant line relative to WT in either darkness or light. For the 0- to 7-day seedlings grown in darkness (7D 0L), white light (0D 7L), or 3D4L, and the low-fluence 3-day seedlings (Supplementary Figures 2, 3), at least three replicates of 10–20 seedlings each were analyzed where the unpaired t-test was used; for some samples, applying Welch's correction was appropriate (GraphPad Prism, v.9). Statistical analyses used for differential gene expression and clustering analyses are described in section 2.12.

3 Results

3.1 Expression of *ADT* genes is tissue-specific and light-regulated in *Arabidopsis*

To obtain insight into tissue localization and regulation of expression of the *ADT* genes, we constructed heat maps using Arabidopsis AtGenExpress public microarray datasets of young Co-0 WT seedlings (www.weigelworld.org ; Figure 1). *ADT* genes are expressed at relatively low levels in most tissues, and in a tissue-specific manner in 7-day seedlings grown in Wc (Figure 1A). Previously reported data using qRT-PCR analyses (Rippert et al., 2009) indicated some similarities, and some major differences with these data, but age and growth conditions including light levels were distinct for the respective information. Given the prior association of some *ADT* genes with light regulation (Warpeha et al., 2006), we assessed the impact of distinct light qualities in 4-day-old seedlings. Each ADT member indicated responsiveness to all light qualities (Figure 1B). Notably, *ADT* genes were expressed at higher levels with a longer irradiation, the exception being *ADT2*, which expresses at higher levels regardless of light condition, with the exception of UV-A, UV-A/B, and R pulse where a longer irradiation (or in darkness, a longer treatment) increased induction. Most *ADTs* expressed at higher levels in longer irradiations of UV-A/B, B, and FR.

In planta tissue localization of fluorescently tagged ADT proteins was localized by exploring each tissue of the seedlings by microscopy. Green fluorescence above background indicated expression comparable to the transcript analysis results (Figure 1A) for 7-day plants. Each *ADT* gene family member GFP reporter construct (35S promoter, except for *ADT3* that utilized the native promoter due to a larger study (Para et al., 2016) was transformed into a corresponding null *adt* mutant. Seedlings were grown under basta selection, under a long-day (16-h light:8-h dark; 16:8) growth condition, then live seedlings were viewed at day 7 post-planting. ADT protein, which may accumulate distinctly based on protein stability and/or turnover relative to 35S promoter-driven gene expression, was observed by microscopy as generally low throughout seedlings, with specific, predominating tissue-specific patterns for each ADT member (Supplementary Figure S1). ADT1-GFP and ADT6-GFP accumulated in cotyledon mesophyll cells, particularly in the chloroplasts (confirmed by fluorescence pattern [21]), but where ADT1 was sporadic throughout the mesophyll (from individual chloroplasts to many chloroplasts), ADT6 was detected in most mesophyll cells in all sections through the cotyledon. Although ADT3-GFP exhibited low expression in newly divided cells and SAM, it was most discernable in the cotyledon epidermal layer, especially at the plasma membrane of pavement cells and in immature guard cells, which confirms reported results for young dark-grown seedlings (Para et al., 2016). ADT4-GFP was most expressed in the upper hypocotyl, occurring largely in plastids. ADT5-GFP was the only ADT with a distinct expression in the root. Null *adt2* is embryonic lethal (El-Azaz et al., 2018), so ADT2 was not studied in this context.

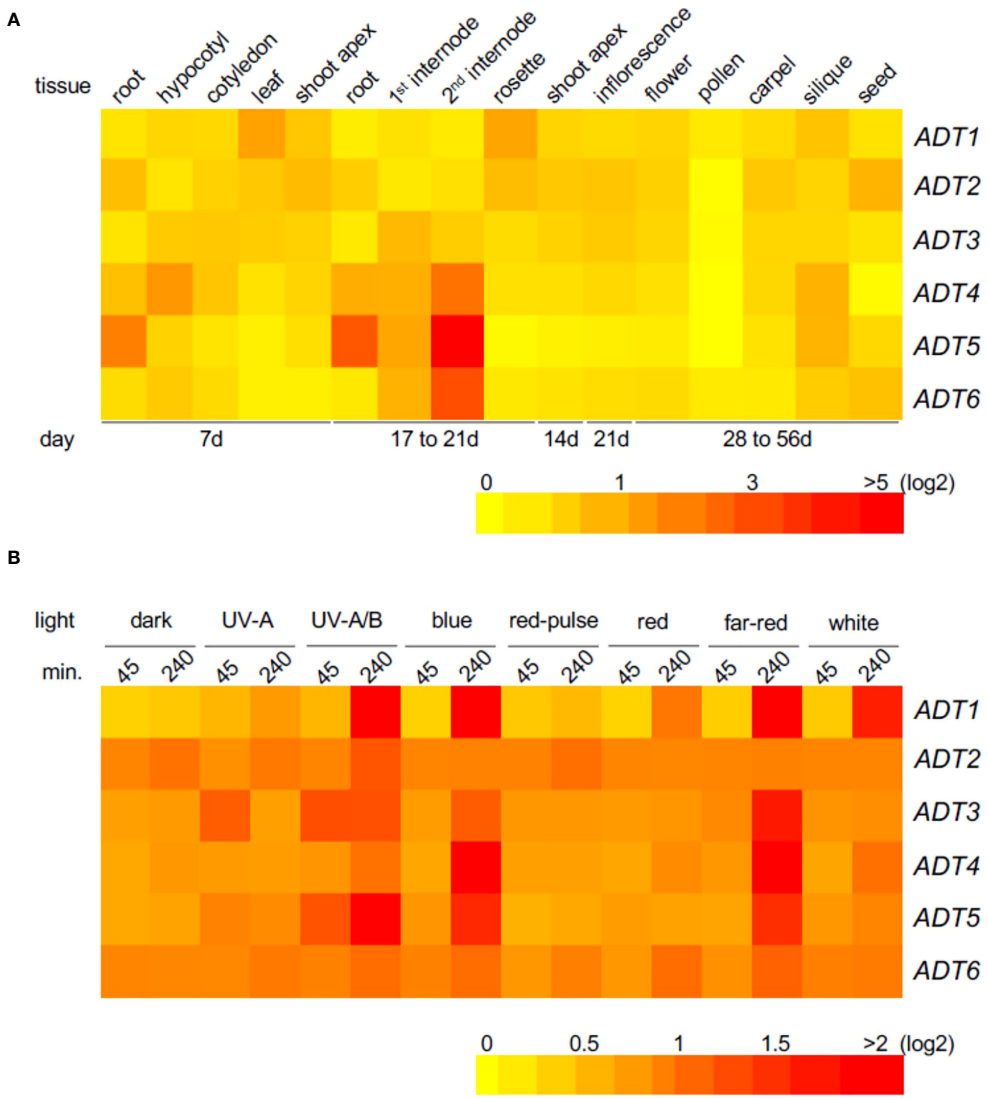

FIGURE 1
Heat map showing the expression of *ADT* genes in various Arabidopsis tissues **(A)** or under different light conditions **(B)**. Mean-normalized values from AtGenExpress expression library (www.weigelworld.org) and BAR Heatmapper *Plus* (http://bar.utoronto.ca) were used for heat map construction. For tissue-specific expression **(A)**, 7-day seedlings were grown in continuous white light (far left) and other ages of seedlings shown under the map **(B)**. Four-day-old seedlings grown on MS medium were treated with specific light for either 45 or 240 min and aerial parts (hypocotyl and cotyledons) were used to extract RNA. Color scale represents log2 expression values; red indicates high expression and yellow denotes low expression.

3.2 Germination phenotypes of *adt* mutants

To elucidate the role of ADT-mediated Phe synthesis during the earliest stage of the seed-to-seedling transition, we investigated the role of ADT in the seed germination process. Given the recognized role of hormones in modulating the timing of seed germination, seeds of *adt* mutants were grown in complete darkness in the absence or presence of a specific hormone in the medium (Figure 2). All *adt* seeds germinated similarly to WT (~100%) by 72 h post-stratification in the absence of exogenous hormone (No Hormone [NH]; Figure 2A). However, *adt5* exhibited a delay in germination compared to WT, whereas *adt6* and *adt3* germinated before WT by 24 h. *adt1* and *adt4* demonstrated germination patterns similar to WT. GA at 1 μM had unique effects on the germination of the *adt* mutants (Figure 2B). *adt6* seeds germinated more quickly than WT. *adt4* germinated similarly to WT, whereas *adt3* and *adt1* germination was delayed but within range of WT responses. Germination of all *adt* mutants in the presence of GA was similar to WT (~100%) by 72 h, except *adt5*, which indicated delay in any germination up to ~36 h, then gradual germination increase over the 72-h period. In response to ACC, *adt6* germinated rapidly within 24 h, similar to the NH condition (Figure 2C). *adt1*, *adt3*, and *adt4* germination were delayed by growth on ACC similarly to WT, with approximately 50% of seeds germinating by 36 h, but between 36 and 72 h, *adt1* germination continued in a linear fashion, behind WT and *adt4*, with 100% germination by 72 h. *adt3* seed germination decreased from 36 to 72 h with just over 60%

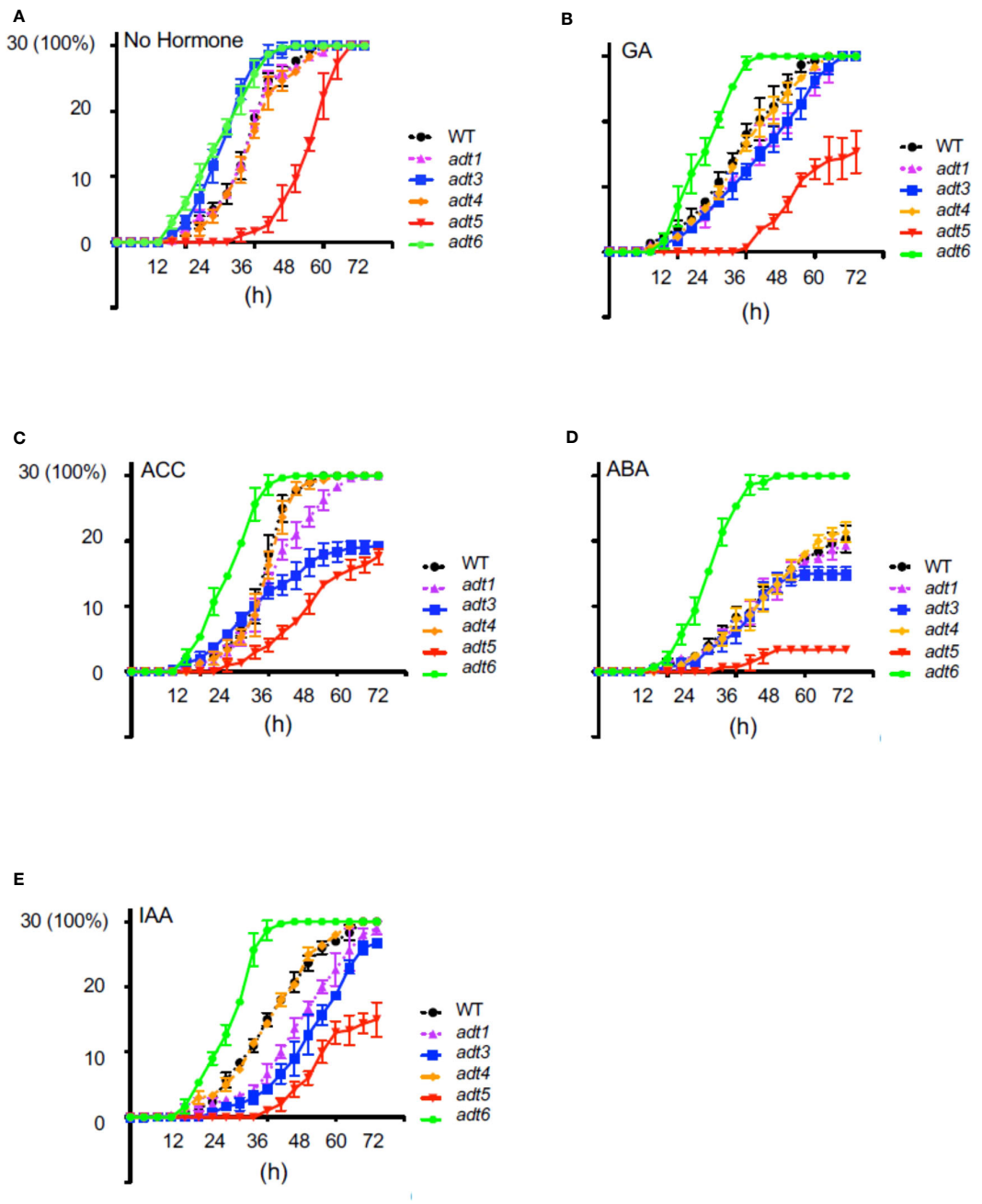

FIGURE 2
Germination of wild-type and *adt* mutants in the absence or presence of hormones. WT or *adt* mutant seeds were grown as described in Methods inclusive of exogenous hormones, shown in the figure. Thirty seeds (*y* axis; 30 seeds germinated = 100%) were sown with **(A)** no exogenous hormone, i.e., No Hormone (Control); **(B)** gibberellic acid (GA) at 1 µM; **(C)** 1-aminocyclopropane-1carboxylic acid (ACC) at 1 µM; **(D)** abscisic acid (ABA) at 500 nm; or **(E)** indole-3-acetic acid (IAA) at 1 µM. Germination was scored every 4 h up to 72 h where resultant data were plotted in GraphPad Prism indicating mean and SD as shown.

fully germinating. *adt5* like NH indicated a slow to start germination process, but then exhibited linear germination over time, with only ~60% germinated by 72 h. ABA at 500 nM caused an expected delay in WT relative to untreated (NH) seeds, with, *adt1*, *adt3*, and *adt4* indicating similar delays, where *adt3* did not fully recover after 48 h (Figure 2D). ABA blocked *adt5* germination, even by 72 h, post-stratification. *adt6* appeared completely insensitive to ABA, germinating at the same rate as NH. In response to IAA, WT was slightly delayed, and *adt1*, *adt3*, and *adt5* were inhibited in increasing effect (i.e., *adt5* was the most inhibited, where the overall profile resembled responses to GA and ACC) (Figure 2E). Considering germination overall with or without hormones, *adt4* had near-identical germination responses as WT. *adt6* was uniquely unresponsive to all hormones, and *adt5* was uniquely delayed in germination in response to all hormones, where ABA appeared to completely shut down germination.

3.3 Role of ADT in regulating far-red block of greening and ABA signaling

Given the impact of ABA on *adt5* germination and that ABA impacts transcription of chloroplast genes by a PP2C-dependent activation of nuclear encoded sigma factors (SIGs) (Woodson et al., 2013; Yamburenko et al., 2015), we examined interplay between ADT family members and plastid development. As phyA is known to regulate sigma factors, especially Sig6 (Oh and Montgomery, 2013), and they are both involved in the plastid development-related FR-BOG response in plants (Alameldin et al., 2020), we assessed FR-BOG-dependent gene expression in a *sig6* mutant (Figure 3).

Our RNA-seq data of the *sig6* mutant line under FR-BOG conditions indicated that *ADT5* was the only ADT gene that was downregulated in the *sig6* mutant line under FR-BOG treatment compared to growth in white light (Figure 3B), suggesting a potential role of ADT5 in the FR-BOG response. To examine phenotypes that may be predicted by the alteration of *ADT5* mRNA levels in a *sig6* mutant under FR-BOG compared to wild type, we tested the greening response of the *adt5* line under FR-BOG. Our results indicated that, like *phyA* and *sig6* that have been previously shown to have an altered greening response in FR-BOG (Alameldin et al., 2020), the *adt5* mutant similarly accumulates chlorophyll under FR-BOG (Figure 4). This result supports a potential role of ADT5 in the chloroplast development process.

To further understand the role of ADT5 in the ABA-dependent chloroplast development process, we investigated ABA-related genes in our RNA-seq dataset. Our data indicate the misregulation of numerous ABA response genes (Figure 3B). Multiple members of the PP2C protein family, known to regulate ABA signaling negatively, are downregulated in *sig6* under FR-BOG conditions [56, 57. 58].

We detected a downregulation of two phenylalanine ammonia-lyase (PAL) genes in a *sig6* mutant under FR-BOG (Figure 3); PAL catalyzes the conversion of phenylalanine to trans-cinnamic acid, the first step of phenylpropanoid biosynthesis leading to diverse plant metabolites reactions (Truman et al., 2007; Widjaja et al.,

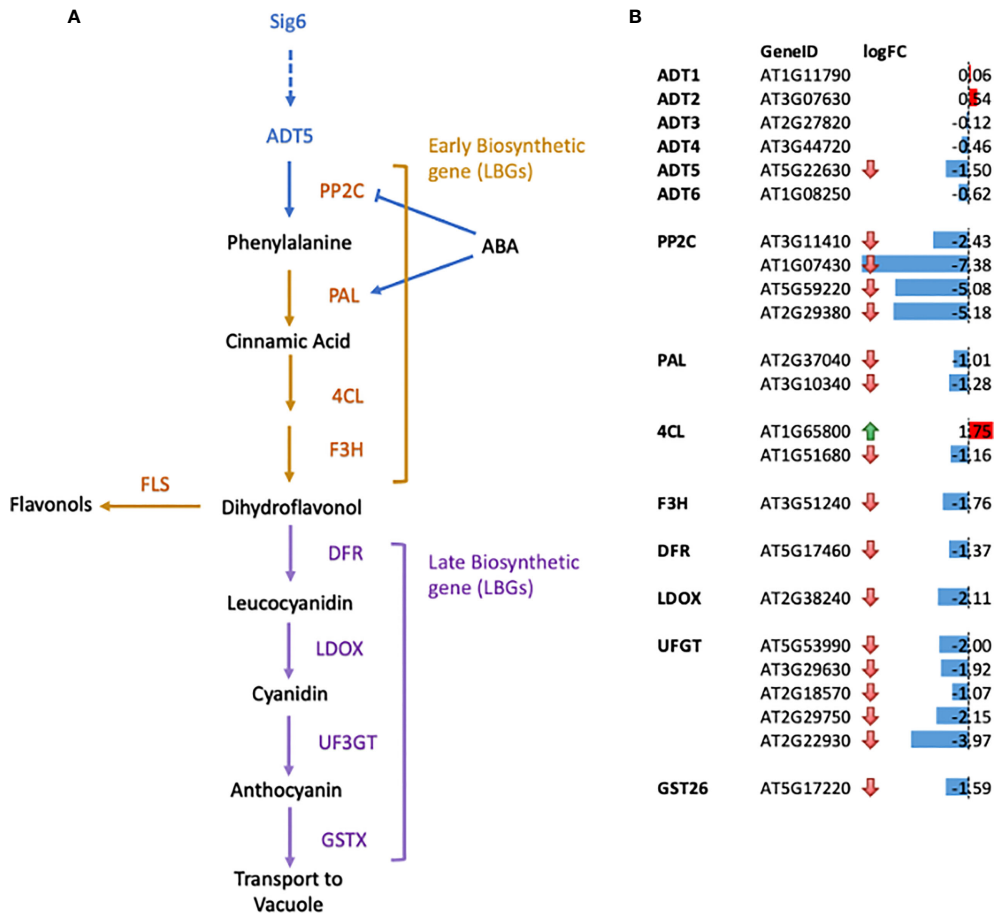

FIGURE 3
Gene expression changes for genes in the flavonoid biosynthetic pathways in *sig6* relative to wild-type under far-red block-of-greening (FR-BOG) conditions. **(A)** Flavonoid biosynthetic pathway. Orange and purple letters indicate the early biosynthetic genes (EBGs) and the late biosynthetic genes (LBGs), respectively. **(B)** Expression of genes involved in flavonoid biosynthesis in *sig6* under FR-BOG. Values are average obtained from four independent RNAseq data experiments. PP2C, protein phosphatase 2C; PAL, phenylalanine ammonia-lyase; 4CL, 4-Coumarate : CoA ligase; F3H, flavonol 3-hydroxylase; F3'H, flavonol 3'-hydroxylase; FLS, flavonol synthase; DFR, dihydroflavonol-4-reductase; LDOX, leucoanthocyanidin dioxygenase; UF3GT, UDP-glucose flavonoid-3-Oglucosyltransferase; GST26, Glutathione S-transferase 26.

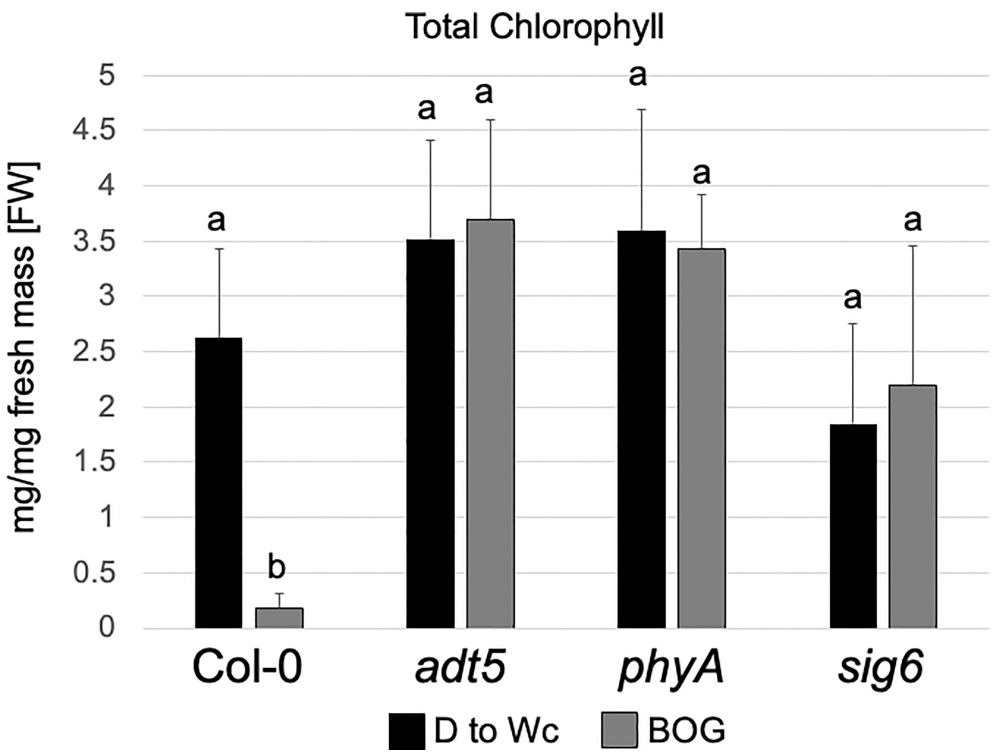

FIGURE 4
Chlorophyll content of wild-type, *adt5*, *phyA*, and *sig6* lines. Chlorophyll content of Col-0 WT, *adt5*, *phyA*, and *sig6* mutant lines was grown at 22°C in darkness (D) for 5 days, then moved to continuous white light (Wc) at 100 µmol m^{-2} s^{-1} for 5 days, i.e., control treatment (D to Wc), or under constant far-red (FRc) illumination at 5 µmol m^{-2} s^{-1} for 5 days, then moved to Wc at 100 µmol m^{-2} s^{-1} for 5 days, i.e., FR block-of-greening (BOG) treatment. Total chlorophyll (mg/mg fresh mass [FW]) was extracted with N,N-dimethylformamide. Data are presented as means (± SD) and were analyzed using a one-way ANOVA, which revealed a significant main effect of genotype ($F_{7,\ 110}$ = 9.09, p < 0.0001), a significant effect of treatment ($F_{1,\ 110}$ = 301.48, p < 0.0001), and a significant interaction between factors ($F_{7,\ 110}$ = 14.46, p < 0.0001). Bars marked with different letters are significantly different (p < 0.05) based on the Tukey–Kramer *post-hoc* test using astatsa.com.

2009). PAL is also involved in the ABA signaling pathway, where PAL was misregulated in *aba3* mutants under oxidative stress. Our data also indicated the downregulation of the Cinnamate 4-hydroxylase *4CL1* gene that controls the last step of the general phenylpropanoid pathway (Li et al., 2015).

Additionally, we detected a downregulation of flavanone 3-hydroxylase (F3H) that is coordinately expressed with chalcone synthase and chalcone isomerases and is involved in flavonoid biosynthesis (Shih et al., 2008). Flavonol synthase 3 (FLS3), involved in the last step of flavonol biosynthesis (Pelletier et al., 1999), was also downregulated in the *sig6* mutant under FR-BOG. Furthermore, five of the UDP-Glycosyltransferase superfamily members' mRNA levels were significantly reduced in the *sig6* mutant under FR-BOG. UDP-Glycosyltransferase superfamily proteins play a central role in the last step of the anthocyanin biosynthesis pathway (Yonekura-Sakakibara et al., 2014). Additionally, the GLUTATHIONE S-TRANSFERASE PHI 12 (GSTF12), which functions as a carrier to transport anthocyanin from the cytosol to tonoplasts (Wagner et al., 2002), was also downregulated in the *sig6* mutant under FR-BOG. Since *adt5* was delayed in germination in response to ABA, and given the fact that ADT5 regulates phenylalanine biosynthesis, our RNA-seq data analysis suggests that ADT5 might play an important role in the anthocyanin biosynthesis pathway.

3.4 *adt* mutant seedlings have unique responses to darkness and white light

After emergence of the seedling from the seed, and prior to emergence into light (presumably under soil or leaf litter in natural contexts), seedling development initiates with rapid stem elongation in darkness. Following emergence into a light environment, photoreceptors perceive ambient light, then initiate the inhibition of stem elongation and promotion of cotyledon expansion, plastid development, and root development. Until the seedling is fully autotrophic, these processes are supported by metabolites stored in the seed, and made in the emerging seedling. We investigated the role of ADTs in darkness, continuous light, or as a result of light-to-dark-transition, from 0 to 7 days.

3.4.1 Seedling development in complete darkness

The *adt1* and *adt4* mutants were not significantly different from WT in shoot or root development in the dark or any light condition tested (Supplementary Figure S2); hence, the remainder of the light study focused on *adt3*, *adt5*, and *adt6* mutants. When grown in Dc (7D0L), hypocotyl (shoot) elongation (shorter; p < 0.001) and root elongation (shorter; p < 0.05) were significantly different for the *adt5* mutant compared to WT (7D0L; Figure 5A). *adt6* mutants

grown in Dc also exhibited shorter shoots relative to WT, but the difference was not significant (p = 0.083), whereas roots were significantly longer than WT (p < 0.01), ultimately resulting in similar shoot+root total lengths for *adt6* and WT (Figure 5A). *adt3* mutant seedlings grew longer in the Dc compared to WT, in both shoot (n.s., p = 0.2665) and root (p < 0.05) lengths, resulting in an overall increased total shoot+root mean length. Although the summed total length of shoot and root were similar for *adt6* and less for *adt5* relative to WT, both *adt5* and *adt6* exhibited reduced shoot:root ratios. Shoot:root ratios can be impacted by environmental conditions and can indicate relative energy contributions to shoot vs. stem elongation (Wilson, 1988).

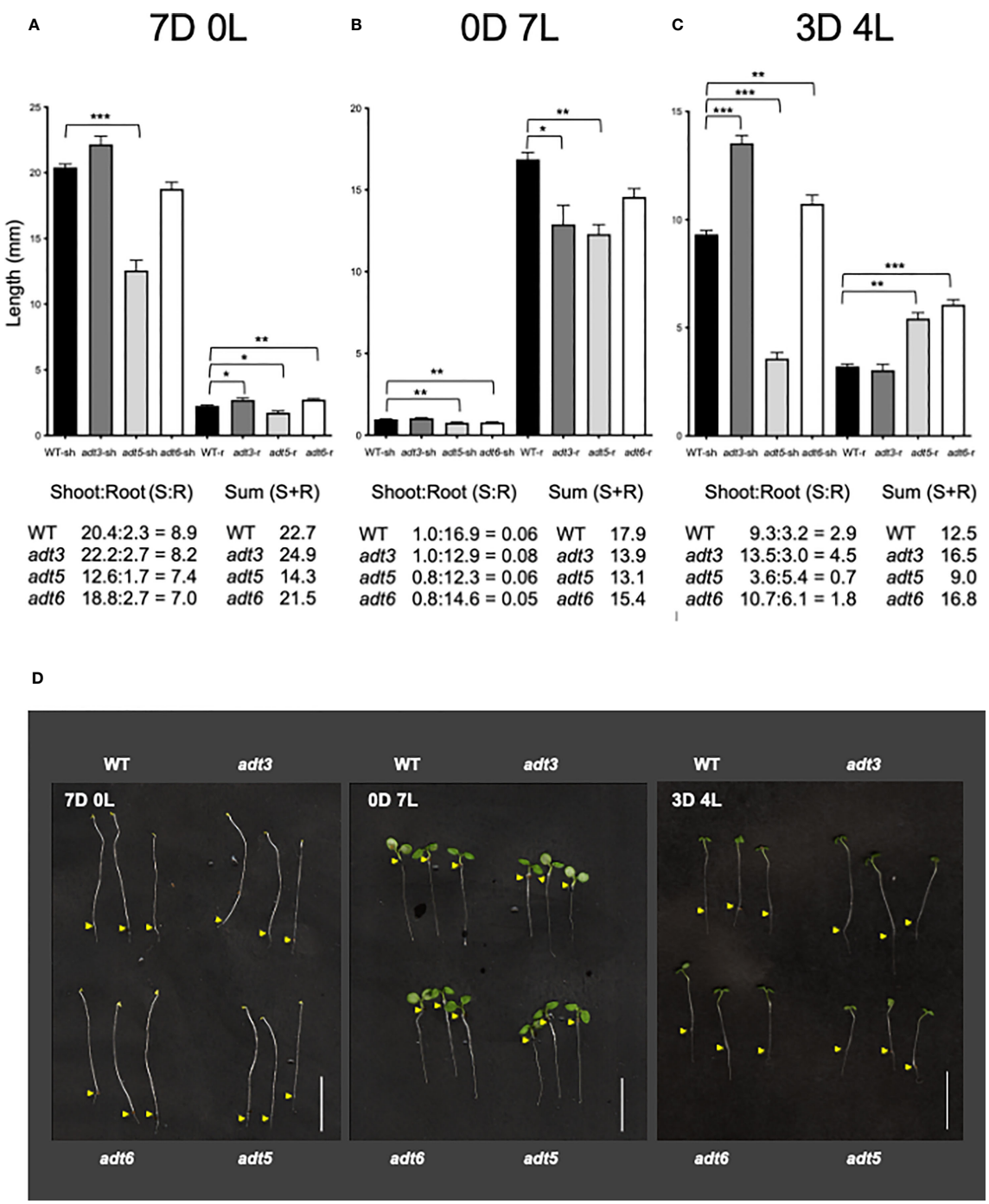

FIGURE 5
Darkness and white light 7-day growth assays. WT and *adt* seedlings were grown vertically on sucrose-free 0.5XMS plates under conditions of **(A)** continuous darkness (7D0L), **(B)** continuous white light (0D7L), or **(C)** a dark–light transition (3 days darkness; 4 days light, 3D4L), maintained at 20° CC. Lengths of shoots (sh) and roots (r) were measured, then bar graphs were made in GraphPad Prism, with differences in mean lengths of roots and shoots compared by unpaired *t*-test, as reported in Results. Lengths of sh and r were summed (shoot + root) in mm. Ratios of shoot:root were also calculated as shown. **(D)** Representative seedlings are shown in the images; scale bar for images indicates 1.0 cm. Yellow arrows indicate the root–shoot junction. *p < 0.05, **p < 0.01., ***p < 0.001.

3.4.2 Seedling development in continuous white light

In continuous white light (0D7L), all roots elongated less than WT [*adt3* (p = 0.0138), *adt5* (p < 0.001), and *adt6* (n.s., p = 0.07) (Figure 5B)]. *adt5* and *adt6* shoot lengths were both less than that observed for WT (p < 0.01 for *adt5* and *adt6*). The ratios of shoot: root lengths for *adt5* and *adt6* were similar to WT in this light regime. *adt3* shoot length was similar to WT (n.s., p = 0.2766), considering that root length resulted in a shoot:root ratio larger than the WT ratio. The sums of the shoot+root length for all *adt* mutant seedlings were less than WT.

3.4.3 Seedling development during a dark-to-light transition

The differences in 7D0L vs. 0D7L were distinct for *adt3, adt5*, and *adt6* mutant seedlings, and led us to test dark-to-light transitions. We tested periods of darkness (D) and periods of white light (L) from 6 days of Dc followed by moving seedlings to 1 day of white light (i.e., 6D:1L), then 5D:2L and so on to 1D:6L. We found that only the regime of 3D:4L resulted in any significant differences between *adt* mutants and WT seedlings (3D4L; Figure 5C). *adt3* exhibited a significantly longer shoot (p < 0.001), but only a marginally shorter root (n.s. p = 0.4796), producing a larger shoot:root ratio and larger shoot+root length compared to WT. *adt5* shoot elongation was less than that measured for WT seedlings (p < 0.001). *adt5* root elongation, however, was greater than WT (p < 0.01), with the shoot:root ratio and total summed shoot+root length of *adt5* being less than those of WT (Figure 5C). Conversely, *adt6* shoot length was longer than WT (p < 0.01), and the root length nearly double that of WT (p < 0.001). This phenotype resulted in a shoot+root length for *adt6* that exceeded WT, whereas the shoot:root ratio was less than WT.

In all three of the light regimes tested, *adt5* had reduced shoot +root lengths. *adt6* in contrast exhibited shoot+root length less than WT in Dc (7D0L) and Wc (0D7L), but greater than WT in the 3D4L condition. If there was darkness in the growth regime (7D0L and 3D4L), *adt3* exhibited greater shoot+root lengths. Representative images of the seedlings in the light regimes including controls are shown in Figure 5D. Given that *adt5* differs from WT in all conditions, whereas *adt3* and *adt6* differ from WT and each other in specific conditions, these data strongly suggest unique light-dependent roles for these ADT family members.

3.5 Monochromatic light-dependent and -independent impacts on hypocotyl elongation in *adt* mutants

Owing to the responses of *adt3*, *adt5*, and *adt6* seedlings in variable light conditions, we measured hypocotyl lengths of these mutants in specific R, FR, or B monochromatic light conditions. Plants were grown at two different fluence rates of continuous R (Rc; 50 and 100 μmol m^{-2} s^{-1}), FR (FRc; 5 and 25 μmol m^{-2} s^{-1}), or B (Bc; 25 and 50 μmol m^{-2} s^{-1}) light with a control set grown in Dc (black bars) for each light condition. A *phyA* mutant was used as a positive control for FR and B light, and a *phyB* mutant was used as a positive control for R light experiments. Of note, *adt3* has been previously shown to have a B-dependent role in Phe synthesis (Warpeha et al., 2006; Warpeha et al., 2008). An insertion mutant of Pirin1, *prn1*, was also included as it is involved in accumulation of phenylpropanoids, and in B- and ABA hormone-dependent signaling (Orozco-Nunnelly et al., 2014). These data are shown in Figure 6 (representative seedlings for conditions are shown Figures 6A–E).

Under an Rc illumination of 50 μmol m^{-2} s^{-1}, *adt5* and *prn1* were longer (p < 0.01 for both) than WT, similar to the *phyB* mutant (p < 0.01), though not to the same magnitude (Figures 6C, F). At a higher fluence of Rc (i.e., 100 μmol m^{-2} s^{-1}), no *adt* mutants were significantly longer than WT (Figure 6I), suggesting a light intensity-dependent role. Under an FRc of 5 μmol m^{-2} s^{-1}, the *adt6* (p < 0.01) mutants were longer than WT, which was similar but to a much lesser degree than the FR-light insensitive *phyA* mutant (p < 0.01; Figures 6D, G). Similar to Rc data, a higher fluence of FRc light did not indicate any significant differences of *adt* mutants and WT (Figure 6J). Under Bc at 25 μmol m^{-2} s^{-1}, *adt3* was longer than WT (p < 0.01), similar to the positive control *phyA* (p < 0.01; Figures 6E, H). *adt5* was shorter than WT (p < 0.01) under these conditions (Figures 6E, H). Markedly, at 50 μmol m^{-2} s^{-1} of Bc, all of the mutants tested were significantly longer than WT (Figure 6K), similar to *phyA*. Notably, among the lines tested, *adt6* exhibited a consistently longer hypocotyl than WT in complete darkness on sucrose-containing medium (Figure 6). These results confirm the input of multiple wavelengths of lights into ADT function during seedling development, as predicted from the gene expression data (Figure 1). As Rc and Bc illumination impacted *adt5* and *adt6* development in hypocotyl inhibition assays on sucrose-containing medium at 7 days, we also examined seedlings during the early post-germination period under a lower fluence rate of Rc or Bc on sucrose-free medium, assessed at 3 days (72 h) post-stratification (Supplementary Figure S3). Shoots and roots of *adt6* were longer than WT under Rc and Bc, and achieved significance for all measurements (p < 0.001); *adt5* was significant for all measurements (Shoots, Bc p < 0.001; Rc p < 0.01) except Rc roots (n.s.).

3.6 Anthocyanin accumulation is impacted in *adt5* mutants

The accumulation of anthocyanins is promoted by light, and anthocyanins are synthesized from the Phe-dependent phenylpropanoid pathway (Chen et al., 2016). Thus, we assessed anthocyanin accumulation in specific single *adt* mutants grown under Wc conditions at the early seedling stage. Anthocyanin levels in the control *phyAphyB* mutant were reduced to 63% of WT levels (Supplementary Figure S4), and the *prn1* mutant that overproduces specific pigments in response to light (Orozco-Nunnelly et al., 2014) was also used as a control. Notably, the *adt5* mutant accumulated only ~70% of WT anthocyanin levels (Supplementary Figure S4). No other mutant had a light-dependent defect in anthocyanin accumulation under our conditions, though *adt5* and *prn1* accumulated less anthocyanins in Dc than that observed for WT (Supplementary Figure S4).

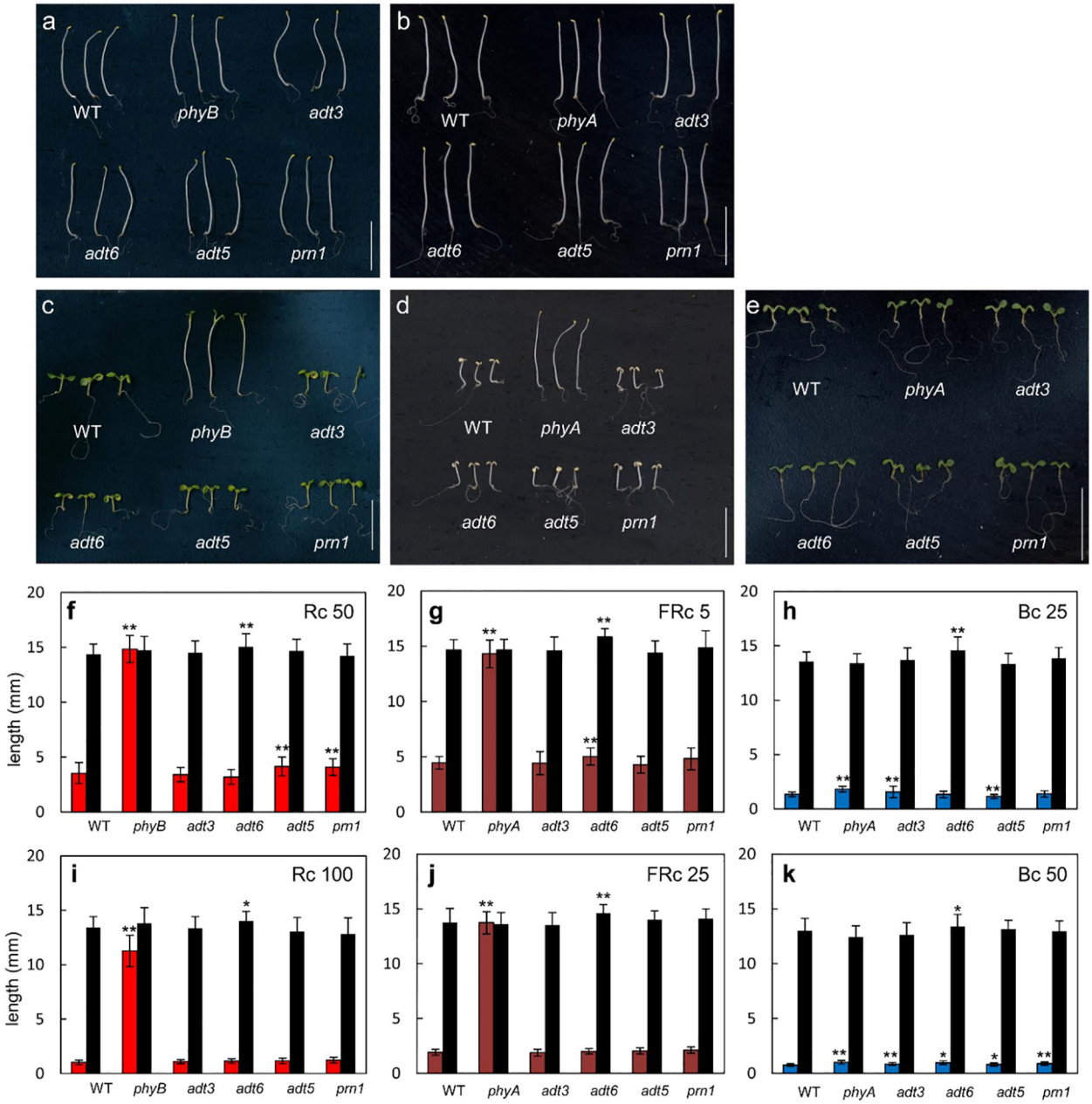

FIGURE 6
Photomorphogenesis of wild-type and *adt* seedlings. WT, *adt*, and *prn1* (control) lines were grown at 22°CC on Phytablend medium containing 1% sucrose for 7 days in **(A, B)** darkness, **(C)** continuous red light (Rc) of 50 μmol m^{-2} s^{-1}, **(D)** continuous far-red light (FRc) of 5 μmol m^{-2} s^{-1}, or **(E)** continuous blue light (Bc) of 25 μmol m^{-2} s^{-1}. *phyB* mutant seedlings are included as control in Rc measurements and *phyA* mutant seedlings in FRc and Bc measurements. Hypocotyl length measurements of WT, *adt*, and *prn1* seedlings under **(F, I)** Rc, **(G, J)** FRc, and **(H, K)** Bc at the indicated fluence rate in μmol m^{-2} s^{-1}; data points represent mean (± SD) of hypocotyl lengths measured for 25 seedlings of each line in each of three independent experiments, i.e., n = 75. Black bars are hypocotyl lengths in dark-grown seedlings. Data analyzed by one-way ANOVA with *post-hoc* Tukey's test; $*p < 0.05$, $**p < 0.01$. Scale bar = 1 cm.

4 Discussion

4.1 ADT5 and ADT6 regulate early developmental responses

There are two aspects of the phenotypes of *adt* mutants that appear particularly important to consider—the germination or early phenotype, where germination is typically completed for WT by 48–72 h post-stratification, and the seedling phenotype, observed herein at 4–7 days. During germination (0–3 days), the available pool of resources, including Phe, stored in the seed to support early growth appears critical, prior to assembly and function of the chloroplasts, where expression of ADTs is deemed important as reviewed (Perkowski and Warpeha, 2019). During seedling development, ADT5 and ADT6 have different actions, which may be based on the tissue in which they primarily occur. As observed in the analysis of germination (Figure 2), it

is clear that *adt5* mutants have difficulty in germination, which may partly be explained in that ADT5 is expressed in the roots (Figure 1; Supplementary S1) where roots emerge first from the seed. *adt5* seeds may possess insufficient resources in the seed to support germination. The inability of *adt5* mutants to overcome dormancy in the dark in response to germination-promoting hormones tested (ACC and GA) provides additional evidence of dependence on photoreceptors, perhaps reinforced by the fact that long irradiations of UV-A/B, blue, and far-red light increase the induced expression of the *ADT5* transcript (Figure 1). The phenotype of *adt5* mutants under FR-BOG conditions mirrored the phenotype of *phyA* and *sig6* (Figure 4), which have previously been implicated in light-responsive, phytochrome-dependent plastid development (Alameldin et al., 2020), further highlighting a role for *ADT5* function in light-dependent, photoreceptor-modulated processes. *adt6* mutants exhibit a phenotype where no hormone had any influence on rapid germination of the mutant in darkness (Figure 2). Primarily protein expression *in planta* appears to be in the cotyledon in the developing mesophyll (Supplementary Figure S1). ADT6 protein may contribute to repressing germination until conditions, in general, are optimal. *ADT6* expression is higher in seeds than *ADT3* and *ADT5* and more similar to *ADT2* (Figure 1A) (Hossain et al., 2018), where its action might be in defense or other activities, which may be important in preparing the embryo for germination.

We explored further the relationship between complete darkness and white light as it impacted hypocotyl and root growth (Figure 5). The observed responses for *adt6* were distinct from those for *adt5*. The amount of darkness versus light affected hypocotyl and root elongation differently, with both Dc and Wc preventing *adt5* from full (compared to WT) expansion in hypocotyls or roots. 3D4L indicated greater expansion of roots for *adt5*, exceeding WT. Any period of darkness (Dc or 3D4L) promoted greater root expansion of *adt6* compared to WT and 3D4L, promoting longer *adt6* hypocotyls. However, 7 days of white light reduced both shoot and root expansion compared to WT, a trend of reduced root+shoot expansion for all three *adt* mutants. *adt3* responses were unique compared to *adt5* and *adt6*, with longer shoots and roots in complete darkness (7D0L), reduced roots in light (0D7L), and increased shoots in 3D4L. Any darkness increased *adt6* roots (7D0L and 3D4L), and any darkness increased *adt3* shoots (7D0L and 3D4L). ADT proteins may have direct influence on auxin transport or directly affect flavonol concentrations in the root:shoot continuum, or in the meristems in different stages of development (Lewis et al., 2011; Liu et al., 2019). An increased exposure to FR or decreased R:FR impacts auxin transport, and is linked to changes in phenylpropanoid-related compounds, including a reduction in anthocyanins and increased lignin in maize (Afifi and Swanton, 2012). *Adt5* mutants accumulated less anthocyanins in Wc (Supplementary Figure S4) in our measurements. Chen et al.'s study of single and multiple ADT gene mutations indicated that ADTs contribute to anthocyanin accumulation, particularly ADT2 at an early stage (Chen et al., 2016).

4.2 Roles of ADT1, ADT2, ADT3, and ADT4 in development

ADT1 and ADT4, while not having dramatic phenotypes apparent in this age of plant development, did indicate unique transcript expression profiles (Figure 1) that coordinated with the observed expression in the GFP fusions (Supplementary Figure S1). ADT2 is important in seed formation and embryo for early survival (Chen et al., 2016). Indeed, both ADT2 and ADT3 (herein and (Para et al., 2016)) indicate impact on earlier processes, with ADT2 being required possibly mostly for seed development (Chen et al., 2016) and defense compounds (Bross et al., 2017) and ADT3 being more important immediately post-germination in development (Para et al., 2016). ADT2 and ADT3 perhaps provide Phe until ADT1, 4, 5, and 6 express in specific tissues of the seedling (photosynthesis in chloroplasts, and roots developing as storage organs). One major event that happens in the seed-to-seedling transition is chloroplast development in the developing leaf cells, where ADT2 and ADT3 may work to coordinate that development, given that different labs have shown that ADT2 (Bross et al., 2017; El-Azaz et al., 2018) and ADT3 (Para et al., 2016) are both required for processes preceding chloroplast development. Phe made via ADTs in general are also recently shown to have a number of specific impacts on photosynthesis and metabolism in older seedlings (~3 weeks old) (Höhner et al., 2018).

4.3 Effect of monochromatic light on ADT functions in young seedlings

Based on the results of the growth studies under monochromatic light, the impact of ADT family proteins on Phe pools may contribute to the photoregulation of hypocotyl elongation. Rc, FRc, and Bc light impact hypocotyl elongation of distinct *adt* mutants relative to WT (Figure 6). This impact may be due to direct regulation of *ADT* gene expression by light (Figure 1B), but could also be due to the general light-associated reduction of Phe pools on growth and development in these mutants. These results suggest an interaction between light and Phe homeostasis. This is further supported by the observed light-impacted differential expression of individual *ADT* genes (Figure 1). In some cases, *adt* mutants and phytochrome mutants have similar light-dependent phenotypes. For example, *phyA* and *adt6* have defects in FR- and B-dependent inhibition of hypocotyl elongation responses at 7 days (Figure 6) and both *phyB* and *adt6* under Rc were different from WT responses. These data suggest potential phytochrome regulation of the light-associated role for ADT6 and also indicated where *adt6* hypocotyls are reduced in 0D7L, but had greater expansion in 7D0L.

The notable and differential defects of *adt* mutants to hormone treatment in germination assays and defects in light responsiveness suggest interplay between light and hormones in the modulation of Phe homeostasis. Light has been shown to regulate a number of hormonal pathways in plants. The integration of GA signaling and light-dependent phytochrome signaling has been previously shown to involve two PHYTOCHOME-INTERACTING FACTOR (PIF) proteins, PIF3 (Feng et al., 2008) and PIF4 (de Lucas et al., 2008). The transcription factor HY5, which is a key regulator of photomorphogenesis (Oyama et al., 1997), also has been linked to hormonal modulation. HY5 impacts GA (Alabadí et al., 2008), auxin (Cluis et al., 2004; Sibout et al., 2006), and ABA (Chen et al., 2008) signaling. Recent studies have also linked G-box-specific binding transcription factor bZIP16 to light, GA, and ABA

signaling through regulating the expression of genes including *PIL5* and *RGL2* (Hsieh et al., 2012). PIL5 (Oh et al., 2006) and RGL2 (Lee et al., 2002) have both been linked to the regulation of seed germination, a phenotype disrupted in *adt* mutants. Light also has a complex regulation of the conversion of ACC to ethylene, dependent on fluence, spectral quality, age of seedlings, and responses to a pulse of light versus continuous irradiations, reviewed in Zdarska et al. (2015). The Rc, FRc, and Bc data of *adt5* or *adt6* compared to WT, as well as the FR-BOG phenotype of *adt5*, indicate that phytochromes and blue light photoreceptors play unique roles with *ADT5* and *ADT6* in development.

4.4 Phe and the seedling transition

Development during the seed-to-seedling transition is an intricate multi-component process in higher plants, requiring energy allocation to rapid development and growth, while the emerging seedling also utilizes energy to sense and respond to environmental signals and to avoid and/or defend against potential detrimental environmental factors. Phe is the first committed precursor of the phenylpropanoid pathway, and genetic and biochemical data indicate that Phe is a concentration-limiting substrate (Margna, 1977; Lee et al., 2002; Rohde et al., 2004; Voll et al., 2004; Warpeha et al., 2008). Phe concentrations are likely coordinated with other phenylpropanoid enzymes, several of which have been shown to peak in expression in 3-day-old white light-grown seedlings (Margna et al., 1989a), a developmental age and growth condition utilized in our experiments. Expression of phenylalanine ammonia-lyase (PAL; EC 4.3.1.5), the enzyme catalyzing the first step of the phenylpropanoid pathway that deaminates L-phenylalanine to trans-cinnamic acid, is highly responsive to environmental and developmental cues and induced early in seedling development (Ohl et al., 1989; Kubasek et al., 1992). *pal1 pal2 pal3 pal4* quadruple mutants of Arabidopsis were severely stunted in growth at the early seedling stage and sterile (Lamb et al., 1989). Depending on the *adt* mutant assessed, the growth of seedlings compared to WT was different, so the location of the Phe accumulation in the seedling (tissue) as well as location in cell types may matter. All data considered suggest that through either direct light-mediated signaling impacts on Phe levels or light-associated disruptions in the regulation of Phe synthesis resulting in reduced Phe pools, ADT-dependent Phe homeostasis impacts the coordination of the regulation of the existing energy budget with growth and development. The expression of each *ADT* appears finely tuned to environmental cues and available resources. Perhaps to prepare the seedling to produce the levels of metabolites and structures required, ADTs evolved as mainly type II isoforms with relaxed regulation to enable the massive production of Phe in the seed-to-seedling transition (El-Azaz et al., 2016; El-Azaz et al., 2022). Because of the uniqueness of responses for each ADT, Phe regulation is likely specific to tissues with respect to age and level of development and, hence, may be critical for promoting the successful establishment of seedlings in dynamic environments.

Data availability statement

The datasets presented in this study can be found in online repositories. The name of the repository and accession number can be found below: NCBI Sequence Read Archive; NCBI Gene Expression Omnibus database: BioProject accession number - PRJNA991474.

Author contributions

KW and BM designed the experiments. DM, HA, SO, BM, and KW performed experiments. DM, HA, SO, BM, and KW analyzed the data. BM, HA, and KW prepared the article with significant contributions from DM and SO. All authors contributed to the article and approved the submitted version.

Funding

This work was supported by the National Science Foundation (grant no MCB-0848113 to KW and MCB-0919100 and MCB-1515002 to BM) and UIC startup funds to KW.

Acknowledgments

We sincerely thank undergraduates Carlos Montero, Jennifer Baek, Anita Chawla, and Shamaila Zaheer, and former graduate students Danielle Orozco-Nunnelly, Lauren Vosseller, and Huini Wu for technical assistance. We thank Bethany Huot for conducting photobiology experiments and providing critical input and feedback on early versions of the manuscript.

Conflict of interest

The authors declare that the research was conducted in the absence of any commercial or financial relationships that could be construed as a potential conflict of interest.

Publisher's note

All claims expressed in this article are solely those of the authors and do not necessarily represent those of their affiliated organizations, or those of the publisher, the editors and the reviewers. Any product that may be evaluated in this article, or claim that may be made by its manufacturer, is not guaranteed or endorsed by the publisher.

Supplementary material

The Supplementary Material for this article can be found online at: https://www.frontiersin.org/articles/10.3389/fpls.2023.1220732/full#supplementary-material

References

Afifi, M., and Swanton, C. (2012). Early physiological mechanisms of weed competition. *Weed Sci.* 60, 542–551. doi: 10.1614/WS-D-12-00013.1

Alabadí, D., Gallego-Bartolomé, J., Orlando, L., García-Cárcel, L., Rubio, V., Martínez, C., et al. (2008). Gibberellins modulate light signaling pathways to prevent Arabidopsis seedling de-etiolation in darkness. *Plant J.* 53, 324–335. doi: 10.1111/j.1365-313X.2007.03346.x

Alameldin, H. F., Oh, S., Hernandez, A. P., and Montgomery, B. L. (2020). Nuclear-encoded sigma factor 6 (SIG 6) is involved in the block of greening response in Arabidopsis thaliana. *Am. J. Bot.* 107 (2), 329–338. doi: 10.1002/ajb2.1423

Alonso, J. M., Stepanova, A. N., Leisse, T. J., Kim, C. J., Chen, H., Shinn, P., et al. (2003). Genome-wide insertional mutagenesis of Arabidopsis thaliana. *Sci.* 301, 653–657. doi: 10.1126/science.1086391

Anders, S., Pyl, P. T., and Huber, W. (2015). HTSeq—a Python framework to work with high-throughput sequencing data. *bioinformatics* 31 (2), 166–169. doi: 10.1093/bioinformatics/btu638

Benjamini, Y., and Hochberg, Y. (1995). Controlling the false discovery rate: a practical and powerful approach to multiple testing. *J. R. Stat. Society: Ser. B (Methodological)* 57 (1), 289–300. doi: 10.1111/j.2517-6161.1995.tb02031.x

Bolger, A. M., Lohse, M., and Usadel, B. (2014). Trimmomatic: a flexible trimmer for Illumina sequence data. *Bioinformatics* 30 (15), 2114–2120. doi: 10.1093/bioinformatics/btu170

Borevitz, J. O., Maloof, J. N., Lutes, J., Dabi, T., Redfern, J. L., Trainer, G. T., et al. (2002). Quantitative trait loci controlling light and hormone response in two accessions of Arabidopsis thaliana. *Genetics.* 160, 683–696. doi: 10.1093/genetics/160.2.683

Bross, C. D., Howes, T. R., Rad, S. A., Kljakic, O., and Kohalmi, S. E. (2017). Subcellular localization of Arabidopsis arogenate dehydratases suggests novel and non-enzymatic roles. *J. Exp. Bot.* 68 (7), 1425–1440. doi: 10.1093/jxb/erx024

Bruns, B., Hahlbrock, K., and Schäfer, E. (1986). Fluence dependence of the ultraviolet-light-induced accumulation of chalcone synthase mRNA and effects of blue and far-red light in cultured parsley cells. *Planta.* 169, 393–398. doi: 10.1007/BF00392136

Chen, Q., Man, C., Li, D., Tan, H., Xie, Y., and Huang, J. (2016). Arogenate dehydratase isoforms differentially regulate anthocyanin biosynthesis in arabidopsis thaliana. *Mol. Plant.* 9 (12), 1609–1619. doi: 10.1016/j.molp.2016.09.010

Chen, H., Zhang, J., Neff, M. M., Hong, S.-W., Zhang, H., Deng, X.-W., et al. (2008). Integration of light and abscisic acid signaling during seed germination and early seedling development. *Proc. Natl. Acad. Sci. U. S. A.* 105, 4495–4500. doi: 10.1073/pnas.0710778105

Cho, M. H., Corea, O. R. A., Yang, H., Bedgar, D. L., Laskar, D. D., Anterola, A. M., et al. (2007). Phenylalanine biosynthesis in Arabidopsis thaliana: Identification and characterization of arogenate dehydratases. *J. Biol. Chem.* 282 (42), 30827–30835. doi: 10.1074/jbc.M702662200

Cluis, C. P., Mouchel, C. F., and Hardtke, C. S. (2004). The Arabidopsis transcription factor HY5 integrates light and hormone signaling pathways. *Plant J.* 38, 332–347. doi: 10.1111/j.1365-313X.2004.02052.x

Corea, O. R. A., Ki, C., Cardenas, C. L., Kim, S. J., Brewer, S. E., Patten, A. M., et al. (2012). Arogenate dehydratase isoenzymes profoundly and differentially modulate carbon flux into lignins. *J. Biol. Chem.* 287, 11446–11459. doi: 10.1074/jbc.M111.322164

de Lucas, M., Davière, J.-M., Rodríguez-Falcón, M., Pontin, M., Iglesias-Pedraz, J. M., Lorrain, S., et al. (2008). A molecular framework for light and gibberellin control of cell elongation. *Nature.* 451, 480–484. doi: 10.1038/nature06520

Dobin, A., Davis, C. A., Schlesinger, F., Drenkow, J., Zaleski, C., Jha, S., et al. (2013). STAR: ultrafast universal RNA-seq aligner. *Bioinformatics* 29 (1), 15–21. doi: 10.1093/bioinformatics/bts635

El-Azaz, J., Cánovas, F. M., Barcelona, B., Ávila, C., and de la Torre, F. (2022). Deregulation of phenylalanine biosynthesis evolved with the emergence of vascular plants. *Plant Physiol.* 188, 134–150. doi: 10.1093/plphys/kiab454

El-Azaz, J., de la Torre, F., Ávila, C., and Cánovas, F. M. (2016). Identification of a small protein domain present in all plant lineages that confers high prephenate dehydratase activity. *Plant J.* 87 (2), 215–229. doi: 10.1111/tpj.13195

El-Azaz, J., Francisco, C., Avila, C., and de la Torre, F. (2018). The arogenate dehydratase ADT2 is essential for seed development in Arabidopsis. *Plant Cell Physiol.* 59, 2409–2420. doi: 10.1093/pcp/pcy200

Farré, E. M., and Weise, S. E. (2012). The interactions between the circadian clock and primary metabolism, Curr. *Opin. Plant Biol.* 15, 293–300. doi: 10.1016/j.pbi.2012.01.013

Feng, S., Martínez, C., Gusmaroli, G., Wang, Y., Zhou, J., Wang, F., et al. (2008). Coordinated regulation of Arabidopsis thaliana development by light and gibberellins. *Nature* 451, 475–479. doi: 10.1038/nature06448

Fischer, R., and Jensen, R. (1987). Arogenate dehydratase. *Methods Enzymol.* 142, 495–502. doi: 10.1016/S0076-6879(87)42061-2

Franklin, K. A., and Quail, P. H. (2010). Phytochrome functions in Arabidopsis development. *J. Exp. Bot.* 61 (1), 11–24. doi: 10.1093/jxb/erp304

Hahlbrock, K., and Scheel, D. (1989). Physiology and molecular biology of phenylpropanoid metabolism. *Annu. Rev. Plant Physiol. Plant Mol. Biol.* 40, 347–369. doi: 10.1146/annurev.pp.40.060189.002023

Höhner, R., Marques, J. V., Ito, T., Amakura, Y., Budgeon, A. D., Weitz, K., et al. (2018). Reduced arogenate dehydratase expression: ramifications for photosynthesis and metabolism. *Plant Physiol.* 177 (1), 115–131. doi: 10.1104/pp.17.01766

Hossain, M. Z., Ishiga, Y., Yamanaka, N., Ogiso-Tanaka, E., and Yamaoka, Y. (2018). Soybean leaves transcriptomic data dissects the phenylpropanoid pathway genes as a defence response against *Phakopsora pachyrhizi Plant Physiol.Biochem.* 132, 424–433. doi: 10.1016/j.plaphy.2018.09.020

Hsieh, W.-P., Hsieh, H.-L., and Wu, S.-H. (2012). Arabidopsis bZIP16 transcription factor integrates light and hormone signaling pathways to regulate early seedling development. *Plant Cell.* 24, 3997–4011. doi: 10.1105/tpc.112.105478

Inskeep, W. P., and Bloom, P. R. (1985). Extinction coefficients of chlorophyll a and b in N, N-dimethylformamide and 80% acetone. *Plant Physiol.* 77, 483–485. doi: 10.1104/pp.77.2.483

Jiao, Y., Ma, L., Strickland, E., and Deng, X. W. (2005). Conservation and divergence of light-regulated genome expression patterns during seedling development in rice and Arabidopsis. *Plant Cell* 17, 3239–3256. doi: 10.1105/tpc.105.035840

Kami, C., Lorrain, S., Hornitschek, P., and Fankhauser, C. (2010). Light-regulated plant growth and development. *Curr. Top. Dev. Biol.* 91, 29–66. doi: 10.1016/S0070-2153(10)91002-8

Kim, S. Y., Warpeha, K. M., and Huber, S. C. (2019). The brassinosteroid receptor kinase, BRI1, plays a role in seed germination and the release of dormancy by cold stratification. *J. Plant Physiol.* 241, 153031. doi: 10.1016/j.jplph.2019.153031

Kliebenstein, D. J. (2004). Secondary metabolites and plant/environment interactions: A view through *Arabidopsis thaliana* tinged glasses. *Plant Cell Environ.* 27 (6), 675–684. doi: 10.1111/j.1365-3040.2004.01180.x

Kubasek, W., Shirley, B., McKillop, a, Goodman, H., Briggs, W., and Ausubel, F. (1992). Regulation of flavonoid biosynthetic genes in germinating arabidopsis seedlings. *Plant Cell* 4, 1229–1236. doi: 10.1105/tpc.4.10.1229

Lamb, C. J., Lawton, M. A., Dron, M., and Dixon, R. A. (1989). Signals and transduction mechanisms for activation of plant defenses against microbial attack. *Cell* 56, 215–224. doi: 10.1016/0092-8674(89)90894-5

Lee, S., Cheng, H., King, K. E., Wang, W., He, Y., Hussain, A., et al. (2002). Gibberellin regulates Arabidopsis seed germination via RGL2, a GAI/RGA-like gene whose expression is up-regulated following imbibition. *Genes Dev.* 16, 646–658. doi: 10.1101/gad.969002

Lewis, D. R., Ramirez, M. V., Miller, N. D., Vallabhaneni, P., Ray, W. K., Helm, R. F., et al. (2011). Auxin and ethylene induce flavonol accumulation through distinct transcriptional networks. *Plant Physiol.* 156, 144–164. doi: 10.1104/pp.111.172502

Li, Y., Yi, J. I., Pysh, K. L., and Chapple., X. X. X. C. (2015). Four isoforms of Arabidopsis 4-coumarate: CoA ligase have overlapping yet distinct roles in phenylpropanoid metabolism. *Plant Physiol.* 169 (4), 2409–2421. doi: 10.1104/pp.15.00838

Liu, Z., Marella, C. B. N., Hartmann, A., Hajirezaei, M. R., and von Wirén, N. (2019). An age-dependent sequence of physiological processes defines developmental root senescence. *Plant Physiol.* 181 (3), 993–1007. doi: 10.1104/pp.19.00809

Love, M. I., Anders, S., and Huber, W. (2017). *Analyzing RNA-seq data with DESeq2. R package reference manual.* (Seattle, WA: Bioconductor).

Love, M. I., Huber, W., and Anders, S. (2014). Moderated estimation of fold change and dispersion for RNA-seq data with DESeq2. *Genome Biol.* 15 (12), 1–21. doi: 10.1186/s13059-014-0550-8

Maeda, H., and Dudareva, N. (2012). The shikimate pathway and aromatic amino acid biosynthesis in plants. *Ann. Rev. Plant Biol. Vol.* 63, 73–105. doi: 10.1146/annurev-arplant-042811-105439

Maranville, E., and Zhu, A. (2000). Assessment of amino-acid substitutions at tryptophan 16 in - galactosidase. *Eur. J. Biochem.* 267, 1495–1501. doi: 10.1046/j.1432-1327.2000.01149.x

Margna, U. (1977). Control at the level of substrate supply—an alternative in the regulation of phenylpropanoid accumulation in plant cells. *Phytochemistry.* 16 (4), 419–426. doi: 10.1016/S0031-9422(00)94321-8

Margna, U., Margna, E., and VainjÄrv, T. (1989a). Influence of nitrogen nutrition on the utilization of L-phenylalanine for building flavonoids in buckwheat seedling tissues. *J. Plant Physiol.* 134 (6), 697–702. doi: 10.1016/S0176-1617(89)80030-6

Margna, U., Vainjärv, T., and Laanest, L. (1989b). Different l-phenylalanine pools available for the biosynthesis of phenolics in buckwheat seedling tissues. *Phytochemistry.* 28, 469–475. doi: 10.1016/0031-9422(89)80034-2

Mayfield, J. D., Folta, K. M., Paul, A.-L., and Ferl, R. J. (2007). The 14-3-3 proteins and influence transition to flowering and early phytochrome response. *Plant Physiol.* 145, 1692–1702. doi: 10.1104/pp.107.108654

Montgomery, B. L., Yeh, K. C., Crepeau, M. W., and Lagarias, J. C. (1999). Modification of distinct aspects of photomorphogenesis via targeted expression of mammalian biliverdin reductase in transgenic Arabidopsis plants. *Plant Physiol.* 121, 629–639. doi: 10.1104/pp.121.2.629

Moran, R. (1982). Formulae for determination of chlorophyllous pigments ex- tracted with N, N-dimethylformamide. *Plant Physiol.* 69, 1376–1381. doi: 10.1104/pp.69.6.1376

Nemhauser, J. L., Hong, F., and Chory, J. (2006). Different plant hormones regulate similar processes through largely nonoverlapping transcriptional responses. *Cell* 126, 467–475. doi: 10.1016/j.cell.2006.05.050

Oh, S., and Montgomery, B. L. (2013). Phytochrome-induced SIG2 expression contributes to photoregulation of phytochrome signalling and photomorphogenesis in Arabidopsis thaliana. *J. Exp. Bot.* 64, 5457–5472. doi: 10.1093/jxb/ert308

Oh, E., Yamaguchi, S., Kamiya, Y., Bae, G., Il Chung, W., and Choi, G. (2006). Light activates the degradation of PIL5 protein to promote seed germination through gibberellin in Arabidopsis. *Plant J.* 47, 124–139. doi: 10.1111/j.1365-313X.2006.02773.x

Ohl, S., Hahlbrock, K., and Schäfer, E. (1989). A stable blue-light-derived signal modulates ultraviolet-light-induced activation of the chalcone-synthase gene in cultured parsley cells. *Planta.* 177, 228–236. doi: 10.1007/BF00392811

Orozco-Nunnelly, D. A., Muhammad, D., Mezzich, R., Lee, B.-S., Jayathilaka, L., Kaufman, L. S., et al. (2014). Pirin1 (PRN1) is a multifunctional protein that regulates quercetin, and impacts specific light and uv responses in the seed-to-seedling transition of *Arabidopsis thaliana*. *PloS One* 9 (4), e93371. doi: 10.1371/journal.pone.0093371

Oyama, T., Shimura, Y., and Okada, K. (1997). The Arabidopsis HY5 gene encodes a bZIP protein that regulates stimulus- induced development of root and hypocotyl. *Genes Dev.* 11, 2983–2995. doi: 10.1101/gad.11.22.2983

Para, A., Muhammad, D., Orozco-Nunnelly, D. A., Memishi, R., Alvarez, S., Naldrett, M. J., et al. (2016). The dehydratase ADT3 affects ROS homeostasis and cotyledon development. *Plant Physiol.* 172 (2), 1045–1060. doi: 10.1104/pp.16.00464

Pelletier, M. K., Burbulis, I. E., and Winkel-Shirley, B. (1999). Disruption of specific flavonoid genes enhances the accumulation of flavonoid enzymes and end-products in Arabidopsis seedlings. *Plant Mol. Biol.* 40 (1), 45–54. doi: 10.1023/A:1026414301100

Perkowski, M. C., and Warpeha, K. M. (2019). Phenylalanine roles in the seed-to-seedling stage: Not just an amino acid. *Plant Sci.* 289, 110223. doi: 10.1016/j.plantsci.2019.110223

Rippert, P., Puyaubert, J., Grisollet, D., Derrier, L., and Matringe, M. (2009). Tyrosine and phenylalanine are synthesized within the plastids in arabidopsis. *Plant Physiol.* 149 (3), 1251–1260. doi: 10.1104/pp.108.130070

Rohde, A., Morreel, K., Ralph, J., Goeminne, G., Hostyn, V., De Rycke, R., et al. (2004). Molecular phenotyping of the pal1 and pal2 mutants of Arabidopsis thaliana reveals far-reaching consequences on phenylpropanoid, amino acid, and carbohydrate metabolism. *Plant Cell* 16, 2749–2771. doi: 10.1105/tpc.104.023705

Ruckle, M. E., DeMarco, S. M., and Larkin, R. M. (2007). Plastid signals remodel light signaling networks and are essential for efficient chloroplast biogenesis in arabidopsis. *Plant Cell Online.* 19, 3944–3960. doi: 10.1105/tpc.107.054312

Shih, C. H., Chu, H., Tang, L. K., Sakamoto, W., Maekawa, M., Chu, I. K., et al. (2008). Functional characterization of key structural genes in rice flavonoid biosynthesis. *Planta* 228 (6), 1043–1054. doi: 10.1007/s00425-008-0806-1

Sibout, R., Sukumar, P., Hettiarachchi, C., Holm, M., Muday, G. K., and Hardtke, C. S. (2006). Opposite root growth phenotypes of hy5 versus hy5 hyh mutants correlate with increased constitutive auxin signaling. *PloS Genet.* 2, 1898–1911. doi: 10.1371/journal.pgen.0020202

Sullivan, J. A., and Deng, X. W. (2003). From seed to seed: The role of photoreceptors in Arabidopsis development. *Dev. Biol.* 260, 289–297. doi: 10.1016/S0012-1606(03)00212-4

Truman, W., Bennett, M. H., Kubigsteltig, I., Turnbull, C., and Grant., M. (2007). Arabidopsis systemic immunity uses conserved defense signaling pathways and is mediated by jasmonates. *Proc. Natl. Acad. Sci.* 104 (3), 1075–1080. doi: 10.1073/pnas.060542310

Tzin, V., and Galili, G. (2010). New Insights into the shikimate and aromatic amino acids biosynthesis pathways in plants. *Mol. Plant.* 3 (6), 956–972. doi: 10.1093/mp/ssq048

Van Heerden, P. S., Neil Towers, G. H., and Lewis, N. G. (1996). Nitrogen metabolism in lignifying Pinus taeda cell cultures. *J. Biol. Chem.* 271, 12350–12355. doi: 10.1074/jbc.271.21.12350

Voll, L. M., Allaire, E. E., Fiene, G., and Weber, A. P. M. (2004). The Arabidopsis phenylalanine insensitive growth mutant exhibits a deregulated amino acid metabolism. *Plant Physiol.* 136, 3058–3069. doi: 10.1104/pp.104.047506

Wagner, U., Edwards, R., Dixon, D. P., and Mauch, F. (2002). Probing the diversity of the Arabidopsis glutathione S-transferase gene family. *Plant Mol. Biol.* 49, no. 5, 515–532. doi: 10.1023/A:1015557300450

Warnasooriya, S. N., and Montgomery, B. L. (2009). Detection of spatial-specific phytochrome responses using targeted expression of biliverdin reductase in Arabidopsis. *Plant Physiol.* 149, 424–433. doi: 10.1104/pp.108.127050

Warpeha, K. M., Gibbons, J., Carol, A., Slusser, J., Tree, R., Durham, W., et al. (2008). Adequate phenylalanine synthesis mediated by G protein is critical for protection from UV radiation damage in young etiolated *Arabidopsis thaliana* seedlings. *Plant Cell Environ.* 31 (12), 1756–1770. doi: 10.1111/j.1365-3040.2008.01878.x

Warpeha, K. M., Lateef, S. S., Lapik, Y., Anderson, M., Lee, B.-S., and Kauffman, L. S. (2006). G-protein-coupled receptor 1, G-protein Gα-subunit 1, and prephenate dehydratase 1 are required for blue light-induced production of phenylalanine in etiolated arabidopsis. *Plant Physiol.* 140 (3), 844–855. doi: 10.1104/pp.105.071282

Warpeha, K. M. F., Marrs, K. A., and Kaufman, L. S. (1989). Blue-light regulation of specific transcript levels in *Pisum sativum*. *Plant Physiol.* 91, 1030–1035. doi: 10.1104/pp.91.3.1030

Warpeha, K. M., and Montgomery, B. L. (2016). Light and hormone interactions in the seed-to-seedling transition. *Environ.Exp. Bot* 121, 56–65. doi: 10.1016/j.envexpbot.2015.05.004

Widjaja, I., Naumann, K., Roth, U., Wolf, N., Mackey, D., Dangl, J. L., et al. (2009). Combining subproteome enrichment and Rubisco depletion enables identification of low abundance proteins differentially regulated during plant defense. *Proteomics* 9 (1), 138–147. doi: 10.1002/pmic.200800293

Wilson, J. B. (1988). A review of evidence on the control of shoot:root ratio, in relation to models. *Ann. Bot.* 61, 433–449. doi: citeulike-article-id:8704709 doi: 10.1093/oxfordjournals.aob.a087575

Woodson, J. D., Perez-Ruiz, J. M., Schmitz, R. J., Ecker, J. R., and Chory, J. (2013). Sigma factor-mediated plastid retrograde signals control nuclear gene expression. *Plant J.* 73, 1–13. doi: 10.1111/tpj.12011

Yamada, T., Matsuda, F., Kasai, K., Fukuoka, S., Kitamura, K., Tozawa, Y., et al. (2008). Mutation of a rice gene encoding a phenylalanine biosynthetic enzyme results in accumulation of phenylalanine and tryptophan. *Plant Cell* 20 (5), 1316–1329. doi: 10.1105/tpc.107.057455

Yamburenko, M. V., Yan, O. Z., and Börner, T. (2015). Abscisic acid affects transcription of chloroplast genes via protein phosphatase 2C-dependent activation of nuclear genes: repression by guanosine-3′-5′-bisdiphosphate and activation by sigma factor 5. *Plant J.* 82 (6), 1030–1041. doi: 10.1111/tpj.12876

Yonekura-Sakakibara, K., Nakabayashi, R., Sugawara, S., Tohge, T., Ito, T., Koyanagi, M., et al. (2014). A flavonoid 3-O-glucoside: 2 ″-O-glucosyltransferase responsible for terminal modification of pollen-specific flavonols in *Arabidopsis thaliana*. *Plant J.* 79 (5), 769–782. doi: 10.1111/tpj.12580

Zdarska, M., Dobisová, T., Gelová, Z., Pernisová, M., Dabravolski, S., Hejátko, J., et al. (2015). Illuminating light, cytokinin, and ethylene signalling crosstalk in plant development. *J. Exp. Bot.* 66 (16), 4913–4931. doi: 10.1093/jxb/erv261

frontiers | Frontiers in Plant Science

TYPE Original Research
PUBLISHED 02 November 2023
DOI 10.3389/fpls.2023.1273235

OPEN ACCESS

EDITED BY
Muhammad Awais Farooq,
Hebei Agricultural University, China

REVIEWED BY
Torsten Möhlmann,
University of Kaiserslautern, Germany
Claus-Peter Witte,
Leibniz University Hannover, Germany

*CORRESPONDENCE
Robert D. Slocum
robert.slocum@goucher.edu

RECEIVED 05 August 2023
ACCEPTED 17 October 2023
PUBLISHED 02 November 2023

CITATION
Slocum RD, Mejia Peña C and Liu Z (2023) Transcriptional reprogramming of nucleotide metabolism in response to altered pyrimidine availability in Arabidopsis seedlings.
Front. Plant Sci. 14:1273235.
doi: 10.3389/fpls.2023.1273235

Transcriptional reprogramming of nucleotide metabolism in response to altered pyrimidine availability in Arabidopsis seedlings

Robert D. Slocum[1]*, Carolina Mejia Peña[2] and Zhongchi Liu[3]

[1]Department of Biological Sciences, Goucher College, Towson, MD, United States, [2]Department of Molecular Biology, Cell Biology, and Biochemistry, Brown University, Providence, RI, United States, [3]Department of Cell Biology and Molecular Genetics, University of Maryland, College Park, MD, United States

In Arabidopsis seedlings, inhibition of aspartate transcarbamoylase (ATC) and *de novo* pyrimidine synthesis resulted in pyrimidine starvation and developmental arrest a few days after germination. Synthesis of pyrimidine nucleotides by salvaging of exogenous uridine (Urd) restored normal seedling growth and development. We used this experimental system and transcriptional profiling to investigate genome-wide responses to changes in pyrimidine availability. Gene expression changes at different times after Urd supplementation of pyrimidine-starved seedlings were mapped to major pathways of nucleotide metabolism, in order to better understand potential coordination of pathway activities, at the level of transcription. Repression of *de novo* synthesis genes and induction of intracellular and extracellular salvaging genes were early and sustained responses to pyrimidine limitation. Since *de novo* synthesis is energetically more costly than salvaging, this may reflect a reduced energy status of the seedlings, as has been shown in recent studies for seedlings growing under pyrimidine limitation. The unexpected induction of pyrimidine catabolism genes under pyrimidine starvation may result from induction of nucleoside hydrolase *NSH1* and repression of genes in the plastid salvaging pathway, diverting uracil (Ura) to catabolism. Identification of pyrimidine-responsive transcription factors with enriched binding sites in highly coexpressed genes of nucleotide metabolism and modeling of potential transcription regulatory networks provided new insights into possible transcriptional control of key enzymes and transporters that regulate nucleotide homeostasis in plants.

KEYWORDS

nucleotide metabolism, pyrimidine, purine, *Arabidopsis*, transcriptome

1 Introduction

Nucleotides play essential roles in the metabolism of all living organisms. They are the building blocks of nucleic acids, function in energy metabolism and cell signaling cascades, and serve as activated intermediates in carbohydrate metabolism (Bar-Peled and O'Neill, 2011) and other diverse processes (Zrenner et al., 2006; Ashihara et al., 2020; Pietrowska-Borek et al., 2020; Witte and Herde, 2020). Previous biochemical and molecular studies have defined metabolic pathways and genes encoding most enzymes involved in pyrimidine and purine nucleotide metabolism in plants (Wagner and Backer, 1992; Zrenner et al., 2006; Ashihara et al., 2020; Witte and Herde, 2020). These pathways comprise *de novo* synthesis, salvaging of preexisting nucleobases or nucleosides, nucleotide synthesis, and catabolism. In addition, nucleobase, nucleoside and nucleotide transporters move these intermediates within and between cells and tissues (Girke et al., 2014; Major et al., 2017).

Coordination between major pathways of nucleotide metabolism has been further characterized through metabolic profiling studies (Ashihara et al., 2020) and functional studies with mutants. For example, antisense-mediated knockdown of UMP synthase expression in the *de novo* pyrimidine synthesis pathway in potato tubers resulted in increased expression of genes involved in pyrimidine salvaging, increased salvaging pathway activities, and increased levels of uridine nucleotides as a compensatory response (Geigenberger et al., 2005). Similar results were obtained for Arabidopsis RNAi lines with decreased expression of aspartate transcarbamoylase (Chen and Slocum, 2008), which regulates *de novo* pyrimidine pathway activities (Schröder et al., 2005; Bellin et al., 2021; Bellin et al., 2023a). Increased expression of pyrimidine salvaging pathway genes and decreased expression of catabolic pathway genes in response to pyrimidine limitation suggested similar compensatory responses that could help maintain pyrimidine homeostasis in these plants. Thus, nucleotide metabolism responds dynamically to changes in pyrimidine synthesis, at least in part, through transcriptional regulation of enzyme activities. Mechanisms by which this occurs have been poorly investigated.

Here, we explored transcriptional control of nucleotide metabolism in Arabidopsis seedlings using genome-wide expression profiling to investigate changes in expression of genes encoding all known enzymes and transporters of nucleotide metabolism in response to changes in pyrimidine availability. Treatment of seedlings with *N*-(phosphonacetyl)-L-aspartate (PALA), a potent and specific inhibitor of aspartate transcarbamoylase (ATC) and *de novo* pyrimidine synthesis (Bassett et al., 2003; Bellin et al., 2021), resulted in severe growth inhibition and developmental arrest of seedlings within a few days of germination. Normal development was restored by supplementation with exogenous uridine (Urd), which is taken up and used to synthesize pyrimidine nucleotides *via* salvage pathway activities (Witte and Herde, 2020). Expression profiling at various times after Urd addition, and mapping of gene expression changes to metabolic pathways, was a highly informative approach to understanding transcriptional regulation of key enzymes and transporters involved in nucleotide homeostasis. We also examined broader effects of this perturbation in nucleotide metabolism on other cellular processes and identified transcription factors (TF) that may participate in transcription regulatory networks controlling these processes. This represents the first comprehensive study of this type, and it has provided important new insights into the regulation of nucleotide metabolism in plants.

2 Materials and methods

2.1 Growth of Arabidopsis cultures and experimental treatments

Arabidopsis thaliana L. seeds (Col-0, Columbia ecotype; stock number CS6673, Arabidopsis Biological Resource Center, Columbus, OH, USA) were surface-sterilized, and approximately 25 seeds were placed into liquid cultures (100 mL of ½× MS medium containing 2.5 mM KH_2PO_4 and 1% (w/v) sucrose in a 250-mL flask). The medium contained supplemental phosphate so that this nutrient was not limiting for nucleotide metabolism during the course of the experiment. After 2 days at 4°C to synchronize seed germination, flasks were placed on a rotary shaker at 100 rpm under fluorescent lights (approximately 100 μE m^{-2} s^{-1}) and a 16L/8D photoperiod at 25°C. The experiment design is shown in Figure 1. PALA (*N*-(phosphonoacetyl)-L-aspartate, NSC #224131-F/30; Developmental Therapeutics Program, National Cancer Institute, NIH, Bethesda, MD, USA) was added to 1 mM final concentration to some of the cultures at day 2. Untreated and 1 mM PALA-containing cultures were harvested 6 h into the light cycle on days 5, 7, 9, and 12. Uracil (Ura), uridine (Urd), and thymidine (Thd) (Sigma-Aldrich; St. Louis, MO, USA) were added to 1 mM final concentrations in some PALA-containing cultures on day 5. Seedlings were harvested on days 7, 9, and 12. Data are representative of two separate experiments, except for gene expression data, which were derived from the second experiment only.

2.2 Determination of tissue chlorophyll contents

Seedlings were weighed, homogenized in 2 mL of 95% (v/v) methanol, then centrifuged at 16,000 × *g*, 10 min. The pellet was reextracted with an equal volume of solvent. Total chlorophyll (*a*+*b*) was determined using the method of Arnon (1949) and expressed on a fresh weight basis. Three biological replicates of 8–10 seedlings each were assayed for each treatment.

2.3 Catabolic pathway activity assay

Day 9 seedlings were removed from liquid culture, briefly rinsed in pH 5.8 potassium phosphate buffer, then blotted dry and weighed. Two seedlings were placed in a capped 75 × 12-mm

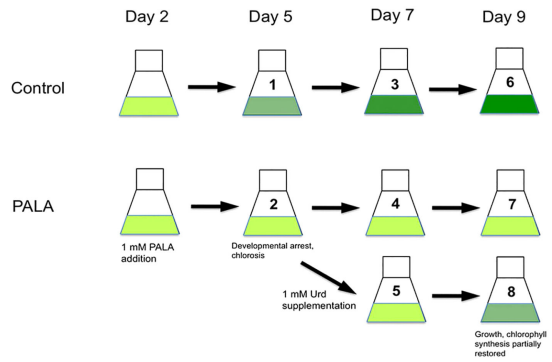

FIGURE 1
Experiment design. At day 2, PALA was added to a final concentration of 1 mM. Control and PALA-treated seedlings were sampled at days 5, 7, and 9. Some cultures containing 1 mM PALA were supplemented with 1 mM Urd at day 5, then seedlings were sampled at day 7 and day 9. For qRT-PCR assays, samples were also collected at the day 5 and 7 time points, and also the day 12 time point (not shown). Developmental and biochemical phenotype and gene expression data were based upon comparisons of PALA-treated, or PALA+Urd supplemented seedlings with untreated control seedlings at each time point.

plastic tube containing 1 mL of the same buffer containing 1 mM unlabeled Ura + 1 μCi [2-^{14}C]-Ura (7.4 GBq mmol^{-1}; Sigma-Aldrich, St. Louis, MO, USA). Following a 16-h incubation at 25°C, seedlings were removed from the tube, rinsed in buffer + 1 mM unlabeled Ura, and homogenized in 1 mL of 10% (v/v) perchloric acid (PCA). PCA-soluble and -insoluble fractions were separated by centrifugation at 16,000 × *g*. PCA-insoluble materials were hydrolyzed overnight in 6 M HCl and the supernatant was collected after 16,000 x *g* centrifugation. Soluble and insoluble fractions were neutralized with KOH, and ^{14}C-label was quantified by scintillation counting. In parallel, a CO_2 capture assay was performed to measure Ura catabolism. Seedlings were placed in tubes containing the same reactants as previously described and 6-mm paper discs saturated with 2 M KOH were mounted inside the tube on a plugged 22-gauge syringe needle, inserted through the tube cap. After the incubation period, the assay was terminated by addition of 1 mL of 10% PCA. The tube was re-capped and any additional release of $^{14}CO_2$ was captured for 6 h. After drying, ^{14}C-label on paper discs was counted directly. Four biological replicates of each assay were used.

2.4 Seedling DNA and RNA contents

Seedling DNA contents were determined using a DAPI assay, as described by Baer et al. (1982). Seedling total RNA was isolated using the Plant RNeasy kit (Qiagen, Valencia, CA), according to the manufacturer's protocol. RNA samples were treated using a TURBO DNA-Free DNase I kit (Thermo Fisher Scientific, Carlsbad, California) to remove genomic DNA contamination. RNA was quantified by A_{260} using a NanoDrop One spectrophotometer.

2.5 qRT-PCR analyses of gene expression

Primer3 was used to design primers to Arabidopsis coding sequences. Unique primer pairs generating 100–150-bp amplicons with T_m = 60.0 ± 2.0°C were designed for each of the target genes and tested for self-complementarity characteristics. For target genes producing alternatively spliced transcripts, primers were designed to amplify all transcripts associated with the gene. Primers were also designed for the five spiking controls and four invariant control genes (see below). Primer sequences and product sizes for all genes are listed in Supplemental Table 1. Primers were synthesized by Operon (Eurofins Genomics, Louisville, KY).

Total RNA (1 μg) was reverse-transcribed (SuperScript III First-Strand Synthesis System; Invitrogen, Carlsbad, CA, USA). Spiking controls (*Bacillus subtilis* transcripts) were added to each sample before cDNA synthesis (per μg total RNA: *lysA*, 0.00002 fmol; *pheB*, 0.0002 fmol; *thrC*, 0.002 fmol; *trpF*, 0.02 fmol; *dapB*, 0.2 fmol). PCR primers were arrayed with sample sets in 384-well optical plates in 10-μL reactions containing 2.5 μL of 0.8 mM primers, 2.5 μL of 1:12.5-diluted sample cDNA, and 5 μL of 2× SYBR Green PCR Master Mix. The master mix and plates were purchased from ABI (Applied Biosystems Inc., Foster City, CA, USA). qPCR analyses were conducted using an ABI Prism 7800HT Sequence Detection System and the SDS v. 2.2.1 software package. PCR amplification steps: 50°C, 2 min; 95°C, 10 min [45 cycles: 95°C, 15 s; 60°C, 1 min]. SYBR Green fluorescence was measured at a threshold value of 0.2, and results were expressed as the C_T value. Dissociation curve analyses confirmed amplification of homogeneous targets. qPCR products were sequenced to confirm target specificity. PCR amplification efficiencies for each template (three biological replicates, two technical replicates of each) were determined using the LinRegPCR v 7.5 analysis package (Ramakers et al., 2003). qBase v. 1.3.5 analysis software (Hellemans et al., 2008) was used to calculate normalized relative quantities (NRQ) from raw expression data (C_T values) with gene-specific efficiency correction and sample-to-sample interrun calibration (IRC) using four reference genes (AT4G26410, AT4G27960, AT5G15710, AT5G46630; Czechowski et al., 2005). Stability of the reference genes under experimental conditions was evaluated using the geNorm algorithm (Vandesompele et al., 2002) within qBase. Expression data for experimental samples were calculated as ratios ± S.E, relative to control samples. Expression data for day 12 seedlings was gathered only for genes analyzed by qRT-PCR.

2.6 RNA-seq analyses

Total RNA sample quality was analyzed using a Agilent Bioanalyzer 2100 platform and prepared for sequencing using a TruSeq cDNA library prep kit (Illumina). Using an Illumina HiSeq 2000 sequencer, an average 53.9 million reads (50 bp, unpaired) per each biological replicate (n = 2) were obtained. Sequencing was performed by Cornell Weill Medical College genomics core (https://

research.weill.cornell.edu/core-facilities/genomics). CLC Genomics Workbench v. 10.0.1 software was used to trim and map reads to exons in the Arabidopsis reference genome (TAIR10.1) using Araport11 annotation (Cheng et al., 2017) and 94.8% of reads mapped to exons and introns. Data set normalization, quality control analyses, and gene differential expression (DE) analyses using the R Bioconductor module DESeq2 were performed according to Veerappa et al. (2019). Differentially expressed genes were defined as those having fold-change values of ≥1.5 (padj ≤ 0.05) in response to treatments, relative to untreated controls. RNA-seq reads data have been deposited in the NCBI Sequence Read Archive (BioProject accession #PRJNA704993). Normalized gene expression data were visualized, hierarchically clustered (1-Pearson, average linkage) and further analyzed using Morpheus (https://software.broadinstitute.org/morpheus/). qRT-PCR expression analyses for 35 genes were used to verify RNA-seq expression data for day 5 and day 7 samples (Supplemental Figure 1).

2.7 Transcription factor enrichment analyses and modeling of transcriptional regulatory networks

ATTED-II (Obayashi et al., 2018) was used to identify the 300 most highly coexpressed Arabidopsis genes with input lists of DE genes functioning in *de novo* synthesis, NTP synthesis, salvaging, catabolism, or nucleobase transport. The PlantRegMap transcription factor (TF) enrichment tool (Tian et al., 2020) was used to identify TF with statistically overrepresented targets in coexpressed genes that were also DE in response to PALA treatment at any time point (day 5, 7, or 9). Lists of significantly enriched TF ($q \leq 0.05$) were further limited to those TF that were also DE in response to PALA treatment.

iRegNet (Shim et al., 2021) was used to suggest transcriptional regulatory networks beyond potential direct regulations identified in target genes. This resource was queried with TF that were induced or repressed by PALA treatment in day 5 seedlings and which also had enriched targets within the highly co-expressed nucleotide metabolism gene cohorts described above (Bonferroni-corrected p-values ≤ 1e−10; 1,000-bp upstream and 1,000-bp downstream flanking sequences of genes were analyzed). iRegNet was also used to explore potential upstream regulons for individual TF and small groups of co-regulated genes.

2.8 Construction of metabolic pathways for Arabidopsis nucleotide metabolism

Metabolic pathways and enzyme and transporter annotation and genes for Arabidopsis nucleotide metabolism were adopted from Zrenner et al. (2006) and Witte and Herde (2020). Pathways described in the present study are also supported by information retrieved from AraCyc (https://biocyc.org/group?id=:ALL-PATHWAYS&org-id=ARA#%20).

3 Results

3.1 The pyrimidine starvation phenotype in Arabidopsis seedlings is reversed by salvaging of exogenous uridine

The experiment design for investigating developmental and biochemical phenotypes related to changes in pyrimidine availability is shown in Figure 1. Treatment with 1 mM PALA beginning at 2 days after germination resulted in developmental arrest of seedlings by day 5 and continued through day 9 and day 12 time points (Figure 2A). Root growth was especially stunted. Seedlings exhibited severe chlorosis, with chlorophyll contents only 25%–30% of that in untreated control seedlings at days 5, 7, and 9 (Figure 2B). At day 9, seedling DNA and RNA contents were 60% and 30% lower than controls, respectively (Figure 2C). This pyrimidine starvation phenotype persisted at day 12, indicating that metabolism of PALA was negligible.

Addition of 1 mM Urd to day 5 cultures containing 1 mM PALA reversed seedling developmental arrest beginning around 9, when increased hypocotyl and primary root growth, expansion of cotyledons, and development of leaves were noted (Figure 2A). Chlorophyll contents were not significantly different from control seedlings by day 7 (Figure 2B). By day 9, DNA contents were the same as controls and RNA contents were 20% higher than in control seedlings (Figure 2C). In cultures grown for an additional 3 days (day 12, 7 days of Urd supplementation), seedling development was nearly indistinguishable from control seedlings at the day 9 stage, including significant lateral root development and two sets of rosette leaves (Figure 2A). In contrast, development of seedlings supplemented with 1 mM Ura was not different from PALA-treated seedlings in day 9 or day 12 cultures. However, at day 7, chlorophyll contents of these seedlings were 80% of those in control seedlings and were not different from controls at day 9 (Figure 2B), suggesting a limited ability to salvage this nucleobase. Seedlings in thymidine-supplemented cultures (not shown) did not look different than PALA-treated seedlings at either day 9 or day 12 (Figure 2A). Chlorophyll contents were also not different from those of PALA-treated seedlings, indicating little salvaging of this nucleoside (Figure 2B).

3.2 Increased uracil catabolism explains poor salvaging of this nucleobase in pyrimidine starved seedlings

The limited salvaging of Ura in PALA-treated day 9 seedlings was supported by assays of [2-^{14}C]-uracil metabolism (Figure 3). In untreated control seedlings, approximately 40% of the label taken up by the plant was recovered as $^{14}CO_2$, a measure of catabolic pathway activity. This was similar to the catabolic activity previously reported for WT Arabidopsis seedlings (Zrenner et al., 2009). PALA treatment increased catabolism of Ura twofold, with decreased labeling of soluble metabolite and insoluble nucleic acid fractions (Figure 3). Interestingly, PALA-treated seedlings took up

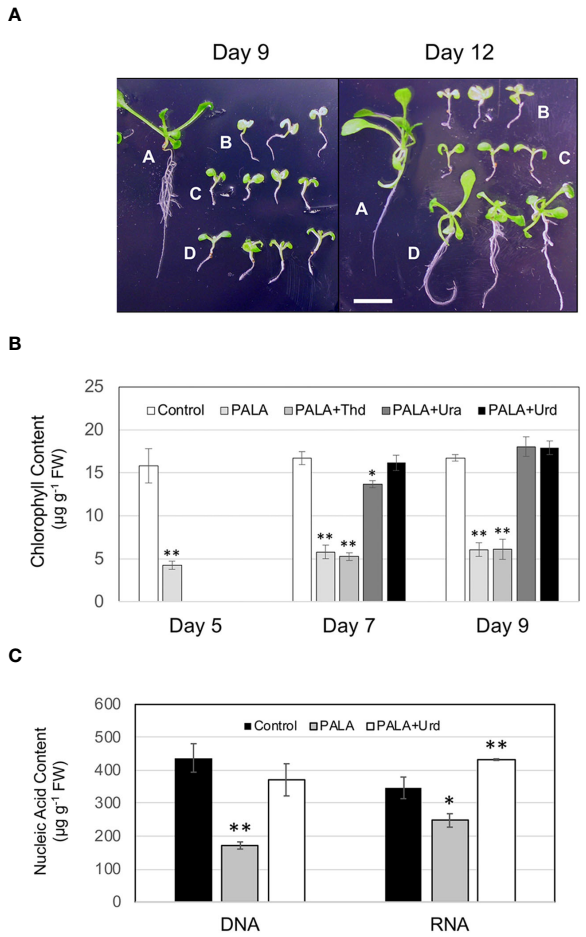

FIGURE 2
Developmental and biochemical phenotypes resulting from changes in pyrimidine availability in Arabidopsis seedlings. **(A)** Effects of PALA ± supplements on seedling growth and development; control **(A)**, 1 mM PALA **(B)**, 1 mM PALA supplemented with either 1 mM Ura **(C)** or 1 mM Urd **(D)** on day 5, then grown for an additional 4 days (day 9) or 7 days (day 12). Scale bar = 0.5 cm. **(B)** Chlorophyll contents of seedlings growing for 5, 7, or 9 days in control medium, or medium containing 1 mM PALA or 1 mM PALA supplemented with 1 mM Thd, 1 mM Ura, or 1 mM Urd on day 5. **(C)** DNA and RNA contents of Arabidopsis seedlings grown in control medium or 1 mM PALA for 9 days, or in 1 mM PALA for 5 days, then supplemented with 1 mM Urd for four additional days. Values are means ± S.E. for three biological replicates. Asterisks mark samples that are significantly different from the untreated control at each timepoint (*$p \leq 0.05$; ** $p \leq 0.01$).

only 75% as much labeled Ura as control seedlings, which may reflect a reduced energy status in their tissues.

3.3 Genome-wide transcriptional profiling reveals biological processes impacted by changes in pyrimidine availability

RNA-seq identified 11,845 unique genes that were differentially expressed (DE) at one or more stages of seedling development (day 5, day 7, day 9) in response to PALA treatment, with or without Urd supplementation. Table 1 summarizes the number of induced and repressed DE genes in response to different experimental treatments at different time points. Remarkably, most genes that remained DE in response to PALA at day 9 were no longer DE after 4 days of Urd supplementation, relative to untreated control seedlings. This condition paralleled the recovery of seedling development.

Clustering of genes by their overall expression profiles (Figure 4) facilitated identification of 12 gene clusters and their enriched GO BioProcess categories that were co-regulated in response to changes in pyrimidine availability over time. Most genes induced by PALA function primarily in abiotic and biotic stress responses. Genes involved in cellular responses to hypoxia or pathogens and in auxin, and Ca^{2+} homeostasis and signaling were regulated beginning at day 5. Genes regulating root development were not induced until day 9, although inhibition of root growth occurred much earlier. In contrast, genes in the cluster 10 expression module were broadly repressed on day 5. Among the genes that belong to cluster 10, many are involved in regulating cell wall loosening during growth, including several expansins and an endoglucanase, and many others that encode proteins which regulate gene expression and cell division activities required for normal seedling growth and development. At day 7, expression of large numbers of genes involved in plastid development and photosynthesis was uniformly decreased. Thus, overall patterns of gene expression supported developmental and biochemical phenotypes but further revealed major abiotic and biotic stress responses resulting from pyrimidine starvation.

3.4 Pyrimidine starvation induces genes regulating synthesis of the phytoalexin camalexin

One early response to pyrimidine starvation was the strongly increased expression of genes encoding enzymes that synthesize the indole glucosinolate camalexin, the major phytoalexin in Arabidopsis which plays an important role in defense against pathogens and herbivores (Supplemental Figure 2; Lemarié et al., 2015). Several genes in this pathway are regulated by MYB51/HIGH INDOLIC GLUCOSINOLATE 1 (Frerigmann et al., 2015), which was shown to be strongly induced at day 5 (Supplemental Figure 2). In contrast, expression of myrosinase 1 and 2, which activate glucosinolates, producing toxic isothiocynante and thiocyanate defense compounds (Shroff et al., 2008), was repressed (Supplemental Figure 2). This suggests that this defense response would be ineffective in PALA-treated seedlings, whereas metabolic diversion of L-tryptophan from auxin synthesis (Zhao, 2012) to camalexin synthesis would be expected to impact root development (Overvoorde et al., 2010) and other auxin-regulated processes.

3.5 Pyrimidine limitation caused reduced expression of genes involved in chloroplast development and photosynthetic pigment synthesis

The severe chlorosis associated with pyrimidine limitation in the light-grown seedlings was previously noted. Genes in chlorophyll

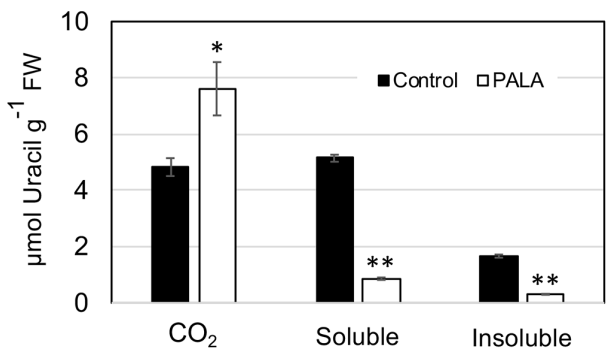

FIGURE 3
Metabolism of [2-^{14}C]-uracil in 9-day-old PALA-treated seedlings. The soluble fraction is free uracil or labeled metabolites in seedling tissues. The insoluble fraction represents incorporation of uracil label into nucleic acids. CO_2 is label released by uracil catabolism. Asterisks mark samples that are significantly different from the control (*$p \leq 0.05$; ** $p \leq 0.01$).

(Supplemental Figure 3) and carotenoid (Supplemental Figure 4) synthesis pathways were coordinately downregulated by PALA treatment by day 7, although genes involved in plastid organization were repressed earlier, beginning on day 5. Protochlorophyllide reductase A (PORA), which functions in phototransformation of protochlorophyllide to chlorophyllide (Liu et al., 2017) was repressed nearly 40-fold in the tetrapyrrole synthesis pathway. Genes encoding MEP pathway enzymes and prenyltransferase activities synthesizing the isoprenoid geranylgeranyl diphosphate (GGPP) precursor for phytyl diphosphate, the phytol tail donor to chlorophyllide *a* in the final step of chlorophyll *a* synthesis (Kim et al., 2013; Kopcsayová and Vranová, 2019), were also repressed. PALA induction of chlorophyll catabolism enzymes chlorophyllase-2 and the magnesium dechelatase STAY-GREEN1 (Hörtensteiner and Kräutler, 2011) on day 5 preceded repression of chlorophyll synthesis genes beginning on day 7 (Supplemental Figure 3) and likely contributed to decreased chlorophyll contents of these seedlings. Expression of GATA1, GATA2, and GLK2, transcription factors which activate genes promoting chlorophyll biosynthesis and photosynthetic membrane organization (Liu et al., 2017; Zubo et al., 2018) was repressed (Supplemental Figure 3). Additionally, numerous genes encoding chlorophyll *a/b* binding proteins of photosystems I and II were repressed (data not shown). For example, *LHCB2.4* transcript levels continued to decrease in response to PALA treatment to only 5% of control levels by day 12, but Urd supplementation on day 5 restored levels of this transcript to 60% of those in control seedlings by day 12 (Supplemental Figure 1).

Carotenoids are also essential photosynthetic pigments which are synthesized from GGPP and repression of isoprenoid pathway genes would limit their production, in addition to the synthesis of isoprenoid-derived hormones abscisic acid and gibberellins (Kopcsayová and Vranová, 2019), which regulate a wide range of physiological and developmental processes. Phytoene synthase, which regulates carotenoid synthesis (Stanley and Yuan, 2019), and other pathway genes were further repressed in response to pyrimidine limitation (Supplemental Figure 4).

3.6 Genes encoding enzymes and transporters of nucleotide metabolism are responsive to changes in pyrimidine availability

Supplemental Table 2 lists 152 genes encoding enzymes or transporters involved in nucleotide metabolism and the co-regulated Arg synthesis pathway. qRT-PCR expression analyses (Supplemental Figure 1) verified the expression of 35 individual genes at day 5 and day 7 time points but also included day 12 expression data, which are not represented in transcriptome datasets. Day 12 expression data identified genes that responded more slowly to changes in pyrimidine availability. In most cases, RNA-seq and qRT-PCR expression data were highly similar.

Among the 2,163 genes that were downregulated by PALA on day 5 but not at later stages, genes in the GO BioProcess category "*de novo*" pyrimidine nucleobase biosynthetic process (GO: 0006207) were the most enriched, although *de novo* purine synthesis genes were also repressed (Supplemental Table 2). Approximately half of the genes involved in nucleotide metabolism and Arg synthesis were DE in response to PALA treatment and expression profiles for most of these genes were reversed by Urd supplementation. Genes that function in salvaging of extracellular nucleotides were strongly induced by pyrimidine starvation, but, unexpectedly, pyrimidine and purine catabolic pathway genes were also induced under limited pyrimidine availability.

Expression data for DE genes were mapped to the *de novo* pyrimidine and purine synthesis pathways (Figure 5) and pathways for pyrimidine (Figure 6) and purine (Figure 7) salvaging (intracellular and extracellular) and catabolism to better understand possible metabolic responses to changes in pyrimidine availability, at the level of transcriptional regulation. Abbreviations for enzymes and transporters are provided in Supplemental Table 2 and abbreviations for pathway intermediates are listed in Supplemental Table 3.

3.6.1 *De novo* synthesis pathways and arginine synthesis

Aspartate transcarbamoylase (ATC), the target of PALA inhibition, catalyzes the committed step in the *de novo* synthesis of pyrimidines in the plastid (Bellin et al., 2021); Figure 5). The remaining four reactions leading to UMP synthesis occur in the cytosol and mitochondrion inner membrane space and UMP is the precursor for synthesis of other pyrimidine nucleotides (Witz et al., 2012; Witte and Herde, 2020). PALA treatment resulted in decreased expression of CPSA, ATC, and DHODH in day 5 seedlings but not at later time points (Supplemental Table 2). PALA decreased UMPS expression in day 7 seedlings, but this response was not observed when day 5 seedlings were supplemented with Urd for 2 days.

Figure 5 also shows the pathway for arginine (Arg) synthesis, which is functionally coupled to *de novo* pyrimidine synthesis at the level of CP utilization by both OTC and ATC (Slocum, 2005). OTC initiates Arg synthesis from Orn, which is usually synthesized from Glu using a cyclic pathway in which the acetyl moiety is conserved

TABLE 1 Numbers of induced and repressed DEG in Arabidopsis seedlings in response to PALA treatment, with or without Urd supplementation at day 5, day 7, and day 9 time points.

Comparison groups	Relative expression (fold change)		Number of DEGs		
Day 5 control vs. PALA	UP	≥2×	1,369	2,365	4,528
		1.5–2×	996		
	DOWN	1.5–2×	1,254	2,163	
		≥2×	909		
Day 7 control vs. PALA	UP	≥2×	2,781	4,081	8,816
		1.5–2×	1,300		
	DOWN	1.5–2×	2,506	4,735	
		≥2×	2,229		
Day 7 control vs. PALA+Urd	UP	≥2×	930	1,663	3,284
		1.5–2×	733		
	DOWN	1.5–2×	1,301	1,621	
		≥2×	320		
Day 9 control vs. PALA	UP	≥2×	1,735	2,541	5,092
		1.5–2×	806		
	DOWN	1.5–2×	904	2,551	
		≥2×	1,647		
Day 9 control vs. PALA+Urd	UP	≥2×	25	149	207
		1.5–2×	124		
	DOWN	1.5–2×	47	58	
		≥2×	11		

(Slocum, 2005; Winter et al., 2015). PALA did not change the expression of any genes encoding the five enzymes in Orn synthesis, although it did increase expression of the NAOD gene in day 9 seedlings (Table S2). This enzyme catalyzes Orn synthesis with metabolism of the acetyl group. Interestingly, expression of the PII sensory protein which activates NAGK was decreased in day 7 seedlings, a response which was partially reversible by Urd. PII exerts major metabolic control of Orn and Arg synthesis *via* Arg end-product inhibition (Ferrario-Méry et al., 2006). Further Arg synthesis from Orn would likely be downregulated since expression of the three enzymes catalyzing these steps (OTC, AS, AL) was repressed. Depression of Arg synthesis would divert CP to *de novo* pyrimidine synthesis, perhaps decreasing PALA inhibition of ATC by competing for substrate binding sites in the enzyme.

The 12-step plastid-localized pathway for *de novo* synthesis of the purine AMP is shown in Figure 5. AMP is exported to the cytosol for further metabolism to other purine nucleotides (Zrenner et al., 2006; Witte and Herde, 2020; see Figure 7, below). Expression of most of these genes was decreased by PALA treatment, except for ASE1, and was reversible by Urd (Supplemental Table 2). Co-expression analyses for genes in the *de novo* pyrimidine and purine synthesis pathways and Arg synthesis pathway (ATTEDII) confirmed that many are coordinately regulated (Figure 5).

3.6.2 Pathways for pyrimidine salvaging and catabolism

Pathways for the synthesis of pyrimidine nucleotides by salvaging of pyrimidine nucleosides and nucleobases, and competing pathways for their catabolism, are shown in Figure 6. Under pyrimidine limitation, UMP may be synthesized directly from Urd by UCK2, which was induced by PALA at day 5 and later stages (Supplemental Table 2). An important source of Urd is the vacuole, where ribonuclease RNS2 facilitates RNA turnover and acid phosphatases further metabolize ribonucleotide products. Urd and Cyd are then exported to the cytosol *via* the tonoplast transporter ENT1, where these nucleosides can be salvaged to UMP and other pyrimidines (Bernard et al., 2011; Hillwig et al., 2011; Witte and Herde, 2020). Both RNS2 and ENT1 were induced by PALA at day 5 but not at later time points, suggesting that changes in activities of this salvaging pathway were an early response to pyrimidine starvation.

Extracellular pyrimidine nucleosides may also be produced by degradation of RNA by RNases and further metabolism of nucleotides by phosphatases (Chen et al., 2000; Robinson et al., 2012), as occurs in the vacuole. Cyd from intracellular or extracellular sources would be metabolized by CDA1, producing Urd (Chen et al., 2016). Although CDA1 transcripts were not

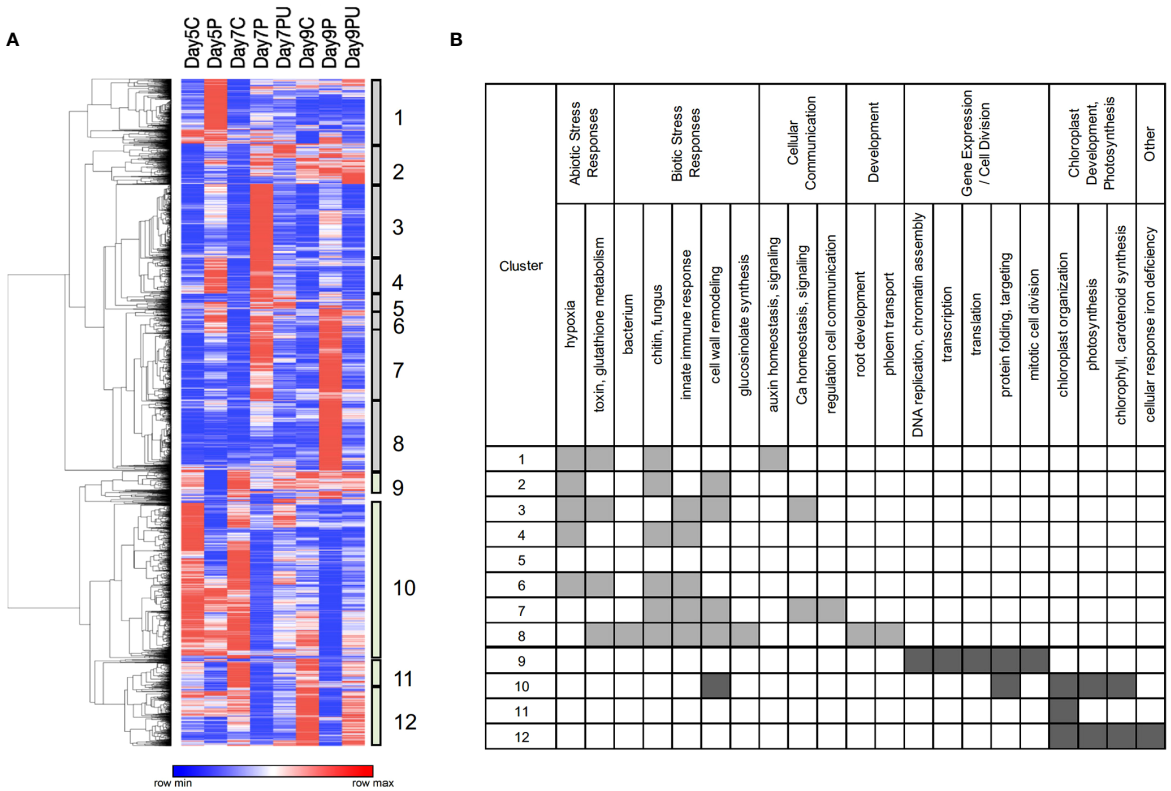

FIGURE 4
Heatmap showing clustering **(A)** of normalized expression values for 6,245 DE genes (FC ≥ 2). Clusters 1–8 show genes with increased expression in response to PALA treatment, with reversal by Urd supplementation, and represent a timeline of early to late responses (left to right). Genes in clusters 9–12 show genes that were repressed by PALA treatment, with Urd reversal, with early to late responses (left to right). Control, PALA treatment, and PALA + Urd treatment (C, P, PU) at days 5, 7, and 9. Statistically overrepresented GO BioProcess categories for genes in each cluster **(B)**.

detected in RNA-seq analyses (Supplemental Table 2), strong CDA1 induction by PALA and repression by Urd was observed in qRT-PCR assays (Supplemental Figure 1). PALA treatment upregulated expression of plasma membrane (PM)-localized ENT3 (Girke et al., 2014) on day 5, and cell-wall-localized ribonuclease RNS1 was among the most strongly upregulated genes at all time points. Extracellular phosphatase NPP3 and apyrases APY5 and APY6, which may function as ecto-phosphatases that regulate extracellular NTP (eNTP) levels (Pietrowska-Borek et al., 2020; Clark et al., 2021) also exhibited strong, early induction by PALA (Supplemental Table 5). Since no PM-localized transporter is known to take up nucleotides directly into plant cells (Major et al., 2017), nucleotide metabolism to nucleosides, or further metabolism to nucleobases, is required for intracellular salvaging to occur (Riewe et al., 2008). Expression of extracellular salvaging genes did not increase when PALA-treated seedlings were supplemented with Urd.

Early induction of genes involved in both intracellular and extracellular salvaging of pyrimidine nucleosides suggest that these processes are highly responsive to changes in pyrimidine availability in the cell. However, expression profiles for genes involved in further metabolism of UMP into uridylates, (deoxy)cytidylates and thymidylates, and downstream processes like nucleic acid synthesis and carbohydrate metabolism (Figure 6) suggest that these processes were repressed, consistent with biochemical data, such as decreased nucleic acid contents of PALA-treated seedlings (Figure 2C). For example, increased expression of UMK1 and UMK4 in response to PALA does not occur until day 7 (Supplemental Table 2), potentially limiting the flux of salvaged UMP into pyrimidine nucleotide pools during early stages of pyrimidine starvation. Downregulation of NDPK1 and CTPS1 would limit UTP availability for RNA synthesis and carbohydrate metabolism. DNA synthesis would be inhibited by decreased DUT expression and increased expression of DHFR-TS3, which inhibits activities of DHFR-TS1 and DHFR-TS2 in thymidylate synthesis (Gorelova et al., 2017). Increased cytosolic thymidine kinase TK1a expression at day 5 could facilitate salvaging of Thd to dTMP, although further incorporation into thymidylates would be inhibited by decreased NDPK1 expression (Supplemental Table 2).

In addition to cytosolic salvaging of Urd, plastid salvaging of Urd is also possible. Recently, Chen et al. (2023) characterized PLASTID NUCLEOSIDE KINASE 1 (PNK1) as an inosine kinase which also functions as a Urd kinase *in vivo*. In PALA-treated seedlings, PNK1 expression decreased at day 7 and was reversible by Urd supplementation (Supplemental Table 4). Uptake of Urd into the plastid implies the existence of an unknown nucleoside transporter in this organelle.

Salvaging of Ura is also possible. Ura can be taken up directly by several PM-localized nucleobase transporters, such as NAT8, whose expression was strongly upregulated by PALA beginning on day 7 (Supplemental Table 2). Cytosolic metabolism of Urd to Ura can also

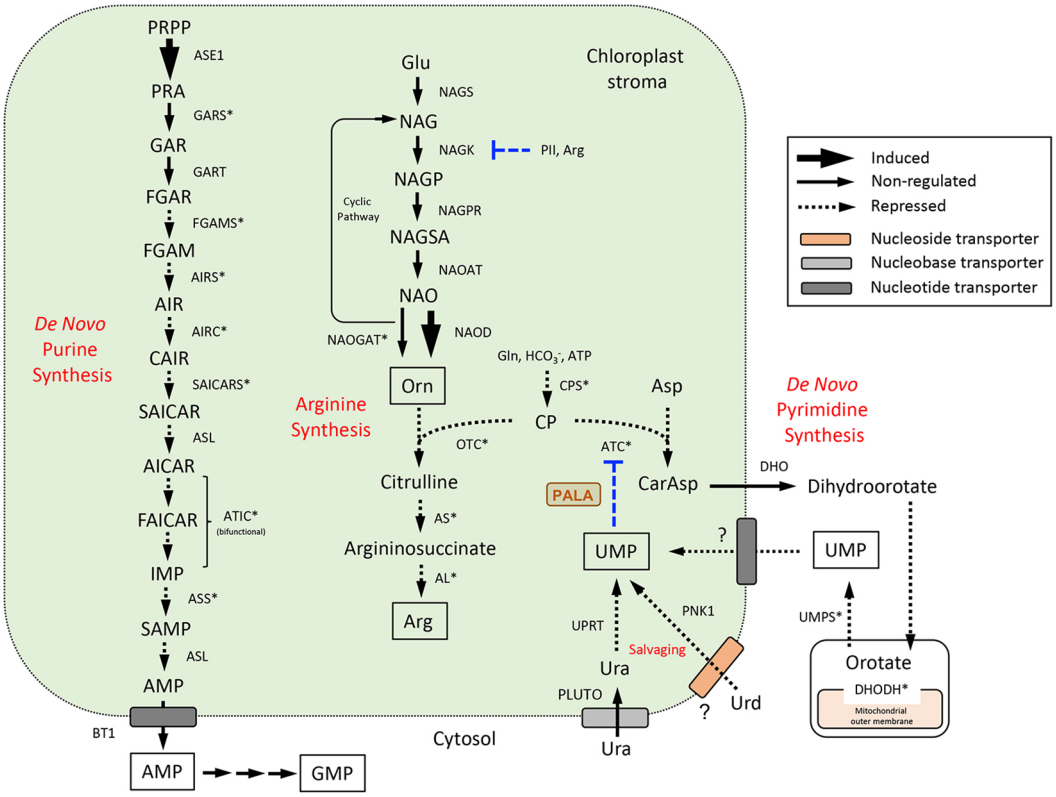

FIGURE 5
De novo purine and pyrimidine synthesis pathways and their subcellular compartmentation in Arabidopsis (Zrenner et al., 2006; Witte and Herde, 2020). Pyrimidine synthesis is integrated with the synthesis of Arg at the level of CP utilization by ATC and OTC. The UMP end product exerts major control over pyrimidine synthesis through allosteric regulation of ATC activity (Belin et al., 2020) and is also formed through uracil salvaging by UPRT or Urd salvaging by PNK1 (see Figure 6). UMP and Orn modulate CPS activities; Arg and the N-sensing regulatory protein PII control Arg synthesis at the NAGK step (Slocum, 2005). Gene expression information is integrated into pathways to show steps that are induced or repressed in response to PALA treatment. Highly coexpressed genes in the three pathways are indicated with an asterisk. PALA inhibition of ATC is shown. Abbreviations used for enzymes and transporters are listed in Supplemental Table 2 and pathway intermediates are listed in Supplemental Table 3.

occur as a result of nucleoside hydrolase NSH1 activity (Jung et al., 2009) and *NSH1* was induced late, on day 9. After uptake into the plastid by the nucleobase transporter PLUTO, Ura is successively metabolized to UMP, UDP, and UTP *via* UPRT, a plastid UMP kinase (PUMPKIN) and NDPK2 (Witz et al., 2012). The plastid salvaging pathway is distinct from the *de novo* synthesis of UMP, which is initiated in the plastid but completed in the cytosol and mitochondrion (Figure 5; Witz et al., 2012). It is also distinct from the UMP product of Urd salvaging in the plastid (Chen et al., 2023). Expression of plastid salvage pathway genes was strongly downregulated by PALA at days 7 and 9 and was reversed by Urd. PLUTO expression was unusual in that it did not change in response to PALA but was downregulated at day 7 by Urd supplementation.

Alternatively, Ura in the plastid may be catabolized by PYD1 to dihydrouracil, which is further metabolized outside of the plastid by PYD2, PYD3, and PYD4, recycling pyrimidine N as NH_3 into general N metabolism (Zrenner et al., 2009). Catabolic pathway genes were upregulated by PALA and this response was reversed by Urd supplementation (Supplemental Table 2). Increased catabolism of labeled Ura in PALA-treated seedlings (Figure 3) provided biochemical evidence in support of gene expression data.

3.6.3 Pathways for purine salvaging and catabolism

Pathways for purine salvaging and catabolism are shown in Figure 7. As for pyrimidine metabolism, coordinated induction of vacuolar RNS2(+phosphatases)/ENT1 and extracellular RNS1 (+phosphatases)/ENT3 genes at day 5 suggests that RNA and nucleotide degradation would provide Ado and Guo for salvaging or catabolism as an early response to pyrimidine limitation. Increased expression of cell wall-localized, purine-specific nucleoside hydrolase *NSH3* (Jung et al., 2011) would facilitate metabolism of the extracellular purine nucleosides to the corresponding nucleobases, Ade and Gua, for uptake by several PM-localized, nucleobase transporters. PALA increased *NSH3* expression more than twofold on day 7, but Urd did not reverse this response. Expression of PUP1 and other purine

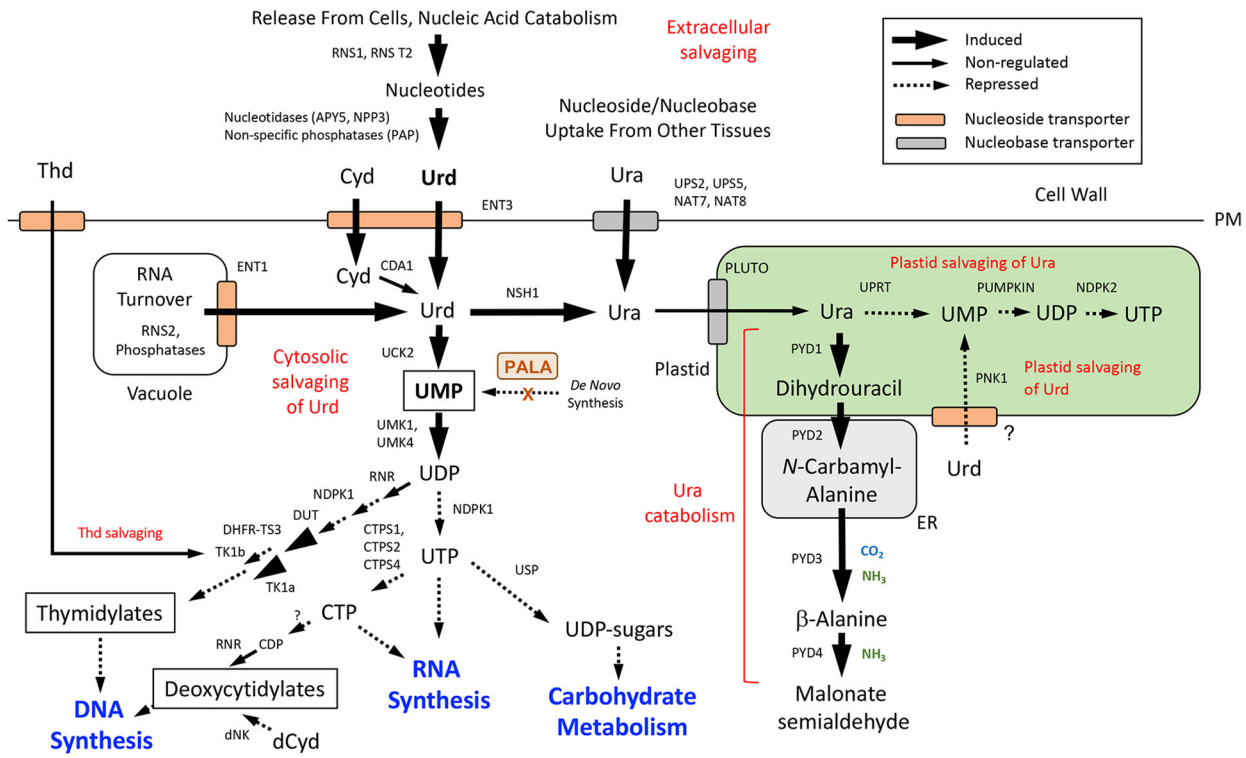

FIGURE 6
Pyrimidine salvaging (intracellular and extracellular) and catabolism. Pathway organization and subcellular compartmentation are according to Witte and Herde (2020). Gene expression information is integrated into pathways to show steps that are induced or repressed in response to PALA treatment. Salvaging of nucleobases derived from RNA turnover in the vacuole and extracellular sources of nucleotides are indicated. Cytosolic salvaging of Cyd (*via* CDA1 and Urd), Urd, and Thd and plastid salvaging pathways for Ura and Urd are shown. Induced salvaging of Cyd to CMP by UCK2 and downstream cytidylates by UMK1/4 and NDPK1 activities is not shown). Further metabolism of UMP into thymidylate, uridylate, and (deoxy)cytidylate precursors of RNA and DNA synthesis and carbohydrate metabolism are also shown. Inhibition of UMP synthesis by PALA inhibition of the *de novo* pathway is indicated (see Figure 5). Abbreviations used for enzymes and transporters are listed in Supplemental Table 2 and pathway intermediates are listed in Supplemental Table 3.

permeases was strongly upregulated by PALA beginning on day 5. In contrast, expression of PUP4 and AtAzg2 transporters increased at day 7 in response to Urd supplementation but not PALA treatment alone. Expression of adenine phosphoribosyltransferase APT2, which metabolizes Ade to AMP, was similarly regulated by Urd but not by PALA, at day 7, but its expression increased at day 9 in PALA-treated seedlings. In contrast, adenosine kinase (ADK1, ADK2; Supplemental Table 5) was not regulated by PALA or Urd. Thus, salvaging of Ade, rather than Ado, may represent the main salvaging activity for adenylates, in response to altered pyrimidine metabolism.

Genes encoding enzymes for the *de novo* synthesis of GMP from AMP in the cytosol, *via* the IMP intermediate (Figure 7), or HGRPT, which salvages Gua directly, were not regulated in response to PALA treatment. Downregulation of *AMK2*, *AMK5*, and *NDPK2* suggests that further metabolism of AMP (derived from *de novo* synthesis or Ade/Ado salvaging) or GMP into adenylate or guanylate pools in the plastid would be inhibited. Although cytosolic GMK2 was induced on day 7, NDPK1 expression decreased on day 5, suggesting that GTP synthesis from GDP would also be limited.

The pathway for purine catabolism is also shown in Figure 7. Xanthosine cannot be salvaged (Yin et al., 2014) so its formation resulting from GSDA deamination of Guo (Dahncke and Witte, 2013) or dephosphorylation by an XMP phosphatase (XMPP; Heinemann et al., 2021) commits it to the catabolic pathway. Most AMP is degraded *via* GMP, which is metabolized to Guo by an unknown GMP phosphatase (Witte and Herde, 2020). Although *GSDA*, *XDH1*, and *ALNS* expression was induced on day 5, *NSH1* and *NSH2* expression increased later, at day 9, which might limit purine catabolism, since the NSH1/NSH2 complex has been shown to constitute the major nucleoside hydrolase activity that degrades xanthosine (Baccolini and Witte, 2019). Decreased expression of *AAH* at day 9 may further limit purine degradation and recycling of purine N to general N metabolism.

3.7 Transcription factors responsive to pyrimidine starvation function mainly in regulation of abiotic and biotic stress responses

Gene expression profiling for transcription factors (TF) which were DE in response to PALA treatment is shown in Figure 8. As in Figure 4, clustering revealed early (day 5) and later (day 7, 9) responses and associated enriched GO BioProcess categories. Most

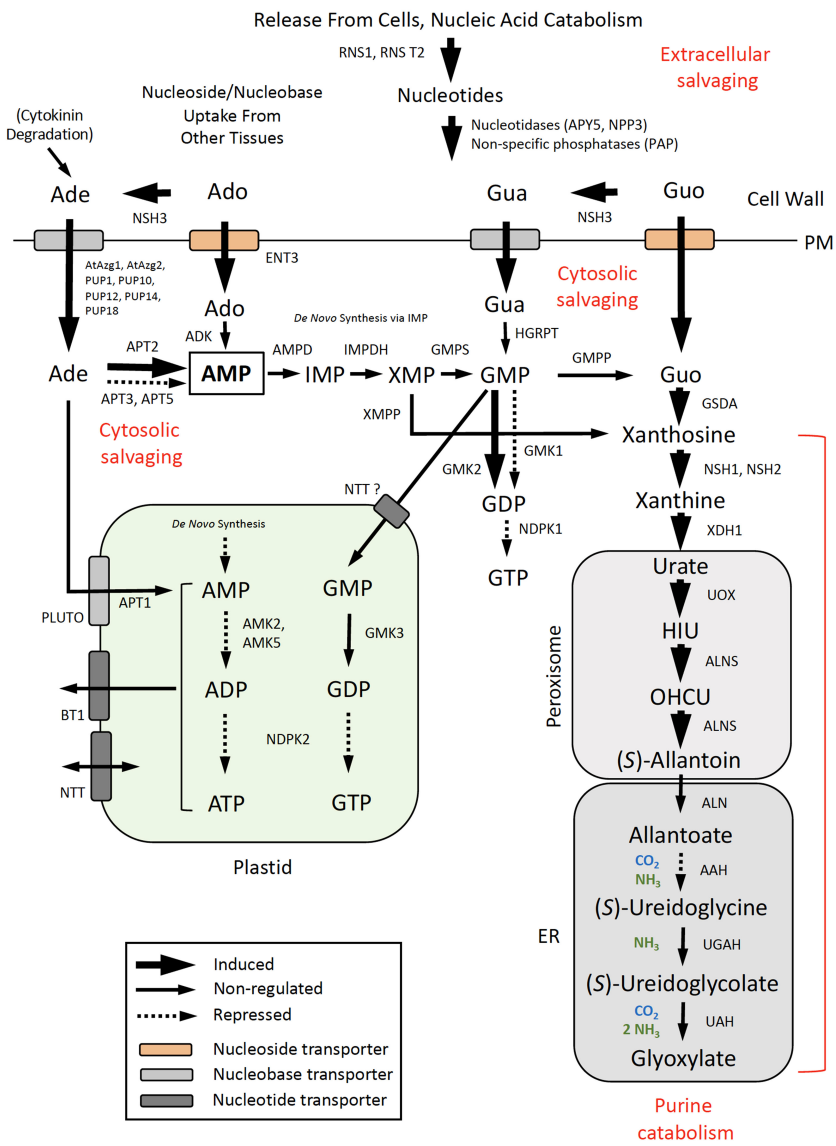

FIGURE 7
Purine salvaging (intracellular and extracellular) and catabolism. Pathway organization and subcellular compartmentation are according to Witte and Herde (2020). Gene expression information is integrated into pathways to show steps that are induced or repressed in response to PALA treatment. Salvaging of Ado and Gua derived from RNA turnover in the vacuole, deoxypurine metabolism, and salvaging of inosine and hypoxanthine are not shown. Abbreviations used for enzymes and transporters are listed in Supplemental Table 2 and pathway intermediates are listed in Supplemental Table 3.

induced TF genes in clusters 1–4 are involved in regulating abiotic and biotic stress responses, consistent with the functional characterization of early regulated genes (Figure 4) and included numerous WRKY and ethylene-responsive TF. Early, repressed TF mainly regulate developmental processes.

3.8 Identification of potential transcriptional regulatory networks for nucleotide metabolism in Arabidopsis

We identified TF with enriched targets (Tian et al., 2020) within individual cohorts of highly coexpressed genes representing the major metabolic pathways of nucleotide metabolism and Arg synthesis. Enriched TF and their target genes are arrayed in Supplemental Table 4, and annotation and expression data for these TF are given in Supplemental Table 5. Many of the co-regulated genes function in different pathways and have common TF targets that may serve to coordinate nucleotide metabolism at the level of transcription. Induction of a large number of ERF TF is correlated with repression of genes involved in nucleotide synthesis and Arg synthesis, and induction of nucleobase transporter genes. Targets for induced WRKY TF are strongly overrepresented in CPSA, whose repression would decrease synthesis of carbamoyl-P, further limiting pyrimidine and Arg synthesis.

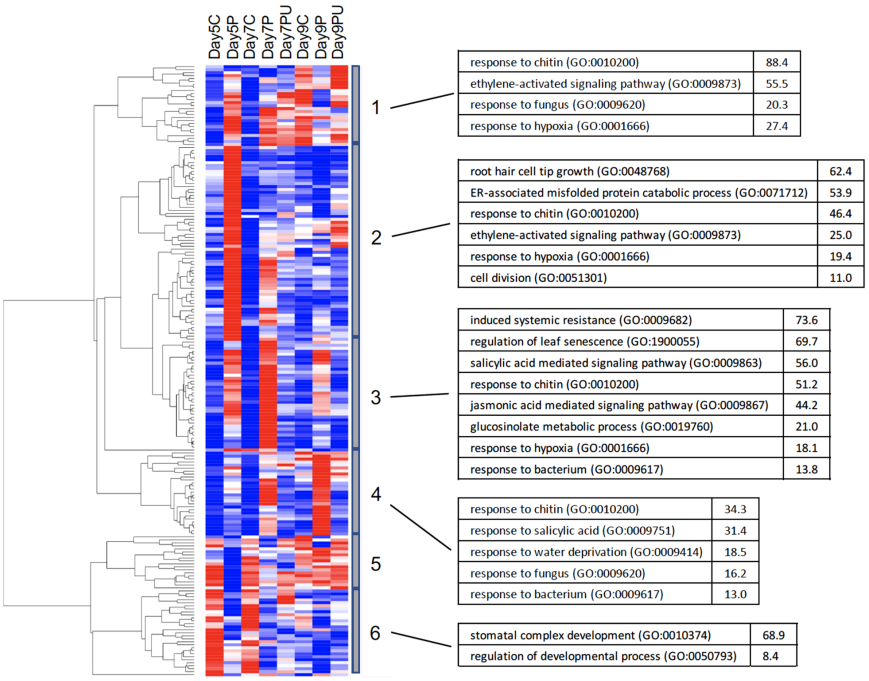

FIGURE 8
Heatmap showing clustering of normalized expression values for 89 DE TF genes (FC ≥ 2). Clusters 1–4 show genes with increased expression in response to PALA treatment, compared with untreated controls. Urd supplementation reversed this response. Genes in clusters 5–6 show the opposite response to PALA and Urd. Control, PALA treatment and PALA + Urd treatment (C, P, PU) at days 5, 7, and 9. Highly overrepresented GO BioProcess categories and fold-enrichment values for each cluster are shown.

To better understand transcriptional control of nucleotide metabolism, we modeled transcriptional regulatory networks for TF whose induction or repression by PALA on day 5 was reversed by Urd. These TF represented the earliest responses to changes in pyrimidine availability. iRegNet (Shim et al., 2021) was used to generate regulatory network graphs for day 5 responses (Figure 9). This resource identifies significantly overrepresented upstream regulators of query genes, integrating gene-to-gene co-expression data to generate realistic regulatory networks. As is shown in Figure 9A, nearly all TF induced by PALA on day 5 are potentially regulated by one or more upstream transcription factors ERF11, ERF105, ZAT10, WRKY33, and WRKY40. Transcription factors repressed by PALA treatment are downstream of ERF039, SPL15, DOF2.4, DOF5.8, and CDF3 (Figure 9B).

Some of the predicted upstream regulators of DE TF are themselves regulated by PALA ± Urd treatments. Several have binding sites that are enriched within co-regulated genes of nucleotide metabolism and, thus, have potential for direct regulations of those genes. Many of the potentially regulated downstream TF in the network graphs also have enriched targets in nucleotide metabolism genes. This information can be used to construct hypothetical regulons for individual genes or groups of genes that may help coordinate metabolic responses to altered pyrimidine levels in seedlings. For example, ASIL2 has binding sites in genes that regulate *de novo* nucleotide synthesis, intracellular and extracellular salvaging, and Arg synthesis activities (Supplemental Table 2) and is repressed by PALA at day 5. A hypothetical transcriptional regulatory network for ASIL2 is shown in Figure 10A. In this model, induction of ethylene-responsive TF, including ABR1, with targets in the same nucleotide metabolism genes, could further coordinate their expression. Additional direct and indirect regulations involving ABR1 are shown in Figure 10B. These network graphs also validate TF enrichment analyses (Supplemental Table 4) as a general approach to identifying nucleotide metabolism genes that are likely to be co-regulated by individual TF.

Attempts to model similar regulatory networks for DE catabolic pathway genes and TF with enriched targets in those genes were unsuccessful. Using all DE catabolic genes (Supplemental Table S2) as queries in iRegNet, the hypothetical regulon shown in Figure 11 was produced. In this model, highly induced WRKY70 and NAC047, which function in abiotic and biotic stress responses, would activate genes of pyrimidine and purine catabolism.

4 Discussion

PALA inhibition of pyrimidine synthesis and Urd supplementation offered a useful model for investigating the effects of altered pyrimidine availability on biochemical, developmental, and transcriptome-level responses in Arabidopsis seedlings.

Pyrimidine starvation led to developmental arrest in seedlings 5 days after germination, when seed stores of pyrimidines were exhausted. Gene expression profiling suggests a nearly complete collapse of anabolic activities and increased catabolic activities in

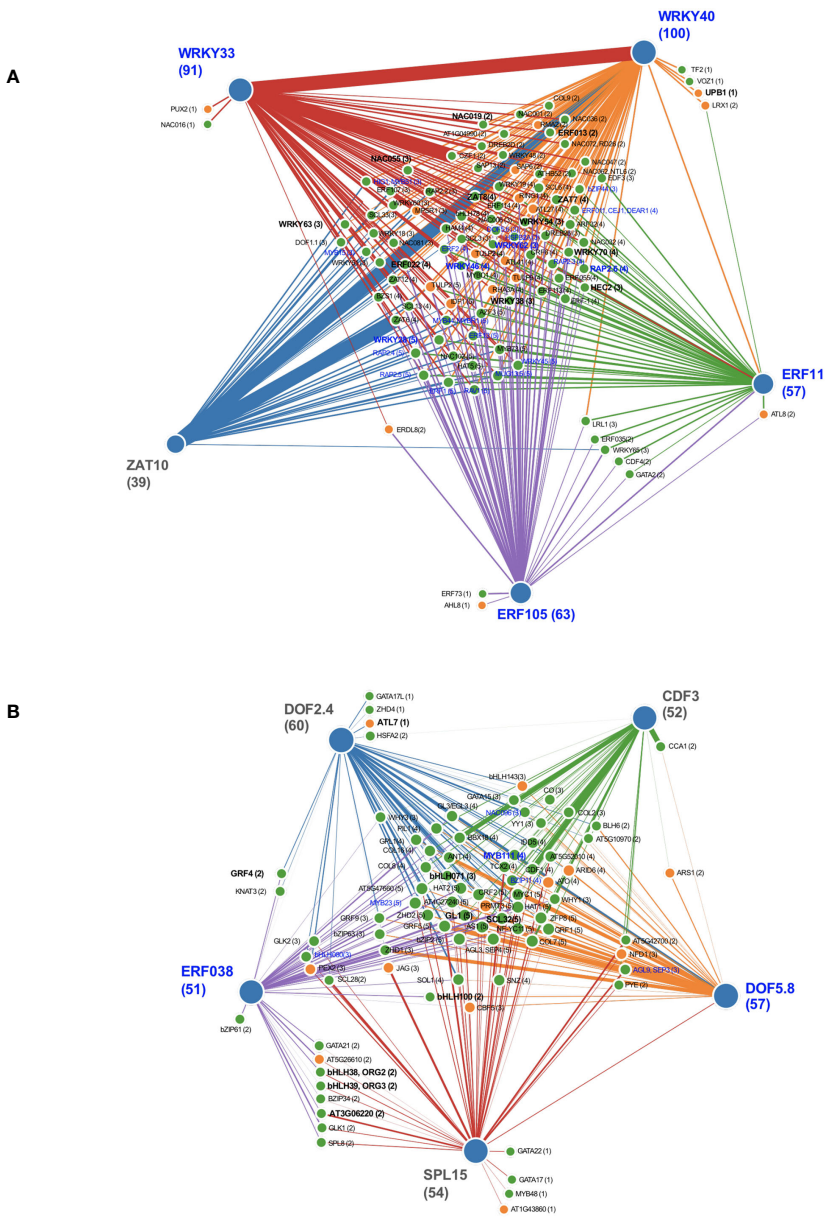

FIGURE 9
Integrative network graphs (iRegNet) showing five highly coexpressed upstream genetic regulators (outer nodes) for differentially expressed TF (FC ≥ 1.5) that were either induced **(A)** or repressed **(B)** by pyrimidine starvation at day 5. Edge thickness indicates strength of co-expression between genes. Induced genes with FC ≥5 on day 5 and repressed genes with FC ≥ 5 on day 7 (bold font) represent the most highly regulated early TF genes. TF with enriched targets in genes of nucleotide metabolism, representing potential downstream regulations, are indicated (blue font).

these seedlings, paralleled by general abiotic and biotic stress responses. One interesting stress response was the strong induction of indole glucosinolate synthesis genes, which may divert L-tryptophan from the synthesis of auxin (Zhao, 2012), an important regulator of root development (Overvoorde et al., 2010). Repression of genes involved in auxin signaling or regulation of auxin homeostasis was one of the earliest responses to PALA treatment. Early inhibition of root growth in pyrimidine starved seedlings was observed in the present study and was also reported in a previous investigation (Schröder et al., 2005).

A general repression of genes involved in chloroplast development and photosynthetic pigment synthesis paralleled strongly decreased chlorophyll contents in PALA-treated seedlings. Impaired plastid functions have been reported in a variety of plant mutants with defects in nucleotide metabolism (Sugimoto et al., 2007; Lange et al., 2008; Mainguet et al., 2009; Chen et al., 2015; Ye et al., 2016; Chen et al., 2018; Ohler et al., 2019) and would significantly impact energy metabolism and major metabolic pathways, including nucleotide synthesis, salvaging, and catabolism activities that reside in this organelle. Bellin et al. (2023b) recently reported a low photosynthetic efficiency and increased production of reactive oxygen species in the ATC knockdown line *atc#1*, which exhibits reduced pyrimidine levels. Additionally, other genes of central energy metabolism (glycolysis,

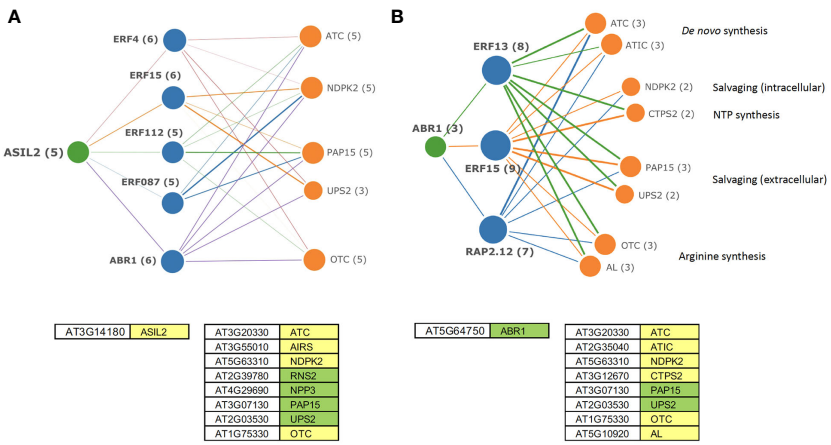

FIGURE 10
Hypothetical regulatory networks for transcription factors ASIL2 **(A)** and ABR1 **(B)**. Edge thickness indicates strength of co-expression between genes. ASIL2 is repressed on day 5. ABR1, a potential downstream target of ASIL2 is induced by day 7. Both TF have binding sites within the nucleotide metabolism genes and may further regulate the downstream targets by induction of ethylene-responsive TF, coordinating synthesis, and salvaging of nucleotides with Arg synthesis. Models were developed based on the DE genes with statistically enriched targets for ASIL2 and ABR1 (AGI numbers; green—induced genes, yellow—repressed genes).

TCA cycle, respiration) were significantly repressed, relative to the Col-0 WT.

Genome-wide gene expression profiling in Arabidopsis seedlings supports some general observations regarding possible transcriptional control of nucleotide metabolism in this plant. In response to pyrimidine starvation, salvaging pathways (intracellular and extracellular) were upregulated and *de novo* synthesis was downregulated. Synthesis of nucleotides by salvaging of preformed nucleobases and nucleosides requires less energy than *de novo* synthesis (Zrenner et al., 2006). Thus, salvaging would be more efficient under conditions of impaired energy metabolism resulting from defects in chloroplast development and photosynthesis, or other energy-generating processes. Ohler et al. (2019) reported that UCK1/UCK2 are responsible for most pyrimidine salvaging *in vivo* and *uck1/uck2* mutants exhibit severe growth inhibition. This suggests that *de novo* pyrimidine synthesis activities alone are insufficient to support normal seedling growth and development (Chen and Thelen, 2011). While knockouts of any genes in the *de novo* pyrimidine pathway are lethal (Schröder et al., 2005), it is clear that salvaging activities alone were able to sustain normal seedling growth and development in the present study, under continued strong inhibition of *de novo* synthesis by PALA. It is interesting to note that moderate genetic repression of each gene in the *de novo* pathway did not produce visible phenotypes in the solanaceous plants tobacco and potato (Schröder et al., 2005). Stronger inhibition of pathway activities was required to significantly reduce nucleotide pool sizes, and this resulted in growth inhibition without large changes in the developmental program, although roots were more sensitive than shoots to pyrimidine limitation. They concluded that the plants compensated for pyrimidine starvation with reduced growth and that even reduced nucleotide pools could sustain basic metabolic processes (Schröder et al., 2005). Strong inhibition of ATC with 1 mM PALA resulted in severe growth inhibition during the first few days after germination, with developmental arrest by day 5, suggesting that nucleotide pools were insufficient to maintain seedling growth. Bassett et al. (2003) had previously shown that growth inhibition of Arabidopsis seedlings on medium containing 0.1 mM PALA occurred much more slowly, reaching developmental arrest by day 12 after germination. The higher PALA concentration used in the present study allowed for transcriptome analyses during early stages of pyrimidine salvaging and recovery of seedling growth and development in a timeframe in which nutrient limitation would not become a factor in the analyses.

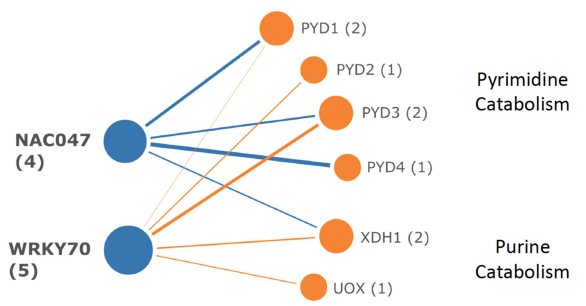

FIGURE 11
Hypothetical regulon for DE genes of pyrimidine and purine catabolism. Transcription factors WRKY70 and NAC047 are highly induced by PALA and could coordinately regulate target gene expression in both pathways, although binding sites for these TF are not statistically overrepresented in the target genes.

It is remarkable that Urd supplementation reversed transcriptome-level responses within the first 2 days. After 4 days, Urd salvaging restored expression of most genes to control levels, in spite of continued PALA inhibition of *de novo* synthesis in these plants, and normal seedling development resumed. Very little is known about mechanisms for sensing nucleotide pool sizes in plant tissues, but it seems clear that they respond quickly and dynamically, even to major perturbations in nucleotide metabolism. Beyond direct Urd uptake from surrounding plant

tissues, it seems clear that extracellular salvaging activities that metabolize nucleic acids and nucleotides, and parallel activities in the vacuole, involving RNA turnover, are tightly coupled to intracellular salvaging activities and would play important roles in salvaging during normal plant growth.

An important finding of this study is that *de novo* pyrimidine and arginine synthesis pathway activities are likely coordinated at the level of transcriptional regulation, in addition to the well-characterized metabolic control of CP allocation to each pathway (Slocum, 2005). Feedback control of ATC and *de novo* pyrimidine synthesis by UMP is well known (Bellin et al., 2021), but the mechanism by which this might occur *in vivo* has been poorly understood, since UMP synthesis in this pathway occurs outside of the plastid (Witz et al., 2012). In contrast, UMP synthesis in the plastid, resulting from Urd salvaging by PNK1 (Chen et al., 2023) or Ura salvage pathway activities (Witz et al., 2012), may regulate ATC activity, thus providing a mechanism to balance salvaging and *de novo* synthesis activities. The observed co-expression of *de novo* pyrimidine and purine synthesis pathway genes was also seen in the present study and may be an important mechanism for regulating pool sizes for these nucleotides.

Induction of pyrimidine catabolism genes, under conditions of severe pyrimidine limitation, was unexpected in PALA-treated seedlings. In two previous studies with ATC knockdown lines with less severe phenotypes (Chen and Slocum, 2008; Bellin et al., 2023a), catabolic pathway genes were repressed. In the present study, enhanced catabolism of labeled Ura in day 9 seedlings may have resulted from repression of Ura salvaging pathway genes, leading to Ura accumulation in the plastid and increased availability to PYD1 and the catabolic pathway. Failure of salvaged UMP/UDP to be further incorporated into downstream nucleotide synthesis (repression of NDPK1, CTPS1 would limit UTP, CTP synthesis) and nucleotide-dependent metabolism, might also favor Urd accumulation in the cytosol where NSH1 would metabolize Urd to Ura for further catabolism in the plastid. The relatively late induction of NSH1 at day 9, and repression of PNK1 at day 7, in PALA-treated seedlings raises an interesting question for further study. Would Urd salvaging have been be less effective if it began on day 9, rather than at the earlier (day 5) time point? Repression of cytosolic NDPK1 and plastid NDPK2 would also limit ATP and GTP synthesis and salvaged AMP/GMP would be channeled toward xanthosine and the catabolic pathway. This might represent a mechanism for balancing purine and pyrimidine catabolism in the seedlings.

Coordination of *de novo* synthesis, salvaging, and catabolic pathway activities is required to balance pyrimidine and purine pool sizes resulting from changing metabolic demands during plant growth and development. However, a recent review of plant nucleotide metabolism (Witte and Herde, 2020) noted the paucity of information regarding transcriptional regulation of these processes. We performed TF enrichment analyses for highly coexpressed genes encoding enzymes and transporters of nucleotide metabolism to identify TF that might be involved in direct regulations of those genes, limiting the analyses to both TF and targets that were DE in response to changes in pyrimidine availability. Further modeling of transcriptional regulatory networks permitted construction of hypothetical ASIL2 and ABR1 regulons that may coordinate key steps in pyrimidine and purine synthesis and salvaging, as well as Arg synthesis. Similarly, WRKY 70 and NAC047 may coordinate expression of pyrimidine and purine catabolism genes. A small number of TF that were strongly induced or repressed by PALA on day 5 may further coordinate downstream TF networks representing nearly all regulated TF with enriched targets in nucleotide metabolism genes. We recognize the limitations of integrating transcriptomic data in systems studies of metabolism (Cavill et al., 2016; Richelle et al., 2019). However, approaches used in the current study may prove useful for further characterizing transcription regulatory networks for plant nucleotide metabolism.

Data availability statement

The datasets presented in this study can be found in online repositories. The names of the repository/repositories and accession number(s) can be found below: https://www.ncbi.nlm.nih.gov/genbank/, PRJNA704993.

Author contributions

RS: Conceptualization, Data curation, Formal Analysis, Funding acquisition, Investigation, Methodology, Project administration, Resources, Software, Supervision, Validation, Visualization, Writing – original draft, Writing – review & editing. CP: Formal Analysis, Investigation, Methodology, Writing – review & editing. ZL: Funding acquisition, Methodology, Project administration, Resources, Software, Supervision, Writing – review & editing.

Funding

The author(s) declare financial support was received for the research, authorship, and/or publication of this article. This work was supported by NSF awards MCB-0516544 to RDS and IOS-0923913 to ZL.

Acknowledgments

We thank Dr. Christopher Town, Plant Genomics, J. Craig Venter Institute and Caren Bartosz, Biological Sciences, Goucher College, for support of qRT-PCR analyses and Julie Caruana, Naval Surface Warfare Center, Dahlgren Division for assistance with RNA-seq analyses.

Conflict of interest

The authors declare that the research was conducted in the absence of any commercial or financial relationships that could be construed as a potential conflict of interest.

The author(s) declared that they were an editorial board member of Frontiers, at the time of submission. This had no impact on the peer review process and the final decision.

Publisher's note

All claims expressed in this article are solely those of the authors and do not necessarily represent those of their affiliated organizations, or those of the publisher, the editors and the reviewers. Any product that may be evaluated in this article, or claim that may be made by its manufacturer, is not guaranteed or endorsed by the publisher.

Supplementary material

The Supplementary Material for this article can be found online at: https://www.frontiersin.org/articles/10.3389/fpls.2023.1273235/full#supplementary-material

References

Arnon, D. I. (1949). Copper enzymes in isolated chloroplasts. Polyphenoloxidase in *Beta vulgaris*. *Plant Physiol.* 24, 1–15. doi: 10.1104/pp.24.1.1

Ashihara, H., Ludwig, I. A., and Crozier, A. (2020). Plant nucleotide metabolism - biosynthesis, degradation, and alkaloid formation. doi: 10.1002/9781119476139

Baccolini, C., and Witte, C. P. (2019). AMP and GMP catabolism in Arabidopsis converge on xanthosine, which is degraded by a nucleoside hydrolase heterocomplex. *Plant Cell* 31, 734–751. doi: 10.1105/TPC.18.00899

Baer, G. R., Meyers, S. P., Molin, W. T., and Schrader, L. E. (1982). A simple and sensitive DNA assay for plant extracts. *Plant Physiol.* 70, 999–1003. doi: 10.1104/PP.70.4.999

Bar-Peled, M., and O'Neill, M. A. (2011). Plant nucleotide sugar formation, interconversion, and salvage by sugar recycling. *Annu. Rev. Plant Biol.* 62, 127–155. doi: 10.1146/annurev-arplant-042110-103918

Bassett, E. V., Bouchet, B. Y., Carr, J. M., Williamson, C. L., and Slocum, R. D. (2003). PALA-mediated pyrimidine starvation increases expression of aspartate transcarbamoylase (*pyrB*) in Arabidopsis seedlings. *Plant Physiol. Biochem.* 41, 695–703. doi: 10.1016/S0981-9428(03)00094-9

Bellin, L., Del Caño-Ochoa, F., Velázquez-Campoy, A., Möhlmann, T., and Ramón-Maiques, S. (2021). Mechanisms of feedback inhibition and sequential firing of active sites in plant aspartate transcarbamoylase. *Nat. Commun.* 12, 1–13. doi: 10.1038/s41467-021-21165-9

Bellin, L., Garza Amaya, D. L., Scherer, V., Pruß, T., John, A., Richter, A., et al. (2023a). Nucleotide imbalance, provoked by downregulation of aspartate transcarbamoylase impairs cold acclimation in Arabidopsis. *Molecules* 28, 1585. doi: 10.3390/MOLECULES28041585/S1

Bellin, L., Melzer, M., Hilo, A., Garza Amaya, D. L., Keller, I., Meurer, J., et al. (2023b). Nucleotide limitation results in impaired photosynthesis, reduced growth and seed yield together with massively altered gene expression. *Plant Cell Physiol.* doi: 10.1093/PCP/PCAD063

Bernard, C., Traub, M., Kunz, H. H., Hach, S., Trentmann, O., and Möhlmann, T. (2011). Equilibrative nucleoside transporter 1 (ENT1) is critical for pollen germination and vegetative growth in Arabidopsis. *J. Exp. Bot.* 62, 4627–4637. doi: 10.1093/JXB/ERR183

Cavill, R., Jennen, D., Kleinjans, J., and Briedé, J. J. (2016). Transcriptomic and metabolomic data integration. *Brief. Bioinform.* 17, 891–901. doi: 10.1093/BIB/BBV090

Chen, C. T., and Slocum, R. D. (2008). Expression and functional analysis of aspartate transcarbamoylase and role of *de novo* pyrimidine synthesis in regulation of growth and development in Arabidopsis. *Plant Physiol. Biochem.* 46, 150–159. doi: 10.1016/j.plaphy.2007.10.016

Chen, D. L., Delatorre, C. A., Bakker, A., and Abel, S. (2000). Conditional identification of phosphate-starvation-response mutants in *Arabidopsis thaliana*. *Planta* 211, 13–22. doi: 10.1007/s004250000271

Chen, F., Dong, G., Ma, X., Wang, F., Zhang, Y., Xiong, E., et al. (2018). UMP kinase activity is involved in proper chloroplast development in rice. *Photosynth. Res.* 137, 53. doi: 10.1007/S11120-017-0477-5

Chen, M., and Thelen, J. J. (2011). Plastid uridine salvage activity is required for photoassimilate allocation and partitioning in Arabidopsis. *Plant Cell* 23, 2991–3006. doi: 10.1105/TPC.111.085829

Chen, M., Herde, M., and Witte, C. P. (2016). Of the nine cytidine deaminase-like genes in Arabidopsis, eight are pseudogenes and only one is required to maintain pyrimidine homeostasis in *vivo*. *Plant Physiol.* 171, 799–809. doi: 10.1104/PP.15.02031

Chen, X., Zhu, L., Xin, L., Du, K., Ran, X., Cui, X., et al. (2015). Rice *stripe1-2* and *stripe1-3* mutants encoding the small subunit of ribonucleotide reductase are temperature sensitive and are required for chlorophyll biosynthesis. *PloS One* 10, e0130172. doi: 10.1371/JOURNAL.PONE.0130172

Chen, X., Kim, S. H., Rhee, S., and Witte, C. P. (2023). A plastid nucleoside kinase is involved in inosine salvage and control of purine nucleotide biosynthesis. *Plant Cell* 35, 510–528. doi: 10.1093/PLCELL/KOAC320

Cheng, C. Y., Krishnakumar, V., Chan, A. P., Thibaud-Nissen, F., Schobel, S., and Town, C. D. (2017). Araport11: a complete reannotation of the *Arabidopsis thaliana* reference genome. *Plant J.* 89, 789–804. doi: 10.1111/tpj.13415

Clark, G., Brown, K. A., Tripathy, M. K., and Roux, S. J. (2021). Recent advances clarifying the structure and function of plant apyrases (nucleoside triphosphate diphosphohydrolases). *Int. J. Mol. Sci.* 22, 3283 doi: 10.3390/ijms22063283

Czechowski, T., Stitt, M., Altmann, T., Udvardi, M. K., and Scheible, W.-R. (2005). Genome-wide identification and testing of superior reference genes for transcript normalization in Arabidopsis. *Plant Physiol.* 139, 5–17. doi: 10.1104/pp.105.063743

Dahncke, K., and Witte, C. P. (2013). Plant purine nucleoside catabolism employs a guanosine deaminase required for the generation of xanthosine in Arabidopsis. *Plant Cell* 25, 4101–4109. doi: 10.1105/TPC.113.117184

Ferrario-Méry, S., Besin, E., Pichon, O., Meyer, C., and Hodges, M. (2006). The regulatory PII protein controls arginine biosynthesis in Arabidopsis. *FEBS Lett.* 580, 2015–2020. doi: 10.1016/j.febslet.2006.02.075

Frerigmann, H., Glawischnig, E., and Gigolashvili, T. (2015). The role of MYB34, MYB51 and MYB122 in the regulation of camalexin biosynthesis in *Arabidopsis thaliana*. *Front. Plant Sci.* 6. doi: 10.3389/fpls.2015.00654

Geigenberger, P., Regierer, B., Nunes-Nesi, A., Leisse, A., Urbanczyk-Wochniak, E., Springer, F., et al. (2005). Inhibition of *de novo* pyrimidine synthesis in growing potato tubers leads to a compensatory stimulation of the pyrimidine salvage pathway and a subsequent increase in biosynthetic performance. *Plant Cell* 17, 2077–2088. doi: 10.1105/tpc.105.033548

Girke, C., Daumann, M., Niopek-Witz, S., and Möhlmann, T. (2014). Nucleobase and nucleoside transport and integration into plant metabolism. *Front. Plant Sci.* 5. doi: 10.3389/FPLS.2014.00443/XML/NLM

Gorelova, V., De Lepeleire, J., Van Daele, J., Pluim, D., Meï, C., Cuypers, A., et al. (2017). Dihydrofolate reductase/thymidylate synthase fine-tunes the folate status and controls redox homeostasis in plants. *Plant Cell* 29, 2831–2853. doi: 10.1105/TPC.17.00433

Heinemann, K. J., Yang, S. Y., Straube, H., Medina-Escobar, N., Varbanova-Herde, M., Herde, M., et al. (2021). Initiation of cytosolic plant purine nucleotide catabolism involves a monospecific xanthosine monophosphate phosphatase. *Nat. Commun.* 12, 1–9. doi: 10.1038/s41467-021-27152-4

Hellemans, J., Mortier, G., De Paepe, A., Speleman, F., and Vandesompele, J. (2008). qBase relative quantification framework and software for management and automated analysis of real-time quantitative PCR data. *Genome Biol.* 8, 1–14. doi: 10.1186/GB-2007-8-2-R19/COMMENTS

Hillwig, M. S., Contento, A. L., Meyer, A., Ebany, D., Bassham, D. C., and MacIntosha, G. C. (2011). RNS2, a conserved member of the RNase T2 family, is necessary for ribosomal RNA decay in plants. *Proc. Natl. Acad. Sci. U. S. A.* 108, 1093–1098. doi: 10.1073/PNAS.1009809108/-/DCSUPPLEMENTAL/PNAS.201009809SI.PDF

Hörtensteiner, S., and Kräutler, B. (2011). Chlorophyll breakdown in higher plants. *Biochim. Biophys. Acta - Bioenerg.* 1807, 977–988. doi: 10.1016/j.bbabio.2010.12.007

Jung, B., Flörchinger, M., Kunz, H. H., Traub, M., Wartenberg, R., Jeblick, W., et al. (2009). Uridine-ribohydrolase is a key regulator in the uridine degradation pathway of Arabidopsis. *Plant Cell* 21, 876. doi: 10.1105/TPC.108.062612

Jung, B., Hoffmann, C., and Möhlmann, T. (2011). Arabidopsis nucleoside hydrolases involved in intracellular and extracellular degradation of purines. *Plant J.* 65, 703–711. doi: 10.1111/J.1365-313X.2010.04455.X

Kim, S., Schlicke, H., Van Ree, K., Karvonen, K., Subramaniam, A., Richter, A., et al. (2013). Arabidopsis chlorophyll biosynthesis: An essential balance between the methylerythritol phosphate and tetrapyrrole pathways. *Plant Cell* 25, 4984–4993. doi: 10.1105/tpc.113.119172

Kopcsayová, D., and Vranová, E. (2019). Functional gene network of prenyltransferases in *Arabidopsis thaliana*. *Molecules* 24, 4556. doi: 10.3390/MOLECULES24244556

Lange, P. R., Geserick, C., Tischendorf, G., and Zrenner, R. (2008). Functions of chloroplastic adenylate kinases in Arabidopsis. *Plant Physiol.* 146, 492. doi: 10.1104/PP.107.114702

Lemarié, S., Robert-Seilaniantz, A., Lariagon, C., Lemoine, J., Marnet, N., Levrel, A., et al. (2015). Camalexin contributes to the partial resistance of *Arabidopsis thaliana* to the biotrophic soilborne protist *Plasmodiophora brassicae*. *Front. Plant Sci.* 6. doi: 10.3389/fpls.2015.00539

Liu, X., Li, Y., and Zhong, S. (2017). Interplay between light and plant hormones in the control of Arabidopsis seedling chlorophyll biosynthesis. *Front. Plant Sci.* 8, 1433 doi: 10.3389/fpls.2017.01433

Mainguet, S. E., Gakière, B., Majira, A., Pelletier, S., Bringel, F., Guérard, F., et al. (2009). Uracil salvage is necessary for early Arabidopsis development. *Plant J.* 60, 280–291. doi: 10.1111/j.1365-313X.2009.03963.x

Major, P., Embley, T. M., and Williams, T. A. (2017). Phylogenetic diversity of NTT nucleotide transport proteins in free-living and parasitic bacteria and Eukaryotes. *Genome Biol. Evol.* 9, 480–487. doi: 10.1093/gbe/evx015

Obayashi, T., Aoki, Y., Tadaka, S., Kagaya, Y., and Kinoshita, K. (2018). ATTED-II in 2018: A plant coexpression database based on investigation of the statistical property of the Mutual Rank Index. *Plant Cell Physiol.* 59, e3. doi: 10.1093/pcp/pcx191

Ohler, L., Niopek-Witz, S., Mainguet, S. E., and Möhlmann, T. (2019). Pyrimidine Salvage: Physiological functions and interaction with chloroplast biogenesis. *Plant Physiol.* 180, 1816–1828. doi: 10.1104/pp.19.00329

Overvoorde, P., Fukaki, H., and Beeckman, T. (2010). Auxin control of root development. *Cold Spring Harb. Perspect. Biol.* 2, a001537. doi: 10.1101/cshperspect.a001537

Pietrowska-Borek, M., Dobrogojski, J., Sobieszczuk-Nowicka, E., and Borek, S. (2020). New insight into plant signaling: Extracellular ATP and uncommon nucleotides. *Cells* 9, 345. doi: 10.3390/cells9020345

Ramakers, C., Ruijter, J. M., Lekanne Deprez, R. H., and Moorman, A. F. M. (2003). Assumption-free analysis of quantitative real-time polymerase chain reaction (PCR) data. *Neurosci. Lett.* 339, 62–66. doi: 10.1016/S0304-3940(02)01423-4

Richelle, A., Joshi, C., and Lewis, N. E. (2019). Assessing key decisions for transcriptomic data integration in biochemical networks. *PloS Comput. Biol.* 15, e1007185. doi: 10.1371/JOURNAL.PCBI.1007185

Riewe, D., Grosman, L., Fernie, A. R., Zauber, H., Wucke, C., and Geigenberger, P. (2008). A cell wall-bound adenosine nucleosidase is involved in the salvage of extracellular ATP in *Solanum tuberosum*. *Plant Cell Physiol.* 49, 1572–1579. doi: 10.1093/pcp/pcn127

Robinson, W. D., Park, J., Tran, H. T., Del Vecchio, H. A., Ying, S., Zins, J. L., et al. (2012). The secreted purple acid phosphatase isozymes AtPAP12 and AtPAP26 play a pivotal role in extracellular phosphate-scavenging by *Arabidopsis thaliana*. *J. Exp. Bot.* 63, 6531–6542. doi: 10.1093/jxb/ers309

Schröder, M., Giermann, N., and Zrenner, R. (2005). Functional analysis of the pyrimidine *de novo* synthesis pathway in solanaceous species. *Plant Physiol.* 138, 1926–1938. doi: 10.1104/pp.105.063693

Shim, S., Park, C. M., and Seo, P. J. (2021). iRegNet: an integrative Regulatory Network analysis tool for *Arabidopsis thaliana*. *Plant Physiol.* 187, 1292–1309. doi: 10.1093/PLPHYS/KIAB389

Shroff, R., Vergara, F., Muck, A., Svatos, A., and Gershenzon, J. (2008). Nonuniform distribution of glucosinolates in *Arabidopsis thaliana* leaves has important consequences for plant defense. *Proc. Natl. Acad. Sci. U.S.A.* 105, 6196–6201. doi: 10.1073/PNAS.0711730105/SUPPL_FILE/0711730105SI.PDF

Slocum, R. D. (2005). Genes, enzymes and regulation of arginine biosynthesis in plants. *Plant Physiol. Biochem.* 43, 729–745. doi: 10.1016/j.plaphy.2005.06.007

Stanley, L., and Yuan, Y. W. (2019). Transcriptional regulation of carotenoid biosynthesis in plants: So many regulators, so little consensus. *Front. Plant Sci.* 10. doi: 10.3389/fpls.2019.01017

Sugimoto, H., Kusumi, K., Noguchi, K., Yano, M., Yoshimura, A., and Iba, K. (2007). The rice nuclear gene, *VIRESCENT 2*, is essential for chloroplast development and encodes a novel type of guanylate kinase targeted to plastids and mitochondria. *Plant J.* 52, 512–527. doi: 10.1111/J.1365-313X.2007.03251.X

Tian, F., Yang, D. C., Meng, Y. Q., Jin, J., and Gao, G. (2020). PlantRegMap: Charting functional regulatory maps in plants. *Nucleic Acids Res.* 48, D1104–D1113. doi: 10.1093/nar/gkz1020

Vandesompele, J., De Preter, K., Pattyn, F., Poppe, B., Van Roy, N., De Paepe, A., et al. (2002). Accurate normalization of real-time quantitative RT-PCR data by geometric averaging of multiple internal control genes. *Genome Biol.* 3, research0034.1. doi: 10.1186/gb-2002-3-7-research0034

Veerappa, R., Slocum, R. D., Siegenthaler, A., Wang, J., Clark, G., and Roux, S. J. (2019). Ectopic expression of a pea apyrase enhances root system architecture and drought survival in Arabidopsis and soybean. *Plant Cell Environ.* 42, 337–353. doi: 10.1111/pce.13425

Wagner, K. G., and Backer, A. I. (1992). Dynamics of nucleotides in plants studied on a cellular basis. *Int. Rev. Cytol.* 134, 1–84. doi: 10.1016/S0074-7696(08)62027-6

Winter, G., Todd, C. D., Trovato, M., Forlani, G., and Funck, D. (2015). Physiological implications of arginine metabolism in plants. *Front. Plant Sci.* 6. doi: 10.3389/fpls.2015.00534

Witte, C. P., and Herde, M. (2020). Nucleotide metabolism in plants. *Plant Physiol.* 182, 63–78. doi: 10.1104/pp.19.00955

Witz, S., Jung, B., Fürst, S., and Möhlmann, T. (2012). *De novo* pyrimidine nucleotide synthesis mainly occurs outside of plastids, but a previously undiscovered nucleobase importer provides substrates for the essential salvage pathway in Arabidopsis. *Plant Cell* 24, 1549–1559. doi: 10.1105/TPC.112.096743

Ye, W., Hu, S., Wu, L., Ge, C., Cui, Y., Chen, P., et al. (2016). *White stripe leaf 12 (WSL12)*, encoding a nucleoside diphosphate kinase 2 (OsNDPK2), regulates chloroplast development and abiotic stress response in rice (*Oryza sativa* L.). *Mol. Breed.* 36, 57. doi: 10.1007/S11032-016-0479-6

Yin, Y., Katahira, R., and Ashihara, H. (2014). Metabolism of purine nucleosides and bases in suspension-cultured *Arabidopsis thaliana* cells. *Chem. Bull.* 3, 925–934.

Zhao, Y. (2012). Auxin biosynthesis: A simple two-step pathway converts tryptophan to indole-3-acetic acid in plants. *Mol. Plant* 5, 334. doi: 10.1093/MP/SSR104

Zrenner, R., Riegler, H., Marquard, C. R., Lange, P. R., Geserick, C., Bartosz, C. E., et al. (2009). A functional analysis of the pyrimidine catabolic pathway in Arabidopsis. *New Phytol.* 183, 117–132. doi: 10.1111/j.1469-8137.2009.02843.x

Zrenner, R., Stitt, M., Sonnewald, U., and Boldt, R. (2006). Pyrimidine and purine biosynthesis and degradation in plants. *Annu. Rev. Plant Biol.* 57, 805–836. doi: 10.1146/annurev.arplant.57.032905.105421

Zubo, Y. O., Blakley, I. C., Franco-Zorrilla, J. M., Yamburenko, M. V., Solano, R., Kieber, J. J., et al. (2018). Coordination of chloroplast development through the action of the GNC and GLK transcription factor families. *Plant Physiol.* 178, 130–147. doi: 10.1104/PP.18.00414

frontiers | Frontiers in Plant Science

TYPE Original Research
PUBLISHED 10 January 2024
DOI 10.3389/fpls.2023.1273620

OPEN ACCESS

EDITED BY
Md Asaduzzaman,
Charles Sturt University, Australia

REVIEWED BY
Gao Wei,
Anhui Agricultural University, China
Wajid Zaman,
Yeungnam University, Republic of Korea
Mohamed Omar Kaseb,
Agricultural Research Center, Egypt

*CORRESPONDENCE
Paul Staswick
pstaswick1@unl.edu

RECEIVED 06 August 2023
ACCEPTED 04 December 2023
PUBLISHED 10 January 2024

CITATION
Dharni JS, Shi Y, Zhang C, Petersen C, Walia H and Staswick P (2024) Growth and transcriptional response of wheat and rice to the tertiary amine BMVE. *Front. Plant Sci.* 14:1273620. doi: 10.3389/fpls.2023.1273620

Growth and transcriptional response of wheat and rice to the tertiary amine BMVE

Jaspinder Singh Dharni[1], Yu Shi[2], Chi Zhang[2], Chris Petersen[3], Harkamal Walia[1] and Paul Staswick[1*]

[1]Department of Agronomy and Horticulture, University of Nebraska, Lincoln, NE, United States, [2]School of Biological Sciences, University of Nebraska, Lincoln, NE, United States, [3]Kamterter Products, LLC, Waverly, NE, United States

Introduction: Seed vigor is largely a product of sound seed development, maturation processes, genetics, and storage conditions. It is a crucial factor impacting plant growth and crop yield and is negatively affected by unfavorable environmental conditions, which can include drought and heat as well as cold wet conditions. The latter leads to slow germination and increased seedling susceptibility to pathogens. Prior research has shown that a class of plant growth regulators called substituted tertiary amines (STAs) can enhance seed germination, seedling growth, and crop productivity. However, inconsistent benefits have limited STA adoption on a commercial scale

Methods: We developed a novel seed treatment protocol to evaluate the efficacy of 2-(N-methyl benzyl aminoethyl)-3-methyl butanoate (BMVE), which has shown promise as a crop seed treatment in field trials. Transcriptomic analysis of rice seedlings 24 h after BMVE treatment was done to identify the molecular basis for the improved seedling growth. The impact of BMVE on seed development was also evaluated by spraying rice panicles shortly after flower fertilization and subsequently monitoring the impact on seed traits.

Results: BMVE treatment of seeds 24 h after imbibition consistently improved wheat and rice seedling shoot and root growth in lab conditions. Treated wheat seedlings grown to maturity in a greenhouse also resulted in higher biomass than controls, though only under drought conditions. Treated seedlings had increased levels of transcripts involved in reactive oxygen species scavenging and auxin and gibberellic acid signaling. Conversely, several genes associated with increased reactive oxygen species/ROS load, abiotic stress responses, and germination hindering processes were reduced. BMVE spray increased both fresh and mature seed weights relative to the control for plants exposed to 96 h of heat stress. BMVE treatment during seed development also benefited germination and seedling growth in the next generation, under both ambient and heat stress conditions.

Discussion: The optimized experimental conditions we developed provide convincing evidence that BMVE does indeed have efficacy in plant growth enhancement. The results advance our understanding of how STAs work at the molecular level and provide insights for their practical application to improve crop growth.

KEYWORDS

tertiary amine, germination, abiotic stress, transcriptome, growth, seed vigor, seed treatment

Introduction

A critical factor determining plant growth and productivity is seed vigor, a complex trait encompassing seed dormancy, viability, germination rate, and seedling establishment. Seeds with low vigor are more susceptible to stress during germination, especially in unfavorable environments (Bewley et al., 2013; Finch-Savage and Bassel, 2016). Rapid and synchronous germination minimizes these detriments and maximizes uniformity at harvest time. Causes of low seed vigor include adverse environmental conditions during seed development and poor seed storage conditions after harvest (Bewley and Black, 2013; Zinsmeister et al., 2020). Seed vigor is an important trait that many plant breeding programs have aimed to improve through incorporation of increased genetic diversity (Lara-Fioreze et al., 2013; Dang et al., 2014; Luo et al., 2021).

A useful technology to reduce germination time and improve germination synchrony is seed priming. This most often involves controlled hydration of seeds to initiate early stages of germination, followed by drying treatments to suspend germination until planting (Osborne, 1983; Halmer, 2004; Hussain et al., 2016). A variety of stress, chemical and bioactive treatments of seeds have also been investigated to enhance seed germination, with or without typical seed priming protocols (Ashraf and Foolad, 2005; Ilyas, 2006; Singh, 2018; Rhaman et al., 2021). One mechanism behind the efficacy of seed priming may involve the enhanced activation of antioxidant defense systems, which help counter the toxic reactive oxygen species that accrue during germination, especially under stress conditions (Gill and Tuteja, 2010; Xu et al., 2011; Khaliq et al., 2015; Hussain et al., 2016; Zheng et al., 2016; Guo et al., 2022). On the other hand, primed seeds are more susceptible to deterioration before planting, reducing their storage longevity (Heydecker and Gibbins, 1977; Tarquis and Bradford, 1992; Chiu et al., 2002).

Several reports have suggested that a class of plant growth regulators known collectively as substituted tertiary amines (STAs) can enhance seedling development and increase crop productivity when used to treat seeds or growing plants (Jung et al., 1975; Hayman and Yokoyama, 1990; Keithly et al., 1990a, b; Keithly and Yokoyama, 1992; Ashraf and Foolad, 2005; Van Pelt, 2007; Qi et al., 2013; Banerjee et al., 2014; Yan, 2015; Wang et al., 2016; Gao et al., 2022). Low-dose application of these compounds to seeds prior to germination reportedly increases root growth and seedling establishment, while foliar application at later stages can enhance photosynthetic efficiency along with yield traits (US9464283B2, Kamtec LLC) (Yokoyama et al., 2015). A recent study reported that foliar application of DCPTA [2-(3,4-dichlorophenoxy) triethylamine] enhanced expression of genes associated with photosynthetic output (Gao et al., 2022).

Despite the positive examples of STAs, other field and greenhouse studies showed no or inconsistent benefits (Hartz et al., 1995; Davies et al., 2004; Singh, 2018). Thus, the early promise of STAs has generally not translated to commercial use. The reasons for the discrepancies in reported efficacy are not clear, although they could be related to differential plant response under variable environmental conditions, or variation in cultivar/genotype response to tertiary amines.

A significant deficiency in our current knowledge of STAs is an understanding of their action at the molecular level. While some effects of STAs are reminiscent of plant hormone activities, STA mode of action does not appear to simply mimic phytohormones (Gausman, 1991; Van Pelt, 2007). Understanding how STAs act at the molecular level could help to explain why positive results have been sporadic and might allow for their use in a more consistently beneficial way.

In this report we optimized conditions under which seed treatment with 2-(N-methyl benzyl aminoethyl)-3-methyl butanoate (BMVE) consistently enhanced rice (*Oryza sativa* L. ssp. Japonica, var. Kitaake) and wheat (*Triticum aestivum*, var. Ruth) seedling growth in the laboratory. We determined the physiological modifications triggered by BMVE seed treatment and examined whether the positive seedling effects were sustained through later vegetative growth under normal and drought conditions. We also investigated the transcriptional changes occurring in seedlings shortly after their treatment with BMVE to gain insight into the underlying molecular mechanism of BMVE actions. Finally, we explored whether BMVE treatment of seeds while they were developing on the plant enhanced germination and plant growth in the next generation. Results from this study show that BMVE has efficacy in improving plant growth when applied at the early seedling stage, and when sprayed on rice panicles during seed development.

Materials and methods

Seed treatment method

The formal name for BMVE is 2-(N-methyl benzyl aminoethyl)-3-methyl butanoate. Before each experiment, freshly prepared BMVE (100mM in ethanol) was used as a stock to further prepare the working solution in distilled water at the specified concentrations. Control solutions for seed treatments used the same volume of 100% ethanol that was used for the 100mM BMVE treatment. Before the treatment, seeds were imbibed for 24 hours in dark. At this point, uniform seeds having an emerged radical of about 2 mm were selected and treatment was applied by soaking the seeds in BMVE or control solution for 3 hours in dark. Following the treatment, seeds were kept on moist paper under dark conditions for an additional 24 hours. The temperatures used for the dark pre- and post-treatment periods was 23°C and 28°C for wheat and rice, respectively. Varieties used in this study were Kitaake (*Oryza sativa* L.), a Japonica rice commonly used in research worldwide and Ruth, a wheat (*Triticum aestivum*) variety developed for the great plains area of the United Sates.

Measurements during early seedling growth

Following seed treatment, seeds were set to grow on wet tissue paper (six layers) in small plastic boxes. Boxes were covered with aluminum foil to maintain dark conditions until measurements. All the material including tissue paper, boxes, and water was sterilized before use. During the preliminary experiment that aimed at tracking wheat shoot growth until 9 days after growth, treated wheat seeds were grown in plastic trays containing small pots filled with autoclaved soil (greenhouse soil mix supplemented with Osmocote fertilizer and Micromax micronutrients). Keeping the growth chamber conditions maintained at day/night temperature (24/18 °C) and light/dark period (14 h/10 h), shoot height of wheat seedlings was measured at indicated timepoints. In subsequent experiments shoot and root lengths were measured at 24 and 48 hours after treatment described above (HAT) while growing in the plastic boxes in the dark. For each timepoint/treatment 16 – 18 seedlings were used for measurements.

RNA extraction, RNA-seq analysis, RT-qPCR

To understand the underlying genetic variation resulting from the BMVE treatment, an RNA-seq study was conducted. BMVE treatment improved seed germination rate for both wheat and rice as early as 24 HAT (see Results) so we chose this time after treatment for transcriptome analysis of rice. Seeds were germinated and treated as described above. The three treatments used for total RNA extraction included a control minus BMVE (C24), BMVE treated (B24), and non-treated seeds harvested immediately after the 24 h of imbibition (C). Three biological replicates consisting of about 25 seedlings each were used for each treatment. At these stages, intact seeds were immediately frozen using liquid nitrogen. Following the collection, seed tissue was ground to a fine powder using liquid nitrogen with a mortar and pestle. Each finely ground tissue sample weighing ~100 mg was used for RNA extraction using Trizol-Phenol method as described in (Chomczynski and Mackey, 1995; Li and Trick, 2005). Upon isolation, RNA was purified using RNeasy MinElute cleanup kit (Qiagen) and subsequently treated with DNase. High quality RNA samples were sequenced in the University of Nebraska, Medical Center core facility (Omaha, NE). RNA libraries were sequenced using 150-bp single-end reads on an Illumina Novaseq 6000. Later, the bioinformatics tools with default settings were deployed including *Fastqc* to test the quality of the reads, *Trimmomatic* for trimming the adapters and removing low quality reads, *Tophat2* to align the RNA-seq reads to the reference genome, *Htseq* to create the read count matrix, and *EdgeR* (bioconductor package) for DEG analysis (Andrews, 2010; Bolger et al., 2014; Anders et al., 2015; Trapnell et al., 2009; Robinson et al., 2010). After obtaining the read counts, the genes expressing differentially between the control and BMVE treatment at 24 HAT were considered to have passed the statistical significance threshold of false discovery rate (fdr) < 0.05, and fold change (FC) greater than 2 or smaller than 0.5. This yielded a list of 474 genes. The read count ratio for specific genes of interest was calculated for control and BMVE treatment at 24 HAT using untreated seeds at 0 HAT as the base line level. These ratios were converted to the z-score values. Gene ontology enrichment analysis for the genes was conducted using bioinformatic tool, ShinyGO (http://ge-lab.org/go/) (Ge et al., 2020).

To confirm the RNAseq results as well as to gain temporal insights into the expression of certain genes, we performed real time quantitative PCR (RT-qPCR) assays. Treatment and stages that have been used for RT-qPCR assays included 2, 6, 12, and 24 HAT for control and BMVE treatment, respectively, along with non-treated uniformly pre-germinated seeds (24 hours after imbibition). SuperScript VILO cDNA synthesis kit (Invitrogen) was used to synthesize cDNA from 1μg of total RNA. RT-qPCR (10 μL) reaction mix prepared using gene-specific primers, SYBR Green Master Mix (Bio-Rad), and template were run on a Lightcycler 480 Real-Time PCR system (Roche). Ubiquitin (*UBQ5*) was used as a reference gene and endogenous control. Thermal cycling conditions were followed as described by Fragkostefanakis et al. (2015). Standard methods for data analysis were followed as described in Livak and Schmittgen (2001). In these RT-qPCR assays, a minimum of two independent biological replicates and three technical replicates were used.

Ground-bed study

The ground-bed study was conducted to investigate if the growth enhancing effects of BMVE observed during germination

and seedling growth were maintained during later vegetative growth stages. Wheat seeds were first treated with BMVE or control treatments at the seedling level as described above. Treated seeds were then grown in plastic cuvette trays filled with soil (greenhouse mix) until transplanted. After 7 days of growth in trays, treated and control seeds were transplanted into the ground bed (UNL Plant Growth Facilities, Lincoln, Nebraska). The ground-bed area was divided into two regions, one each for well-watered (WW) and water-limited (WL) conditions. In each region, 3 plots of 90x45 cm each, spaced at 20 cm, were randomly assigned to BMVE and control treatments (Supplementary Figure 1A). The spacing between the seedlings was set at 18x15 cm. Each plot had 24 wheat plants.

Irrigation of the plots

The soil composition of the ground-bed was a silty clay loam. The calculated percentage of volumetric water content (VWC), field capacity (FC), and permanent wilting point (PWP) for this soil type were reported as 77.356 $SMP^{-0.181}$, 41.08%, and 20.588%, respectively. Plant available water (PAW) was calculated by subtracting PWP from FC which equates to 20.49%. Manageable allowable water depletion for this soil type was 35% of PAW depleted from FC which is 33.9%. It implies that severe drought stress begins when VWC dips lower than 33.9%. Surface drip pipes were used to water the plots throughout the experiment. To monitor the irrigation, water sensors were deployed at three depths (1, 2, and 3 feet) at two locations in each region. Volumetric water content was monitored every day and irrigation decisions were made accordingly. The ground-bed was located inside the greenhouse where the major source of water loss was evapotranspiration. Hence, it was difficult to impose complete drought conditions during the duration of the experiment. However, the water sensor data corresponding to WL plots indicated a declining trend for the VWC at 1 ft (Supplementary Figure 1B). Regularly applied irrigation to WW plots kept the VWC constant over time (Supplementary Figure 1B). Data from water sensors indicated that water requirements were met for WW plots whereas WL plots began experiencing drought at about 45 d.

Phenotyping

For digital phenotyping, a recently developed aerial gantry imaging system was used to image the plots twice a week (Palli et al., 2019). The gantry imaging platform is an autonomous/semi-autonomous navigation system equipped with a trolley carrying camera suspended over the plots to capture crop canopy images (Palli et al., 2019). Imaging data were further processed in MATLAB to compute the pixel sum of the canopies. Later, the pixel sum was used as a proxy to characterize the aboveground biomass content of the plants. To complement the 2-D imaging data from the gantry system, manual measurements were taken alongside digital phenotyping once a week starting from week 2 to 9 after transplanting. These measurements include height (length of the longest leaf), number of tillers, and number of leaves. Due to the complexity in efficiently counting the large number of leaves, leaf counting was carried out only until 7 weeks after transplanting (WAT). At the end of week 9, plants were harvested to measure fresh weight following which the plants were oven dried at 70°C for 7 days to measure dry weight.

BMVE rice panicle spray

The BMVE spray study was conducted to determine the effect of BMVE application during post-fertilization events on rice seed development and on germination in the next generation. As the rice seed developmental phase is very sensitive to high temperatures, we incorporated heat stress into the study to test if the BMVE treatment moderated the stress-mediated detrimental effects on seed

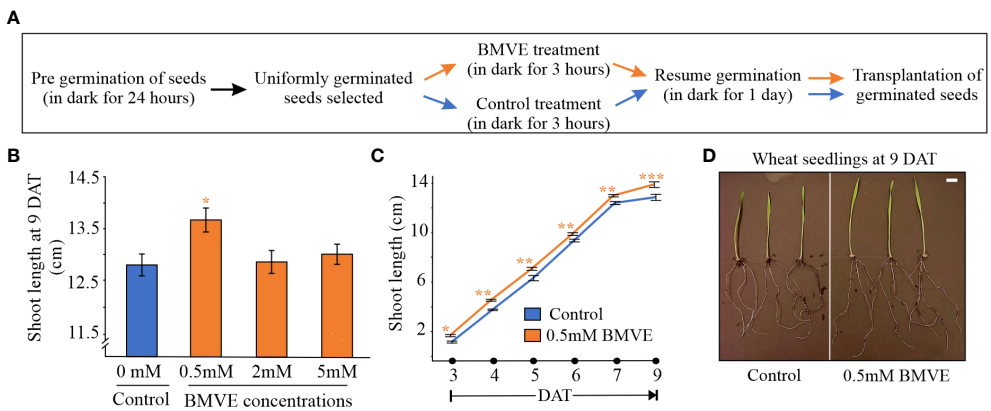

FIGURE 1
BMVE wheat seedling treatment. **(A)** Protocol for treating crop seeds with BMVE. **(B)** BMVE concentration effect on wheat shoot length 9 days after treatment (DAT). **(C)** Shoot length from 3 to 9 DAT. Statistical analysis is by Student's t-test (α= 0.050); n = 16 per treatment/timepoint for shoot length data; ± bars represent standard error. Level of significances corresponding to p-value < 0.05, 0.01, or 0.001 are denoted by '*', '**', or '***', respectively. Similar results were obtained from two independent experiments. **(D)** Representative wheat seedlings at 9 DAT. White bar represents 1 cm.

development. Rice plants were grown in control conditions until flowering. During the onset of the flowering phase, panicles were carefully tracked and florets were marked upon the completion of fertilization (Dharni et al., 2022). Twenty-four hours after fertilization (HAF) of marked florets, subsets of plants were sprayed with BMVE or control solutions. To avoid spray drift, collar sheets were used around the panicles. Due to the highly sensitive nature of seeds to external treatments around the time of fertilization, the BMVE concentration used for spray was 0.1 mM instead of 0.5mM, which was used earlier for mature seed treatment. Immediately after the spray at 24 HAF, half of the plants for each treatment were kept in the control greenhouse (16 h light and 8 h dark at 28 ± 1°C and 23 ± 1°C) while the rest were moved to a greenhouse with high day and night temperatures (HDNT; 16 h light and 8 h dark at 36 ± 1°C and 32 ± 1°C). In total we had four treatment combinations; control treated/control environment, BMVE treated/control environment, control treated/HDNT environment, and BMVE treated/HDNT environment. A minimum of 3 plants per treatment combination was used and multiple seeds per plant were recovered. We first measured the fresh weight (FW) of developing seeds at 1, 2, and 4 days after treatment (DAT), and then measured the dry weight (DW) of seeds oven dried at 40 °C for 10 days.

Another set of similarly treated plants was grown to maturity under control conditions. Stressed counterparts of this set were also moved back to the control environment after being exposed to HDNT stress for 1, 2, and 4 d after treatment (DAT), respectively. These sets of plants were used to measure mature yield traits of marked seeds including mature seed weight, and morphometric parameters (length, width) for all four treatment combinations. For morphometric assessments, 50 marked seeds per treatment combination were first scanned with the WinRhizo scanner, and then analyzed using *SeedExtractor* (Zhu et al., 2021a). Later, we conducted germination assays using the harvested seeds from plants corresponding to all four treatment combinations. After surface sterilization, 45 seeds per treatment were germinated in 3 separate plastic boxes (as discussed above) and were considered germinated when their shoot length reached at least 0.2 cm. Following this criterion, seed germination was scored at 36, 60, and 84 hours after beginning of imbibition. Once ~99% germination was achieved both the root and shoot length of seedlings were measured using a ruler.

Results

Wheat seedling treatment with BMVE enhances early seedling growth

In earlier work we aimed to characterize the efficacy of one representative STA called BMVE (US9464283B2, Kamtec LLC) (Yokoyama et al., 2015). When mature dry wheat seeds were coated with BMVE we saw inconsistent results on the subsequent growth of plants in greenhouse studies (Singh, 2018). We hypothesized this may be due to inherent variability in the timing of seed germination among the relatively small number of seeds tested, and/or to suboptimal BMVE treatment conditions, either of which could obscure detection of potential beneficial effects. Therefore, we developed an improved protocol for wheat seed treatment that involved imbibing seeds for 24 h, selecting for uniformly germinated seeds (radical around 2 mm), followed by soaking these seeds in BMVE or control solution for 3 h. Growth was then continued for 24 h in the dark, followed by transplantation to soil and growth in the light (Figure 1A).

To identify a BMVE concentration producing a positive effect, seeds were treated with 0, 0.5, 2 or 5mM BMVE, and shoot height was measured 9 days after treatment (DAT) following growth in soil. Greater shoot length was seen from the 0.5 mM BMVE treatment (p-value < 0.05), whereas higher concentrations were not effective (Figures 1B, D). We next determined whether positive BMVE effects were detectable at earlier times. A significant increase in shoot length was seen as early as 3 DAT and for each time point after that up to 9 DAT, when the maximum difference was observed (Figure 1C). To test for even earlier effects on both roots and shoots, treated seedlings were incubated on moist germination paper under dark conditions. A significant increase in shoot length was seen at 24 h after treatment (HAT) (Figure 2A). Primary root length enhancement was detected at 48 h after treatment (Figure 2B). Figure 2C shows a representative sample of wheat seedlings grown to 48 HAT. Similar results were obtained from two independent experiments.

Seedling treatment confers tolerance to water limitation in mature plants

To learn whether the positive effect of BMVE on seedling growth translates to later stages of vegetative growth, a larger study with wheat was conducted in which control and BMVE treated wheat seedlings were transferred to a greenhouse ground bed. After 7 d of growth in soil, treated seedlings were transplanted to the ground-bed and growth was monitored using an overhead gantry imaging system as well as by manual phenotyping. Both well-watered (WW) and a water-limited (WL) stress condition were evaluated. Three plot repetitions were randomly assigned to each of the seed treatments (Control and BMVE) under each irrigation regime, and each plot contained 24 healthy wheat plants (Supplementary Figure 1A). Importantly, although water was withheld from the beginning for the WL treatment, a soil water deficit was not evident until around 34 days after transplanting (DATP) and did not reach the severe drought stage until about 51 DATP (Supplementary Figure 1B). 2-D imaging was carried out twice a week from 28 to 52 DATP. In previous studies, pixel sum has been used as a proxy to estimate the biomass content of the imaged plants (Chen et al, 2014.; Hartmann et al., 2011; Fahlgren et al., 2015; Zhu et al., 2021b).

Our results show that under WW condition there is no significant difference in pixel count for plants from the BMVE treatment versus the controls (Figure 3A). However, under WL conditions pixel count for BMVE treated plants was significantly higher than for control plants for days 49 and 52, time points when plants were experiencing severe drought (Supplementary Figure 1). Manual measurements gave similar results in that BMVE had no beneficial effect under WW conditions for any trait measured, with

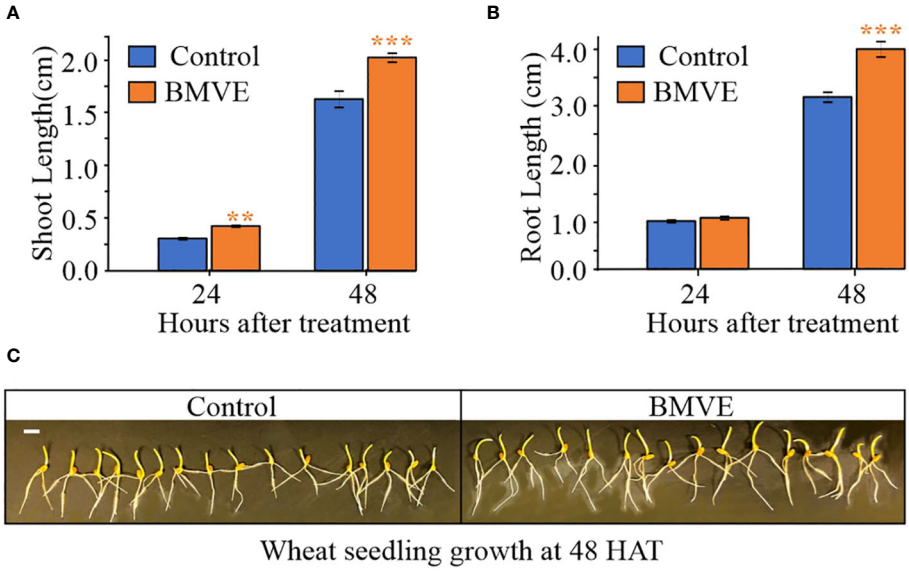

FIGURE 2
Effect of BMVE (0.5 mM) on early wheat seedling growth. Parts **(A)** and **(B)** represent average wheat shoot and primary root lengths at 24 and 48 HAT. For statistical analysis, a student's t-test was conducted (α= 0.050); n = 16 to 20 per treatment/timepoint for shoot and root length data; ± bars represent standard error. Level of significances corresponding to p-value < 0.05, 0.01, or 0.001 are denoted by '*', '**', or '***', respectively. **(C)** visual of germinating wheat seeds at 48 HAT. Horizontal white bar represents 1 cm.

the exception that height was modestly higher for BMVE treatment at 52 DATP (Figure 3B). Under WL the number of leaves and tillers was significantly greater for BMVE treated plants beginning at 28 and 35 DAP, respectively. This is around the time when drought was becoming evident. Plant height was only greater at 52 d and counting of leaf number was not feasible after 42 DATP because of the large number of leaves by that time. End point measurement of fresh and dry weights at 52 DATP confirmed the results of the pixel count data analysis, yielding a significant difference for BMVE treatment only under WL conditions (Figure 3C). These results

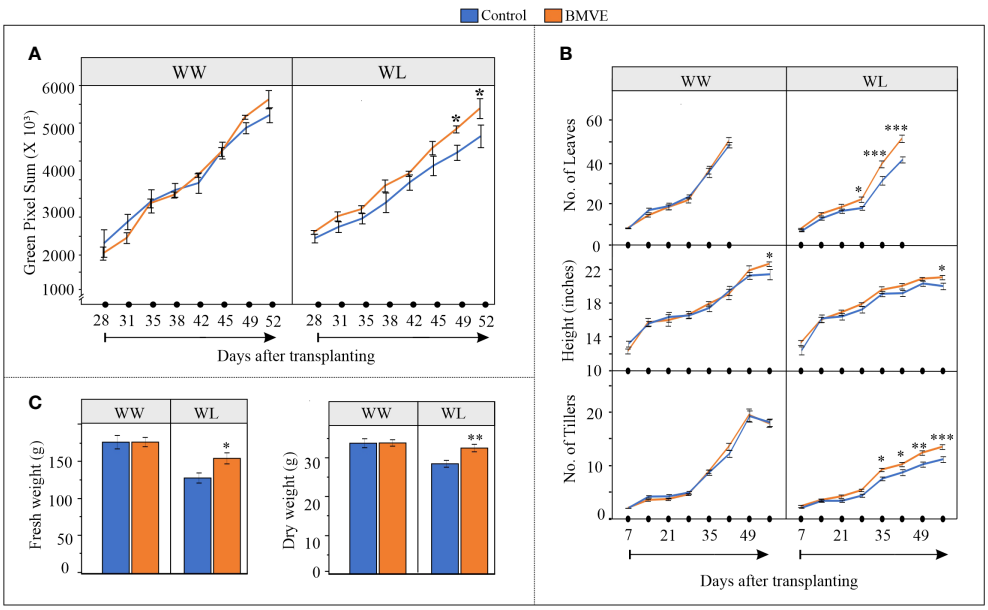

FIGURE 3
Impact of BMVE seed treatment on plants grown in a greenhouse ground-bed. **(A)** Digital imaging measurements captured by an automated gantry system were processed to calculate the aboveground green pixels. **(B)** Parameters documented manually during plant growth including number of leaves, plant height, and number of tillers. n = 12 per treatment/per water condition/per timepoint **(C)** Fresh and dry weights of the harvested above ground biomass at 56 days after transplanting. n = 16 per replicate/per treatment/per water conditions, and three replicates per treatment were used. For statistical analysis, a student's t-test was conducted (α= 0.050); ± bars represent standard error. Level of significances corresponding to p-value < 0.05, 0.01, or 0.001 are denoted by '*', '**', or '***', respectively.

show that the positive BMVE effect on seedlings continued to older plants, but only when water deficit was apparent in the soil.

BMVE enhances rice seedling growth

We next tested whether the wheat seedling treatment protocol yielded similar results in rice. Rice seedlings treated with BMVE (0.5mM) also exhibited significantly higher shoot and root length at 48 HAT (Figure 4A). At 24 HAT shoot and root length were not significantly higher for BMVE treated rice seedlings. Representative rice seedlings at 48 HAT are shown in (Figure 4B). Two independent experiments gave similar results, showing that BMVE enhances seedling growth in at least two major crops.

BMVE alters the transcriptome of rice seedlings

We hypothesized that transcriptome changes after BMVE treatment of seedlings would precede the first noticeable enhancement of shoot and root growth at 48 HAT. To capture these early alterations, RNA-seq analysis was performed on rice seedlings corresponding to the 24 HAT growth stage for both the control and BMVE treatment, which we refer to as C24 and B24, respectively. Seedlings that were only imbibed for 24 h and not treated with BMVE were also sampled at that time point (C0) to decipher the differential temporal changes in gene expression that result from BMVE treatment. A total of 472 differentially expressed genes were identified between B24 and C24 (FDR adjusted p-value 0.05). Among the 472 total genes, 194 showed increased transcript level (FC > 2) while 278 genes showed decreased transcripts (FC < 0.5).

An overview of altered biological pathways between C24 and B24 was obtained through gene ontology (GO) enrichment analysis. This yielded 22 and 10 unique genes for upregulated and downregulated classes, respectively, with most genes falling within multiple GO terms (Supplementary Table 1). About 75% of the up-regulated genes were overrepresented among 20 GO terms, with enrichment ranging from about 9 to 48-fold (Figure 5). Most of the enriched GO terms in the upregulated category were associated with detoxifying processes, responses to toxic substances, development, and hormonal activity. On the other hand, about 20% of downregulated genes were grouped into 15 GO terms with enrichment ranging from around 1 to 1300-fold. Largely, these downregulated GO terms were associated with stress responses including abiotic, biotic, and water deprivation (Figure 5).

Transcripts associated with reducing ROS load are elevated by BMVE

GO term enrichment revealed that classes corresponding to 'cellular response to toxic substances, detoxification, monooxygenase

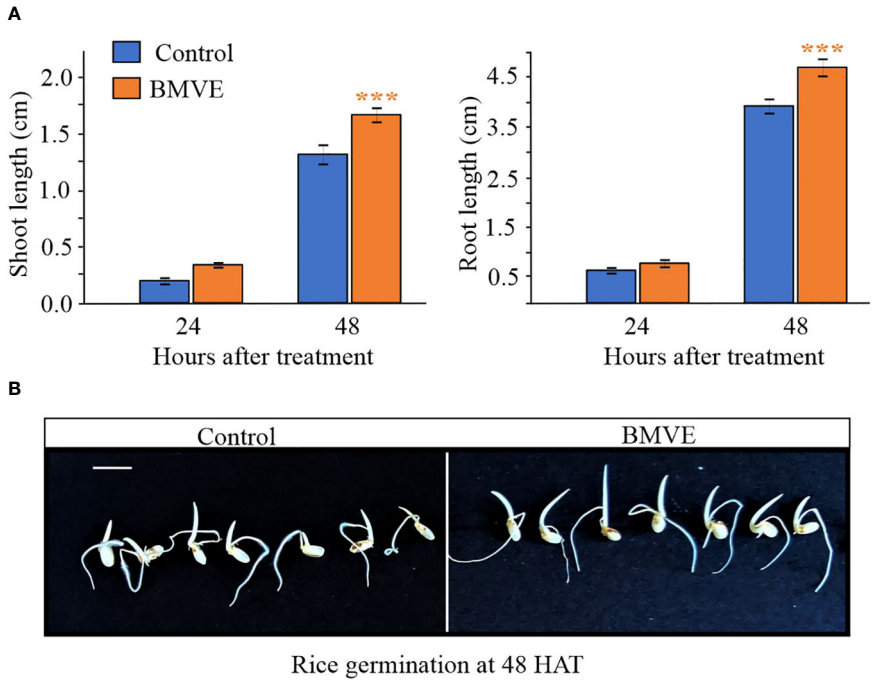

FIGURE 4
Growth of rice seedlings treated with BMVE. **(A)** Shoot and root lengths at 24 and 48 HAT. For statistical analysis, a student's t-test was conducted (α= 0.050); n = 16 to 20 per treatment/timepoint for shoot and root length data; ± bars represent standard error. Level of significances corresponding to p-value < 0.05, 0.01, or 0.001 are denoted by '*', '**', or '***', respectively. The experiment was repeated twice, and similar results were obtained. **(B)** representative germinating rice seeds at 48 HAT. Horizontal white bar represents 1 cm.

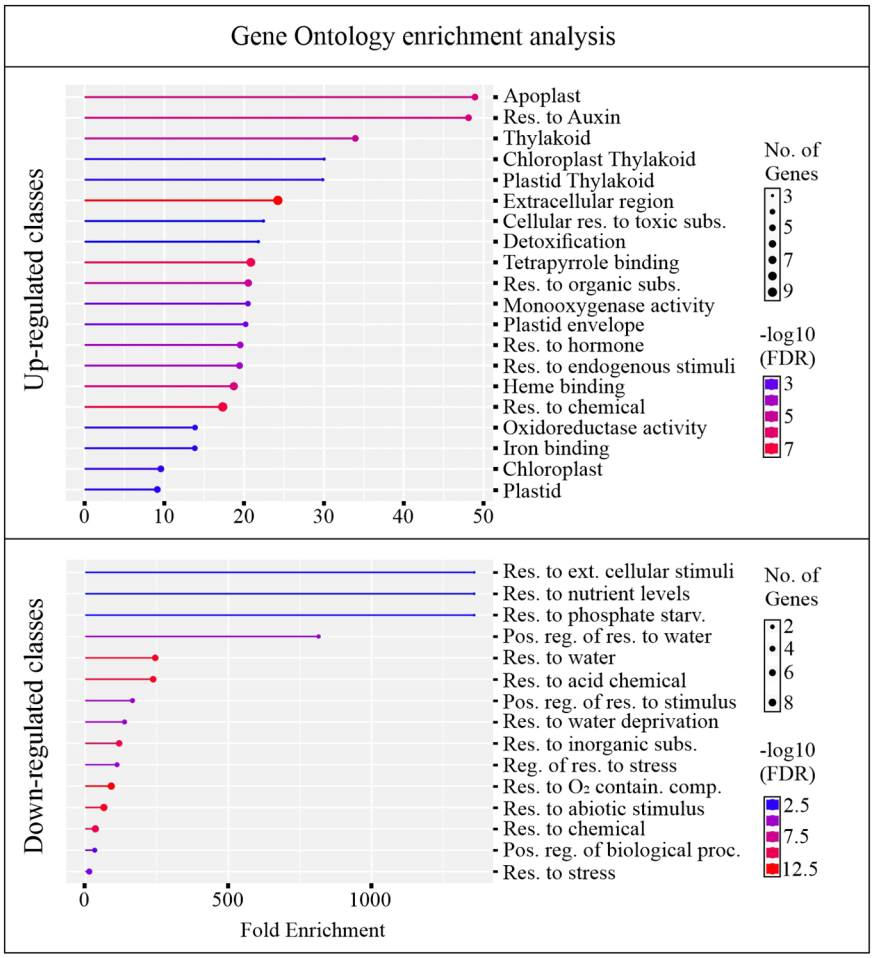

FIGURE 5
Gene ontology (GO) enrichment. The analysis was conducted for genes differently regulating between BMVE, and control treated rice seeds at 24 HAT. The genes passing the statistical threshold of p-value < 0.05, false discovery rate (fdr) < 0.05, and fold change greater or less than 2 were considered for this analysis.

activity, and oxidoreductase activity' were enriched with genes exhibiting increased transcript abundance (Figure 5). Figure 6 shows the FC of genes discovered by GO enrichment (labeled in bold). Rapid breakdown and oxidation of nutrient reserves during seed germination results in accumulation of reactive oxygen species (ROS) that can delay or prevent seedling growth (Kurek et al., 2019; Thakur and Vasudevan, 2019). Activation of antioxidant systems such as peroxidases (PRXs), catalases (CATs), and superoxide dismutases (SODs) facilitate ROS removal and counteract potential molecular damage (Dietz et al., 2016; Steinbrecher and Leubner-Metzger, 2017; Noctor et al., 2018; Kurek et al., 2019; Marks et al., 2022). Several peroxidases (PRXs) and Cytochrome P450 genes appeared in our GO analysis results (Supplementary Table 1) and these are generally known to be involved in H_2O_2 metabolism and enhancing the activity of compounds with increased antioxidant activity (Almagro et al., 2009; Pandian et al., 2020; Rao et al., 2020; Zhang et al., 2022). Other upregulated categories in the GO analysis included apoplast, chloroplast, extracellular region, heme binding, plastid, response to hormone, and response to chemical (Figure 5). These classes include genes such as *DIM/DWF1 (LOC_Os04g48200)*, *Dirigent (LOC_Os11g42500)*, *OsGLP3-3 (LOC_Os03g58980)*, *OsLhcb2 (LOC_Os03g39610)*, and *OsPSK5 (LOC_Os03g47230)* that are important for maintaining antioxidant systems and regulating ROS production (Thamil Arasan et al., 2013; Han J. et al., 2014; Li et al., 2016; Nahirñak et al., 2019; Jiang et al., 2021; Yang et al., 2006) (Supplementary Table 1).

To assess how BMVE perturbs the normal temporal changes in early seedling transcripts. Figure 7 shows transcript abundance for control and BMVE treatment compared to C0, expressed as z-scores. For example, PRX125 transcript normally increases over 24 h of seedling growth (C0/C0 vs. C24/C0), but BMVE treatment enhances the increase (B24/C0). On the other hand, the expression of some Cytochrome P450s (*CYP86A7-2*, *CYP96E*, *CYP76M1*), PRX (*LOC_Os04g51300*), and *PSK5* is reduced in seedlings from C0 to C24, but BMVE treatment either increases or maintains the expression of these transcripts over the first 24 h (Figure 7). Overall, these results suggest that one effect of BMVE treatment is to help reduce the ROS load, allowing for more vigorous seedling growth at this stage.

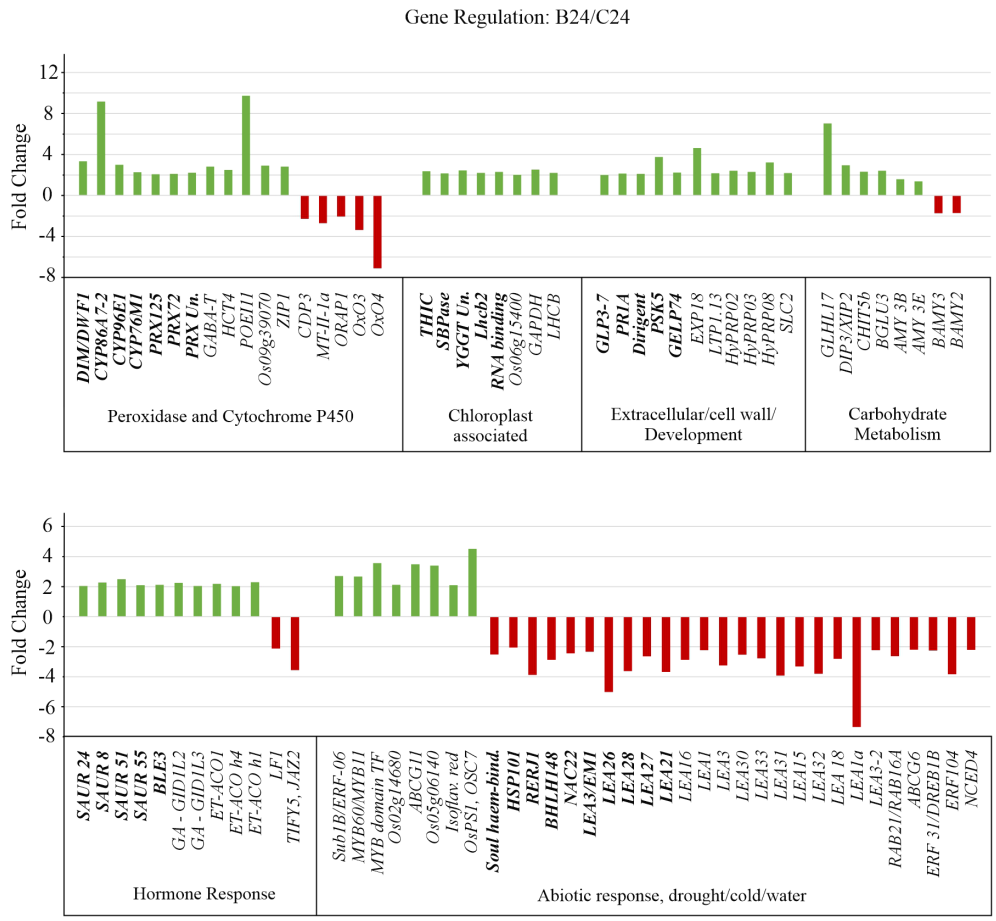

FIGURE 6
Gene expression altered by BMVE treatment in comparison to control treatment at 24 HAT. Transcript differences with p-value < 0.05, false discovery rate (fdr) < 0.05, and > 2-fold change were included in the analysis. Unique genes recovered from Gene Ontology (GO) enrichment analysis are shown in bold, additional differentially regulated gene shown in plain text.

Transcripts associated with cell elongation and growth are elevated by BMVE

Other genes identified by GO analysis in the upregulated classes include four small auxins up RNAs (*SAUR*) *8, 24, 51*, and *55* (Figures 6, 7, Supplementary Table 1). Although their function is unclear, *SAUR* genes respond quickly to exogenous and endogenous auxin and they are expressed predominantly in developing tissues, especially the elongating hypocotyl (Gee et al., 1991; Jain et al., 2006). *OsBLE3* (*LOC_Os05g15630*) is another upregulated auxin responsive gene reported that was reported to be involved in cell elongation in rice through dual regulation by brassinolide and auxin (Yang et al., 2006). The Calvin-Benson cycle gene, *SBPase* (*LOC_Os04g16680*), was also upregulated for B24. Mutation in this gene results in decreased chlorophyll content during the seedling stage in rice (Li et al., 2020). Additionally, *SBPase* is known to be upregulated by chitosan treatment, which positively impacts plant carbon metabolism and photosynthetic components ultimately leading to enhanced plant growth and development (Chamnanmanoontham et al., 2015). Consistent with the physiological observation, several genes associated with growth are up regulated by BMVE treatment.

Several transcripts associated with abiotic stress are reduced by BMVE

Ten unique down-regulated genes were grouped by GO enrichment into abiotic stress response categories. Most of the genes in this category normally exhibit higher expression over time (Figure 7, C0 vs. C24). However, for B24 their transcript levels are significantly less as compared to C24. The abscisic acid (ABA) inducible genes *OsNAC22 (LOC_Os03g04070), Osbhlh148 (LOC_Os03g53020)*, and *LEA26 (LOC_Os11g26750)* are known to modulate stress tolerance responses through ABA dependent signaling pathways (Seo et al., 2011; Hong et al., 2016; Verma et al., 2017). *OsEm1/OsLEA3 (LOC_Os05g28210)* encodes an ABA regulated small hydrophilic plant seed protein whose expression is reduced in the embryos dissected from germinating seeds and co-expresses with the genes belonging to *LEA* or dehydrin protein family (Hattori et al., 1995; Han C. et al., 2014). In addition to *OsEm1*, all other *LEA 21, 26, 27, and 28* genes exhibited decreased expression in BMVE treated seeds at 24 HAT (Figure 7). *OsRERJ1* is involved in rice shoot growth inhibition mediated by jasmonic acid (Kiribuchi et al., 2004), and its expression was also reduced under BMVE treatment. In summary, BMVE treatment shifted the normal

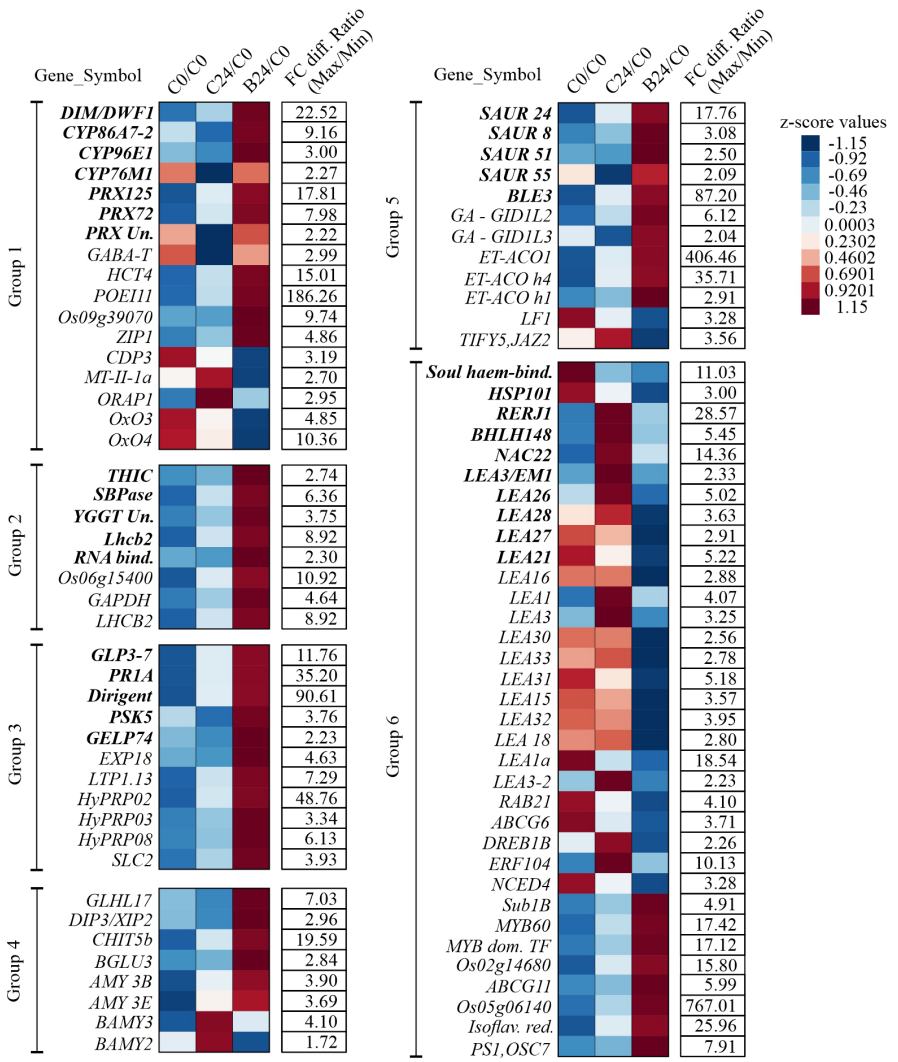

FIGURE 7
Temporal expression of the genes for C24 and B24 in comparison to untreated seeds (C0). Magnitude of the expression differences is depicted by z-score of the ratios calculated by dividing the average transcript reads for both the treatments at 24 HAT with the read count for untreated control seeds. Fold change differences in the ratios between maximum and minimum values per row are provided in the column 'FC diff. Ratio (Max/Min)'. 'C0', 'C24', and 'BM24' represent untreated control, control at 24 HAT and BMVE treatment at 24 HAT, respectively. Unique genes recovered from Gene Ontology (GO) enrichment analysis are shown in bold fonts, additional differentially regulated genes are in plain text. Genes representing common functions are clustered together into six groups. Group 1: Peroxidases, cytochrome P450s, and detoxification associated genes; Group 2: Chloroplast and thylakoid associated genes; Group 3: Extracellular region, cell wall, and development associated genes; Group 4: Carbohydrate (CHO) metabolism; Group 5: Hormonal response; Group 6: Response to stress (abiotic, biotic, water, and chemical).

trajectory of many transcripts by increasing levels for genes involved in antioxidant activity and auxin/growth responses, while reducing transcripts for abiotic stress response.

BMVE modulates additional genes involved in seed germination processes

To broaden the scope of the analysis we identified 58 additional genes not identified by GO analysis that were nevertheless significantly affected by BMVE and were associated with the major GO classes (shown as regular font in Figures 6, 7). These belonged to the classes including oxidoreductase activity, detoxification, cell wall development, carbohydrate metabolism, hormone, and response to abiotic/biotic stresses (Figures 6, 7).

Among these are three genes, *GABA-T* (*LOC_Os02g02210*), *HCT4* (*LOC_Os06g08640*), and *POEI11* (*LOC_Os10g05950*) that are involved in monooxygenase and oxidoreductase activity. *HCT4* and *POEI11* normally increase over time, while *GABA-T* declines (C0 vs. C24), but in each case BMVE treatment resulted in higher transcript levels (C24 vs. B24). (Wu et al., 2006; Kim et al., 2012; You et al., 2014). Activity of *GABA-T* defends against environmental stress by preventing cell death and restricting the accumulation of reactive oxygen intermediates (Wu et al., 2006). *HCT4* is involved in catalyzing the biosynthesis of cinnamic acid conjugates that function as antioxidants (Zhao and Moghadasian, 2010; Kim et al., 2012). Expression of two heavy metal detoxifying

genes i.e., *LOC_Os09g39070* and *ZIP1*, involved in aluminum, zinc, cadmium, and copper stress tolerance mechanisms in plants was also increased for B24 (Wang et al., 2014; Liu et al., 2019). In contrast, the expression of the genes (*CDP3*, *MT-II-1a*, *ORAP1*, *OxO3*, and *OxO4*) that are either induced by or promote production of hydrogen peroxide was reduced for BMVE treated seeds (Hu et al., 2003; L. Zhou et al., 2005; Ueda et al., 2015; Peng et al., 2022). Over time, *CDP3*, *OXO3*, and *OXO4* exhibited a slight decline in transcript levels for control seeds, however BMVE treatment led to even greater reductions (Figure 7).

Hormonal signaling plays a vital role during germination and early seedling growth (Ni et al., 2001; Seo et al., 2009; Ren and Gray, 2015; Sun et al., 2020). In addition to the SAUR class genes mentioned earlier, our analysis revealed additional differentially genes. Genes involved in ethylene biosynthesis, such as 1-aminocyclopropane-1-carboxylate oxidase *ACO1* (*LOC_Os09g27820*), *ACO homolog 1* (*LOC_Os08g30100*), *& ACO homolog 4* (*LOC_Os08g30080*), were upregulated for BMVE treated seeds at 24 HAT (Figure 6). In contrast, ethylene response factors *ERF-104* (*LOC_Os08g36920*) and *ERF3/DREB1b* (labeled *DREB1B* in Figure 7) (*LOC_Os09g35010*) are normally elevated as seedling development progresses (C0 vs. C24) (Figure 7), but BMVE essentially eliminates the increase during this time (B24). *ERF-104* is associated with cold stress response (Li et al., 2018) and *ERF3/DREB1b* are associated with cold and drought. This is consistent with the reduction of several other stress associated transcripts mentioned earlier. On the other hand, an *APETALA2* transcription factor *ERF-063*, commonly known as *Sub1b* showed higher transcript levels for BMVE treated seeds at 24 HAT (Figure 7).

The 9-cis-epoxycarotenoid dioxygenase (*OsNCED4*; *LOC_Os07g05940*), a major gene involved in ABA biosynthesis, normally declines during germination and in our experiment the reduction is evident from C0 to C24 (Figure 7). However, BMVE treatment results in an even greater reduction in its transcript levels. During the process of seed germination an antagonistic reaction occurs between abscisic acid (ABA) and gibberellic acid (GA), where the former is known to repress germination (Müller et al., 2006; Golldack et al., 2013; Liu et al., 2016; Liu and Hou, 2018). *OsLF1* (*LOC_Os01g51610*), *a B3 DNA* binding domain-containing protein that negatively regulates GA metabolism and promotes the ABA biosynthesis (Guo et al., 2013) also shows this pattern of enhanced downregulation by BMVE (Figure 7). Another ABA inducible gene that is involved in jasmonic acid signaling i.e., *TIFY5/JAZ2* (*LOC_Os07g05830*) (Ye et al., 2009) showed reduced transcript levels for BMVE treated seeds (Figure 7). On the other hand, two gibberellic acid receptors, *GID1L2* (*LOC_Os07g06860*) and *GID1L3* (*LOC_Os01g06220*) showed increased transcript abundance for BMVE treated seeds at 24 HAT (Figure 7) (Hartweck and Olszewski, 2006).

All of the differentially expressed *LEA* genes (including *LEA 3, 21, 26, 27*, and *28* from the GO enrichment analysis) showed reduced transcript levels for BMVE treated seeds at 24 h (Figures 6, 7). Their expression either increases or slightly decreases over time for control seeds. *LEA* genes are normally expressed in response to ABA, dehydration, and salt stress, reinforcing our observation that in general, stress-related transcripts are reduced by BMVE treatment (Chandler and Robertson, 1994; Bray, 1997; Shinozaki, 2000; Wang et al., 2007).

Exceptions to this trend are genes involved in salt stress (*ABCG11*: *LOC_Os05g02890*; *LOC_Os05g06140*) and biotic stress (*Isoflavone reductase*: *LOC_Os01g01650*; *PS1/OSC7*: *LOC_Os11g08569*) tolerance, which showed upregulation for B24 (Figure 7). *ABCG11* is highly responsive to salt stress in rice, and its deficiency reduces the lipid metabolism in roots which further impact suberin biosynthesis (Panikashvili et al., 2010; Matsuda et al., 2012). A study comparing the difference in salt tolerance between barley and rice reported a higher expression of *LOC_Os05g06140* in the salt tolerant barley accession 'XZ26' (Fu et al., 2019). *Isoflavone reductase* upregulates in rice to defend against bacterial leaf blight disease and *PS1/OSC7* is a member of the gene family '2,3-oxidosqualene cyclase' which catalyzes the first step in triterpene biosynthesis required for protection against pathogen and pests (Thimmappa et al., 2014; Peng et al., 2015; Xue et al., 2018).

Studies have shown that expansins operate as cell wall loosening proteins and are known to mediate coleoptile elongation under anoxic conditions (Cho and Kende, 1997; Lee et al., 2001; Magneschi et al., 2009). One such gene is the *OsEXP 18* (*LOC_Os03g06040*) gene from the 'Expansin' family and showed higher transcript levels for B24 (Figure 7). *SLC2* (*LOC_Os09g39720*) plays an important role in shoot development and salicylic acid production in rice (Liu et al., 2020). The expression of this gene normally increases over time (C24 versus C0), however, it exhibits even higher levels for BMVE treated seeds indicative of growth advancement (Figures 6, 7). Three 'PS Calvin cycle' related genes, '*Glyceraldehyde-3-phosphate dehydrogenase* (*GAPDH; LOC_Os04g38600*), *LOC_Os01g73540, and chlorophyll A-B binding protein* (*LOC_Os03g39610*)', also showed higher transcript abundance for BMVE treated seeds (Figure 7). The upregulation of various growth associated genes for BMVE treatment at 24 HAT is consistent with the advancement in seedling growth observed at 48 HAT.

BMVE modulates transcript abundance of carbohydrate metabolism genes

According to the triphasic model for seed germination, the TCA cycle or aerobic respiration is usually recovered during phase III at 50 hours after imbibition (Bewley, 1997). This phase is marked by the initiation of rapid cell division and increased energy demand resulting in increased activity of α-amylases following the breakdown of starch reserves (He and Yang, 2013). The induction of α-amylases during the initial stages of seed germination is regulated by ethylene (ET) and gibberellic acid (GA) (Sun et al., 2020). In general, the activity of ET and GA during seed germination promotes the expression of α-amylases while impeding the β-amylases (Sun et al., 2020). To explore further the changes in energy status among the rapidly (BMVE treated) and slow growing (control treated) seeds, we searched for all the DEGs related to starch metabolism. Our results indicated that two each of α and β-amylases consistently exhibited higher (*AMY3B:*

LOC_Os09g28420, and *AMY3E: LOC_Os08g36900*) and lower (*BAMY2: LOC_Os03g04770*, and *BAMY3: LOC_Os10g41550*) expression trends (Figure 7). Additionally, the genes belong to *Glycosyl Hydrolase* family including *BGLU3: LOC_Os01g59840, CHIT5b: LOC_Os11g27400, DIP3/XIP2: LOC_Os05g15850*, and *GLHL17: LOC_Os01g71380* have higher transcript levels for BMVE treated seeds (Figure 6). The upregulation of amylase and glycosyl hydrolase genes is further evidence that seedling growth is advanced by BMVE treatment of seedlings.

Evidence for earlier transcriptional changes

Transcriptome data for 24 HAT indicates that BMVE-induced acceleration of seedling growth correlates with up-regulation of growth-related hormonal genes and transcription factors, starch regulatory genes, and enzymes involved in anaerobic pathways. To validate these results and test whether BMVE stimulated genes prior to 24 HAT, six were evaluated by qPCR at 2, 6, 12 and 24 HAT (Figure 8). The results for 24 h aligned closely with the transcriptomic results, validating the overall accuracy of whole transcriptome data. BMVE increased the transcript abundance of genes associated with ethylene biosynthesis (*ACO 1)*, cell wall loosening (*EXP 18*), an auxin responsive factor (*SAUR 51*), a glycosyl hydrolase gene that degrades the callose deposited in the grain cell wall (*GLHL17*), and a major carbohydrate (CHO) metabolism gene (*AMY 3B*). Five of the upregulated transcripts showed no increase prior to 24 HAT. The exception was *EXP18*, which was significantly elevated relative to the control at 12 HAT.

In contrast, NCED was negatively affected by BMVE as early as 2 HAT. At 24 HAT qPCR indicated no difference for this treatment from BMVE treatment, although whole transcriptome analysis suggested a roughly 2-fold decline at 24 HAT. ABA activity negatively regulates the process of seed germination during very earlier stages and the ABA synthesis enzyme *NCED4* normally declines during germination (Figure 7) (Huo et al., 2013). Our results showing that BMVE treatment accelerates the early loss of *NCED4* transcripts suggests that early hormonal changes may regulate later gene and metabolic responses that are associated with growth.

BMVE rescues rice seed grain parameters under heat stress

Embryo and endosperm development are sensitive to high temperature, which can negatively impact seed viability, germination, and seedling growth in the next generation (Warner and Erwin, 2005; Jagadish et al., 2007; Arshad et al., 2017; Paul et al., 2020). We investigated whether BMVE application to rice florets shortly after fertilization impacts development of the resulting seeds that were then exposed to heat stress during the embryo/endosperm development phase.

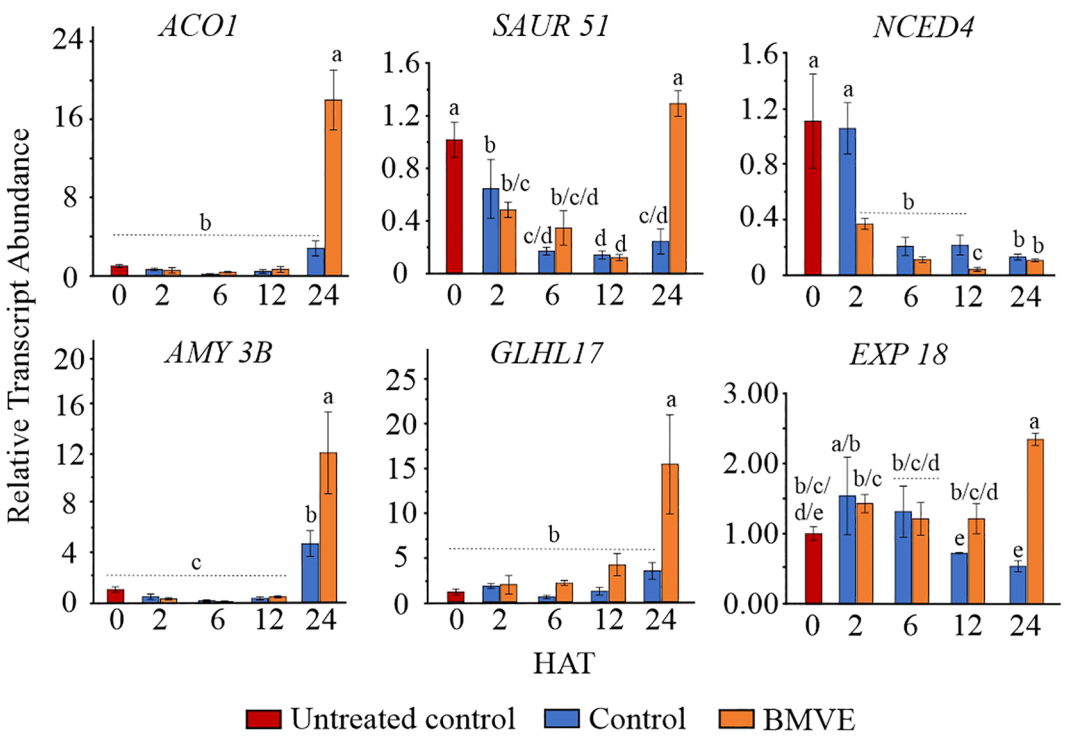

FIGURE 8
Gene expression analysis by real time quantitative PCR (RT-qPCR). At 2, 6, 12, and 24 hours after treatment (HAT) for both control and BMVE treatments, the relative transcript abundance of these genes was calculated against the transcript abundance of untreated control seeds at 0 HAT. These genes included aminocyclopropane-1-carboxylate (ACO1), small auxin up RNA (SAUR51), 9-cis-epoxycarotenoid dioxygenase (NCED4), α-amylase (AMY3B), glycosyl hydrolase family protein (GLHL17), and an expansin family protein (EXP18). For statistical analysis, a student's t-test was conducted (α= 0.050); ± bars represent the standard error; values not connected by same letter are significantly different.

We marked recently fertilized florets and then whole panicles were sprayed 24 h later with BMVE (100 uM) or control solution (Dhatt et al., 2021; Dharni et al., 2022). Plants were then moved to control (28 ± 1 °C and 23 ± 1 °C light and dark, respectively) or high day and night temperature (HDNT; 36 ± 1°C and 32 ± 1°C light and dark, respectively) (Figure 9A). To avoid the more damaging impacts of severe heat stress, we chose a moderate stress regime following the BMVE treatment (Figure 9A). Plants were heat stressed for 24, 48 or 96 h corresponding to 48, 72 and 120 HAF, respectively. Developing seed weight for 24 and 48 HS showed non-significant differences between control and BMVE treated seeds under both ambient and HDNT conditions (Figure 9B). Developing seed weight for 48 HS was significantly higher than non-heat stressed seeds for both the control and BMVE treatments, probably due to precocious cellularization under this moderate level of heat stress (Chen et al., 2016; Begcy et al., 2018). For plants exposed to a 96 h of HDNT, BMVE treatment led to significantly higher FW of developing seeds. The experiment was repeated twice, and similar results were obtained.

Separate sets of similarly treated plants were grown to maturity to assess mature grain seed traits including weight and morphometrics of the marked grains. These plants had been moved back to control conditions after exposing them to the indicated HDNT regimes (Figure 9A). Mature grain weights were not significantly different for any treatment for 24 and 48 HS (Figure 9B). In contrast with fresh weight at 96 h, mature grain weight from control plants was negatively affected following the 96 HS treatment. However, BMVE treatment of these developing seeds restored the mature seed weight to that of non-heat stressed plants. This shows that BMVE treatment negates the detrimental impact of the 96 h HS imposed at the time of early seed development.

As a positive effect of BMVE treatment was only seen for 96 h HS, mature seeds from this time were used to conduct morphometric analysis. Grain length, width, and area are the major determinants of grain size and quality parameters, and contribute to final grain yield (Tan et al., 2000; Huang et al., 2013). BMVE treatment of developing seeds led to significantly greater grain length, in both ambient and heat stress conditions (Table 1). Grain width and area were unaffected by BMVE for the seeds developed under ambient conditions. However, the reduction in width caused by HS was restored to ambient level by BMVE, and grain area was significantly greater under HS for BMVE treatment compared with control. These results are consistent with the increased mature seed weight seen for BMVE treated seeds that experienced the 96 HS treatment.

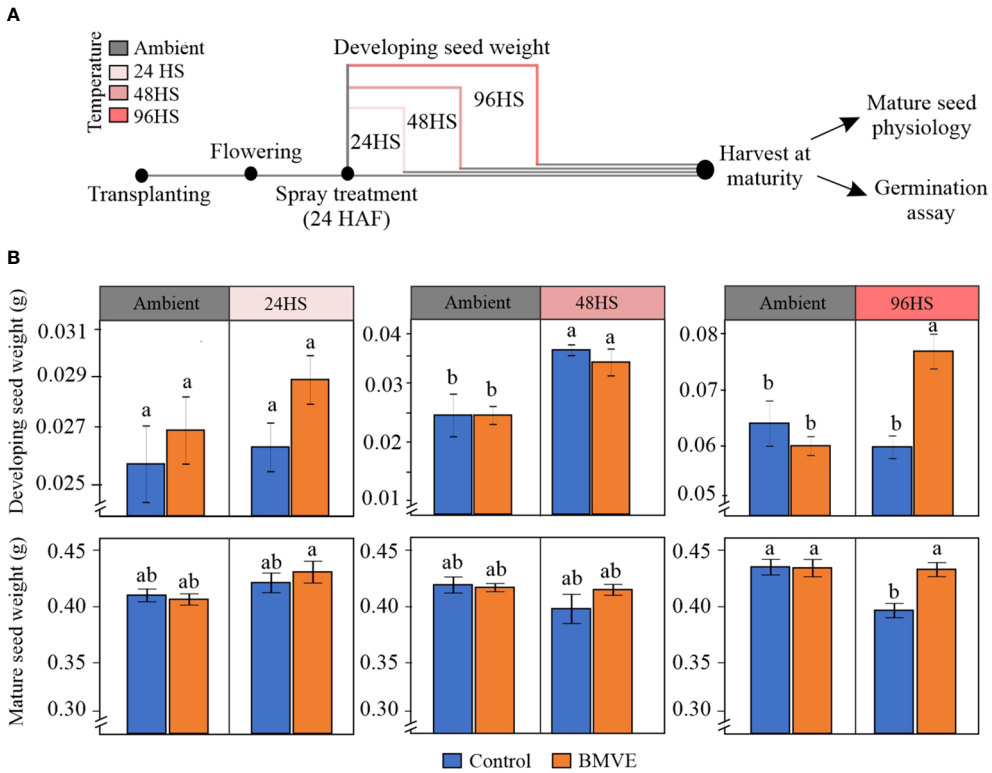

FIGURE 9
Effect of BMVE treatment on the rice grain development under heat stress (HS) conditions. **(A)** pictogram illustrating heat stress regime. Florets were marked at the time of fertilization, and 24 hours after fertilization (HAF) spray treatments were applied (BMVE: 0.1 mM and control). Following the spray, plants subjected to ambient (28 ± 1 °C and 23 ± 1 °C, light: dark) and heat stress (HDNT; 36 ± 1°C and 32 ± 1°C, light: dark) conditions. These plants were evaluated for developing seed weights at 24, 48, and 96 hours after the heat stress along with respective controls. Additionally, separate sets of plants were moved back to ambient conditions upon the completion of each type of stress regime and subjected to grow until maturity facilitating mature seed data collection. **(B)** shows the developing and mature seed weights from the plants that received above-mentioned treatments. For statistical analysis, a student's t-test was conducted (α= 0.050); n = 40 – 50 seeds per treatment/timepoint from 8 replicates (developing grain weight) and 60 – 80 seeds per treatment from 8 replicates (mature grain weight); ± bars represent the standard error; values not connected by same letter are significantly different. The whole experiment was repeated twice.

TABLE 1 Grain morphometrics data of mature grains from ambient temperature-control spray, ambient temperature-BMVE spray, heat stress-control spray, and heat stress-BMVE spray conditions.

Temperature	Ambient		Heat stress	
Spray	Control	BMVE	Control	BMVE
Grain length	4.87 ± 0.03[b]	5.01 ± 0.03[a]	4.86 ± 0.03[b]	5.05 ± 0.03[a]
Grain width	2.96 ± 0.02[a]	3.00 ± 0.02[a]	2.89 ± 0.02[c]	3.01 ± 0.02[a]
Grain area	11.41 ± 0.13[b]	11.72 ± 0.12[ab]	11.02 ± 0.13[c]	11.78 ± 0.12[a]

For statistical analysis, a student's t-test was conducted (α= 0.050) for each morphometric parameter individually; n=50-60 marked seeds; ± represents the standard deviation; values not connected by same letter are significantly different.

BMVE treatment of developing seeds enhances germination

We next tested whether the enhanced seed parameters resulting from BMVE treatment translated to increased seed germination and seedling vigor in the next generation. Seeds were considered to have germinated when the radicle emerged and the plumule reached the length of at least 0.2 cm. Seeds that developed following the BMVE treatment germinated faster than the untreated seeds from the heat stressed plants, correlating with the enhanced values for all parameters that were measured for these seeds (Figure 10A). Although grain length was the only morphometric trait affected by BMVE for non-heat stressed plants, BMVE treatment also enhanced germination of these seeds. For both temperature conditions BMVE treated seeds achieved more than 90% of germination by 60 hours whereas control treated seeds achieved only about 70% germination by that time. By 84 h all the seeds under observation were germinated, indicating the HS treatment was not severe enough to affect viability. Also evident is that this moderate HS treatment increased germination rate for both the control and BMVE treatments, consistent with previous findings (Begcy et al., 2018).

As expected from the faster germination rate for seeds that developed on BMVE treated plants, both the shoot and root length of these seedlings were significantly higher than the controls at 84 h after germination (Figures 10B, C). For the non-BMVE seeds, the shoot length was significantly higher for seeds that developed under HS as compared to ambient conditions while no differences were observed for root length. This is consistent with previous findings that moderate HS during the seed development phase accelerates the seed germination process in the next generation (Begcy et al., 2018). BMVE treatment of developing seeds leads to higher root and shoot growth in the next generation regardless of temperature treatment, suggesting that BMVE triggers biological processes that lead to increased seed vigor.

Discussion

Because treatment of dry seeds reportedly increases final yield of several crop plants, a reasonable hypothesis is that BMVE affects early stages of seedling development, with positive effects extending throughout plant growth (Yokoyama et al., 2015; Kamtec LLC, unpublished). To address the earlier issues of inconsistencies in our own evaluation of BMVE seed treatment (Singh, 2018), we developed a new treatment protocol based on the triphasic model of seed germination (Bewley, 1997; Yang et al., 2007). Phase 1 corresponds to the rapid uptake of water by a dry seed and lasts up to 20 hours after imbibition (HAI) (Bewley, 1997; Howell et al., 2009). Phase II lasts from 20 - 50 HAI and is considered the most critical, as most of the metabolic reactions required for germination occur during this window (Yang et al., 2007; He and Yang, 2013). Phase III begins 50 HAI onwards in which another rapid water uptake takes place followed by radical protrusion (Yang et al., 2007). We hypothesized that as a beneficial seed treatment BMVE targets phase II. To enhance treatment efficacy, we imbibed the seeds for 24 hours prior to BMVE treatment. In addition to targeting the early metabolically active phase II, this allowed for the selection of seeds at the same stage of germination for subsequent BMVE treatment, minimizing the confounding effects of natural variability in germination rate among seeds. We also optimized the BMVE concentration for treatment under this condition. Together, this gave repeatable beneficial effects of BMVE on wheat and rice seedling shoot and root length as early as 48 HAT (24 HAT for wheat shoots) in our relatively small-scale laboratory experiments.

When BMVE treated wheat seedlings that were grown in well-watered soil for up to 52 days after transplanting, the advantage observed during the early seedling growth was not evident for the parameters measured during the vegetative growth phase. However, we did not obtain final grain yield data, which might still have shown a significant difference in the end. In contrast to plants with sufficient water, the benefit of BMVE treatment became evident as early as 35 days after transplanting (number of leaves and tillers) when the plants began to experience drought conditions (Figure 3). Total biomass determined by RGB imaging corroborated this result, beginning at 49 DAP, when drought had become severe. The higher biomass observed for BMVE treatment under the WL condition could be primarily due to increased tillering, although the final tiller number for BMVE treatments under WL conditions were still lower than that of the WW treatment. Further testing that includes final yield data and grain parameters would help to better understand the benefits of BMVE seedling treatment. We also acknowledge that other crop species may not respond similarly to BMVE.

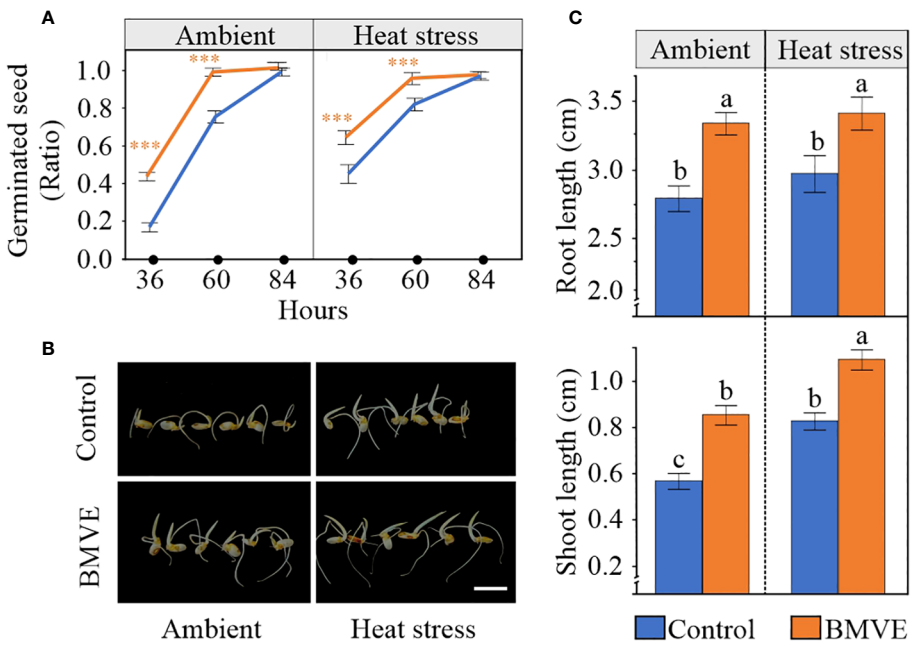

FIGURE 10
Effect of BMVE treatment of developing rice seeds in the next-generation. **(A)** Germination ratio for seeds from ambient and 96 h HS at 36, 60, and 84 hours after germination (HAG). **(B)** Representative rice seed germination at 84 HAG. Horizontal white bar represents 1 cm. **(C)** Root and shoot lengths at 84 HAG,for seeds germinated following the indicated treatment and temperature conditions. Statistical analysis was a student's t-test (α= 0.050); n = 46 to 48 seeds per treatment; $\pm$ represents the standard error. Level of significances corresponding to p-value < 0.001 is indicated by ***.

These results suggest that BMVE is most beneficial under abiotic stress conditions, based both on our physiological experiments and from the number of stress-related genes affected by BMVE. DCPTA is another STA that has been reported to ameliorate drought stress following foliar application (Xie et al., 2017). Anecdotal observations also suggest that these compounds are more likely to be beneficial under stress conditions in field experiments (Kamtec, LLC, unpublished). Differential environmental stress conditions may partly explain the discrepancies in past field studies that sometimes showed no beneficial effect of STA treatment.

Our demonstration of altered seedling growth parameters coupled with the transcriptome results suggest that early changes in gene expression mediate the BMVE effect. Specifically, transcripts associated with photosynthesis, carbohydrate metabolism, cell growth and hormones regulating growth were all increased 24 h after BMVE treatment relative to the control. Several peroxidase and cytochrome protective enzyme transcripts were also elevated. Early seed germination leads to a nutrient deprived state, resulting in rapid mobilization and oxidation of nutrient reserves. ROS species are a detrimental by-product of these oxidation processes (Thakur and Vasudevan, 2019). To facilitate seed germination, antioxidant systems are activated to scavenge free radicles (Steinbrecher and Leubner-Metzger, 2017; Marks et al., 2022). Hence, antioxidant activity is considered a reliable indicator of robust seed germination and seedling performance (Corbineau, 2012). One of the observed results of seed priming is higher activity of antioxidant defense mechanisms, which presumably contributes to more rapid and synchronous germination and more uniform crop stands (Jisha et al., 2013; Hussain et al., 2016). Notably, our transcriptome analysis results revealed that BMVE treatment not only increased the expression of genes that are involved in antioxidant and detoxification activities but also reduced the expression of those that promote the production of free radicles, in particular, H_2O_2 (Figures 6, 7). This suggests that BMVE treatment might mimic some of the priming effects seen during early seedling growth, which ultimately enables accelerated development of seedlings. It would be important in future studies to evaluate whether any of the transcriptomic changes we observed persist into the mature plant, or if other genes change their pattern of expression as plants mature.

We cannot rule out the possibility that BMVE also has a direct biochemical effect on early seedling metabolism that does not require altered gene expression. Yokoyama and Keithly (1991) proposed that DCPTA [2-(3,4-dichlorophenoxy) triethylamine] modifies carotenoid content in plants and mold (*Phycomyces blakesleeana*) directly by modifying enzyme activity, as well as indirectly by changing gene expression for an extended period. Evidence for the latter is that carotenoid changes persisted after several serial transfers to culture media lacking DCPTA. Gao et al. (2022) reported that foliar spraying of mung bean plants resulted in increased SOD, POD, and CAT enzyme activities within 7 days, although the mechanism for this increase was not reported.

One of the more notable trends seen from the transcriptome analysis was how BMVE treatment changes the normal temporal

trajectory of gene expression (Figure 7). For instance, expression of cytochrome P450s (*CYP86A7-2*, *CYP96E1*, *CYP76M1*) and PRX (*LOC_Os04g51300*) declines over 24 h for untreated seedlings (C0 vs. C24), while BMVE maintains these transcripts at 24 h. Similar trends were observed for other genes that are involved in ROS scavenging (*GABA-T*), development (*PSK5*), carbohydrate metabolism (*GLHL17* and *DIP3/XIP2*), and hormonal activities (*SAUR55* and *GID1L3*). In contrast, BMVE treatment greatly reduces the expression of some genes that exhibit minimal reduction over time for the control seeds. For instance, expression of the H_2O_2 promoting genes (*CDP3*, *OXO3*, and *OXO4*) declines normally as evident from the control seeds C0 vs. C24) but BMVE treatment led to a further reduction in transcript levels (Figure 7). A similar pattern was observed for the upregulated genes in all other classes where the expression normally increases over time, but even higher levels were usually observed for BMVE treated seedlings. Higher activity of antioxidants enhance plant growth by fostering their tolerance capabilities, suggesting this is an important mechanism of BMVE activity (Gill and Tuteja, 2010).

Most transcripts for stress associated genes (response to stress, abiotic/water/chemical) were reduced for BMVE treated seedlings (Figures 6, 7). For example, *RERJ1*, *bHLH148*, *NAC22*, *LEA3*, *LEA1*, and *ERF104* transcripts increased over time for control seedlings, however, the levels for B24 were lower than for C24 (Figure 7). For other stress associated genes, such as *Soul haem-binding*, *HSP101*, *LEAs*, *RAB21*, *ABCG6*, and *NCED4*, transcript level declined over time for control seeds, but the reduction was even greater for BMVE treated seedlings (Figure 7). There were exceptions to this trend. Genes associated with drought response (*MYB60*, and *LOC_Os11g03440*, another MYB60 ortholog), and abiotic stress (LOC_Os02g14680, *ABCG11*, *LOC_Os05g06140*) and biotic stress tolerance (*isoflavone reductase*, *PS1*/*OSC7*) exhibited higher transcript levels for B24 compared to C24 (Figures 6, 7). However, it should be noted that these genes could also have roles that are beneficial to growth in the absence to stress, in which case their upregulation would be consistent with the physiological data.

It might seem counterintuitive that reduction in several stress associated genes is correlated with enhanced growth. However, this may not be causal to the BMVE effect, rather, a result of BMVE treated seedlings experiencing less stress due to the enhanced antioxidant activity. Although antioxidant levels were not directly measured in this study, the BMVE mediated upregulation of genes associated with antioxidant mechanisms could explain the reduced expression of stress associated genes.

We cannot distinguish between the possibility that the BMVE-potentiated changes in transcript abundance are a direct cause of enhanced seedling growth, or whether the changes simply reflect a more advanced stage of growth at B24 versus C24. This may well be the case for several gene transcripts associated with development, chloroplast, and carbohydrate metabolism that normally increase (C0 vs. C24), but their levels are even higher for B24 (faster growing). Gao et al. (2022) observed that increased photosynthetic capacity in mung bean following foliar application of DCPTA was correlated with increased transcript levels for sucrose synthase, fructokinase, and beta-fructofuranosidase. However, whether DCPTA directly caused the increased gene expression in this case is unclear due to the 7 d delay between DCPTA application and transcript analysis.

We suspect that early changes in some genes we observed are causal for enhanced seedling growth. As mentioned earlier, ABA negatively regulates seed germination and the ABA synthesis enzyme transcript *NCED4* normally declines during germination (Figure 8) (Huo et al., 2013). Our results showed that BMVE treatment leads to an earlier repression of *NCED4* transcripts (nearly 3-fold within 2 HAT) compared to no loss for the control at 2 HAT. (2 HAT corresponds to 24 h imbibition, plus 3 h BMVE treatment, followed by 2 h further growth). By 6 HAT the control transcript level had declined to a similar level as the BMVE treatment. It seems unlikely that accelerated seedling growth was itself responsible for the BMVE mediated decline in *NCED4* transcript at 2 HAT, since rice shoot and root growth enhancement were only detectible at 48 HAT. This suggests that early hormonal changes in response to BMVE may regulate metabolic responses that then translate to faster growth. Genes associated with increased antioxidant activity following BMVE treatment may also have a causative role, as similar activity is associated with seed priming treatments that enhance germination and seedling vigor. Future studies could explore additional genes at early time points to help identify candidate causal regulatory genes in the BMVE response.

Robust seed germination and seedling growth are dependent on events that occur early in seed development on the mother plant (Lopes and Larkins, 1993; Luo and Tucker, 2001). Proper endosperm development is crucial as it provides mechanical support during early embryo growth and it is a storage site for nutrient reserves that facilitate subsequent seed germination (Lopes and Larkins, 1993). Exposure to heat stress during endosperm development alters the initiation of endosperm cellularization, impacting mature grain characteristics (Folsom et al., 2014; Chen et al., 2016; Begcy et al., 2018).

The positive association of BMVE seedling treatment with stress responses prompted us to examine its effect on seed development under heat stress. Developing seed weight showed no change between the control and BMVE treatment when the duration of HS imposed was up to 48 hours (Figure 9B). The probable reason behind the higher seed weight at 48 HS as compared to the ambient conditions could be the precocious endosperm cellularization caused by moderate heat stress (Chen et al., 2016; Begcy et al., 2018). Under the moderate heat stress used in our study cellularization of seeds begins around 48 HAF and completes by 72 HAF, respectively, whereas under ambient conditions it completes by 96 HAF (Folsom et al., 2014; Chen et al., 2016). For 96 HS, BMVE application significantly improved the developing grain weight. This suggests that BMVE might be accelerating seed development under HS conditions. Interestingly, the mature seed weight, which was not changed for 24 and 48 HS between BMVE and control treatments, showed a significant drop for the control

seeds under 96 HS. This is in line with a previous study that reported precocious cellularization under HS results in smaller seed size and reduced mature grain weight (Folsom et al., 2014). In contrast, BMVE treatment restored the mature grain weight to the ambient levels for 96 HS seeds (Figure 9). This suggests that during the comparatively longer 96 HS exposure only the control treated seeds would have gone through the precocious cellularization, and the BMVE treated seeds might have developed normally. Future evaluation of developing and mature seeds under scanning electron microscope should validate the processes related to cellularization, grain filling, and starch composition.

BMVE treatment during seed development increased grain length under both temperature treatments (Table 1). Grain width and area exhibited no change between control and BMVE treatment but were significantly lower for the control seeds developed under HS. Mohammed et al. (2013) showed that exposure to higher temperatures during the rice reproductive phase reduces the thickness of mature grains. The decline we observed for mature weight for the control seeds that developed under HS could be due to reduced grain size parameters including width and area (Figure 9B, Table 1). This showed that the BMVE treatment improves grain length in general and negates the detrimental impact of HS on the grain width and area.

Seeds that developed under 96 HS exhibited early germination (Figure 10A), probably due to altered ABA sensitivity or increased starch levels caused by exposure to non-terminal moderate HS (Begcy et al., 2018). However, despite the temperature conditions that the seeds were exposed to during the post-fertilization period, BMVE treated seeds exhibited faster germination rates as compared to control treated seeds (Figure 10). This led to significantly higher root and shoot lengths in both temperature treatment groups. For the control seedlings, the significantly higher shoot length under HS further supported the growth promoting effect of moderate HS explained by Begcy et al. (2018). Overall, the evidence suggests that irrespective of the temperature treatment, BMVE applied soon after fertilization alters metabolic activity in a way that enhances seed germination vigor in the next generation. Exploring gene expression changes in developing seeds could elucidate the mechanisms for this activity.

One caveat in our results is that, as whole panicles were sprayed with BMVE we do not know whether BMVE had a direct effect on the developing seeds. Panicles are a significant source of photosynthate, both transported and locally produced, so it is possible that the treatment affected the plant's capacity to supply resources to developing seeds. This would be in line with reports that STAs do enhance photosynthetic processes when applied to mature plants (Keithly et al., 1990a, b; Yokoyama et al., 2015; Gao et al., 2022.).

In summary, the optimized experimental conditions we developed provide convincing molecular and biological evidence that BMVE does indeed have efficacy in plant growth enhancement. Because of its laborious nature, the protocol is not suitable for large scale industrial applications, but it identifies conditions under which further exploration of the mechanism of STA activity can be explored. Increased expression of genes involved in antioxidant activity and early modification of genes associated with hormonal regulation may be key players driving accelerated seedling growth. BMVE application during early seed development also enhances germination and seedling growth in the next generation, under both ambient and HS conditions. To our knowledge this is the most comprehensive study tying gene regulatory effects to plant growth enhancement by STAs. It provides a base of new knowledge that points to avenues to further explore the molecular mechanisms of STA activity, which could lead to the development of practical applications.

Data availability statement

The original contributions presented in the study are included in the article/Supplementary Material, further inquiries can be directed to the corresponding author/s.

Author contributions

PS: Conceptualization, Formal analysis, Funding acquisition, Investigation, Methodology, Project administration, Supervision, Writing – review & editing. JSD: Data curation, Investigation, Methodology, Writing – original draft. YS: Formal analysis, Writing – review & editing. CZ: Formal analysis, Supervision, Writing – review & editing. CP: Funding acquisition, Supervision, Writing – review & editing. HW: Conceptualization, Investigation, Methodology, Supervision, Validation, Writing – review & editing.

Funding

The author(s) declare financial support was received for the research, authorship, and/or publication of this article. This research is a contribution of the University of Nebraska Agricultural Research Division, supported in part by the USDA National Institute of Food and Agriculture, Hatch project NEB 22-357. The project was generously supported by a gift from Kamterter Products, LLC, Waverly, Nebraska, USA.

Conflict of interest

Author CP was employed by the company Kamterter Products, LLC.

The remaining authors declare that the research was conducted in the absence of any commercial or financial relationships that could be construed as a potential conflict of interest.

This study received funding from Kamterter Products, LLC. The funder had the following involvement in the study: provided the chemical compound used in the study, offered unpublished

information and suggestions useful to carrying out the research, reviewed the manuscript and suggested improvements.

The author(s) declared that they were an editorial board member of Frontiers, at the time of submission. This had no impact on the peer review process and the final decision.

Publisher's note

Supplementary material

The Supplementary Material for this article can be found online at: https://www.frontiersin.org/articles/10.3389/fpls.2023.1273620/full#supplementary-material

References

Almagro, L., Gómez Ros, L. V., Belchi-Navarro, S., Bru, R., Ros Barceló, A., and Pedreño, M. A. (2009). Class III peroxidases in plant defence reactions. *J. Exp. Bot.* 60 (2), 377–390. doi: 10.1093/jxb/ern277

Anders, S., Pyl, P. T., and Huber, W. (2015). HTSeq—a Python framework to work with high-throughput sequencing data. *bioinformatics* 31 (2), 166–169. doi: 10.1093/bioinformatics/btu638

Andrews, S. (2010). *FastQC: a quality control tool for high throughput sequence data*. Available at: http://www.bioinformatics.babraham.ac.uk/projects/fastqc/.

Arshad, M. S., Farooq, M., Asch, F., Krishna, J. S. V., Prasad, P. V. V., and Siddique, K. H. M. (2017). Thermal stress impacts reproductive development and grain yield in rice. *Plant Physiol. Biochem.* 115, 57–72. doi: 10.1016/j.plaphy.2017.03.011

Ashraf, M., and Foolad, M. R. (2005). Pre-sowing seed treatment—A shotgun approach to improve germination, plant growth, and crop yield under saline and non-saline conditions. *Adv. Agron.* 88, 223–271. doi: 10.1016/S0065-2113(05)88006-X

Banerjee, S., Yuan, X., Germida, J. J., and Vujanovic, V. (2014). Gene expression patterns in wheat coleorhiza under cold- and biological stratification. *Microbiological Res.* 169 (7–8), 616–622. doi: 10.1016/J.MICRES.2013.09.016

Begcy, K., Sandhu, J., and Walia, H. (2018). Transient heat stress during early seed development primes germination and seedling establishment in rice. *Front. Plant Sci.* 9. doi: 10.3389/fpls.2018.01768

Bewley, J. D. (1997). Seed germination and dormancy. *Plant Cell* 9 (7), 1055–1066. doi: 10.1105/tpc.9.7.1055

Bewley, J. D., Bradford, K. J., Hilhorst, H. W., and Nonogaki, H. (2013). *Seeds: physiology of development and germination and dormancy, 3rd Edition.* (New York, NY: Springer), 133–181. doi: 10.1007/978-1-4614-4693-4

Bolger, A. M., Lohse, M., and Usadel, B. (2014). Trimmomatic: a flexible trimmer for Illumina sequence data. *Bioinformatics* 30 (15), 2114–2120. doi: 10.1093/bioinformatics/btu170

Bray, E. A. (1997). Plant responses to water deficit. *Trends Plant Sci.* 2 (2), 48–54. doi: 10.1016/S1360-1385(97)82562-9

Chamnanmanoontham, N., Pongprayoon, W., Pichayangkura, R., Roytrakul, S., and Chadchawan, S. (2015). Chitosan enhances rice seedling growth via gene expression network between nucleus and chloroplast. *Plant Growth Regul.* 75 (1), 101–114. doi: 10.1007/s10725-014-9935-7

Chandler, P. M., and Robertson, M. (1994). Gene expression regulated by abscisic acid and its relation to stress tolerance. *ANNU.REV.PLANT PHYSIOL.PLANT MOL.BIOL.* 45, 113–141. doi: 10.1146/annurev.pp.45.060194.000553

Chaudhury, A. M., Koltunow, A., Payne, T., Luo, M., Tucker, M. R., Dennis, E. S., et al (2001). Control of early seed development. *Annu. Rev. Cell Dev. Biol.* 17 (1), 677–699. doi: 10.1146/annurev.cellbio.17.1.677

Chen, C., Begcy, K., Liu, K., Folsom, J. J., Wang, Z., Zhang, C., et al. (2016). Heat stress yields a unique MADS box transcription factor in determining seed size and thermal sensitivity. *Plant Physiol.* 171 (1), 606–622. doi: 10.1104/pp.15.01992

Chen, D., Neumann, K., Friedel, S., Kilian, B., Chen, M., Altmann, T., et al. (2014). Dissecting the phenotypic components of crop plant growth and drought responses based on high-throughput image analysis. *Plant Cell* 26 (12), 4636–4655. doi: 10.1105/tpc.114.129601

Chiu, K. Y., Chen, C. L., and Sung, J. M. (2002). Effect of priming temperature on storability of primed sh-2 sweet corn seed. *Crop Sci.* 42 (6), 1996–2003. doi: 10.2135/cropsci2002.1996

Cho, H. T., and Kende, H. (1997). Expansins in deepwater rice internodes. *Plant Physiol.* 113 (4), 1137–1143. doi: 10.1104/pp.113.4.1137

Chomczynski, P., and Mackey, K. (1995). Short technical reports. Modification of the TRI reagent procedure for isolation of RNA from polysaccharide-and proteoglycan-rich sources. *Biotechniques* 19 (6), 942–945.

Corbineau, F. (2012). Markers of seed quality: From present to future. *Seed Sci. Res.* 22 (SUPPL. 1), S61–S68). doi: 10.1017/S0960258511000419

Dang, X., Thi, T. G. T., Dong, G., Wang, H., Edzesi, W. M., and Hong, D. (2014). Genetic diversity and association mapping of seed vigor in rice (Oryza sativa L.). *Planta* 239 (6), 1309–1319. doi: 10.1007/s00425-014-2060-z

Davies, F. S., Zalman, G. R., Stover, E., and Ciliento, S. (2004). EcoLyst application timing and juice corrected soluble solids (Brix) of processing oranges and grapefruit in florida. *HortTechnology horttech* 14 (2), 207–212. doi: 10.21273/HORTTECH.14.2.0207

Dharni, J. S., Dhatt, B. K., Paul, P., Gao, T., Awada, T., Bacher, H., et al. (2022). A non-destructive approach for measuring rice panicle-level photosynthetic responses using 3D-image reconstruction. *Plant Methods* 18 (1), 126. doi: 10.1186/s13007-022-00959-y

Dhatt, B. K., Paul, P., Sandhu, J., Hussain, W., Irvin, L., Zhu, F., et al. (2021). Allelic variation in rice Fertilization Independent Endosperm 1 contributes to grain width under high night temperature stress. *New Phytol.* 229 (1), 335–350. doi: 10.1111/nph.16897

Dietz, K.-J., Mittler, R., and Noctor, G. (2016). Recent progress in understanding the role of reactive oxygen species in plant cell signaling. *Plant Physiol.* 171 (3), 1535–1539. doi: 10.1104/pp.16.00938

Fahlgren, N., Gehan, M. A., and Baxter, I. (2015). Lights, camera, action: high-throughput plant phenotyping is ready for a close-up. *Curr. Opin. Plant Biol.* 24, 93–99. doi: 10.1016/J.PBI.2015.02.006

Finch-Savage, W. E., and Bassel, G. W. (2016). Seed vigour and crop establishment: Extending performance beyond adaptation. *J. Exp. Bot.* 67 (3), 567–591. doi: 10.1093/jxb/erv490

Folsom, J. J., Begcy, K., Hao, X., Wang, D., and Walia, H. (2014). Rice *fertilization-independent endosperm1* regulates seed size under heat stress by controlling early endosperm development. *Plant Physiol.* 165 (1), 238–248. doi: 10.1104/pp.113.232413

Fragkostefanakis, S., Simm, S., Paul, P., Bublak, D., Scharf, K. D., and Schleiff, E. (2015). Chaperone network composition in Solanum lycopersicum explored by transcriptome profiling and microarray meta-analysis. *Plant Cell Environ.* 38 (4), 693–709. doi: 10.1111/pce.12426

Fu, L., Shen, Q., Kuang, L., Wu, D., and Zhang, G. (2019). Transcriptomic and alternative splicing analyses reveal mechanisms of the difference in salt tolerance between barley and rice. *Environ. Exp. Bot.* 166, 103810. doi: 10.1016/j.envexpbot.2019.103810

Gao, Y., Zhang, X., Wang, X., Zhang, Q., Tang, H., Qiu, T., et al. (2022). Exogenous DCPTA treatment increases mung bean yield by improving carbon metabolism pathway and up-regulating photosynthetic capacity and antioxidants. *Front. Plant Sci.* 13, 796694. doi: 10.3389/fpls.2022.796694

Gausman, H. W., Quisenberry, J. E., and Yokoyama, H. (1991). Introduction to effects of plant biochemical regulators. In *Plant Biochemical Regulators*. H. W. Gausman editor. (Boca Raton, FL: CRC Press), 1–16.

Ge, S. X., Jung, D., and Yao, R. (2020). ShinyGO: a graphical gene-set enrichment tool for animals and plants. *Bioinformatics* 36 (8), 2628–2629. doi: 10.1093/bioinformatics/btz931

Gee, M. A., Hagenib, G., and Guilfoyleb, T. J. (1991). Tissue-specific and organ-specific expression of soybean auxin-responsive transcripts GH3 and SAURs. *Plant Cell* 3 (4), 419–430. doi: 10.1105/tpc.3.4.419

Gill, S. S., and Tuteja, N. (2010). Reactive oxygen species and antioxidant machinery in abiotic stress tolerance in crop plants. *Plant Physiol. Biochem.* 48 (12), 909–930. doi: 10.1016/j.plaphy.2010.08.016

Golldack, D., Li, C., Mohan, H., and Probst, N. (2013). Gibberellins and abscisic acid signal crosstalk: Living and developing under unfavorable conditions. *Plant Cell Rep.* 32 (7), 1007–1016. doi: 10.1007/s00299-013-1409-2

Guo, X., Hou, X., Fang, J., Wei, P., Xu, B., Chen, M., et al. (2013). The rice *GERMINATION DEFECTIVE 1*, encoding a B3 domain transcriptional repressor, regulates seed germination and seedling development by integrating GA and carbohydrate metabolism. *Plant J.* 75, 403–416. doi: 10.1111/tpj.12209

Guo, X., Zhi, W., Feng, Y., Zhou, G., and Zhu, G. (2022). Seed priming improved salt-stressed sorghum growth by enhancing antioxidative defense. *PloS One* 17 (2), e0263036. doi: 10.1371/journal.pone.0263036

Halmer, P. (2004). Methods to improve seed performance in the field. *Handb. Seed Physiol.*, 125–165.

Han, C., He, D., Li, M., and Yang, P. (2014). In-depth proteomic analysis of rice embryo reveals its important roles in seed germination. *Plant Cell Physiol.* 55 (10), 1826–1847. doi: 10.1093/pcp/pcu114

Han, J., Tan, J., Tu, L., and Zhang, X. (2014). A peptide hormone gene, *GhPSK* promotes fibre elongation and contributes to longer and finer cotton fibre. *Plant Biotechnol. J.* 12 (7), 861–871. doi: 10.1111/pbi.12187

Hartmann, A., Czauderna, T., Hoffmann, R., Stein, N., and Schreiber, F. (2011). HTPheno: An image analysis pipeline for high-throughput plant phenotyping. *BMC Bioinf.* 12 (1), 148. doi: 10.1186/1471-2105-12-148

Hartweck, L. M., and Olszewski, N. E. (2006). Rice GIBBERELLIN INSENSITIVE DWARF1 is a gibberellin receptor that illuminates and raises questions about GA signaling. *Plant Cell* 18 (2), 278–282. doi: 10.1105/tpc.105.039958

Hartz, T. K., Kies, L. J., Baameur, A., and May, D. M. (1995). DCPTA ineffective as a production aid on field-grown tomato and pepper. *HortScience* 30 (1), 78–79. doi: 10.21273/hortsci.30.1.78

Hattori, T., Terada, T., and Hamasuna, S. (1995). Regulation of the Osem gene by abscisic acid and the transcriptional activator VP1: analysis of cis-acting promoter elements required for regulation by abscisic acid and VP1. *Plant J.* 7 (6), 913–925. doi: 10.1046/j.1365-313X.1995.07060913.x

Hayman, E., and Yokoyama, H. (1990). Enhanced germination rates and growth of DCPTA-treated guayule seed. *HortScience* 25 (12), 1614–1615. doi: 10.21273/HORTSCI.25.12.1614

He, D., and Yang, P. (2013). Proteomics of rice seed germination. *Front. Plant Sci.* 4 (JUL). doi: 10.3389/fpls.2013.00246

Heydecker, W., and Gibbins, B. M. (1977). The 'priming' of seeds. *Symposium Seed Problems Horticulture* 83, 213–224. doi: 10.17660/ActaHortic.1978.83.29

Hong, Y., Zhang, H., Huang, L., Li, D., and Song, F. (2016). Overexpression of a stress-responsive NAC transcription factor gene ONAC022 improves drought and salt tolerance in rice. *Front. Plant Sci.* 7, 4. doi: 10.3389/fpls.2016.00004

Howell, K. A., Narsai, R., Carroll, A., Ivanova, A., Lohse, M., Usadel, B., et al. (2009). Mapping metabolic and transcript temporal switches during germination in rice highlights specific transcription factors and the role of RNA instability in the germination process. *Plant Physiol.* 149 (2), 961–980. doi: 10.1104/pp.108.129874

Hu, X., Bidney, D. L., Yalpani, N., Duvick, J. P., Crasta, O., Folkerts, O., et al. (2003). Overexpression of a gene encoding hydrogen peroxide-generating oxalate oxidase evokes defense responses in sunflower. *Plant Physiol.* 133 (1), 170–181. doi: 10.1104/pp.103.024026

Huang, R., Jiang, L., Zheng, J., Wang, T., Wang, H., Huang, Y., et al. (2013). Genetic bases of rice grain shape: So many genes, so little known. *Trends Plant Sci.* 18 (4), 218–226. doi: 10.1016/j.tplants.2012.11.001

Huo, H., Dahal, P., Kunusoth, K., McCallum, C. M., and Bradford, K. J. (2013). Expression of *9-cis-EPOXYCAROTENOID DIOXYGENASE4* is essential for thermoinhibition of lettuce seed germination but not for seed development or stress tolerance. *Plant Cell* 25 (3), 884–900. doi: 10.1105/tpc.112.108902

Hussain, S., Khan, F., Cao, W., Wu, L., and Geng, M. (2016). Seed priming alters the production and detoxification of reactive oxygen intermediates in rice seedlings grown under sub-optimal temperature and nutrient supply. *Front. Plant Sci.* 7 (APR2016). doi: 10.3389/fpls.2016.00439

Ilyas, S. (2006). Review : seed treatments using matriconditioning to improve vegetable seed quality. *Jurnal Agronomi Indonesia (Indonesian Journal of Agronomy)* 34 (2).

Jagadish, S., Craufurd, P., and Wheeler, T. (2007). High temperature stress and spikelet fertility in rice (Oryza sativa L.). *J. Exp. Bot.* 58 (7), 1627–1635. doi: 10.1093/jxb/erm003

Jain, M., Tyagi, A. K., and Khurana, J. P. (2006). Genome-wide analysis, evolutionary expansion, and expression of early auxin-responsive SAUR gene family in rice (Oryza sativa). *Genomics* 88 (3), 360–371. doi: 10.1016/j.ygeno.2006.04.008

Jiang, D., Hou, J., Gao, W., Tong, X., Li, M., Chu, X., et al. (2021). Exogenous spermidine alleviates the adverse effects of aluminum toxicity on photosystem II through improved antioxidant system and endogenous polyamine contents. *Ecotoxicology Environ. Saf.* 207, 111265. doi: 10.1016/j.ecoenv.2020.111265

Jisha, K. C., Vijayakumari, K., and Puthur, J. T. (2013). Seed priming for abiotic stress tolerance: an overview. *Acta Physiologiae Plantarum* 35 (5), 1381–1396. doi: 10.1007/s11738-012-1186-5

Jung, J., Koenig, K., Rentzea, C., and Zeeh, B. (1975). *Plant growth regulators*. Available at: https://www.google.com/patents/US3,905,798.

Keithly, J. H., Yokoyama, H., and Gausman, H. W. (1990a). Effect of 2-(3,4-dichlorophenoxy)triethylamine (DCPTA) on the growth and development of sugarbeet. *Plant Sci.* 68, 57–64. doi: 10.1016/0168-9452(90)90152-E

Keithly, J., and Yokoyama, H. (1992). Promotive effects of DCPTA on seedling development and growth of radish. *J. Am. Soc. Hortic. Sci.* 117 (2), 294–297. doi: 10.21273/JASHS.117.2.294

Keithly, J. H., Yokoyama, H., and Gausman, H. (1990b). Enhanced yield of tomato in response to 2-(3,4-dichlorophenoxy)triethylamine (DCPTA). *Plant Growth Regul.* 9 (2), 127–136. doi: 10.1007/BF00027440

Khaliq, A., Aslam, F., Matloob, A., Hussain, S., Geng, M., Wahid, A., et al. (2015). Seed priming with selenium: Consequences for emergence, seedling growth, and biochemical attributes of rice. *Biol. Trace Element Res.* 166 (2), 236–244. doi: 10.1007/s12011-015-0260-4

Kim, I. A., Kim, B. G., Kim, M., and Ahn, J. H. (2012). Characterization of hydroxycinnamoyltransferase from rice and its application for biological synthesis of hydroxycinnamoyl glycerols. *Phytochemistry* 76, 25–31. doi: 10.1016/j.phytochem.2011.12.015

Kiribuchi, K., Sugimori, M., Takeda, M., Otani, T., Okada, K., Onodera, H., et al. (2004). RERJ1, a jasmonic acid-responsive gene from rice, encodes a basic helix-loop-helix protein. *Biochem. Biophys. Res. Commun.* 325 (3), 857–863. doi: 10.1016/j.bbrc.2004.10.126

Kurek, K., Plitta-Michalak, B., and Ratajczak, E. (2019). Reactive oxygen species as potential drivers of the seed aging process. *Plants* 8 (6), 174. doi: 10.3390/plants8060174

Lara-Fioreze, A. C. C., Tomaz, C. A., Fioreze, S. L., Pilon, C., and Zanotto, M. D. (2013). Genetic diversity among progenies of Crambe abyssinica Hochst for seed traits. *Ind. Crops Products* 50, 771–775. doi: 10.1016/j.indcrop.2013.07.039

Lee, Y., Choi, D., and Kende, H. (2001). Expansins: Ever-expanding numbers and functions. *Curr. Opin. Plant Biol.* 4 (6), 527–532. doi: 10.1016/S1369-5266(00)00211-9

Li, C., Li, N., Huang, R., Chen, C., Guo, J., Yang, X., et al. (2020). A single nucleotide substitution at the 3′-end of SBPase gene involved in Calvin cycle severely affects plant growth and grain yield in rice. *BMC Plant Biol.* 20 (1), 345. doi: 10.1186/s12870-020-02541-x

Li, J., Qin, R., Xu, R., et al. (2018). Isolation and identification of five cold-inducible promoters from *Oryza sativa*. *Planta* 247, 99–111. doi: 10.1007/s00425-017-2765-x

Li, Z., and Trick, H. N. (2005). Rapid method for high-quality RNA isolation from seed endosperm containing high levels of starch. *BioTechniques* 38 (6), 872–876. doi: 10.2144/05386BM05

Li, L., Xu, X., Chen, C., and Shen, Z. (2016). Genome-wide characterization and expression analysis of the Germin-like protein family in rice and arabidopsis. *Int. J. Mol. Sci.* 17 (10). doi: 10.3390/ijms17101622

Liu, X., Cai, W. J., Yin, X., Yang, D., Dong, T., Feng, Y. Q., et al. (2020). Two SLENDER and CRINKLY LEAF dioxygenases play an essential role in rice shoot development. *J. Exp. Bot.* 71 (4), 1387–1401. doi: 10.1093/jxb/erz501

Liu, X. S., Feng, S. J., Zhang, B. Q., Wang, M. Q., Cao, H. W., Rono, J. K., et al. (2019). OsZIP1 functions as a metal efflux transporter limiting excess zinc, copper and cadmium accumulation in rice. *BMC Plant Biol.* 19 (1), 1–16. doi: 10.1186/s12870-019-1899-3

Liu, Xu, and Hou, X. (2018). Antagonistic regulation of ABA and GA in metabolism and signaling pathways. *Front. Plant Sci.* 9. doi: 10.3389/fpls.2018.00251

Liu, Xu, Hu, P., Huang, M., Tang, Y., Li, Y., Li, L., et al. (2016). The NF-YC-RGL2 module integrates GA and ABA signalling to regulate seed germination in Arabidopsis. *Nat. Commun.* 7 (1), 1–14. doi: 10.1038/ncomms12768

Livak, K. J., and Schmittgen, T. D. (2001). Analysis of relative gene expression data using real-time quantitative PCR and the 2– ΔΔCT method. *methods* 25 (4), 402–408. doi: 10.1006/meth.2001.1262

Lopes, M. A., and Larkins, B. A. (1993). Endosperm origin, development, and function. *Plant Cell* 5 (10), 1383–1399. doi: 10.1105/tpc.5.10.1383

Luo, T., Zhang, Y., Zhang, C., Nelson, M. N., Yuan, J., Guo, L., et al. (2021). Genome-Wide Association Mapping Unravels the Genetic Control of Seed Vigor under Low-Temperature Conditions in Rapeseed (Brassica napus L.). *Plants* 10 (3), 426. doi: 10.3390/plants10030426

Magneschi, L., Kudahettige, R. L., Alpi, A., and Perata, P. (2009). Expansin gene expression and anoxic coleoptile elongation in rice cultivars. *J. Plant Physiol.* 166 (14), 1576–1580. doi: 10.1016/j.jplph.2009.03.008

Marks, Z. D., Cowley, J. M., Burton, R. A., and Bianco-Miotto, T. (2022). The role of oxidative stress in seed priming to improve germination and vigour. *BioRxiv* 2022-06. doi: 10.1101/2022.06.05.494903

Matsuda, S., Funabiki, A., Furukawa, K., Komori, N., Koike, M., Tokuji, Y., et al. (2012). Genome-wide analysis and expression profiling of half-size ABC protein subgroup G in rice in response to abiotic stress and phytohormone treatments. *Mol. Genet. Genomics* 287 (10), 819–835. doi: 10.1007/s00438-012-0719-3

Mohammed, R., Cothren, J. T., and Tarpley, L. (2013). High night temperature and abscisic acid affect rice productivity through altered photosynthesis, respiration and spikelet fertility. *Crop Sci.* 53 (6), 2603–2612. doi: 10.2135/cropsci2013.01.0060

Müller, K., Tintelnot, S., and Leubner-Metzger, G. (2006). Endosperm-limited Brassicaceae Seed Germination: Abscisic Acid Inhibits Embryo-induced Endosperm Weakening of Lepidium sativum (cress) and Endosperm Rupture of Cress and Arabidopsis thaliana. *Plant Cell Physiol.* 47 (7), 864–877. doi: 10.1093/pcp/pcj059

Nahirñak, V., Rivarola, M., Almasia, N. I., Barrios Barón, M. P., Hopp, H. E., Vile, D., et al. (2019). Snakin-1 affects reactive oxygen species and ascorbic acid levels and hormone balance in potato. *PloS One* 14 (3), e0214165. doi: 10.1371/journal.pone.0214165

Ni, D. A., Wang, L. J., Ding, C. H., and Xu, Z. H. (2001). Auxin distribution and transport during embryogenesis and seed germination of Arabidopsis. *Cell Res.* 11 (4), 273–278. doi: 10.1038/sj.cr.7290096

Noctor, G., Reichheld, J.-P., and Foyer, C. H. (2018). ROS-related redox regulation and signaling in plants. *Semin. Cell Dev. Biol.* 80, 3–12. doi: 10.1016/j.semcdb.2017.07.013

Osborne, D. J. (1983). Biochemical control systems operating in the early hours of germination. *Can. J. Bot.* 61 (12), 3568–3577. doi: 10.1139/b83-406

Palli, P., Liew, C. T., Drozda, A., Mwunguzi, H., Pitla, S. K., Walia, H., et al. (2019). Robotic gantry for automated imaging, sensing, crop input application, and highthroughput analysis. In *2019 ASABE Annual International Meeting (p. 1)*. American Society of Agricultural and Biological Engineers. doi: 10.13031/aim.201901519

Pandian, B. A., Sathishraj, R., Djanaguiraman, M., Prasad, P. V. V., and Jugulam, M. (2020). Role of cytochrome P450 enzymes in plant stress response. *Antioxidants* 9 (5), 454. doi: 10.3390/antiox9050454

Panikashvili, D., Shi, J. X., Bocobza, S., Franke, R. B., Schreiber, L., and Aharoni, A. (2010). The arabidopsis DSO/ABCG11 transporter affects cutin metabolism in reproductive organs and suberin in roots. *Mol. Plant* 3 (3), 563–575. doi: 10.1093/mp/ssp103

Paul, P., Dhatt, B. K., Sandhu, J., Hussain, W., Irvin, L., Morota, G., et al. (2020). Divergent phenotypic response of rice accessions to transient heat stress during early seed development. *Plant Direct* 4 (1), e00196. doi: 10.1002/pld3.196

Peng, H., Chen, Z., Fang, Z., Zhou, J., Xia, Z., Gao, L., et al. (2015). Rice Xa21 primed genes and pathways that are critical for combating bacterial blight infection. *Sci. Rep.* 5 (1), 1–12. doi: 10.1038/srep12165

Peng, L., Sun, S., Yang, B., Zhao, J., Li, W., Huang, Z., et al. (2022). Genome-wide association study reveals that the cupin domain protein OsCDP3.10 regulates seed vigour in rice. *Plant Biotechnol. J.* 20 (3), 485–498. doi: 10.1111/pbi.13731

Qi, R., Gu, W., Zhang, J., Hao, L., and Zhang, M. (2013). Exogenous diethyl aminoethyl hexanoate enhanced growth of corn and soybean seedlings through altered photosynthesis and phytohormone. *Australian J. Crop. Sci.* 7 (13), 2021–2028. doi: 10.3316/informit.805375472242393

Rao, M. J., Xu, Y., Tang, X., Huang, Y., Liu, J., Deng, X., et al. (2020). antioxidants csCYT75B1, a citrus CYTOCHROME P450 gene, is involved in accumulation of antioxidant flavonoids and induces drought tolerance in transgenic arabidopsis. *Mdpi.Com* 9 (2), 161. doi: 10.3390/antiox9020161

Ren, H., and Gray, W. M. (2015). SAUR proteins as effectors of hormonal and environmental signals in plant growth. *Mol. Plant* 8 (8), 1153–1164. doi: 10.1016/j.molp.2015.05.003

Rhaman, M. S., Rauf, F., Tania, S. S., Karim, M. M., Sagar, A., Robin, A. H. K., et al. (2021). Seed priming and exogenous application of salicylic acid enhance growth and productivity of okra (Abelmoschus esculentus L.) by regulating photosynthetic attributes. *J. Exp. Biol. Agric. Sci.* 9 (6), 759–769. doi: 10.18006/2021.9(6).759.769

Robinson, M. D., McCarthy, D. J., and Smyth, G. K. (2010). edgeR: a Bioconductor package for differential expression analysis of digital gene expression data. *Bioinformatics* 26 (1), 139–140. doi: 10.1093/bioinformatics/btp616

Seo, J.-S., Joo, J., Kim, M.-J., Kim, Y.-K., Nahm, B. H., Song, S. I., et al. (2011). OsbHLH148, a basic helix-loop-helix protein, interacts with OsJAZ proteins in a jasmonate signaling pathway leading to drought tolerance in rice. *Plant J.* 65 (6), 907–921. doi: 10.1111/j.1365-313X.2010.04477.x

Seo, M., Nambara, E., Choi, G., and Yamaguchi, S. (2009). Interaction of light and hormone signals in germinating seeds. *Plant Mol. Biol.* 69 (4), 463–472. doi: 10.1007/s11103-008-9429-y

Shinozaki, K. (2000). Molecular responses to dehydration and low temperature: differences and cross-talk between two stress signaling pathways. *Curr. Opin. Plant Biol.* 3 (3), 217–223. doi: 10.1016/S1369-5266(00)80068-0

Singh, J. (2018) *Biological Activity of a Tertiary Amine Plant Growth Regulator, BMVE, in Arabidopsis thaliana and Wheat (Triticum Aestivum)*. Available at: https://digitalcommons.unl.edu/agronhortdiss/153/.

Steinbrecher, T., and Leubner-Metzger, G. (2017). The biomechanics of seed germination. *J. Exp. Bot.* 68 (4), 765–783. doi: 10.1093/jxb/erw428

Sun, M., Tuan, P. A., Izydorczyk, M. S., and Ayele, B. T. (2020). Ethylene regulates post-germination seedling growth in wheat through spatial and temporal modulation of ABA/GA balance. *J. Exp. Bot.* 71 (6), 1985–2004. doi: 10.1093/jxb/erz566

Tan, Y. F., Xing, Y. Z., Li, J. X., Yu, S. B., Xu, C. G., and Zhang, Q. (2000). Genetic bases of appearance quality of rice grains in Shanyou 63, an elite rice hybrid. *Theor. Appl. Genet.* 101 (5–6), 823–829. doi: 10.1007/s001220051549

Tarquis, A. M., and Bradford, K. J. (1992). Prehydration and priming treatments that advance germination also increase the rate of deterioration of lettuce seeds. *J. Exp. Bot.* 43 (3), 307–317. doi: 10.1093/jxb/43.3.307

Thakur, N., and Vasudevan, S. N. (2019). Role of enzymatic antioxidants in seed science and technology: A review. *~ 3503 ~ J. Pharmacognosy Phytochem.* 8 (4), 3503–3507.

Thamil Arasan, S. K., Park, J. I., Ahmed, N. U., Jung, H. J., Hur, Y., Kang, K. K., et al. (2013). Characterization and expression analysis of dirigent family genes related to stresses in Brassica. *Plant Physiol. Biochem.* 67, 144–153. doi: 10.1016/j.plaphy.2013.02.030

Thimmappa, R., Geisler, K., Louveau, T., O'Maille, P., and Osbourn, A. (2014). Triterpene biosynthesis in plants. *Annu. Rev. Plant Biol.* 65, 225–257. doi: 10.1146/annurev-arplant-050312-120229

Trapnell, C., Pachter, L., and Salzberg, S. L. (2009). TopHat: discovering splice junctions with RNA-Seq. *Bioinformatics* 25 (9), 1105–1111. doi: 10.1093/bioinformatics/btp120

Ueda, Y., Siddique, S., and Frei, M. (2015). A novel gene, OZONE-RESPONSIVE APOPLASTIC PROTEIN1, enhances cell death in ozone stress in rice. *Plant Physiol.* 169 (1), 873–889. doi: 10.1104/pp.15.00956

Van Pelt, R. (2007). Substituted tertiary amine plant bioregulators affect yield and pigment content of paprika. *J. Vegetable Sci.* 12 (3), 63–71. doi: 10.1300/J484v12n03_06

Verma, G., Dhar, Y. V., Srivastava, D., Kidwai, M., Chauhan, P. S., Bag, S. K., et al. (2017). Genome-wide analysis of rice dehydrin gene family: Its evolutionary conservedness and expression pattern in response to PEG induced dehydration stress. *PLoS One* 12 (5), e0176399. doi: 10.1371/journal.pone.0176399

Wang, Y., Gu, W., Xie, T., Li, L., Sun, Y., Zhang, H., et al. (2016). Mixed compound of DCPTA and CCC increases maize yield by improving plant morphology and up-regulating photosynthetic capacity and antioxidants. *PLoS One* 11 (2), e0149404. doi: 10.1371/journal.pone.0149404

Wang, Z. Q., Xu, X. Y., Gong, Q. Q., Xie, C., Fan, W., Yang, J. L., et al. (2014). Root proteome of rice studied by iTRAQ provides integrated insight into aluminum stress tolerance mechanisms in plants. *J. Proteomics* 98, 189–205. doi: 10.1016/j.jprot.2013.12.023

Wang, X. S., Zhu, H. B., Jin, G. L., Liu, H. L., Wu, W. R., and Zhu, J. (2007). Genome-scale identification and analysis of LEA genes in rice (Oryza sativa L.). *Plant Sci.* 172 (2), 414–420. doi: 10.1016/j.plantsci.2006.10.004

Warner, R. M., and Erwin, J. E. (2005). Naturally occurring variation in high temperature induced floral bud abortion across Arabidopsis thaliana accessions. *Plant Cell Environ.* 28 (10), 1255–1266. doi: 10.1111/j.1365-3040.2005.01361.x

Wu, C., Zhou, S., Zhang, Q., Zhao, W., and Peng, Y. (2006). Molecular cloning and differential expression of an γ-aminobutyrate transaminase gene, OsGABA-T, in rice (Oryza sativa) leaves infected with blast fungus. *J. Plant Res.* 119 (6), 663–669. doi: 10.1007/s10265-006-0018-3

Xie, T., Gu, W., Meng, Y., Li, J., Li, L., Wang, Y., et al. (2017). Exogenous DCPTA ameliorates simulated drought conditions by improving the growth and photosynthetic capacity of maize seedlings. *Sci. Rep.* 7 (1), 12684. doi: 10.1038/s41598-017-12977-1

Xu, S., Hu, J., Li, Y., Ma, W., Zheng, Y., and Zhu, S. (2011). Chilling tolerance in Nicotiana tabacum induced by seed priming with putrescine. *Plant Growth Regul.* 63 (3), 279–290. doi: 10.1007/s10725-010-9528-z

Xue, Z., Tan, Z., Huang, A., Zhou, Y., Sun, J., Wang, X., et al. (2018). Identification of key amino acid residues determining product specificity of 2,3-oxidosqualene cyclase in Oryza species. *New Phytol.* 218 (3), 1076–1088. doi: 10.1111/nph.15080

Yan, M. (2015). Seed priming stimulate germination and early seedling growth of Chinese cabbage under drought stress. *South Afr. J. Bot.* 99, 88–92. doi: 10.1016/J.SAJB.2015.03.195

Yang, P., Li, X., Wang, X., Chen, H., Chen, F., and Shen, S. (2007). Proteomic analysis of rice (Oryza sativa) seeds during germination. *Proteomics* 7 (18), 3358–3368. doi: 10.1002/pmic.200700207

Yang, G., Nakamura, H., Ichikawa, H., Kitano, H., and Komatsu, S. (2006). OsBLE3, a brassinolide-enhanced gene, is involved in the growth of rice. *Phytochemistry* 67 (14), 1442–1454. doi: 10.1016/j.phytochem.2006.05.026

Ye, H., Du, H., Tang, N., Li, X., and Xiong, L. (2009). Identification and expression profiling analysis of TIFY family genes involved in stress and phytohormone responses in rice. *Plant Mol. Biol.* 71 (3), 291–305. doi: 10.1007/s11103-009-9524-8

Yokoyama, H., Chan, J. H., Oyama, P. S., Hov, L. J., Petersen, C. L., Vu, D., et al. (2015). *Signaling compositions, methods, and systems for effecting plant burndown and herbicide enhancement*. U.S. Patent No. 8,999,890. (Washington, DC: U.S. Patent and Trademark Office). Available at: https://www.google.com/patents/US8999890.

Yokoyama, H., and Keithly, J. H. (1991). Service, US department of agriculture, pasadena, california. *Plant Biochem. Regulators* 21, 19.

You, J., Zong, W., Hu, H., Li, X., Xiao, J., and Xiong, L. (2014). A STRESS-RESPONSIVE NAC1-regulated protein phosphatase gene rice *protein phosphatase18* modulates drought and oxidative stress tolerance through abscisic acid-independent reactive oxygen species scavenging in rice. *Plant Physiol.* 166 (4), 2100–2114. doi: 10.1104/pp.114.251116

Zhang, C., Zhang, J., Liu, H., Qu, X., Wang, J., He, Q., et al. (2022). Transcriptomic analysis reveals the role of FOUR LIPS in response to salt stress in rice. *Plant Mol. Biol.* 110 (1-2), 37–52. doi: 10.1007/s11103-022-01282-9

Zhao, Z., and Moghadasian, M. H. (2010). Bioavailability of hydroxycinnamates: A brief review of in *vivo* and in *vitro* studies. *Phytochem. Rev.* 9 (1), 133–145. doi: 10.1007/s11101-009-9145-5

Zheng, M., Tao, Y., Hussain, S., Jiang, Q., Peng, S., Huang, J., et al. (2016). Seed priming in dry direct-seeded rice: consequences for emergence, seedling growth and associated metabolic events under drought stress. *Plant Growth Regul.* 78 (2), 167–178. doi: 10.1007/s10725-015-0083-5

Zhou, G. K., Xu, Y. F., and Liu, J. Y. (2005). Characterization of a rice class II metallothionein gene: Tissue expression patterns and induction in response to abiotic factors. *J. Plant Physiol.* 162 (6), 686–696. doi: 10.1016/j.jplph.2004.11.006

Zhu, F., Paul, P., Hussain, W., Wallman, K., Dhatt, B. K., Sandhu, J., et al. (2021a). SeedExtractor: an open-source GUI for seed image analysis. *Front. Plant Sci.* 11. doi: 10.3389/fpls.2020.581546

Zhu, F., Saluja, M., Dharni, J. S., Paul, P., Sattler, S. E., Staswick, P., et al. (2021b). PhenoImage : An open-source graphical user interface for plant image analysis. *Plant Phenome J.* 4 (1), e20015. doi: 10.1002/ppj2.20015

Zinsmeister, J., Leprince, O., and Buitink, J. (2020). Molecular and environmental factors regulating seed longevity. *Biochem. J.* 477 (2), 305–323. doi: 10.1042/BCJ20190165

frontiers | Frontiers in Plant Science

TYPE Original Research
PUBLISHED 02 February 2024
DOI 10.3389/fpls.2024.1336689

Check for updates

OPEN ACCESS

EDITED BY
Muhammad Awais Farooq,
Hebei Agricultural University, China

REVIEWED BY
Xianhai Zhao,
Brookhaven National Laboratory (DOE),
United States
Raquel Iglesias Fernández,
Polytechnic University of Madrid, Spain

*CORRESPONDENCE
Aying Zhang
ayzhang@njau.edu.cn

RECEIVED 11 November 2023
ACCEPTED 18 January 2024
PUBLISHED 02 February 2024

CITATION
Xiang Y, Zhao C, Li Q, Niu Y, Pan Y, Li G, Cheng Y and Zhang A (2024) Pectin methylesterase 31 is transcriptionally repressed by ABI5 to negatively regulate ABA-mediated inhibition of seed germination. *Front. Plant Sci.* 15:1336689.
doi: 10.3389/fpls.2024.1336689

Pectin methylesterase 31 is transcriptionally repressed by ABI5 to negatively regulate ABA-mediated inhibition of seed germination

Yang Xiang[1], Chongyang Zhao[1], Qian Li[1], Yingxue Niu[1], Yitian Pan[1], Guangdong Li[1], Yuan Cheng[1] and Aying Zhang[1,2]*

[1]College of Life Sciences, State Key Laboratory of Crop Genetics & Germplasm Enhancement and Utilization, Nanjing Agricultural University, Nanjing, China, [2]Sanya Institute of Nanjing Agricultural University, Nanjing Agricultural University, Sanya, China

Pectin methylesterase (PME), a family of enzymes that catalyze the demethylation of pectin, influences seed germination. Phytohormone abscisic acid (ABA) inhibits seed germination. However, little is known about the function of PMEs in response to ABA-mediated seed germination. In this study, we found the role of *PME31* in response to ABA-mediated inhibition of seed germination. The expression of *PME31* is prominent in the embryo and is repressed by ABA treatment. Phenotype analysis showed that disruption of *PME31* increases ABA-mediated inhibition of seed germination, whereas overexpression of *PME31* attenuates this effect. Further study found that ABI5, an ABA signaling bZIP transcription factor, is identified as an upstream regulator of PME31. Genetic analysis showed that PME31 functions downstream of ABI5 in ABA-mediated seed germination. Detailed studies showed that ABI5 directly binds to the *PME31* promoter and inhibits its expression. In the plants, *PME31* expression is reduced by ABI5 in ABA-mediated seed germination. Taken together, *PME31* is transcriptionally inhibited by ABI5 and negatively regulates ABA-mediated seed germination inhibition. These findings shed new light on the mechanisms of PMEs in response to ABA-mediated seed germination.

KEYWORDS
abscisic acid, seed germination, PME31, ABI5, transcription repression

Introduction

Seed germination is a vital step in plant growth and development and impacts the crop yield. The timing and rate of seed germination are controlled by a variety of internal and external factors (Graeber et al., 2012; Mei et al., 2023). Abscisic acid (ABA) and gibberellin acid (GA) are the primary internal factors that regulate the transition from dormancy to germination (Singh and Datta, 2023). ABA promotes seed dormancy and represses seed germination. GA is essential for the release of dormancy and for the initiation of germination. They antagonistically modulate seed germination, which is at least in part regulated by the balance and sensitivity to ABA and GA (Shu et al., 2013; Loades et al., 2023). In adverse environmental conditions, such as drought, high salinity, and extreme temperatures, ABA dominates the dormant state. The mechanisms of ABA-mediated seed germination inhibition have been investigated (Graeber et al., 2012; Tuan et al., 2018; Sharma et al., 2023). For instance, ABA reduces the water potential on the seed surface and water uptake to hinder seed germination (Berry and Bewley, 1992; Grainge et al., 2022). ABA also represses cell division and regulates the ion transport of seeds in seed germination (Liu et al., 2022). Besides, ABA modulates gene expression and regulates the activity of enzymes, such as amylases and protein kinases, to control seed germination (Xue et al., 2021; Li et al., 2022; Loades et al., 2023).

ABA initiates the cell response by activating downstream signaling genes. Several components have been identified in ABA signaling pathway, including PYRABACTIN RESISTANCE (PYR1)/PYR1-LIKE (PYL)/REGULATORY COMPONENT OF ABSCISIC ACID RECEPTOR (RCAR), SNF1-related protein kinase 2s (SnRK2s), protein phosphatases 2C (PP2Cs), ABSCISIC ACID INSENSITIVE3 (ABI3), ABSCISIC ACID INSENSITIVE4 (ABI4), and ABSCISIC ACID INSENSITIVE5 (ABI5) (Yan et al., 2020; Zhao et al., 2020). Among these, bZIP transcription factor ABI5 performs a crucial part in ABA-mediated seed germination (Lopez-Molina et al., 2001; Liu and Stone, 2010; Rushton et al., 2012; Nie et al., 2022). The *abi5* mutants showed insensitivity to ABA in seed germination, while *ABI5* overexpressors exhibited hypersensitivity (Lopez-Molina et al., 2001), suggesting that ABI5 positively regulated ABA-mediated seed germination inhibition. Studies showed that ABI5 directly regulated downstream target genes by binding to the G-box (ACGT) motif (Bi et al., 2017; Zhao et al., 2020). Bi et al. (2017) discovered that ABI5 was bound to the G-box of *CAT1* promoter and activated *CAT1* expression during seed germination. ABI5 also modulated the expression of ABA receptor genes (*PYL11* and *PYL12*) by directly binding to their promoters in ABA-mediated seed germination (Zhao et al., 2020). A key negative regulator of GA signaling DELLA protein RGL2 was directly bound to the *ABI5* promoter to promote its expression (Liu et al., 2016). Furthermore, ABI5 interacted with AFP, KEG, and MIEL1 in regulating seed germination (Liu and Stone, 2010; Nie et al., 2022). These studies demonstrated that ABI5 modulated seed germination in various manner.

Pectin methylesterase (PME) catalyzes the demethylation of pectin and alters cell wall structure and characteristics. The *PME* gene family is a large and diverse group with at least 66 members in *Arabidopsis thaliana* (Weber et al., 2013). Approximately 75% of Arabidopsis *PME* genes had tissue- and stress-specific expression profiles. The *PME* expression pattern showed the diversity of their involvement in cell wall modification throughout the development as well as stress responses (Pelloux et al., 2007; Huang et al., 2017). *PMEs* influence plant growth and development by changing the biomechanical features of the cell wall (Hongo et al., 2012; Zúñiga-Sánchez et al., 2014; Huang et al., 2017; Zhang et al., 2023). For instance, *PME35* reduced the degree of methylation in pectin and affected the mechanical characteristics of the stem cell wall (Hongo et al., 2012). Mutation of *PME3* influenced cell wall structure and zinc ion absorption (Weber et al., 2013). *PMEs* also play an important role in response to abiotic stresses. *PME34* improved plant heat tolerance by promoting stomatal opening, and increased water evaporation and temperature regulation capabilities under high-temperature conditions (Huang et al., 2017). *PME31* positively regulated salt stress tolerance (Yan et al., 2018). Brassinosteroids (BRs) modulated total PME activity in Arabidopsis by regulating *PME41* expression under chilling stress (Qu et al., 2011). Seed germination is intimately connected to the degree of pectin methylesterification. The demethylesterification of pectin promoted seed coat rupture and endosperm release (Müller et al., 2013). Zúñiga-Sánchez et al. (2014) found that the DUF642 gene *BIIDXI* improved PME activity to enhance Arabidopsis seed germination performance. In addition, PME activity was inhibited when garden cress seeds were treated with ABA (Scheler et al., 2015), indicating that ABA influenced PME activity in seed germination. However, the role of ABA and *PME* genes in seed germination is still unknown.

Here, we showed the role of PME31 in ABA-mediated seed germination inhibition. *PME31* negatively modulated ABA-mediated seed germination inhibition. We further identified the upstream regulator of *PME31*, an ABA-signaling bZIP transcription factor ABI5. We found that *PME31* expression was inhibited by ABI5 in ABA-mediated seed germination. Our findings shed light on the mechanisms of PMEs in response to ABA-mediated seed germination.

Materials and methods

Plant material and growth conditions

The Arabidopsis Biological Resource Center (ABRC) provided *Arabidopsis thaliana* L. Heynh. Ecotype Columbia (Col-0), Landsberg *erecta* (Ler-0), *pme31-1* (SALK_074820), *pme31-2* (CS25163), *abi3-1* (CS24), *abi4-1* (CS8104) and *abi5-1* (CS8105). The *abi5-1 pme31-1* double mutant was created through a genetic cross between *pme31-1* and *abi5-1*. The identified primers were listed in Supplementary Table S1. Seeds were planted in 1/2 MS medium and grew in a light incubator at 22°C/20°C (day/night), with a photoperiod of 16 h/8 h (day/night) and photosynthetic active radiation of 200 μmol m^{-2} s^{-1}. Seeds were stratified at 4°C in darkness for various times (0, 12, 24, 36, 48 h) to detect *PME31* gene expression in seed germination. Samples were collected and promptly preserved in liquid nitrogen for analysis.

Generation of transgenic plants

To generate *PME31*-overexpressing plants, the coding sequence of *PME31* with specific primers (Supplementary Table S1) was amplified and inserted into the pEarleyGate 101 vector from Earley et al. (2006). To investigate *PME31* tissue-specific expression, the *PME31* promoter sequence (2142 bp) was cloned into the pMD19-T vector (Takara, Japan) and inserted into the pGWB3 vector from Nakagawa et al. (2007) (Supplementary Table S1). The reporter *GUS* gene was driven by the *PME31* promoter (*proPME31:GUS*). The recombinant vectors were transformed into *Agrobacterium tumefaciens* strain GV3101. Transgenic plants were created by floral dip transformation (Clough and Bent, 1998). Positive plants were screened on 1/2 MS medium with 50 μg mL^{-1} Basta. Homozygous T3 transgenic plants were selected and collected for further analysis. *ABI5* overexpressors were obtained from the Arashare platform. *ABI5* was overexpressed by a β-estradiol-inducible promoter (Coego et al., 2014). *ABI4* overexpressor was obtained from Yan et al. (2020).

Histochemical staining for β-glucuronidase (GUS) activity

The peeled seeds, rosette leaves, and roots of the *proPME31:GUS* transgenic plants were placed in GUS staining solution (10 mg mL X-Gluc, 0.1 M Na_2HPO_4-NaH_2PO_4 pH 7.0, 0.1% Triton X-100, 8 mM β-mercaptoethanol, 0.5 mM $K_3[Fe(CN)_6]$, 0.5 mM $K_4[Fe(CN)_6]$) and vacuum-infiltrated for 30 min. The samples were stained at 37°C overnight and decolorized with 75% ethanol. The images were taken using a stereomicroscope (Optec SZ680, China).

Real-time quantitative PCR (RT-qPCR) analyses

Total RNA was extracted from plant materials using TRIzol Reagent (CoWin Biotech, China). RNAs were then reverse-transcribed into cDNA by the 5×All-In-One MasterMix Kit (Abm Inc., China). The cDNA was amplified using the CFX96 Touch Real-Time PCR System (Bio-Rad, USA). The reaction system was 20 μL, containing 10μL AceQ qPCR SYBR Green Master Mix (Vazyme, China), 1.0 μL of each primer, 100 ng cDNA. The amplification conditions were as follows: 95 ° for 10 min; 95 ° for 15 s; 60 ° for 1 min, 40 Cycles. The internal reference was *Actin2*. The details of the specific primers were listed in Supplementary Table S1. The relative expression of each gene was calculated using the $2^{-\Delta\Delta Ct}$ method (Livak and Schmittgen, 2001).

Determination of PME activity

PME activity was determined using a PME activity assay kit (Thermo Fisher Scientific, USA). Samples were extracted from seeds with PBS buffer (0.01 M, pH7.4). The protein samples were centrifuged at 12,000g for 20 min and collected supernatants. Protein concentration was measured by Bradford assays (Bradford, 1976). Samples were measured according to the manufacturer's instructions. After the reaction, the absorbance value was measured at 450nm. The PME activity was calculated using the standard curve.

Assays for seed germination and cotyledon greening

Assays for seed germination and cotyledon greening were performed as previously described (Yan et al., 2020). Each transgenic plant had more than 100 seeds collected simultaneously. After sterilization, seeds were sown on 1/2 MS medium either with or without 0.5 μM ABA. Once the radicle had emerged from the testa, the seed germination rate was recorded every 12 h. After 72 h, the cotyledon greening rate was measured. To investigate PME31 in response to ABA at the seedling stage, five-day-old seedlings were transferred to 1/2 MS medium with or without 10 μM ABA and then kept in an incubator under normal conditions for 14 d. Time to 50% germination and the percentage of maximum germination were recorded.

Yeast-one-hybrid assays (Y1H)

Y1H assays were performed as previously described (Zhou et al., 2020; Xiang et al., 2021a). The pLacZi-proPME31 and pB42AD-ABI5 constructs were transformed into yeast strain EGY48. Transformants were screened on SD/−Trp−Ura plates and cultured in SD/−Trp−Ura/Gal/Raf/X-Gal (80 μg mL^{-1}) plates for color development. The β-galactosidase activity was detected using a β-Galactosidase Assay Kit (Beyotime, Shanghai, China). The β-galactosidase activity was calculated as previously described (Xiang et al., 2021a). The pLacZi and pB42AD vectors were used as the negative control.

Electrophoretic mobility shift assays (EMSA)

EMSA was performed as previously described (Xiang et al., 2021b). The coding sequence of *ABI5* was inserted into the pET-30a vector (Novagen, USA). His-ABI5 proteins were expressed in *Escherichia coli* Rosetta (DE3) for 6 h at 24°C following being induced with 0.5 mM isopropyl-1-thio-β-D-galactopyranoside (IPTG). The recombined proteins were purified using the MagnetHis™ protein purification system (Promega, USA) and eluted with elution buffer (100 mM HEPES, 500 mM imidazole, pH7.5). The probe contained the ttaCACGTag sequence (−945 to −954 bp) and was labeled using an EMSA Probe Biotin Labeling Kit (Beyotime, Shanghai, China). EMSAs were performed using a Chemiluminescent EMSA Kit (Beyotime, Shanghai, China). The unlabeled probe (Comp) and the mutated probe (mComp) were used as competitors (Supplementary Table S1).

Luciferase assays

The *PME31* promoter was inserted into the p1381-LUC vector from Xiang et al. (2021a) (Supplementary Table S1). The coding sequence of *ABI5* was recombined into the pCAMBIA1300-221-3×flag vector (generated by insertion of a *35S* promoter and a Flag tag into the pCAMBIA1300 vector) from Xiang et al. (2021a) (Supplementary Table S1). The recombinant plasmids were transformed into *Agrobacterium tumefaciens* strain GV3101. The *proPME31:LUC-35S:REN* reporter was infiltrated into tobacco (*Nicotiana benthamiana*) leaves. After infiltration for 72 h, the LUC signals were imaged using a Tanon 5200 multi-chemiluminescent imaging system (Tanon, China). The tobacco leaves were collected and frozen in liquid nitrogen. The luciferase activities were detected using a Dual Luciferase Reporter Gene Assay Kit (Yeasen, Shanghai, China). The LUC/REN ratio was used to calculate the relative promoter activity.

Accession numbers

The genes in this study have the following IDs: *PME31*, AT3G29090; *ABI5*, AT2G36270; *Actin2*, AT3G18780; *ABI3*, AT3G24650; *ABI4*, AT2G40220.

Results

The expression pattern of *PME31* during seed germination

To investigate the tissue-specific expression of *PME31*, transgenic plants with *PME31* promoter-driven GUS reporters were generated. Different tissues from various development stages were collected and stained by GUS histochemical staining. The peeled seeds were obtained from Arabidopsis seed at 12 h imbibition. The Arabidopsis seed embryo exhibited a blue color. When Arabidopsis grew to 10 days old, the rosette leaves and roots were stained by GUS and showed that the leaf vasculature and primary root displayed a blue color (Figure 1A). The results suggested *PME31* was expressed in embryo, leaf vasculature, and primary root in Arabidopsis.

We next determined the expression pattern of *PME31* during seed germination. After imbibition, the *PME31* expression had a significant accumulation at 12 h imbibition and then decreased at 36 h and 48 h imbibition compared with dry seeds (Figure 1B). It suggested that *PME31* have an impact on seed germination. Previous studies showed that seed germination is tightly controlled by ABA (Zhao et al., 2020). To investigate whether *PME31* is involved in ABA-mediated seed germination, seeds were treated with ABA. The *PME31* expression decreased in ABA treatment for 12 h and was maintained until 48 h. The results showed that *PME31* expression was downregulated under ABA treatment (Figure 1C).

Disruption of *PME31* promotes ABA-mediated inhibition of seed germination

To investigate whether *PME31* is involved in ABA-mediated seed germination, we screened two *pme31* mutants by PCR identification. The insertion site of the *pme31-1* mutant was in exon, while that of the *pme31-2* mutant was in 5'-UTR. RT-qPCR analysis showed that the expression of *PME31* decreased in the *pme31-2* mutant (Supplementary Figure S1). Thus, *PME31* was knocked out in the *pme31-1* mutant and knocked down in the *pme31-2* mutant. Under normal conditions, the *pme31-1* and *pme31-2* mutants had similar cotyledon greening rates and germination rates compared with the Col-0. However, the cotyledon greening rate and germination rate of *pme31-1* and *pme31-2* mutants were significantly lower than that of Col-0 under ABA treatment (Figures 2A–C). Moreover, the time to 50% germination of *pme31-1* and *pme31-2* mutants was higher compared with the Col-0 under ABA treatment (Figure 2D). The percentage of maximum germination had no significant difference in the Col-0, *pme31-1*, and *pme31-2* mutants (Figure 2E). The results suggested that disruption of *PME31* increased sensitivity to ABA during seed germination.

To further test whether *PME31* respond to ABA in the seedling stage, five-day-old seedlings were treated with ABA. Under normal conditions, the growth phenotype of *pme31-1* and *pme31-2* seedlings was not significantly different from Col-0. When supplemented with 10 μM ABA, there was also no significant difference in Col-0, *pme31-1*, and *pme31-2* seedlings (Figures 2F, G), indicating that the *PME31* mutation did not affect sensitivity to ABA in Arabidopsis seedlings. The above results suggested that disruption of *PME31* improves ABA-mediated inhibition of seed germination.

Overexpression of *PME31* attenuates ABA-mediated inhibition of seed germination

To further elucidate the role of *PME31* in ABA-mediated seed germination, we created transgenic plants overexpressing *PME31* under the control of the *35S* promoter (Supplementary Figure S2A). RT-qPCR analysis showed that transgenic plants overexpressing *PME31* (OE-*PME31*#3 and OE-*PME31*#4) had higher *PME31* expression (Supplementary Figure S2B). Under normal conditions, *PME31* overexpressors showed a similar cotyledon greening rate and germination rate as Col-0. Under ABA treatment conditions, the cotyledon greening rate and germination rate in *PME31* overexpressors were significantly higher than that in Col-0 (Figures 3A–C). The time to 50% germination of *PME31* overexpressors was lower compared with the Col-0 under ABA treatment (Figure 2D). The percentage of maximum germination had no significant difference in the Col-0 and *PME31* overexpressors (Figure 2E). It indicated that *PME31* overexpression reduced ABA-mediated inhibition of seed germination.

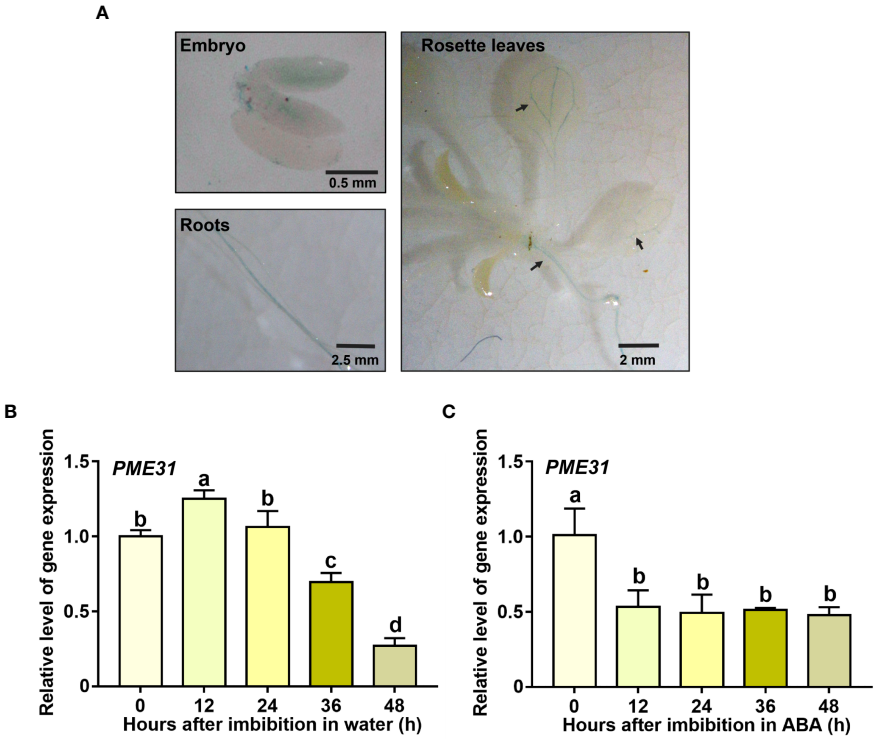

FIGURE 1
The expression pattern of *PME31* in different tissue and seed germination. **(A)** Tissue-specific expression analysis of *PME31* using GUS histochemical staining. The peeled seeds were obtained from Arabidopsis seed at 12 h imbibition. The rosette leaves and roots were obtained from 10-day-old Arabidopsis seedlings on 1/2 MS medium. The tissues were stained in GUS staining solution and vacuum-infiltrated for 30 min. The samples were stained at 37°C overnight and decolorized with 75% ethanol. The images were taken. **(B)** The expression of *PME31* during seed germination. Seeds were imbibed at 25°C in darkness for various times (0, 12, 24, 36, 48 d). **(C)** The expression of *PME31* in the presence of ABA during seed germination. Seeds were imbibed at 25°C in darkness and treated with 0.5 μM ABA. The gene expression of *PME31* was determined using RT-qPCR. *Actin2* was used as the internal reference. Data are means (± SD) of three biological replicates. Different letters indicate significant differences at $P < 0.05$ according to two-way ANOVA (Tukey's multiple comparison test).

We then investigated the effect of *PME31* overexpression on Arabidopsis seedlings treated with ABA. Under normal conditions, the primary root length of OE-*PME31*#3 and OE-*PME31*#4 was similar to that of Col-0, but with the addition of 10 μM ABA, the primary root length of OE-*PME31*#3 and OE-*PME31*#4 was longer than that of the Col-0 (Figures 3F, G). Those results showed that *PME31* overexpression reduces ABA-mediated inhibition of seed germination.

ABI5 directly binds to the *PME31* promoter and inhibits its expression

To identify upstream regulators of PME31, the *PME31* promoter was used as bait in a yeast-one-hybrid (Y1H) screen. The results showed that a bZIP transcription factor ABI5 was identified. ABI5 plays a vital role in seed germination, early seedling growth, and abiotic stresses in the presence of ABA (Skubacz et al., 2016). To investigate whether *PME31* was regulated by other ABI transcription factors, we analyzed the *PME31* expression in seeds of *abi3-1*, *abi4-1* mutants, and *ABI4* overexpressor and found that the *PME31* expression had no significant difference in those mutants (Supplementary Figure S4).

We then performed Y1H assays to test if ABI5 directly binds to the *PME31* promoter. As shown in Figure 4A, the color turned blue in EGY48 yeast cells transformed with pB42AD-ABI5 and pLacZi-proPME31 constructs, but not in yeast cells with other constructs. β-Galactosidase assays showed that yeast cells transformed with pB42AD-ABI5 and pLacZi-proPME31 had higher β-galactosidase activity compared with yeast cells transformed with other constructs (Figure 4B), suggesting that ABI5 directly binds to the *PME31* promoter.

We next search ABI5 binding elements in the promoters of *PME31* by using the Plant Promoter Analysis Navigator (PlantPAN; http://PlantPAN2.itps.ncku.edu.tw) (Chow et al., 2016) and found that the putative binding sequence TTACACGTAG located in −945 to −954 bp. We performed EMSAs to verify whether ABI5 directly binds to the TTACACGTAG sequence of the *PME31* promoter. The 50-bp oligonucleotide containing the TTACACGTAG sequence (−945 to −954 bp) was synthesized and labeled as a probe. When the His-ABI5 protein was incubated with the labeled probe, the protein-DNA complex with a slower migration speed was observed. When the His-ABI5 protein was incubated with the unlabeled probe, the protein-DNA binding was

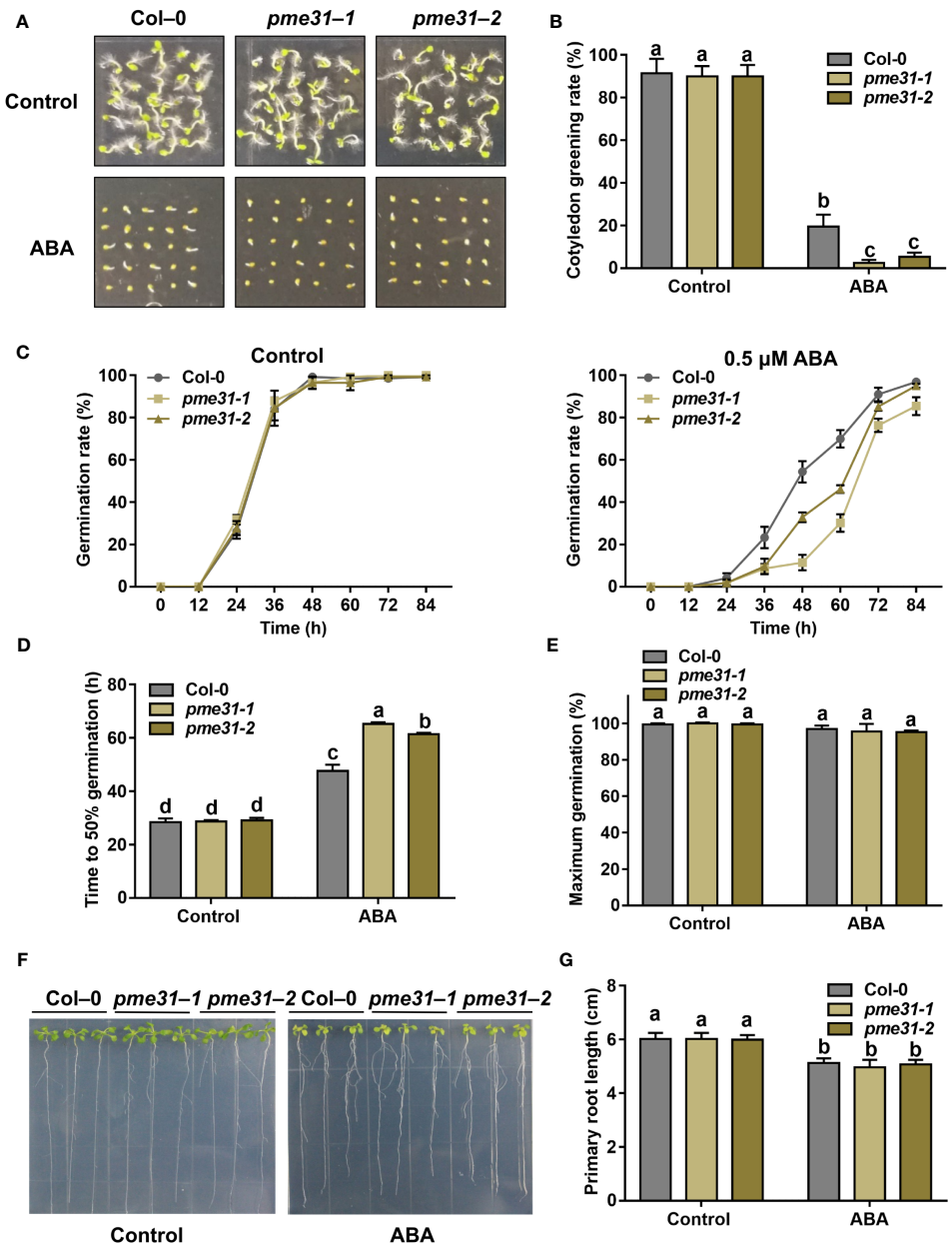

FIGURE 2
Disruption of *PME31* improves ABA-mediated inhibition of seed germination. **(A)** Phenotype of seed germination in Col-0 and *pme31* mutants treated with ABA. Seeds were sown on 1/2 MS medium with or without 0.5 μM ABA, and photographs were taken at 48 h of seed germination. **(B)** Green cotyledons rate was recorded after 72 h. **(C)** Germination rate of Col-0 and *pme31* mutants. Seeds were sown on 1/2 MS medium with or without 0.5 μM ABA. The seed germination rate was recorded every 12 h. **(D)** Time to 50% gemination of Col-0 and *pme31* mutants. **(E)** The percentage of maximum germination of Col-0 and *pme31* mutants. Seeds were sown on 1/2 MS medium with 0.5 μM ABA. **(F)** Phenotype of seedlings in Col-0 and *pme31* mutants treated with ABA. Five-day-old seedlings were selected and transferred to 1/2 MS medium with or without 10 μM ABA and placed in an incubator with normal conditions for 14 d. **(G)** Primary root length was recorded after growing for 14 d. Data are means (± SD) of three biological replicates. Different letters indicate significant differences at $P < 0.05$ according to two-way ANOVA (Tukey's multiple comparison test).

suppressed, but not with the mutated probe (Figure 4C). These results showed that ABI5 directly binds to the TTACACGTAG sequence of the *PME31* promoter.

To test if ABI5 was an activator or a repressor of *PME31*, we then performed luciferase assays. The effector was generated by the coding sequence of *ABI5* inserted into the pCAMBIA1300-221-3×flag vector. The reporter was generated by the *PME31* promoter fusing with LUC (Figure 4D). Tobacco leaves were infiltrated with the *proPME31*:LUC-35S:REN reporter and the *35S:ABI5* effector. The results showed that ABI5 inhibited LUC activity under the control of the *PME31* promoter (Figures 4E, F). Overall, those results indicated that ABI5 directly binds to the *PME31* promoter and acts as a transcriptional repressor of the *PME31* gene.

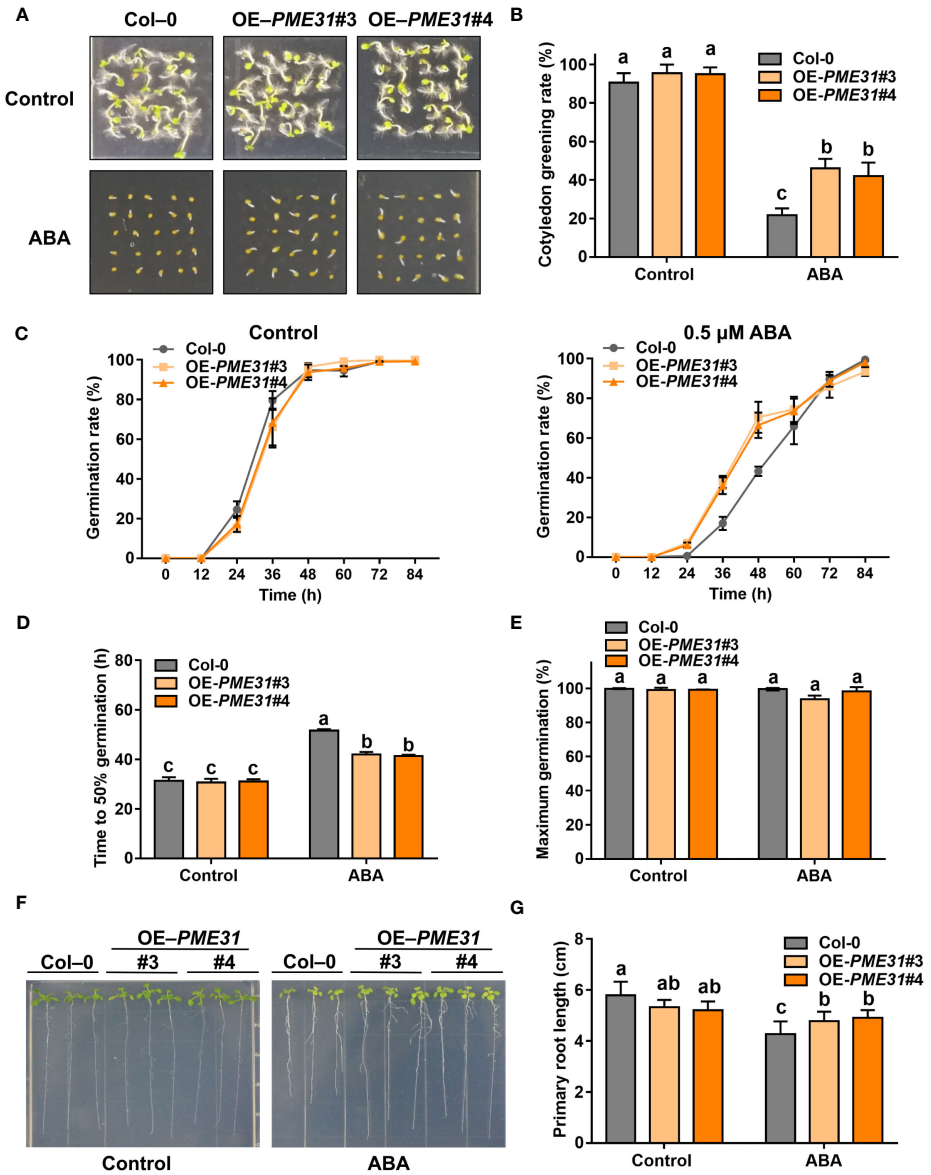

FIGURE 3
PME31 overexpression reduces ABA-mediated inhibition of seed germination. **(A)** Phenotype of seed germination in Col-0 and *PME31* overexpressors treated with ABA. Seeds were sown on 1/2 MS medium with or without 0.5 μM ABA, and photographs were taken at 48 h of seed germination. **(B)** Green cotyledons rate was recorded after 72 h. **(C)** Germination rate of Col-0 and *PME31* overexpressors mutants. Seeds were sown on 1/2 MS medium with or without 0.5 μM ABA. The seed germination rate was recorded every 12 h. **(D)** Time to 50% gemination of Col-0 and *PME31* overexpressors. **(E)** The percentage of maximum germination of Col-0 and *PME31* overexpressors. Seeds were sown on 1/2 MS medium with 0.5 μM ABA. **(F)** Phenotype of seedlings in Col-0 and *PME31* overexpressors treated with ABA. Five-day-old seedlings were selected and transferred to 1/2 MS medium with or without 10 μM ABA and placed in an incubator with normal conditions for 14 d. **(G)** Primary root length was recorded after growing for 14 d. Data are means (± SD) of three biological replicates. Different letters indicate significant differences at $P < 0.05$ according to two-way ANOVA (Tukey's multiple comparison test).

PME31 acts genetically downstream of ABI5 in ABA-mediated seed germination

To dissect the genetic relationship between PME31 and ABI5, we crossed *pme31-1* with *abi5-1* and analyzed seed germination in Col-0, *pme31-1*, *abi5-1*, and *abi5-1 pme31-1* mutants under ABA treatment. Under normal conditions, the cotyledon greening rate and germination rate had no significant difference in *pme31-1*, *abi5-1*, and *abi5-1 pme31-1* compared with the Col-0. Under ABA treatment conditions, the cotyledon greening rate and germination rate of *abi5-1* were higher than that of the Col-0. It indicated *abi5-1* was insensitive to ABA-mediated inhibition of seed germination. The cotyledon greening rate and germination rate of *pme31-1* were lower than that of Col-0 and *abi5-1*, while that of *abi5-1 pme31-1* were intermediate between *pme31-1* and *abi5-1* (Figures 5A–C). The time to 50% germination of *abi5-1 pme31-1* mutant was more than that of *abi5-1* and less than that of *pme31-1* (Figure 5D). The percentage of maximum germination had no significant difference in those

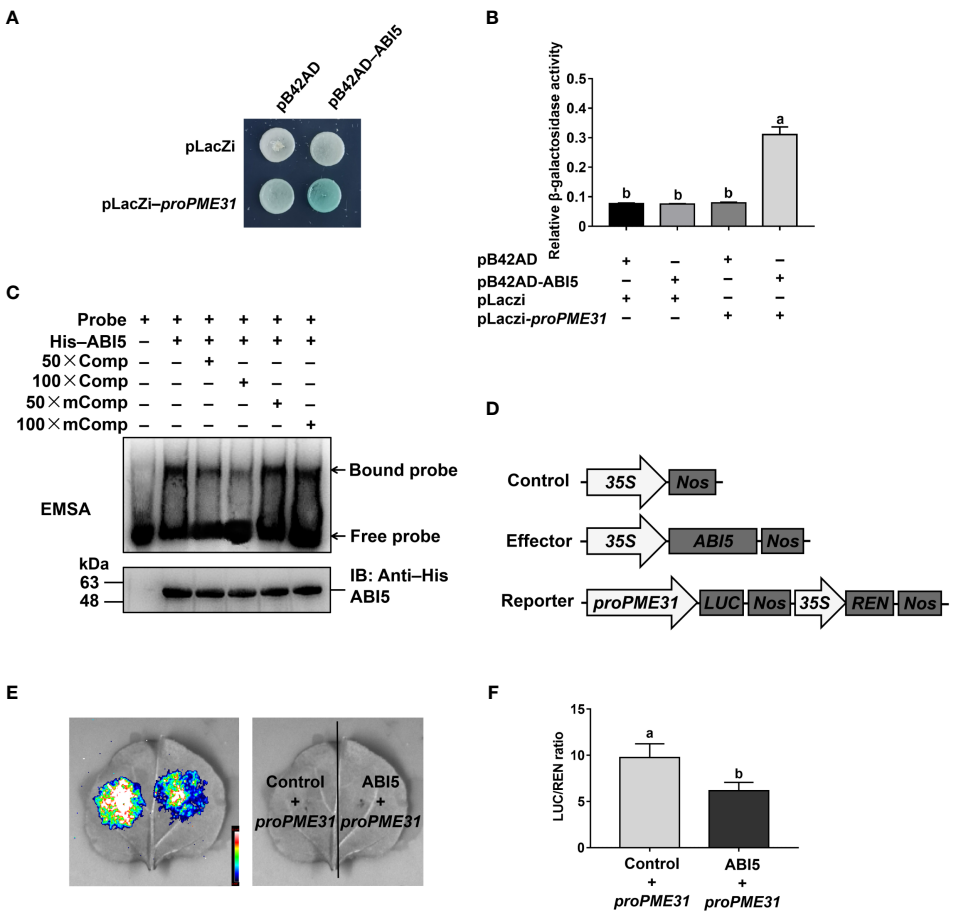

FIGURE 4
ABI5 directly binds to the *PME31* promoter and represses its expression. **(A)** Yeast-one-hybrid assays showing ABI5 directly binding to the promoter of *PME31*. The pLacZi-*proPME31* constructs were transformed with pB42AD-ABI5 into yeast strain EGY48. Transformants were screened on SD/−Trp−Ura plates and cultured on SD/−Trp−Ura/Gal/Raf/X-Gal (80 μg mL^{-1}) for blue color development at 30°C for 3 d. The pLacZi and pB42AD vectors were used as the negative control. **(B)** β-Galactosidase activity in **(A)**. **(C)** Electrophoretic mobility shift assays showing ABI5 directly binding to the promoter of *PME31*. The 50-bp oligonucleotide containing the ttaCACGTag sequence (−945 to −954 bp) was synthesized and labeled as a probe. The 50× and 100× unlabeled probes (Comp) and 100× mutated probes (mComp) were used as competitors. **(D)** Schematic diagram of the effector and reporter constructs. The coding sequence of ABI5 was inserted into the pCAMBIA1300-221-3×flag vector to generate an effector. The *PME31* promoter was fused with LUC to generate a reporter. **(E)** Luciferase assays showing ABI5 acted as a transcriptional repressor of *PME31*. The *proPME31:LUC-35S:REN* reporter was infiltrated into tobacco leaves. The LUC signals were imaged. **(F)** LUC and REN activities. The relative activity of the promoter was calculated by the LUC/REN ratio. Data are means (± SD) of three biological replicates. Different letters indicate significant differences at $P < 0.05$ according to two-way ANOVA (Tukey's multiple comparison test).

mutants (Figure 5E). Taken together, those results showed that PME31 acts genetically downstream of ABI5 in ABA-mediated seed germination.

PME31 expression is reduced by ABI5 in ABA-mediated seed germination

To further explore the effect of ABI5 on *PME31* expression in the plants, we examined the *PME31* expression in the *abi5-1* mutant and *ABI5* overexpressors during seed germination. Under normal conditions, *PME31* expression in the *abi5-1* mutant was significantly lower than in the wild-type. *PME31* expression increased significantly in the *abi5-1* mutant after 12 h imbibition. After 12 h imbibition, the *PME31* expression had a significant increase in the *abi5-1* mutant (Figure 6A). We then examined the *PME31* expression in *ABI5* overexpressors. *ABI5* overexpression was driven by a β-estradiol-inducible promoter. The *ABI5* expression was significantly increased in the presence of β-estradiol treatment (Figure 6B). After 12 h imbibition with β-estradiol induction, the *PME31* expression was significantly reduced in *ABI5* overexpressors compared with the Col-0 (Figure 6C). Therefore, ABI5 decreases *PME31* expression in seed germination.

Discussion

Endospermic seeds, such as Arabidopsis, tobacco, and garden cress, often germinate in a two-step process: after the initial phase of water uptake by the dry seeds (imbibition), testa rupture (TR) occurs and is subsequently followed by endosperm rupture (ER)

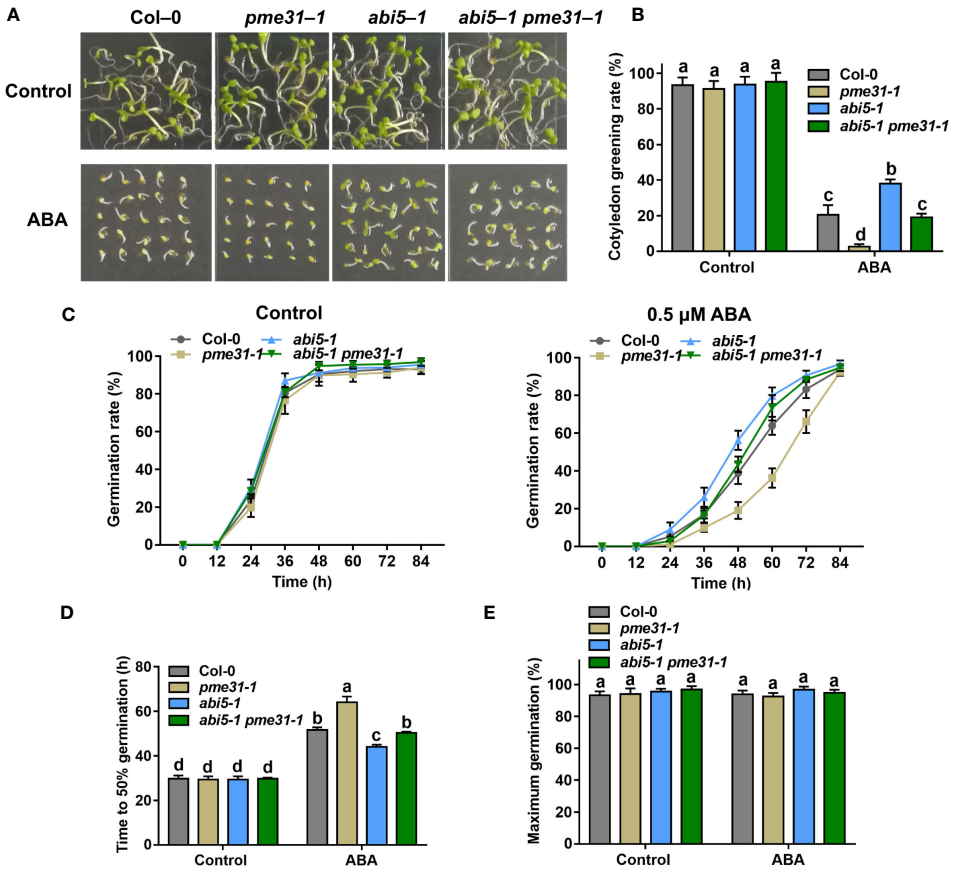

FIGURE 5
PME31 acts genetically downstream of ABI5 in ABA-mediated inhibition of seed germination. **(A)** Phenotype of seed germination in Col-0, *pme31-1, abi5-1, abi5-1 pme31-1* mutants treated with ABA. Seeds were sown on 1/2 MS medium with or without 0.5 μM ABA, and photographs were taken at 48 h of seed germination. **(B)** Green cotyledons rate was recorded after 72 h. **(C)** Germination rate of Col-0, *pme31-1, abi5-1, abi5-1 pme31-1* mutants. Seeds were sown on 1/2 MS medium with or without exogenous ABA (0.5 μM). The seed germination rate was recorded every 12 h. **(D)** Time to 50% gemination of Col-0, *pme31-1, abi5-1, abi5-1 pme31-1* mutants. **(E)** The percentage of maximum germination of Col-0, *pme31-1, abi5-1, abi5-1 pme31-1* mutants. Seeds were sown on 1/2 MS medium with 0.5 μM ABA. Data are means (± SD) of three biological replicates. Different letters indicate significant differences at $P < 0.05$ according to two-way ANOVA (Tukey's multiple comparison test).

(Müller et al., 2006; Linkies et al., 2010). Cell walls are highly dynamic structures that provide mechanical support to plant cells. Hemicelluloses bind and crosslink with pectin in cell walls to generate a methylesterified hydrated matrix. Modifications of pectin are important to the process of TR and ER. PMEs regulate the methylesterification status of pectins by removing the methyl group of pectin. It results in an anionically charged matrix and alters the structure properties of the cell wall (Müller et al., 2013; Chandrasekaran et al., 2022). In garden cress, exogenous PME treatment increased testa permeability and promoted TR (Scheler et al., 2015). Salanenka et al. (2009) found that the activity of PMEs was associated with endosperm weakening in cucumber seeds, suggesting PMEs were closely related to seed germination. *PME* genes were more than 66 members in *Arabidopsis*. Most *PME* genes displayed tissue- and stress-specific expression profiles in plant development and stress responses (Pelloux et al., 2007; Weber et al., 2013; Huang et al., 2017; Tang et al., 2023). For instance, Weber et al. (2013) found that the root cell size in the *pme3* mutant seedlings was smaller in the presence of Zn^{2+}. PbrPME44 greatly inhibited pollen tube growth and alleviated the increase in methyl-esterified pectin levels caused by PbrS–RNase (Tang et al., 2023). Previous studies showed that PME activity was close to seed germination. The increased PME activity improved the demethylesterification of pectin to facilitate the release of endosperm and promote seed germination (Müller et al., 2013). Scheler et al. (2015) found that ABA suppressed PME activity during seed germination. However, the mechanism of *PMEs* in response to ABA-mediated seed germination remains unknown. Studies showed that disruption of *PME31* reduced the release of seed coat mucilage and salt stress tolerance (Yan et al., 2018; Zhang et al., 2023), but the role of *PME31* in seed germination is not clear. In this study, we found that the *PME31* expression is prominent in the embryo and was downregulated in the presence of ABA (Figure 1). Phenotype analysis showed that *PME31* negatively regulated ABA-mediated seed germination inhibition (Figures 2 and 3). We further identified an upstream regulator of PME31, ABI5, which is an ABA signaling bZIP transcription factor (Figure 4A). *PME31* expression was downregulated in the *abi5-1* mutant, while it had a significant increase in the *abi5-1* mutant after 12 h imbibition. In seeds of *abi3-1*, *abi4-1* mutants, and *ABI4*

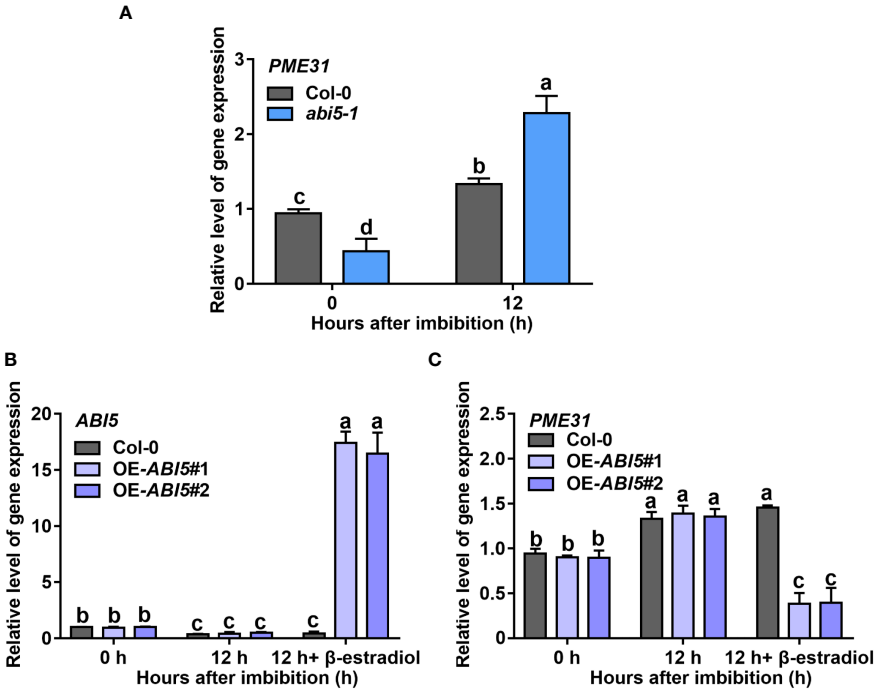

FIGURE 6
ABI5 decreases *PME31* expression in ABA-mediated seed germination **(A)** The expression of *PME31* in the *abi5-1* mutant. **(B)** The expression of *ABI5* in *ABI5* overexpressors. **(C)** The expression of *PME31* in *ABI5* overexpressors. Seeds were imbibed at 25°C in darkness for 12 h. The expression of *ABI5* was induced with or without 10 μM β-estradiol. *Actin2* was used as the internal reference. Data are means (± SD) of three biological replicates. Different letters indicate significant differences at P < 0.05 according to two-way ANOVA (Tukey's multiple comparison test).

overexpressor, the *PME31* expression had no significant difference (Figure 6A; Supplementary Figure S4). It suggested that *PME31* expression is mainly influenced by ABI5.

ABA inhibits seed germination and hinders post-germination growth at early developmental stages in plants. Studies have shown that ABI5 negatively regulated ABA-mediated seed germination (Lopez-Molina et al., 2001; Bi et al., 2017; Zhao et al., 2020). ABI5 interacted with a variety of factors, including functional proteins, transcription factors, and enzymes, to regulate seed germination. For instance, the circadian clock proteins PSEUDO-RESPONSE REGULATOR5 (PRR5) collaborated with ABI5 to increase ABA signaling and inhibit seed germination (Yang et al., 2021). In addition, ABA relieved the interaction of C-type Cyclin1;1 (CycC1;1) and inhibition of ABI5, which activated ABI5 activity in the ABA responses and inhibited seed germination (Guo et al., 2022). ABI5 also was bound to the target genes in ABA-mediated seed germination. ABI5 could bind to the promoters of *ABI3*, *CAT1*, and *PYR/PYL/RCAR* genes to influence their gene expression during seed germination (Lopez-Molina et al., 2002; Bi et al., 2017; Zhao et al., 2020). However, whether ABI5 transcriptionally

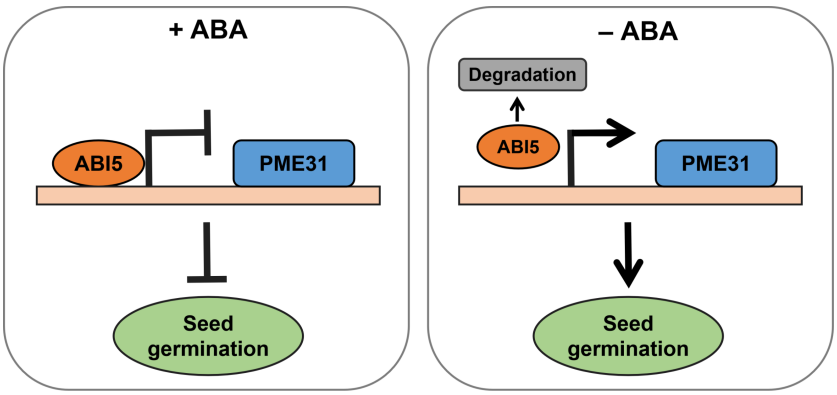

FIGURE 7
A working model for transcriptional repression of *PME31* by ABI5 in ABA-mediated seed germination As seed germination proceeded, ABA content and ABI5 protein level reduced, and the reduced ABI5 alleviated its transcriptional repression of *PME31*, thereby responding to the ABA-mediated seed germination.

regulates *PMEs* expression is not clear. We found that ABI5 was directly bound to the *PME31* promoter and suppressed its expression (Figure 4). Meanwhile, genetic analysis revealed that ABI5 acted upstream of PME31 in ABA-mediated seed germination (Figure 5). Furthermore, ABI5 reduced *PME31* expression in plant seed germination (Figure 6). Consequently, it suggested that ABI5 was directly bound and downregulated *PME31* expression in ABA-mediated seed germination.

The stability of ABI5 is strictly regulated as an important regulator of ABA-responsive genes during seed germination (Lopez-Molina et al., 2001; Nie et al., 2022). ABA elevated the stability of the ABI5 protein, but 26S proteasomes quickly broke down the protein when ABA was removed (Lopez-Molina et al., 2001). Numerous factors regulated the degradation of ABI5. For instance, ABI five binding protein (AFP) promoted ABI5 protein degradation (Lopez-Molina et al., 2003). ABA facilitated ABI5 accumulation by inducing the ubiquitination and proteasomal degradation of KEG (Liu and Stone, 2010). Moreover, the ubiquitin E3 ligase MIEL1 interacted with and ubiquitinated ABI5 to facilitate its degradation in the process of seed germination (Nie et al., 2022). It has been proved that as seeds germinate, the amount of ABA and the level of ABI5 protein gradually drop (Price et al., 2003; Zhao et al., 2020). We therefore hypothesized that as seed germination proceeds, ABA content and ABI5 protein level decrease, and the reduced ABI5 alleviates its transcriptional repression of *PME31*, thereby responding to the ABA-mediated seed germination (Figure 7).

In conclusion, *PME31* is transcriptionally repressed by ABI5 to negatively regulate ABA-mediated seed germination inhibition. Our findings shed light on the mechanisms that *PME31* is in response to ABA-mediated seed germination.

Data availability statement

The original contributions presented in the study are included in the article/Supplementary Files, further inquiries can be directed to the corresponding author/s.

Author contributions

YX: Data curation, Formal analysis, Funding acquisition, Investigation, Methodology, Software, Writing – original draft, Writing – review & editing. CZ: Data curation, Investigation, Writing – original draft, Writing – review & editing. QL: Data curation, Investigation, Writing – original draft, Writing – review & editing. YN: Data curation, Methodology, Writing – original draft, Writing – review & editing. YP: Data curation, Investigation, Methodology, Writing – original draft. GL: Data curation, Investigation, Methodology, Writing – original draft. YC: Data curation, Investigation, Methodology, Writing – original draft. AZ: Funding acquisition, Writing – review & editing.

Funding

The author(s) declare financial support was received for the research, authorship, and/or publication of this article. This study was supported by National Natural Science Foundation of China (32201707), the Fundamental Research Funds for the Central Universities (KYQN2023025), Natural Science Foundation of Jiangsu Province (BK20220999), China Postdoctoral Science Foundation (2021M701739, 2023T160323), Jiangsu Funding Program for Excellent Postdoctoral Talent (2022ZB330), Open Competition Mechanism to Select the Best Candidates Fund of Jiangsu Province (JBGS[2021]012), Key Research and Development Program of Ningxia Hui Autonomous Region (2023BCF01009), and the Achievement Transformation Fund Project of Hainan Research Institute of Nanjing Agricultural University (NAUSY-CG-YB07).

Acknowledgments

We gratefully acknowledge Professor Jingwei Yan from Zhejiang Agriculture and Forestry University for providing ABI4 overexpressor.

Conflict of interest

The authors declare that the research was conducted in the absence of any commercial or financial relationships that could be construed as a potential conflict of interest.

Publisher's note

Supplementary material

The Supplementary Material for this article can be found online at: https://www.frontiersin.org/articles/10.3389/fpls.2024.1336689/full#supplementary-material

References

Berry, T., and Bewley, J. D. (1992). A role for the surrounding fruit tissues in preventing the germination of tomato (*Lycopersicon esculentum*) seeds. *Plant Physiol.* 100, 951–957. doi: 10.1104/pp.100.2.951

Bi, C., Ma, Y., Wu, Z., Yu, Y. T., Liang, S., Lu, K., et al. (2017). Arabidopsis ABI5 plays a role in regulating ROS homeostasis by activating CATALASE 1 transcription in seed germination. *Plant Mol. Biol.* 94, 197–213. doi: 10.1007/s11103-017-0603-y

Bradford, M. M. (1976). A rapid and sensitive method for the quantitation of microgram quantities of protein utilizing the principle of protein-dye binding. *Anal. Biochem.* 72, 248–254. doi: 10.1016/0003-2697(76)90527-3

Chandrasekaran, U., Zhao, X., Luo, X., Wei, S., and Shu, K. (2022). Endosperm weakening: The gateway to a seed's new life. *Plant Physiol. Bioch.* 178, 31–39. doi: 10.1016/j.plaphy.2022.02.016

Chow, C. N., Zheng, H. Q., Wu, N. Y., Chien, C. H., Huang, H. D., Lee, T. Y., et al. (2016). PlantPAN 2.0: an update of plant promoter analysis navigator for reconstructing transcriptional regulatory networks in plants. *Nucleic Acids Res.* 44, 1154–1160. doi: 10.1093/nar/gkv1035

Clough, S. J., and Bent, A. F. (1998). Floral dip: a simplified method for Agrobacterium-mediated transformation of Arabidopsis thaliana. *Plant J.* 16, 735–743. doi: 10.1046/j.1365-313x.1998.00343.x

Coego, A., Brizuela, E., Castillejo, P., Ruíz, S., Koncz, C., del Pozo, J. C., et al. (2014). The TRANSPLANTA collection of Arabidopsis lines: a resource for functional analysis of transcription factors based on their conditional overexpression. *Plant J.* 77, 944–953. doi: 10.1111/tpj.12443

Earley, K. W., Haag, J. R., Pontes, O., Opper, K., Juehne, T., Song, K., et al. (2006). Gateway-compatible vectors for plant functional genomics and proteomics. *Plant J.* 45, 616–629. doi: 10.1111/j.1365-313X.2005.02617.x

Graeber, K. A. I., Nakabayashi, K., Miatton, E., Leubner-Metzger, G., and Soppe, W. J. J. (2012). Molecular mechanisms of seed dormancy. *Plant Cell Environ.* 35, 1769–1786. doi: 10.1111/j.1365-3040.2012.02542.x

Grainge, G., Nakabayashi, K., Steinbrecher, T., Kennedy, S., Ren, J., Iza, F., et al. (2022). Molecular mechanisms of seed dormancy release by gas plasma-activated water technology. *J. Exp. Bot.* 73, 4065–4078. doi: 10.1093/jxb/erac150

Guo, J. X., Song, R. F., Lu, K. K., Zhang, Y., Chen, H. H., Zuo, J. X., et al. (2022). CycC1;1 negatively modulates ABA signaling by interacting with and inhibiting ABI5 during seed germination. *Plant Physiol.* 190, 2812–2827. doi: 10.1093/plphys/kiac456

Hongo, S., Sato, K., Yokoyama, R., and Nishitani, K. (2012). Demethylesterification of the primary wall by PECTIN METHYLESTERASE35 provides mechanical support to the Arabidopsis stem. *Plant Cell* 24, 2624–2634. doi: 10.1105/tpc.112.099325

Huang, Y. C., Wu, H. C., Wang, Y. D., Liu, C. H., Lin, C. C., Luo, D. L., et al. (2017). PECTIN METHYLESTERASE34 contributes to heat tolerance through its role in promoting stomatal movement. *Plant Physiol.* 174, 748–763. doi: 10.1104/pp.17.00335

Li, H., Li, X., Wang, G., Zhang, J., and Wang, G. (2022). Analysis of gene expression in early seed germination of rice: landscape and genetic regulation. *BMC Plant Biol.* 22, 70. doi: 10.1186/s12870-022-03458-3

Linkies, A., Graeber, K., Knight, C., and Leubner-Metzger, G. (2010). The evolution of seeds. *New Phytol.* 186, 817–831. doi: 10.1111/j.1469-8137.2010.03249.x

Liu, H., and Stone, S. L. (2010). Abscisic acid increases Arabidopsis ABI5 transcription factor levels by promoting KEG E3 ligase self-ubiquitination and proteasomal degradation. *Plant Cell* 22, 2630–2641. doi: 10.1105/tpc.110.076075

Liu, X., Hu, P., Huang, M., Tang, Y., Li, Y., Li, L., et al. (2016). The NF-YC-RGL2 module integrates GA and ABA signalling to regulate seed germination in *Arabidopsis*. *Nat. Commun.* 7, 12768. doi: 10.1038/ncomms12768

Liu, Z., Ma, C., Hou, L., Wu, X., Wang, D., Zhang, L., et al. (2022). Exogenous SA affects rice seed germination under salt stress by regulating Na^+/K^+ balance and endogenous GAs and ABA homeostasis. *Int. J. Mol. Sci.* 23, 3293. doi: 10.3390/ijms23063293

Livak, K. J., and Schmittgen, T. D. (2001). Analysis of relative gene expression data using real-time quantitative PCR and the 2–ΔΔCT method. *Methods* 25, 402–408. doi: 10.1006/meth.2001.1262

Loades, E., Pérez, M., Turečková, V., Tarkowská, D., Strnad, M., Seville, A., et al. (2023). Distinct hormonal and morphological control of dormancy and germination in Chenopodium album dimorphic seeds. *Front. Plant Sci.* 14. doi: 10.3389/fpls.2023.1156794

Lopez-Molina, L., Mongrand, S., Kinoshita, N., and Chua, N. H. (2003). AFP is a novel negative regulator of ABA signaling that promotes ABI5 protein degradation. *Genes Dev.* 17, 410–418. doi: 10.1101/gad.1055803

Lopez-Molina, L., Mongrand, S., McLachlin, D. T., Chait, B. T., and Chua, N. H. (2002). ABI5 acts downstream of ABI3 to execute an ABA-dependent growth arrest during germination. *Plant J.* 32, 317–328. doi: 10.1046/j.1365-313X.2002.01430.x

Lopez-Molina, L., Mongrand, S., and Nam-Hai, C. (2001). A postgermination developmental arrest checkpoint is mediated by abscisic acid and requires the ABI5 transcription factor in Arabidopsis. *Proc. Natl. Acad. Sci. U.S.A.* 98, 4782–4787. doi: 10.1073/pnas/081594298

Mei, S., Zhang, M., Ye, J., Du, J., Jiang, Y., and Hu, Y. (2023). Auxin contributes to jasmonate-mediated regulation of abscisic acid signaling during seed germination in Arabidopsis. *Plant Cell* 35, 1110–1133. doi: 10.1093/plcell/koac362

Müller, K., Levesque-Tremblay, G., Bartels, S., Weitbrecht, K., Wormit, A., Usadel, B., et al. (2013). Demethylesterification of cell wall pectins in Arabidopsis plays a role in seed germination. *Plant Physiol.* 161, 305–316. doi: 10.1104/pp.112.205724

Müller, K., Tintelnot, S., and Leubner-Metzger, G. (2006). Endosperm-limited Brassicaceae seed germination: abscisic acid inhibits embryo-induced endosperm weakening of *Lepidium sativum* (cress) and endosperm rupture of cress and *Arabidopsis thaliana*. *Plant Cell Physiol.* 47, 864–877. doi: 10.1093/pcp/pcj059

Nakagawa, T., Kurose, T., Hino, T., Tanaka, K., Kawamukai, M., Niwa, Y., et al. (2007). Development of series of gateway binary vectors, pGWBs, for realizing efficient construction of fusion genes for plant transformation. *J. Biosci. Bioeng.* 104, 34–41. doi: 10.1263/jbb.104.34

Nie, K., Zhao, H., Wang, X., Niu, Y., Zhou, H., and Zheng, Y. (2022). The MIEL1-ABI5/MYB30 regulatory module fine tunes abscisic acid signaling during seed germination. *J. Integr. Plant Biol.* 64, 930–941. doi: 10.1111/jipb.13234

Pelloux, J., Rusterucci, C., and Mellerowicz, E. (2007). New insights into pectin methylesterase structure and function. *Trends Plant Sci.* 12, 267–277. doi: 10.1016/j.tplants.2007.04.001

Price, J., Li, T. C., Kang, S. G., Na, J. K., and Jang, J. C. (2003). Mechanisms of glucose signaling during germination of Arabidopsis. *Plant Physiol.* 132, 1424–1438. doi: 10.1104/pp.103.020347

Qu, T., Liu, R., Wang, W., An, L., Chen, T., Liu, G., et al. (2011). Brassinosteroids regulate pectin methylesterase activity and *AtPME41* expression in Arabidopsis under chilling stress. *Cryobiology* 63, 111–117. doi: 10.1016/j.cryobiol.2011.07.003

Rushton, D. L., Tripathi, P., Rabara, R. C., Lin, J., Ringler, P., Boken, A. K., et al. (2012). WRKY transcription factors: key components in abscisic acid signalling. *Plant Biotechnol. J.* 10, 2–11. doi: 10.1111/j.1467-7652.2011.00634.x

Salanenka, Y. A., Goffinet, M. C., and Taylor, A. G. (2009). Structure and histochemistry of the micropylar and chalazal regions of the perisperm-endosperm envelope of cucumber seeds associated with solute permeability and germination. *J. Am. Soc Hortic. Sci.* 134, 479–487. doi: 10.21273/JASHS.134.4.479

Scheler, C., Weitbrecht, K., Pearce, S. P., Hampstead, A., Büttner-Mainik, A., Lee, K. J. D., et al. (2015). Promotion of testa rupture during garden cress germination involves seed compartment-specific expression and activity of pectin methylesterases. *Plant Physiol.* 167, 200–215. doi: 10.1104/pp.114.247429

Sharma, E., Majee, M., and Penfield, S. (2023). Seed germination variability: why do genetically identical seeds not germinate at the same time? *J. Exp. Bot.* 74, 3462–3475. doi: 10.1093/jxb/erad101

Shu, K., Zhang, H., Wang, S., Chen, M., Wu, Y., Tang, S., et al. (2013). ABI4 regulates primary seed dormancy by regulating the biogenesis of abscisic acid and gibberellins in Arabidopsis. *PloS Genet.* 9, e1003577. doi: 10.1371/journal.pgen.1003577

Singh, D., and Datta, S. (2023). BBX30/miP1b and BBX31/miP1a form a positive feedback loop with ABI5 to regulate ABA-mediated postgermination seedling growth arrest. *New Phytol.* 238, 1908–1923. doi: 10.1111/nph.18866

Skubacz, A., Daszkowska-Golec, A. , and Szarejko, I. (2016). The role and regulation of ABI5 (ABA-Insensitive 5) in plant development, abiotic stress responses and phytohormone crosstalk. *Front. Plant Sci.* 71884. doi: 10.3389/fpls.2016.01884

Tang, C., Wang, P., Zhu, X., Qi, K., Xie, Z., Zhang, H., et al. (2023). Acetylation of inorganic pyrophosphatase by S-RNase signaling induces pollen tube tip swelling by repressing pectin methylesterase. *Plant Cell* 35, 3544–3565. doi: 10.1093/plcell/koad162

Tuan, P. A., Kumar, R., Rehal, P. K., Toora, P. K., and Ayele, B. T. (2018). Molecular mechanisms underlying abscisic acid/gibberellin balance in the control of seed dormancy and germination in cereals. *Front. Plant Sci.* 9. doi: 10.3389/fpls.2018.00668

Weber, M., Deinlein, U., Fischer, S., Rogowski, M., Geimer, S., Tenhaken, R., et al. (2013). A mutation in the *Arabidopsis thaliana* cell wall biosynthesis gene pectin methylesterase 3 as well as its aberrant expression cause hypersensitivity specifically to Zn. *Plant J.* 76, 151–164. doi: 10.1111/tpj.12279

Xiang, Y., Bian, X., Wei, T., Yan, J., Sun, X., Han, T., et al. (2021a). ZmMPK5 phosphorylates ZmNAC49 to enhance oxidative stress tolerance in maize. *New Phytol.* 232, 2400–2417. doi: 10.1111/nph.17761

Xiang, Y., Sun, X., Bian, X., Wei, T., Han, T., Yan, J., et al. (2021b). The transcription factor ZmNAC49 reduces stomatal density and improves drought tolerance in maize. *J. Exp. Bot.* 72, 1399–1410. doi: 10.1093/jxb/eraa507

Xue, X., Du, S., Jiao, F., Xi, M., Wang, A., Xu, H., et al. (2021). The regulatory network behind maize seed germination: Effects of temperature, water, phytohormones, and nutrients. *Crop J.* 9, 718–724. doi: 10.1016/j.cj.2020.11.005

Yan, J., Fang, L., Yang, L., He, H., Huang, Y., Liu, Y., et al. (2020). Abscisic acid positively regulates L-arabinose metabolism to inhibit seed germination through ABSCISIC ACID INSENSITIVE4-mediated transcriptional promotions of MUR4 in *Arabidopsis thaliana*. *New Phytol.* 225, 823–834. doi: 10.1111/nph.16149

Yan, J., He, H., Fang, L., and Zhang, A. (2018). Pectin methylesterase31 positively regulates salt stress tolerance in Arabidopsis. *Biochem. Biophys. Res. Commun.* 496, 497–501. doi: 10.1016/j.bbrc.2018.01.025

Yang, M., Han, X., Yang, J., Jiang, Y., and Hu, Y. (2021). The Arabidopsis circadian clock protein PRR5 interacts with and stimulates ABI5 to modulate abscisic acid signaling during seed germination. *Plant Cell* 33, 3022–3041. doi: 10.1093/plcell/koab168

Zhang, X., Guo, H., Xiao, C., Yan, Z., Ning, N., Chen, G., et al. (2023). PECTIN METHYLESTERASE INHIBITOR18 functions in stomatal dynamics and stomatal dimension. *Plant Physiol.* 192, 1603–1620. doi: 10.1093/plphys/kiad145

Zhao, H., Nie, K., Zhou, H., Yan, X., Zhan, Q., Zheng, Y., et al. (2020). ABI5 modulates seed germination via feedback regulation of the expression of the PYR/PYL/RCAR ABA receptor genes. *New Phytol.* 228, 596–608. doi: 10.1111/nph.16713

Zhou, C., Lin, Q., Lan, J., Zhang, T., Liu, X., Miao, R., et al. (2020). WRKY transcription factor OsWRKY29 represses seed dormancy in rice by weakening abscisic acid response. *Front. Plant Sci.* 11, 691. doi: 10.3389/fpls.2020.00691

Zúñiga-Sánchez, E., Soriano, D., Martínez-Barajas, E., Orozco-Segovia, A., and Alicia, G. D. (2014). BIIDXI, the At4g32460 DUF642 gene, is involved in pectin methyl esterase regulation during *Arabidopsis thaliana* seed germination and plant development. *BMC Plant Biol.* 14, 338. doi: 10.1186/s12870-014-0338-8

frontiers | Frontiers in Plant Science

TYPE Original Research
PUBLISHED 08 February 2024
DOI 10.3389/fpls.2024.1344383

OPEN ACCESS

EDITED BY
Zhou Li,
Sichuan Agricultural University, China

REVIEWED BY
Lei Wang,
Chinese Academy of Sciences (CAS), China
Szilvia Veres,
University of Debrecen, Hungary

*CORRESPONDENCE
Anca Macovei
anca.macovei@unipv.it

RECEIVED 25 November 2023
ACCEPTED 22 January 2024
PUBLISHED 08 February 2024

CITATION
Dueñas C Jr, Pagano A, Calvio C, Srikanthan DS, Slamet-Loedin I, Balestrazzi A and Macovei A (2024) Genotype-specific germination behavior induced by sustainable priming techniques in response to water deprivation stress in rice.
Front. Plant Sci. 15:1344383.
doi: 10.3389/fpls.2024.1344383

Genotype-specific germination behavior induced by sustainable priming techniques in response to water deprivation stress in rice

Conrado Dueñas Jr[1], Andrea Pagano[1], Cinzia Calvio[1], Dhanush Srikanth Srikanthan[1], Inez Slamet-Loedin[2], Alma Balestrazzi[1] and Anca Macovei[1]*

[1]Department of Biology and Biotechnology 'L. Spallanzani', University of Pavia, Pavia, Italy, [2]Trait and Genome Engineering Cluster, Rice Breeding Innovations, International Rice Research Institute, Metro Manila, Philippines

Water stress brought about by climate change is among the major global concerns threatening food security. Rice is an important staple food which requires high water resources. Being a semi-aquatic plant, rice is particularly susceptible to drought. The aim of this work was to develop techniques directed to promote rice resilience to water deprivation stress during germination by implementing specific seed priming treatments. Five popular Italian rice varieties were subjected to priming treatments using novel, sustainable solutions, like poly-gamma-glutamic acid (γ-PGA), denatured γ-PGA (dPGA), and iron (Fe) pulsing, alone or in combination. The effect of the developed priming methods was tested under optimal conditions as well as under water deprivation stress imposed by polyethylene glycol (PEG) treatments. The priming efficacy was phenotypically determined in terms of germination behavior by measuring a series of parameters (germinability, germination index, mean germination time, seed vigor index, root and shoot length, germination stress tolerance index). Biochemical analyses were carried out to measure the levels of iron uptake and accumulation of reactive oxygen species (ROS). Integrative data analyses revealed that the rice varieties exhibited a strong genotype- and treatment-specific germination behavior. PEG strongly inhibited germination while most of the priming treatments were able to rescue it in all varieties tested except for Unico, which can be defined as highly stress sensitive. Molecular events (DNA repair, antioxidant response, iron homeostasis) associated with the transition from seed to seedling were monitored in terms of changes in gene expression profiles in two varieties sensitive to water deprivation stress with different responses to priming. The investigated genes appeared to be differentially expressed in a genotype-, priming treatment-, stress- and stage-dependent manner. The proposed seed priming treatments can be envisioned as sustainable and versatile agricultural practices that could help in addressing the impact of climate challenges on the agri-food system.

KEYWORDS

poly-gamma glutamic acid (γ-PGA), polyethylene glycol (PEG), iron pulsing, seed germination, gene expression, antioxidant response, DNA damage response

1 Introduction

Re-emergence of global hunger is related to increasing obstacles in agricultural food production associated with the climate change scenario (https://www.fao.org/publications/sofi/2022/en/). Actions to mitigate these challenges are envisioned in the Sustainable Development Goals (SDG) Agenda 2030, mainly in SDG#2 - Zero hunger. Rice has high potential for aiding the accomplishment of SDG#2 due to its global consumption. This staple crop contributes to 35 - 59% of the daily caloric intake for billions of people, being the third most cultivated crop in the world (Sperotto et al., 2012). As a semiaquatic plant, rice is particularly sensitive to drought, a condition progressively worsening in the current climate scenario (Shahzad et al., 2021; Habib-Ur-Rahman et al., 2022). Hence, there is a need to develop strategies that could mitigate drought stress, starting from the germination stage (Panda et al., 2021).

Seed germination is one of the most important processes in the life of the plant, marking the transition from the quiescent state to a metabolically active state, initiating a series of biophysical, biochemical and molecular changes leading to radicle emergence and subsequent seedling growth (Han and Yang, 2015; Macovei et al., 2017; Yu et al., 2021). Within the agricultural context, optimal seed germination ensures seedling vigor and subsequently high yields during harvest, which are however negatively influenced by water deprivation stress (Osakabe et al., 2014; Reed et al., 2022). In the case of rice, numerous drought stress-related studies have been conducted at the reproductive stage due to its direct relation to yield (Rang et al., 2011; He and Serraj, 2012; Favreau et al., 2023; Lou et al., 2023) while less attention has been given to the germination stage.

Mature seeds contain an embryo in a quiescent state, characterized by reduced metabolism, although transcriptional and post-transcriptional modifications in response to the environmental signals remain partially active to sense and start the germination process under favorable conditions (Holdsworth et al., 2008). Seed germination is a triphasic process, where phase I is characterized by rapid water uptake, which in rice, corresponds to the first 20 h of imbibition. Phase II (lag phase) spans from 20 to 48 h, whereas phase III, representative of radicle emergence, starts after 48 h from imbibition (Yang et al., 2007). Complex physiological and biochemical events are involved in the transition from the dry, quiescent seed to the metabolically active state, including an intermediary state called pre-germinative metabolism, characterized by highly dynamic changes in carbohydrate metabolism, signal transduction, DNA synthesis, gene expression, regulation of redox homeostasis, and DNA repair (Howell et al., 2009; Macovei et al., 2017; Sano et al., 2022). Moreover, the *de novo* transcription happening during the early stages of germination is further subjected to additional regulation during seedling establishment (Rajjou et al., 2012; Sano et al., 2012). During the reactivation of the seed metabolism, reactive oxygen species (ROS) are produced at high levels due to rapid water uptake, and this can be potentially harmful if their levels pass a certain threshold (Baily et al., 2008, Pagano et al., 2022). To maintain ROS balance, the activation of antioxidant defense mechanisms are required to ensure successful seedling development (Kranner et al., 2010; Rajjou et al., 2012; Pagano et al., 2023). Moreover, efficient activation of the DNA damage response (DDR) pathway is necessary to repair DNA damage and safeguard seedling genome integrity (Balestrazzi et al., 2011; Pagano et al., 2017; Waterworth et al., 2019).

Generally, water deprivation stress can occur when water availability is low, potentially triggering loss of turgor pressure at a cellular level. In an agronomic context, water deprivation stress represents only a part of the complex drought conditions which highly restricts plant growth by reducing cellular elongation and expansion, detrimentally affecting seedling development and germination (Bhandari et al., 2023). Rice is highly sensitive to dry conditions during germination and the early phases of seedling growth. Low water potential in the soil prevents seedling from absorbing water, reducing seedling vigor (Kruthika and Jithesh, 2023; Székely et al., 2023). The effects of water deprivation stress include altered membrane transport, disruption of metabolic processes, decreased ATP synthesis, leading to aborted germination, or severe seedling growth reduction (Batlang et al., 2013; Oladosu et al., 2019; Kota et al., 2023). Transcriptional and hormonal activities, along with ROS levels, are highly affected when imbibition and seedling development occur during water stress conditions (Ishibashi et al., 2018; Kawaguchi et al., 2023).

Water deprivation stress at the germination stage can be addressed through several practices that include seed treatments to induce osmoprotection, limiting ROS accumulation, or enhancing the seed repair response. Among these treatments, seed priming is envisaged as a sustainable, cost-effective, and easy to use technique dedicated to improve seed germination even under adverse conditions. Seed priming is a pre-sowing technique that involves controlled imbibition, allowing seeds to reach the early stages of germination without radicle protrusion, followed by subsequent drying (Paparella et al., 2015; Devika et al., 2021). These treatments allow increased and uniform germination by acting on enhancing enzyme activation, metabolite production, repair of damaged DNA and osmotic regulation (Gerna et al., 2018; Forti et al., 2020a; Forti et al., 2020b; Wang et al., 2022). Even upon exposure to drought stress, this technique can speed up seedling emergence through the regulation of metabolic process in the early phases of germination (Marthandan et al., 2020). In rice, different priming methods, including hydropriming (Nakao et al., 2020), nanopriming (Waqas Mazhar et al., 2022), chemical priming applied through the use of salt solutions (Ali et al., 2021), plant extracts (Khan et al., 2022) or plant growth elicitors (Samota et al., 2017), have been applied and were shown to mitigate the effects of drought stress at different levels. Although the research in this field is steadily advancing, there is still the need to understand how priming works at a molecular level, and develop strategies that could mitigate water deprivation stress starting from the germination stage, taking into consideration also the intraspecific genetic variability (Pagano et al., 2023).

The priming protocols developed in this study utilize novel seed priming agents, namely, poly-gamma-glutamic acid (γ-PGA), denatured γ-PGA (dPGA), and iron (Fe) pulsing, applied to five economically important Italian rice varieties. Polyethylene glycol (PEG) was used to simulate water deprivation stress, as this is an inert and water-binding polymer with a non-ionic and impermeable long chain which mimics water and osmotic stress (Perez-Fernandez et al., 2006). γ-PGA, used as a chemical priming agent,

has the potential to alleviate the effect of water stress due to its hygroscopic and water-holding qualities (Ogunleye et al., 2015). Additionally, dPGA can be used as a nutripriming agent given that it is constituted of single glutamic acid molecules released upon γ-PGA degradation. The combination of Fe pulsing with either γ-PGA or dPGA was also conducted to investigate a possible cumulative effect on rice germination under water deprivation stress. Phenotyping (germination, seedling growth, and stress parameters), biochemical (ROS detection, Fe quantification), and molecular analyses (gene expression profiling), were carried out to investigate the effect of priming and stress conditions on rice germination.

2 Materials and methods

2.1 Seed materials and water stress treatments

A selection of five popular Italian rice (*Oryza sativa* L.) varieties, namely Carnaroli, Cerere, Unico, Lomello, and Apollo, were used for the current study. Seeds were kindly supplied by Sardo Piemontese Sementi (Sa.Pi.Se, https://sapise.it/) and the University of Pavia Botanical Garden Plant Germplasm Bank (https://terraeambiente.dip.unipv.it/it/dipartimento/risorse/banca-del-germoplasma-vegetale).

To impose water deprivation stress during seed germination, a 25% PEG6000 (polyethylene glycol) solution was used to simulate an osmotic potential of -1215.9 kPa (Stanley and Strey, 2003) while distilled water (0 kPa) was used as a non-stress control. Before selecting this concentration, preliminary trials using 15%, 20% and 25% PEG were carried out on the Lomello variety. Petri dishes, containing 30 seeds/replicate, lined with a two-layer filter paper and 7 ml of PEG6000 or water, were placed in a growth chamber at 26°C under dark for two days and subsequently at 16 h light/8 h dark cycle for 10 days. The light conditions included a photon flux density of 150 µmol $m^{-2}s^{-1}$ and 70–80% relative humidity inside the containers. The system was laid out in a complete randomized design with three replicates.

2.2 Extraction of poly-gamma glutamic acid and denatured PGA

Recovery of crude γ-PGA was conducted by adapting a protocol from Massaiu et al. (2019). *Bacillus subtilis* strain PB5390 (Ermoli et al., 2021) was streaked on an LB plate and incubated at 37° overnight for single colonies. A pre-culture was prepared by incubating 6 colonies in LB liquid media containing 0.5% glucose at 37° with 233 rpm shaking for 8 h. The OD was measured at 600 nm to calculate the volume of the pre-culture that was added to the E-medium (40 g L^{-1} $KC_5H_8NO_4$, 12 g L^{-1} $Na_3C_6H_5O_7$, 80 g L^{-1} glucose, 0.104 g L^{-1} $MnSO_4$, 0.5 g L^{-1} $MgSO_4$, 7 g L^{-1} K_2HPO_4, 0.04 g L^{-1} CaCl, 0.004 g L^{-1} FeCl, 0.05 g L^{-1} tryptophan, 0.05 g L^{-1} phenylalanine). The culture was incubated in the same conditions for 60 h. The culture was centrifuged (8,000 rpm, 15 min, 10°C) and the supernatant was collected. γ-PGA was precipitated with three volumes of cold methanol and kept at -20°C for 16 h. The mixture was later centrifuged to recover the γ-PGA pellet. The pellet was resuspended in 100 mM NaCl. The concentration of isolated crude γ-PGA was measured using a spectrophotometer at 216 nm in a quartz cuvette. A standard calibration curve with commercial γ-PGA was used to compute its concentration in g L^{-1}. Absorbance measurement was carried out via the NanoPhotometer UV/Vis spectrophotometer (Implen, Schatzbogen, München, Germany), using 100 mM NaCl as blank. Denatured γ-PGA (dPGA) was prepared by incubating the extracted γ-PGA in a 120° oven for 72 h.

2.3 Priming treatments

For γ-PGA and dPGA priming treatments, sets of 30 rice seeds were placed in an open mouth flat bottomed tube and filled with 3 ml of 1 g L^{-1} γ-PGA or dPGA. Floating seeds on the surface were gently tapped to ensure total submergence in the soaking solution. The seeds were soaked for 16 hours at room temperature before direct sowing in Petri plates containing 25%PEG solution or water.

The iron (Fe) pulsing protocol used in this study was adapted from Dey et al. (2021). A volume of 3 ml of water was poured into an open mouth-flat bottom tube containing 30 rice seeds per replicate. The seeds were soaked for 16 hours at room temperature. Afterward, the seeds were sown directly on 85 mm plastic Petri dishes lined with 2 filter papers soaked in 7 ml of 10 mM ferrous sulphate heptahydrate ($FeSO_4.7H_20$). Alternatively, iron pulsing was combined with either γ-PGA (treatment PGA-Fe) or with dPGA (treatment dPGA-Fe) priming. For the PGA-Fe and dPGA-Fe priming, water was replaced with a soaking solution of either 0.001 g L^{-1} γ-PGA or 0.001 g L^{-1} dPGA. The sowing for Fe treatment started after soaking from Day 0 of the experiment. After 3 days, the seeds were transferred to new Petri plates with 2 filter papers and 7 ml of distilled water (non-stressed condition) or 25%PEG (stressed condition) and allowed to grow for a duration of 10 days.

Water soaking (WS) was included among the treatments to serve as a control for distinguish between the effect of the different agents used (PGA, dPGA, Fe) from that of water. Moreover, WS can also be considered as a priming treatment and it was previously used as a traditional pre-sowing technique in rice cultivation (Farooq et al., 2006). For the WS treatment, rice seeds were soaked in water for 16 hours at room temperature and subsequently directly sown in the 25%PEG- or water-containing Petri dishes.

A schematic representation of the experimental design based on different priming protocols and germination in the presence of 25% PEG-induced stress or non-stress conditions is given in Figure 1.

2.4 Phenotyping analyses

The number of germinated seeds was recorded at 24 h intervals. Seeds were considered as germinated when they reached the S2 stage, when both the plumule and radicle were 2 mm long (Counce et al., 2000). Different sets of parameters were collected and calculated to evaluate germination performance, seedling growth, and stress tolerance (Kader, 2005; Ranal and Santana, 2006;

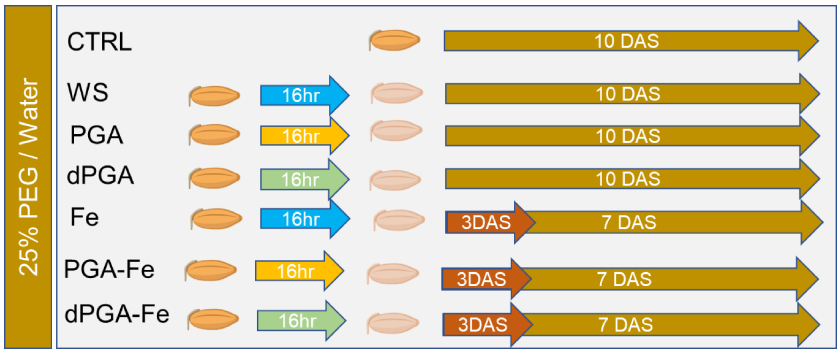

FIGURE 1
Overview of the experimental system developed to compare the effects of proposed seed priming protocols on the germination behavior of Italian rice varieties under 25%PEG-induced stress or non-stress (water) conditions. CTRL, unprimed control; WS, water soaking; PGA, poly-gamma-glutamic acid; dPGA, denatured poly-gamma-glutamic acid; Fe, iron pulsing; DAS, days after sowing. Blue arrow indicates that seeds were soaked for 16 h in water. Yellow arrow indicates that seeds were soaked for 16 h in PGA. Green arrow indicates that seeds were soaked for 16 h in dPGA.

Mahmood et al., 2022). For the evaluation of germination performance, the following parameters were used: germinability (G%), germination index (GI), mean germination time (MGT), and synchronization index (Z). To assess seedling growth, root length (Root), shoot length (Shoot), and seedling vigor index I (VII), were used. To test the water deprivation stress resilience or sensitivity, several tolerance indices were selected as follows: germination water stress tolerance index calculated at 7 days (GDTIMax), shoot length water stress tolerance index (SLWTI), and root length water stress tolerance index (RLWTI). The formulas used for the calculations of each parameter and the explanation of the obtained values are given in Supplementary Table 1. Measurements of shoot and root length were taken using the ImageJ program (https://imagej.nih.gov/ij/download.html).

2.5 Histochemical staining for Fe and H_2O_2 detection

The presence of Fe in the embryo axis was evaluated using Perl's Prussian staining protocol adapted from Shobhana et al. (2013). Seedlings were removed from the plates after 10 days from sowing, thoroughly washed with water, and soaked in Perl's stain containing 2% potassium ferrocyanide ($K_4[Fe(CN)_6]$) and 2% hydrochloric acid (HCl), for 30 min at room temperature under dark and vacuum conditions. Blue color develops in the presence of Fe in the tissue.

The levels of hydrogen peroxide (H_2O_2) in the embryo axis tissue were evaluated using the 3,3'-diaminobenzidine (DAB) staining method (Macovei et al., 2010). The DAB solution was prepared at a 0.005 g L^{-1} concentration by dissolving 3,3'-diaminobenzidine tetrahydrochloride in Tris-Buffered Saline (TBS, 50 mM Tris-Cl, pH 7.5, 150 mM NaCl) buffer. At the end of the treatments, 10-day old seedlings were soaked in 0.005 g L^{-1} DAB stain for 1 h under dark and vacuum conditions. Brown color develops in the presence of H_2O_2 in the tissue.

For both types of histochemical staining methods, a semi-quantitative approach was carried out to estimate the presence of Fe or H_2O_2 in the embryo axis, and data are presented as fold change to control. The intensity color gradient was measured using the ImageJ program.

2.6 RNA extraction and cDNA synthesis

Samples from the PEG-induced stress were collected at 3 time points, namely 16 h, 3 and 7 days after sowing (DAS), along with the embryo axis extracted from dry (untreated) mature seeds. Relatively 80 to 90 mg of tissue for embryo axis and 100 to 150 mg of tissue for seedlings were grinded in liquid N and collected into 1.5 ml tubes. For RNA isolation the TRIzol extraction method was applied following manufacturer's indications. A volume of 750 µl of TRIzol reagent (Thermo Fisher Scientific, Monza, Italy) was added to each tube, vortexed for 5 s, and incubated in ice for 5 min. A volume of 150 µl chloroform was added, gently mixed, incubated for 3 min on ice, and centrifuged at 10,000 rpm for 15 min at 4°C. The upper phase was collected and transferred to new 1.5 ml tubes and an equal volume of isopropanol was added. The samples were incubated at -20°C for 20 min then centrifuged with the same settings and the supernatant was discarded to collect the RNA pellet. The pellet was washed with 500 µl ice-cold 70% ethanol and centrifuged, followed by two additional washes with 500 µl ice cold absolute ethanol. Finally, the pellet was air dried and resuspended in nuclease-free water. The concentration of each RNA sample was measured using a Biowave spectrophotometer (Biochrom Ltd., England), and the integrity of RNA samples was assessed on agarose gel. For cDNAs synthesis, the RevertAid First Strand cDNA Synthesis Kit (ThermoFisher Scientific, Monza, Italy) was used, according to the manufacturer's recommendations.

2.7 Quantitative real-time PCR

The qRT-PCR reactions were carried out on a CFX Duet Real-time PCR system machine (Bio-rad Laboratories Inc., Milan, Italy) using the Maxima SYBR Green qPCR Master Mix (Thermo Fisher Scientific, Monza, Italy) as indicated by the manufacturer. The machine was operated using the Bio-rad CFX maestro software

(Bio-rad Laboratories Inc.) and the following amplification conditions were applied: denaturation at 95°C, 10 min, and 40 cycles of 95°C, 15 s and 60°C, 30 s, final extension at 72°C, 30 s.

Oligonucleotide primers (Supplementary Table 2) were designed using Primer3plus (https://www.primer3plus.com/index.html) and subsequently verified with Oligo Analyzer (https://eu.idtdna.com/calc/analyzer), and Primer-Blast (https://www.ncbi.nlm.nih.gov/tools/primer-blast/index.cgi?GROUP_TARGET=on). The list of investigated genes include: *LigVI (DNA LIGASE VI), FPG (FORMAMIDOPYRIMIDINE-DNA GLYCOSYLASE), NBS1 (NIJMEGEN BREAKAGE SYNDROME 1 MUTATED GENE), OGG1 (8-OXOGUANINE DNA GLYCOSYLASE), OPT7 (OLIGOPEPTIDE TRANSPORTER 7), PARP1 (POLY [ADP-RIBOSE] POLYMERASE 1), RAD51 (RADIATION SENSITIVE PROTEIN 51), TDP1α (TYROSYL-DNA PHOSPHODIESTERASE 1α), TDP1ß (TYROSYL-DNA PHOSPHODIESTERASE 1β), AoX1b (ALTERNATIVE OXIDASE 1B), APX6 (ASCORBATE PEROXIDASE 6), Cu/ZnSOD (CU/ZN SUPEROXID DISMUTASE), SODFe (FE SUPEROXID DISMUTASE), MIR (MITOCHONDRIAL-IRON REGULATED), NAS1 (NICOTIANAMINE SYNTHASE 1), NRAMP1 (NATURAL RESISTANCE-ASSOCIATED PROTEIN 1), VIT1 (VACUOLAR IRON TRANSPORTER), AAP1 (ASPARTATE AMINOTRANSFERASE 1), C3H50 (CYSTEINE 2 HISTIDINE).* The *25sRNA* was selected as a reference gene given that it was previously reported to be stable across different growth conditions and developmental stages in rice (Jain et al., 2006). The Thomsen method was used for relative quantification of transcript accumulation using the efficiency value of 1.8 (Thomsen et al., 2010). All reactions were carried out in triplicates. For data representation, Z-score was calculated on the linearized Ct values and used to generate heatmaps using the OriginPro 2023b software (OriginLab Corporation, Northampton, MA, USA).

2.8 Statistical analyses

Statistical analyses were carried out using the Statistical Tool for Agricultural Research 2.0.1 (STAR 2.0.1) software. Significant differences among varieties and treatments were determined though a two-way ANOVA (Analysis of Variance) method. The significance of the results was evaluated at a 0.05% level ($p \leq 0.05$) using the Least Significant Difference (LSD) or Tukey's Honest Significant Difference (HSD) tests. Means with the same designated letters are indicated as not significantly different. For the qRT-PCR data, the Student *t*-test (*, $p \leq 0.05$) was used for statistical interpretation where each priming treatment was compared to the non-primed control (CTRL). A Principal Component Analysis (PCA) was conducted using the Originpro 2023b software (https://www.originlab.com/2023), following user's guide specifications.

3 Results

3.1 Seed priming mitigates the negative effect of water stress during germination

Seed of Apollo, Carnaroli, Cerere, Lomello, and Unico varieties were treated with either water (WS), PGA, dPGA, Fe, PGA-Fe-, and dPGA-Fe. An unprimed control (CTRL) was also used. Primed and unprimed seeds were sown in Petri dishes under control conditions and PEG-induced stress. To evaluate the effect of the priming protocols, several germination parameters were analyzed.

In the absence of stress, no significant changes were observed in terms of germination percentage between the priming treatments and unprimed seeds (Supplementary Figure 1). The WS treatment showed a significant effect on the germination of all the tested varieties, specifically in terms of GI (Supplementary Table 3). A genotype-dependent effect of priming was observed. In Apollo, WS and PGA-Fe treatments decreased the germination time (MGT) by a day while the root length of seedlings from WS-, PGA-Fe-, and dPGA-Fe-treated seeds were significantly longer than the CTRL. The PGA, PGA-Fe, and dPGA-Fe treatments also resulted in high vigor (VII) values. For Carnaroli, increased shoot growth was observed in seedlings from WS- and dPGA-Fe-treated seeds while VII was improved only after WS treatment. The Cerere variety showed enhanced root and shoot length following WS, PGA, and dPGA treatments. The MGT decreased by 3 days in the Lomello variety, leading to a significant increase in root length following WS application. Treatments with PGA-Fe and dPGA-Fe also increased root length in Lomello. Unico showed no change in germination parameters across all priming methods applied, except for the GI values that were slightly improved upon WS treatments. Germinability (Gmax) and synchronicity (Z) did not significantly vary throughout the priming treatments in all varieties.

To simulate water deprivation stress, a PEG concentration of 25%, corresponding to -1215.9 kPa (Stanley and Strey, 2003), reported as the maximal limit in previous studies in rice (Islam et al., 2018; Sobahan et al., 2022) was used in this study. A preliminary test, conducted on the Lomello variety (Supplementary Figure 2) using 15%, 20%, and 25% PEG, indicated that 25% PEG allowed a better distinction between primed and unprimed seeds. Therefore, this concentration was chosen for subsequent analyses. Among the tested varieties, Lomello was identified as water deprivation stress tolerant as it showed germination values of 32.33 ± 5.03% under simulated drought, while Apollo, Carnaroli, Cerere, and Unico were classified as stress-sensitive since they did not germinate under these conditions (Supplementary Table 4, CTRL Gmax). However, the germinability of Apollo and Cerere seeds was rescued by iron pulsing (Fe) alone or in combination with PGA (PGA-Fe) and dPGA (dPGA-Fe). Significantly improved Gmax, GI, and VII values were registered following these priming techniques under PEG stress. The significant difference in MGT observed for Carnaroli and Cerere may be attributed to the events taking place during the first phases of germination, started during the 16 h soaking treatments applied before stress induction, while the CTRL was represented by dry seeds. The Unico variety can be considered as highly susceptible to water deprivation stress since even after the priming treatments seeds it did not germinate in the presence of PEG.

Since there was an increase in germinability among the stress-sensitive varieties upon priming, the germination water stress tolerance index (GWTI), root length, shoot length, and seedling vigor (VII) were assessed. Figure 2 shows the graphical progression of calculated values for each variety, while the statistical significance

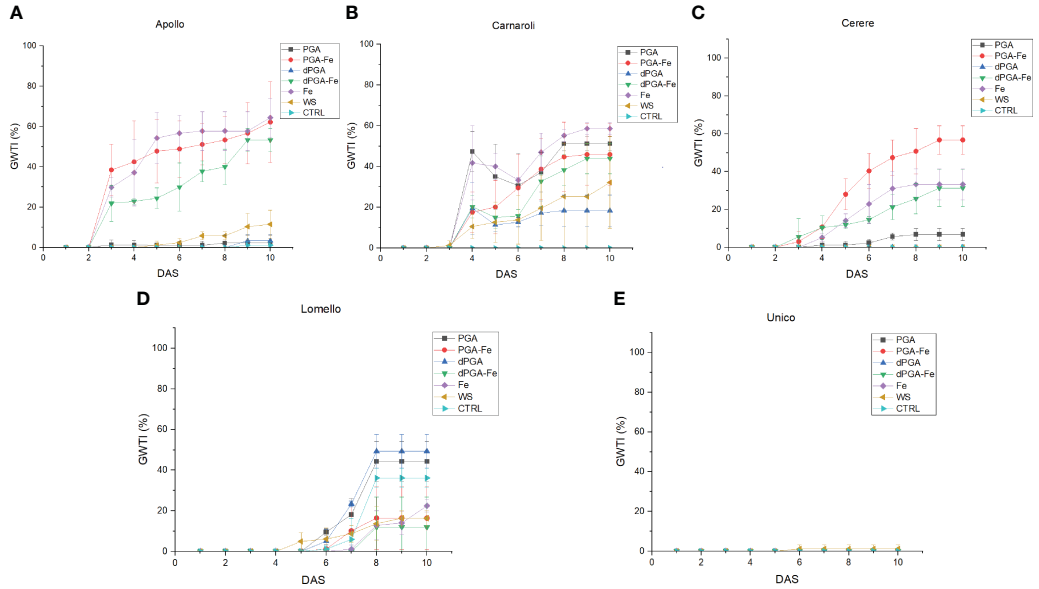

FIGURE 2
Germination water stress tolerance index (GWTI) for **(A)** Apollo, **(B)** Carnaroli, **(C)** Cerere, **(D)** Lomello, and **(E)** Unico. Data represent the means ± st.dev. of three independent replicates of 30 seeds each. CTRL, unprimed control; PGA, poly-gamma-glutamic acid; dPGA, denatured poly-gamma-glutamic acid; Fe, iron pulsing; WS, water soaking; DAS, days after sowing. Statistical analysis is provided in Supplementary Table 5.

is provided in Supplementary Table 5. Overall, the previously observed trend was maintained among varieties also for these parameters. In terms of GWTI, Apollo showed a significant enhancement after treatments when Fe was applied either alone or in combination with PGA (PGA-Fe) and dPGA (dPGA-Fe) (Figure 2A). Carnaroli showed improved GWTI for most treatments (except dPGA) when compared to the CTRL conditions, and this was particularly significant for Fe pulsed seeds, reaching 58% at 10 DAS (Figure 2B). Cerere achieved elevated GWTI values up to 57%, specifically for the PGA-Fe-treated seeds (Figure 2C). For the highly-tolerant Lomello variety (Figure 2D) and the highly-sensitive Unico variety (Figure 2E), no significant changes were observed in terms of calculated GWTI values.

When considering the calculated stress vigor indexes (Figure 3) similar patterns were observed among varieties. The elevated root length upon PEG-induced stress indicates that all seed priming treatments (except WS) applied on Carnaroli (Figure 3B), and iron pulsing (Fe, PGA-Fe, and dPGA-Fe) applied on Cerere (Figure 3C) and Apollo (Figure 3A), were able to mitigate the negative effect of water stress. The stress-tolerant Lomello variety showed significant differences compared to the CTRL for PGA and Fe pulsing treatments (Figure 3D), while no growth was registered in the case of Unico (Figure 3E) variety.

Overall, the proposed seed priming treatments were able to improve rice germination under both stress and non-stress conditions in a genotype-specific manner. The 25% PEG-induced stress strongly inhibited germination while most of the priming treatments were able to rescue it in all varieties tested except for Unico, which can be defined as highly sensitive to water deprivation stress. Importantly, the identification of Lomello as being highly stress tolerant and responsive to priming may help in enhancing its adoption not only for cultivation but also in breeding programs to further promote this trait.

3.2 The genotype-specific responses to priming are supported by PCA integrative analyses

To better evidence the genotype-specific behavior, an integrative analysis was carried out by applying a Principal Component Analysis (PCA) based on all the germination parameters collected from 1 to 10 DAS. Two PCA clusters were generated relative to the data regarding non-stressed (Figure 4A) and stressed (Figure 4B) conditions. The two principal components (PC) contributed to 70.76% (in which 47.38% belongs to PC1 and 23.38% belongs to PC2) of the observed variability for non-stressed conditions and 79.86% (in which 67.31% belongs to PC1 and 12.55% belongs to PC2) of the variability in case of PEG-induced stress. The clustering pattern obtained from the germination behavior of the seeds grown under optimal condition (Figure 4A) grouped the varieties according to the genetic clades described by Mongiano et al. (2018); namely, Carnaroli and Lomello were grouped around G2 clade, Apollo to G4, while Cerere and Unico were grouped to clade G5.

On the other side, the clustering pattern based on the data collected from PEG-induced stress revealed a treatment-based grouping (Figure 4B). Apollo and Cerere were grouped closely as responsive to iron treatments (Fe, PGA-Fe, and dPGA-Fe), while Carnaroli clustered separately since this variety was responsive to most seed treatments. Unico, was placed close to Apollo, and Cerere, forming the group of varieties sensitive to PEG-induced stress, as reflected from all the germination data. The difference

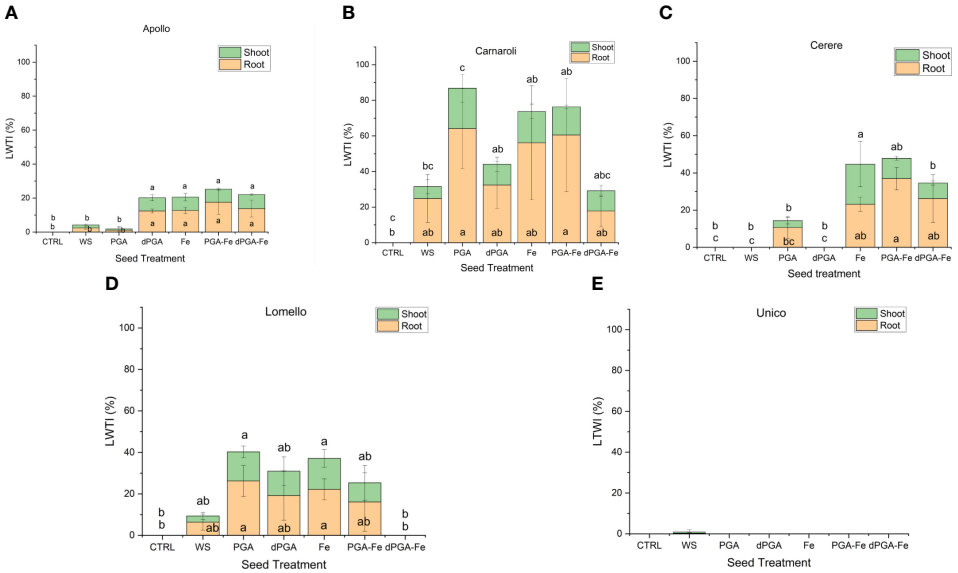

FIGURE 3
Calculated vigor tolerance indexes under stress in terms of shoot and root length (LTWI, length tolerance water stress index) for **(A)** Apollo, **(B)** Carnaroli, **(C)** Cerere, **(D)** Lomello, and **(E)** Unico. Data represent the means ± st.dev. of three independent replicates of 30 seeds each. CTRL, unprimed control; PGA, poly-gamma-glutamic acid; dPGA, denatured poly-gamma-glutamic acid; Fe, iron pulsing; WS, water soaking; DAS, days after sowing. Samples followed by different letters indicate statistically significant ($p \leq 0.05$) differences determined using the ANOVA Tukey's test.

between Unico and the other sensitive varieties consists in the fact that while Apollo and Cerere were positively affected by priming, Unico was not. Lomello represented another cluster as majority of the germination parameters investigated pointed towards an enhanced tolerance to water deprivation stress. Its position close to Carnaroli is in agreement with the fact that the priming treatments resulted in a further improvement of stress tolerance.

Based on the PCA results, it can be inferred that the G2 clade (including Lomello and Carnaroli) is a potential source of genetic materials that can be used for developing water deprivation stress tolerant varieties. Results from this analysis suggest that the trends in priming responsiveness could reflect the breeding treads presented by Mongiano et al. (2018).

3.3 Determination of iron and hydrogen peroxide accumulation during the imposed treatments

Perls Prussian blue staining was performed to measure Fe accumulation in 10 DAS seedlings while DAB staining was used to measure the accumulation of H_2O_2.

Based on the results of Perls Prussian blue staining, it can be observed that, as expected, only the Fe-related priming methods (Fe, PGA-Fe, and dPGA-Fe) displayed Fe accumulation in the germinating seedlings (Figure 5). High levels of Fe can be detected in the Cerere variety both in the absence (Figure 5A) and presence of PEG (Figure 5B). This provides further evidence in support of the previous observation regarding the high response of this variety to

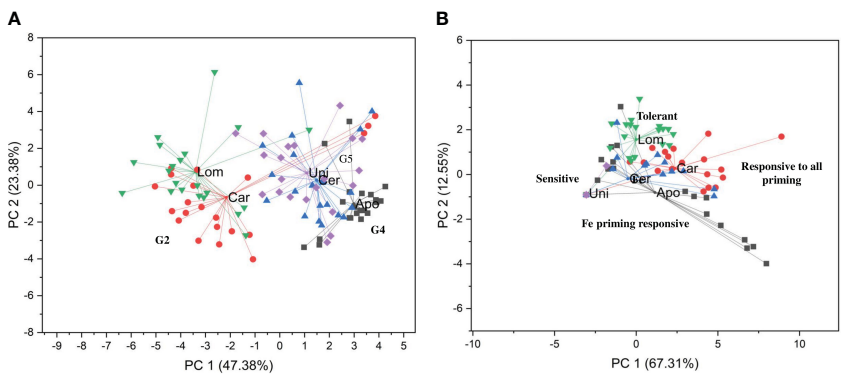

FIGURE 4
PCA clustering generated using all germination parameters collected from 1 to 10 DAS for the five Italian rice varieties and seed priming treatments. **(A)** PCA plot for optimal germination conditions. **(B)** PCA plot for PEG-induced water stress. Lom, Lomello; Car, Carnaroli; Uni, Unico; Apo, Apollo; Cer, Cerere; G2, G4, G5 genetic clades described by Mongiano et al. (2018) for variety development.

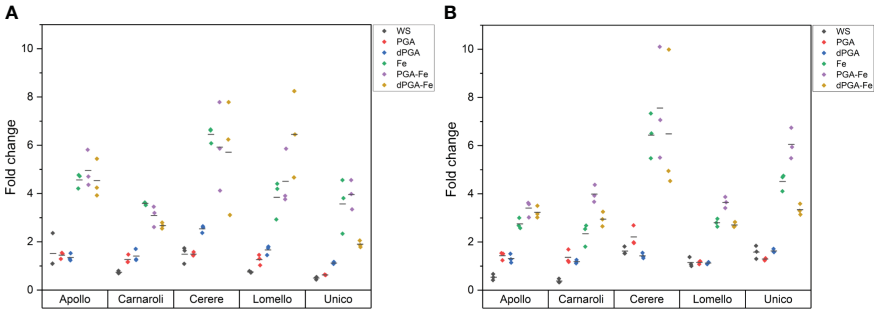

FIGURE 5
Semiquantitative measurement of iron accumulation through Perls Prussian Blue staining in 10 DAS rice seedlings in the **(A)** absence and **(B)** presence of 25% PEG-induced stress. Horizontal bars indicate the average fold change with respect to the control from the three replicates. PGA, poly-gamma-glutamic acid; dPGA, denatured poly-gamma-glutamic acid; Fe, iron pulsing; WS, water soaking.

priming treatments that includes Fe pulsing (Fe, PGA-Fe, dPGA-Fe). In the absence of stress, most varieties accumulated high Fe levels in the seedlings, except for Carnaroli, which is less responsive to Fe pulsing as evidenced by the phenotyping data. Under PEG-induced stress, Fe levels seem to decrease in most varieties, except Cerere and Unico (Figure 5B). This may be due to the fact that Fe requirement is generally enhanced during stress as Fe is needed to supply the energy and redox power necessary to support seedling growth and antioxidant activity (Rout and Sahoo, 2015).

It is well-known that overproduction of ROS can be observed during water stress while stress tolerance is associated with the ability to reduce ROS by increased activity of the antioxidant defense mechanism (Wang et al., 2019). In seeds, accumulation of H_2O_2 is also necessary to activate germination since ROS can modulate metabolic and hormone signaling pathways that induce germination (Farooq et al., 2021).

In the case of DAB staining, similar levels of H_2O_2 are observed in the presence and absence of stress (Figure 6). This may indicate that the proposed priming treatments were effective in balancing ROS production during seedling growth both under optimal and stress conditions. In terms of varieties tested, Apollo showed the lowest observed values in the absence of stress (Figure 6A). Considering the priming treatments, dPGA and dPGA-Fe resulted in the highest levels of H_2O_2 accumulation in the seedlings of Cerere and Lomello varieties. In the presence of PEG stress (Figure 6B), accumulation of H_2O_2 was induced by Fe pulsing, specifically for Carnaroli and Lomello varieties. In the case of Apollo, PGA and dPGA also resulted in enhanced H_2O_2 accumulation compared to non-stress conditions.

In conclusion, the semiquantitative measurement of Fe and H_2O_2 levels in seedlings supported the genotype-specific responses to water deprivation stress and priming treatments.

3.4 Changes in gene expression profiles in response to priming and water deprivation stress during the transition from seed to seedlings

To further investigate the observed genotype-specific responses to priming and water stress, qRT-PCR analyses were conducted on genes selected on the basis of the available literature and a preliminary data mining approach (Supplementary Figure 3). These genes belong to specific processes like DNA damage response (DDR), antioxidant defense mechanism (ADM), and Fe and Zn homeostasis (Fe/Zn). Additionally, few genes related to drought stress response and amino acid transport (SAAT) were included. DDR genes were selected because DNA damage can accumulate during the early pre-germinative phase, when rapid water uptake generates enhanced ROS production (Rajjou et al., 2012; Pagano et al., 2023). This damage must be repaired prior to cell division to minimize induction of mutations and inhibition of seedling growth and development (Waterworth et al., 2015; Waterworth et al., 2022), therefore DDR genes are envisioned as hallmarks of the seed repair response (Pagano et al., 2019; Forti et al., 2020a; Forti et al., 2020b). Rice genes associated with the antioxidant defense were evaluated as further indicators of stress tolerance (Wang et al., 2019; Panda et al., 2021). Fe/Zn related genes were selected to evaluate metal homeostasis during germination as these are important minerals for metabolic processes during germination. This is in agreement with the fact that the supply of ferrous ions as a priming treatment lead to positive effect on germination, as evidenced by the phenotypic and biochemical analyses.

To address the transition phase from seed to seedlings, the expression of the selected genes was evaluated in Carnaroli and Cerere varieties at different timepoints during germination; namely, in dry seeds (CTRL, 0 h), during seed imbibition (16 h) and at radicle protrusion (3 DAS), both in presence and absence of stress. The two varieties were selected since they exhibited sensitivity to water deprivation stress and responded differently to the imposed priming methods. Specifically, Carnaroli showed efficient responses to all the priming methods while Cerere's response was mostly related to the presence of iron (Fe, PGA-Fe, dPGA-Fe).

During seed imbibition (16 h), only WS, PGA, and dPGA priming treatments were considered in the absence of stress because this was the timepoint selected for stopping the imposed soaking treatments before proceeding with Fe pulsing and subsequent sowing on water or PEG-containing plates. Control dry, non-primed seeds (CLTR, 0 h) are also included in this comparison. The results are presented as a heatmap (Figure 7) where the blue color indicates low expression while red color indicates high gene expression. In the Carnaroli variety, the *PARP1, APX6, SOD-Fe,*

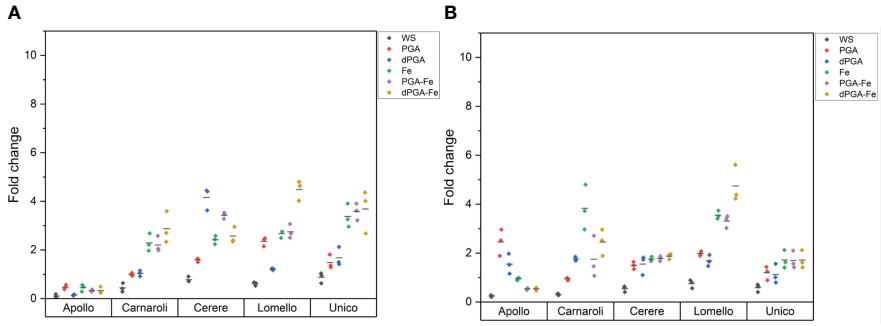

FIGURE 6
Semiquantitative measurement of H_2O_2 staining through DAB staining in 10 DAS rice seedlings in the **(A)** absence and **(B)** presence of 25% PEG-induced stress. Horizontal bars indicate the average fold change with respect to the control from the three replicates. PGA, poly-gamma-glutamic acid; dPGA, denatured poly-gamma-glutamic acid; Fe, iron pulsing; WS, water soaking.

NAS1, NRAMP1 and *MIR* genes were highly expressed in dry seeds (Figure 7B, CTRL). Changes in the expression patterns of the investigated genes were observed in response to the different priming treatments. The WS treatment resulted in a significant upregulation mainly of DDR-related genes (*NBS1, RAD51, TDP1α, LigIV*), and SAAT-related genes (*C3H50, AAP1*). Differently, some of the ADM (*SOD-Fe*) and Fe/Zn-related genes (*MIR*) were downregulated. The PGA priming resulted in significant upregulation of *NBS1*, *AOX1b*, *SOD-Cu/Zn*, and *C3H50* genes and downregulation of *PARP1*, *SOD-Fe*, *NAS1*, *NRAMP1* and *MIR* genes. Further downregulation was observed following dPGA priming where mostly the Fe/Zn homeostasis was involved (*NAS1, NRAMP1, MIR*) along with few DDR (*PARP1*) and ADM (*APX6, SOD-Cu/Zn*) genes. In the Cerere variety, all the tested genes were expressed at low levels in dry seeds (Figure 7B, CTRL). In this case, the priming treatments that mostly induced the expression of the genes were dPGA and WS while PGA resulted in a slight upregulation of only few DDR-related genes (*NBS1, PARP1, FPG*). In the case of dPGA, all tested genes were significantly upregulated compared to CTRL, whereas the WS treatment induced the expression of most ADM-, Fe/Zn- and SAAT-related genes.

At 3 DAS, the gene espression pattern was investigated in response to all priming methods in the presence and absence of PEG-induced stress (Figure 8). In this case, the CTRL samples represent seedlings obtained from unprimed seeds. The genotype-specific expression pattern is again quite evident by observing the data obtained under optimal conditions (Figures 8A, C) while PEG induced specific changes mosty when considering the different priming treatments (Figures 8B, C). In Carnaroli at 3 DAS, all the genes were already highly expressed in the CTRL samples (Figure 8A). The priming treatment resulting in a further upregulation of most genes (except for *AOX1b* wich is downregulated) in the dPGA-Fe combination. The Fe and PGA-

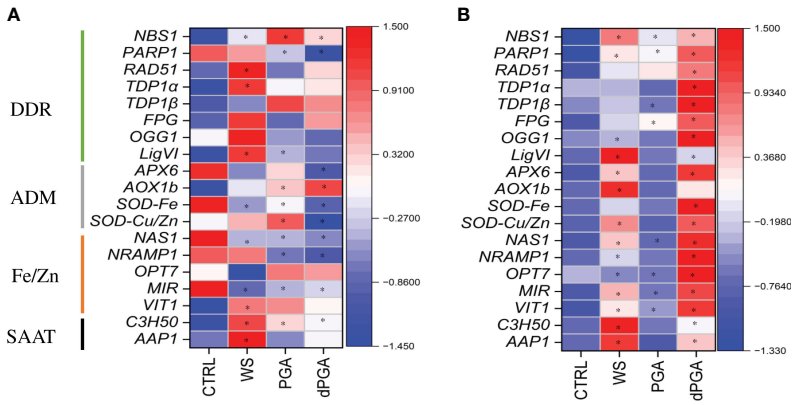

FIGURE 7
Heatmaps representing the expression patterns of the selected genes during seed imbibition (16 h) in **(A)** Carnaroli and **(B)** Cerere seeds subjected to priming treatments. *$p \leq 0.05$ as indicated by the Student *t*-test. CTRL, dry seeds, unprimed control; WS, water soaking; PGA, poly-gamma-glutamic acid; dPGA, denatured poly-gamma-glutamic acid; *LigVI, DNA LIGASE VI; FPG, FORMAMIDOPYRIMIDINE-DNA GLYCOSYLASE; NBS1, NIJMEGEN BREAKAGE SYNDROME 1 MUTATED GENE; OGG1, 8-OXOGUANINE DNA GLYCOSYLASE; OPT7, OLIGOPEPTIDE TRANSPORTER 7; PARP1, POLY [ADP-RIBOSE] POLYMERASE 1; RAD51, RADIATION SENSITIVE PROTEIN 51; TDP1α, TYROSYL-DNA PHOSPHODIESTERASE 1α; TDP1ß, TYROSYL-DNA PHOSPHODIESTERASE 1β; AoX1b, ALTERNATIVE OXIDASE 1B; APX6, ASCORBATE PEROXIDASE 6; Cu/ZnSOD, CU/ZN SUPEROXID DISMUTASE; SODFe, FE SUPEROXID DISMUTASE; MIR, MITOCHONDRIAL-IRON REGULATED; NAS1, NICOTIANAMINE SYNTHASE 1; NRAMP1, NATURAL RESISTANCE-ASSOCIATED PROTEIN 1; VIT1, VACUOLAR IRON TRANSPORTER; AAP1, ASPARTATE AMINOTRANSFERASE 1; C3H50, CYSTEINE 2 HISTIDINE.*

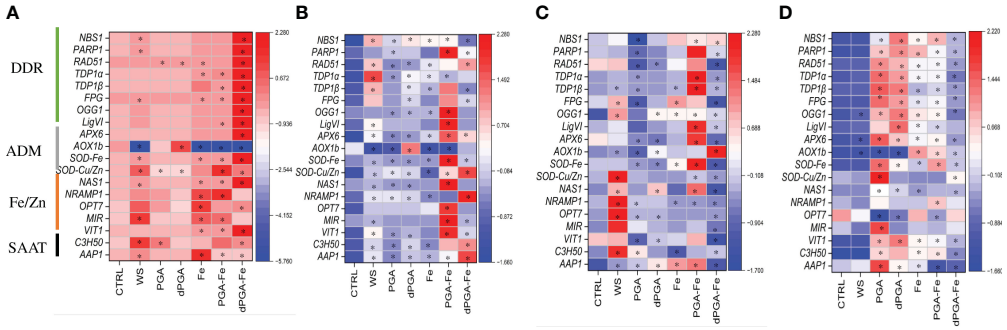

FIGURE 8
Heatmaps representing the expression patterns of selected genes at 3 days after sowing in presence/absence of priming and PEG stress. **(A)** Carnaroli seedlings under optimal conditions. **(B)** Carnaroli seedlings under PEG-induced stress. **(C)** Cerere seedlings under optimal conditions. **(D)** Cerere seedlings under PEG-induced stress. *$p \leq 0.05$ as indicated by the Student *t*-test. CTRL, dry seeds, unprimed control; WS, water soaking; PGA, poly-gamma-glutamic acid; dPGA, denatured poly-gamma-glutamic acid; Fe, iron pulsing; *LigVI, DNA LIGASE VI; FPG, FORMAMIDOPYRIMIDINE-DNA GLYCOSYLASE; NBS1, NIJMEGEN BREAKAGE SYNDROME 1 MUTATED GENE; OGG1, 8-OXOGUANINE DNA GLYCOSYLASE; OPT7, OLIGOPEPTIDE TRANSPORTER 7; PARP1, POLY [ADP-RIBOSE] POLYMERASE 1; RAD51, RADIATION SENSITIVE PROTEIN 51; TDP1α, TYROSYL-DNA PHOSPHODIESTERASE 1α; TDP1ß, TYROSYL-DNA PHOSPHODIESTERASE 1β; AoX1b, ALTERNATIVE OXIDASE 1B; APX6, ASCORBATE PEROXIDASE 6; Cu/ZnSOD, CU/ZN SUPEROXID DISMUTASE; SODFe, FE SUPEROXID DISMUTASE; MIR, MITOCHONDRIAL-IRON REGULATED; NAS1, NICOTIANAMINE SYNTHASE 1; NRAMP1, NATURAL RESISTANCE-ASSOCIATED PROTEIN 1; VIT1, VACUOLAR IRON TRANSPORTER; AAP1, ASPARTATE AMINOTRANSFERASE 1; C3H50, CYSTEINE 2 HISTIDINE.*

Fe treatments also resulted in upregulation of Fe/Zn-related genes. Differently, under PEG stress, all the genes were poorly expressed in the CTRL samples for this variety (Figure 8B). Significant gene upregulation was mainly observed following PGA-Fe priming while DDR-related genes were induced also by WS. As for Cerere, the genes were expressed at low levels in CTRL samples both in the presence or absence of stress (Figures 8C, D). Under optimal conditions, WS mostly induced a significant upregulation of Fe/Zn-related genes while the PGA-Fe priming lead to the upregulation of DDR and ADM genes (Figure 8C). Differently, upon PEG stress the priming treatments that generally induce gene upregulation were PGA and dPGA (Figure 8C). Gene upregulation was also observed following Fe pulsing (alone or in combination) but at a lower extent.

To investigate if the gene expression trends persisted, 7 DAS seedlings grown under PEG-induced stress were evaluated (Supplementary Figure 4). At this timepoint, results were similar in the two varieties. Namely, the CTRL samples were charaterized by high levels of gene expression wherease, in most cases, the priming treatments resulted in downregulation. In Carnaroli, upregulated genes included *NRAMP1* and *OPT7* in response to PGA, and *SOD-Cu/Zn* and *AAP1* in response to Fe and dPGA-Fe. In Cerere, the only upregulated gene was *AOX1b* following dPGA priming.

To summarize, the different germinative behaviour was supported by genotype-specific gene expression patterns following the transition from seeds to seedlings. Specific genes were induced by specific priming treatments both in presence and absence of PEG stress. At 16 h, WS-induced gene upregulation was present in the Carnaroli variety while dPGA mostly affected gene expression in Cerere. PEG treatments added another layer of complexity to the investigated system. In Carnaroli, most genes were downregulated by PEG at 3 DAS in CTRL samples, in agreement with the seeds not being able to germinate under stress in the absence of priming, in contrast with the high expression recorded under optimal conditions. In Cerere, WS stimulates gene expression at 3 DAS under optimal conditions while PGA and dPGA induce the expression of genes under PEG stress. Although it seems difficult to correlate the germination behaviour with the gene expression patters, it can be stated that all genes tested were differentially expressed in a genotype-, priming-, stress- and stage-dependent manner.

4 Discussion

In the current study, different seed priming treatments were developed to improve rice germination under water deprivation stress. Given the empirical nature of priming protocols and the influence that the genetic base can have on the efficacy of these treatments, five varieties of high economic impact in the Mediterranean area were tested. In a context where erratic climate changes highly affect crop productivity, screening for tolerant varieties along with the possible applications of easy-to-use, sustainable, and economic treatments to enhance germination and yield is of utmost importance.

The priming protocols developed in this study utilize novel seed priming agents like poly-gamma-glutamic acid (PGA), denatured γ-PGA (dPGA), applied alone or in combination with iron pulsing (Fe). PGA is a biodegradable, non-immunogenic and non-toxic anionic homopolymer made-up of D- and L-glutamic acid units linked by γ-amide bonds (Kimura et al., 2004; Ogunleye et al., 2015). It is mainly produced and secreted by *Bacillus* species (Osera et al., 2009). When released in the environment, γ-PGA contributes to biofilm formation and can help other organisms survive under adverse conditions (Yu et al., 2016). Additionally, the release of glutamic acid subunits from the long polymeric chains can represent a source of carbon and nitrogen (Ogunleye et al., 2015). Since it is biodegradable and non-toxic, γ-PGA has been utilized in

a wide array of applications in agriculture, cosmetics, and medical industries. In agriculture, its application generates a positive impact on plant growth, soil microbial community, nitrogen pools, and water/fertilizer use efficiency (Xu et al., 2013; Zhang et al., 2017). Recent reports associated its use to drought tolerance in several plant species, including rapeseed (Xu et al., 2020) and corn (Yin et al., 2018). Currently, there is no report proposing the use of γ-PGA as a seed priming treatment nor has this been tested on rice. Nevertheless, agricultural byproducts, including rice bran, have been used to enhance bacterial PGA production through fermentation (Tang et al., 2015; Song et al., 2019). Moreover, the denatured PGA (formed by single or few glutamic acid residues) can be envisioned as nutripriming, as an exogenous source of glutamic acid. This compound is used by plant cells for the production of GABA (gamma-aminobutyric acid), a key player in the plant response to drought as well as nitrogen mobilizer in germinating seeds (Seifikalhor et al., 2019). Iron pulsing was previously applied to rice seeds by using a ferrous salt ($FeSO_4$), and this treatment proved to be favorable during germination (Dey et al., 2021). It also promoted seedling growth by facilitating photosynthesis and nitrogen assimilation, leading to increased chlorophyll content, more efficient activity of the antioxidant system, and ultimately improved yield.

To test whether these priming methods could aid rice seeds germinate better under water deprivation stress, polyethylene glycol (PEG) was used; this agent is widely used to regulate the osmotic potential due to the high hydrophilicity that allows it to sequester water molecules. Previous reports indicated PEG as an ideal system for germination screening due to its high molecular weight that prevents its entry through the plant cell walls while simulating water retention (Islam et al., 2018; Sobahan et al., 2022). According to a 100-rice variety screening study (Islam et al., 2018), as well as other more recent reports (Sobahan et al., 2022), 25% PEG is considered the highest concentration that can be utilized for water stress simulation. Data collected in the present work on multiple parameters related to germination efficiency (G%, GI, MGT, Z), seedling growth (root, shoot, VII) and stress resilience (GDTIMax, SLWTI, RLWTI), evidenced a genotype-specific germination behavior. Carnaroli was responsive to all the priming methods, whereas Cerere and Apollo showed positive changes in the germinative behavior under the treatment with Fe, PGA-Fe, and dPGA-Fe. While the strong genotype-dependent effect of seed priming is an acknowledged feature of these treatments (Harris et al., 2001; Pradhan et al., 2015; Bhardwaj et al., 2021), it also represents a major drawback for designing efficient and universal protocols as it delays the search for common hallmarks of seed quality (Pagano et al., 2023). This was reported also in rice where a recent study investigated the genetic diversity of hydropriming applied under different soil moisture conditions (Nakao et al., 2020). The authors considered 27 genotypes, including *O. sativa* and *O. glaberrima*, representative of either wetland or dryland conditions, and reported wide genotypic differences in priming efficiency with the upland rice showing better responsiveness (Nakao et al., 2020). In our study, the application of integrative PCA further reinforced the genotype-dependent effect while also allowing to attribute each variety to the specific genetic clades that take into consideration the main breeding trends (Mongiano et al., 2018); To this purpose the G2 clade includes Carnaroli and Lomello, G4 includes Apollo, and G5 includes Cerere and Unico. Importantly, under PEG-induced stress, it was possible to also distinguish tolerant (e.g., Lomello) and sensitive (Carnaroli, Cerere, Apollo) or highly sensitive (Unico) varieties. When semiquantitative measurement of Fe and H_2O_2 levels were carried out in seedlings, the genotype-specific responses to water stress and priming treatments were further reinforced. The fact that H_2O_2 has not accumulated in stressed seedlings when priming was applied further supports the protective effect of the proposed treatments. This is in agreement with other studies carried out in rice showing that different priming techniques (hydropriming, application of selenium or salicylic acid) were able to lower ROS production under heavy metal pollution and nutrient starvation, leading to improved germination (Khan et al., 2020).

A schematic representation of the response to PEG-induces stress and the effect of seed priming treatments developed in this study is provided in Figure 9, taking into consideration the phenotyping and molecular analyses. The data pinpoints the clade distinction between the five popular rice Italian varieties along with their sensitivity/tolerance to water deprivation stress, and their responsiveness to priming. Differences observed among the varieties may be related to their seed type and breeding programs. Carnaroli, a variety obtained through hybridization and part of the G2 clade, is characterized by long grains. Cerere, a variety obtained through mutagenesis and part of the G5 clade, is characterized by the presence of short oval grains (Mongiano et al., 2018). Our study shows that both varieties are sensitive to PEG-induced stress while enhanced tolerance is gained after priming, possibly because it differentially modulates the expression of genes involved in the seed stress response.

To further explore the genotype-dependent response to priming, a targeted gene expression profile study was carried out on Carnaroli and Cerere varieties particularly focusing on the transition from seed to seedlings. A panel of genes was investigated to cover processes related to DDR, antioxidant defense, Fe/Zn homeostasis and stress response. Among the genes associated with DDR, *NBS1* (Nijmegen breakage syndrome 1 mutated gene), is a component of the MRN (MRE11-RAD50-NBS1) double-strand breaks sensor complex, while *RAD51* is directly involved in HR (homologous recombination) (Banerjee and Roy, 2021). Additional genes involved in BER (Base Excision Repair) were also selected as this type of repair pathway is often associated with damage induced by accumulation of ROS (Roldán-Arjona and Ariza, 2009). The *FPG* (formamidopyrimidine-DNA glycosylase) gene, encoding for a DNA repair enzyme that excises oxidized purines from damaged DNA, and the *OGG1* (8-oxoguanine glycosylase) gene, involved in the removal of 8-oxoG products, were proven to be highly induced during seed imbibition in multiple species (Macovei et al., 2011; Forti et al., 2021; Kowalik and Groszyk, 2023). The two *TDP1* (tyrosyl-DNA phosphodiesterase 1) genes, *TDP1α* and *TDP1β*, encoding enzymes involved in hydrolyzing phosphodiester bond formed between topoisomerase I and the 3'-DNA, were proved to be highly active during seed imbibition as well as seedling growth under stress (Macovei et al., 2010; Gualtieri et al., 2021). *PARP1* (poly-(ADP-ribose) polymerase 1) gene plays an important role in mediating the

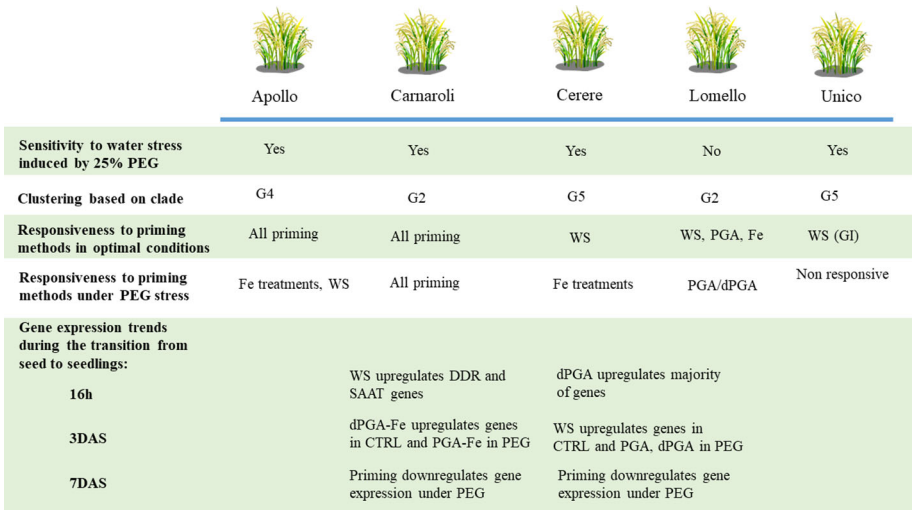

	Apollo	Carnaroli	Cerere	Lomello	Unico
Sensitivity to water stress induced by 25% PEG	Yes	Yes	Yes	No	Yes
Clustering based on clade	G4	G2	G5	G2	G5
Responsiveness to priming methods in optimal conditions	All priming	All priming	WS	WS, PGA, Fe	WS (GI)
Responsiveness to priming methods under PEG stress	Fe treatments, WS	All priming	Fe treatments	PGA/dPGA	Non responsive
Gene expression trends during the transition from seed to seedlings:					
16h		WS upregulates DDR and SAAT genes	dPGA upregulates majority of genes		
3DAS		dPGA-Fe upregulates genes in CTRL and PGA-Fe in PEG	WS upregulates genes in CTRL and PGA, dPGA in PEG		
7DAS		Priming downregulates gene expression under PEG	Priming downregulates gene expression under PEG		

FIGURE 9
Overview of the main results obtained in the current study. The sensitivity/tolerance to water deprivation stress and responsiveness to priming treatments is considered for each investigated variety. Varietal clustering based on genetic clades is provided. Gene expression trends during the transition from seed to seedling are provided for the Carnaroli and Cerere varieties.

response to DNA damage during gametophyte development (Banerjee and Roy, 2021). The *LigVI* (DNA ligase VI) gene is a plant-specific ligase essential for DNA ligase-mediated rejoining of single- and double-strand breaks, previously identified as a major determinant of seed quality in *A. thaliana* (Waterworth et al., 2010). Antioxidant-related genes, such as *APX6*, encoding for an ascorbate peroxidase isoform found in the mitochondria which participates in H_2O_2 detoxification, was shown to have a more stable expression compared with other isoforms (Rossatto et al., 2017). The *AOX1b* gene encodes an alternative oxidase known to be induced by several stresses, including oxidative stress caused by H_2O_2 exposure (Feng et al., 2009). The superoxide dismutases *SOD-Fe* and *SOD-Cu/Zn* were proven to be highly expressed in rice during salt and/or osmotic stress (Rosatto et al., 2017). For Fe/Zn genes, *NAS1* (nicotianamine synthase 1) is the gene related to Fe and Zn uptake and transport and it is highly expressed during the early stage of germination in rice (Nozoye et al., 2007). The *NRAMP1* (natural resistance-associated macrophage protein 1) gene is also associated with metal transport, being part of an important protein transporter family, highly expressed during germination (Nozoye et al., 2007). The *OPT7* (iron deficiency-regulated oligopeptide transporter 7) gene is associated with transport of ferrous ions bound to nicotianamine (Bashir et al., 2015). Another metal transporter coding gene is *VIT1* (vacuolar iron transporter), associated with Fe accumulation and reallocation during seed development and germination (Eroglu et al., 2017). Among other stress-related genes, *C3H50* (Cystenin3-Histidine50) encodes a zinc finger protein, highly induced by drought in rice via post-transcription regulation of messenger RNAs (Seong et al., 2020). This gene showed the highest expression among various C3H orthologs, especially in roots during drought stress, maybe because it has the highest number of drought-responsive elements (DRE). The *AAP1* (amino acid transporter protein 1) gene, encoding for a member of the AAT protein family, was shown to absorb and translocate a wide variety of amino acids (Ji et al., 2020). Therefore, the genes selected for this investigation cover broad aspects of the seed response to stress both during imbibition and seedling establishment. The data collected in this study indicate that these genes are differentially expressed in Carnaroli and Cerere both from the point of view of the temporal transition as well as considering the priming methods and stress treatment (Figure 9). When considering seed imbibition, the WS treatment mostly resulted in gene upregulation in Carnaroli, while in Cerere dPGA had the same effect. At the radicle protrusion stage (3 DAS), further differences were evidenced among the two varieties, as the investigated genes are highly expressed in Carnaroli while low expression values were obtained for Cerere under control conditions. Under PEG-induced stress, PGA-Fe and dPGA-Fe treatments had a greater influence on the gene expression in Carnaroli, while in Cerere mostly PGA and dPGA priming affected the expression of some genes. However, these differences subsided at later seedling development (7 DAS), when the majority of genes were downregulated by priming. This may indicate that, at a molecular level, the priming effect is fundamental during the early phases of gemination to boost seed germination and stress response.

Given the results obtained in this study, the proposed seed priming treatments can be envisioned as sustainable and versatile practices to help addressing the impact of water deprivation stress in rice. Considering the observed genotype-specific differences, further varieties should be screened and the priming treatments can be tested also in relation to other types of stress. Ultimately, filed trials should be envisioned to ascertain the effect of these priming methods on final yield under drought conditions.

Data availability statement

The original contributions presented in the study are included in the article/Supplementary Material. Further inquiries can be directed to the corresponding author.

Author contributions

CD: Data curation, Formal analysis, Investigation, Methodology, Validation, Writing – review & editing. AP: Data curation, Formal analysis, Validation, Writing – review & editing. CC: Formal analysis, Supervision, Visualization, Writing – review & editing. DS: Formal analysis, Methodology, Writing – review & editing. IS-L: Funding acquisition, Investigation, Resources, Visualization, Writing – review & editing. AB: Resources, Validation, Writing – review & editing. AM: Conceptualization, Data curation, Investigation, Supervision, Writing – original draft.

Funding

The author(s) declare financial support was received for the research, authorship, and/or publication of this article. IS-L, CD, and AM acknowledged funding received for Rice Research provided through the International Rice Research Institute (IRRI), Philippines. AM acknowledged the FRG (Fondo Ricerca Giovani) funds received through the University of Pavia from the Italian Ministry of Education and Research (MUR). CD was supported by a PhD scholarship received through the Dipartimenti di Eccellenza Program (2018-2022) - Department of Biology and Biotechnology 'L. Spallanzani', University of Pavia, provided by MUR.

Acknowledgments

The authors would like to acknowledge Dr. Carlo Minoia and his team at SA.PI.SE (Sardo Piemontese Sementi) Coop. Agricola (https://sapise.it/), as well as Prof. Graziano Rossi and Prof. Andrea Mondoni from the University of Pavia, Botanical Garden Plant Germplasm Bank (https://terraeambiente.dip.unipv.it/it/dipartimento/risorse/banca-del-germoplasma-vegetale), for kindly providing the seed materials used in this study.

Conflict of interest

The authors declare that the research was conducted in the absence of any commercial or financial relationships that could be construed as a potential conflict of interest.

The author(s) declared that they were an editorial board member of Frontiers, at the time of submission. This had no impact on the peer review process and the final decision.

Publisher's note

Supplementary material

The Supplementary Material for this article can be found online at: https://www.frontiersin.org/articles/10.3389/fpls.2024.1344383/full#supplementary-material

References

Ali, L. G., Nulit, R., Ibrahim, M. H., and Yien, C. Y. S. (2021). Efficacy of KNO_3, SiO_2 and SA priming for improving emergence, seedling growth and antioxidant enzymes of rice (*Oryza sativa*), under drought. *Sci. Rep.* 11 (1), 3864. doi: 10.1038/s41598-021-83434-3

Bailly, C., El-Maarouf-Bouteau, H., and Corbineau, F. (2008). From intracellular signaling networks to cell death: the dual role of reactive oxygen species in seed physiology. *C.R. Biol.* 331 (10), 806–814. doi: 10.1016/j.crvi.2008.07.022

Balestrazzi, A., Confalonieri, M., Macovei, A., and Carbonera, D. (2011). Seed imbibition in *Medicago truncatula* Gaertn.: Expression profiles of DNA repair genes in relation to PEG-mediated stress. *J. Plant Physiol.* 168 (7), 706–713. doi: 10.1016/j.jplph.2010.10.008

Banerjee, S., and Roy, S. (2021). An insight into understanding the coupling between homologous recombination mediated DNA repair and chromatin remodeling mechanisms in plant genome: an update. *Cell Cycle* 20 (18), 1760–1784. doi: 10.1080/15384101.2021.1966584

Bashir, K., Ishimaru, Y., Itai, R. N., Senoura, T., Takahashi, M., An, G., et al. (2015). Iron deficiency regulated OsOPT7 is essential for iron homeostasis in rice. *Plant Mol. Biol.* 88 (1-2), 165–176. doi: 10.1007/s11103-015-0315-0

Batlang, U., Baisakh, N., Ambavaram, M. M., and Pereira, A. (2013). Phenotypic and physiological evaluation for drought and salinity stress responses in rice. *Methods Mol. Biol.* 956, 209–225. doi: 10.1007/978-1-62703-194-3_15

Bhandari, U., Gajurel, A., Khadka, B., Thapa, I., Chand, I., Bhatta, D., et al. (2023). Morpho-physiological and biochemical response of rice (*Oryza sativa* L.) to drought stress: A review. *Heliyon* 9 (3), e13744. doi: 10.1016/j.heliyon.2023.e13744

Bhardwaj, A., Sita, K., Sehgal, A., Bhandari, K., Kumar, S., Prasad, P. V. V., et al. (2021). Heat priming of lentil (*Lens culinaris* Medik.) seeds and foliar treatment with γ-aminobutyric acid (GABA), confers protection to reproductive function and yield traits under high-temperature stress environments. *Int. J. Mol. Sci.* 22, 5825. doi: 10.2135/cropsci2000.402436x

Counce, P. A., Keisling, T. C., and Mitchell, A. J. (2000). A uniform, objective, and adaptive system for expressing rice development. *Crop Sci.* 40 (2), 436-443. doi: 10.2135/cropsci2000.402436x

Devika, O. S., Singh, S., Sarkar, D., Barnwal, P., Suman, J., and Rakshit, A. (2021). Seed priming: a potential supplement in integrated resource management under fragile intensive ecosystems. *Front. Sustain. Food Syst.* 5. doi: 10.3389/fsufs.2021.654001

Dey, S., Paul, S., Nag, A., Banerjee, R., Gopal, G., Mukherjee, A., et al. (2021). Iron-pulsing, a novel seed invigoration technique to enhance crop yield in rice: A journey from lab to field aiming towards sustainable agriculture. *Sci. Total Environ.* 769, 144671. doi: 10.1016/j.scitotenv.2020

Ermoli, F., Bontà, V., Vitali, G., and Calvio, C. (2021). SwrA as global modulator of the two-component system DegSU in *Bacillus subtilis*. Res. *Microbiol* 172 (6), 103877. doi: 10.1016/j.resmic.2021.103877

Eroglu, S., Giehl, R. F., Meier, B., Takahashi, M., Terada, Y., Ignatyev, K., et al. (2017). Metal tolerance protein 8 mediates manganese homeostasis and iron reallocation during seed development and germination. *Plant Physiol.* 174 (3), 1633–1647. doi: 10.1104/pp.16.01646

Farooq, M., Barsa, S. M., and Wahid, A. (2006). Priming of field-sown rice seed enhances germination, seedling establishment, allometry and yield. *Plant Growth Regul.* 49, 285–294. doi: 10.1007/s10725-006-9138-y

Farooq, M. A., Zhang, X., Zafar, M. M., Ma, W., and Zhao, J. (2021). Roles of reactive oxygen species and mitochondria in seed germination. *Front. Plant Sci.* 12. doi: 10.3389/fpls.2021.781734

Favreau, B., Gaal, C., Pereira de Lima, I., Droc, G., Roques, S., Sotillo, A., et al. (2023). A multi-level approach reveals key physiological and molecular traits in the response of

two rice genotypes subjected to water deficit at the reproductive stage. *Plant Environ. Interact.* 4 (5), 229–257. doi: 10.1002/pei3.10121

Feng, H. Q., Li, H. Y., and Sun, K. (2009). Enhanced expression of alternative oxidase genes is involved in the tolerance of rice (*Oryza sativa* L.) seedlings to drought stress. *Z Naturforsch. CJ Biosci.* 64 (9-10), 704–710. doi: 10.1515/znc-2009-9-1016

Forti, C., Ottobrino, V., Bassolino, L., Toppino, L., Rotino, G. L., Pagano, A., et al. (2020a). Molecular dynamics of pre-germinative metabolism in primed eggplant (*Solanum melongena* L.) seeds. *Hortic. Res.* 7 (1), 87. doi: 10.1038/s41438-020-0310-8

Forti, C., Shankar, A., Singh, A., Balestrazzi, A., Prasad, V., and Macovei, A. (2020b). Hydropriming and biopriming improve *Medicago truncatula* seed germination and upregulate DNA repair and antioxidant genes. *Genes (Basel)* 11 (3), 242. doi: 10.3390/genes11030242

Forti, C., Ottobrino, V., Doria, E., Bassolino, L., Toppino, L., Rotino, G. L., et al. (2021). Hydropriming applied on fast germinating Solanum villosum Miller seeds: Impact on pre-germinative metabolism. *Front Plant Sci.* 12, 639336. doi: 10.3389/fpls.2021.639336

Gerna, D., Roach, T., Arc, E., Stöggl, W., Limonta, M., Vaccino, P., et al. (2018). Redox poise and metabolite changes in bread wheat seeds are advanced by priming with hot steam. *Biochem. J.* 475 (23), 3725–3743. doi: 10.1042/BCJ20180632

Gualtieri, C., Gianella, M., Pagano, A., Cadeddu, T., Araújo, S., Balestrazzi, A., et al. (2021). Exploring microRNA signatures of DNA damage response using an innovative system of genotoxic stress in *Medicago truncatula* seedlings. *Front. Plant Sci.* 12. doi: 10.3389/fpls.2021.645323

Habib-Ur-Rahman, M., Ahmad, A., Raza, A., Hasnain, M. U., Alharby, H. F., Alzahrani, Y. M., et al. (2022). Impact of climate change on agricultural production; Issues, challenges, and opportunities in Asia. *Front. Plant Sci.* 13. doi: 10.3389/fpls.2022.925548

Han, C., and Yang, P. (2015). Studies on the molecular mechanisms of seed germination. *Proteomics* 15 (10), 1671–1679. doi: 10.1002/pmic.201400375

Harris, D., Pathan, A. K., Gothkar, P., Joshi, A., Chivasa, W., and Nyamudeza, P. (2001). On-farm seed priming: using participatory methods to revive and refine a key technology. *Agric. Syst.* 69, 151–164. doi: 10.1016/S0308-521X(01)00023-3

He, H., and Serraj, R. (2012). Involvement of peduncle elongation, anther dehiscence and spikelet sterility in upland rice response to reproductive-stage drought stress. *Environm. Exp. Bot.* 75, 120–127. doi: 10.1016/j.envexpbot.2011.09.004

Holdsworth, M. J., Finch-Savage, W. E., Grappin, P., and Job, D. (2008). Post-genomics dissection of seed dormancy and germination. *Trends Plant Sci.* 13 (1), 7–13. doi: 10.1016/j.tplants.2007.11.002

Howell, K. A., Narsai, R., Carroll, A., Ivanova, A., Lohse, M., Usadel, B., et al. (2009). Mapping metabolic and transcript temporal switches during germination in rice highlights specific transcription factors and the role of RNA instability in the germination process. *Plant Physiol.* 149, 961–980. doi: 10.1104/pp.108.129874

Ishibashi, Y., Yuasa, T., and Iwaya-Inoue, M. (2018). Mechanisms of maturation and germination in crop seeds exposed to environmental stresses with a focus on nutrients, water status, and reactive oxygen species. *Adv. Exp. Med. Biol.* 1081, 233–257. doi: 10.1007/978-981-13-1244-1_13

Islam, M. M., Kayesh, E., Zaman, E., Urmi, T. A., and Haque, M. M. (2018). Evaluation of rice (*Oryza sativa* L.) genotypes for drought tolerance at germination and early seedling stage. *Agriculturists* 16 (1), 44–54. doi: 10.3329/agric.v16i1.37533

Jain, M., Nijhawan, A., Tyagi, A. K., and Khurana, J. P. (2006). Validation of housekeeping genes as internal control for studying gene expression in rice by quantitative real-time PCR. *Biochem. Biophys. Res. Commun.* 345 (2), 646–651. doi: 10.1016/j.bbrc.2006.04.140

Ji, Y., Huang, W., Wu, B., Fang, Z., and Wang, X. (2020). The amino acid transporter AAP1 mediates growth and grain yield by regulating neutral amino acid uptake and reallocation in *Oryza sativa.* J. *Exp. Bot.* 71 (16), 4763–4777. doi: 10.1093/jxb/eraa256

Kader, M. A. (2005). A comparison of seed germination calculation formulae and the associated interpretation of resulting data. *J. Proc. - R. Soc New SOouth Wales* 138, 65–75. doi: 10.5962/p.361564

Kawaguchi, R., Suriyasak, C., Matsumoto, R., Sawada, Y., Sakai, Y., Hamaoka, N., et al. (2023). Regulation of reactive oxygen species and phytohormones in osmotic stress tolerance during seed germination in indica rice. *Front. Plant Sci.* 14. doi: 10.3389/fpls.2023.1186960

Khan, F., Hussain, S., Khan, S., and Geng, M. (2020). Seed priming improved antioxidant defense system and alleviated Ni-induced adversities in rice seedlings under N, P, or K deprivation. *Front. Plant Sci.* 11. doi: 10.3389/fpls.2020.565647

Khan, S., Ibrar, D., Bashir, S., Rashid, N., Hasnain, Z., Nawaz, M., et al. (2022). Application of Moringa leaf extract as a seed priming agent enhances growth and physiological attributes of rice seedlings cultivated under water deficit regime. *Plants (Basel).* 11 (3), 261. doi: 10.3390/plants11030261

Kimura, K., Tran, L. S. P., Uchida, I., and Itoh, Y. (2004). Characterization of *Bacillus subtilis* γ-glutamyltransferase and its involvement in the degradation of capsule poly-γ-glutamate. *Microbiol* 150 (12), 4115–4123. doi: 10.1099/mic.0.27467-0

Kota, S., Vispo, N. A., Quintana, M. R., Cabral, C. L. U., Centeno, C. A., Egdane, J., et al. (2023). Development of a phenotyping protocol for combined drought and salinity stress at seedling stage in rice. *Front. Plant Sci.* 14. doi: 10.3389/fpls.2023.1173012

Kowalik, S., and Groszyk, J. (2023). Profiling of barley, wheat, and rye FPG and OGG1 genes during grain germination. *Int. J. Mol. Sci.* 24 (15), 12354. doi: 10.3390/ijms241512354

Kranner, I., Minibayeva, F. V., Beckett, R. P., and Seal, C. E. (2010). What is stress? Concepts, definitions and applications in seed science. *New Phytol.* 188 (3), 655–673. doi: 10.1111/j.1469-8137.2010.03461.x

Kruthika, N., and Jithesh, M. N. (2023). Morpho-physiological profiling of rice (*Oryza sativa*) genotypes at germination stage with contrasting tolerance to salinity stress. *J. Plant Res.* 136 (6), 907–930. doi: 10.1007/s10265-023-01491-3

Lou, D., Lu, S., Chen, Z., Lin, Y., Yu, D., and Yang, X. (2023). Molecular characterization reveals that OsSAPK3 improves drought tolerance and grain yield in rice. *BMC Plant Biol.* 23 (1), 53. doi: 10.1186/s12870-023-04071-8

Macovei, A., Balestrazzi, A., Confalonieri, M., and Carbonera, D. (2010). The tyrosyl-DNA phosphodiesterase gene family in *Medicago truncatula* Gaertn: bioinformatic investigation and expression profiles in response to copper- and PEG-mediated stress. *Planta* 232 (2), 393–407. doi: 10.1007/s00425-010-1179-9

Macovei, A., Balestrazzi, A., Confalonieri, M., Faé, M., and Carbonera, D. (2011). New insights on the barrel medic MtOGG1 and MtFPG functions in relation to oxidative stress response in planta and during seed imbibition. *Plant Physiol. Biochem.* 49 (9), 1040–1050. doi: 10.1016/j.plaphy.2011.05.007

Macovei, A., Pagano, A., Leonetti, P., Carbonera, D., Balestrazzi, A., and Araújo, S. S. (2017). Systems biology and genome-wide approaches to unveil the molecular players involved in the pre-germinative metabolism: implications on seed technology traits. *Plant Cell Rep.* 36 (5), 669–688. doi: 10.1007/s00299-016-2060-5

Mahmood, T., Iqbal, M. S., Li, H., Nazir, M. F., Khalid, S., Sarfraz, Z., et al. (2022). Differential seedling growth and tolerance indices reflect drought tolerance in cotton. *BMC Plant Biol.* 22 (1), 331. doi: 10.1186/s12870-022-03724-4

Marthandan, V., Geetha, R., Kumutha, K., Renganathan, V. G., Karthikeyan, A., and Ramalingam, J. (2020). Seed priming: a feasible strategy to enhance drought tolerance in crop plants. *Int. J. Mol. Sci.* 21 (21), 8258. doi: 10.3390/ijms21218258

Massaiu, I., Pasotti, L., Sonnenschein, N., Rama, E., Cavaletti, M., Magni, P., et al. (2019). Integration of enzymatic data in *Bacillus subtilis* genome-scale metabolic model improves phenotype predictions and enables in silico design of poly-γ-glutamic acid production strains. *Microb. Cell Fact.* 18 (1), 1–20. doi: 10.1186/s12934-018-1052-2

Mongiano, G., Titone, P., Tamborini, L., Pilu, R., and Bregaglio, S. (2018). Evolutionary trends and phylogenetic association of key morphological traits in the Italian rice varietal landscape. *Sci. Rep.* 8 (1), 13612. doi: 10.1038/s41598-018-31909-1

Nakao, Y., Sone, C., and Sakagami, J. I. (2020). Genetic diversity of hydro priming effects on rice seed emergence and subsequent growth under different moisture conditions. *Genes (Basel)* 11 (9), 994. doi: 10.3390/genes11090994

Nozoye, T., Inoue, H., Takahashi, M., Ishimaru, Y., Nakanishi, H., Mori, S., et al. (2007). The expression of iron homeostasis-related genes during rice germination. *Plant Mol. Biol.* 64, 35–47. doi: 10.1007/s11103-007-9132-4

Ogunleye, A., Bhat, A., Irorere, V. U., Hill, D., Williams, C., and Radecka, I. (2015). Poly-γ-glutamic acid: production, properties and applications. *Microbiol* 161 (Pt 1), 1–17. doi: 10.1099/mic.0.081448-0

Oladosu, Y., Rafii, M. Y., Samuel, C., Fatai, A., Magaji, U., Kareem, I., et al. (2019). Drought resistance in rice from conventional to molecular breeding: a review. *Int. J. Mol. Sci.* 20 (14), 3519. doi: 10.3390/ijms20143519

Osakabe, Y., Osakabe, K., Shinozaki, K., and Tran, L. S. (2014). Response of plants to water stress. *Front. Plant Sci.* 5. doi: 10.3389/fpls.2014.00086

Osera, C., Amati, G., Calvio, C., and Galizzi, A. (2009). SwrAA activates poly-γ-glutamate synthesis in addition to swarming in *Bacillus subtilis*. *Microbiol* 155 (7), 2282–2287. doi: 10.1099/mic.0.026435-0

Pagano, A., Araújo, S. S., Macovei, A., Leonetti, P., and Balestrazzi, A. (2017). The seed repair response during germination: Disclosing correlations between DNA repair, antioxidant response, and chromatin remodeling in *Medicago truncatula.* Front. *Plant Sci.* 8. doi: 10.3389/fpls.2017.01972

Pagano, A., de Sousa Araújo, S., Macovei, A., Dondi, D., Lazzaroni, S., and Balestrazzi, A. (2019). Metabolic and gene expression hallmarks of seed germination uncovered by sodium butyrate in *Medicago truncatula*. *Plant Cell Environ.* 42 (1), 259–269. doi: 10.1111/pce.13342

Pagano, A., Folini, G., Pagano, P., Sincinelli, F., Rossetto, A., Macovei, A., et al. (2022). ROS accumulation as a hallmark of dehydration stress in primed and overprimed *Medicago truncatula* seeds. *Agronomy* 12, 268. doi: 10.3390/agronomy12020268

Pagano, A., Macovei, A., and Balestrazzi, A. (2023). Molecular dynamics of seed priming at the crossroads between basic and applied research. *Plant Cell Rep.* 42 (4), 657–688. doi: 10.1007/s00299-023-02988-w

Panda, D., Mishra, S. S., and Behera, P. K. (2021). Drought tolerance in rice: focus on recent mechanisms and approaches. *Rice Sci.* 28 (2), 119–132. doi: 10.1016/j.rsci.2021.01.002

Paparella, S., Araújo, S. S., Rossi, G., Wijayasinghe, M., Carbonera, D., and Balestrazzi, A. (2015). Seed priming: state of the art and new perspectives. *Plant Cell Rep.* 34, 1281–1293. doi: 10.1007/s00299-015-1784-y

Pérez-Fernández, M. A., Calvo-Magro, E., and Ferrer-Castán, D. (2006). Simulation of germination of pioneer species along an experimental drought gradient. *J. Environm. Biol.* 27 (4), 679–685.

Pradhan, N., Prakash, P., Manimurugan, C., Tiwari, S. K., Sharma, R., and Singh., P. (2015). Screening of tomato genotypes using osmopriming with PEG 6000 under salinity stress. *Res. Environ. Life Sci.* 8, 245–250.

Rajjou, L., Duval, M., Gallardo, K., Catusse, J., Bally, J., Job, C., et al. (2012). Seed germination and vigor. *Annu. Rev. Plant Biol.* 63, 507–533. doi: 10.1146/annurev-arplant-042811-105550

Ranal, M. A., and Santana, D. G. D. (2006). How and why to measure the germination process? *Braz. J. Bot.* 29, 1–11. doi: 10.1590/S0100-84042006000100002

Rang, Z. W., Jagadish, S. V. K., Zhou, Q. M., Craufurd, P. Q., and Heuer, S. (2011). Effect of high temperature and water stress on pollen germination and spikelet fertility in rice. *Environm. Exp. Bot.* 70 (1), 58–65. doi: 10.1016/j.envexpbot.2010.08.009

Reed, R. C., Bradford, K. J., and Khanday, I. (2022). Seed germination and vigor: ensuring crop sustainability in a changing climate. *Heredity (Edinb)* 128 (6), 450–459. doi: 10.1038/s41437-022-00497-2

Roldán-Arjona, T., and Ariza, R. R. (2009). Repair and tolerance of oxidative DNA damage in plants. *Mutat. Res.* 681 (2-3), 169–179. doi: 10.1016/j.mrrev.2008.07.003

Rossatto, T., do Amaral, M. N., Benitez, L. C., Vighi, I. L., Braga, E. J. B., de Magalhães Júnior, A. M., et al. (2017). Gene expression and activity of antioxidant enzymes in rice plants, cv. BRS AG, under saline stress. *Physiol. Mol. Biol. Plants.* 23, 865–875. doi: 10.1007/s12298-017-0467-2

Rout, G. R., and Sahoo, S. (2015). Role of iron in plant growth and metabolism. *Rev. Agric. Sci.* 3, 1–24. doi: 10.7831/ras.3.1

Samota, M. K., Sasi, M., Awana, M., Yadav, O. P., Amitha Mithra, S. V., Tyagi, A., et al. (2017). Elicitor-induced biochemical and molecular manifestations to improve drought tolerance in rice (*Oryza sativa* L.) through seed-priming. *Front. Plant Sci.* 8. doi: 10.3389/fpls.2017.00934

Sano, N., Lounifi, I., Cueff, G., Collet, B., Clément, G., Balzergue, S., et al. (2022). Multi-omics approaches unravel specific features of embryo and endosperm in rice seed germination. *Front. Plant Sci.* 13. doi: 10.3389/fpls.2022.867263

Sano, N., Permana, H., Kumada, R., Shinozaki, Y., Tanabata, T., Yamada, T., et al. (2012). Proteomic analysis of embryonic proteins synthesized from long-lived mRNAs during germination of rice seeds. *Plant Cell Physiol.* 53, 687–698. doi: 10.1093/pcp/pcs024

Seifikalhor, M., Aliniaeifard, S., Hassani, B., Niknam, V., and Lastochkina, O. (2019). Diverse role of γ-aminobutyric acid in dynamic plant cell responses. *Plant Cell Rep.* 38 (8), 847–867. doi: 10.1007/s00299-019-02396-z

Seong, S. Y., Shim, J. S., Bang, S. W., and Kim, J. K. (2020). Overexpression of OsC3H10, a CCCH-zinc finger, improves drought tolerance in rice by regulating stress-related genes. *Plants* 9 (10), 1298. doi: 10.3390/plants9101298

Shahzad, A., Ullah, S., Dar, A. A., Sardar, M. F., Mehmood, T., Tufail, M. A., et al. (2021). Nexus on climate change: agriculture and possible solution to cope future climate change stresses. *Environ. Sci. Pollut. Res. Int.* 28 (12), 14211–14232. doi: 10.1007/s11356-021-12649-8

Shobhana, V. G., Senthil, N., Kalpana, K., Abirami, B., Sangeetha, J., Saranya, B., et al. (2013). Comparative studies on the iron and zinc contents estimation using atomic absorption spectrophotometer and grain staining techniques (PRussian Blue and DTZ) in maize germplasms. *J. Plant Nutr.* 36 (2), 329–342. doi: 10.1080/01904167.2012.744419

Sobahan, M. A., Akter, N., and Rana, M. M. (2022). Polyethylene glycol mediated drought stress impacts on germination, growth and accumulation of proline in rice (Oryza sativa L.). *SAARC Journal of Agriculture* 20 (1), 107-119. doi: 10.3329/sja.v20i1.60544

Song, D. Y., Reddy, L. V., Charalampopoulos, D., and Wee, Y. J. (2019). Poly-(γ-glutamic acid) production and optimization from agro-industrial bioresources as renewable substrates by Bacillus sp. *FBL-2 through response surface methodology. Biomolecules.* 9 (12), 754. doi: 10.3390/biom9120754

Sperotto, R. A., Ricachenevsky, F. K., de Abreu Waldow, V., and Fett, J. P. (2012). Iron biofortification in rice: it's a long way to the top. *Plant Sci.* 190, 24–39. doi: 10.1016/j.plantsci.2012.03.004

Stanley, C. B., and Strey, H. H. (2003). Measuring osmotic pressure of poly (ethylene glycol) solutions by sedimentation equilibrium ultracentrifugation. *Macromolecules* 36 (18), 6888–6893. doi: 10.1021/ma034079e

Székely, Á., Szalóki, T., Lantos, C., Pauk, J., and Jancsó, M. (2023). Data of germination ability of tetraploid rice lines under multiple stress factors. *Data Brief.* 48, 109235. doi: 10.1016/j.dib.2023.109235

Tang, B., Lei, P., Xu, Z., Jiang, Y., Xu, Z., Liang, J., et al. (2015). Highly efficient rice straw utilization for poly-(γ-glutamic acid) production by *Bacillus subtilis* NX-2. *Bioresour. Technol.* 193, 370–376. doi: 10.1016/j.biortech.2015.05.110

Thomsen, R., Sølvsten, C. A. E., Linnet, T. E., Blechingberg, J., and Nielsen, A. L. (2010). Analysis of qPCR data by converting exponentially related Ct values into linearly related X0 values. *J. Bioinform. Comput. Biol.* 8 (5), 885–900. doi: 10.1142/s0219720010004963

Wang, X., Liu, H., Yu, F., Hu, B., Jia, Y., Sha, H., et al. (2019). Differential activity of the antioxidant defense system and alterations in the accumulation of osmolyte and reactive oxygen species under drought stress and recovery in rice (*Oryza sativa* L.) tillering. *Sci. Rep.* 9 (1), 8543. doi: 10.1038/s41598-019-44958-x

Wang, W., Zhang, C., Zheng, W., Lv, H., Li, J., Liang, B., et al. (2022). Seed priming with protein hydrolysate promotes seed germination via reserve mobilization, osmolyte accumulation and antioxidant systems under PEG-induced drought stress. *Plant Cell Rep.* 41 (11), 2173–2186. doi: 10.1007/s00299-022-02914-6

Waqas Mazhar, M., Ishtiaq, M., Hussain, I., Parveen, A., Hayat Bhatti, K., Azeem, M., et al. (2022). Seed nano-priming with Zinc Oxide nanoparticles in rice mitigates drought and enhances agronomic profile. *PloS One* 17 (3), e0264967. doi: 10.1371/journal.pone.0264967

Waterworth, W. M., Bray, C. M., and West, C. E. (2015). The importance of safeguarding genome integrity in germination and seed longevity. *J. Exp. Bot.* 66 (12), 3549–3558. doi: 10.1093/jxb/erv080

Waterworth, W. M., Bray, C. M., and West, C. E. (2019). Seeds and the art of genome maintenance. *Front. Plant Sci.* 10. doi: 10.3389/fpls.2019.00706

Waterworth, W. M., Masnavi, G., Bhardwaj, R. M., Jiang, Q., Bray, C. M., and West, C. E. (2010). A plant DNA ligase is an important determinant of seed longevity. *Plant J.* 63 (5), 848–860. doi: 10.1111/j.1365-313X.2010.04285.x

Waterworth, W. M., Latham, R., Wang, D., Alsharif, M., and West, C. E. (2022). Seed DNA damage responses promote germination and growth in Arabidopsis thaliana. *Proc. Nat. Acad. Sci.* 119 (30), e2202172119. doi: 10.1073/pnas.2202172119

Xu, Z., Ma, J., Lei, P., Wang, Q., Feng, X., and Xu, H. (2020). Poly-γ-glutamic acid induces system tolerance to drought stress by promoting abscisic acid accumulation in *Brassica napus* L. *Sci. Rep.* 10 (1), 252. doi: 10.1038/s41598-019-57190-4

Xu, Z., Wan, C., Xu, X., Feng, X., and Xu, H. (2013). Effect of poly (γ-glutamic acid) on wheat productivity, nitrogen use efficiency and soil microbes. *Acta Agric. Scand. B Soil Plant Sci.* 13 (3), 744–755. doi: 10.1080/09064710.2013.849752

Yang, P., Li, X., Wang, X., Chen, H., Chen, F., and Shen, S. (2007). Proteomic analysis of rice (*Oryza sativa*) seeds during germination. *Proteomics* 7, 3358–3368. doi: 10.1002/pmic.200700207

Yin, A., Jia, Y., Qiu, T., Gao, M., Cheng, S., Wang, X., et al. (2018). Poly-γ-glutamic acid improves the drought resistance of maize seedlings by adjusting the soil moisture and microbial community structure. *Appl. Soil Ecol.* 129, 128–135. doi: 10.1016/j.apsoil.2018.05.008

Yu, F., Li, M., He, D., and Yang, P. (2021). Advances on post-translational modifications involved in seed germination. *Front. Plant Sci.* 12. doi: 10.3389/fpls.2021.642979

Yu, Y., Yan, F., Chen, Y., Jin, C., Guo, J. H., and Chai, Y. (2016). Poly-γ-glutamic acids contribute to biofilm formation and plant root colonization in selected environmental isolates of Bacillus subtilis. *Front. Microbiol.* 7. doi: 10.3389/fmicb.2016.01811

Zhang, L., Yang, X., Gao, D., Wang, L., Li, J., Wei, Z., et al. (2017). Effects of poly-γ-glutamic acid (γ-PGA) on plant growth and its distribution in a controlled plant-soil system. *Sci. Rep.* 7 (1), 6090. doi: 10.1038/s41598-017-06248-2

frontiers | Frontiers in Plant Science

TYPE Original Research
PUBLISHED 08 February 2024
DOI 10.3389/fpls.2024.1336116

Check for updates

OPEN ACCESS

EDITED BY
Alma Balestrazzi,
University of Pavia, Italy

REVIEWED BY
Mohammad Shah Jahan,
Sher-e-Bangla Agricultural University,
Bangladesh
Chao Li,
Northwest A&F University, China

*CORRESPONDENCE
Dong Liang
liangeast@sicau.edu.cn
Hui Xia
susanxia_2001@163.com

RECEIVED 10 November 2023
ACCEPTED 22 January 2024
PUBLISHED 08 February 2024

CITATION
Zhang X, Huang T, Liang Y, Hussain S, Peng R, Wang T, Deng H, Wang J, Lv X, Liang D and Xia H (2024) Melatonin and 14-hydroxyed brassinosteroid combined promote kiwifruit seedling growth by improving soil microbial distribution, enzyme activity and nutrients uptake.
Front. Plant Sci. 15:1336116.
doi: 10.3389/fpls.2024.1336116

Melatonin and 14-hydroxyed brassinosteroid combined promote kiwifruit seedling growth by improving soil microbial distribution, enzyme activity and nutrients uptake

Xiaoli Zhang, Ting Huang, Yan Liang, Shafiq Hussain, Rui Peng, Tong Wang, Honghong Deng, Jin Wang, Xiulan Lv, Dong Liang* and Hui Xia*

College of Horticulture, Sichuan Agricultural University, Chengdu, China

Kiwifruit, a nutrient-dense fruit, has become increasingly popular with consumers in recent decades. However, kiwifruit trees are prone to stunted growth after a few years of planting, called early tree decline. In this study, melatonin (MT), pollen polysaccharide (SF), 14-hydroxyed brassinosteroid (14-HBR) were applied alone or in combination to investigate their influence on plant growth, nutrition absorption and rhizosphere bacterial abundance in kiwifruit seedlings. The results revealed that MT, SF and 14-HBR alone treatments significantly increased leaf chlorophyll content, photosynthetic capacity and activities of dismutase and catalase compared with the control. Among them, MT treatment significantly increased the dry root biomass by 35.7%, while MT +14-HBR treatment significant enhanced the dry shoot biomass by 36.9%. Furthermore, both MT and MT+14-HBR treatments markedly improved the activities of invertase, urease, protease and phosphatase in soil, as well as the abundance of Proteobacteria and Acidobacteria in rhizosphere microorganisms based on 16S rDNA sequencing. In addition, MT treatment improved the content of available K and organic matter in soil, and increased the uptake of P, K and Fe by seedlings. In summary, 14-HBR and MT combined had the best effect on promoting rhizosphere bacterial distribution, nutrient absorption and plant growth. These findings may provide valuable guidance for solving growth weakness problem in kiwifruit cultivation.

KEYWORDS

kiwifruit, melatonin, 14-hydroxyed brassinosteroid, mineral nutrients, soil microorganisms

1 Introduction

Kiwifruit (*Actinidia chinensis*) is a deciduous vine fruit tree in *Actinidia* Lindl. of Actinidiaceae family. Over the past century, kiwifruit has been successfully domesticated from wild growth to large-scale cultivation, and the kiwifruit industry has flourished worldwide (Liang et al., 2019). As a nutrient-dense fruit, kiwifruit is rich in vitamin C, dietary fiber, and mineral nutrients and phenolic compounds, *etc.*, thus favored by increasing consumers (Richardson et al., 2018). China, where the fruit originated, has also developed into the world's largest kiwifruit producer since 2010, and now accounts for more than 60% of the world's planted area (Ferguson and Huang, 2007). However, in large-scale kiwifruit cultivation, there appeared a decline of tree potential after a few years of planting, called early kiwifruit decline. It was mainly manifested as the cessation of vegetative growth, the decline of fruit yield in the overground, and the loss of fibrous roots or the decay of structural roots in the underground (Bardi, 2020). The possible causes of early kiwifruit decline have been suggested to be associated with root waterlogging, soil anoxic conditions or soil pathogenic microorganisms (Donati et al., 2020). Nevertheless, effective countermeasures for this issue are still lacking.

Plant growth regulators (PGRs) are organic compounds that are synthesized artificially (or extracted from natural organisms) and have similar functions as plant hormones in regulating growth and development (Ahmad et al., 2016; Mohanta et al., 2018). PGRs are widely used in agricultural production to achieve the purpose of increasing yield, improving crop quality and enhancing stress resistance by effectively regulating crops growth process (Spaepen et al., 2014; Kudoyarova et al., 2019). Multiple PGRs have been reported to positively regulate different physiological and biochemical processes in plants under normal and stressed conditions. Melatonin (MT), a newly discovered phytohormone, is involved in diverse plant development process, including root and stem growth, photosynthesis, callus formation, flowering, leaf senescence retardation, reactive oxygen species metabolism, and plant defense system (Jahan et al., 2023; Tan et al., 2014; Zhang et al., 2014). Moreover, MT application enhanced the decomposition of soil organic matter by increasing the activity of soil microbes and enzymes, hence contributing to the improvement of root morphology, root structure, and plant growth (Liang et al., 2018; Li et al., 2018). 14-Hydroxyed brassinosteroid (14-HBR), an important group of plant steroid hormones, performs a crucial role in various physiological functions of plants (Zhang et al., 2013; Ahammed et al., 2020). The application of brassinosteroids enhanced plant growth and biomass accumulation by improving antioxidant enzyme activity under unfavorable environmental conditions (Hussain et al., 2019; Ahammed et al., 2020). Furthermore, it efficiently enhanced the uptake of essential nutrients (N, P, K, Ca, Mg, Fe, Zn, etc.) by improving ion homeostasis in leaves and roots under extreme environmental conditions (Liu et al., 2014; Anwar et al., 2018). Pollen polysaccharide is a novel PGR containing essential nutrients for plant growth and development (Wang et al., 2013). However, little information about its beneficial role in different physiological and biochemical processes occurring in plants is known so far.

Rhizosphere microorganisms, predominantly bacteria, are tightly attached to the rhizosphere soil. The environment influences the composition and abundance of rhizosphere microorganisms, and there are interactions between microorganisms and plant hosts (Zhang et al., 2017). During plant growth, apoptosis roots and secretions serve as crucial sources of nutrition and energy for rhizosphere microorganisms. In comparison to non-rhizosphere soil, rhizosphere soil provides better water status and aeration conditions, thereby creating an optimal microenvironment for the proliferation of these microorganisms. These interactions significantly impact microbial population structure and contribute to the overall health of plant hosts. Numerous microbes in the rhizosphere act as guardians of plant health by protecting plants against pathogens and helping in nutrient acquisition from the soil (Bai et al., 2022).

However, the effect of the above-mentioned PGRs on kiwifruit growth and rhizosphere microorganisms is not well understood so far. In this study, three treatments of single MT, 14-HBR, SF, and two combined treatments MT+SF, 14-HBR+MT were designed to evaluate their effects on plant growth index, soil rhizosphere microbial abundance, and plant uptake of mineral nutrients. We hope the results can lay a foundation for the further wide application of the new PGRs and provide a reference for solving the problem of early kiwifruit decline.

2 Materials and methods

2.1 Plant preparation and treatment

A pot experiment was conducted in the greenhouse of Sichuan Agricultural University, Chengdu, China. One-year-old kiwifruit (*Actinidia chinensis*) seedlings were planted in pots (30×22 ×32cm), each filled with approximately 10.0 kg orchard soil and placed in a greenhouse with natural sunlight. Soil properties were as fellow: pH 7.08, organic matter 21.38 g/kg, total nitrogen 1.15 g/kg, total phosphorus 1.13 g/kg, total potassium 12.23 g/kg, alkali hydrolysis nitrogen 104.30 mg/kg, available phosphorus 9.87 mg/kg, available potassium 79.03 mg/kg. A total of 144 seedlings, one in each pot, were divided into six groups for treatment. Every treatment contained 15 pots as replicates. The seedlings were treated with: 1) water (CK), 2) 100 μM melatonin solution (MT), 3) pollen polysaccharide diluted 200 times (SF), 4) 14-hydroxyed brassinosteroid diluted 1500 times (14-HBR), 5) 50 μM melatonin + 14-hydroxyed brassinosteroid diluted 1500 times (MT + HBR), and 6) pollen polysaccharide diluted 200 times + 50 μM melatonin (SF+ MT), respectively. The concentration of MT was based to our previous study (Liang et al., 2019), and the concentration of 14-HBR and SF was referred to the manufacturer's recommended concentration and our preliminary experiments. The treatments were applied three times at 15 days intervals, 200 mL each time. After two months, soil and plant samples were taken for parameters determination. Part of the leaf and soil samples were stored at -80°C for DNA/RNA extraction.

2.2 Determination of plant growth parameters

The plant height, stem diameter, root length, and the fresh weight of shoot or root were recorded at 60 d after treatment. The dry weight of shoot and roots were measured after drying to a constant weight at 80°C in an oven.

2.3 Determination of root vitality and soil organic matter content

Roots deoxidation capacity was calculated by using the triphenyltetrazolium chloride method (Zhang et al., 2017). Soil organic matter content was estimated following the procedure illustrated by Mylavarapu and Zinati (2009).

2.4 Photosynthetic pigment content measurement

The content of chlorophyll a (Chl *a*), chlorophyll b (Chl *b*), total chlorophyll and carotenoid were measured following the procedure described by Liang et al. (2018). Fresh leaf samples (0.5 g) were cut into pieces and immersed in 10 mL of ethanol and acetone (1:1, v/v) solution, and kept under dark conditions for 24 hours. Leaf sap was collected and utilized for the measurement of Chl *a*, Chl *b*, and carotenoid content at 470, 646, and 663 nm, respectively, using a spectrophotometer (Thermo Fisher Scientific, USA).

2.5 Assay of gas exchange parameters

On day 10 of the drought treatment, the leaf gas exchange parameters, including net photosynthetic rate (Pn), transpiration rate (Tr), stomatal conductance (Gs), and intercellular CO_2 concentration (Ci), were measured on fully expanded leaves between 9:00 am to 11:00 am using a portable device LI-COR (Model LI-6400, LI-COR Inc., USA). A red/blue LED light source and a constant flow rate of 500 mL·min^{-1} and CO^2 concentration of ca. 400 μmol·mol^{-1} under a PAR of 1000 μmol·m^{-2}s^{-1} were used.

2.6 Determination of antioxidant enzyme activity in leaves

The activities of superoxide dismutase (SOD), peroxidase (POD), and catalase (CAT) were measured following the method of Wang and Huang (2015). 0.2 g of leaf samples were homogenized in a precooled 50 mM phosphate buffer PBS (pH 7.8) containing 1% (w/v) polyvinyl pyrrolidone PVP, 2.0 mM dithiothreitol (DTT) and 0.1 mM ethylene-diaminetetraacetic (EDTA). After centrifugation at 4°C, the supernatant was collected. POD activity was measured at 470 nm using hydrogen peroxide and guaiacol as substrates. SOD activity was estimated by monitoring the phytochemical decline of nitroblue tetrazolium (NBT) at 560 nm. CAT activity determined by recording the decrease in absorbance at 240 nm resulting from the decomposition of hydrogen peroxide (H_2O_2).

2.7 Gene expression assay

The total RNA was extracted using the Mini RNA Isolation I Kit (Beijing Tianmo Sci & Tech Development Co., Ltd, China) according to the manufacturer's instructions. The first strand cDNA was obtained by reverse transcribing RNA with PrimeScriptTM RT reagent Kit with gDNA eraser (Perfect Real Time) (Takara, Tokyo, Japan). The gene-specific primers were designed using Primer Premier5 and synthesized by Tsingke Biotechnology Co., Ltd (Beijing, China, Supplementary Table 1), *Actin* was used as the reference. Quantitative Real-time PCR was performed on the CFX96 Real-Time System C1000 Thermal Cycler (Bio-RAD, Hercules, CA, USA) using an SYBR® Premix Ex TaqTM II (Tli RnaseH Plus) kit (TaKaRa, Tokyo, Japan). The reaction conditions were as follows: 95 °C for 30 s, followed by 40 cycles of 95 °C for 5 s, and at 52 °C to 55 °C for 30 s. Each sample was subjected to three replicates. The $2^{-\Delta\Delta CT}$ method was used to calculate the relative mRNA expression level using *Actin* as the reference (Zhou et al., 2022).

2.8 Determination of soil enzymes activities

The activity of different soil enzymes was measured according to the methods described by Wang et al. (Wang Y. et al., 2016), and the activity of proteinase was estimated according to the method of Ladd and Butler (Ladd and Butler, 1972). Invertase, urease, proteinase, and phosphatase activities were represented as the amount (mg) of glucose, ammonia-nitrogen, and phenol respectively that was released per gram of dry soil in 24 h.

2.9 Estimation of the nutrients content in leaves and soil

Leaf samples were oven-dried at 65°C for two days, weighed, and immediately digested in a sulfuric acid solution. Soil samples were air-dried and ground and sieved (< 1 mm) to determine available nutrient content. The content of alkali nitrogen was determined by the alkaline diffusion method. Available phosphorus was extracted with sodium bicarbonate and determined by Mo-Sb anti-colorimetric method, and the content of available potassium was determined by atomic absorption spectrophotome-try (Greger et al., 2018). The concentrations of Zn, Mn, Cu, and Fe were estimated by ICP-MS (7900 Mass Spectrophotometer, Agilent, Santa Clara, CA, USA). Soil organic matter was determined by the potassium dichromate oxidation method.

2.10 Soil bacterial communities analysis based on 16S rDNA sequencing

DNA was extracted from the soil samples (1.0 g) using the E.Z.N.A.®Stool DNAKit (D4015, Omega, Inc., USA) according to the manufacturer's instructions. The region of V3-V4, V4, and V4-V5 of 16S rDNA was amplified. The PCR products were purified by AMPure XT beads (Beckman Coulter Genomics, Danvers, MA, USA) and quantified by Qubit (Invitrogen, Carlsbad, CA, USA). The amplicon pools were prepared for sequencing and the size and quantity of the amplicon library were assessed on Agilent 2100 Bioanalyzer (Agilent, USA) and with the Library Quantification Kit for Illumina (Kapa Biosciences, Woburn, MA, USA), respectively. The libraries were sequenced on the NovaSeq PE250 platform.

Samples were sequenced on an Illumina NovaSeq platform according to the manufacturer's recommendations, provided by LC-Bio. Paired-end reads were assigned to samples based on their unique barcode and truncated by cutting off the bar-code and primer sequence. Paired-end reads were merged using FLASH. Quality fil-tering on the raw reads was performed under specific filtering conditions to obtain high-quality clean tags according to the fqtrim (v0.94) (https://ccb.jhu.edu/software/fqtrim/index.shtml). After quality-filtering, the obtained sequences were clustered operational taxonomic units (OTUs) at a similarity of 97% using Usearch (version 7.0 http://drive5.com/usearch/). Then feature sequences was normalized using the relative abundance of each sample according to SILVA (release 132, http://www.arb-silva.de) classifier at a confidence threshold of 70%. Alpha diversity and beta diversity were calculated by QIIME2 (https://qiime2.org/), the stacked bar chart were drawn by the R package (v3.5.2). The blast was used for sequence alignment, and the feature sequences were annotated with the SILVA database for each representative sequence (Li et al., 2018).

2.11 Statistical analysis

Data were presented as mean ± standard deviation (SD). One way ANOVA was adopted for statistical analysis using SPSS 20.0 software. Tukey's multiple range test was used to compare the differences between treatments at $P < 0.05$ level.

3 Results

3.1 Effect of PGRs on morphological parameters

All treatments increased the plant growth parameters, including plant height, stem diameter, root length and root vitality compared with CK (Table 1). Among the single treatments, MT showed the most obvious effect on promoting root length by 25.2%. The combined treatment of MT and 14-hydroxyed brassinosteroid (14-HBR) further improved the growth promotion of aboveground parts, with plant height and stem diameter increased by 9.1% and 5.6% compared with MT, respectively. Consistent with the growth parameters, each PGR treatment increased the accumulation of fresh and dry weight in both roots and shoots of seedlings. MT treatment had the most significant effect on root dry mass, increasing by 35.7%, while MT+14-HBR treatment had the most significant effect on shoot dry mass accumulation, increasing by 37.0% (Table 1).

3.2 Effect of PGRs on photosynthetic pigments and gas exchange parameters

Our results revealed that all treatments significantly improved the content of photosynthetic pigments in leaves. MT enhanced the content of Chl *a*, Chl *b*, total chlorophyll, and carotenoids by 35.81%, 80%, 48.93%, or 36.36%, respectively (Figures 1A-D). For the gas exchange parameter Pn, Tr, Gs, and Ci, treatments MT, SF+MT and MT+14-HBR all had good improvement effects. MT+14-HBR had the best effect, Pn, Gs, Tr and Ci were increased by 59.44%, 84.61%, 44.15% and 4.92% compared with the control, respectively (Figures 1E-H).

3.3 Effect of PGRs on antioxidant enzyme activity and expression of related genes

All PGR treatments improved the antioxidant activities of CAT and SOD, but 14-HBR and SF+MT did not increase the enzyme activity of POD. MT and MT+14-HBR had the most significant effect, increasing SOD, POD and CAT activities by 42.02%, 36.52% and 47.32%, respectively (Figure 2A). Moreover, the expression level of related genes encoding these antioxidants were investigated by qRT-PCR. The expression level of *SOD*, *SOD[Cu-Zn]*, *POD2*, *CAT1* and *CAT6* in MT and MT+14-HBR treatments were significantly up-regulated compared with the control (Figure 2B).

3.4 Effect of PGRs on soil enzyme activities

Soil enzymes are associated with nutrient cycling and play a vital role in maintaining soil fertility. The highest values for soil invertase, urease, protease, and phosphatase activity were recorded in MT and MT+14-HBR treatments (Figure 3). MT significantly increased the activity of invertase, urease, protease, and phosphatase by 84.21%, 97.66%, 98.75%, and 33.87%, respectively. In addition, MT+14-HBR treatment also enhanced the activity of the above-mentioned enzymes.

3.5 Effect of PGRs on mineral nutrients in the soil

Different PGRs treatments significantly increased soil nutrient contents as shown in Figure 4. The maximum values for soil nitrogen (N), phosphorus (P), potassium (K), zinc (Zn), copper

TABLE 1 Effect of PGRs application on morphological parameters and biomass accumulation in kiwifruit seedlings.

Treatment	Plant height (cm)	Stem diameter (mm)	Root length (cm)	Root vitality (μg/g·h)	Biomass			
					Shoot (g FW)	Root (g FW)	Shoot (g DW)	Root (g DW)
CK	79.0± 1.8 b	4.3± 0.2 b	10.7± 0.9 b	35.2± 3.2 c	172.5± 5.1 b	77.3± 1.1 c	33.6± 2.9 b	14.1± 1.0 b
MT	101.1± 9.9 a	5.3± 0.3 a	13.4± 1.3 a	84.0± 7.2 a	216.4± 9.3 a	96.6± 1.0 a	45.2 ± 2.1 a	19.1± 2.4 a
SF	92.0± 8.8 ab	4.8± 0.2 ab	11.2± 0.9 b	47.7± 3.7 bc	196.1± 5.4 ab	86.0± 4.8 b	40.0 ± 2.4 ab	16.7± 2.2 ab
14-HBR	98.2± 7.6 ab	4.8± 0.3 ab	11.5± 0.5 b	54.0± 4.6 bc	190.0± 14.8 ab	86.6± 0.9 b	37.0 ± 7.9 ab	16.8± 1.9 ab
SF+MT	98.2± 1.4 ab	5.2± 0.5 ab	11.6± 0.6 b	61.5± 5.4 b	208.4± 11.5 a	91.4± 3.3 ab	40.4 ± 1.1 ab	17.7± 0.8 ab
MT+14-HBR	110.3± 2.3 a	5.6± 0.3 a	12.6± 1.2 ab	92.9± 8.7 a	218.4± 1.9 a	95.5± 1.5 a	46.0 ± 1.8 a	19.0± 0.8 a

Values are the mean ± SD (n=5). CK: H_2O; MT: 100 μM melatonin; SF: 200× pollen polysaccharide; 14-HBR: 1500× 14-hydroxyed brassinosteroid; SF+MT: 200× SF + 50 μM MT; MT+14-HBR: 50 μM MT + 1500×14-HBR. Different letters indicate significant differences (P<0.05) between treatments estimated by Tukey's multiple range test.

(Cu), and organic matter content were observed in MT+14-HBR. The MT+14-HBR significantly increased the N, P, K, and organic matter content by 10.48%, 17.36%, 43.54%, or 22.34% than CK. In addition, the highest values for soil Fe and Mn were recorded in MT. The MT significantly enhanced the soil Fe by 13.94% and Mn by 11.50% compared with CK.

3.6 Effect of PGRs on microorganism diversity in soil

All nutrients absorbed by plants must pass through the roots, and the structure of rhizosphere microorganisms affects the uptake of soil nutrients by the roots. Rhizosphere bacterial diversity was therefore analyzed based on 16S rDNA sequencing. 2697-3012 operational taxonomic units (OTUs) were detected in each treated soil sample, with the coverage larger than 0.96, indicating that the depths of sequencing could meet the requirements (Supplementary Table 2). A total of 31 phyla of rhizosphere bacteria were detected from soil samples, Proteobacteria, Acidobacteria, Gemmatimonadetes, Planctomycetes, Verrucomicrobia, and Chloroflexi were the dominant bacterial communities in all treatment soil samples, accounting for 80.21%. However, there were differences in the abundance of bacterial communities among treatments. Compared with the control, all PGR treatments enhanced the relative abundance of Proteobacteria and Acidobacteria, and the highest abundance was recorded in MT +14-HBR at 38.92% and 24.96%, respectively (Figure 5A). Bacterial

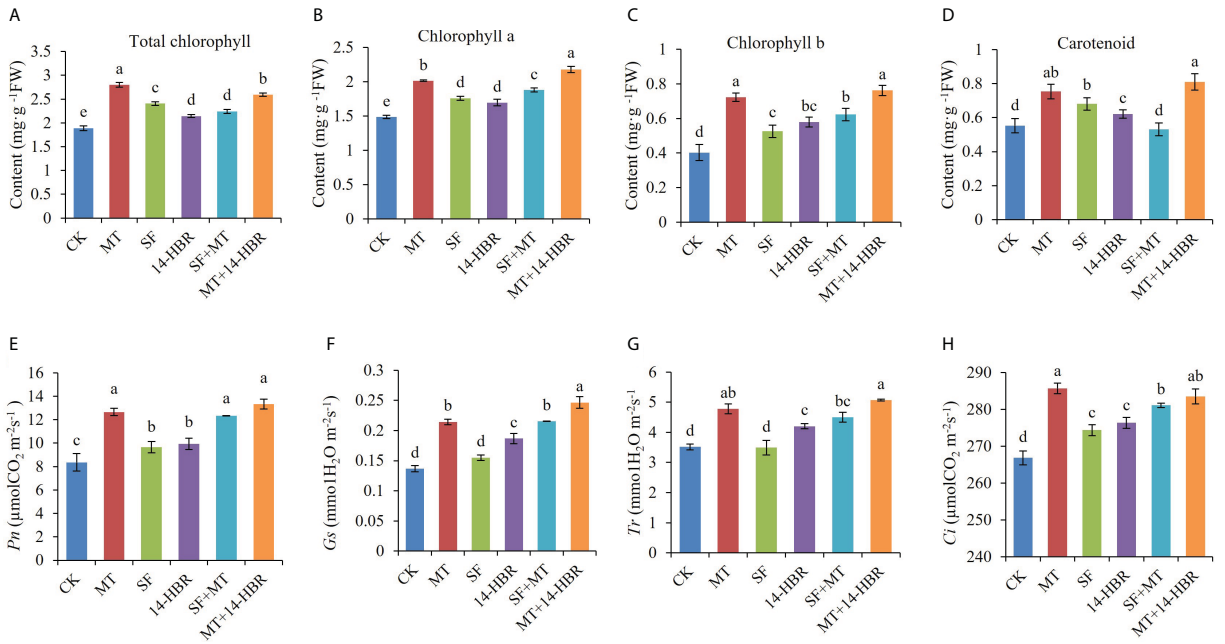

FIGURE 1
Effect of PGRs application on photosynthetic pigments **(A-D)** and gas exchange parameters **(E-H)** in kiwifruit leaves. Pn: net photosynthetic rate; Gs: stomatal conductance; Tr: transpiration rate; Ci, intercellular CO_2 concentration. CK: H_2O; MT: 100 μM melatonin; SF: 200× pollen polysaccharide; 14-HBR: 1500× 14-hydroxyed brassinosteroid; SF+MT: 200× SF + 50 μM MT; MT+14-HBR: 50 μM MT + 1500×14-HBR. Different letters indicate significant differences (*P*<0.05) between treatments estimated by Tukey's multiple range test.

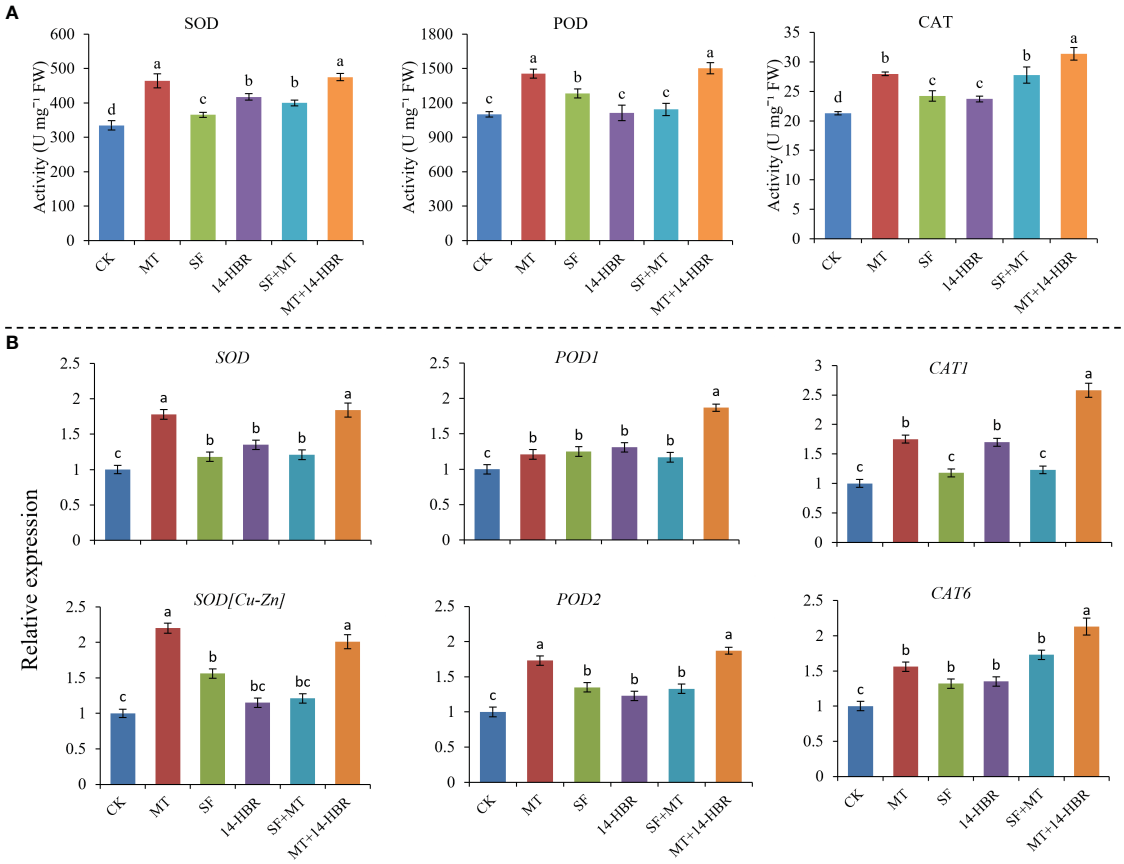

FIGURE 2
Effect of PGRs application on antioxidant enzyme activities **(A)** and gene expression **(B)**. CAT: catalase, POD: peroxidase, SOD: superoxide dismutase. CK: H_2O; MT: 100 μM melatonin; SF: 200× pollen polysaccharide; 14-HBR: 1500× 14-hydroxyed brassinosteroid; SF+MT: 200× SF + 50 μM MT; MT +14-HBR: 50 μM MT + 1500×14-HBR. Different letters indicate significant differences (P<0.05) between treatments estimated by Tukey's multiple range test.

communities with significant abundance differences between treatments were analyzed. Chloroflexi, Spirochaetes had the highest abundance in CK; Planctomycetes, Chasmydiae and BRC1 had the highest abundance in MT treatment; Dadabacteria and Actinobacteria had the highest abundance in HBR treatment; Firmicures and Candidatus_Saccharibacteria had the highest abundance in SF treatment; While MT+HBR treatment had more bacterial communities with moderate abundance (Figure 5B).

At the genus level, the dominant communities in all soil samples included Subgroup 6, Subgroup 2, Gemmatimonadaceae, Acidobacteriales, and Sphingomonas (Figure 6A). The bacterial composition among different soil samples was generally the same, but the proportions of each genus were fluctuation (Supplementary Figure 1, Supplementary Table 3). For instance, JG36-GS-52 was found only in MT and MT+14-HBR treatments. Lamia and Sphingobacteriaceae were detected in all soil treatments except SF and control treatments. Among all soil treatments, only the SF treatment soil did not show an abundance of Prosthecobacter and Luteolibacter bacterial groups. Soil samples in MT and MT+14-HBR treatments showed the highest abundance of Proteobacteria, Myxococcales, Desulfarculaceae Bdellovibrio, Subgroup 22, Bryobacter, Rokubacteriales, and Anaerolineae, respectively. All PGR treatments significantly increased the abundance of Bradyrhizobium, Alphaproteo-bacteria, Dongia, bacteriap-25, Acidobacteriaceae, and Gemmatirosa compared with the control (Figure 6B, Supplementary Figure 1).

3.7 Effect of PGRs on the absorption of nutrients

PGRs application improved nutrient contents of N, P, K, Zn, Fe, Mn and Cu in seedling leaves (Figure 7). MT and MT+14-HBR treatments significantly improved the contents of N, P, K, Fe, Mn in leaves, and SF had the best effect to increase the content of Zn and Cu than other treatments. Our findings related to leaf nutrient contents revealed that MT among alone treatments and MT+14-HBR in combined treatments showed the most promising results with a beneficial effect on multiple nutrients.

4 Discussion

In this study, the effect of three PGRs, melatonin (MT), pollen polysaccharide (SF), 14-hydroxyed brassinosteroid (14-HBR) on plant growth, nutrient uptake and rhizosphere microbiota

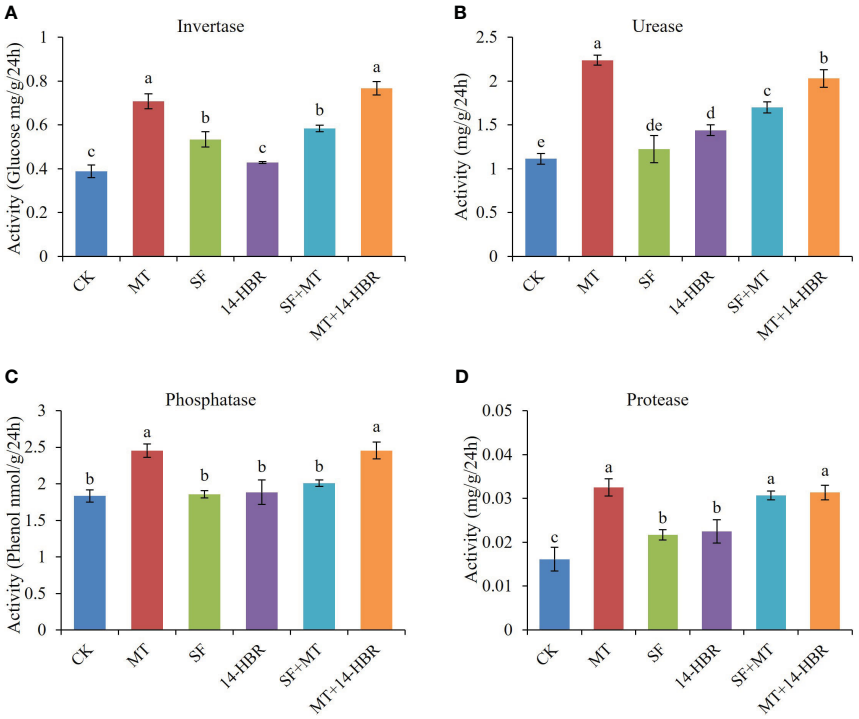

FIGURE 3
Effect of PGRs application on soil enzyme activity of invertase **(A)**, urease **(B)**, protease **(C)**, and phosphatase **(D)**. CK: H_2O; MT: 100 μM melatonin; SF: 200× pollen polysaccharide; 14-HBR: 1500× 14-hydroxyed brassinosteroid; SF+MT: 200× SF + 50 μM MT; MT+14-HBR: 50 μM MT + 1500×14-HBR. Different letters indicate significant differences (P<0.05) between treatments estimated by Tukey's multiple range test.

distribution in kiwifruit seedlings were investigated, since they play a crucial role in plant development (Chmur and Bajguz, 2021; Sun et al., 2021). We expected to find an effective way to promote plant growth and provide a reference for overcoming the early tree decline in large-scale kiwifruit cultivation, which was reported mainly due to root damage (Donati et al., 2020).

Overall, our results showed that MT, SF and 14-HBR all can increase chlorophyll content, photosynthesis capacity, and promote the kiwifruit seedling growth with an increase of shoot height, stem diameter, root length, and vitality and biomass of root and shoot, as reported in previous studies about the role of melatonin and brassinosteroid (Vardhini and Anjum, 2015; Wei et al., 2015). However, there are few reports about the application of pollen polysaccharide and 14-HBR on plant growth to date. 14-HBR is a natural brassinosteroid product derived from rape pollen that is more active than the other four chemically synthesized brassinolide compounds, including 24-epibrassinolide, 22, 23, 24-epibrassinolide, 28-epibrassinolide and 28-homobrassinolide. Pollen polysaccharide are extracted from the pollen of different plants and is rich in amino acids, proteins, vitamins, flavonoids and other beneficial ingredients (provided by the producer). Herein, our results showed that SF had a comparable effect with 14-HBR on promoting plant growth. Like other PGRs, they increased chlorophyll content, the pigment responsible for photosynthesis to capture and transmit solar energy in plants (Arnao and Hernández-Ruiz, 2009), enhanced net photosynthetic rate to provide more C-source to synthesis for the plant, thus to promoter accumulation of biomass in the plant (Szafrańska et al., 2016; Wang L. et al., 2016; Cui et al., 2017). Encouragingly, melatonin had a stronger effect than SF and 14-HBR almost in all growth parameters. To some extent, it supported melatonin as a master regulator in plants as suggested by Arnao and Hernández-Ruiz (2019).

Since soil environmental microecology is proposed as the main cause for early vine decline in kiwifruit (Donati et al., 2020), we paid special attention to the effects of PGR on soil enzyme activities and rhizosphere microorganisms. Our results showed an improvement in enzyme activity of invertase, urease and phosphatase induced by the addition of all three PGRs, with the treatments MT and MT+14-HBR most, followed by SF+MT. Melatonin have much stronger effect on enhancing urease activity than other PRGs, it may dependent on concentration in certain range, resulting a better effect of 100 μm MT than 50μm MT and 14-HBR (Figure 3). Improving soil enzyme activity can provide more nutrients such as sugar and glucose, carbon dioxide and ammonia, inorganic phosphorus to plants and rhizosphere microorganisms, making the soil more healthy (Gianfreda et al., 2005; Krajewska, 2009; Mikhailouskaya and Bogdevitch, 2009).

Soil microorganisms perform important functions in the environment via involvement in various biological as well as physio-chemical reactions occurring in soil, thus directly contributing toward soil fertility and ecosystem stability (Critter et al., 2004). In the present study, we detected significant differences in bacterial composition between the control and PGR treatments; all PGR treatments enhanced the relative abundance of Proteobacteria and Acidobacteria, whose community structures could be used as a bacterial indicator for farmland (Kim et al., 2021). Proteobacteria and Acidobacteria were the dominant bacteria in the rhizosphere of kiwifruit as reported by Liu et al.

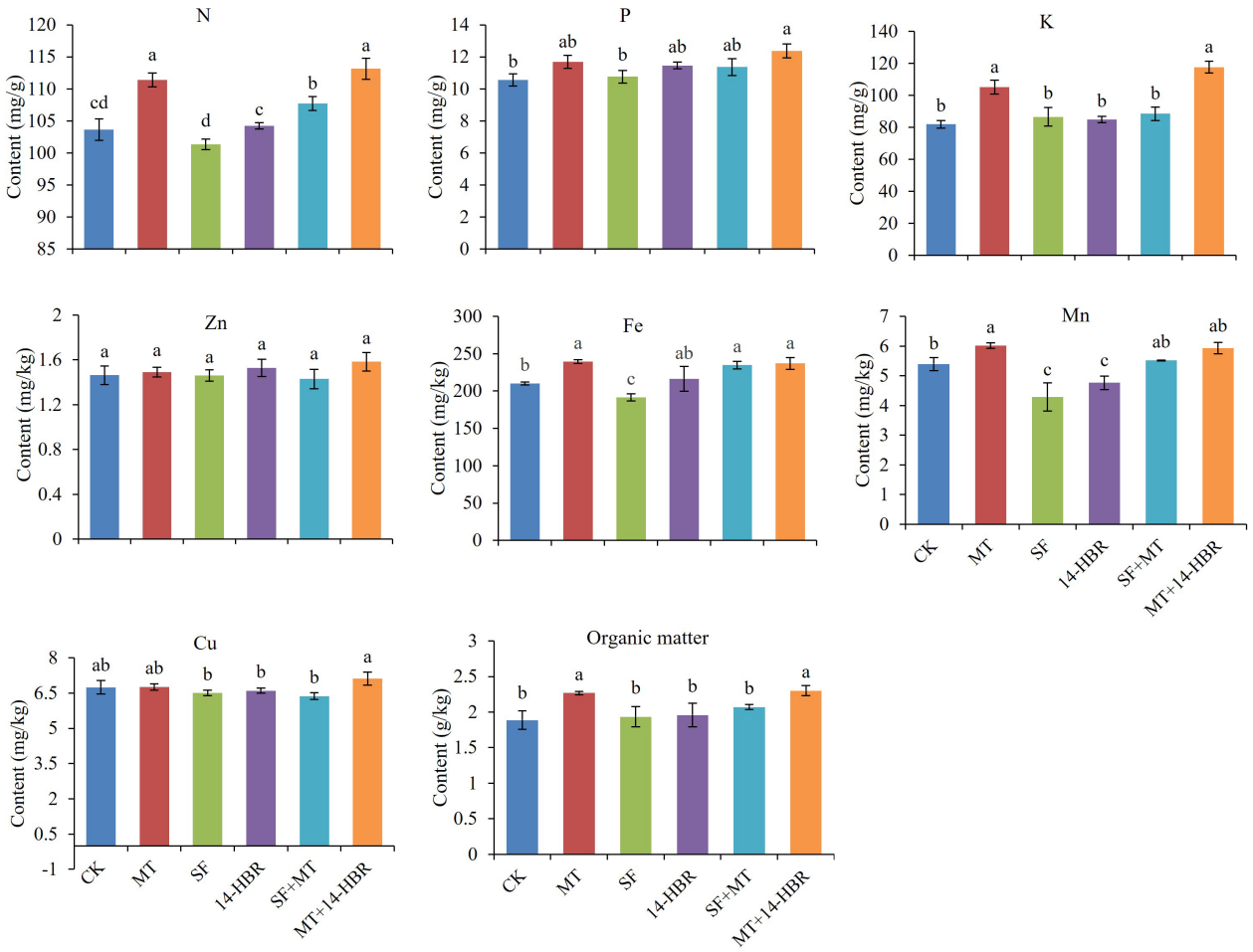

FIGURE 4
Effect of PGRs application on the content of available nitrogen (N), potassium (K), phosphorus (P), zinc (Zn), iron (Fe), manganese (Mn), copper (Cu), and organic matter in the soil. CK: H_2O; MT: 100 μM melatonin; SF: 200× pollen polysaccharide; 14-HBR: 1500× 14-hydroxyed brassinosteroid; SF +MT: 200× SF + 50 μM MT; MT+14-HBR: 50 μM MT + 1500×14-HBR. Different letters indicate significant differences (P<0.05) between treatments estimated by Tukey's multiple range test.

(2020). The enhanced abundance of Proteobacteria and Acidobacteria may be explained by enhanced soil organic matter content observed in our study (Trivedi et al., 2013). Proteobacteria, taxonomically classified as copiotrophs, exhibit rapid growth under nutrient-sufficient conditions due to their utilization of labile carbon for metabolic activities and proliferation (Fierer et al., 2007; Trivedi et al., 2013). The phylum Acidobacteria is highly abundant in the rhizosphere and contributes to polysaccharides degradation and carbon cycling (Ward et al., 2009). While the maximum relative abundance for Gemmatimonadetes, Verrucomicrobia, and Chloroflexi was recorded in the control, similar findings were reported by Li et al. (2018), where more abundance of Verrucomicrobia was detected in melatonin-free replant soil. These results suggest that a high abundance of these bacteria may act negatively and hinder the process of decomposition and nutrient cycling ultimately reducing the growth of plants as evident from our biomass data, however, this needs to be elucidated further in detail.

At the genus level, the bacterial composition among different soil samples was the same, however, the proportion of each genus showed fluctuation (Figure 6, Supplementary Table 1). For instance, JG36-GS-52 was found only in MT and MT+14-HBR treatments. Lamia and Sphingobacteriaceae were detected in all soil treatments except SF and the control. In contrast to other soil treatments, MT and MT +14-HBR treatments showed the highest abundance of Proteobacteria, Myxococcales, Desulfarculaceae Bdellovibrio, Subgroup 22, Bryobacter, Rokubacteriales, and Anaerolineae, respectively. All PGR treatments significantly enhanced the abundance of Bradyrhizobium, Alphaproteobacteria, Dongia, bacterial-25, Acidobacteriaceae, and Gemmatirosa compared with the control (Figure 6). Bradyrhizobium was reported to be the predominant in the root nodules of mung bean (Quiza et al., 2015; Hakim et al., 2021). However, the detailed mechanism by which MT and MT+14-HBR enriched the rhizosphere bacterial communities demands further in-depth studies.

Mineral nutrients are absorbed by roots from the rhizosphere in an ionic state regulated by various transport proteins. Different macronutrients (N, P, K) and micronutrients (Zn, Cu, Mn, Fe) have been reported to play indispensable functions in different physiochemical processes occurring in plants (Maathuis and Diatloff,

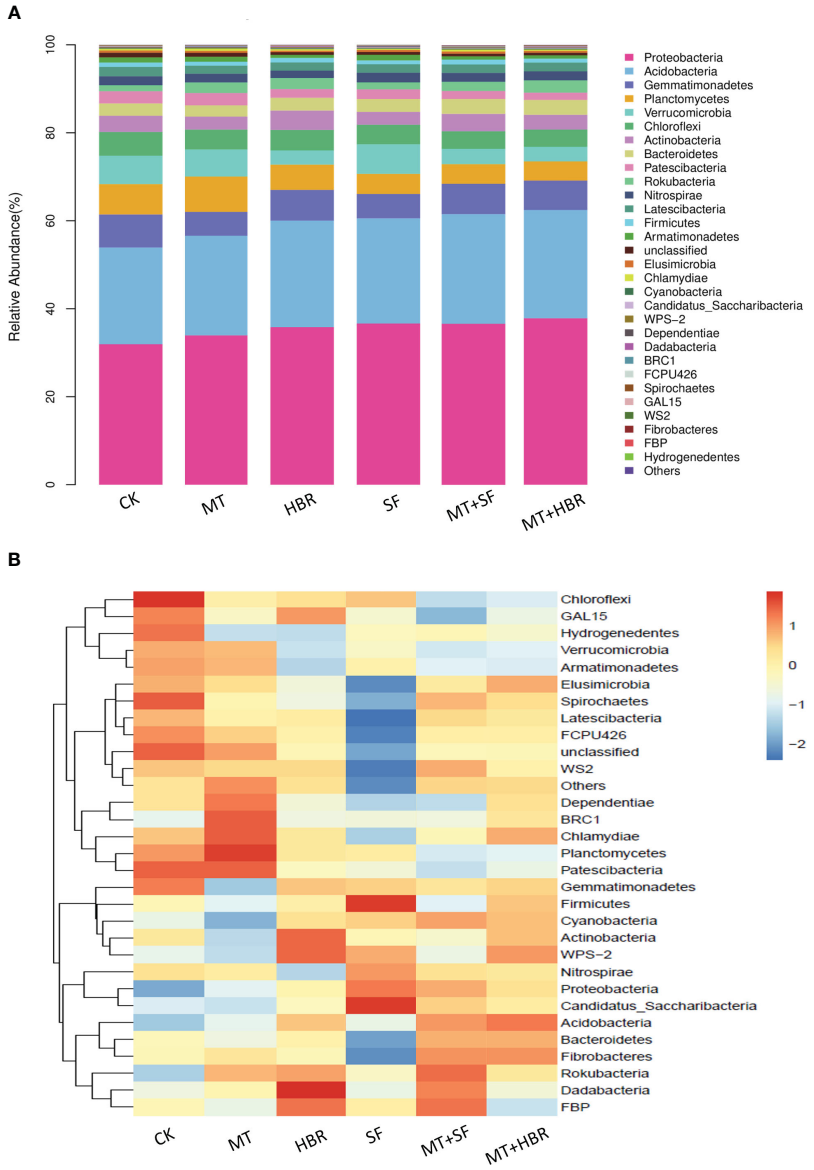

FIGURE 5
Stacked bar chart **(A)** and heatmap **(B)** of bacterial community diversity in treated soil samples at the phylum level. CK: H_2O; MT: 100 μM melatonin; SF: 200× pollen polysaccharide; 14-HBR: 1500× 14-hydroxyed brassinosteroid; SF+MT: 200× SF + 50 μM MT; MT+HBR: 50 μM MT + 1500×14-HBR.

2013; Victor Roch et al., 2019). Our results revealed that exogenous application of MT among alone treatments and MT+14-HBR in combined treatments significantly enhanced leaf and soil mineral nutrient contents as well as soil organic matter content (Figures 5, 7). Our results were parallel to the previous study (Cheng et al., 2021), where the application of brassinosteroid enhanced growth via nutrient homeostasis in soybean seedlings under normal conditions. Similar findings have also been illustrated that enhanced soil organic matter content with manure and growth regulator (NAA) combination in tomatoes (Naz et al., 2018). Our results suggested that MT and MT +14-HBR regulated improvement in mineral nutrient and organic matter content might be the result of enhanced soil enzymatic and microbial activities contributing towards better nutrient availability in soil and leaf as evident from our soil enzymatic and microbial results (Figures 4–6). Previous studies have also proved the role of soil enzymes and beneficial microbes in nutrient cycling and retaining soil fertility status (Cui et al., 2016; Li et al., 2018).

In summary, our findings showed that the application of MT and MT+14-HBR significantly enhanced the growth parameters, biomass accumulation, photosynthetic pigments and antioxidant enzyme activity compared with the control. In addition, MT and MT+14-HBR treatments markedly increased the soil enzyme activities and soil mineral nutrient content, and improved nutrient absorption by plants. Furthermore, the highest abundance of bacterial communities at phylum and genus levels was recorded in MT and MT+14-HBR treated soils. The results suggested that MT and MT+14-HBR induced improvement in morphology and physiochemical attributes of kiwifruit seedlings were associated with significant enrichment of rhizosphere with beneficial bacterial communities and soil enzymes contributing towards enhanced nutrient cycling,

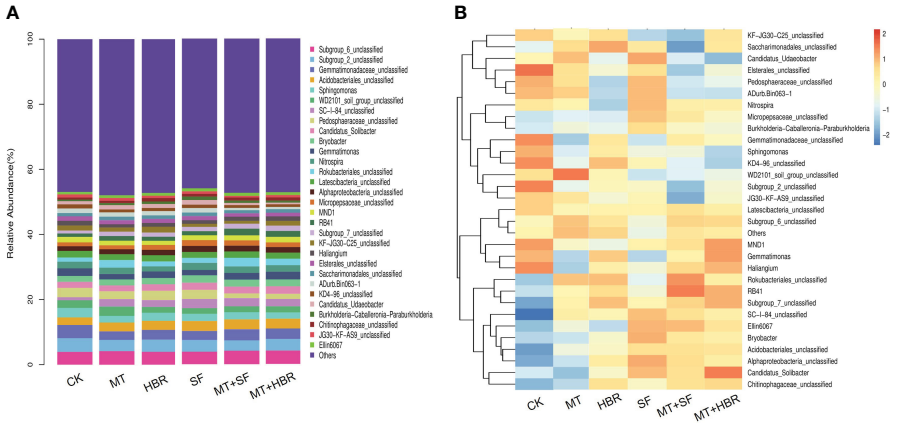

FIGURE 6
Stacked bar chart **(A)** and heatmap **(B)** of bacterial community diversity in treated soil samples at the genus level. CK: H_2O; MT: 100 μM melatonin; SF: 200× pollen polysaccharide; 14-HBR: 1500× 14-hydroxyed brassinosteroid; SF+MT: 200× SF + 50 μM MT; MT+14-HBR: 50 μM MT + 1500×14-HBR.

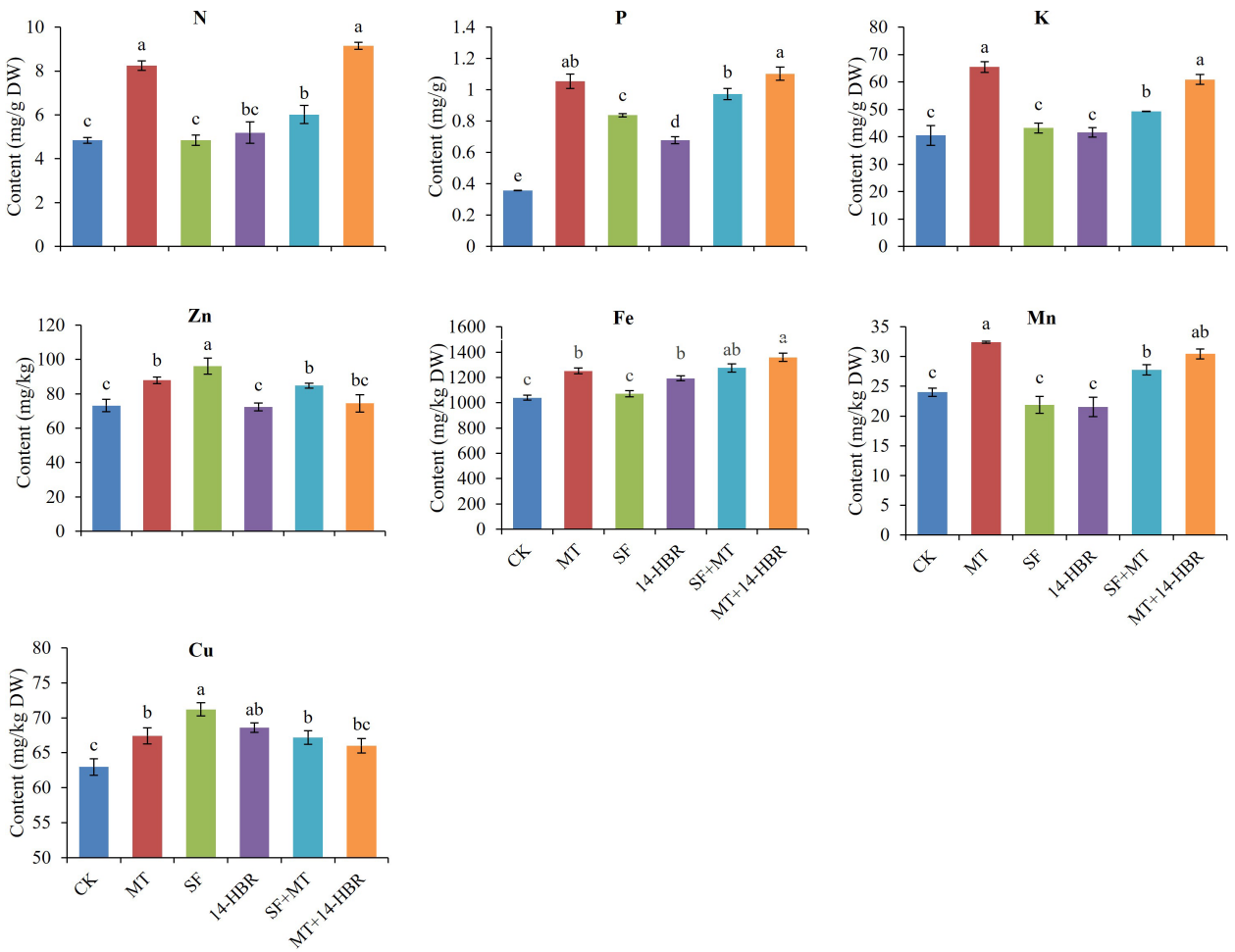

FIGURE 7
Effect of PGRs application on the content of nutrients in leaves of kiwifruit seedlings. CK: H_2O; MT: 100 μM melatonin; SF: 200× pollen polysaccharide; 14-HBR: 1500× 14-hydroxyed brassinosteroid; SF+MT: 200× SF + 50 μM MT; MT+14-HBR: 50 μM MT + 1500×14-HBR. Different letters indicate significant differences (P<0.05) between treatments estimated by Tukey's multiple range test.

degradation of organic matter, soil fertility, and ultimately improvement of plant growth.

Data availability statement

The data presented in the study are deposited in the NCBI Sequence Read Archive Bioproject repository, accession number PRJNA842376. https://www.ncbi.nlm.nih.gov/sra/?term=PRJNA842367.

Author contributions

XZ: Methodology, Validation, Writing – original draft. TH: Investigation, Methodology. YL: Investigation, Methodology. SH: Data curation, Investigation, Methodology, Writing – original draft. RP: Investigation, Methodology. TW: Investigation, Methodology. HD: Methodology, Validation. JW: Methodology, Resources. XL: Resources, Supervision. DL: Funding acquisition. HX: Funding acquisition, Supervision, Validation, Writing – review & editing.

Funding

The author(s) declare financial support was received for the research, authorship, and/or publication of this article. This work was supported by funds received from the Sichuan Science and Technology Program (2022YFH0049, 2022-YF05-0065-SN, 2023YFH0003, 23CGZH0007 and 2023ZHCG0098).

Conflict of interest

The authors declare that the research was conducted in the absence of any commercial or financial relationships that could be construed as a potential conflict of interest.

Publisher's note

All claims expressed in this article are solely those of the authors and do not necessarily represent those of their affiliated organizations, or those of the publisher, the editors and the reviewers. Any product that may be evaluated in this article, or claim that may be made by its manufacturer, is not guaranteed or endorsed by the publisher.

Supplementary material

The Supplementary Material for this article can be found online at: https://www.frontiersin.org/articles/10.3389/fpls.2024.1336116/full#supplementary-material

References

Ahammed, G. J., Li, X., Liu, A., and Chen, S. (2020). Brassinosteroids in plant tolerance to abiotic stress. *J. Plant Growth Regul.* 39 (4), 1451–1464. doi: 10.1007/s00344-020-10098-0

Ahmad, P., Rasool, S., Gul, A., Sheikh, S. A., Akram, N. A., Ashraf, M., et al. (2016). Jasmonates: multifunctional roles in stress tolerance. *Front. Plant Sci.* 7. doi: 10.3389/fpls.2016.00813

Anwar, A., Liu, Y., Dong, R., Bai, L., Yu, X., and Li, Y. (2018). The physiological and molecular mechanism of brassinosteroid in response to stress: a review. *Biol. Res.* 51, 46. doi: 10.1186/s40659-018-0195-2

Arnao, M., and Hernández-Ruiz, J. (2009). Protective effect of melatonin against chlorophyll degradation during the senescence of barley leaves. *J. Pineal Res.* 46, 58–63. doi: 10.1111/j.1600-079X.2008.00625.x

Arnao, M. B., and Hernández-Ruiz, J. (2019). Melatonin: A new plant hormone and/or a plant master regulator? *Trends Plant Sci.* 24(1), 38–48. doi: 10.1016/j.tplants.2018.10.010

Bai, B., Liu, W., Qiu, X., Zhang, J., Zhang, J., and Bai, Y. (2020). Early kiwifruit decline: A soil-borne disease syndrome or a climate change effect on plant–soil relations? *Front. Agron.* 2. doi: 10.3389/fagro.2020.00003

Bardi, L. (2020). Early kiwifruit decline: A soil-borne disease syndrome or a climate change effect on plant–soil relations? *Front. Agron.* 2. doi: 10.3389/fagro.2020.00003

Cheng, L., Li, M., Min, W., Wang, M., Chen, R., and Wang, W. (2021). Optimal brassinosteroid levels are required for soybean growth and mineral nutrient homeostasis. *Int. J. Mol. Sci.* 22, 8400. doi: 10.3390/ijms22168400

Chmur, M., and Bajguz, A. (2021). Brassinolide enhances the level of brassinosteroids, protein, pigments, and monosaccharides in wolffia arrhiza treated with brassinazole. *Plants* 10, 1311. doi: 10.3390/plants10071311

Critter, S. A., Freitas, S. S., and Airoldi, C. (2004). Microcalorimetric measurements of the metabolic activity by bacteria and fungi in some Brazilian soils amended with different organic matter. *Thermochimica Acta* 417 (2), 275–281. doi: 10.1016/j.tca.2003.09.033

Cui, G., Zhao, X., Liu, S., Sun, F., Zhang, C., and Xi, Y. (2017). Beneficial effects of melatonin in overcoming drought stress in wheat seedlings. *Plant Physiol. Biochem.* 118, 138–149. doi: 10.1016/j.plaphy.2017.06.014

Cui, Z., Ojaghian, M., Tao, Z., Kakar, K., Zeng, J., Zhao, W., et al. (2016). Multiplex PCR assay for simultaneous detection of six major bacterial pathogens of rice. *J. Appl. Microbiol.* 120, 1357–1367. doi: 10.1111/jam.13094

Donati, I., Cellini, A., Sangiorgio, D., Caldera, E., Sorrenti, G., and Spinelli, F. (2020). Pathogens associated to kiwifruit vine decline in Italy. *Agriculture* 10 (4), 119. doi: 10.3390/agriculture10040119

Ferguson, A. R., and Huang, H. (2007). Genetic resources of kiwifruit: domestication and breeding. *Hortic. Rev.* 33, 1–121. doi: 10.1002/9780470168011.ch1

Fierer, N., Bradford, M. A., and Jackson, R. B. (2007). Toward an ecological classification of soil bacteria. *Ecology* 88, 1354–1364. doi: 10.1890/05-1839

Gianfreda, L., Rao, M. A., Piotrowska, A., Palumbo, G., and Colombo, C. (2005). Soil enzyme activities as affected by anthropogenic alterations: intensive agricultural practices and organic pollution. *Sci. Total Environ.* 341, 265–279. doi: 10.1016/j.scitotenv.2004.10.005

Greger, M., Landberg, T., and Veculik, M. (2018). Silicon influences soil availability and accumulation of mineral nutrients in various plant species. *Plants* 7 (2), 41. doi: 10.3390/plants7020041

Hakim, S., Imran, A., and Mirza, M. S. (2021). Phylogenetic diversity analysis reveals Bradyrhizobium yuanmingense and Ensifer aridi as major symbionts of mung bean (Vigna radiata L.) in Pakistan. *Braz. J. Microbiol.* 52, 311–324. doi: 10.1007/s42770-020-00397-9

Hussain, M., Khan, T. A., Yusuf, M., and Fariduddin, Q. (2019). Silicon-mediated role of 24-epibrassinolide in wheat under high-temperature stress. *Environ. Sci. pollut. Res.* 26 (17), 17163–17172. doi: 10.1007/s11356-019-04938-0

Jahan, M. S., Zhao, C. J., Shi, L. B., Liang, X. R., Jabborova, D., Nasar, J., et al. (2023). Physiological mechanism of melatonin attenuating to osmotic stress tolerance in soybean seedlings. *Front. Plant Sci.* 14. doi: 10.3389/fpls.2023.1193666

Kim, H. S., Lee, S. H., Jo, H. Y., Finneran, K. T., and Kwon, M. J. (2021). Diversity and composition of soil Acidobacteria and Proteobacteria communities as a bacterial indicator of past land-use change from forest to farmland. *Sci. Total Environ.* 797, 148944. doi: 10.1016/j.scitotenv.2021.148944

Krajewska, B. (2009). Ureases I. Functional, catalytic and kinetic properties: A review. *J. Mol. Catalysis B: Enzymatic* 59 (1-3), 9–21. doi: 10.1016/j.molcatb.2009.01.003

Kudoyarova, G., Arkhipova, T., Korshunova, T., Bakaeva, M., Loginov, O., and Dodd, I. C. (2019). Phytohormone mediation of interactions between plants and non-symbiotic growth promoting bacteria under edaphic stresses. *Front. Plant Sci.* 10. doi: 10.3389/fpls.2019.01368

Ladd, J. N., and Butler, J. H. A. (1972). Short-term assays of soil proteolytic enzyme activities using proteins and dipeptide derivatives as substrates. *Soil Biol. Biochem.* 4 (1), 19–30. doi: 10.1016/0038-0717(72)90038-7

Li, C., Zhao, Q., Gao, T., Wang, H., Zhang, Z., Liang, B., et al. (2018). The mitigation effects of exogenous melatonin on replant disease in apple. *J. Pineal Res.* 65, e12523. doi: 10.1111/jpi.12523

Liang, D., Ni, Z., Xia, H., Xie, Y., Lv, X., Wang, J., et al. (2019). Exogenous melatonin promotes biomass accumulation and photosynthesis of kiwifruit seedlings under drought stress. *Scientia Hortic.* 246, 34–43. doi: 10.1016/j.scienta.2018.10.058

Liang, D., Shen, Y., Ni, Z., Wang, Q., Lei, Z., Xu, N., et al. (2018). Exogenous melatonin application delays senescence of kiwifruit leaves by regulating the antioxidant capacity and biosynthesis of flavonoids. *Front. Plant Sci.* 9. doi: 10.3389/fpls.2018.00426

Liu, J., Gao, H., Wang, X., Zheng, Q., Wang, C., Wang, X., et al. (2014). Effects of 24-epibrassinolide on plant growth, osmotic regulation and ion homeostasis of salt-stressed canola. *Plant Biol.* 16 (2), 440–450. doi: 10.1111/plb.12052

Liu, Z., Guo, Q., Feng, Z., Liu, Z., Li, H., Sun, Y., et al. (2020). Long-term organic fertilization improves the productivity of kiwifruit (*Actinidia chinensis* Planch.) through increasing rhizosphere microbial diversity and network complexity. *Appl. Soil Ecol.* 147, 103426. doi: 10.1016/j.apsoil.2019.103426

Maathuis, F. J., and Diatloff, E. (2013). Roles and functions of plant mineral nutrients. *Methods Mol. Biol.* 953, 1–21. doi: 10.1007/978-1-62703-152-3_1

Mikhailouskaya, N., and Bogdevitch, I. (2009). Relations of enzyme activities with different fractions of soil organic matter. *Polish J. Soil Sci.* 42, 175–182. doi: 10.1007/978-1-62703-152-3_1

Mohanta, T. K., Bashir, T., Hashem, A., Abd_Allah, E. F., Khan, A. L., and Al-Harrasi, A. S. (2018). Early events in plant abiotic stress signaling: interplay between calcium, reactive oxygen species and phytohormones. *J. Plant Growth Regul.* 37, 1033–1049. doi: 10.1007/s00344-018-9833-8

Mylavarapu, R. S., and Zinati, G. M. (2009). Improvement of soil properties using compost for optimum parsley production in sandy soils. *Scientia Hortic.* 120 (3), 426–430. doi: 10.1016/j.scienta.2008.11.038

Naz, M., Khan, Q. U., Khan, M. J., Sayal, O. U., Afridi, A., and Sayal, A. U. (2018). Impact of foliar NPK and NAA blended with organic material on tomato yield attributes and properties of soil. *Pak J. Agr Res.* 31, 323–331. doi: 10.17582/journal.pjar/2018/31.4.323.331

Quiza, L., St-Arnaud, M., and Yergeau, E. (2015). Harnessing phytomicrobiome signaling for rhizosphere microbiome engineering. *Front. Plant Sci.* 6. doi: 10.3389/fpls.2015.00507

Richardson, D. P., Ansell, J., and Drummond, L. N. (2018). The nutritional and health attributes of kiwifruit: a review. *Eur. J. Nutr.* 57, 2659–2676. doi: 10.1007/s00394-018-1627-z

Spaepen, S., Bossuyt, S., Engelen, K., Marchal, K., and Vanderleyden, J. (2014). Phenotypical and molecular responses of *Arabidopsis thaliana* roots as a result of inoculation with the auxin-producing bacterium *Azospirillum brasilense*. *New Phytol.* 201 (3), 850–861. doi: 10.1111/nph.12590

Sun, C., Liu, L., Wang, L., Li, B., Jin, C., and Lin, X. (2021). Melatonin: A master regulator of plant development and stress responses. *J. Integr. Plant Biol.* 63 (1), 126–145. doi: 10.1111/jipb.12993

Szafrańska, K., Reiter, R. J., and Posmyk, M. M. (2016). Melatonin application to *Pisum sativum* L. seeds positively influences the function of the photosynthetic apparatus in growing seedlings during paraquat-induced oxidative stress. *Front. Plant Sci.* 7. doi: 10.3389/fpls.2016.01663

Tan, D. X., Zheng, X., Kong, J., Manchester, L. C., Hardeland, R., Kim, S. J., et al. (2014). Fundamental issues related to the origin of melatonin and melatonin isomers during evolution: relation to their biological functions. *Int. J. Mol. Sci.* 15 (9), 15858–15890. doi: 10.3390/ijms150915858

Trivedi, P., Anderson, I. C., and Singh, B. K. (2013). Microbial modulators of soil carbon storage: integrating genomic and metabolic knowledge for global prediction. *Trends Microbiol.* 21, 641–651. doi: 10.1016/j.tim.2013.09.005

Vardhini, B. V., and Anjum, N. A. (2015). Brassinosteroids make plant life easier under abiotic stresses mainly by modulating major components of antioxidant defense system. *Front. Environ. Sci.* 2. doi: 10.3389/fenvs.2014.00067

Victor Roch, G., Maharajan, T., Ceasar, S. A., and Ignacimuthu, S. (2019). The role of PHT1 family transporters in the acquisition and redistribution of phosphorus in plants. *Crit. Rev. Plant Sci.* 38, 171–198. doi: 10.1080/07352689.2019.1645402

Wang, B., Diao, Q., Zhang, Z., Liu, Y., Gao, Q., Zhou, Y., et al. (2013). Antitumor activity of bee pollen polysaccharides from Rosa rugosa. *Mol. Med. Rep.* 7 (5), 1555–1558. doi: 10.3892/mmr.2013.1382

Wang, Y., Fu, F., Li, J., Wang, G., Wu, M., Zhan, J., et al. (2016). Effects of seaweed fertilizer on the growth of *Malus hupehensis* Rehd. seedlings, soil enzyme activities and fungal communities under replant condition. *Eur. J. Soil Biol.* 75, 1–7. doi: 10.1016/j.ejsobi.2016.04.003

Wang, X. K., and Huang, J. L. (2015). *Principles and Techniques of Plant Physiology and Biochemistry Experiments* (Beijing: Higher Education Press).

Wang, L., Liu, J., Wang, W., and Sun, Y. (2016). Exogenous melatonin improves growth and photosynthetic capacity of cucumber under salinity-induced stress. *Photosynthetica* 54, 19–27. doi: 10.1007/s11099-015-0140-3

Ward, N. L., Challacombe, J. F., Janssen, P. H., Henrissat, B., Coutinho, P. M., Wu, M., et al. (2009). Three genomes from the phylum Acidobacteria provide insight into the lifestyles of these microorganisms in soils. *Appl. Environ. Microbiol.* 75, 2046–2056. doi: 10.1128/AEM.02294-08

Wei, W., Li, Q. T., Chu, Y. N., Reiter, R. J., Yu, X. M., Zhu, D. H., et al. (2015). Melatonin enhances plant growth and abiotic stress tolerance in soybean plants. *J. Exp. Bot.* 66, 695–707. doi: 10.1093/jxb/eru392

Zhang, R., Sun, Y., Liu, Z., Jin, W., and Sun, Y. (2017). Effects of melatonin on seedling growth, mineral nutrition, and nitrogen metabolism in cucumber under nitrate stress. *J. Pineal Res.* 62 (4), e12403. doi: 10.1111/jpi.12403

Zhang, H. J., Zhang, N. A., Yang, R. C., Wang, L., Sun, Q. Q., Li, D. B., et al. (2014). Melatonin promotes seed germination under high salinity by regulating antioxidant systems, ABA and GA_4 interaction in cucumber (*Cucumis sativus* L.). *J. Pineal Res.* 57 (3), 269–279. doi: 10.1111/jpi.12167

Zhang, Y., Zhu, X., Ding, H., Yang, S., and Chen, Y. (2013). Foliar application of 24-epibrassinolide alleviates high-temperature-induced inhibition of photosynthesis in seedlings of two melon cultivars. *Photosynthetica* 51, 341–349. doi: 10.1007/s11099-013-0031-4

Zhou, Y., Xia, H., Liu, X., Lin, Z., Guo, Y., Deng, H., et al (2022). Identification of suitable reference genes for qRT-PCR normalization in kiwifruit.. *Horticulturae* 8, 170.

frontiers | Frontiers in Plant Science

TYPE Original Research
PUBLISHED 07 March 2024
DOI 10.3389/fpls.2024.1308553

OPEN ACCESS

EDITED BY
Muhammad Awais Farooq,
Hebei Agricultural University, China

REVIEWED BY
Chiara Amitrano,
University of Naples Federico II, Italy
Ademola Emmanuel Adetunji,
South African Environmental Observation Network (SAEON), South Africa

*CORRESPONDENCE
Yanhua Huang
yanhuah@iastate.edu;
yanhua.huang@bayer.com

RECEIVED 09 October 2023
ACCEPTED 22 January 2024
PUBLISHED 07 March 2024

CITATION
Huang Y, Chang Y, Ni Z and Wang L (2024) Environmental parameters factors exploration on lettuce seed germination with hydrogel. *Front. Plant Sci.* 15:1308553.
doi: 10.3389/fpls.2024.1308553

Environmental parameters factors exploration on lettuce seed germination with hydrogel

Yanhua Huang[1]*, Yanbin Chang[2], Zheng Ni[2] and Lizhi Wang[2]

[1]Department of Industrial and Manufacturing Systems Engineering, Iowa State University, Ames, IA, United States, [2]School of Industrial Engineering and Management, Oklahoma State University, Stillwater, OK, United States

Lettuce (*Lactuca sativa*) germination is sensitive to environmental conditions. Recently, hydrogel has received increased attention as an alternative media to soil for seed germination. Compared to soil seeding, hydrogel-aided germination provides more controlled seeding environments. However, there are still challenges preventing hydrogel-aided seed germination from being widely used in industry production or academic studies, such as hydrogel formulation variations, seeding operation standardization, and germination evaluation. In this study, we tested how the combination of multiple environmental conditions affect lettuce seed germination time, which is measured as the time needed for the first pair of leaves to appear (leaf emergence) or, alternatively, the third leaf to appear (leaf development). We found that germination time and success rate of two lettuce varieties (Iceberg A and Butter Crunch) showed different sensitivities to pH, Hoagland formulations and concentrations, light intensity, and hydrogel content. We have conducted statistical analysis on the correlation between germination time and these environmental conditions.

KEYWORDS

hydroponics, lettuce, hydrogel, Hoagland, germination, timing, operations

1 Introduction

Hydroponics applications have drawn significant attention recently based on several benefits, including water efficiency (Corrado et al., 2021), nutrient control (Yang and Kim, 2020), space optimization (Peiro et al., 2020), continuous production (Magwaza et al., 2020), improved crop quality (Shrivastava et al., 2023), and local food production (Gentry, 2019). Compared with traditional agriculture, hydroponic-based cultivation recycled the nutrient liquid to re-water the crop. A study showed a 64% reduction in water usage in hydroponically cultivated lettuce compared to soil-based cultivation (Majid et al., 2021). Without soil, the nutrients only come from circulated water. The nutrient conditions can be completely controlled by tailoring nutrients to specific plant requirements (Velazquez-Gonzalez et al., 2022). Automated water circulation systems are implemented in most of the hydroponic systems recently reported by the literature (Saad et al., 2021). Nutrient

compositions, pH, temperatures, and watering timing within the water circulation system can be monitored and controlled via sensors and switches (Sihombing et al., 2019). Since most of the hydroponic systems are deployed indoors to enable complete environmental control, it also possesses the advantage of optimized space usage, continuous production, and enabling local food production. Commercial-grade hydroponic systems are profitable to ensure the viability of the business. Space optimization and continuous production are two common approaches to improve profitability (Tetreault et al., 2023). It also reduces the system's dependency on the local climate. With air conditioning, atmosphere modification (CO_2 and O_2), and lighting control, hydroponic systems can produce suitable environmental conditions for crops regardless of the geological location (Zhang et al., 2022), therefore enabling local food production, reducing the duration between farms and dining tables.

Lettuce (*Lactuca sativa*) is attractive as a hydroponic crop in both industry production and academic research due to its fast growth (Lee et al., 2021), high yield (El-Nakhel et al., 2020), high water content (Majid et al., 2021), simple nutrient requirement (Sapkota et al., 2019), and lower temperature requirement (Gentry, 2019). For example, most of the lettuce varieties matured within 40 days (Zabel et al., 2020), with an average fresh weight of 150 g (Ezziddine and Liltved, 2021) with no less than 93% water content (Zabel et al., 2020). The simple nutrient requirement of hydroponically growing lettuce also reduces the production cost, enlarging the profit margins (Hosseini et al., 2021). With lower temperature preference, grown lettuce uses less heat to maintain the environmental temperature. Thus, it also reduces energy costs in cold locations like Sweden (Gentry, 2019). With these advantages, lettuce is one of the most popular crops grown hydroponically.

Germination time estimation is important for both industry production and academic research. It provides important time prediction to facilitate planning and scheduling, allocating resources, minimizing risks, simulating crop growth, predicting yield, and seed breeding. In the controlled environment agriculture industry, thin profit margins require tight operation scheduling and low-risk tolerance. Accurate germination estimation is helpful for the logistics, including transplanting, irrigation, modifying nutrients, and pre-setting lighting conditions. Germination has been studied on rice looking for cold tolerance genetic loci in detail (Thapa et al., 2020). Barley germination was also studied to identify loci associated with drought tolerance (Moursi et al., 2020). These insights can furthermore improve predicting and simulating accuracies for breeding research and genomic selections (Amini et al., 2022; Moeinizade et al., 2022; Wang, 2022).

Compared to soil cultivation, hydrogel is capable of providing more controlled seeding environment. As a mixture of hydrophilic polymers and water, most hydrogels are capable of retaining large amount of water, which provides the essential elements for seeds to germinate. Hydrogel has been validated for seed germination (Huang et al., 2022). With full control of its formulation, it provides similar mechanical pressure to seed as the physical contact of soil (Gao et al., 2021); delivers water and nutrients consistently (Ma et al., 2019); retains water from evaporation (Oladosu et al., 2022); protects seeds from water, temperature, and salt stress (Fadiji et al., 2022); protects seeds from diseases like bacteria, pathogens, and fungi (Tang et al., 2021); and provides a non-toxic and bio-active environment (Fiorati et al., 2021). Despite these benefits, hydrogel-aided seed germination also faces several challenges. Compared with seed germination cubes such as gro-blocks (Barnett, 1986), hydrogel is much expensive. However, it also provides more benefits than gro-block, including temperature stress protection, nutrient customization, root phenotype visualization, and tunable mechanical gripping (An et al., 2022).

In this study, we conducted three experiments to explore the sensitivity of lettuce seed germination to environmental parameters, including hydrogel formulation, nutrient composition, pH, and light intensity during the germination process.

2 Materials and methods

2.1 Materials

Methylcellulose (MC) hydrogel was donated by J. Rettenmaier & Söhne (Schoolcraft, MI). All other chemicals were purchased from Thermo Fisher Scientific (Waltham, MA). Iceberg A lettuce (*Lactuca sativa* var. *crispa*, crisphead group) and Butter Crunch lettuce (*Lactuca sativa* var. *capitata*, butterhead group) were purchased from Burpee Garden Products Co (Warminster, PA). We used two versions of modified Hoagland solutions, formulated as listed in Table 1 (MH1) and in Table 2 (MH2) according to Brechner et al. (1996).

TABLE 1 Modified Hoagland solution 1 (MH1) formula for 100 L.

Chemicals	Mass (mg)
Sulfuric acid	0.1
Sodium phosphate tribasic dodecahydrate	37,704.8
Ammonium molybdate tetrahydrate	3.4
Iron(II) sulfate heptahydrate	507.2
Calcium hydroxide	38,924.1
Manganese(II) chloride	26.0
Iron(III) chloride	0.4
Potassium tetraborate tetrahydrate	78.1
Copper sulfate pentahydrate	5.5
Ammonium chloride	0.1
Ethylenediaminetetraacetic acid (EDTA)	19,454.0
Zinc nitrate hexahydrate	10.5
Potassium hydroxide	39,635.7
Manganese(II) chloride	22.5
Magnesium sulfate	24,043.3
Ammonium nitrate	60,120.2

TABLE 2 Modified Hoagland solution 2 (MH2) formula for 100 L, based on Brechner et al. (1996).

Chemicals	Mass (mg)
Calcium nitrate	47,404.92
Potassium nitrate	43,096.86
Ammonium nitrate	1,365.57
Sprint 330 iron—DTPA	913.63
Monobasic potassium phosphate	13,265.57
Potassium sulfate	1,064.82
Magnesium sulfate	11,997.54
Magnesium(II) chloride	41.62
Zinc sulfate	56.09
Boric Acid	90.71
Copper(II) sulfate pentahydrate	9.10
Ammonium molybdate	5.85

2.2 Experimental design

Three trials were designed to test the germination performance of two varieties of lettuce in different environmental conditions.

Trial 1: Germination with MH1 solution

In Trial 1, Iceberg A and Butter Crunch lettuce seeds were seeded in a 96-well plate with 200 μL conditioned MH1 to directly evaluate the different performances of the conditioned Hoagland solution. To facilitate the water absorption and swelling process during the germination initiation stage, reduced concentrations of MH1 were chosen to reduce the osmotic pressure over the seed's skin, including one-third, one-fourth, and one-fifth of the original Hoagland solution concentration. To explore the impacts of acidity to the germination results, different diluted MH1's pH values were used at 4, 5, 6, and 7 with 2% error. Deionized waters (DI) with different pH were also used to germinate seeds as the control group. For each condition, three seeds were placed in different wells as replicates. The germination process was executed under 25°C with par 30, 2,000 lumens, 5,000K LED lights at all times to stimulate germination. The motivation of using continuous light in Trial 1 is the discovery that seed germination rate of *Arabidopsis thaliana* responded positively to continuous red light (Millar et al., 2010), although it was in microgravity.

Trial 2: Germination with MH1-formulated hydrogel

Trial 2 aims to verify the compatibility between modified MH1 and MC hydrogel. Since the mechanical strength of hydrogels is directly related to the concentration of non-single valent cation salt, lower dry MC powder content (6% w/w) was mixed with the different concentrations of MH1 when formulating the hydrogel for seed germination substrate, compared to the previous minimum of 8% (Jiang et al., 2021). Seeding orientation variations were also varied, differentiated between vertical and horizontal scenarios. In the previous study, seeds with horizontal orientation swelled and sprouted superior to other orientations in terms of swelling ratio and sprout length (Huang et al., 2022). In this study, for each well of the six-well plate with lid, 0.6 g of MC powder were mixed with 1.4 mL of different conditioned Hoagland solutions used in Trial 1 to formulate 2 g of hydrogel. pH modification was conducted by adding hydrochloric acid and sodium hydroxide, since sulfur (S) in sulfuric acid and potassium (K) in potassium hydroxide are key nutrients in the MH1. In each well, 12 seeds were seeded vertically and four horizontally, 1 mm below the top surface of the cast hydrogel. There was a 24-h wait between hydrogel formulation and seeding due to the homogenization of the ions and migration and cross-linking of the hydrogel polymer chain. The germination process was executed under 21°C with mixed LED lights ranging from 4,000 K to 5,500,K at all times.

Trial 3: Germination with MH2-formulated hydrogel

In Trial 3, seed germination was carried out in the MC hydrogel with non-full factorial formula modification mapping based on MH2 for a maximum of 8 days. The formula mapping parameters and their conditions are listed in Table 3. Prior to adding MC powders, pH was measured. A total of 50 gels were cast in the ×100, 100-mm plastic Petri dish with a lid. After six Iceberg A lettuce seeds were seeded in each hydrogel, all 50 hydrogels were placed under two 24-W 5,000 K LED lights for 8 days without changing positions. The light photosynthetic photon flux density (PPFD) of each dish was logged for data analysis. We explored the following independent variable as experimental matrix:

- MH2: concentration times of original MH2 condition; unit, X;
- NH_4NO_3: ammonium nitrate beyond MH2 formulation; unit, ppm;
- KOH: addition of potassium hydroxide beyond MH2 formulation; unit, ppm;
- PO_4: addition of phosphate ions beyond MH2 formulation; unit, ppm;
- Citric: addition of citric acid; unit, ppm;
- MC: weight percentage of MC polymer used in the hydrogel formulation; unit, %. w/w;
- pH: acidity/alkalinity of the formulation; unitless;
- PPFD: light photosynthetic photon flux density; unit μmol/s/m^2.

2.3 Germination score

Based on previously used metrics for germination performance (Brechner et al., 1996; Egbuikwem et al., 2020), we propose a germination score as a performance metric, which requires the following definition of germination time (D) and success rate (R).

- Leaf emergence D_2: average number of days needed for the first pair of leaves to appear, capped at day 8.
- Leaf development D_3: average number of days needed for the third leaf to appear, capped at day 10.
- D_T: average number of days between the first pair of leaves and the third leaf.
- Germination rate R_2: percent of seeds that have reached leaf emergence by the eighth day of germination.

10.3389/fpls.2024.1308553

TABLE 3 A total of 50 non-full factorial formulas for methyl cellulose hydrogels based on modified Hoagland solution 2.

No.	MH2 (x)	NH_4NO_3 (ppm)	KOH (ppm)	KH_2PO_4 (ppm)	K_2HPO_4 (ppm)	Citric Acid (ppm)	MC (%, w/w)
1	0	0	10	0	5	20	6
2	0	0	30	0	5	10	8
3	0	0	30	5	20	50	10
4	0	5	10	5	20	20	6
5	0	5	20	10	80	10	8
6	0	5	30	0	5	50	10
7	0	10	0	0	5	10	10
8	0	10	0	5	20	50	8
9	0	10	20	5	20	20	10
10	0	35	0	10	80	10	6
11	0	35	10	10	80	20	8
12	0	35	20	10	80	50	6
13	0.5	0	0	5	20	20	8
14	0.5	0	10	5	20	10	10
15	0.5	0	20	0	5	20	8
16	0.5	0	30	10	80	10	6
17	0.5	5	0	5	20	50	8
18	0.5	5	0	10	80	50	10
19	0.5	5	20	0	5	20	10
20	0.5	10	10	0	5	50	6
21	0.5	10	30	0	5	10	8
22	0.5	10	30	10	80	20	6
23	0.5	35	10	10	80	50	10
24	0.5	35	20	0	5	10	10
25	0.5	35	30	5	20	10	6
26	1	0	0	5	20	10	6
27	1	0	0	10	80	20	10
28	1	0	20	0	5	50	10
29	1	5	10	0	5	10	8
30	1	5	10	10	80	10	8
31	1	5	20	5	20	50	6
32	1	10	10	5	20	10	10
33	1	10	20	10	80	50	6
34	1	10	30	10	80	20	8
35	1	35	0	0	5	20	6
36	1	35	30	0	5	20	10
37	1	35	30	5	20	50	8
38	1.5	0	10	10	80	50	10

(Continued)

10.3389/fpls.2024.1308553

TABLE 3 Continued

No.	MH2 (x)	NH_4NO_3 (ppm)	KOH (ppm)	KH_2PO_4 (ppm)	K_2HPO_4 (ppm)	Citric Acid (ppm)	MC (%, w/w)
39	1.5	0	20	10	80	10	8
40	1.5	0	30	0	5	50	6
41	1.5	5	0	0	5	10	6
42	1.5	5	10	0	5	20	6
43	1.5	5	30	5	20	20	10
44	1.5	5	30	10	80	10	10
45	1.5	10	0	10	80	20	10
46	1.5	10	10	0	5	50	8
47	1.5	10	20	5	20	10	6
48	1.5	35	0	0	5	50	8
49	1.5	35	10	5	20	10	10
50	1.5	35	20	5	20	20	8

- Germination rate R_3: percent of seeds that have reached leaf development by the 10th day of germination.
- Germination score $G_2 = (8 - D_2) \cdot R_2$.
- Germination score $G_3 = (10 - D_3) \cdot R_3$.

3 Results and discussions

3.1 Trial 1 results

The Iceberg A and Butter Crunch lettuce seeds in the 96-well plate are shown in Figure 1. The germination time D_2, success rate R_2, and germination score G_2 for the two varieties are show in Figures 2A, B. The shortest average germination time D_2 for Iceberg A was 2.167 days, which was under the condition of pH being 6 or 7 and MH1 concentration being one-fifth level of original conditions. Butter Crunch lettuce had a lower germination success rate and took a longer time to germinate. There were four cases that Butter Crunch lettuce could not germinate, inducing 0, 1/3, and 1/4 MH1 solution at pH = 4 and 1/5 MH1 at pH =7, which are indicated by the black blocks in Figure 2B.

Germination solution impacted the germination rate of the two varieties differently. Seeds require absorbing a significant amount of water before reactivating their bio-activity from dormancy. An overcharged nutrient solution may depress the swelling process, which delays or prohibits seeds from germination. On the other hand, changing pH can alter enzyme activities at the cell membrane.

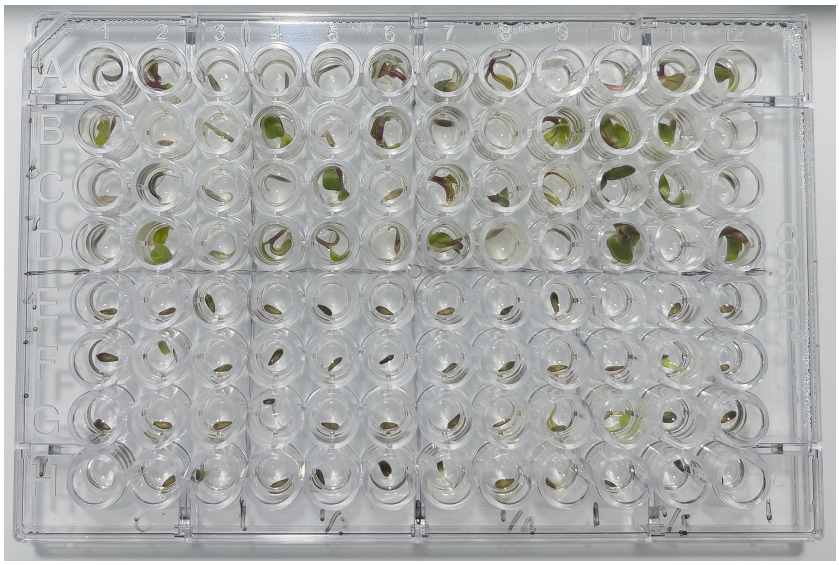

FIGURE 1
In Trial 1, day 4 of Iceberg A (top half) and day 3 of Butter Crunch (bottom half) lettuce germination without MC hydrogel in a 96-well plate.

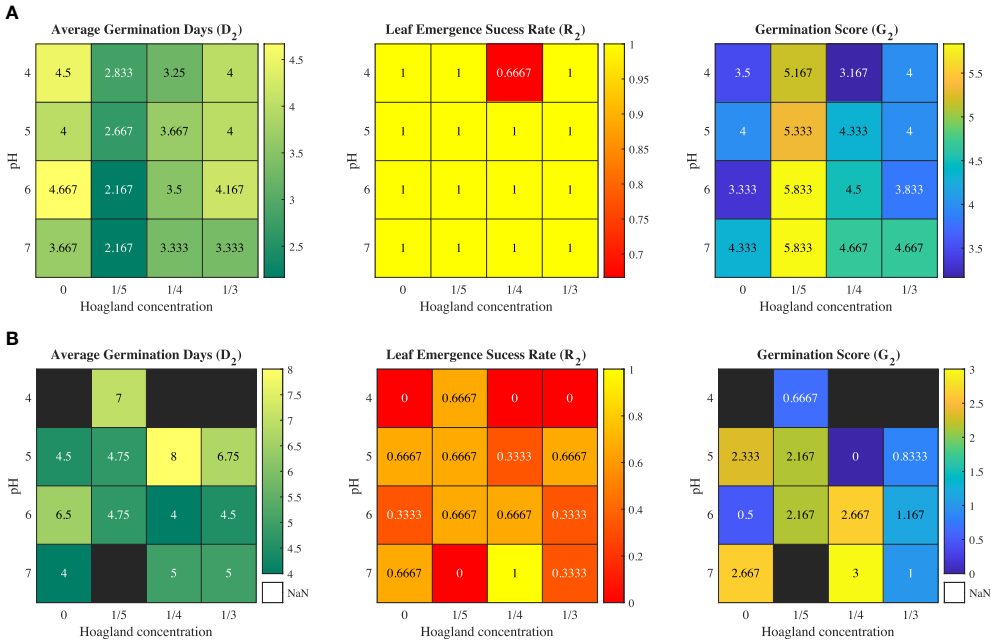

FIGURE 2
Trial 1: Heat maps of average germination time (D2), success rate (R2), and germination score (G2) for leaf emergence without methylcellulose hydrogel for **(A)** Iceberg A lettuce and **(B)** Butter Crunch lettuce.

Unsuitable pH conditions could lead to calcium or magnesium ions disorder and delayed germination (Borhannuddin Bhuyan et al., 2019).

3.2 Trial 2 results

Figure 3 shows the Iceberg A and Butter Crunch lettuce seeds in the six-well plate with MH1-formulated MC hydrogel. The germination time D_2, success rate R_2, and germination score G_2 for the two varieties are show in Figures 4A, B. These figures showed that the shortest germination times D_2 for Iceberg A and Butter Crunch were 3.625 days and 6.5 days, respectively, which were noticeably longer than the respective 2.167 days and 4 days from Trial 1. Germination score G_2 also showed similar trends.

The presence of the MC hydrogel impacted seed germination significantly. When seeded in hydrogels, the seed experienced mechanical compression during germination. Due to the water retention from the hydrogel, less water was available for seeds to

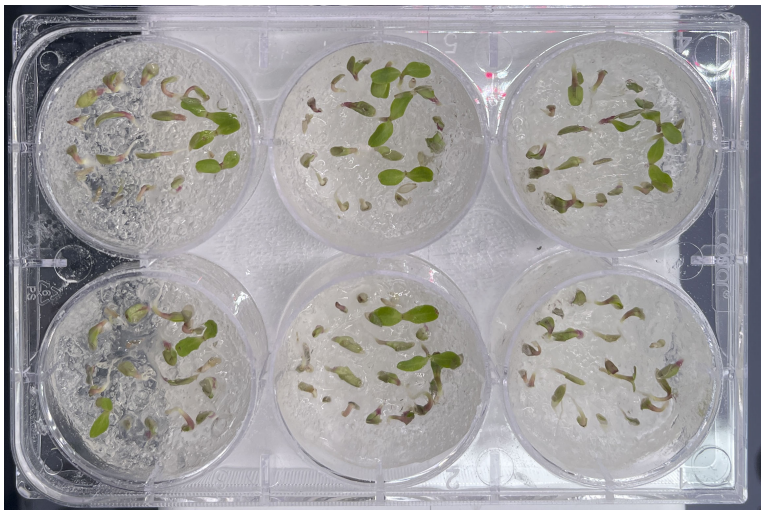

FIGURE 3
In Trial 2, day 3 of Iceberg A lettuce germination with methyl cellulose hydrogel formulated with modified Hoagland solution 1 in six-well plate. In each well, the center four seeds were seeded horizontally, and the rest were seeded vertically.

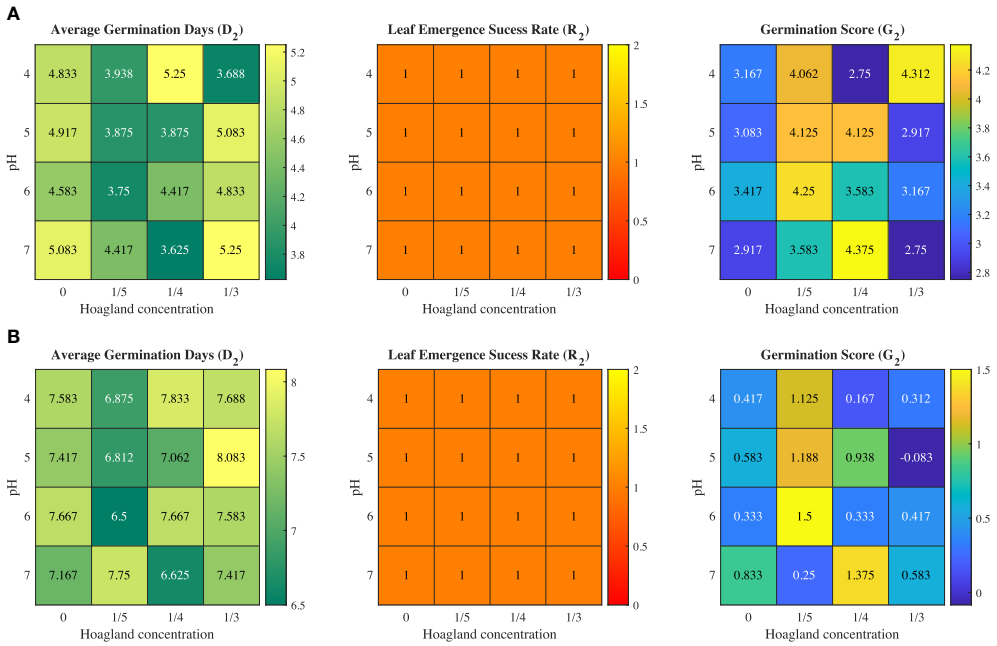

FIGURE 4
Trial 2: Heat maps of average germination time (D2), success rate (R2), and germination score (G2) leaf emergence with MC hydrogel for **(A)** Iceberg A lettuce and **(B)** Butter Crunch lettuce.

swell, therefore delaying the germination process (Bauli et al., 2021). However, hydrogel significantly improved germination success rate. Compared with 56% without hydrogel, germination with MH1-formulated hydrogel provide a 64% of success rate. However, the increase in average germination time offsets the improvement of the success rate role in the germination score.

When seeded in hydrogel, seed orientation significantly impacts the average germination time. Since the dimension of the lettuce seeds is relatively small compared to soybean, it is difficult to distinguish from hilum up or down without a desktop microscope or magnifying glass (Huang et al., 2022). It is safe to plant the seed sideways to ensure less discrepancy induced from

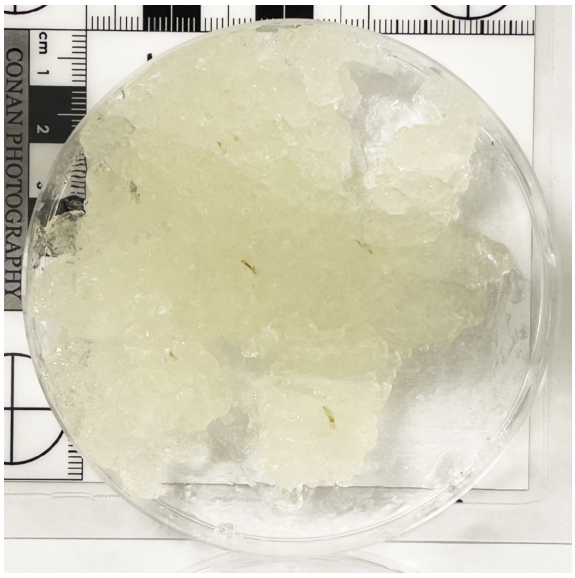

FIGURE 5
In Trial 3, day 0 of seeded Iceberg A lettuce in methyl cellulose hydrogel formulated with modified Hoagland solution 2 No. 9.

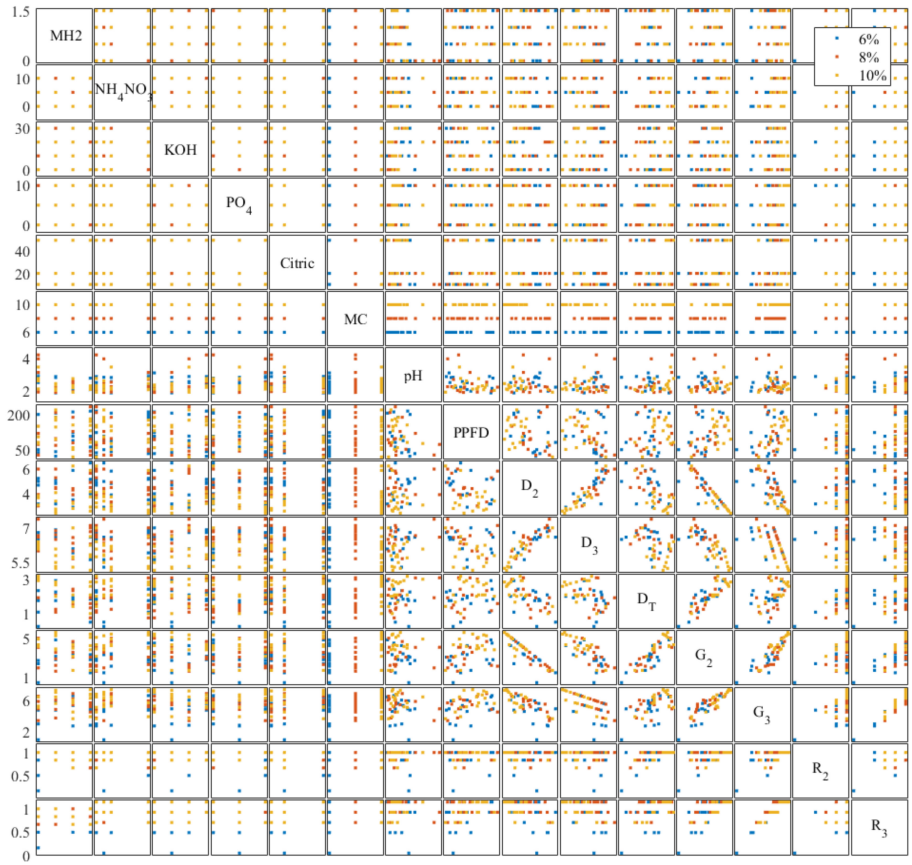

FIGURE 6
Trial 3: multivariate scatter plot (each dot represents the average of six replicate seeds' condition germinated in one of the 50 gels as listed in Table 3) between controlled formulation variables and germination evaluators on the modified Hoagland 2-formulated methyl cellulose hydrogels. Controlled formulation variables and germination evaluators' descriptions can be found in Table 3 and *Section 2.3*, respectively.

seed orientation, as shown in Figure 3. Based on the results, we found that excess sodium and chlorine-rich MH1 formulation posed salt stress to germination.

3.3 Trial 3 results

In Trial 3, we used a different version of Hoagland formula, MH2, with reduced sodium (Na) and chlorine (Cl) in the nutrient solution. Although inexpensive, Na and Cl salts can significantly shift the osmotic pressure, which depresses swelling (Serrano and Gaxiola, 1994). The MH2 formula has only one ingredient, manganese (II) chloride ($MnCl_2$), which contained Na or Cl. Since Mn is a micronutrient in the Hoagland formula, the amount of Cl is negligible. Six Iceberg A lettuce seeds were seeded together in a 10 × 10 mm.

Petri dish with 30 mL MH2-formulated hydrogel, as shown in Figure 5. We only used Iceberg A seeds in Trial 3 because they failed to germinate in several cases in Trial 1 and had a much higher germination score than Butter Crunch in both Trials 1 and 2. Since the previous set showed that pH impacted the germination significantly, we altered the pH by adding different amounts of KOH and citric acid to avoid Na and Cl toxicity. Since nitrogen (N), phosphorus (P), and potassium (K) are the three macronutrients being studied extensively, minor N, P, and K modifications based on the MH2 formula were also introduced in the design of experiments.

More parameters were added in the experimental design to further explore the potential of hydrogel in the perspective of assisting lettuce seed germination. It was found (Millar et al., 2010) that seed responds to photonic energy significantly under microgravity conditions. Previous studies showed significant differences when seeds were sprouted in hydrogels with different polymer concentrations (Huang et al., 2022). In this study, we experimented with the same condition (6, 8, and 10% w/w hydrogel content).

Comparing MH1- with MH2-formulated hydrogels, average germination time (D_2) were shortened from 4.46 days to 4.25 days, validating the chlorine toxicity delay. The average D_3 was 6.28 days. In comparison, the standard industrial estimate is 7–10 days (Hamilton, 2018), and 10 days (Egbuikwem et al., 2020) and 11 (Brechner et al., 1996) days for pre-transplantation.

We analyzed the correlation between all controlling variables and evaluators to understand the effectiveness of independent variables on seed germination. Previous studies showed environmental factors impacting on lettuce germination including

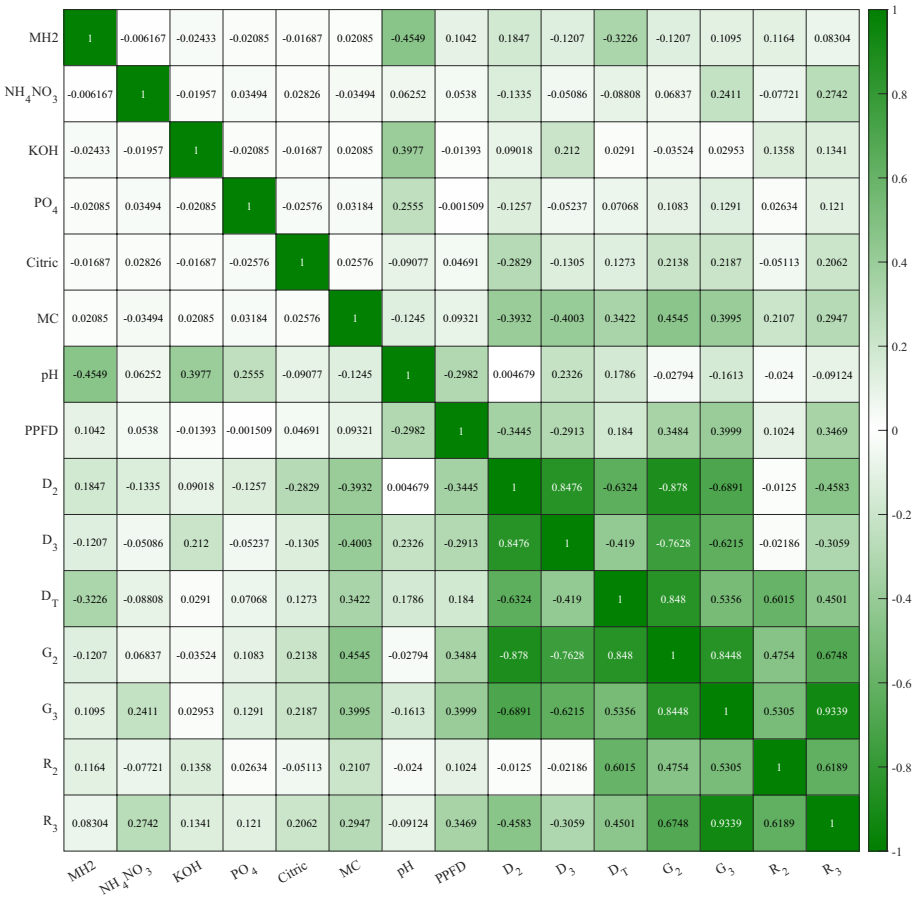

FIGURE 7
Trial 3: correlations between controlled formulation variables and germination evaluators on the modified Hoagland solution 2-formulated methyl cellulose hydrogels.

temperature (Hayashi et al., 2008), lighting conditions (Li et al., 2021), oxygen content (Yasin and Andreasen, 2016), and CO_2 content (Luo, 2020). The multivariate scatter plot and correlation coefficients are shown in Figures 6, 7. As grouped with MC content (%, w/w) in Figure 6, scatter plot D_2 vs. D_3, D_T vs. G_2, and G_2 vs. G_3 showed clear color trends that indicate a high correlation between these evaluators and MC content. KOH and PO_4 showed 0.3977 and 0.2555 correlations, respectively, with pH in Figure 7. The correlation between pH and KOH alternation is expected. As phosphate salts are acting as buffer, the addition of KOH increases the pH. Cellulose-based hydrogels change their mechanical integrity during the pH change, as demonstrated in Jiang et al. (2021). A −0.4549 correlation between pH and MH2 signifies the buffering capability of Hoagland solution. MH2 concentration had a −0.3226 correlation with D_T. Both pH and MH2 correlations confirm that chlorine toxicity from MH2 significantly reduced the germination progress.

Similar to post-germination plant modeling, light stress also depresses the seed germination process significantly after PPFD exceeds certain levels. Figures 8A, B show that G_2 and G_3 reached maximum at 152.30 μmol/s/m^2 and 166.14 μmol/s/m^2, respectively.

MC content plays an important role during the germination process. Figure 9 suggested that germination score G_2 had a positive correlation with hydrogel content between 6% and 10%. Figure 10 shows how the average D_2, D_3, and D_T change under different hydrogel content between 6% and 10%. When hydrogel content increased, the porosity of fully swelled hydrogel also increased due to water content decrease; thus, additional oxygen could be trapped and defused in the hydrogel for roots' immediate access. Increased porosity provides additional space for roots to expand, which also reduce germination times D_2 and D_3 and increase germination scores G_2 and G_3. The air and space increases are crucial during the swelling process for seeds' respiration and volume span. Higher hydrogel content also led to an increase in D_T because it suppressed nutrient absorption and delayed the nutrient source transformation from seeding to cloning stages.

4 Conclusion

In this study, we experimentally explored the effects of multiple environmental parameters on lettuce seed germination. We found that pH, light intensity, cultivation substrate hardness, and porosity have the largest influences on lettuce seed germination with respect to germination time and success rate. In the meantime, MC hydrogel reduced the germination time by providing beneficial conditions for

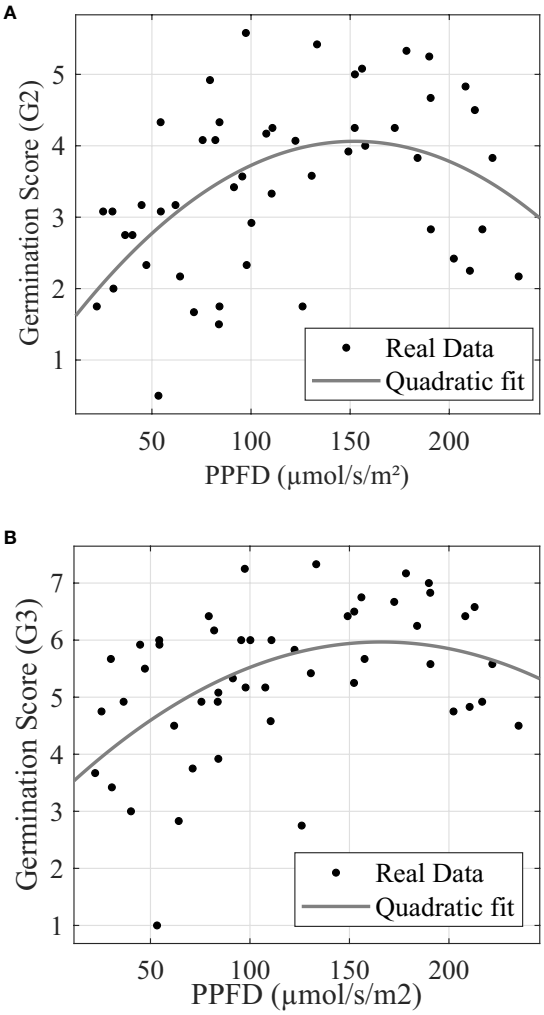

FIGURE 8
Trial 3: Leaf emergence **(A)** and leaf development **(B)** response to photonic energy presents stress. **(A)** G_2 response to photosynthetic photon flux density. **(B)** G_3 response to photosynthetic photon flux density.

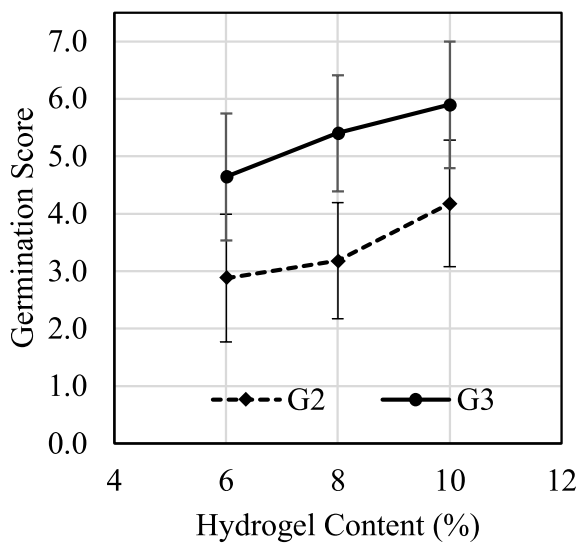

FIGURE 9
Trial 3: G2 and G3 response to hydrogel concentration.

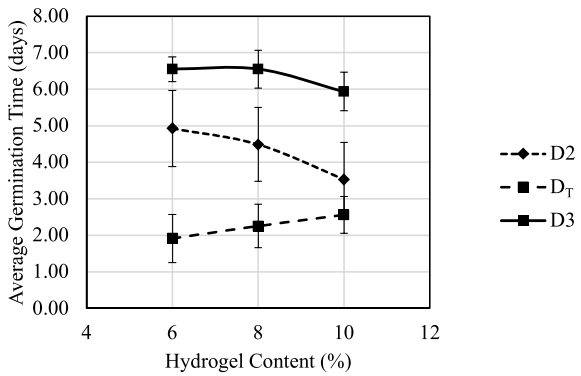

FIGURE 10
Trial 3: D2, D3, and D_T response to hydrogel concentration.

the seed to undergo soil-less germination, including the benefits of regulating water, nutrient supply to oxygen access, and carbon dioxide absorption, providing mechanical grip to protect against diseases.

This study is not without its limitations. For example, we conducted all experiments under the same temperature and humidity conditions without exploring their impact on germination. Salt stress from N, P, and K was also studied within a relatively narrow range. Future research should explore the effects of more environmental parameters over wider ranges on germination. Understanding such effects will not only provide more scientific insight on plant physiology but also commercial value for the controlled environment industry.

Data availability statement

The original contributions presented in the study are included in the article/supplementary material. Further inquiries can be directed to the corresponding author.

Author contributions

YH: Conceptualization, Data curation, Formal analysis, Investigation, Methodology, Validation, Visualization, Writing – original draft, Writing – review & editing. YC: Data curation, Methodology, Writing – review & editing, Formal analysis. ZN: Data curation, Methodology, Writing – review & editing, Formal analysis. LW: Funding acquisition, Project administration, Supervision, Writing – review & editing, Formal analysis, Methodology, Resources.

Funding

The author(s) declare financial support was received for the research, authorship, and/or publication of this article. This work was partially supported by NSF and USDA (#1830478, #1842097, #2021-67021-35329) and by the Plant Sciences Institute at Iowa State University.

Acknowledgments

The authors are grateful to Dr. Maria Salas Fernandez for plant physiology discussions, Mr. Ryan Losh assistance in taking images and collecting data, and Mr. Pete Lelonek for his laboratory management and technical support.

Conflict of interest

The authors declare that the research was conducted in the absence of any commercial or financial relationships that could be construed as a potential conflict of interest.

Publisher's note

All claims expressed in this article are solely those of the authors and do not necessarily represent those of their affiliated organizations, or those of the publisher, the editors and the reviewers. Any product that may be evaluated in this article, or claim that may be made by its manufacturer, is not guaranteed or endorsed by the publisher.

References

Amini, F., Hu, G., Wang, L., and Wu, R. (2022). The l-shaped selection algorithm for multitrait genomic selection. *Genetics* 221. doi: 10.1093/genetics/iyac069

An, B., Wang, Y., Huang, Y., Wang, X., Liu, Y., Xun, D., et al. (2022). Engineered living materials for sustainability. *Chem. Rev.* 123, 2349–2419. doi: 10.1021/acs.chemrev.2c00512

Barnett, J. P. (1986). *Producing southern pine seedlings in containers* (US Department of Agriculture, Forest Service, Southern Forest Experiment Station), 59.

Bauli, C. R., Lima, G. F., de Souza, A. G., Ferreira, R. R., and Rosa, D. S. (2021). Eco-friendly carboxymethyl cellulose hydrogels filled with nanocellulose or nanoclays for agriculture applications as soil conditioning and nutrient carrier and their impact on cucumber growing. *Colloids Surf. A: Physicochem. Eng. Aspects* 623, 126771. doi: 10.1016/j.colsurfa.2021.126771

Borhannuddin Bhuyan, M. H. M., Hasanuzzaman, M., Nahar, K., Mahmud, J. A., Parvin, K., Bhuiyan, T. F., et al. (2019). *Plants behavior under soil acidity stress: insight into morphophysiological, biochemical, and molecular responses* (Springer International Publishing), 35–82. doi: 10.1007/978-3-030-06118-02

Brechner, M., Both, A., and Staff, C. (1996). Hydroponic lettuce handbook. *Cornell Controlled Environ. Agric.* 834, 504–509.

Corrado, G., Micco, V. D., Lucini, L., Miras-Moreno, B., Senizza, B., Zengin, G., et al. (2021). Isosmotic macrocation variation modulates mineral efficiency, morpho-physiological traits, and functional properties in hydroponically grown lettuce varieties (lactuca sativa l.). *Front. Plant Sci.* 12. doi: 10.3389/fpls.2021.678799

Egbuikwem, P. N., Mierzwa, J. C., and Saroj, D. P. (2020). Assessment of suspended growth biological process for treatment and reuse of mixed wastewater for irrigation of edible crops under hydroponic conditions. *Agric. Water Manage.* 231, 106034. doi: 10.1016/j.agwat.2020.106034

El-Nakhel, C., Petropoulos, S. A., Pannico, A., Kyriacou, M. C., Giordano, M., Colla, G., et al. (2020). The bioactive profile of lettuce produced in a closed soilless system as configured by combinatorial effects of genotype and macrocation supply composition. *Food Chem.* 309, 125713. doi: 10.1016/j.foodchem.2019.125713

Ezziddine, M., and Liltved, H. (2021). Quality and yield of lettuce in an open-air rooftop hydroponic system. *Agronomy* 11, 2586. doi: 10.3390/agronomy11122586

Fadiji, A. E., Santoyo, G., Yadav, A. N., and Babalola, O. O. (2022). Efforts towards overcoming drought stress in crops: Revisiting the mechanisms employed by plant growth-promoting bacteria. *Front. Microbiol.* 13. doi: 10.3389/fmicb.2022.962427

Fiorati, A., Linciano, C., Galante, C., Raucci, M. G., and Altomare, L. (2021). Bioactive hydrogels: Design and characterization of cellulose-derived injectable composites. *Materials* 14, 4511. doi: 10.3390/ma14164511

Gao, Y., Zhao, X., Han, X., Wang, P., and Zheng, W. J. (2021). Soft actuator based on metal/hydrogel nanocomposites with anisotropic structure. *Macromol. Chem. Phys.* 223, 2100117. doi: 10.1002/macp.202100117

Gentry, M. (2019). Local heat, local food: Integrating vertical hydroponic farming with district heating in Sweden. *Energy* 174, 191–197. doi: 10.1016/j.energy.2019.02.119

Hamilton, K. (2018). "Struggling with lettuce: Germination," in *Extension Master Gardener Volunteers of Durham County Blog.* Available at: https://durhammastergardeners.com/2018/09/06/struggling-with-lettucegermination/.

Hayashi, E., Aoyama, N., and Still, D. W. (2008). Quantitative trait loci associated with lettuce seed germination under different temperature and light environments. *Genome* 51, 928–947. doi: 10.1139/g08-077

Hosseini, H., Mozafari, V., Roosta, H. R., Shirani, H., van de Vlasakker, P. C. H., and Farhangi, M. (2021). Nutrient use in vertical farming: Optimal electrical conductivity of nutrient solution for growth of lettuce and basil in hydroponic cultivation. *Horticulturae* 7, 283. doi: 10.3390/horticulturae7090283

Huang, Y., Yu, L., Jiang, L., Shi, X., and Qin, H. (2022). 3d printing of hydrogel-based seed planter for in-space seed nursery. *Manuf. Lett.* 33, 103–108. doi: 10.1016/j.mfglet.2022.07.045

Jiang, X., Huang, Y., Cheng, Y., Zhang, Z., Shi, X., and Qin, H. (2021). Effects of lyophilization on the release profiles of 3d printed delivery systems fabricated with carboxymethyl cellulose hydrogel. *Polymers* 13, 749. doi: 10.3390/polym13050749

Lee, E., Rout, P. R., and Bae, J. (2021). The applicability of anaerobically treated domestic wastewater as a nutrient medium in hydroponic lettuce cultivation: Nitrogen toxicity and health risk assessment. *Sci. Total Environ.* 780, 146482. doi: 10.1016/j.scitotenv.2021.146482

Li, J., Wu, T., Huang, K., Liu, Y., Liu, M., and Wang, J. (2021). Effect of LED spectrum on the quality and nitrogen metabolism of lettuce under recycled hydroponics. *Front. Plant Sci.* 12. doi: 10.3389/fpls.2021.678197

Luo, A. (2020). Evaluation of romaine lettuce (lactuca sativa l. Cv. Parris island) production under an elevated carbon dioxide (CO2) gas environment generated from compost materials. [Ph.D. thesis]. Dalhousie University.

Ma, L., Shi, Y., Siemianowski, O., Yuan, B., Egner, T. K., Mirnezami, S. V., et al. (2019). Hydrogel-based transparent soils for root phenotyping in *vivo*. *Proc. Natl. Acad. Sci.* 116, 11063–11068. doi: 10.1073/pnas.1820334116

Magwaza, S. T., Magwaza, L. S., Odindo, A. O., and Mditshwa, A. (2020). Hydroponic technology as decentralised system for domestic wastewater treatment and vegetable production in urban agriculture: A review. *Sci. Total Environ.* 698, 134154. doi: 10.1016/j.scitotenv.2019.134154

Majid, M., Khan, J. N., Shah, Q. M. A., Masoodi, K. Z., Afroza, B., and Parvaze, S. (2021). Evaluation of hydroponic systems for the cultivation of lettuce (lactuca sativa l., var. longifolia) and comparison with protected soil-based cultivation. *Agric. Water Manage.* 245, 106572. doi: 10.1016/j.agwat.2020.106572

Millar, K. D. L., Kumar, P., Correll, M. J., Mullen, J. L., Hangarter, R. P., Edelmann, R. E., et al. (2010). A novel phototropic response to red light is revealed in microgravity. *New Phytol.* 186, 648–656. doi: 10.1111/j.1469-8137.2010.03211.x

Moeinizade, S., Hu, G., and Wang, L. (2022). A reinforcement learning approach to resource allocation in genomic selection. *Intell. Syst. Appl.* 14, 200076. doi: 10.1016/j.iswa.2022.200076

Moursi, Y. S., Thabet, S. G., Amro, A., Dawood, M. F. A., Baenziger, P. S., and Sallam, A. (2020). Detailed genetic analysis for identifying QTLs associated with drought tolerance at seed germination and seedling stages in barley. *Plants* 9, 1425. doi: 10.3390/plants9111425

Oladosu, Y., Rafii, M. Y., Arolu, F., Chukwu, S. C., Salisu, M. A., Fagbohun, I. K., et al. (2022). Superabsorbent polymer hydrogels for sustainable agriculture: A review. *Horticulturae* 8, 605. doi: 10.3390/horticulturae8070605

Peiro, E., Pannico, A., Colleoni, S. G., Bucchieri, L., Rouphael, Y., Pascale, S. D., et al. (2020). Air distribution in a fully-closed higher plant growth chamber impacts crop performance of hydroponicallygrown lettuce. *Front. Plant Sci.* 11. doi: 10.3389/fpls.2020.00537

Saad, M. H. M., Hamdan, N. M., and Sarker, M. R. (2021). State of the art of urban smart vertical farming automation system: Advanced topologies, issues and recommendations. *Electronics* 10, 1422. doi: 10.3390/electronics10121422

Sapkota, S., Sapkota, S., and Liu, Z. (2019). Effects of nutrient composition and lettuce cultivar on crop production in hydroponic culture. *Horticulturae* 5, 72. doi: 10.3390/horticulturae5040072

Serrano, R., and Gaxiola, R. (1994). Microbial models and salt stress tolerance in plants. *Crit. Rev. Plant Sci.* 13, 121–138. doi: 10.1080/07352689409701911

Shrivastava, A., Nayak, C. K., Dilip, R., Samal, S. R., Rout, S., and Ashfaque, S. M. (2023). Automatic robotic system design and development for vertical hydroponic farming using IoT and big data analysis. *Mater. Today: Proc.* 80, 3546–3553. doi: 10.1016/j.matpr.2021.07.294

Sihombing, P., Zarlis, M., and Herriyance, (2019). "Automatic nutrition detection system (ANDES) for hydroponic monitoring by using micro controller and smartphone android," in *2019 Fourth International Conference on Informatics and Computing (ICIC)* (IEEE). doi: 10.1109/icic47613.2019.8985851

Tang, T.-C., Tham, E., Liu, X., Yehl, K., Rovner, A. J., Yuk, H., et al. (2021). Hydrogel-based biocontainment of bacteria for continuous sensing and computation. *Nat. Chem. Biol.* 17, 724–731. doi: 10.1038/s41589-021-00779-6

Tetreault, J., Fogle, R. L., Fogarty, S., and Guerdat, T. (2023). Coupled aquaponics: Optimizing hydraulic retention times using a parallel unit process water treatment approach. *Front. Hortic.* 2. doi: 10.3389/fhort.2023.1140998

Thapa, R., Tabien, R. E., Thomson, M. J., and Septiningsih, E. M. (2020). Genome-wide association mapping to identify genetic loci for cold tolerance and cold recovery during germination in rice. *Front. Genet.* 11. doi: 10.3389/fgene.2020.00022

Velazquez-Gonzalez, R. S., Garcia-Garcia, A. L., Ventura-Zapata, E., Barceinas-Sanchez, J. D. O., and Sosa-Savedra, J. C. (2022). A review on hydroponics and the technologies associated for medium- and small-scale operations. *Agriculture* 12, 646. doi: 10.3390/agriculture12050646

Wang, L. (2022). The leave-worst-k-out criterion for cross validation. *Optim. Lett.* 17, 545–560. doi: 10.1007/s11590-022-01894-6

Yang, T., and Kim, H.-J. (2020). Comparisons of nitrogen and phosphorus mass balance for tomato-, basil-, and lettuce-based aquaponic and hydroponic systems. *J. Clean. Prod.* 274, 122619. doi: 10.1016/j.jclepro.2020.122619

Yasin, M., and Andreasen, C. (2016). Effect of reduced oxygen concentration on the germination behavior of vegetable seeds. *Hortic. Environ. Biotechnol.* 57, 453–461. doi: 10.1007/s13580-016-0170-1

Zabel, P., Zeidler, C., Vrakking, V., Dorn, M., and Schubert, D. (2020). Biomass production of the EDEN ISS space greenhouse in Antarctica during the 2018 experiment phase. *Front. Plant Sci.* 11. doi: 10.3389/fpls.2020.00656

Zhang, S., Guo, Y., Li, S., Ke, Z., Zhao, H., Yang, J., et al. (2022). Investigation on environment monitoring system for a combination of hydroponics and aquaculture in greenhouse. *Inf. Process. Agric.* 9, 123–134. doi: 10.1016/j.inpa.2021.06.006

frontiers | Frontiers in Plant Science

TYPE Original Research
PUBLISHED 08 March 2024
DOI 10.3389/fpls.2024.1358312

Check for updates

OPEN ACCESS

EDITED BY
Ewa M. Kalemba,
Polish Academy of Sciences, Poland

REVIEWED BY
Raquel Iglesias Fernández,
Polytechnic University of Madrid, Spain
Carol Baskin,
University of Kentucky, United States

*CORRESPONDENCE
Jake O. Chandler
jake.chandler@rhul.ac.uk;
j.o.chandler@lancaster.ac.uk
Gerhard Leubner-Metzger
Gerhard.Leubner@rhul.ac.uk

RECEIVED 19 December 2023
ACCEPTED 19 February 2024
PUBLISHED 08 March 2024

CITATION
Arshad W, Steinbrecher T, Wilhelmsson PKI, Fernandez-Pozo N, Pérez M, Mérai Z, Rensing SA, Chandler JO and Leubner-Metzger G (2024) *Aethionema arabicum* dimorphic seed trait resetting during transition to seedlings. *Front. Plant Sci.* 15:1358312. doi: 10.3389/fpls.2024.1358312

Aethionema arabicum dimorphic seed trait resetting during transition to seedlings

Waheed Arshad [1], Tina Steinbrecher [1], Per K.I. Wilhelmsson [2], Noe Fernandez-Pozo [2,3], Marta Pérez [1], Zsuzsanna Mérai [4], Stefan A. Rensing [2,5,6], Jake O. Chandler [1]* and Gerhard Leubner-Metzger [1,7]*

[1]Seed Biology and Technology Group, Department of Biological Sciences, Royal Holloway University of London, Egham, United Kingdom, [2]Plant Cell Biology, Faculty of Biology, University of Marburg, Marburg, Germany, [3]Department Plant Breeding and Physiology, Institute for Mediterranean and Subtropical Horticulture "La Mayora" (IHSM-CSIC-UMA), Málaga, Spain, [4]Gregor Mendel Institute of Molecular Plant Biology, Austrian Academy of Sciences, Vienna Biocenter (VBC), Vienna, Austria, [5]Centre for Biological Signalling Studies (BIOSS), University of Freiburg, Freiburg, Germany, [6]Faculty of Chemistry and Pharmacy, University of Freiburg, Freiburg, Germany, [7]Laboratory of Growth Regulators, Faculty of Science, Palacký University and Institute of Experimental Botany, Czech Academy of Sciences, Olomouc, Czechia

The transition from germinating seeds to emerging seedlings is one of the most vulnerable plant life cycle stages. Heteromorphic diaspores (seed and fruit dispersal units) are an adaptive bet-hedging strategy to cope with spatiotemporally variable environments. While the roles and mechanisms of seedling traits have been studied in monomorphic species, which produce one type of diaspore, very little is known about seedlings in heteromorphic species. Using the dimorphic diaspore model *Aethionema arabicum* (Brassicaceae), we identified contrasting mechanisms in the germination responses to different temperatures of the mucilaginous seeds (M^+ seed morphs), the dispersed indehiscent fruits (IND fruit morphs), and the bare non-mucilaginous M^- seeds obtained from IND fruits by pericarp (fruit coat) removal. What follows the completion of germination is the pre-emergence seedling growth phase, which we investigated by comparative growth assays of early seedlings derived from the M^+ seeds, bare M^- seeds, and IND fruits. The dimorphic seedlings derived from M^+ and M^- seeds did not differ in their responses to ambient temperature and water potential. The phenotype of seedlings derived from IND fruits differed in that they had bent hypocotyls and their shoot and root growth was slower, but the biomechanical hypocotyl properties of 15-day-old seedlings did not differ between seedlings derived from germinated M^+ seeds, M^- seeds, or IND fruits. Comparison of the transcriptomes of the natural dimorphic diaspores, M^+ seeds and IND fruits, identified 2,682 differentially expressed genes (DEGs) during late germination. During the subsequent 3 days of seedling pre-emergence growth, the number of DEGs was reduced 10-fold to 277 root DEGs and 16-fold to 164 shoot DEGs. Among the DEGs in early seedlings were hormonal regulators, in particular for auxin, ethylene, and gibberellins. Furthermore, DEGs were identified for water and ion transporters, nitrate transporter and assimilation enzymes, and cell wall remodeling protein genes encoding enzymes targeting xyloglucan and pectin. We conclude that the

transcriptomes of seedlings derived from the dimorphic diaspores, M^+ seeds and IND fruits, undergo transcriptional resetting during the post-germination pre-emergence growth transition phase from germinated diaspores to growing seedlings.

KEYWORDS

fruit and seed heteromorphism, bet-hedging strategy, diaspore dimorphism, seed seedling transition, transcriptome resetting, seedling stress resilience, pre-emergence growth, pericarp-imposed dormancy

1 Introduction

The transition from germinating seeds to emerging seedlings is one of the most vulnerable plant life cycle stages, which depends on seed and seedling phenotypic plasticity and complex interactions with environmental cues (Fenner, 1987; Walck et al., 2011; Gardarin et al., 2016). Seed germination and fruit germination depend on basic requirements for water, oxygen, and an appropriate temperature and are generally considered to be completed by radicle protrusion (visible germination). Germination is further spread over time by dormancy mechanisms, which block germination under favorable conditions so that germination occurs when conditions for establishing a new plant generation are likely to be suitable (Finch-Savage and Leubner-Metzger, 2006; Baskin and Baskin, 2014; Finch-Savage and Footitt, 2017). Successful seedling establishment and spreading seedling emergence over time, therefore, depend primarily on germination timing; in addition, post-germination seedling traits are of major importance. What follows the completion of germination is the pre-emergence seedling growth phase, which may be prone to increasing post-germination stress in the soil environment, and consequently, seeds/seedlings are often lost and fail to establish during this stage (Moles and Westoby, 2006; Finch-Savage and Bassel, 2016; Gardarin et al., 2016). Pre-emergence seedling growth is heterotrophic growth in which the seeds' storage reserves are used to establish a root and to fuel shoot elongation until the seedling emerges from the soil and switches to greening and self-nourishing autotrophic growth (Fenner, 1987; Finch-Savage and Bassel, 2016; Ha et al., 2017; Smolikova et al., 2022). While the roles and mechanisms of seedling traits have been studied in monomorphic species, which produce one type of diaspore (dispersed seeds or fruits), very little is known about seedlings in heteromorphic species.

Diaspore (seed/fruit) heteromorphism is the production by an individual plant of two (dimorphism) or more distinct kinds of seeds and/or fruits that differ in morphological (e.g., mass, shape, and color), dispersal ability (e.g., dormancy and mode of dispersal), and other diaspore properties (Imbert, 2002; Baskin and Baskin, 2014; Baskin et al., 2014). Heteromorphic diaspore traits have been proposed to be an adaptive bet-hedging strategy to cope with spatiotemporally variable environments. Distinct dormancy breaking requirements of the morphs cause differences in germination timing, and consequently, seedling emergence is spread over time and space (Maun and Payne, 1989; Lu et al., 2017a; b; Arshad et al., 2019; Lu et al., 2020). For example, comparison of seedlings derived from the dimorphic seeds of the cold desert halophyte *Suaeda corniculata* demonstrated that seedlings from black seeds emerged in July and August, and those from brown seeds emerged in May, and these dimorphic seedlings also differed in size and root/shoot ratio (Cao et al., 2012; Yang et al., 2015). Seedlings derived from dimorphic seeds of *Atriplex centralasiatica* and other *Suaeda* species differed in salinity tolerance (Xu et al., 2011; Zhang et al., 2021; Cao et al., 2022; Song et al., 2023). Whether seedlings derived from dimorphic seeds also differ in responsiveness to other abiotic stress factors such as heat or drought has not been investigated.

Here, we exploit the diaspore dimorphism of *Aethionema arabicum* (Figure 1), an annual member of the earliest diverging sister tribe within the Brassicaceae, in which seed and fruit dimorphism was associated with a switch to an annual life history (Lenser et al., 2016; Mohammadin et al., 2017; Chandler et al., 2024). *Ae. arabicum* is adapted to arid and semiarid environments, its life-history strategy appears to be a blend of bet-hedging and phenotypic plasticity (Bhattacharya et al., 2019b), and it exhibits true seed and fruit dimorphism with no intermediate morphs (Lenser et al., 2016). Two distinct fruit types are produced on the same infructescence: dehiscent (DEH) fruits, with four to six mucilaginous (M^+) seeds, and indehiscent (IND) fruits, each containing a single non-mucilaginous (M^-) seed. Upon maturity, DEH fruits shatter, releasing the M^+ seeds, while the dry IND fruits are dispersed in their entirety by abscission. Two very contrasting biophysical and ecophysiological dispersal mechanisms of the *Ae. arabicum* dimorphic diaspores were revealed (Arshad et al., 2019). Dehiscence of large fruits leads to the release of M^+ seed diaspores, which adhere to substrata via seed coat mucilage, thereby preventing dispersal (anti-telechory). IND fruit diaspores (containing non-mucilaginous seeds) disperse by wind or water currents, promoting dispersal (telechory) over a longer range. The pericarp properties confer enhanced dispersal ability and degree of dormancy to the IND fruit morph to support telechory, while the M^+ seed morph supports anti-telechory. The germination of M^+ seeds of some *Ae. arabicum* accessions is inhibited by light, while other *Ae. arabicum* accessions, including the widely used TUR (Turkey) accession, germinate equally well in continuous light and darkness (Merai et al., 2019). Dimorphic fruits and seeds of the *Ae. arabicum*

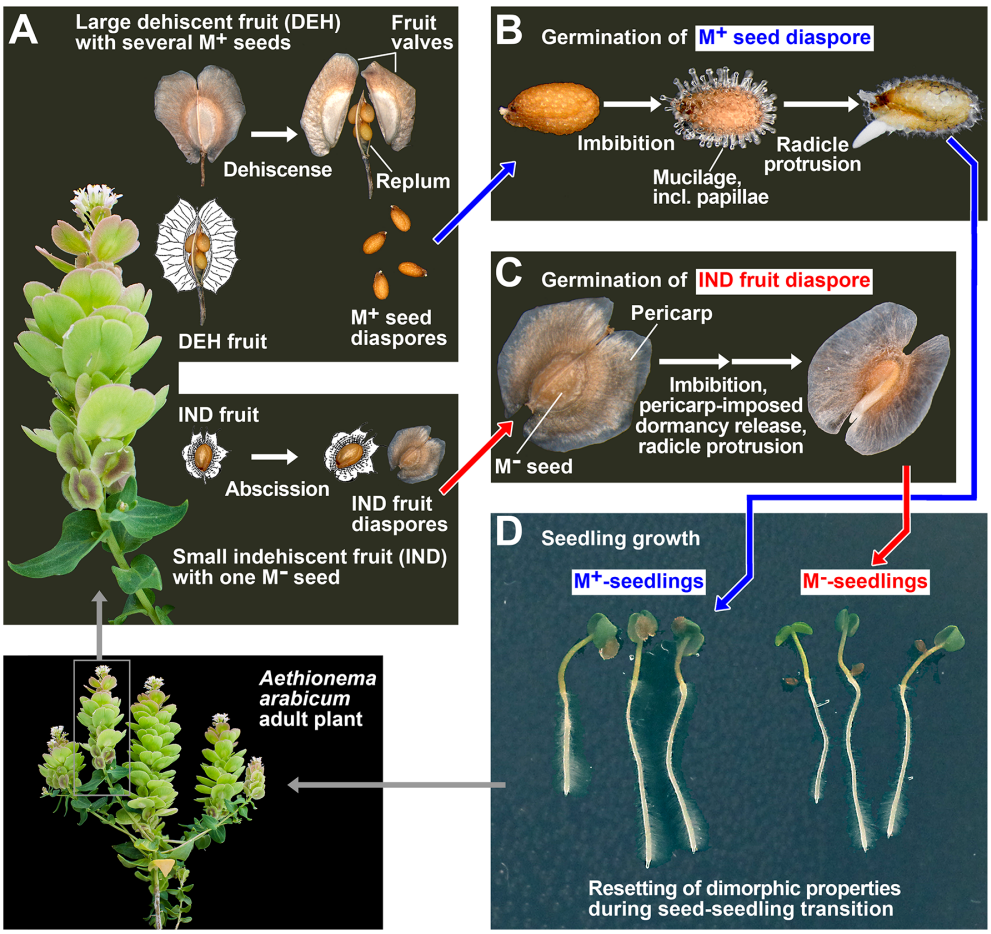

FIGURE 1
Annual life cycle of the dimorphic diaspore model *Aethionema arabicum*. **(A)** Dimorphic fruit and seed development and dispersal of the M^+ seed and IND fruit diaspores. **(B)** Germination of the M^+ seed diaspore. **(C)** Germination of the IND fruit diaspore. **(D)** Seedling growth of M^+ and M^- seedlings derived from the M^+ and M^- seeds, respectively. Resetting of the dimorphism during pre-emergence growth leads to adult plants that are indistinguishable regarding their M^+ or IND origin. These plants restart producing dimorphic diaspores during reproduction. Rearranged and redrawn using parts from Arshad et al. (2019).

TUR accession differ in their molecular mechanisms throughout their development on the mother plant, in the mature dry state upon dispersal, and in dormancy and germination properties during imbibition (Lenser et al., 2018; Arshad et al., 2019; Wilhelmsson et al., 2019; Nichols et al., 2020; Arshad et al., 2021; Steinbrecher and Leubner-Metzger, 2022; Chandler et al., 2024). We demonstrate here that the seedlings of the *Ae. arabicum* TUR accession derived from the dimorphic diaspores (M^+ seeds and IND fruits) differ during their pre-emergence growth and undergo resetting of their transcriptomes during the transition from germinated diaspores to early seedlings.

2 Results

2.1 Resetting of distinct *Ae. arabicum* dimorphic diaspore responses to abiotic stresses during the seed-to-seedling transition phase

Figure 1 shows the life cycle of the annual *Ae. arabicum*, which is characterized by the production and dispersal of dimorphic diaspores. The M^+ seed diaspore is dispersed by dehiscence (pod shatter), and upon imbibition, it produces a mucilaginous layer during germination (Figure 1B). The IND fruit diaspore is dispersed by abscission and constitutes an indehiscent fruit in which the single M^- seed is covered by the pericarp (fruit coat), which confers coat dormancy and prevents or delays germination (Figure 1C). Earlier work with *Ae. arabicum* TUR (Chandler et al., 2024) revealed the molecular and morphological mechanisms underpinning the distinct dormancy and germination responses of the dimorphic diaspores to different imbibition temperatures. A comparison of the maximal germination percentages (G_{max}) and the germination rates (speed) of germination (GR_{50}; i.e., the inverse of the time of the diaspore population to reach 50% radicle protrusion) identified 14°C as the optimal temperature for the highest germination speed of the M^+ seed morphs, the bare M^- seeds (manually extracted from IND fruits by pericarp removal), and the IND fruit morphs (Supplementary Figure 1). The IND fruit morph, however, exhibited a degree of pericarp-imposed dormancy across the entire temperature window. Thus, our initial physiological experiments investigating the effects of abiotic stress factors on seedling growth focused on comparing M^+ and M^- seedlings derived from germinated M^+ and bare M^- seeds, respectively. These experiments, involving the removal of the

pericarp to obtain exposed M^- seeds, align with dimorphic systems (see the Introduction) characterized by true seeds of distinct colors as diaspores. In such systems, the resulting seedlings exhibit differential responses to salinity, with the unique seedling reactions having already been established during dimorphic seed development (Xu et al., 2011; Zhang et al., 2021; Cao et al., 2022; Song et al., 2023). In our subsequent comparative biomechanical and transcriptome analyses with *Ae. arabicum* TUR, we compared the seed–seedling transition phase and early growth of seedlings derived from germinated M^+ seeds, bare M^- seeds, and IND fruits. Adult plants grown from M^+ and M^- seedlings are indistinguishable from each other and produce dimorphic diaspores (Figure 1).

To study the effects of thermal stress on M^+ and M^- seedling growth independently from the temperature effects on dimorphic diaspore germination (Supplementary Figure 1), M^+ and M^- seeds were imbibed at an optimal germination temperature, and seeds that had just completed germination (1-mm radicle protrusion visible) were transferred to agar plates for conducting the seedling growth assay (Figure 2). M^+ and M^- seedlings grown on vertical agar plates at 14°C, 20°C, 24°C, 30°C, and 35°C were compared for their root and shoot lengths at the times indicated [in "hat" (hours after transfer)], and seedling growth rates were calculated. Though the total seedling length differed significantly in several cases between the morphs, the difference was very small, and there was no overall morph-specific physiological response. Similarly, seedling growth rates did not differ between the M^+ and M^- morphs (Figure 2A). The fastest seedling growth rate was observed at 72 hat, and 30°C was identified as the temperature for fastest growth leading to the longest seedlings at 240 hat (Figure 2B; Supplementary Figure 2). Fresh and dry weights of separated root and shoot tissue at the end of the experiment (10 days) revealed a strong temperature response ($p < 0.001$), with the highest masses observed at 30°C (Supplementary Figure 2). Together with seedling lengths, growth rates, and fresh weights, the most optimal seedling growth condition considered was thus 30°C, likely corresponding with the maximum climatic temperatures of sites in Turkey from which *Ae. arabicum* TUR was collected (Arshad et al., 2019). At 35°C, there were slight indications that M^+ seedlings had greater vigor, with a higher mean shoot fresh and dry weight than M^- seedlings (Supplementary Figure 2). Temperature, therefore, had a profound effect on M^+ and M^- seedling growth, in particular on post-germination pre-emergence growth until 72 hat (Figure 2).

To study the effect of osmotic stress on the growth of *Ae. arabicum* M^+ and M^- seedlings, their growth was analyzed at lowered water potentials using high-molecular-weight polyethylene glycol (PEG). After more than 3 weeks of vertical growth, seedling morphs did not differ in their total length and growth rates under three different concentrations of PEG (Supplementary Figure 3). Taken together, no differences in the physiological responses of M^+ and M^- seedlings derived from M^+ seeds and bare M^- seeds to temperature and reduced water potential were identified. This suggests that during the seed–seedling transition, the observed dimorphic diaspore trait differences observed in abiotic stress responses (Lenser et al., 2016, 2018; Arshad et al., 2019; Wilhelmsson et al., 2019; Bhattacharya et al., 2019a, b; Arshad et al., 2020, 2021; Fernandez-Pozo et al., 2021; Chandler et al., 2024) may be reset to a large extent. To test this hypothesis, we conducted transcriptome analysis.

2.2 Comparative RNA-seq analysis of late germination and post-germination pre-emergence seedling growth reveals gradual resetting of transcriptomes

Figure 3A depicts the experimental design for the RNA-seq analysis in which we compared the transcriptomes during the late germination phase with those during early seedling growth. Samples were collected from imbibed *Ae. arabicum* M^+ seeds, M^- seeds, and IND fruits at $T_{1\%}$, i.e., the time for the onset of the completion of germination of a seed population, and at $T_{100\%}$, i.e., the time when the entire population had completed germination by visible radicle protrusion (Figure 3A). It is known from previous work (Wilhelmsson et al., 2019; Arshad et al., 2021; Chandler et al., 2024) that the pericarp of imbibed IND fruits is dead tissue that does not contain any RNA and that dry seed and germination transcriptomes until $T_{1\%}$ differ considerably between the dimorphic diaspores. The physiological sampling times for $T_{1\%}$ and $T_{100\%}$ of M^+ seeds, bare M^- seeds, and IND fruits are indicated in Figure 3A. Diaspores that had just completed germination (1-mm radicle protrusion) were transferred to agar plates at $T_{100\%}$ (0 hat) for conducting the seedling growth assay. Root and shoot tissues were harvested from seedling samples at key physiological stages (72 hat and 240 hat) during early seedling growth (Figure 3).

The 72-hat pre-emergence growth samples correspond to the maximal growth rate, and 72 hat was associated with the onset of cotyledon greening by chlorophyll accumulation (Figure 3B). Between 6 and 10 days, the growth rates of M^+ and M^- seedlings derived from germinated M^+ seeds and bare M^- seeds, respectively, remained roughly equal. M^+ and M^- seedlings derived from germinated M^+ seeds and bare M^- seeds had straight hypocotyls. In contrast to this, seedlings derived from IND fruits often exhibited a bent lower hypocotyl connected with an overall slower shoot and root growth (Figure 4A). To investigate if morph caused a long-lasting effect on the biomechanical properties of the hypocotyls, we conducted comparative hypocotyl tensile tests of 15-day-old seedlings (Figure 4B). No significant differences in the hypocotyl breaking force were evident between the seedlings derived from germinated M^+ seeds, bare M^- seeds, and IND fruits (Figure 4C). The observed difference in hypocotyl shape (bent versus straight) and the slower shoot and root growth of IND fruit-derived seedlings, therefore, did not affect the hypocotyl biomechanical properties at this stage of seedling growth.

To provide insights into the association between RNA-seq samples, datasets were visualized using principal component analysis (PCA), based on the 500 genes with the highest variance. Replicate RNA-seq samples clustered tightly by diaspore and by organ (root and shoot) type (Figure 5A). As expected, three distinct clusters were separated primarily by the derivation of the samples from seed, root, or shoot tissue based on the first two components, explaining 48% and 44% of the variability. In this combined analysis

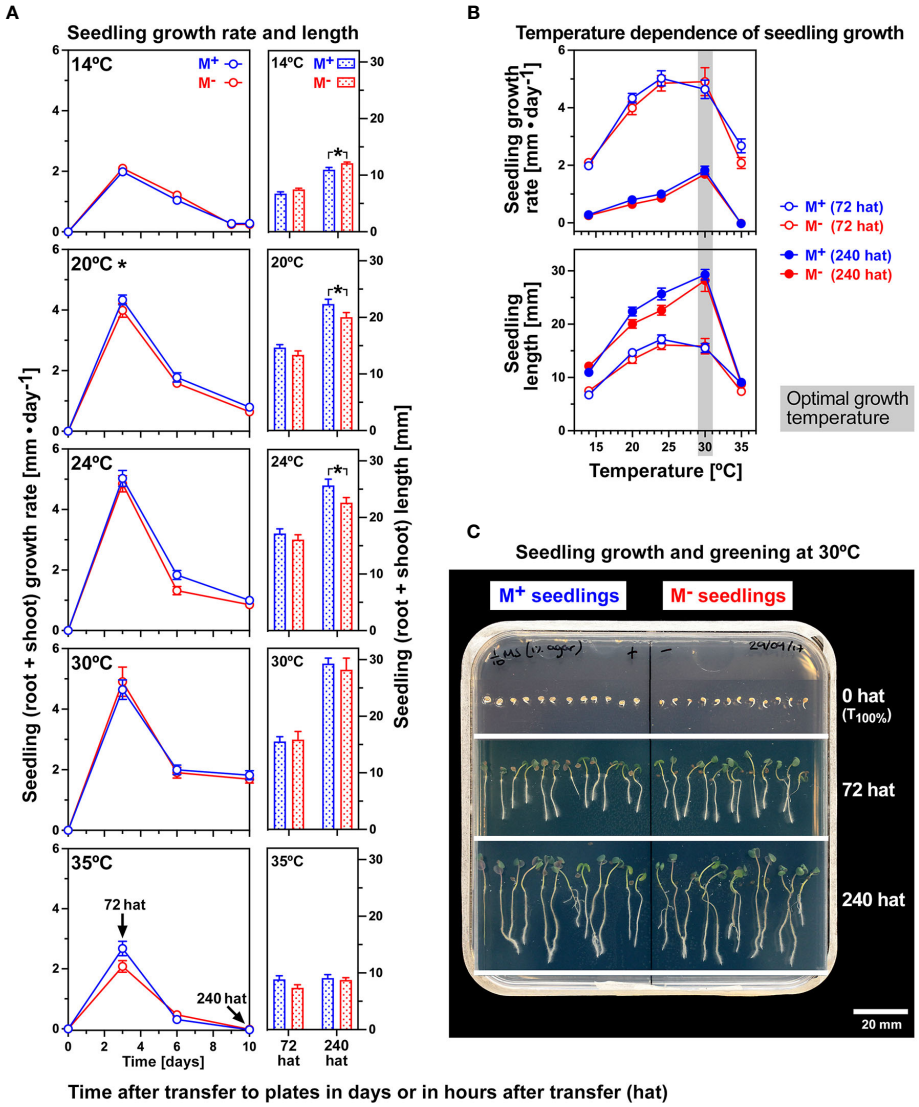

FIGURE 2
The effect of a range of constant temperatures on the growth of *Aethionema arabicum* M^+ and M^- seedlings. **(A)** M^+ and M^- seedlings were grown on vertical agar plates at constant temperatures as indicated. Seedling growth was scored over time starting at 0 hat (hours after transfer). The mean ± SEM (N = 3 plates, each with seven seedlings) of seedling growth rates over time and seedling lengths at 72 and 240 hat are presented; for further details, see Supplementary Figure 2. ANOVA of growth rates revealed that morph had no effect overall at 14°C ($p = 0.114$), 24°C ($p = 0.089$), 30°C ($p = 0.959$), or 35°C ($p = 0.217$), while at 20°C ($p = 0.027$), M^+ seedlings grew at a faster rate than M^- seedlings. Statistical analysis (unpaired t-test) of day 10 M^+ and M^- seedlings demonstrated that the slightly different lengths between M^+ and M^- seedlings were significant (*) at 14°C (M^- seedlings slightly longer, $p = 0.012$), 20°C (M^- seedlings slightly shorter, $p = 0.049$), and 24°C (M^- seedlings slightly shorter, $p = 0.040$), while no significant length difference was obtained at 30°C and 35°C. **(B)** Temperature dependence of seedling growth rate and seedling length at 72 and 240 hat. The optimal seedling growth temperature (30°C) is indicated. ANOVA of 72 and 240-hat seedling growth rates and seedling length across the entire temperature range revealed no significant differences between the morphs (M^+ versus M^-). **(C)** M^+ and M^- seedlings were grown on vertical agar plates in continuous white light (170 $\mu mol \cdot m^{-2} \cdot s^{-1}$). Seedling growth assays were conducted with seedlings derived from germinated M^+ and M^- seeds, which were selected for transfer to agar plates containing media based on 1-mm protrusion of the radicle (0 hat).

(Figure 5A), IND samples at $T_{100\%}$ (germinated diaspores) remain distinct from all other tissues and time points. Separation of samples involved in key processes of germination ($T_{1\%}$ and $T_{100\%}$), root growth (72 and 240 hat), and shoot growth (72 and 240 hat) revealed comparative transcriptome profiles between the morphs in greater detail (Figure 5). Clear differences were observed with IND samples, such that both $T_{1\%}$ and $T_{100\%}$ samples clustered separately from M^+ and M^- seed samples. M^+ and M^- seed samples, however, showed tight correlations throughout the course of germination (Figure 5B). As seedlings, differences between morphs appear to be smaller. M^+ and M^- samples clustered together during the two time points during root (Figure 5C) and shoot (Figure 5D) growth. IND root samples remain distinct from M^+ and M^- samples. However, transcriptional profiles of IND shoot tissue suggest that while samples at 72 hat remain as a separate cluster, by 240 hat, there is a tendency toward greater similarity of M^+ and M^- samples.

Cleaned RNA-seq reads mapped to the *Ae. arabicum* genome were obtained for 23,594 genes (Supplementary Dataset 1). To

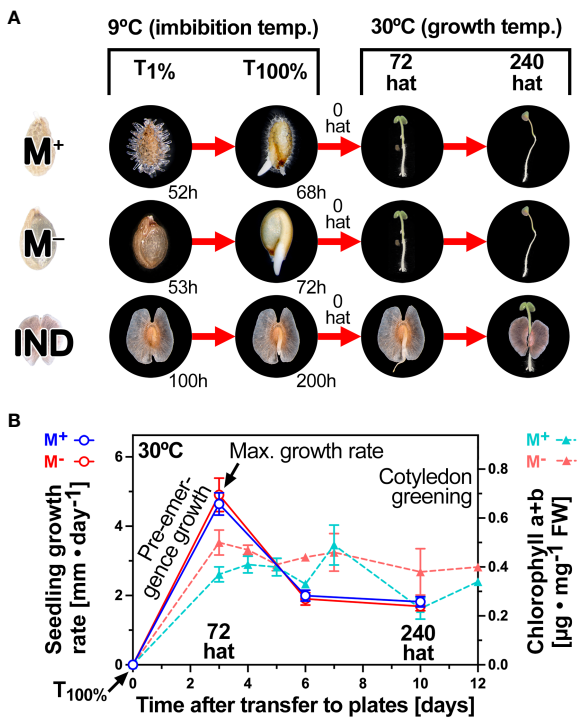

FIGURE 3
Diaspore germination and seedling growth phases for the comparative transcriptome analysis. **(A)** Overall experimental design for comparative RNA-seq analysis of diaspore germination and seedling establishment. Time points were selected during completion of germination ($T_{1\%}$ and $T_{100\%}$; times of these are indicated), early [72 hat (hours after transfer)], and late (240 hat) seedling growth. Within-root and within-shoot tissue pairwise comparisons were based on the effect of the seed morph (M^+ seed vs. bare M^- seed), the effect of the pericarp (M^- seed vs. IND fruit), and the ecological dispersal unit (M^+ seed vs. IND fruit). **(B)** Key events and phases of seedling growth at the optimal temperature (30°C) and time course analysis of chlorophyll accumulation during cotyledon greening. Error bars = ± 1 SEM. N = 3, each with 10 replicate seedlings.

make the transcript abundance data easily and publicly accessible, a gene expression atlas was generated, which was implemented in the *Ae. arabicum* genome database (DB) (Fernandez-Pozo et al., 2021) at https://plantcode.cup.uni-freiburg.de/aetar_db/index.php. The *Ae. arabicum* gene expression atlas includes the transcriptome results of this work and work published earlier (Merai et al., 2019; Wilhelmsson et al., 2019; Arshad et al., 2021; Chandler et al., 2024) and allows adding future transcriptome datasets. The transcript abundance data for the 23,594 *Ae. arabicum* genes were further investigated, and differentially expressed genes (DEGs; Supplementary Dataset 1) were detected in a strict consensus (overlap) approach using an adjusted p-value cutoff set to 0.001 (Wilhelmsson et al., 2019). Pairwise comparisons of M^+ seeds vs. bare M^- seeds (seeds only), M^+ seeds vs. IND fruits (natural dispersal units), and M^- vs. IND (pericarp effect) allowed transcriptome exploration of the dimorphic syndrome during seed germination and seedling growth. Comparisons showed that M^+ and M^- seed transcriptomes became remarkably similar during the completion of germination (Figure 6A; Supplementary Table 1). A total of 180 and 55 DEGs were detected at $T_{1\%}$ and $T_{100\%}$, respectively, while after 72 hat, the seedling transcriptomes were almost identical in the root (three DEGs) and shoot (two DEGs). By contrast, comparisons between the natural diaspores, M^+ seed vs. IND fruit, showed a much higher number of DEGs during germination. A total of 2,041 DEGs during $T_{1\%}$ increased to 2,682 by $T_{100\%}$, thereafter reducing 10-fold (277 root DEGs) and 16-fold (164 shoot DEGs) by 72 hat. By 240 hat, the time of true leaf emergence for seedlings, differences between M^+ seed vs. IND fruit-derived seedlings were only evident from 60 DEGs in root samples and 10 DEGs in shoot samples (Figure 6B; Supplementary Table 1).

Interestingly, a similar but more pronounced pattern of DEGs was observed in the comparison of the pericarp effect (bare M^- seed vs. IND fruit) on M^- seed germination and seedling growth (Figure 6C; Supplementary Table 1). The number of DEGs at $T_{1\%}$ was similar to that detected in the M^+ vs. IND comparison (2,041 vs. 1,938). The greatest differences were observed at $T_{100\%}$ (3,228 DEGs) at the onset of pre-emergence growth. Here, the number of upregulated DEGs in M^- seeds increased 1.4-fold (to 1,220 DEGs), while the number of downregulated DEGs increased 1.9-fold (to 2,008 DEGs). As seedlings progressed through root and shoot growth, the pericarp imposed a total of 347 root-specific DEGs at 72 hat, while shoot-specific DEGs were lower (64). By 240 hat, differences in shoot samples comprised four up- and four downregulated DEGs, while 62 up- and 69 downregulated DEGs were detected in the root tissues (Figure 6C; Supplementary Table 1). Taken together, these results suggest the tendency toward transcriptional "resetting" of seedling morphs mainly during the post-germination pre-emergence growth phase.

In the ecologically relevant comparison (M^+ seed vs. IND fruit), shoot resetting occurred earlier (by 72 hat), and root resetting occurred later (differences still evident at 240 hat). Comparison of M^+/IND DEG lists (Supplementary Dataset 1) between the $T_{100\%}$ (germinated diaspores) and the $T_{1\%}$ (ungerminated diaspores) time points revealed that about one-third of the DEGs are overlapping and two-thirds are unique to either $T_{100\%}$ or $T_{1\%}$ (Figure 7A). Comparison of the M^+/IND and M^-/IND DEG lists at $T_{100\%}$ revealed that while the majority of the DEGs are overlapping, there is also a considerable number of DEGs unique to either M^+/IND or M^-/IND (Figure 7A). For the ecologically relevant comparison (M^+/IND), the comparison between the $T_{100\%}$ seed and the 72-hat seedling state delivered root and shoot DEGs common and unique for pre-emergence seedling growth (Figure 7B). Comparison of M^+/IND DEG lists during pre-emergence seedling growth revealed that most of the DEGs at 72 hat are unique for root and shoot, a finding that strongly suggests that the two compartments are distinct (Figure 7C). To investigate the effect of the pericarp on the pre-emergence seedling growth at M^+/IND and M^-/IND, DEG lists for root and shoot at 72 hat were compared and delivered DEG lists representing pericarp-dependent and pericarp-independent mechanisms (Figure 7B; Supplementary Dataset 1). These comparative DEG lists (M^+/IND vs. M^-/IND) contained for roots a total of 190 up- and 226 downregulated genes and for shoots a total of 43 up- and 138 downregulated genes.

To gain insight into the processes differing during the transition from germinated diaspores to early seedlings derived from M^+, M^-, and IND, Gene Ontology (GO) term enrichment analysis of DEG

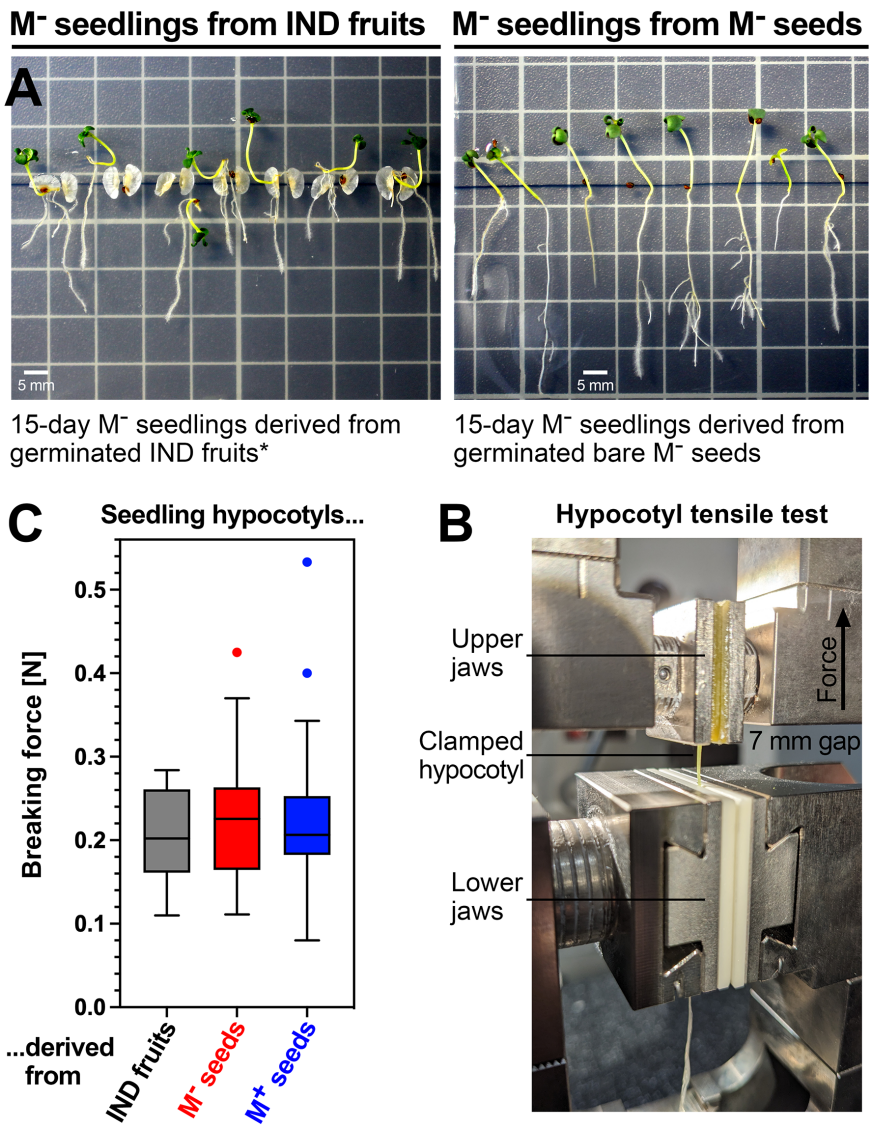

FIGURE 4
Comparative biomechanical analysis of *Aethionema arabicum* seedlings derived from M^+ seeds, M^- seeds, and IND fruits. **(A)** Fifteen-day-old seedlings from germinated (0 hat) IND fruits (*left panel*) and bare M^- seeds (*right panel*). * IND pericarps of germinated fruits (at 0 hat) were manually split open to aid seedling growth. Note that seedlings derived from IND fruits often had bent lower hypocotyls and, in general, grew slower compared to seedlings derived from M^- seeds, which had straight hypocotyls. **(B)** Hypocotyl tensile test. **(C)** Hypocotyl breaking forces of 15-day-old seedlings derived from IND fruits, bare M^- seeds, and M^+ seeds. Box plots with Tukey's whiskers of hypocotyl breaking forces are presented from force-displacement data obtained using N = 42 (M^+), N = 38 (M^-), and N = 15 (IND) seedlings. The hypocotyls show no significant difference in their breaking force.

lists was performed comparing M^+ seeds versus IND fruits and M^- seeds versus IND for the $T_{100\%}$ (germinated diaspores) and the 72 hat (root and shoot separately) stages (Figure 8; Supplementary Figure 4, Supplementary Dataset 2). Broadly, selected identified GO terms were categorized by key processes identified as differing between seedlings originating from the different diaspores (Figure 8; Supplementary Figure 4). For example, genes up in roots of seedlings 72 hat derived from M^+ or M^- seeds compared to IND diaspores were significantly enriched in GO terms related to nitrates (e.g., nitrate assimilation), cell wall (e.g., cellulose catabolic process), and transport (e.g., regulation of ion transport) (clusters 1 and 5). Interestingly, some cell wall and nitrate-related terms (e.g., cell wall pectin metabolic process and nitrate transport) were enriched in genes more highly expressed in 72-hat seedlings derived from IND compared to M^+ and M^- (clusters 8 and 5). A pronounced effect of pericarp at the $T_{100\%}$ stage was evident in the enrichment of abiotic stress-related GO terms "response to oxidative stress", "response to salt stress", and "anaerobic respiration". Terms identifying hormone signaling (e.g., ethylene, auxin, gibberellin, and ABA) were also identified (Figure 8; Supplementary Figure 4; Supplementary Dataset 2). Overall, it was evident that pericarp presence at the diaspore stage was a driver of differences in gene expression, with similar differences evident when comparing M^+ or M^- seeds against IND diaspores. However, some contrasts were more evident when comparing 72-hat seedlings derived from M^+ to IND (rather than M^- to IND),

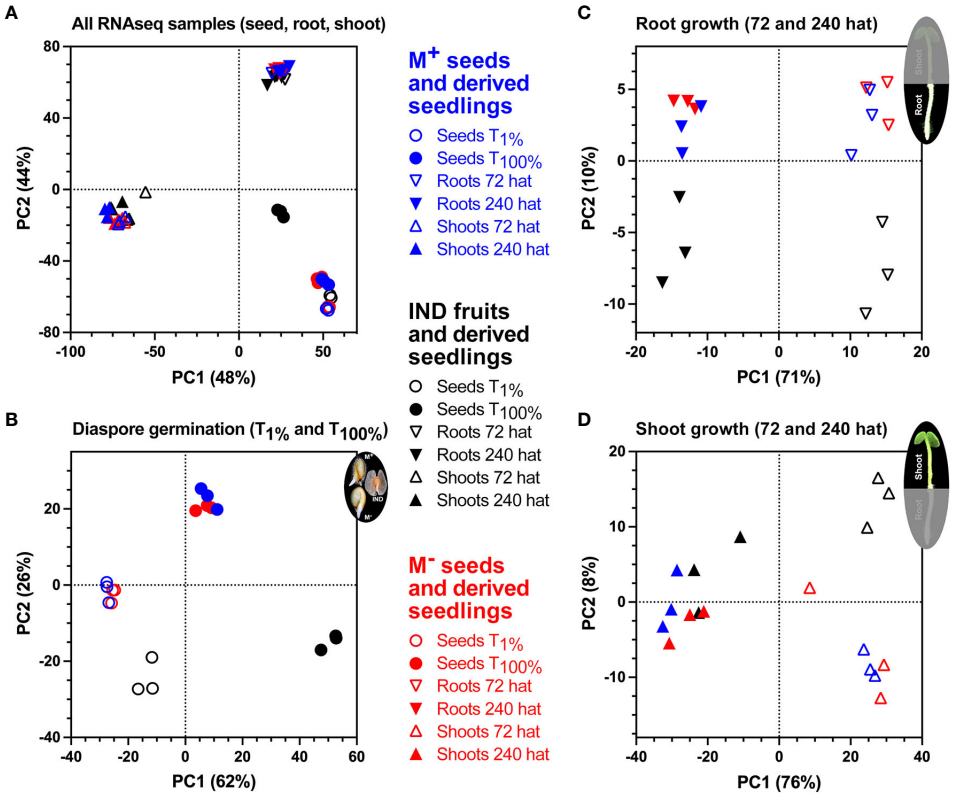

FIGURE 5
Principal component analysis (PCA) of *Aethionema arabicum* seed and seedling RNA-seq samples. **(A)** PCA of RNA-seq samples obtained during M^+ seed, M^- seed, and IND fruit germination and seedling establishment. Colors indicate morph, while symbols indicate seed, root, or shoot tissue at 1% germination ($T_{1\%}$), 100% germination ($T_{100\%}$), or 72 or 240 hours after transfer (hat) to seedling growth plates. **(B)** PCA of RNA-seq samples during diaspore germination. **(C)** PCA of RNA-seq samples during seedling root growth at 72 and 240 hat. **(D)** PCA of RNA-seq samples during seedling shoot growth at 72 and 240 hat.

suggesting seed morph-specific responses that were not dependent on pericarp presence at imbibition, particularly evident in the enrichment of GO terms "flavonol biosynthetic process" and "anthocyanin-containing compound biosynthetic process". The pre-emergence seedling growth DEGs from these lists of enriched GO categories (Figure 8; Supplementary Figure 4) and a comparison to early seed germination and dormancy (Chandler et al., 2024) are the focus of the following analysis into the resetting of dimorphic expression patterns.

2.3 Resetting of dimorphic expression patterns of hypoxia and hormone-related genes

In earlier work, we identified morph-specific expression patterns of hormone-related genes during seed and fruit development (Arshad et al., 2021) and dormancy and germination of the dimorphic diaspores (Chandler et al., 2024). This revealed the importance of ABA metabolism and signaling in dimorphic diaspore development and germination, and key roles for ABA and hypoxia in imposing pericarp-imposed dormancy in IND fruits. Figure 9A shows that when IND fruits were compared to M^+ and M^- seeds, the distinct expression patterns of hypoxia-responsive genes in seeds were reset during the transition from the germination ($T_{100\%}$) to the early seedling (72 hat) phase. This was evident for the hypoxia-regulated transcription factor (TF) genes, such as *AearNAC102* and *AearERF71/73*, and downstream genes, such as the ethanolic fermentation enzyme gene *AearADH1a* (Chandler et al., 2024). The *Ae. arabicum* genes presented in Figure 9A were identified as part of the core hypoxia-responsive gene list derived from hypoxia-treated *Arabidopsis thaliana* seedlings (Christianson et al., 2009; Gasch et al., 2016; Lee and Bailey-Serres, 2019), and the resetting of their expression patterns, therefore, also indicates the absence of hypoxia once the M^- seedlings have emerged from the IND pericarp. Most genes involved in ethylene biosynthesis, 1-aminocyclopropane-1-carboxylic acid (ACC) oxidase (ACO) and ACC synthase (ACS), and many genes encoding ethylene response factor (ERF) TFs also exhibited resetting during pre-emergence seedling growth (Figure 9A; Supplementary Figure 5A). However, for genes encoding the ACC oxidases AearACO2 and AearACO4, the ethylene receptor AearETR2, and several ERF TFs (AearERF2, AearERF11, AearERF113/RAP2.6, and AearRAP2.11), distinct transcript abundances were retained in 72-hat shoots or roots (Supplementary Figure 5A). The *A. thaliana* homologs of these ERF TFs are known to be involved in the control of seedling growth by modulating ABA, ethylene, gibberellin, and auxin signaling (Kim

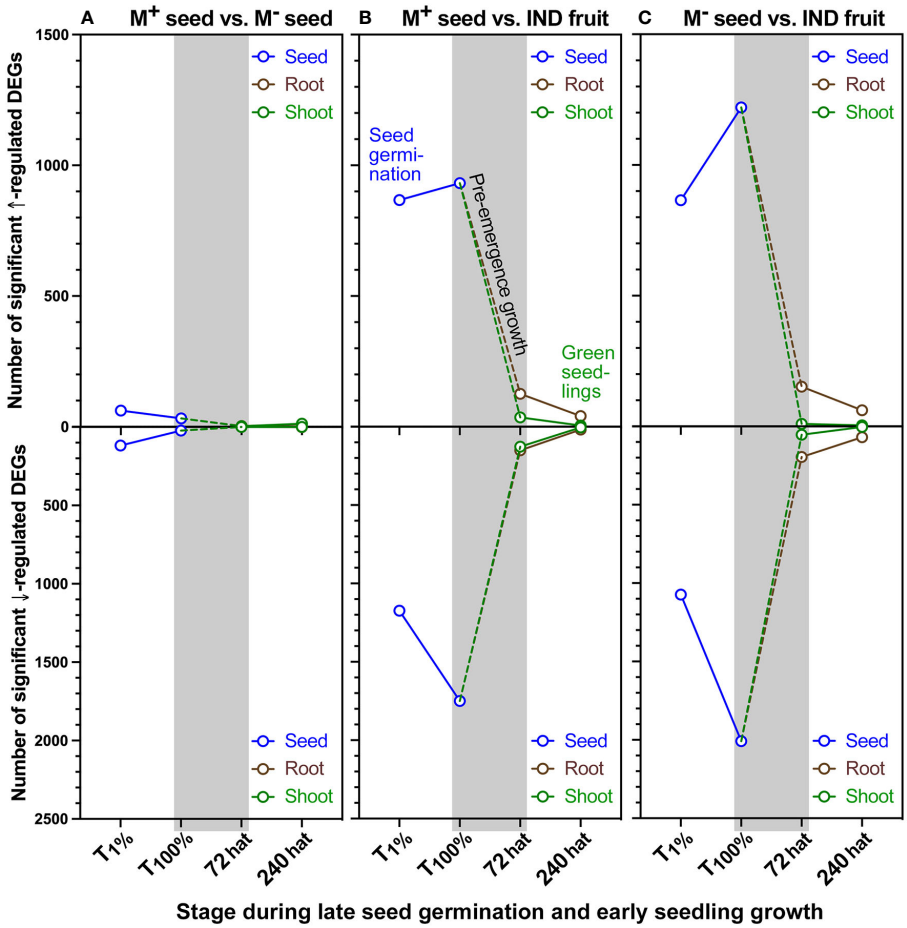

FIGURE 6
Number of differentially expressed genes (DEGs) identified during the developmental transition from germination to seedling establishment of *Aethionema arabicum*. Total number of DEGs detected during the developmental transition from germination to seedling establishment. Shown are DEGs upregulated (↑) and downregulated (↓) based on pairwise comparisons of **(A)** M^+ seed vs. M^- seed (M^+/M^-), **(B)** M^+ seed vs. IND fruit (M^+/IND), and **(C)** M^- seed vs. IND fruit (M^+/IND). In all comparisons, the second treatment type was the baseline to which the first treatment was compared as transcript abundance ratio, i.e., M^+/M^-, M^+/IND, and M^-/IND. The dashed line indicates a hypothetical trajectory of DEGs for the corresponding tissues. DEG detection was performed using the pipeline-adjusted p-value cutoff set to 0.001 as previously described by Wilhelmsson et al. (2019). Symbols indicate seed, root, or shoot tissue at 1% germination ($T_{1\%}$), 100% germination ($T_{100\%}$), or 72 or 240 hours after transfer (hat) to seedling growth plates. For further details, see Supplementary Table 1 and Supplementary Dataset 1.

et al., 2012; Zhou et al., 2016; Lorrai et al., 2018; Zhu et al., 2020; Templalexis et al., 2022). AtRAP2.11 is, in addition, known as a major regulator of potassium and nitrate transporters in responses to low-nutrient conditions (Kim et al., 2012; Meng et al., 2016; Templalexis et al., 2022).

In contrast to ethylene-related genes, for all ABA-related metabolism and signaling genes, as well as for the PYR/PYL/RCAR-type ABA receptor genes, resetting of their expression was complete in 72-hat seedlings (Figure 9B; Supplementary Figure 5B). An exception was the ABA-responsive element (ABRE)-binding protein/factor (ABF) *AearAREB3b* for which higher transcript abundances prevailed in 72-hat M^- seedling shoots, but this difference disappeared in 240-hat seedlings (Supplementary Figure 5B). Morph-specific expression patterns for ABA biosynthesis [e.g., 9-*cis*-epoxycarotenoid dioxygenase (NCED) genes] and ABF-type TFs, and ABA contents were a hallmark during the dimorphic seed/fruit development (Lenser et al., 2018; Arshad et al., 2021) and in imbibed dimorphic diaspores (Chandler et al., 2024). Differences in ABA relations were, therefore, most important between dimorphic diaspores but became less important between M^+ and M^- seedlings since they were reset during pre-emergence seedling growth. In contrast to this, distinct expression patterns for gibberellin (GA)-related genes prevailed in 72-hat seedlings (Figure 9B; Supplementary Figure 6A). The transcript abundances for the GA 3-oxidase (biosynthesis of bioactive GA) gene *AearGA3ox1* and the *AearGID1b* gene encoding a GA receptor were higher in 72-hat M^- seedling shoots derived from IND fruits compared to M^+ seedling shoots, suggesting that GA biosynthesis and sensitivity differ between the morphs during early seedling growth. Similarly, the transcript abundances of GASA ("GA-stimulated *Arabidopsis*") genes known to be stimulated by GA and regulated by DELLA repressor proteins (Zhang and Wang, 2017) were higher in 72-hat M^- seedling roots derived from IND fruits compared to M^+ seedling roots, while genes for DELLA

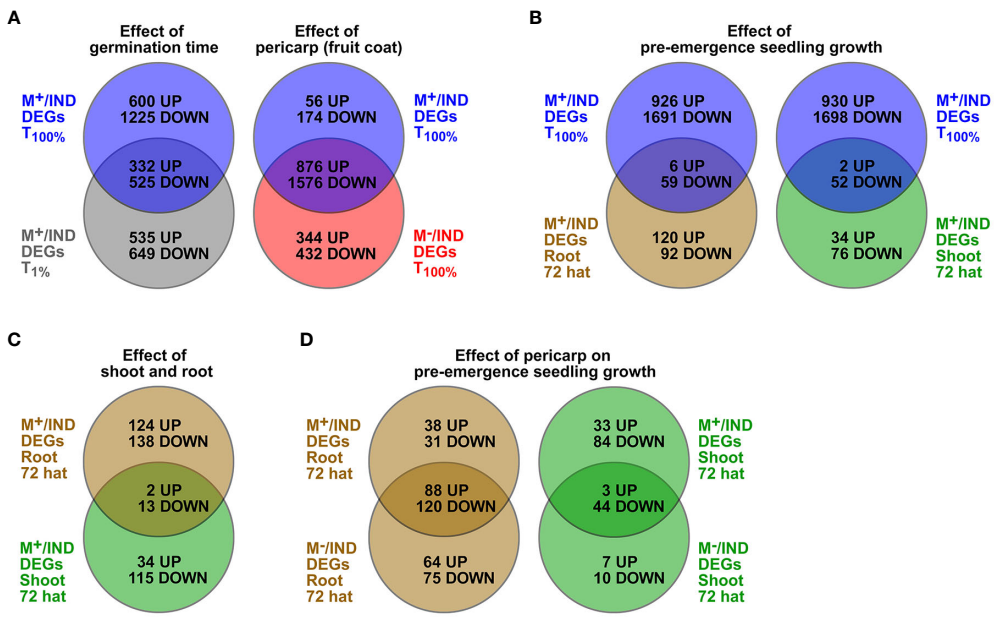

FIGURE 7
Comparative analysis of *Aethionema arabicum* differentially expressed gene (DEG) lists presented as Venn diagrams. **(A)** Effects of germination time and pericarp as comparisons of the list of M^+/IND DEGs at $T_{100\%}$ (*blue circle*) to either M^+/IND at $T_{1\%}$ (*grey circle*) or M^-/IND at $T_{100\%}$ (*red circle*). **(B)** Effect of pre-emergence growth by comparisons of the list of M^+/IND DEGs at $T_{100\%}$ (blue circle) M^+/IND 72-hat DEG lists of roots (*brown circle*) or shoots (*green circle*). **(C)** Effect of shoot and root. **(D)** Effect of pericarp on pre-emergence seedling growth by comparing M^+/IND 72-hat DEG lists with M^-/IND 72-hat DEG lists for roots (*brown circle*) and shoots (*green circle*). Seed, root, or shoot tissue at 1% germination ($T_{1\%}$), 100% germination ($T_{100\%}$), or 72 or 240 hours after transfer (hat) to seedling growth plates was compared. For gene lists of overlapping and unique DEGs, see Supplementary Dataset 1.

repressor proteins did not differ between the morphs (Figure 9B; Supplementary Figure 6A). In general, ABA has an inhibitory and GA has a promoting role in the complex hormonal control of seedling shoot and root growth (Ahammed et al., 2020). We conclude from the *Ae. arabicum* results that for most genes, resetting occurs during the post-germination pre-emergence growth phase ($T_{100\%}$ seeds to 72-hat seedlings) but also that several ethylene and GA-related genes involved in hormonal interactions are among the DEGs in 72-hat seedlings for which resetting occurs later during seedling growth (Figure 7).

That *Ae. arabicum* shoot and root development changed during pre-emergence seedling, which was also evident from the chlorophyll accumulation (Figure 3), the DEG list comparison (Figure 7D), and the shoot-specific induction of chlorophyll-related genes (Supplementary Figure 7A). Interestingly, these chlorophyll-related genes were DEGs in 72-hat shoots with lower expression in M^- seedlings derived from IND fruits. Ethylene, GA, and ABA interact with auxin to regulate seedling growth differently in shoots and roots (Belin et al., 2009; Hu et al., 2017; Ahammed et al., 2020). Auxin/indole-3-acetic acid (Aux/IAA) proteins (IAAs) repress auxin-inducible genes by inhibiting auxin response TFs (ARFs). In *Ae. arabicum*, several ARFs and Aux/IAA proteins were DEGs during late germination with lower (ARFs) and higher (IAAs) transcript abundances in germinated IND fruits ($T_{100\%}$) when compared with germinated M^+ and M^- seeds (Figure 10A and Supplementary Figure 6B). With the exception of *AearARF6*, which was more highly expressed in IND fruit-derived 72-hat and 240-hat seedling shoots, these expression differences had disappeared in 72-hat seedlings. The *A. thaliana* dormancy/auxin-associated protein is known to be involved in the auxin sensitivity of seedlings (Johnson et al., 2015); its *Ae. arabicum* homolog was more highly expressed in germinated IND fruits (Figure 10B). Small auxin-upregulated RNA (SAUR) genes are auxin-responsive genes involved in cell elongation growth and other processes (Stortenbeker and Bemer, 2019). An example in *A. thaliana* seeds is *AtSAUR11*, which accumulates eightfold in the endosperm as compared to the embryo (Dekkers et al., 2013). In general, the differential expression of *Ae. arabicum* SAUR genes during late germination ($T_{100\%}$) was reset in 72-hat seedlings (Figure 10B; Supplementary Figure 6B). A notable exception was *AearSAUR11* for which the transcript abundance was high in germinated IND fruits ($T_{100\%}$) and increased further >10-fold in 72-hat M^- seedling shoots derived from IND fruit as compared to M^+ seedling shoots (Figure 10B).

2.4 Dimorphic expression of transporter genes for water, auxin, nitrate, and flavonoids

Polar auxin transport and auxin homeostasis are key to seedling shoot and root growth and are facilitated by tightly regulated efflux [PIN (PIN-FORMED proteins) and PILS (PIN-LIKES)] and influx (AUX1) carriers, which coordinate cell type-specific asymmetric subcellular auxin localization and local auxin gradients across tissues (Belin et al., 2009; Hu et al., 2017; Yi et al., 2021; Bogaert et al., 2022; Feraru et al., 2022; Nakabayashi et al., 2022; Waidmann et al., 2023). Several auxin carriers including *AearAUX1*, *AearABCG36* (Figure 10B), *AearPILS5*, and *AearPILS6* (Figure 11A) were

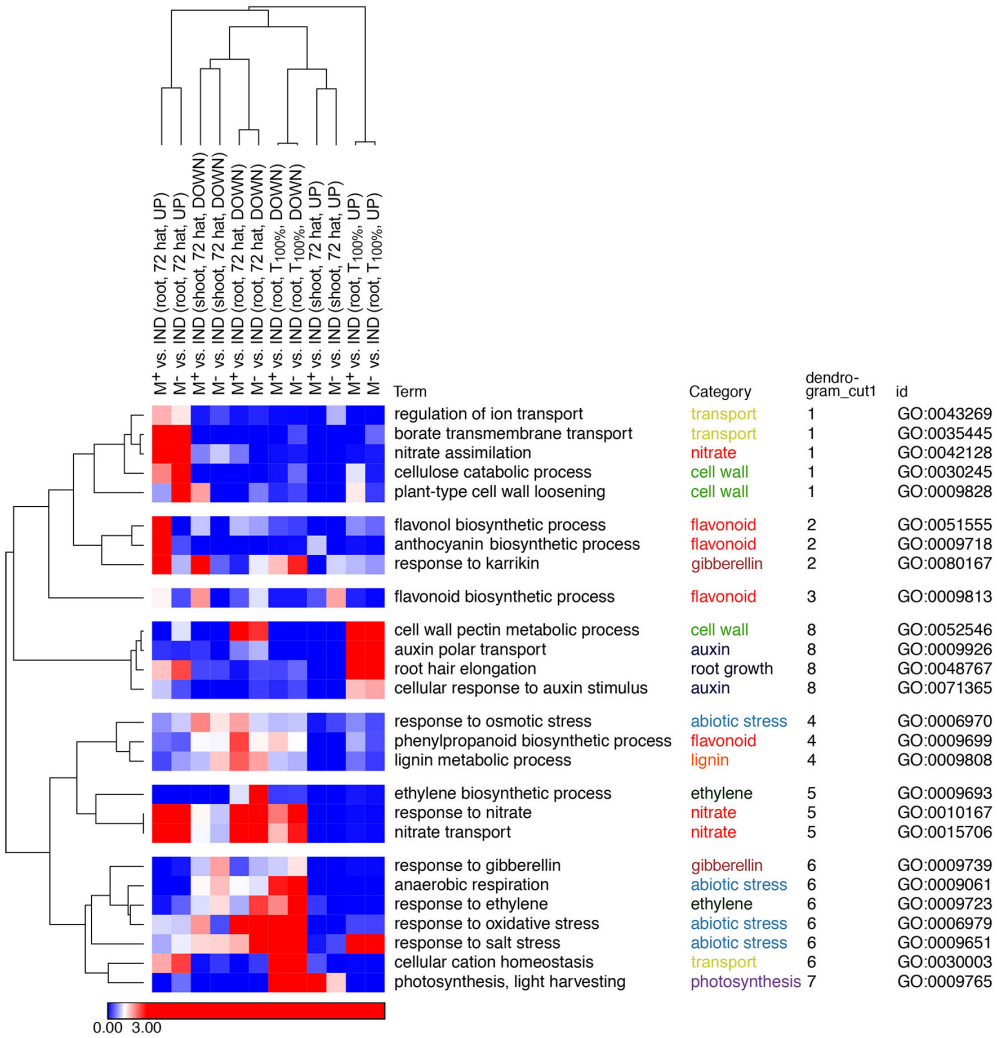

FIGURE 8
Gene Ontology (GO) term enrichment in differentially expressed gene (DEG) lists. GO terms were selected and assigned categories, and enrichment scores [log(1/p-value)] were clustered hierarchically by 1-Pearson correlation using Morpheus (https://software.broadinstitute.org/morpheus/). GO terms representative of each cluster are shown here, with all selected GO terms shown in Supplementary Figure 4, and full GO term enrichment p-values for all DEG lists can be found in Supplementary Dataset 2. Blue indicates non-significantly enriched values ($p > 0.05$), with white representing the significant cutoff ($p = 0.05$) and red indicating where GO terms are significantly enriched in the DEG lists ($p < 0.05$), saturated at $p = 0.001$. Hierarchical clustering was redone with selected GO terms, and the original cluster was based on dendrogram cut Supplementary Figure 4 as indicated.

identified as DEGs during late germination ($T_{100\%}$), but their expression difference was reset during seedling pre-emergence growth. In contrast to these auxin transporters, *AearPILS3*, which was also a DEG in germinated diaspores ($T_{100\%}$), remained as a DEG in shoots at 72 hat (Figure 11A). *AearPILS7* was not expressed during diaspore germination, but it was induced afterward and identified as a DEG in roots during pre-emergence seedling growth. The transcript abundances for *AearPILS7* were lower in 72-hat and 240-hat seedling roots derived from germinated IND fruits as compared to seedling roots derived from germinated M^+ and M^- seeds (Figure 11A). In *A. thaliana* seedlings, *AtPILS7* is involved in fine-tuning stress-responsive root auxin signaling in response to phosphate availability and regulation of phosphate transporter gene expression (Yi et al., 2021). In phylogenies across the plant kingdom, the PILS protein sequences of embryophytes plus green algae form a clade distinct from the PIN proteins, and the seven *A. thaliana* and other embryophyte PILS protein sequences are distributed over two PILS subclades 2 and 3 (Feraru et al., 2012; Bogaert et al., 2022). Figure 11B shows a family-wide phylogenetic analysis of Brassicaceae PILS protein sequences with the five identified *Ae. arabicum* protein sequences distributed across the two subclades (one in subclade 2 and four in subclade 3). In addition to PIN and PILS efflux carriers, which are specific for indole-3-acetic acid (IAA) transport, ABCG36 is known to act as a plasma membrane located exporter for the IAA precursor indole-3-butyric acid (Geisler et al., 2017; Aryal et al., 2019; Nakabayashi et al., 2022). Based on the *AearABCG36* expression patterns, it is a germination DEG that is reset during pre-emergence growth (Figure 10B).

Auxin and other hormones regulate the transition from germination to seedling growth by affecting the expression patterns of water and ion transporters (Yi et al., 2021; Tan et al., 2022; Templalexis et al., 2022). This includes aquaporins, e.g., plasma membrane intrinsic proteins (PIPs) and tonoplast intrinsic proteins

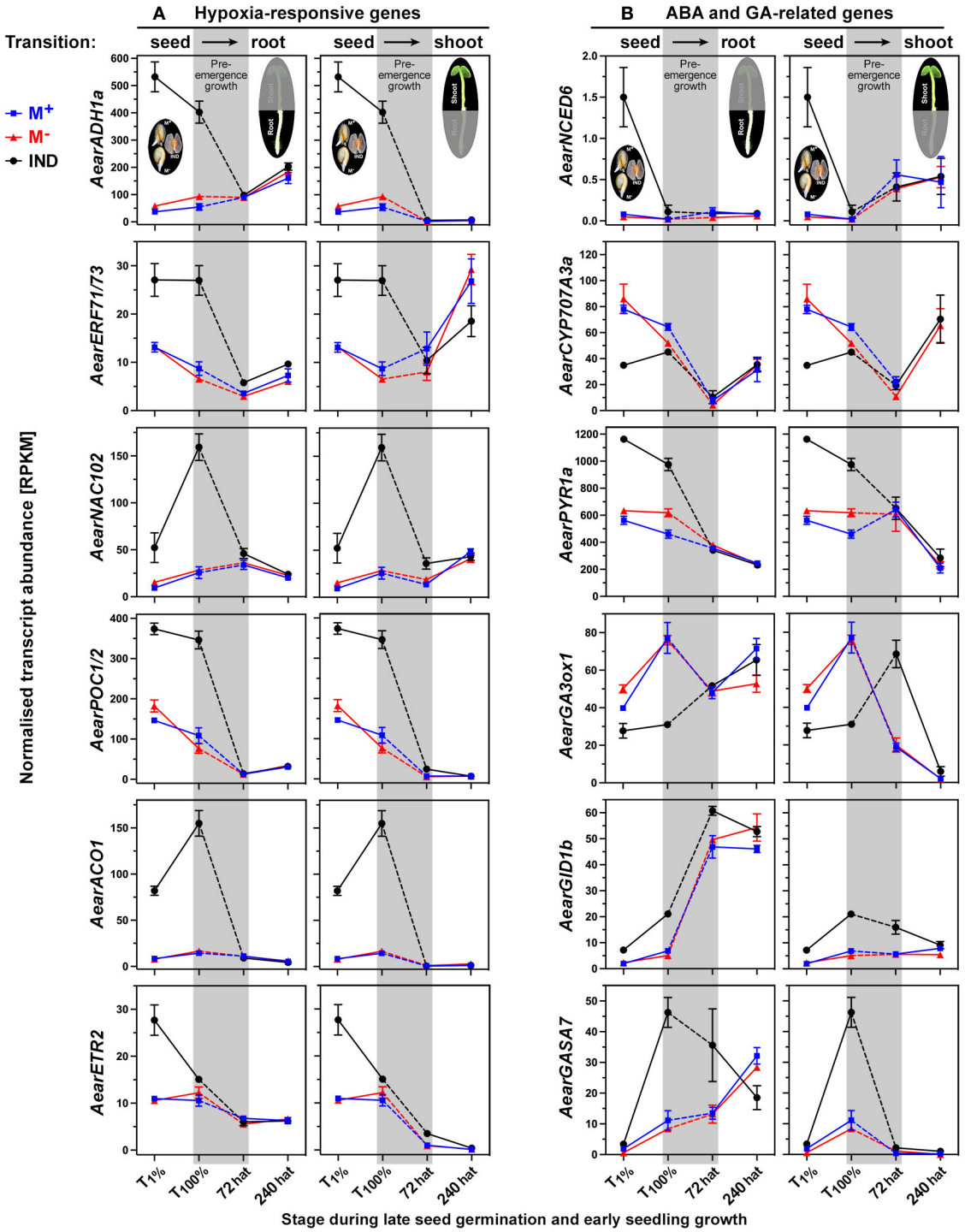

FIGURE 9
Comparative spatiotemporal analysis of transcript abundance patterns of selected *Aethionema arabicum* differentially expressed genes (DEGs). **(A)** Hypoxia-responsive genes. **(B)** Abscisic acid (ABA) and gibberellin (GA)-related genes. M^+ seeds, M^- seeds, and IND fruits were imbibed in dH_2O under darkness at 9°C, sampled, and harvested at $T_{1\%}$ and $T_{100\%}$. Diaspores that had completed germination (1-mm radicle protrusion) were transferred (at 0 hat, hours after transfer) to vertical plates for the seedling growth assay at 30°C in continuous white light (for details, see Figure 2). RNA-seq mean ± SEM values of three biological replicates are presented, and each replicate consisted of 90 seeds or tissue (root or shoot) from 12 seedlings. The pre-emergence growth phase leading from germinated diaspores ($T_{100\%}$) to seedlings at 72 and 240 hours after transfer (hat) is shaded gray; seed–seedling transition RNA-seq values for roots (*left panels*) and shoots (*right panels*) are presented. *AearPOC1/2* is the cumulative sum of *AearPOC1* plus *AearPOC2* transcript abundances. Seed, root, or shoot tissue at 1% germination ($T_{1\%}$), 100% germination ($T_{100\%}$), or 72 or 240 hours after transfer (hat) to seedling growth plates was compared. For gene abbreviations and IDs, see Supplementary Table 2.

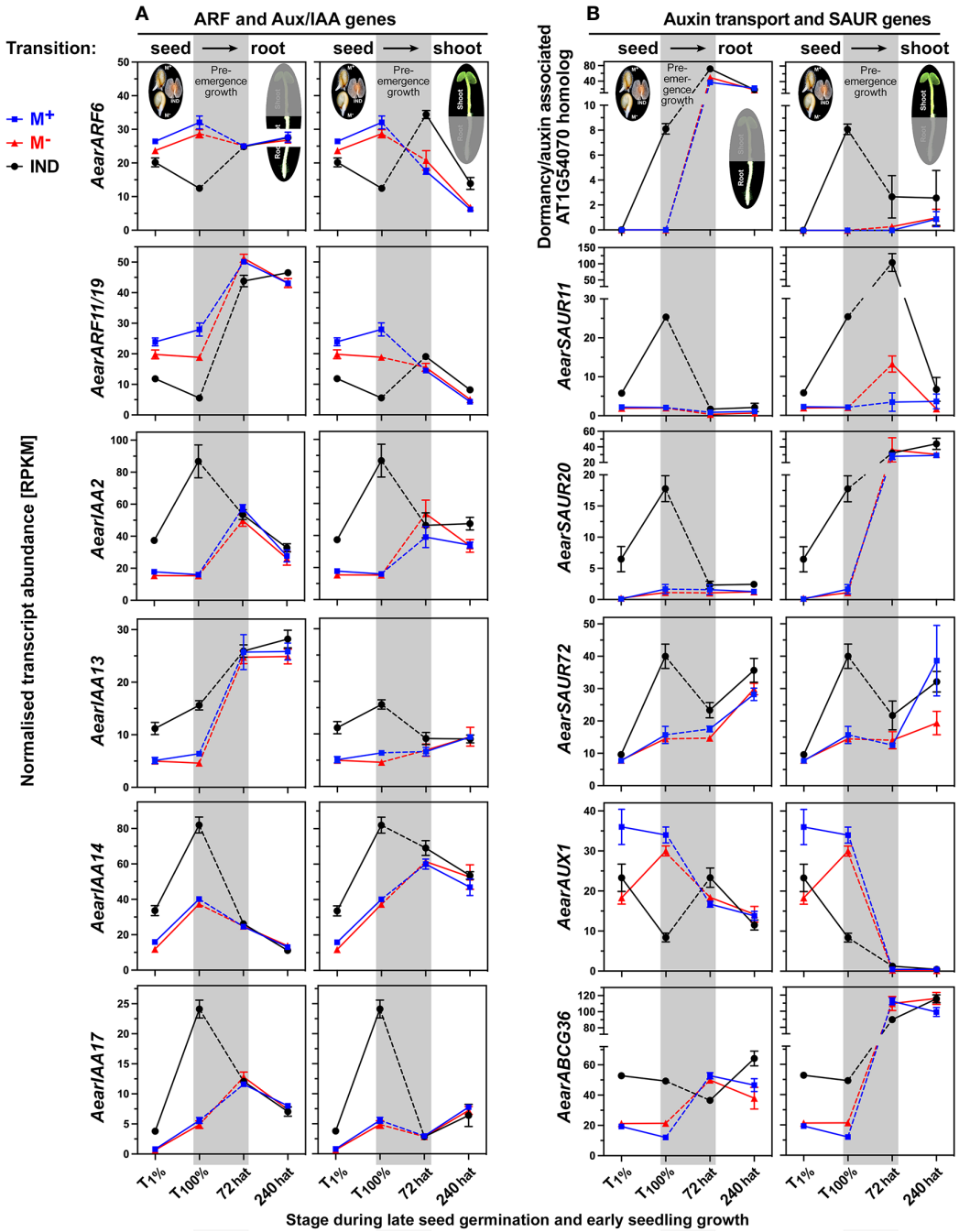

FIGURE 10
Comparative spatiotemporal analysis of transcript abundance patterns of auxin-related *Aethionema arabicum* differentially expressed genes (DEGs). **(A)** Auxin response factor (ARF) and auxin/indole-3-acetic acid (Aux/IAA) genes. **(B)** Auxin/dormancy-associated and small auxin-upregulated RNA (SAUR) genes. RNA-seq mean ± SEM values of three biological replicates are presented; for details, see Figure 9 and main text. For gene abbreviations and IDs, see Supplementary Table 2.

(TIPs), transporting water, ammonia (NH_3), and other solutes (Loqué et al., 2005; Footitt et al., 2019; Hoai et al., 2020). Figure 12A shows that the transcript abundances of *AearPIP3A/2;7* and *AearPIP1E/1;4* were more highly expressed in IND fruits during late germination ($T_{100\%}$) and remained higher in 72-hat seedling roots derived from IND fruits as compared to seedling roots derived from M^+ and M^- seeds. *AearTIP1,4*, for which the *A. thaliana* homolog is regulated by ABA in seeds (Footitt et al., 2019), and *AearTIP1/1,1* were reset during pre-emergence growth (Figure 12A). In contrast to this, expression of the NH_3 transporter genes *AearTIP2;3a* and *AearTIP2;3b* was higher in IND fruits during late germination ($T_{100\%}$) and remained higher in 72-hat seedling roots derived from IND fruits as compared to seedling roots derived from M^+ and M^- seeds (Figure 12A). In *A. thaliana* seedlings, root high-affinity nitrate (NO_3^-) transporters such as NRT2 interact with polar auxin transport (Wang et al., 2023a). *AearNTR2* and *AearNTR3.1* were not expressed during *Ae. arabicum* germination, and

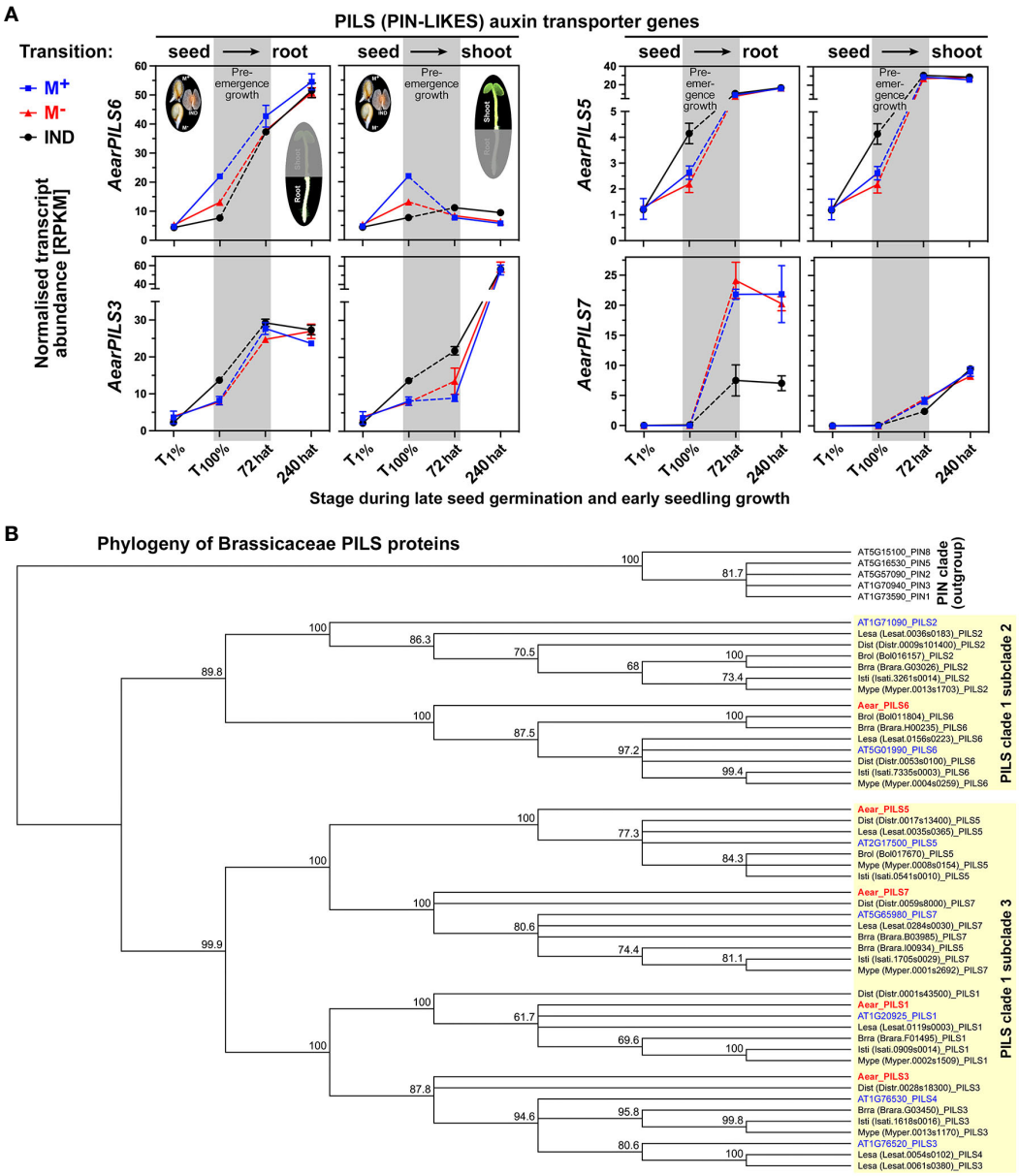

FIGURE 11
Comparative spatiotemporal analysis of transcript abundance patterns and phylogeny of PILS auxin transporter genes. **(A)** Expression patterns of *Aethionema arabicum PILS* genes. RNA-seq mean ± SEM values of three biological replicates are presented; for details, see Figure 9. **(B)** Phylogenetic tree of the predicted amino acid sequences of Brassicaceae PILS (PIN-FORMED-LIKES) auxin efflux carrier. Known and putative amino acid PILS sequences were aligned using ClustalW, and Neighbor-Joining trees were built as described in the Materials and Methods. Naming of PILS sequences was as follows: species as four-letter code (Brra, *Brassica rapa*; Brol, *Brassica oleracea*; Dist, *Diptychocarpus strictus*; Isti, *Isatis tinctoria*; Lesa, *Lepidium sativum*; Mype, *Myagrum perfoliatum*), gene identifier in brackets, and naming based on highest sequence similarity with the *Arabidopsis thaliana* PILS sequences (*in blue*). For *Aethionema arabicum PILS* gene (*in red*) identifier, see Supplementary Table 2. Species selection was based on Brassicaceae phylogeny in which *Aethionema* is the sister to all Brassicaceae, *Arabidopsis* and *Lepidium* represent core Brassicaceae lineage I, the two *Brassica* species represent the lineage II Brassicaceae, and *Isatis* and *Myagrum* represent lineage II Isatideae (Franzke et al., 2011).

their root-specific induction in 72-hat seedlings was lower in roots derived from IND fruits (Figure 12B).

Nitrate and potassium transporter gene expression in *A. thaliana* seedlings is mediated by auxin and the ERF TF RAP2.11 in responses to low-nutrient conditions (Kim et al., 2012; Meng et al., 2016; Templalexis et al., 2022). The expression patterns of *AearRAP2.11* (Supplementary Figure 5A) and the transporters for nitrate *AearNTR2* (Figure 12B) and potassium *AearKUP3* (Supplementary Figure 7A) showed reduced transcript abundances in 72-hat roots derived from IND fruits, which suggest a role of RAP2.11 in the regulation of potassium and nitrate relations during pre-emergence seedling growth. Key enzymes for nitrate assimilation include nitrate reductase (NR) and nitrite reductase (NRI) for which the expression is regulated by hormones and abiotic stresses (Tang et al., 2022). As for the nitrate transporters, also the genes for nitrate assimilation enzymes *AearNR1*, *AearNR2*, and *AearNIR1* were not expressed during germination, and their induction in 72-hat seedling roots was lower in roots derived from IND fruits (Figure 12B). This suggests that nitrate

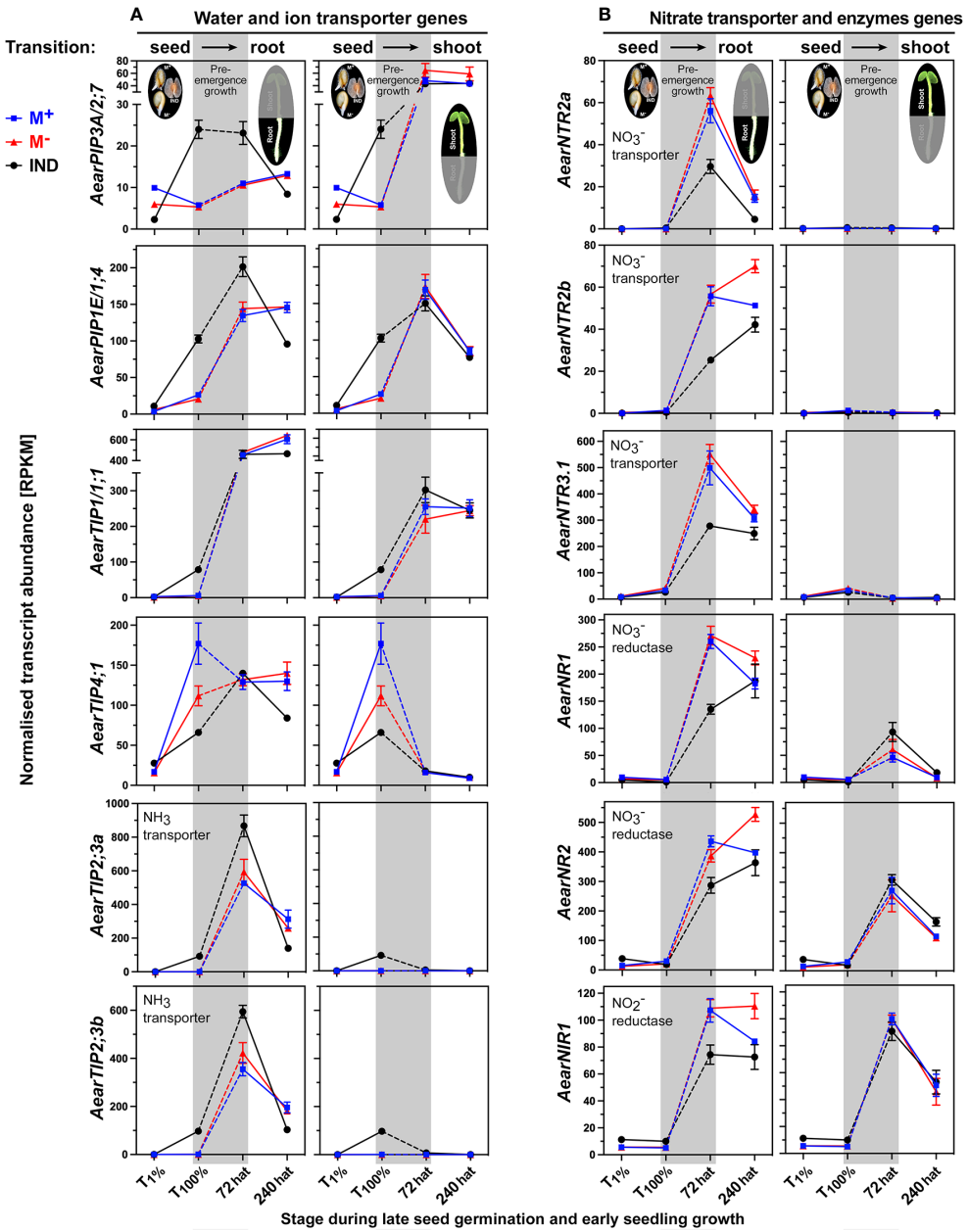

FIGURE 12
Comparative spatiotemporal analysis of transcript abundance patterns of *Aethionema arabicum* transporter and enzyme differentially expressed genes (DEGs). **(A)** Water and ion transporter genes. **(B)** Nitrate transporter and enzyme genes. RNA-seq mean ± SEM values of three biological replicates are presented; for details, see Figure 9 and main text. For gene abbreviations and IDs, see Supplementary Table 2.

transport and assimilation differ in 72-hat roots of seedlings derived from IND fruits and M^+ seeds and that instead of resetting, a distinct reprogramming occurred.

The dimorphic expression patterns of genes encoding enzymes of the flavonoid biosynthesis pathway and proanthocyanidin (PA) accumulation are examples of root-specific DEGs during *Ae. arabicum* pre-emergence growth at 72 hat for which the transcript abundances were higher in seedlings derived from M^+ seeds as compared to seedlings derived from M^- seeds or IND fruits (Figure 13). In *A. thaliana*, mutations in many of the flavonoid biosynthetic genes as well as in genes of the MYB-bHLH-WDR (MBW) protein complex regulating flavonoid biosynthesis lead to "transparent testa (tt)" mutant phenotypes with reduced seed dormancy (Lepiniec et al., 2006; Macgregor et al., 2015; Xu et al., 2015). *A. thaliana TT19* encodes a glutathione-*S*-transferase (GST)-like protein that functions as a carrier to transport anthocyanin and PA precursors and is involved in the accumulation of PAs in the seed coat (Kitamura et al., 2010; Sun et al., 2012). The *AearGSTF12/TT19* transcript abundances during seed germination were high in IND fruits, while there was no expression during M^+ and M^- seed germination (Figure 13A). This expression pattern changed during seedling pre-emergence growth associated with the induction of the flavonoid

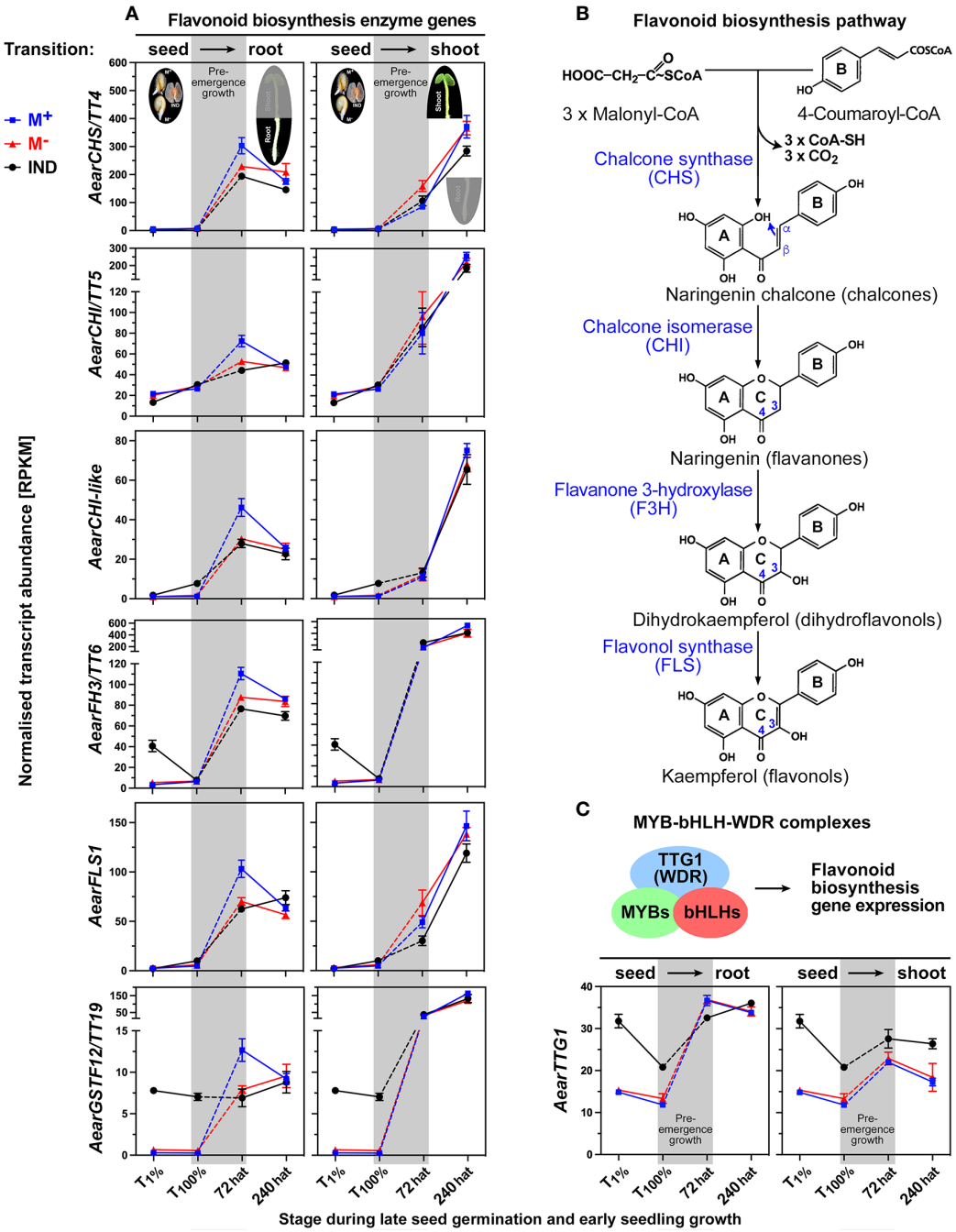

FIGURE 13
Comparative spatiotemporal analysis of transcript abundance patterns of *Aethionema arabicum* flavonoid biosynthesis pathway genes. **(A)** Flavonoid biosynthesis enzymes and the *GSTF12/TT19* transporter gene for proanthocyanidin precursor molecules. RNA-seq mean ± SEM values of three biological replicates are presented; for details, see Figure 9 and main text. **(B)** Simplified scheme of the flavonoid biosynthesis pathway. **(C)** Transcriptional control of the flavonoid biosynthesis pathway by MYB-bHLH-WDR complexes. For abbreviations, see main text. For gene abbreviations and IDs, see Supplementary Table 2.

biosynthetic pathway enzymes, which led to higher expression in 72-hat roots of seedlings derived from M^+ seeds.

The induction of the flavonoid biosynthesis pathway (Figure 13B) genes by the MBW complex was associated with enhanced expression of the WDR protein AearTTG1 (Figure 13C). Its expression pattern during germination supports a role in the enhanced expression of *AearGSTF12/TT19* in IND fruits, but it does not explain the higher expression of *AearGSTF12/TT19* and the flavonoid biosynthesis pathway enzymes in M^+ seed-derived seedling roots at 72 hat (Figure 13A). No bHLH and no MYB TF with enhanced expression

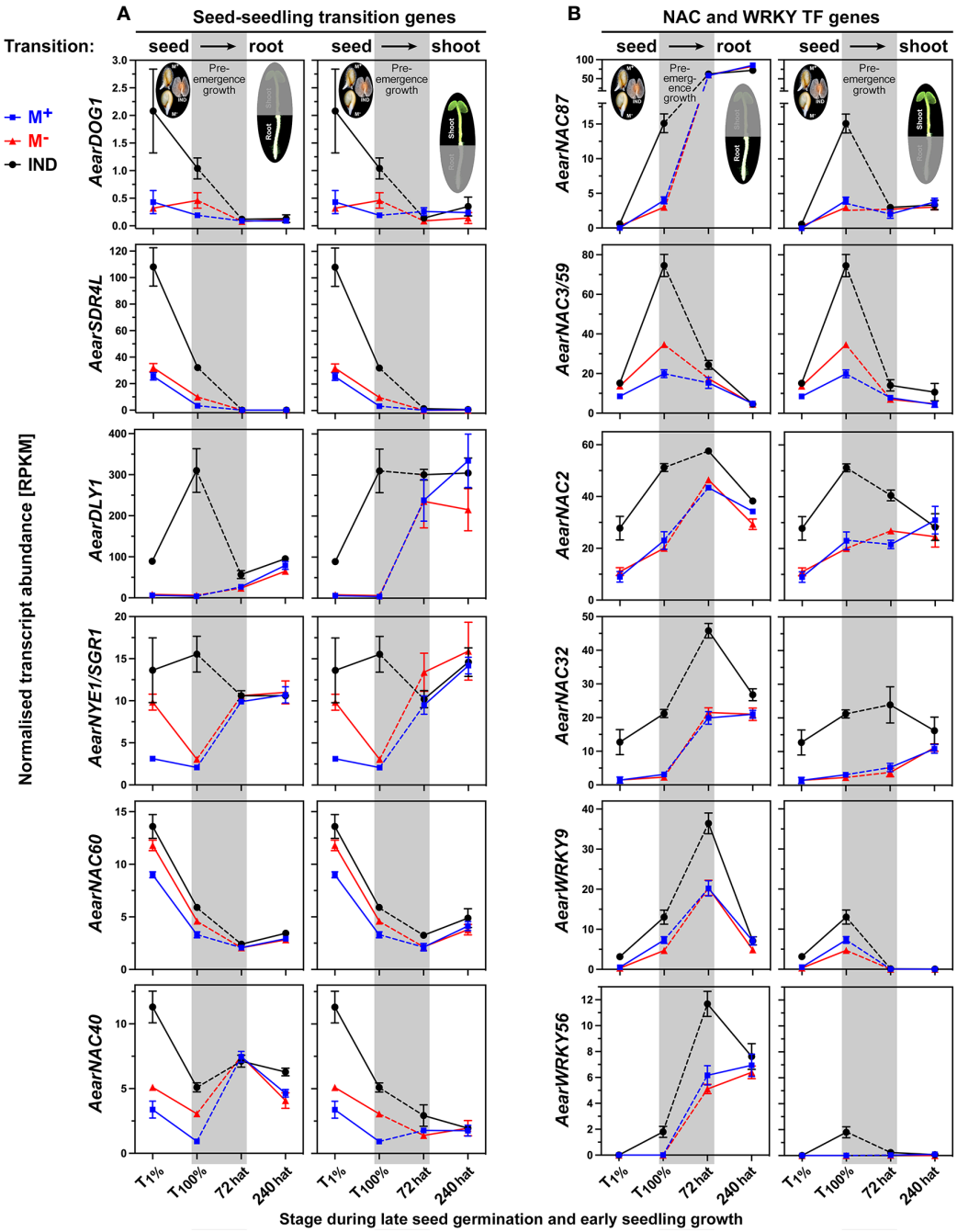

FIGURE 14
Comparative spatiotemporal analysis of transcript abundance patterns of *Aethionema arabicum* differentially expressed genes (DEGs). **(A)** Seed–seedling transition genes. **(B)** NAC and WRKY transcription factor (TF) genes. RNA-seq mean ± SEM values of three biological replicates are presented; for details, see Figure 9 and main text. For gene abbreviations and IDs, see Supplementary Table 2.

in M^+ seed-derived seedling roots at 72 hat were identified. Several *Ae. arabicum* MYB TFs were identified as DEGs during late seed germination ($T_{100\%}$) with higher expression in IND fruits compared to imbibed M^+ and M^- seeds, but for all of them, resetting occurred during pre-emergence growth (Supplementary Figures 8A, B). Among these DEGs is MYB30, which is a key TF in *A. thaliana* seeds and seedlings integrating ABA, ethylene, and reactive oxygen species (ROS) signaling (Mabuchi et al., 2018; Khedia et al., 2019; Maki et al., 2019; Nie et al., 2022; Zhang et al., 2023). Other DEGs are presented and discussed in Supplementary Figure 7B.

2.5 Resetting of maturation and dormancy genes, TFs, and seed–seedling transition markers

Dormancy and maturation gene expression usually decline during the germination of non-dormant seeds. In *A. thaliana* and other species, the transcript abundances for the *Delay of Germination 1* (*DOG1*) and *Seed Dormancy 4-Like* (*SDR4L*) decline in imbibed non-dormant seeds (Graeber et al., 2014; Wu et al., 2022), while *Dormancy-associated protein Like 1* (*DLY1*) and *Non-Yellowing 1/Stay-Green 1* (*NYE1/SGR1*) exhibit more complex expression patterns during seed imbibition (Rae et al., 2014; Wilhelmsson et al., 2019). The transcript abundances of *AearDOG1*, *AearSDR4L*, *Aear DLY1*, and *Aear NYE1/SGR1* were higher in imbibed IND fruits as compared to imbibed M^+ and M^- seeds and declined for *AearDOG1* and *AearSDR4L* (Figure 14A). The observed expression difference during germination for all four genes disappeared during pre-emergence growth, and this resetting led to roughly equal transcript abundances in 72-hat seedlings.

Germin (GER) and germin-like proteins are expressed in seeds, but their functions are largely unknown (Membre et al., 2000). In *Ae. arabicum*, *AearGER3* is a DEG during late germination, but not in seedlings, where it is expressed in a shoot-specific manner (Supplementary Figure 9A). Late embryogenesis-abundant (LEA) proteins accumulate late in seed development and play major roles in desiccation tolerance (Hundertmark and Hincha, 2008; Zinsmeister et al., 2020; Smolikova et al., 2022). Most genes encoding LEA proteins are known to be ABA-induced, and their transcript abundances decline during seed germination. Consistent with the ABA inducibility and higher ABA contents in IND fruits (Chandler et al., 2024), the transcript abundances of *Ae. arabicum LEA* genes were higher in imbibed IND fruits as compared to M^+ and M^- seeds (Supplementary Figure 9). Expression patterns of specific LEA and Heat Shock Protein (HSP) genes are presented in detail in Supplementary Figure 9.

For most *Ae. arabicum* TFs, which were identified as DEGs between IND fruit and M^+ seed diaspores during the germination phase, resetting of the expression pattern was observed during the post-germination pre-emergence phase (Supplementary Figure 8). Examples where the expression differences during late germination ($T_{100\%}$) persisted or were even intensified into the seedling phase include the auxin and ethylene-related TF genes *AearARF6* and *AearERF113* presented earlier (Figure 10A; Supplementary Figure 5A). Resetting during the post-germination pre-emergence phase was also observed for NAC (NAM, ATAF, and CUC) TFs involved in hypoxia responses (*AearNAC102*, Figure 9A) and for *AearNAC40* and *AearNAC60* (Figure 14A), which, in *A. thaliana*, are functionally redundant in the inhibition of dormancy (Song et al., 2022). Homologs of *AearNAC3/59* (Figure 14B) and *AearNAC87* (Figure 14B) are known for being involved in the primary root growth of *A. thaliana* seedlings, for being expressed in the endosperm during germination (Dekkers et al., 2013), and for controlling programmed cell death during root growth (Huysmans et al., 2018). In contrast to these NAC TFs, higher transcript abundances in IND fruit diaspores during germination were maintained for *AearNAC2* and *AearNAC32*, and this difference was further intensified at the 72-hat seedling state (Figure 14B). In *A. thaliana*, NAC2 has a role in integrating environmental and hormone (auxin and ethylene) stimuli during seedling root growth (He et al., 2005) and integration of auxin signaling (Park et al., 2011), and NAC32 has a role in upstream TF in the control of seedling root elongation and ROS signaling (Maki et al., 2019).

The WRKY9 and WRKY40 TFs are known as central repressors of ABA signaling during *A. thaliana* seed germination and seedling growth (Wang et al., 2021) and of ROS and stress signaling (Shin and Schachtman, 2004; Van Aken et al., 2013; Arjmand et al., 2023). In *Ae. arabicum*, *AearWRKY9* and *AearWRKY40* were identified as DEGs more highly expressed in germinating IND fruits as compared to M^+ seeds, and this expression pattern was retained in 72-hat seedlings (Figure 14B, Supplementary Figure 8C). WRKY51 and WRKY56 belong to a subgroup of WRKY TFs involved in controlling auxin transport during *A. thaliana* root development (Templalexis et al., 2022). *AearWRKY51* and *AearWRKY56* are DEGs with higher expression in IND fruits during the germination of the *Ae. arabicum* dimorphic diaspores (Figure 14A, Supplementary Figure 8C). While resetting of this expression difference during pre-emergence growth was observed for *AearWRKY51*, it was retained and further intensified for *AearWRKY56* in 72-hat seedling roots (Figure 14B). Expression patterns of other TFs including homeobox TFs controlling seed-to-seedling phase transition node regulators and the plant-specific AT-rich sequence zinc-binding protein (PLATZ) TFs are presented in detail in Supplementary Figure 8. Taken together, both resetting and intensification of differential expression patterns were observed during the seed-to-seedling transition for TFs from several distinct gene families. For the TFs that were identified as DEGs at the seedling stage expression, the transcript abundances were always higher in seedlings derived from IND fruits and lower in seedlings derived from M^+ seeds.

2.6 Resetting of cell wall remodeling protein gene expression during seed–seedling transition

Cell expansion growth is driven by water uptake, which is restricted unless cell wall loosening is achieved by the action of cell wall remodeling proteins (CWRPs) or apoplastic ROS (Finch-Savage and Leubner-Metzger, 2006; Steinbrecher and Leubner-Metzger, 2017; 2018). Expansins are CWRPs that disrupt non-covalent bonds that tether cell wall matrix polysaccharides to the surface of cellulose microfibrils or each other. Expansins are required for endosperm weakening and embryo elongation during germination and seedling growth (Voegele et al., 2011; Graeber et al., 2014; Boron et al., 2015; Cosgrove, 2016; Ilias et al., 2019). In agreement with the slower germination of *Ae. arabicum* IND fruits as compared to M^+ seeds, the expression of *AearEXPA2* and most other expansins was lower in imbibed IND fruits (Figure 15A; Supplementary Figure 10A). Resetting during post-germination pre-emergence growth was observed for most expansins, which were DEGs during germination, but other expansins also exhibited differential expression in seedling roots. Xyloglucan remodeling enzymes involved in seed germination include α-xylosidase (αXYL)

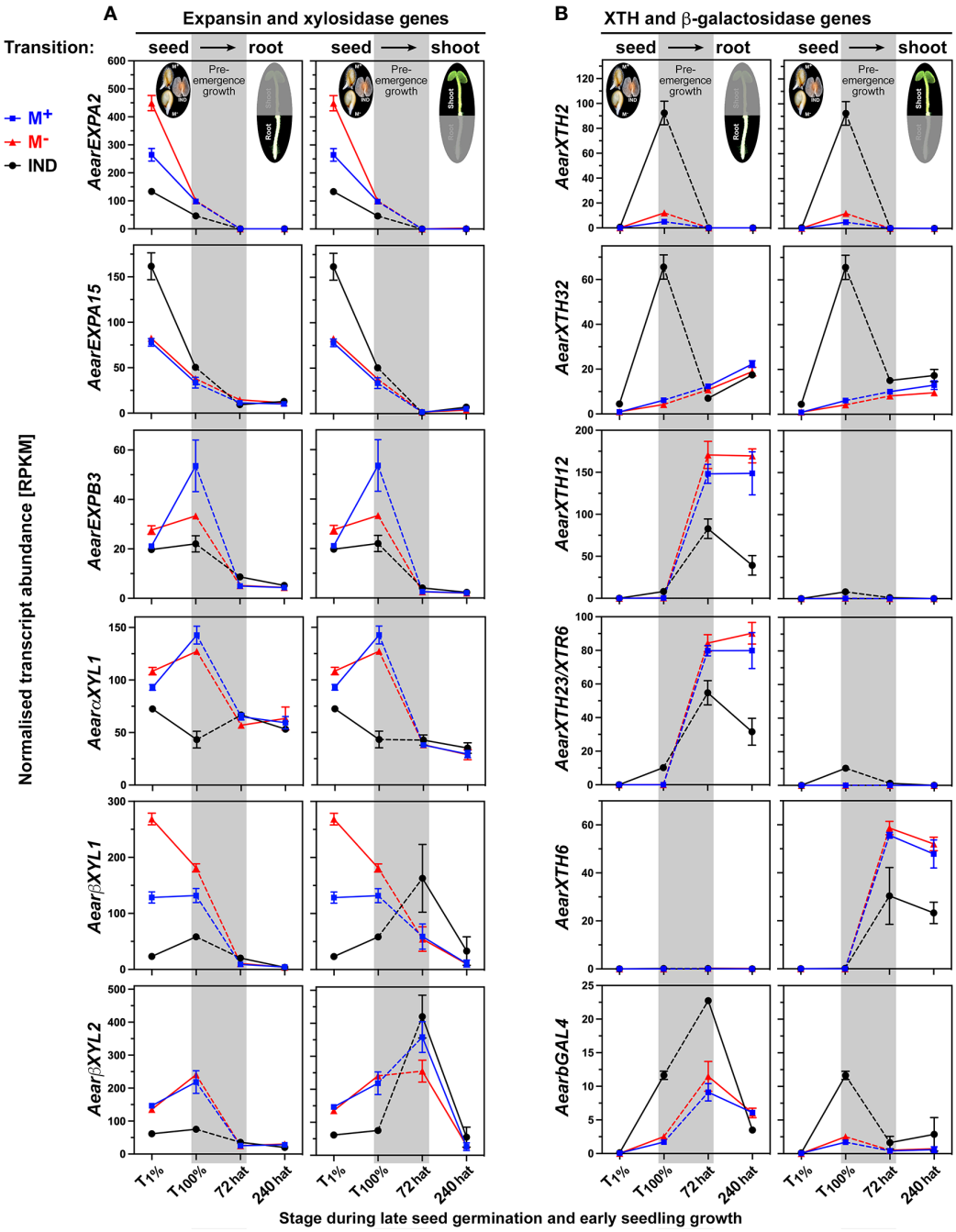

FIGURE 15
Comparative spatiotemporal analysis of transcript abundance patterns of *Aethionema arabicum* differentially expressed genes (DEGs) encoding cell wall remodeling proteins. **(A)** Expansin and xylosidase genes. **(B)** Xyloglucan endotransglucosylase/hydrolase (XTH) and β-galactosidase genes. RNA-seq mean ± SEM values of three biological replicates are presented; for details, see Figure 9 and main text. For gene abbreviations and IDs, see Supplementary Table 2.

(Shigeyama et al., 2016), β-xylosidase (βXYL) (Arsovski et al., 2009), and xyloglucan endotransglucosylase/hydrolase (XTH) (Voegele et al., 2011; Endo et al., 2012; Graeber et al., 2014; Steinbrecher and Leubner-Metzger, 2017; Holloway et al., 2021). In agreement with roles in imbibed *Ae. arabicum* dimorphic diaspores, *AearαXYL1*, *AearβXYL1*, and *AearβXYL2* are DEGs during germination with lower expression in IND fruits (Figure 15A). Resetting during post-germination pre-emergence growth leads to roughly similar expression in seedlings derived from germinated IND fruits and M^+ seeds.

Earlier work by Chandler et al. (2024) demonstrated that during early germination (until $T_{1\%}$), the cumulative expression of all XTHs in imbibed *Ae. arabicum* dimorphic diaspores is lower in IND fruits compared to M^+ and M^- seeds. Interestingly, the transcript abundances of many *AearXTH* genes increased in IND fruits during the late germination (until $T_{100\%}$), and these were,

therefore, identified as germination DEGs (Figure 15B; Supplementary Figure 10A). In general, resetting during post-germination pre-emergence growth was observed for XTH genes, but *AearXTH12*, *AearXTH23*, *AearXTH31*, and *AearXTH26* were DEGs during seedling growth, and their transcript abundances were lower in 72-hat seedling roots derived from germinated IND fruits compared to seedling roots derived from M^+ or M^- seeds. In *A. thaliana* seedlings, *AtXTH23* is known to be involved in root development and adaptation to salt stress (Xu et al., 2020), gene induction is induced by touch and darkness (Lee et al., 2005), and *AtXTH12* and *AtXTH26* exhibit only endotransglucosylase activity (Maris et al., 2010). In contrast to *AearXTH2*, *AearXTH23*, *AearXTH26*, and *AearXTH31*, the transcript abundances of *AearXTH24* were higher in 72-hat seedling roots derived from germinated IND fruits (Figure 15B; Supplementary Figure 10A). In *A. thaliana* seedlings, overexpression of AtXTH24 is known for its role in promoting hypocotyl growth of etiolated seedlings (Dhar et al., 2022). In *A. thaliana* seedlings, *AtXTH6* is known to be regulated by ABA and auxins (Overvoorde et al., 2005; Huang et al., 2007). In *Ae. arabicum* seedlings, *AearXTH6* is specifically expressed in seedling shoots and lower in 72-hat and 240-hat seedling shoots derived from germinated IND fruits (Figure 15B).

β-Galactosidases have β-1,4-galactose in xyloglucan side chains as targets (Steinbrecher and Leubner-Metzger, 2017; Moneo-Sanchez et al., 2019; Steinbrecher and Leubner-Metzger, 2022). In *Ae. arabicum*, resetting during post-germination pre-emergence growth was not observed for *AearβGAL4*, and the expression remained higher in 72-hat seedlings derived from IND fruits (Figure 15B). In *A. thaliana* seedlings, βGAL4's involvement in cell wall changes is associated with the cessation of cell elongation and increased rigidity (Moneo-Sánchez et al., 2016). β-Galactosidases also have β-1,4-galactan in cell wall pectin (rhamnogalacturonan) as a target. Pectins are complex cell wall matrix polysaccharides characterized by α-1,4-linked galacturonic acid and a dynamic degree of methylesterification, and β-galactosidase and various other cell wall remodeling enzymes target pectin (Cao, 2012; Daher and Braybrook, 2015; Scheler et al., 2015). Their expression patterns in *Ae. arabicum* are presented in detail in Supplementary Figure 10. Taken together, CWRP gene expression in the dimorphic diaspore model *Ae. arabicum* revealed either resetting or distinct expression patterns (as DEG in seedlings) during the seed–seedling transition.

3 Discussion

3.1 The dimorphic diaspore syndrome and distinct seedling responses to abiotic stresses

The hormonal interactions during seed germination/dormancy (GA-ABA antagonism dominant) and early seedling growth (auxin-ethylene interactions dominant) differ fundamentally (Finch-Savage and Leubner-Metzger, 2006; Linkies and Leubner-Metzger, 2012; Hu et al., 2017; Ahammed et al., 2020; Smolikova et al., 2022; Wang et al., 2023b). Seedlings during pre-emergence growth may encounter increasing post-germination stress in the soil environment, and consequently, seeds/seedlings often fail to establish during this stage (Moles and Westoby, 2006; Finch-Savage and Bassel, 2016; Gardarin et al., 2016). It is clear from many dimorphic diaspore systems that the germination/dormancy traits of the two distinct morphs differ in their responses to environmental cues including abiotic stresses and that the underpinning molecular (hormonal, transcriptomic, and epigenetic) mechanisms differ (Xu et al., 2011; Zhou et al., 2015; Lu et al., 2015a, b; Lenser et al., 2016; Wilhelmsson et al., 2019; Arshad et al., 2021; Gianella et al., 2021; Zhang et al., 2021; Cao et al., 2022; Loades et al., 2023; Song et al., 2023; Chandler et al., 2024). Whether or not seedlings derived from dimorphic diaspores differ in their molecular responses has been far less investigated. Very little is known about if and when these differences disappear by resetting during seedling growth and whether or not these seedling differences were already induced during the dimorphic seed development on the mother plant and then retained during imbibition.

Comparative analysis of seedlings derived from *Atriplex* and *Suaeda* dimorphic seeds that were distinct in seed color revealed that seedlings were also distinct in responses to salinity and certain molecular features (Xu et al., 2011; Zhang et al., 2021; Cao et al., 2022; Song et al., 2023). Among the enriched functional gene categories that differed in the seedling transcriptomes were genes encoding inorganic ion transport, hormone metabolism, transport and signaling, TFs and signal transduction components, CWRPs, lipid metabolism, redox, and osmotic homeostasis. In these systems, dimorphic seeds differing in color, size, and dormancy were dispersed by pod shattering from dehiscent fruits. A conclusion from these publications is that the observed differences in salinity tolerance of the dimorphic seedlings were already initiated during seed development on the mother plant. Compared to this, the situation in the *Ae. arabicum* dimorphic diaspore system is different in that seedlings derived from either M^+ or bare M^- seeds did not show any obvious differences in a range of constant temperature or osmotic stress (Figure 2; Supplementary Figures 3, 4). What is different in the *Ae. arabicum* M^+ seed and the IND fruit morph system is the presence of the pericarp, which is known to impose coat dormancy and delay the germination of imbibed IND fruits (Lenser et al., 2016; Chandler et al., 2024).

Pericarp removal experiments with monocarpic species demonstrated that beyond seed traits, the pericarp can also affect seedling establishment and performance (Hu et al., 2009; Mamut et al., 2014; Zhou et al., 2015; Lu et al., 2015b; Lu et al., 2017b; a; Ignatz et al., 2019). Interestingly, in *Ae. arabicum*, the pericarp restraint led to different growth of hypocotyls derived from imbibed IND fruits as compared to M^+ and M^- seedlings derived from M^+ and bare M^- seeds (Figure 4). This pericarp effect on pre-emergence seedling growth delivered a 5–20-fold higher number of DEGs from the M^+/IND and M^-/IND comparisons (Figures 7, 8) as compared to the 23 DEGs obtained in the M^+/M^- seedling comparison. The pericarp, therefore, plays an important role in the phenotypic plasticity of the *Ae. arabicum* dimorphic diaspores and has a

significant downstream effect on the root and shoot transcriptomes of M^- seedlings derived from IND fruits. Details about the identified *Ae. arabicum* DEGs were already described in the Results section. The following discussion, therefore, focuses on general aspects and selected major functional DEG categories of the transcriptome resetting process.

3.2 Transcriptome resetting during pre-emergence growth and DEG persistence in seedlings

For the majority of the 1,900–2,000 M^+/IND and M^-/IND DEGs at the completion of germination ($T_{100\%}$), resetting occurred during pre-emergence seedling growth and is completed in 72-hat seedlings (Figures 7, 8). Examples of this include all hypoxia-responsive and many hormone-related genes (see Section 2.3), as well as dormancy, maturation, LEA, and HSP genes (see Section 2.5). However, a considerable number of ethylene, GA, and auxin-related genes either persisted as a DEG in 72-hat seedling or developed into a DEG during pre-emergence seedling growth ($T_{100\%}$ to 72-hat seedling roots or shoots). This includes enhanced transcript expression for the ethylene-forming enzyme gene *AearACO2* in 72-hat seedlings derived from IND fruits (Supplementary Figure 5), GA-related genes including encoding the bioactive GA_4-forming enzyme *AearGA3ox1*, the GA receptor *AearGID1b* (Figure 9B), and several auxin-related genes including *AearSAUR11* (Figure 10B). Ethylene, GA, and ABA interact with auxin to regulate seedling growth differently in shoots and roots (Belin et al., 2009; Hu et al., 2017; Ahammed et al., 2020; Wang et al., 2023b). ACO2 is known for its role in counteracting ABA effects in seeds (Linkies et al., 2009; Linkies and Leubner-Metzger, 2012) and in promoting apical hook formation in seedling shoots (Wang et al., 2023b), and ethylene mediates the ABA inhibition on seedling root growth (Ahammed et al., 2020). Flavonoid biosynthesis pathway genes (Figure 13) exhibited a distinct expression pattern from most other DEGs with a root-specific upregulation in 72-hat M^+ seedlings derived from germinated M^+ seeds. The role of flavonoids in M^+ seedlings as compared to M^- seedlings and the distinct regulation by MBW protein complexes remain to be elucidated by future research.

ERF and ARF TFs are involved in the control of seedling growth by modulating ABA, ethylene, gibberellin, and auxin signaling (Kim et al., 2012; Zhou et al., 2016; Lorrai et al., 2018; Zhu et al., 2020; Templalexis et al., 2022). In agreement with the role of distinct hormonal signaling in M^+ and M^- *Ae. arabicum* seedlings, transcripts for *AearARF6* and several ERF TFs are DEGs in 72-hat seedling roots or shoots (Figure 9; Supplementary Figure 5). ARF and ERF TFs were also identified as DEGs in seedlings derived from the dimorphic (black versus brown) seeds of *Suaeda aralocaspica* (Cao et al., 2022). Resetting for the majority of the *Ae. arabicum* TF DEGs during pre-emergence seedling growth was completed at 72 hat (Figure 14; Supplementary Figure 8). Notable exceptions were two NAC (*AearNAC2* and *AearNAC32*) and two WRKY (*AearWRKY9* and *AearWRKY40*) TF genes for which higher transcript abundances in IND fruit diaspores during germination persisted at the 72-hat seedling state (Figure 14B). In *A. thaliana* seedling growth, these TFs are involved in integrating environmental and hormonal stimuli (see Section 2.5). Taken together, transcriptomes of M^+ and M^- *Ae. arabicum* seedlings derived from germinated M^+ seeds and IND fruits differ in the expression of genes involved in ethylene and GA metabolism, hormone signaling, and for various TFs with roles in integrating environmental and hormonal stimuli.

3.3 Dimorphic expression patterns of auxin/ion transporter and CWRP genes in seedlings

Precise auxin distribution patterns and polar transport are required for the control of root and hypocotyl growth and development (Teale et al., 2006; Hu et al., 2017; Wang et al., 2023b). The PILS auxin carriers are known to be involved in intracellular auxin homeostasis (Feraru et al., 2012, 2019; Bogaert et al., 2022; Feraru et al., 2022). In *Ae. arabicum*, several auxin carriers were DEGs during late germination ($T_{100\%}$), but their expression difference was reset during seedling pre-emergence growth (Figures 9, 10). *AearPILS3*, in addition, remained a DEG at 72 hat where it was more highly expressed only in seedling shoots derived from IND fruits. *AearPILS7* became a root-specific DEG at 72 and 240 hat, where it was more highly expressed only in seedling roots derived from IND fruits. Seedlings derived from IND fruits differed from M^+ and M^- seedlings derived from germinated M^+ seeds and bare M^- seeds, respectively, in that their lower hypocotyls were often bent and not straight and that their hypocotyl and root growth was slower (Figure 4). We speculate that differences in auxin biosynthesis, signaling, and transport play a major role in this altered seedling growth phenotype. This phenotype was, however, not connected with a difference in hypocotyl mechanics (fracture force) of 15-day-old *Ae. arabicum* seedlings (Figure 4). Microtensile measurements of *A. thaliana* seedlings (Saxe et al., 2016) demonstrated that hypocotyls differed mechanically between early (day 4) and later (day 5–7) seedlings, but there were no differences among the later seedlings (Saxe et al., 2016). It seems, therefore, that despite the slower growth and the bent hypocotyls of IND fruit-derived *Ae. arabicum* seedlings, possible mechanical differences between pre-emergence (72 hat) have already disappeared in later (>240 hat) seedlings.

Downstream of the hormonal regulation are distinct expression patterns in seedlings derived from IND fruits for water and ion transporters (Figure 12) potentially affecting the turgor pressure and for CWRP genes (Figure 15) potentially affecting the cell wall extensibility. The rapid and uniform seedling growth depends on cell expansion, which requires cell wall loosening by the action of CWRPs or apoplastic ROS (Finch-Savage and Leubner-Metzger, 2006; Steinbrecher and Leubner-Metzger, 2017; 2018). Among the CWRP DEGs in *Ae. arabicum* seedlings were genes encoding enzymes that target xyloglucan (βGAL4 and XTHs) and pectin (Figure 15, Supplementary Figure 10). *AearXTH12*, *AearXTH23*, and *AearXTH6* were less expressed in 72-hat and 240-hat seedlings derived from IND fruits as compared to M^+ and M^- seedlings

derived from germinated M^+ and M^- seeds. XTHs are known to affect seedling vigor (Ducatti et al., 2022) and hypocotyl growth (Miedes et al., 2013; Dhar et al., 2022), and *AtXTH6* is known to be regulated by ABA and auxins in seedlings (Overvoorde et al., 2005; Huang et al., 2007). Morph-specific differential expression of other xyloglucan remodeling enzymes was observed during *Ae. arabicum* fruit and seed development (Steinbrecher and Leubner-Metzger, 2022), dimorphic diaspore germination (Chandler et al., 2024), and dimorphic seedling growth (this work). CWRP gene expression in the dimorphic diaspore model *Ae. arabicum*, therefore, revealed either resetting or distinct expression patterns (as DEG in seedlings) during seed–seedling transition. Taken together, we conclude that the transcriptomes of seedlings derived from the dimorphic diaspores, M^+ seeds and IND fruits, undergo transcriptional resetting during the post-germination pre-emergence growth transition phase from germinated diaspores to growing seedlings.

4 Materials and methods

4.1 Plant material and germination assays

Plants of *Ae. arabicum* (L.) Andrz. ex DC. were grown from accessions TUR ES1020 (from Turkey) as described by Chandler et al. (2024). Mature M^+ seeds and IND fruits were harvested, further dried over silica gel for 1 week, and stored for a few months at −20°C in air-tight containers. For germination assays, dry mature seeds (M^+ or M^-) or IND fruits were placed in 3-cm Petri dishes containing two layers of filter paper, 3 mL deionized water (dH_2O), and 0.1% Plant Preservative Mixture (Plant Cell Technology, Washington, DC, USA). Temperature response profiles (Supplementary Figure 1) were obtained by incubating plates on a GRD1-LH temperature gradient plate device (Grant Instruments Ltd., Cambridge, UK). Subsequent germination assays were conducted by incubating plates in MLR-350 Versatile Environmental Test Chambers (Sanyo-Panasonic, Bracknell, UK) at the indicated imbibition temperature as described by Chandler et al. (2024). Seed germination, scored as radicle emergence, of three biological replicates of 30 seeds or fruits was analyzed.

4.2 Seedling growth assays

Seedling growth assays were conducted using just-germinated seeds (1-mm radicle protrusion visible; obtained from surface-sterilized seeds germinated in darkness at 9°C), which were selected for transfer to 12 cm × 12 cm plates containing media based on 1-mm protrusion of the radicle. As medium autoclaved 1% (w/v) agar in 1/10 Murashige and Skoog (MS) basal medium (M5519, Sigma, Darmstadt, Germany) was used. For the seedling growth assays, plates were incubated vertically in constant white light (170 $\mu mol \cdot m^{-2} \cdot s^{-1}$) in MLR-350 Versatile Environmental Test Chambers (Sanyo-Panasonic, Bracknell, UK) at a constant temperature, as indicated (Figure 2; Supplementary Figure 2). For seedling growth assays during osmotic stress (Supplementary Figure 3), water potentials were lowered using high-molecular-weight polyethylene glycol (PEG6000; 26603.293, VWR, Radnor, PA, USA) using an overlay method (Van Der Weele et al., 2000; Verslues and Bray, 2004). Seedling growth assay constant temperatures were 14°C for osmotic stress, and temperatures for the thermal stress experiments were between 14°C and 35°C.

4.3 Biochemical and biomechanical analyses

The chlorophyll content of seedlings grown horizontally at 30°C was determined after extracting pigments from leaf tissues homogenized in methanol at room temperature for 15 min while shaking at 1,000 rpm on a thermomixer (S8012-0000, Starlab, Milton Keynes, UK). The obtained extracts were centrifuged for 5 min at 14,000 *g*. The absorbance of the supernatants was determined at 750 nm, 665 nm, and 652 nm using a microplate reader (Spark® 10M, Tecan, Zürich, Switzerland) and subsequently used to calculate chlorophyll contents (Porra et al., 1989). For the biomechanical analyses (Steinbrecher and Leubner-Metzger, 2017), just-germinated *Ae. arabicum* seeds (M^+ and M^-) and IND fruits were transferred to agar plates as described above and grown for 15 days under constant white light at 30°C. IND fruits were manually split open just after the completion of germination (radicle protruding the pericarp) at 0 hat. To conduct biomechanical analyses of hypocotyls, seedlings were clamped, leaving a 7-mm gap between the jaws of a single-column tensile testing machine (Zwick Roell ZwickiLine Z0.5, Ulm, Germany). A constant speed for separation was set at 5 mm/min. Force-displacement data were obtained, and hypocotyl breaking forces were calculated (Figure 4).

4.4 RNA extraction for RNA-seq transcriptome analysis

A sampling of imbibed M^+ seeds, M^- seeds, and IND fruits for molecular analyses was described by Chandler et al. (2024). Three biological replicates of samples each corresponding to 20-mg dry weight of seed material were pulverized in liquid N_2 using mortar and pestle. Extraction of total RNA was performed as described by Graeber et al. (2011). Sampling and RNA extraction were performed of root and shoot tissue from seedlings grown at 30°C (grown from pre-germinated seeds at 9°C in darkness). Tissue was homogenized at 6,500 rpm using a Precellys 24 (Bertin Instruments, CNIM Group, Paris, France). Seed and shoot total RNA was isolated using a protocol modified by Chang et al. (1993). After the addition of RNA extraction buffer [2% (w/v) hexadecyltrimethylammonium bromide (CTAB), 2% (w/v) polyvinylpolypyrrolidone (PVP), 100 mM Tris-HCl pH 8.0, 25 mM ethylenediaminetetraacetic acid (EDTA), 2 M NaCl, and 2% (v/v) β-mercaptoethanol], samples were incubated at 65°C for 10 min with intermittent vortexing. Chloroform:isoamylalcohol (24:1) extractions were repeated three times. After the addition of 10 M LiCl to a final concentration of 2 M, RNA was precipitated overnight at 4°C and then dissolved in NaCl-Tris-EDTA (STE)

buffer [1 M NaCl, 0.5% (w/v) sodium dodecyl sulfate (SDS), 10 mM Tris-HCl pH 8.0, and 1 mM EDTA]. Three further chloroform: isoamylalcohol (24:1) extractions were then performed before precipitation in 100% (v/v) ethanol overnight at −80°C. Samples were then centrifuged for 20 min at 4°C. After the removal of the aqueous phase, the RNA pellets were washed with 70% (v/v) ethanol. Samples were centrifuged for 20 min, the ethanol was carefully removed, and the RNA was subsequently dissolved in RNase-free water. Genomic DNA was removed by DNase-I (QIAGEN, Valencia, CA, USA) digestion in solution, followed by additional purification using columns (QIAGEN RNeasy Kit). Shoot tissue RNA was isolated using the RNeasy Plant Mini Kit (QIAGEN) and manufacturer's instructions. RNA quantity and purity were determined using a NanoDrop™ spectrophotometer (ND-1000, ThermoScientific™, Wilmington, DE, USA) and an Agilent 2100 Bioanalyzer with the RNA 6000 Nano Kit (Agilent Technologies, Santa Clara, CA, USA) using the 2100 Expert Software to calculate RNA Integrity Number (RIN) values.

4.5 Analysis of RNA-seq transcriptome data

Transcriptome assembly, data trimming, filtering, read mapping, feature counting, and DEG detection were performed using the pipeline previously described by Wilhelmsson et al. (2019). PCA was performed using R (R Core Team, 2021) and the Bioconductor package DESeq2 (Love et al., 2014) and plotPCA on log(x + 1)-transformed RPKM values with non-zero values in at least one sample. GO term enrichment in DEG lists was calculated with R package topGO using the elim method with Fisher's exact test (Alexa and Rahnenfuhrer, 2021). Gene identifiers and symbols are according to earlier publications of the *Ae. arabicum* genome (version 2.5) and transcriptome (Wilhelmsson et al., 2019; Arshad et al., 2021; Chandler et al., 2024), and the *Ae. arabicum* web portal (https://plantcode.cup.uni-freiburg.de/aetar_db/index.php) links this to the current (Fernandez-Pozo et al., 2021) and future genome DB and gene expression atlas.

4.6 Phylogenetic analysis

To identify Brassicaceae PILS genes (Figure 11), the *A. thaliana* sequences (Yi et al., 2021; Bogaert et al., 2022; Waidmann et al., 2023) were used, and BLAST analyses were conducted via Phytozome (Goodstein et al., 2012). The combined information of the BLAST analyses was used to conduct the phylogenetic analysis with known and putative PILS amino acid sequences aligned using ClustalW (BLOSUM cost matrix, Gap open cost 10, Gap extend cost 0.1), and Neighbor-Joining trees (Saitou and Nei, 1987) were built using Geneious 8.1.9 Tree Builder (Geneious, San Diego, CA, USA) using Jukes-Cantor distance. Consensus support (minimum 20%) was determined using bootstrap (1,000).

4.7 Statistical analysis

Data are expressed as mean ± 1 SEM. Statistical analysis of experiments was performed using the GraphPad Prism software (v.7.0a; San Diego, CA, USA) for the analysis of variance (ANOVA) and unpaired t-test procedures. For studies examining abiotic stress effects, data were analyzed by two-way ANOVA, with seedling morph and seedling age (time) as between-group factors. Multiple comparisons were performed using Sidak's *post-hoc* correction in GraphPad Prism. Results were considered statistically significant if the p-value was less than 0.05.

Data availability statement

The RNAseq data are deposited at the NCBI Sequencing Read Archive (SRA), BioProject PRJNA639399, https://www.ncbi.nlm.nih.gov/bioproject/PRJNA639399; metadata about the RNAseq samples are also available in Supplementary Dataset 1. Original germination and biomechanics datasets are available at figshare https://doi.org/10.17637/rh.24856305.v2. All other data presented or analyzed in this published article, including accession number(s), are available online through the Supplementary Material.

Author contributions

WA: Conceptualization, Data curation, Formal analysis, Funding acquisition, Investigation, Methodology, Writing – original draft, Writing – review & editing. TS: Conceptualization, Data curation, Formal analysis, Funding acquisition, Investigation, Methodology, Supervision, Writing – review & editing PW: Data curation, Formal analysis, Investigation, Methodology, Software, Writing – review & editing. NF: Data curation, Formal analysis, Investigation, Methodology, Software, Visualization, Writing – review & editing. MP: Data curation, Formal analysis, Investigation, Methodology, Writing – review & editing. ZM: Data curation, Investigation, Methodology, Writing – review & editing. SR: Conceptualization, Data curation, Formal analysis, Funding acquisition, Investigation, Methodology, Resources, Supervision, Writing – review & editing. JC: Conceptualization, Data curation, Formal analysis, Investigation, Methodology, Supervision, Visualization, Writing – original draft, Writing – review & editing. GL: Conceptualization, Data curation, Formal analysis, Funding acquisition, Investigation, Methodology, Project administration, Resources, Supervision, Writing – original draft, Writing – review & editing.

Funding

The author(s) declare financial support was received for the research, authorship, and/or publication of this article. This work is part of the ERA-CAPS "SeedAdapt" consortium project which was led

by GL-M, and funded by grants from the Biotechnology and Biological Sciences Research Council (BBSRC) to GL-M (BB/M00192X/1), from the Natural Environment Research Council (NERC) through a Doctoral Training Grant to WA (NE/L002485/1), from the Deutsche Forschungsgemeinschaft (DFG) SR (RE 1697/8-1), from Ministerio de Ciencia e Innovación (MCIN/AEI/10.13039/501100011033) and the European Social Fund to NFP (RYC2020-030219-I and PID2021-125805OA-I00), from the Austrian Science Fund (FWF) to ZM (FWF I3979-B25). We also acknowledge the support of DataPLANT to SAR (NFDI 7/1 -42077441) as part of the German National Research Data Infrastructure.

Acknowledgments

We acknowledge the support of Lincy Fernandez, Katja Sperber, Teresa Lenser, Samik Bhattacharya, Sara Mayland-Quellhorst, Setareh Mohammadin, Safina Khan, Christopher Grosche, Giles Grainge, Thomas Holloway, Kazumi Nakabayashi, and Michael Ignatz in discussions, harvesting of diaspores, and other tasks. The authors are grateful for the excellent support of the Next Generation Sequencing Unit of the Vienna BioCenter Core Facilities (VBCF).

Conflict of interest

The authors declare that the research was conducted in the absence of any commercial or financial relationships that could be construed as a potential conflict of interest.

Publisher's note

Supplementary material

The Supplementary Material for this article can be found online at: https://www.frontiersin.org/articles/10.3389/fpls.2024.1358312/full#supplementary-material

SUPPLEMENTARY DATA SHEET 1
RNA-seq RPKM values, gene annotations, DEGs, raw counts, and SRA accessions.

SUPPLEMENTARY DATA SHEET 2
GO term enrichment analysis.

SUPPLEMENTARY FIGURE S1
Dimorphic diaspore responses of Aethionema arabicum to temperature.

SUPPLEMENTARY FIGURE S2
Effect of a range of constant temperatures on the growth of Aethionema arabicum M+ and M- seedlings.

SUPPLEMENTARY FIGURE S3
Effect of water potential (osmotica) on the growth of Aethionema arabicum M + and M- seedlings.

SUPPLEMENTARY FIGURE S4
Enrichment scores for selected GO terms significantly enriched in at least one selected DEG list.

SUPPLEMENTARY FIGURE S5
Comparative spatiotemporal analysis of transcript abundance patterns of selected Aethionema arabicum ethylene and ABA-related DEGs.

SUPPLEMENTARY FIGURE S6
Comparative spatiotemporal analysis of transcript abundance patterns of selected Aethionema arabicum GA and auxin-related DEGs.

SUPPLEMENTARY FIGURE S7
Comparative spatiotemporal analysis of transcript abundance patterns of Aethionema arabicum chlorophyll-related and transporter DEGs.

SUPPLEMENTARY FIGURE S8
Comparative spatiotemporal analysis of transcript abundance patterns of Aethionema arabicum transcription factor (TF) DEGs.

SUPPLEMENTARY FIGURE S9
Comparative spatiotemporal analysis of transcript abundance patterns of Aethionema arabicum germin, LEA and HSP DEGs.

SUPPLEMENTARY FIGURE S10
Comparative spatiotemporal analysis of transcript abundance patterns of Aethionema arabicum cell wall remodelling protein (CWRP) DEGs.

SUPPLEMENTARY TABLE S1
Number of Aethionema arabicum DEGs identified.

SUPPLEMENTARY TABLE S2
Aethionema arabicum gene names and IDs.

References

Ahammed, G. J., Gantait, S., Mitra, M., Yang, Y. X., and Li, X. (2020). Role of ethylene crosstalk in seed germination and early seedling development: A review. *Plant Physiol. Biochem.* 151, 124–131. doi: 10.1016/j.plaphy.2020.03.016

Alexa, A., and Rahnenfuhrer, J. (2021). topGO: Enrichment analysis for Gene Ontology. *R package version 2.44.0.*

Arjmand, M. P., Lahiji, H. S., Golfazani, M. M., and Biglouei, M. H. (2023). New insights on the regulatory network of drought-responsive key genes in. *Genetica* 151, 29–45. doi: 10.1007/s10709-022-00177-3

Arshad, W., Lenser, T., Wilhelmsson, P. K. I., Chandler, J. O., Steinbrecher, T., Marone, F., et al. (2021). A tale of two morphs: developmental patterns and mechanisms of seed coat differentiation in the dimorphic diaspore model *Aethionema arabicum* (Brassicaceae). *Plant J.* 107, 166–181. doi: 10.1111/tpj.15283

Arshad, W., Marone, F., Collinson, M. E., Leubner-Metzger, G., and Steinbrecher, T. (2020). Fracture of the dimorphic fruits of *Aethionema arabicum* (Brassicaceae). *Botany* 98, 65–75. doi: 10.1139/cjb-2019-0014

Arshad, W., Sperber, K., Steinbrecher, T., Nichols, B., Jansen, V., Leubner-Metzger, G., et al. (2019). Dispersal biophysics and adaptive significance of dimorphic diaspores in the annual *Aethionema arabicum* (Brassicaceae). *New Phytol.* 221, 1434–1446. doi: 10.1111/nph.15490

Arsovski, A. A., Popma, T. M., Haughn, G. W., Carpita, N. C., Mccann, M. C., and Western, T. L. (2009). *AtBXL1* encodes a bifunctional beta-D-xylosidase/alpha-L-arabinofuranosidase required for pectic arabinan modification in Arabidopsis mucilage secretory cells. *Plant Physiol.* 150, 1219–1234. doi: 10.1104/pp.109.138388

Aryal, B., Huynh, J., Schneuwly, J., Siffert, A., Liu, J., Alejandro, S., et al. (2019). ABCG36/PEN3/PDR8 is an exporter of the auxin precursor, indole-3-butyric acid, and involved in auxin-controlled development. *Front. Plant Sci.* 10, 899. doi: 10.3389/fpls.2019.00899

Baskin, C. C., and Baskin, J. M. (2014). *Seeds - Ecology, biogeography, and evolution of dormancy and germination* (San Diego, London: Academic Press).

Baskin, J. M., Lu, J. J., Baskin, C. C., Tan, D. Y., and Wang, L. (2014). Diaspore dispersal ability and degree of dormancy in heteromorphic species of cold deserts of northwest China: A review. *Perspect. Plant Ecol. Evol. System.* 16, 93–99. doi: 10.1016/j.ppees.2014.02.004

Belin, C., Megies, C., Hauserova, E., and Lopez-Molina, L. (2009). Abscisic acid represses growth of the Arabidopsis embryonic axis after germination by enhancing auxin signaling. *Plant Cell* 21, 2253–2268. doi: 10.1105/tpc.109.067702

Bhattacharya, S., Mayland-Quellhorst, S., Muller, C., and Mummenhoff, K. (2019a). Two-tier morpho-chemical defence tactic in Aethionema via fruit morph plasticity and glucosinolates allocation in diaspores. *Plant Cell Environ.* 42, 1381–1392. doi: 10.1111/pce.13462

Bhattacharya, S., Sperber, K., Ozudogru, B., Leubner-Metzger, G., and Mummenhoff, K. (2019b). Naturally-primed life strategy plasticity of dimorphic *Aethionema arabicum* facilitates optimal habitat colonization. *Sci. Rep.* 9, 16108. doi: 10.1038/s41598-019-52520-y

Bogaert, K. A., Blomme, J., Beeckman, T., and De Clerck, O. (2022). Auxin's origin: do PILS hold the key? *Trends Plant Sci.* 27, 227–236. doi: 10.1016/j.tplants.2021.09.008

Boron, A. K., Van Loock, B., Suslov, D., Markakis, M. N., Verbelen, J. P., and Vissenberg, K. (2015). Over-expression of AtEXLA2 alters etiolated arabidopsis hypocotyl growth. *Ann. Bot.* 115, 67–80. doi: 10.1093/aob/mcu221

Cao, D., Baskin, C. C., Baskin, J. M., Yang, F., and Huang, Z. (2012). Comparison of germination and seed bank dynamics of dimorphic seeds of the cold desert halophyte *Suaeda corniculata* subsp. mongolica. *Ann. Bot.* 110, 1545–1558. doi: 10.1093/aob/mcs205

Cao, J. (2012). The pectin lyases in *Arabidopsis thaliana*: Evolution, selection and expression profiles. *PloS One* 7, e46944. doi: 10.1371/journal.pone.0046944

Cao, J., Li, X. R., Chen, L., He, M. X., and Lan, H. Y. (2022). The developmental delay of seedlings with cotyledons only confers stress tolerance to *Suaeda aralocaspica* (Chenopodiaceae) by unique performance on morphology, physiology, and gene expression. *Front. Plant Sci.* 13, 844430. doi: 10.3389/fpls.2022.844430

Chandler, J. O., Wilhelmsson, P. K. I., Fernandez-Pozo, N., Graeber, K., Arshad, W., Pérez, M., et al. (2024). The dimorphic diaspore model *Aethionema arabicum* (Brassicaceae): Distinct molecular and morphological control of responses to parental and germination temperatures. *Plant Cell* 36, in press. doi: 10.1101/2023.12.14.571707

Chang, S., Puryear, J., and Cairney, J. (1993). A simple and efficient method for isolating RNA from pine trees. *Plant Mol. Biol. Rep.* 11, 113–116. doi: 10.1007/BF02670468

Christianson, J. A., Wilson, I. W., Llewellyn, D. J., and Dennis, E. S. (2009). The low-oxygen induced NAC domain transcription factor ANAC102 affects viability of *Arabidopsis thaliana* seeds following low-oxygen treatment. *Plant Physiol.* 149, 1724–1738. doi: 10.1104/pp.108.131912

Cosgrove, D. J. (2016). Plant cell wall extensibility: connecting plant cell growth with cell wall structure, mechanics, and the action of wall-modifying enzymes. *J. Exp. Bot.* 67, 463–476. doi: 10.1093/jxb/erv511

Daher, F. B., and Braybrook, S. A. (2015). How to let go: pectin and plant cell adhesion. *Front. Plant Sci.* 6, 523. doi: 10.3389/fpls.2015.00523

Dekkers, B. J. W., Pearce, S., Van Bolderen-Veldkamp, R. P. M., Marshall, A., Wider, P., Gilbert, J., et al. (2013). Transcriptional dynamics of two seed compartments with opposing roles in Arabidopsis seed germination. *Plant Physiol.* 163, 205–215. doi: 10.1104/pp.113.223511

Dhar, S., Kim, J., Yoon, E. K., Jang, S., Ko, K., and Lim, J. (2022). SHORT-ROOT controls cell elongation in the etiolated Arabidopsis hypocotyl. *Mol. Cells* 45, 243–256. doi: 10.14348/molcells.2021.5008

Ducatti, K. R., Batista, T. B., Hirai, W. Y., Luccas, D. A., Moreno, L. D., Guimaraes, C. C., et al. (2022). Transcripts expressed during germination are associated with vigor in soybean seeds. *Plants-Basel* 11, 1310. doi: 10.3390/plants11101310

Endo, A., Tatematsu, K., Hanada, K., Duermeyer, L., Okamoto, M., Yonekura-Sakakibara, K., et al. (2012). Tissue-specific transcriptome analysis reveals cell wall metabolism, flavonol biosynthesis and defense responses are activated in the endosperm of germinating *Arabidopsis thaliana* seeds. *Plant Cell Physiol.* 53, 16–27. doi: 10.1093/pcp/pcr171

Fenner, M. (1987). Seedlings. *New Phytol.* 106, 35–47. doi: 10.1111/j.1469-8137.1987.tb04681.x

Feraru, E., Feraru, M. I., Barbez, E., Waidmann, S., Sun, L., Gaidora, A., et al. (2019). PILS6 is a temperature-sensitive regulator of nuclear auxin input and organ growth in *Arabidopsis thaliana*. *Proc. Natl. Acad. Sci. United States America* 116, 3893–3898. doi: 10.1073/pnas.1814015116

Feraru, E., Feraru, M. I., Moulinier-Anzola, J., Schwihla, M., Santos, J. F. D., Sun, L., et al. (2022). PILS proteins provide a homeostatic feedback on auxin signaling output. *Development* 149, dev200929. doi: 10.1242/dev.200929

Feraru, E., Vosolsobe, S., Feraru, M. I., Petrasek, J., and Kleine-Vehn, J. (2012). Evolution and structural diversification of PILS putative auxin carriers in plants. *Front. Plant Sci.* 3, 227. doi: 10.3389/fpls.2012.00227

Fernandez-Pozo, N., Metz, T., Chandler, J. O., Gramzow, L., Merai, Z., Maumus, F., et al. (2021). *Aethionema arabicum* genome annotation using PacBio full-length transcripts provides a valuable resource for seed dormancy and Brassicaceae evolution research. *Plant J.* 106, 275–293. doi: 10.1111/tpj.15161

Finch-Savage, W. E., and Bassel, G. W. (2016). Seed vigour and crop establishment: extending performance beyond adaptation. *J. Exp. Bot.* 67, 567–591. doi: 10.1093/jxb/erv490

Finch-Savage, W. E., and Footitt, S. (2017). Seed dormancy cycling and the regulation of dormancy mechanisms to time germination in variable field environments. *J. Exp. Bot.* 68, 843–856. doi: 10.1093/jxb/erw477

Finch-Savage, W. E., and Leubner-Metzger, G. (2006). Seed dormancy and the control of germination. *New Phytol.* 171, 501–523. doi: 10.1111/j.1469-8137.2006.01787.x

Footitt, S., Clewes, R., Feeney, M., Finch-Savage, W. E., and Frigerio, L. (2019). Aquaporins influence seed dormancy and germination in response to stress. *Plant Cell Environ.* 42, 2325–2339. doi: 10.1111/pce.13561

Franzke, A., Lysak, M. A., Al-Shehbaz, I. A., Koch, M. A., and Mummenhoff, K. (2011). Cabbage family affairs: the evolutionary history of Brassicaceae. *Trends Plant Sci.* 16, 108–116. doi: 10.1016/j.tplants.2010.11.005

Gardarin, A., Coste, F., Wagner, M. H., and Durr, C. (2016). How do seed and seedling traits influence germination and emergence parameters in crop species? A comparative analysis. *Seed Sci. Res.* 26, 317–331. doi: 10.1017/S0960258516000210

Gasch, P., Fundinger, M., Muller, J. T., Lee, T., Bailey-Serres, J., and Mustroph, A. (2016). Redundant ERF-VII transcription factors bind to an evolutionarily conserved *cis*-motif to regulate hypoxia-responsive gene expression in Arabidopsis. *Plant Cell* 28, 160–180. doi: 10.1105/tpc.15.00866

Geisler, M., Aryal, B., Di Donato, M., and Hao, P. C. (2017). A critical view on ABC transporters and their interacting partners in auxin transport. *Plant Cell Physiol.* 58, 1601–1614. doi: 10.1093/pcp/pcx104

Gianella, M., Bradford, K. J., and Guzzon, F. (2021). Ecological, (epi)genetic and physiological aspects of bet-hedging in angiosperms. *Plant Reprod.* 34, 21–36. doi: 10.1007/s00497-020-00402-z

Goodstein, D. M., Shu, S. Q., Howson, R., Neupane, R., Hayes, R. D., Fazo, J., et al. (2012). Phytozome: a comparative platform for green plant genomics. *Nucleic Acids Res.* 40, D1178–D1186. doi: 10.1093/nar/gkr944

Graeber, K., Linkies, A., Steinbrecher, T., Mummenhoff, K., Tarkowská, D., Turečková, V., et al. (2014). *DELAY OF GERMINATION 1* mediates a conserved coat dormancy mechanism for the temperature- and gibberellin-dependent control of seed germination. *Proc. Natl. Acad. Sci. United States America* 111, E3571–E3580. doi: 10.1073/pnas.1403851111

Graeber, K., Linkies, A., Wood, A. T., and Leubner-Metzger, G. (2011). A guideline to family-wide comparative state-of-the-art quantitative RT-PCR analysis exemplified with a Brassicaceae cross-species seed germination case study. *Plant Cell* 23, 2045–2063. doi: 10.1105/tpc.111.084103

Ha, J. H., Han, S. H., Lee, H. J., and Park, C. M. (2017). Environmental adaptation of the heterotrophic-to-autotrophic transition: The developmental plasticity of seedling establishment. *Crit. Rev. Plant Sci.* 36, 128–137. doi: 10.1080/07352689.2017.1355661

He, X. J., Mu, R. L., Cao, W. H., Zhang, Z. G., Zhang, J. S., and Chen, S. Y. (2005). AtNAC2, a transcription factor downstream of ethylene and auxin signaling pathways, is involved in salt stress response and lateral root development. *Plant J.* 44, 903–916. doi: 10.1111/j.1365-313X.2005.02575.x

Hoai, P. T. T., Tyerman, S. D., Schnell, N., Tucker, M., Mcgaughey, S. A., Qiu, J. E., et al. (2020). Deciphering aquaporin regulation and roles in seed biology. *J. Exp. Bot.* 71, 1763–1773. doi: 10.1093/jxb/erz555

Holloway, T., Steinbrecher, T., Pérez, M., Seville, A., Stock, D., Nakabayashi, K., et al. (2021). Coleorhiza-enforced seed dormancy: a novel mechanism to control germination in grasses. *New Phytol.* 229, 2179–2191. doi: 10.1111/nph.16948

Hu, Y. M., Vandenbussche, F., and van der Straeten, D. (2017). Regulation of seedling growth by ethylene and the ethylene-auxin crosstalk. *Planta* 245, 467–489. doi: 10.1007/s00425-017-2651-6

Hu, X. W., Wang, Y. R., and Wu, Y. P. (2009). Effects of the pericarp on imbibition, seed germination, and seedling establishment in seeds of *Hedysarum scoparium* Fisch. et Mey. *Ecol. Res.* 24, 559–564. doi: 10.1007/s11284-008-0524-y

Huang, D. Q., Jaradat, M. R., Wu, W. R., Ambrose, S. J., Ross, A. R., Abrams, S. R., et al. (2007). Structural analogs of ABA reveal novel features of ABA perception and signaling in Arabidopsis. *Plant J.* 50, 414–428. doi: 10.1111/j.1365-313X.2007.03056.x

Hundertmark, M., and Hincha, D. K. (2008). LEA (late embryogenesis abundant) proteins and their encoding genes in *Arabidopsis thaliana*. *BMC Genomics* 9, 118. doi: 10.1186/1471-2164-9-118

Huysmans, M., Buono, R. A., Skorzinski, N., Radio, M. C., De Winter, F., Parizot, B., et al. (2018). NAC transcription factors ANAC087 and ANAC046 control distinct aspects of programmed cell death in the Arabidopsis columella and lateral root cap. *Plant Cell* 30, 2197–2213. doi: 10.1105/tpc.18.00293

Ignatz, M., Hourston, J. E., Tureckova, V., Strnad, M., Meinhard, J., Fischer, U., et al. (2019). The biochemistry underpinning industrial seed technology and mechanical processing of sugar beet. *Planta* 250, 1717–1729. doi: 10.1007/s00425-019-03257-5

Ilias, I. A., Negishi, K., Yasue, K., Jomura, N., Morohashi, K., Baharum, S. N., et al. (2019). Transcriptome-wide effects of expansin gene manipulation in etiolated Arabidopsis seedling. *J. Plant Res.* 132, 159–172. doi: 10.1007/s10265-018-1067-0

Imbert, E. (2002). Ecological consequences and ontogeny of seed heteromorphism. *Perspect. Plant Ecol. Evol. System.* 5, 13–36. doi: 10.1078/1433-8319-00021

Johnson, K. L., Ramm, S., Kappel, C., Ward, S., Leyser, O., Sakamoto, T., et al. (2015). The Tinkerbell (Tink) mutation identifies the dual-specificity MAPK phosphatase INDOLE-3-BUTYRIC ACID-RESPONSE5 (IBR5) as a novel regulator of organ size in Arabidopsis. *PloS One* 10, e0131103. doi: 10.1371/journal.pone.0131103

Khedia, J., Agarwal, P., and Agarwal, P. K. (2019). Deciphering hydrogen peroxide-induced signalling towards stress tolerance in plants. *3 Biotech.* 9, 395. doi: 10.1007/s13205-019-1924-0

Kim, M. J., Ruzicka, D., Shin, R., and Schachtman, D. P. (2012). The AP2/ERF transcription factor RAP2.11 modulates plant response to low-potassium conditions. *Mol. Plant* 5, 1042–1057. doi: 10.1093/mp/sss003

Kitamura, S., Matsuda, F., Tohge, T., Yonekura-Sakakibara, K., Yamazaki, M., Saito, K., et al. (2010). Metabolic profiling and cytological analysis of proanthocyanidins in immature seeds of Arabidopsis thaliana flavonoid accumulation mutants. *Plant J.* 62, 549–559. doi: 10.1111/tpj.2010.62.issue-4

Lee, T. A., and Bailey-Serres, J. (2019). Integrative analysis from the epigenome to translatome uncovers patterns of dominant nuclear regulation during transient stress. *Plant Cell* 31, 2573–2595. doi: 10.1105/tpc.19.00463

Lee, D., Polisensky, D. H., and Braam, J. (2005). Genome-wide identification of touch- and darkness-regulated Arabidopsis genes: a focus on calmodulin-like and XTH genes. *New Phytol.* 165, 429–444. doi: 10.1111/j.1469-8137.2004.01238.x

Lenser, T., Graeber, K., Cevik, O. S., Adiguzel, N., Donmez, A. A., Grosche, C., et al. (2016). Developmental control and plasticity of fruit and seed dimorphism in *Aethionema arabicum*. *Plant Physiol.* 172, 1691–1707. doi: 10.1104/pp.16.00838

Lenser, T., Tarkowska, D., Novak, O., Wilhelmsson, P. K. I., Bennett, T., Rensing, S. A., et al. (2018). When the BRANCHED network bears fruit: How carpic dominance causes fruit dimorphism in *Aethionema*. *Plant J.* 94, 352–371. doi: 10.1111/tpj.13861

Lepiniec, L., Debeaujon, I., Routaboul, J. M., Baudry, A., Pourcel, L., Nesi, N., et al. (2006). Genetics and biochemistry of seed flavonoids. *Annu. Rev. Plant Biol.* 57, 405–430. doi: 10.1146/annurev.arplant.57.032905.105252

Linkies, A., and Leubner-Metzger, G. (2012). Beyond gibberellins and abscisic acid: how ethylene and jasmonates control seed germination. *Plant Cell Rep.* 31, 253–270. doi: 10.1007/s00299-011-1180-1

Linkies, A., Müller, K., Morris, K., Turečková, V., Cadman, C. S. C., Corbineau, F., et al. (2009). Ethylene interacts with abscisic acid to regulate endosperm rupture during germination: A comparative approach using *Lepidium sativum* and *Arabidopsis thaliana*. *Plant Cell* 21, 3803–3822. doi: 10.1105/tpc.109.070201

Loades, E., Perez, M., Tureckova, V., Tarkowska, D., Strnad, M., Seville, A., et al. (2023). Distinct hormonal and morphological control of dormancy and germination in *Chenopodium album* dimorphic seeds. *Front. Plant Sci.* 14, 1156794. doi: 10.3389/fpls.2023.1156794

Loqué, D., Ludewig, U., Yuan, L. X., and Von Wirén, N. (2005). Tonoplast intrinsic proteins AtTIP2;1 and AtTIP2;3 facilitate NH_3 transport into the vacuole. *Plant Physiol.* 137, 671–680. doi: 10.1104/pp.104.051268

Lorrai, R., Gandolfi, F., Boccaccini, A., Ruta, V., Possenti, M., Tramontano, A., et al. (2018). Genome-wide RNA-seq analysis indicates that the DAG1 transcription factor promotes hypocotyl elongation acting on ABA, ethylene and auxin signaling. *Sci. Rep.* 8, 15895. doi: 10.1038/s41598-018-34256-3

Love, M. I., Huber, W., and Anders, S. (2014). Moderated estimation of fold change and dispersion for RNA-seq data with DESeq2. *Genome Biol.* 15, 550. doi: 10.1186/s13059-014-0550-8

Lu, J. J., Dong, W. J., Tan, D. Y., Baskin, C. C., and Baskin, J. M. (2020). Dormancy and germination of the trimorphic achenes of a cold desert annual: spreading the risk over time. *AoB Plants* 12, plaa056. doi: 10.1093/aobpla/plaa056

Lu, J. J., Tan, D. Y., Baskin, J. M., and Baskin, C. C. (2015a). Post-release fates of seeds in dehiscent and indehiscent siliques of the diaspore heteromorphic species *Diptychocarpus strictus* (Brassicaceae). *Perspect. Plant Ecol. Evol. System.* 17, 255–262. doi: 10.1016/j.ppees.2015.04.001

Lu, J. J., Tan, D. Y., Baskin, C. C., and Baskin, J. M. (2017a). Delayed dehiscence of the pericarp: role in germination and retention of viability of seeds of two cold desert annual Brassicaceae species. *Plant Biol.* 19, 14–22. doi: 10.1111/plb.12457

Lu, J. J., Tan, D. Y., Baskin, C. C., and Baskin, J. M. (2017b). Role of indehiscent pericarp in formation of soil seed bank in five cold desert Brassicaceae species. *Plant Ecol.* 218, 1187–1200. doi: 10.1007/s11258-017-0760-8

Lu, J. J., Zhou, Y. M., Tan, D. Y., Baskin, C. C., and Baskin, J. M. (2015b). Seed dormancy in six cold desert Brassicaceae species with indehiscent fruits. *Seed Sci. Res.* 25, 276–285. doi: 10.1017/S0960258515000215

Mabuchi, K., Maki, H., Itaya, T., Suzuki, T., Nomoto, M., Sakaoka, S., et al. (2018). MYB30 links ROS signaling, root cell elongation, and plant immune responses. *Proc. Natl. Acad. Sci. United States America* 115, E4710–E4719. doi: 10.1073/pnas.1804233115

Macgregor, D. R., Kendall, S. L., Florance, H., Fedi, F., Moore, K., Paszkiewicz, K., et al. (2015). Seed production temperature regulation of primary dormancy occurs through control of seed coat phenylpropanoid metabolism. *New Phytol.* 205, 642–652. doi: 10.1111/nph.13090

Maki, H., Sakaoka, S., Itaya, T., Suzuki, T., Mabuchi, K., Amabe, T., et al. (2019). ANAC032 regulates root growth through the MYB30 gene regulatory network. *Sci. Rep.* 9, 11358. doi: 10.1038/s41598-019-47822-0

Mamut, J., Tan, D.-Y., Baskin, C. C., and Baskin, J. M. (2014). Role of trichomes and pericarp in the seed biology of the desert annual *Lachnoloma lehmannii* (Brassicaceae). *Ecol. Res.* 29, 33–44. doi: 10.1007/s11284-013-1098-x

Maris, A., Kaewthai, N., Eklof, J. M., Miller, J. G., Brumer, H., Fry, S. C., et al. (2010). Differences in enzymic properties of five recombinant xyloglucan endotransglucosylase/hydrolase (XTH) proteins of *Arabidopsis thaliana*. *J. Exp. Bot.* 62, 261–271. doi: 10.1093/jxb/erq263

Maun, M. A., and Payne, A. M. (1989). Fruit and seed polymorphism and its relation to seedling growth in the genus *Cakile*. *Can. J. Bot.* 67, 2743–2750. doi: 10.1139/b89-353

Membre, N., Bernier, F., Staiger, D., and Berna, A. (2000). *Arabidopsis thaliana* germin-like proteins: common and specific features point to a variety of functions. *Planta* 211, 345–354. doi: 10.1007/s004250000277

Meng, S., Peng, J. S., He, Y. N., Zhang, G. B., Yi, H. Y., Fu, Y. L., et al. (2016). NRT1.5 mediates the suppression of nitrate starvation-induced leaf senescence by modulating foliar potassium level. *Mol. Plant* 9, 461–470. doi: 10.1016/j.molp.2015.12.015

Merai, Z., Graeber, K., Wilhelmsson, P., Ullrich, K. K., Arshad, W., Grosche, C., et al. (2019). *Aethionema arabicum*: a novel model plant to study the light control of seed germination. *J. Exp. Bot.* 70, 3313–3328. doi: 10.1093/jxb/erz146

Miedes, E., Suslov, D., Vandenbussche, F., Kenobi, K., Ivakov, A., van der Straeten, D., et al. (2013). Xyloglucan endotransglucosylase/hydrolase (XTH) overexpression affects growth and cell wall mechanics in etiolated Arabidopsis hypocotyls. *J. Exp. Bot.* 64, 2481–2497. doi: 10.1093/jxb/ert107

Mohammadin, S., Peterse, K., Van De Kerke, S. J., Chatrou, L. W., Donmez, A. A., Mummenhoff, K., et al. (2017). Anatolian origins and diversification of *Aethionema*, the sister lineage of the core Brassicaceae. *Am. J. Bot.* 104, 1042–1054. doi: 10.3732/ajb.1700091

Moles, A. T., and Westoby, M. (2006). Seed size and plant strategy across the whole life cycle. *Oikos* 113, 91–105. doi: 10.1111/j.0030-1299.2006.14194.x

Moneo-Sanchez, M., Alonso-Chico, A., Knox, J. P., Dopico, B., Labrador, E., and Martin, I. (2019). beta-(1,4)-Galactan remodelling in Arabidopsis cell walls affects the xyloglucan structure during elongation. *Planta* 249, 351–362. doi: 10.1007/s00425-018-3008-5

Moneo-Sánchez, M., Izquierdo, L., Martín, I., Labrador, E., and Dopico, B. (2016). Subcellular location of subfamily a1 β-galactosidases and developmental regulation of transcript levels of their coding genes. *Plant Physiol. Biochem.* 109, 137–145. doi: 10.1016/j.plaphy.2016.09.016

Nakabayashi, K., Walker, M., Irwin, D., Cohn, J., Gurda, S., Garcia, L., et al. (2022). The phytotoxin myrigalone A triggers a phased detoxification programme and inhibits Lepidium sativum seed germination via multiple mechanisms including interference with auxin homeostasis. *Int. J. Mol. Sci.* 23, 4618. doi: 10.3390/ijms23094618

Nichols, B. S., Leubner-Metzger, G., and Jansen, V. (2020). Between a rock and a hard place: adaptive sensing and site-specific dispersal. *Ecol. Lett.* 23, 1370–1379. doi: 10.1111/ele.13564

Nie, K. L., Zhao, H. Y., Wang, X. P., Niu, Y. L., Zhou, H. P., and Zheng, Y. (2022). The MIEL1-ABI5/MYB30 regulatory module fine tunes abscisic acid signaling during seed germination. *J. Integr. Plant Biol.* 64, 930–941. doi: 10.1111/jipb.13234

Overvoorde, P. J., Okushima, Y., Alonso, J. M., Chan, A., Chang, C., Ecker, J. R., et al. (2005). Functional genomic analysis of the AUXIN/INDOLE-3-ACETIC ACID gene family members in *Arabidopsis thaliana*. *Plant Cell* 17, 3282–3300. doi: 10.1105/tpc.105.036723

Park, J., Kim, Y. S., Kim, S. G., Jung, J. H., Woo, J. C., and Park, C. M. (2011). Integration of auxin and salt signals by the NAC transcription factor NTM2 during seed germination in Arabidopsis. *Plant Physiol.* 156, 537–549. doi: 10.1104/pp.111.177071

Porra, R. J., Thompson, W. A., and Kriedemann, P. E. (1989). Determination of accurate extinction coefficients and simultaneous-equations for assaying chlorophyll-a and chlorophyll-b extracted with 4 different solvents - Verification of the concentration of chlorophyll ctandards by atomic-absorption spectroscopy. *Biochim. Biophys. Acta* 975, 384–394. doi: 10.1016/S0005-2728(89)80347-0

Rae, G. M., Uversky, V. N., David, K., and Wood, M. (2014). DRM1 and DRM2 expression regulation: potential role of splice variants in response to stress and environmental factors in Arabidopsis. *Mol. Genet. Genomics* 289, 317–332. doi: 10.1007/s00438-013-0804-2

R Core Team. (2021). *R: A language and environment for statistical computing*. Vienna, Austria: R Foundation for Statistical Computing. Available at: https://www.R-project.org/.

Saitou, N., and Nei, M. (1987). The neighbor-joining method - a new method for reconstructing phylogenetic trees. *Mol. Biol. Evol.* 4, 406–425. doi: : 10.1093/oxfordjournals.molbev.a040454

Saxe, F., Weichold, S., Reinecke, A., Lisec, J., Döring, A., Neumetzler, L., et al. (2016). Age effects on hypocotyl mechanics. *PloS One* 11, 0167808. doi: 10.1371/journal.pone.0167808

Scheler, C., Weitbrecht, K., Pearce, S. P., Hampstead, A., Buettner-Mainik, A., Lee, K., et al. (2015). Promotion of testa rupture during garden cress germination involves seed compartment-specific expression and activity of pectin methylesterases. *Plant Physiol.* 167, 200–215. doi: 10.1104/pp.114.247429

Shigeyama, T., Watanabe, A., Tokuchi, K., Toh, S., Sakurai, N., Shibuya, N., et al. (2016). alpha-Xylosidase plays essential roles in xyloglucan remodelling, maintenance of cell wall integrity, and seed germination in *Arabidopsis thaliana*. *J. Exp. Bot.* 67, 5615–5629. doi: 10.1093/jxb/erw321

Shin, R., and Schachtman, D. P. (2004). Hydrogen peroxide mediates plant root cell response to nutrient deprivation. *Proc. Natl. Acad. Sci. United States America* 101, 8827–8832. doi: 10.1073/pnas.0401707101

Smolikova, G., Strygina, K., Krylova, E., Vikhorev, A., Bilova, T., Frolov, A., et al. (2022). Seed-to-seedling transition in *Pisum sativum* L.: a transcriptomic approach. *Plants (Basel)* 11, 1686. doi: 10.3390/plants11131686

Song, J. Q., Wang, H. F., Chu, R. W., Zhao, L. T., Li, X. X., An, S., et al. (2023). Differences in physiological characteristics, seed germination, and seedling establishment in response to salt stress between dimorphic seeds in the halophyte *Suaeda liaotungensis*. *Plants* 12, 1408. doi: 10.3390/plants12061408

Song, S., Willems, L., Jiao, A., Zhao, T., Schranz, M. E., and Bentsink, L. (2022). The membrane associated NAC transcription factors ANAC060 and ANAC040 are functionally redundant in the inhibition of seed dormancy in *Arabidopsis thaliana*. *J. Exp. Bot.* 73, 5514–5528. doi: 10.1093/jxb/erac232

Steinbrecher, T., and Leubner-Metzger, G. (2017). The biomechanics of seed germination. *J. Exp. Bot.* 68, 765–783. doi: 10.1093/jxb/erw428

Steinbrecher, T., and Leubner-Metzger, G. (2018). Tissue and cellular mechanics of seeds. *Curr. Opin. Genet. Dev.* 51, 1–10. doi: 10.1016/j.gde.2018.03.001

Steinbrecher, T., and Leubner-Metzger, G. (2022). Xyloglucan remodelling enzymes and the mechanics of plant seed and fruit biology. *J. Exp. Bot.* 73, 1253–1257. doi: 10.1093/jxb/erac020

Stortenbeker, N., and Bemer, M. (2019). The SAUR gene family: the plant's toolbox for adaptation of growth and development. *J. Exp. Bot.* 70, 17–27. doi: 10.1093/jxb/ery332

Sun, Y., Li, H., and Huang, J. R. (2012). Arabidopsis TT19 functions as a carrier to transport anthocyanin from the cytosol to tonoplasts. *Mol. Plant* 5, 387–400. doi: 10.1093/mp/ssr110

Tan, P. P., Du, X. H., Shang, Y. J., Zhu, K. K., Joshi, S., Kaur, K., et al. (2022). Ion transporters and their exploration for conferring abiotic stress tolerance in plants. *Plant Growth Regul.* 96, 1–23. doi: 10.1007/s10725-021-00762-0

Tang, X. L., Peng, Y., Li, Z., Guo, H. W., Xia, X. L., Li, B. S., et al. (2022). The regulation of nitrate reductases in response to abiotic stress in Arabidopsis. *Int. J. Mol. Sci.* 23, 1202. doi: 10.3390/ijms23031202

Teale, W. D., Paponov, I. A., and Palme, K. (2006). Auxin in action: signalling, transport and the control of plant growth and development. *Nat. Rev. Mol. Cell Biol.* 7, 847–859. doi: 10.1038/nrm2020

Templalexis, D., Tsitsekian, D., Liu, C., Daras, G., Simura, J., Moschou, P., et al. (2022). Potassium transporter TRH1/KUP4 contributes to distinct auxin-mediated root system architecture responses. *Plant Physiol.* 188, 1043–1060. doi: 10.1093/plphys/kiab472

Van Aken, O., Zhang, B. T., Law, S., Narsai, R., and Whelan, J. (2013). AtWRKY40 and AtWRKY63 modulate the expression of stress-responsive nuclear genes encoding mitochondrial and chloroplast proteins. *Plant Physiol.* 162, 254–271. doi: 10.1104/pp.113.215996

Van Der Weele, C. M., Spollen, W. G., Sharp, R. E., and Baskin, T. I. (2000). Growth of *Arabidopsis thaliana* seedlings under water deficit studied by control of water potential in nutrient-agar media. *J. Exp. Bot.* 51, 1555–1562. doi: 10.1093/jexbot/51.350.1555

Verslues, P. E., and Bray, E. A. (2004). LWR1 and LWR2 are required for osmoregulation and osmotic adjustment in Arabidopsis. *Plant Physiol.* 136, 2831–2842. doi: 10.1104/pp.104.045856

Voegele, A., Linkies, A., Müller, K., and Leubner-Metzger, G. (2011). Members of the gibberellin receptor gene family *GID1* (*GIBBERELLIN INSENSITIVE DWARF1*) play distinct roles during *Lepidium sativum* and *Arabidopsis thaliana* seed germination. *J. Exp. Bot.* 62, 5131–5147. doi: 10.1093/jxb/err214

Waidmann, S., Beziat, C., Ferreira Da Silva Santos, J., Feraru, E., Feraru, M. I., Sun, L., et al. (2023). Endoplasmic reticulum stress controls PIN-LIKES abundance and thereby growth adaptation. *Proc. Natl. Acad. Sci. United States America* 120, e2218865120. doi: 10.1073/pnas.2218865120

Walck, J. L., Hidayati, S. N., Dixon, K. W., Thompson, K., and Poschlod, P. (2011). Climate change and plant regeneration from seed. *Global Change Biol.* 17, 2145–2161. doi: 10.1111/gcb.2011.17.issue-6

Wang, T. J., Huang, S. Z., Zhang, A. I., Guo, P., Liu, Y. T., Xu, C. M., et al. (2021). JMJ17-WRKY40 and HY5-ABI5 modules regulate the expression of ABA-responsive genes in Arabidopsis. *New Phytol.* 230, 567–584. doi: 10.1111/nph.17177

Wang, Y. C., Peng, Y., and Guo, H. W. (2023b). To curve for survival: Apical hook development. *J. Integr. Plant Biol.* 65, 324–342. doi: 10.1111/jipb.13441

Wang, Y., Yuan, Z., Wang, J., Xiao, H., Wan, L., Li, L., et al. (2023a). The nitrate transporter NRT2.1 directly antagonizes PIN7-mediated auxin transport for root growth adaptation. *Proc. Natl. Acad. Sci. United States America* 120, e2221313120. doi: 10.1073/pnas.2221313120

Wilhelmsson, P. K. I., Chandler, J. O., Fernandez-Pozo, N., Graeber, K., Ullrich, K. K., Arshad, W., et al. (2019). Usability of reference-free transcriptome assemblies for detection of differential expression: a case study on *Aethionema arabicum* dimorphic seeds. *BMC Genomics* 20, 95. doi: 10.1186/s12864-019-5452-4

Wu, T., Alizadeh, M., Lu, B. L., Cheng, J. K., Hoy, R., Bu, M. Y., et al. (2022). The transcriptional co-repressor SEED DORMANCY 4-LIKE (AtSDR4L) promotes the embryonic-to-vegetative transition in Arabidopsis thaliana. *J. Integr. Plant Biol.* 64, 2075–2096. doi: 10.1111/jipb.13360

Xu, W. J., Dubos, C., and Lepiniec, L. (2015). Transcriptional control of flavonoid biosynthesis by MYB-bHLH-WDR complexes. *Trends Plant Sci.* 20, 176–185. doi: 10.1016/j.tplants.2014.12.001

Xu, P. P., Fang, S., Chen, H. Y., and Cai, W. M. (2020). The brassinosteroid-responsive xyloglucan endotransglucosylase/hydrolase 19 (XTH19) and XTH23 genes are involved in lateral root development under salt stress in Arabidopsis. *Plant J.* 104, 59–75. doi: 10.1111/tpj.14905

Xu, J., Yin, H. X., Yang, L. L., Xie, Z. X., and Liu, X. J. (2011). Differential salt tolerance in seedlings derived from dimorphic seeds of *Atriplex centralasiatica*: from physiology to molecular analysis. *Planta* 233, 859–871. doi: 10.1007/s00425-010-1347-y

Yang, F., Baskin, J. M., Baskin, C. C., Yang, X., Cao, D., and Huang, Z. (2015). Effects of germination time on seed morph ratio in a seed-dimorphic species and possible ecological significance. *Ann. Bot.* 115, 137–145. doi: 10.1093/aob/mcu210

Yi, C. Y., Wang, X. C., Chen, Q., Callahan, D. L., Fournier-Level, A., Whelan, J., et al. (2021). Diverse phosphate and auxin transport loci distinguish phosphate tolerant from sensitive Arabidopsis accessions. *Plant Physiol.* 187, 2656–2673. doi: 10.1093/plphys/kiab441

Zhang, H., Hu, M. F., Ma, H. Y., Jiang, L., Zhao, Z. Y., Ma, J. B., et al. (2021). Differential responses of dimorphic seeds and seedlings to abiotic stresses in the halophyte *Suaeda salsa*. *Front. Plant Sci.* 12, 630338. doi: 10.3389/fpls.2021.630338

Zhang, S. C., and Wang, X. J. (2017). One new kind of phytohormonal signaling integrator: Up-and-coming GASA family genes. *Plant Signaling Behav.* 12, e1226453. doi: 10.1080/15592324.2016.1226453

Zhang, Y. Y., Xie, Y. F., Shi, H. F., Zhuang, Y. F., Zheng, Y., Lin, H. H., et al. (2023). MYB30 regulates submergence tolerance by repressing ethylene biosynthesis via ACS7 in Arabidopsis. *Plant Cell Physiol.* 64, 814–825. doi: 10.1093/pcp/pcad041

Zhou, Y. M., Lu, J. J., Tan, D. Y., Baskin, C. C., and Baskin, J. M. (2015). Seed germination ecology of the cold desert annual *Isatis violascens* (Brassicaceae): two levels of physiological dormancy and role of the pericarp. *PloS One* 10, e0140983. doi: 10.1371/journal.pone.0140983

Zhou, X., Zhang, Z. L., Park, J., Tyler, L., Yusuke, J., Qiu, K., et al. (2016). The ERF11 transcription factor promotes internode elongation by activating gibberellin biosynthesis and signaling. *Plant Physiol.* 171, 2760–2770. doi: 10.1104/pp.16.00154

Zhu, Y. F., Huang, P. C., Guo, P. C., Chong, L., Yu, G. B., Sun, X. L., et al. (2020). CDK8 is associated with RAP2.6 and SnRK2.6 and positively modulates abscisic acid signaling and drought response in. *New Phytol.* 228, 1573–1590. doi: 10.1111/nph.16787

Zinsmeister, J., Leprince, O., and Buitink, J. (2020). Molecular and environmental factors regulating seed longevity. *Biochem. J.* 477, 305–323. doi: 10.1042/BCJ20190165

frontiers | Frontiers in Plant Science

TYPE Original Research
PUBLISHED 31 July 2024
DOI 10.3389/fpls.2024.1427086

OPEN ACCESS

EDITED BY
Anket Sharma,
Texas Tech University, United States

REVIEWED BY
Muthusamy Ramakrishnan,
Nanjing Forestry University, China
Amit Kumar Mishra,
Mizoram University, India

*CORRESPONDENCE
K. Raja Reddy
krreddy@pss.msstate.edu

RECEIVED 03 May 2024
ACCEPTED 11 July 2024
PUBLISHED 31 July 2024

CITATION
Thenveettil N, Bheemanahalli R, Reddy KN, Gao W and Reddy KR (2024) Temperature and elevated CO_2 alter soybean seed yield and quality, exhibiting transgenerational effects on seedling emergence and vigor. *Front. Plant Sci.* 15:1427086.
doi: 10.3389/fpls.2024.1427086

Temperature and elevated CO_2 alter soybean seed yield and quality, exhibiting transgenerational effects on seedling emergence and vigor

Naflath Thenveettil[1], Raju Bheemanahalli[1], Krishna N. Reddy[2], Wei Gao[3] and K. Raja Reddy[1*]

[1]Department of Plant and Soil Sciences, Mississippi State University, Mississippi State, MS, United States, [2]United States Department of Agriculture - Agricultural Research Service (USDA-ARS), Crop Production Systems Research Unit, Stoneville, MS, United States, [3]United States Department of Agriculture - Ultraviolet B (USDA UVB) Monitoring and Research Program, Department of Ecosystem Science and Sustainability, Colorado State University, Fort Collins, CO, United States

Introduction: Environmental conditions play a prime role in the growth and development of plant species, exerting a significant influence on their reproductive capacity. Soybean is sensitive to high temperatures during flowering and seed developmental stages. Little is known about the combined environmental effect of temperature and CO_2 on seed yield and quality and its future generation.

Methods: A study was conducted to examine the effect of temperature (22/14°C (low), 30/22°C (optimum), and 38/30°C (high)), and CO_2 (420 ppm (ambient; aCO_2) and 720 ppm (elevated; eCO_2)) on seed yield, quality, and transgenerational seedling vigor traits of soybean cultivars (DS25-1 and DS31-243) using Soil-Plant-Atmospheric-Research facility.

Results: A significant temperature effect was recorded among yield and quality attributes. At high-temperature, the 100-seed weights of DS25-1 and DS31-243 declined by 40% and 24%, respectively, over the optimum temperature at aCO_2. The harvest index of varieties reduced by 70% when exposed to high temperature under both aCO2 and eCO_2, compared to the optimum temperature at aCO_2. The seed oil (- 2%) and protein (8%) content altered when developed under high temperature under aCO_2. Maximum sucrose (7.5%) and stachyose (3.8%) accumulation in seeds were observed when developed under low temperatures and eCO_2. When the growing temperature increased from optimum to high, the seed oleic acids increased (63%), while linoleic and linolenic acids decreased (- 28% and - 43%, respectively). Significant temperature and CO_2 effects were observed in progenies with the highest maximum seedling emergence (80%), lesser time to 50% emergence (5.5 days), and higher seedling vigor from parents grown at low-temperature treatment under eCO_2.

Discussion: Exposure of plants to 38/30°C was detrimental to soybean seed yield, and eCO_2 levels did not compensate for this yield loss. The high temperature during seed developmental stages altered the chemical

composition of the seed, leading to an increased content of monounsaturated fatty acids. The findings suggest that parental stress can significantly impact the development of offspring, indicating that epigenetic regulation or memory repose may be at play.

KEYWORDS

CO_2, seed yield, seed quality, seedling vigor response index, temperature, transgenerational effect

1 Introduction

Climate change is an ongoing process, and the Industrial Revolution has substantially intensified the challenges confronting Earth's climate (NOAA, 2021). The trajectory of CO_2 levels in the atmosphere shows that the beginning of the industrial age increased the abundance of CO_2 by around 45% (Buis, 2019), bringing it up to 420 ppm. The global surface temperature has risen by 1.09°C in the last decade compared to 1850-1900, with a faster increase since 1970 than any other 50-year window during the previous 2000 years (Pachauri et al., 2014; Calvin et al., 2023). Due to these climate changes, the ten hottest years occurred in the last 15 years, and the summer of 2023 is confirmed to be the warmest on record (Copernicus Climate Change Service, 2023). In addition, the climate models project global differences in temperature means and extremes if global warming reaches 1.5°C (IPCC, 2018). Recent studies have highlighted that developed countries exhibit higher vulnerability (8-11%) to climate change than developing countries (Lesk et al., 2016; Altieri and Nicholls, 2017). Over the years, global extreme climate events have increased, causing an economic loss of over 220 billion USD in 2022 (CRED, 2023).

Environmental conditions play a prime role in the growth and development of plant species, exerting a significant influence on their reproductive capacity (Raza et al., 2019). Among the critical abiotic factors, temperature, water, and light play a crucial role in shaping plant physiology and reproductive processes. Temperature beyond 30°C can adversely affect plant growth and physiology, leading to a reduction in photosynthesis, flowering, and seed development, ultimately resulting in yield loss (Hatfield and Prueger, 2015). Conversely, sub-optimal temperatures can impede germination and growth rates, hampering overall plant development (Szczerba et al., 2021). Given the concurrent likelihood of changes in CO_2 and temperature, it is critical to quantify the interactions between these two climate variables. While enhanced photosynthetic and agronomic growth has been reported under eCO_2, accompanied by reduced water use efficiency and nitrogen and protein accumulation (Taub, 2010), the specific effects under varying temperature conditions remain understudied.

Soybean is an important crop with a global production of 399.5 million metric tons (USDA-FAS, 2023). The U.S. stands second in world soybean production after Brazil, encompassing 86.3 million acres (MSPB, 2023) and boasting a U.S. export value of 34.37 billion USD (USDA-FAS, 2023). The crop is widely utilized in food, livestock, and industrial sectors due to its high nutritional value and contributes 90% of the U.S. oil seed production. The optimal temperature of soybeans is estimated to be around 25-30°C (Alsajri et al., 2020), and any deviation has the potential to impact plant growth.

Given the relatively lower optimal temperature (26°C) for anthesis and seed development compared to the vegetative stage (30°C), the reproductive stage is the most critical and thermally sensitive phase for soybean development (Hatfield et al., 2011). Consequently, comprehending the temperature-induced responses in soybean becomes imperative for the development of effective mitigation strategies. A study by Tacarindua et al. (2013) reported that a 3°C rise from the ambient temperature during flowering to the early seed-filling stage in soybean led to a 27% reduction in dry matter accumulation, accompanied by decreased photosynthesis and stomatal conductance. Similarly, cold stress during the flowering stage in soybean leads to the non-opening of flowers, leading to inadequate pollination and subsequent lower pod set or production of barren pods (Ohnishi et al., 2010). Temperature fluctuations also impact seed quality, with documented instances of decreased protein and increased oil accumulation (Bellaloui et al., 2015; Mourtzinis et al., 2017; Poudel et al., 2023).

Over the past century, the average annual temperature in soybean growing regions rose1°C (Zhao et al., 2017), resulting in a 26% yield reduction (Sharma et al., 2022), emphasizing heightened concerns for the reproductive and seed-filling stages in soybean. While plants exhibit direct responses to the growing environment, their phenotypes can also be influenced by ancestral environmental conditions (Uller, 2008). Existing research underscores that certain environmental stress effects can be transmitted to progenies, adversely impacting their growth and development (Tielborger and Petru, 2010; Cendán et al., 2013). Numerous studies on *Arabidopsis thaliana* suggest that plant's transgenerational memory plays a crucial role in delivering stress-induced responses, with offspring adaptation to specific stress conditions influenced by the parent's stress response (Suter and Widmer, 2013). Wijewardana et al. (2019) demonstrated the transgenerational impact of drought stress in soybeans, which led to reduced maximum seed germination, seed germination rate, and overall seedling performance in the F_1 generation. Similarly, Alsajri

et al. (2022) reported a reduced seed germination rate in progenies under extreme growth temperatures. To date, no information is available on the transgenerational effects of temperature and CO_2 on soybean.

Furthermore, limited studies have been dedicated to understanding the relationship between seed composition and seedling performance. It has been proposed that increased seed mass will better support the early seedling establishment (Zas et al., 2013). In this study, we looked at the individual seed-to-seedling dynamics within the framework of seed chemical composition, with a specific focus on elucidating the correlation between per-seed composition and the growth and development of seedlings. Therefore, the present study hypothesized that the two soybean cultivars possessing heat and drought-tolerant traits differentially respond to temperature and CO_2 stress and that the effect of these stresses is transgenerational. Additionally, we also postulate that the per-seed chemical composition determines the seedling vigor. The objectives of the study were (1) to quantify the effect of temperature and CO_2 on soybean seed yield and quality, (2) to determine the transgenerational effect of temperature and CO_2 on seed emergence and seedling vigor, and (3) to draw the relationship between per-seed chemical composition and seedling vigor.

2 Materials and methods

The study was conducted in the Soil-Plant-Atmosphere-Research (SPAR) facility at the Environmental Plant Physiology Laboratory, Mississippi State University, MS, USA, from 2022 to 2023. The SPAR chambers precisely manipulate and monitor the CO_2 and temperature through an automated control system (Supplementary Figure 1). At the same time, the plants are being grown under natural sunlight conditions, unlike other controlled environmental growth chambers. The units contain a metal bin and a chamber with Plexiglass (1.27 cm thickness) housing the plant canopy, permitting 97% visible solar radiation. A heating and cooling system controls the temperature inside the chamber. The CO_2 levels are monitored by a CO_2 analyzer and adjusted through the control system. The details and specifications of the SPAR units have been presented by Reddy et al. (2001).

2.1 Experimental details

The study selected heat-tolerant (DS25-1) and drought-tolerant (DS31-243) soybean cultivars with indeterminate growth habits belonging to maturity Group IV. The research comprised two distinct experiments designed to comprehensively examine the effects of temperature and CO2 on soybean seed yield and quality and the influence of these treatments on the subsequent performance of the progeny.

2.1.1 Experiment I: temperature and CO_2 effect on seed yield and quality of soybean

2.1.1.1 Experimental setup

Seeds of DS25-1 and DS31-243 were sown in polyvinyl chloride (PVC) pots (15 × 46 cm; 8-liter capacity) filled with a mixture of a 3:1 ratio of fine sand and topsoil by volume (87% sand, 2% clay, and 11% silt). The pots consisted of a hole of 1 cm diameter at the bottom and were filled with 250g of gravel to facilitate easy drainage. Twenty pots were arranged in 10 columns × 2 rows within each SPAR unit, accommodating 10 pots for each cultivar. Four seeds of two cultivars were sown in alternative columns for randomization. The plants were thinned to one plant per pot at the two-leaf stage. The units were maintained at day/night temperatures of 30/22°C. In contrast, the CO_2 of three SPAR units was maintained at 420 ppm, and another three units were maintained at 720 ppm to imitate the future environment. The pots were irrigated thrice a day with full-strength modified Hoagland's nutrient solution (Hewitt, 1953) for an adequate supply of water and nutrients. Throughout the experiment, the irrigation volume was adjusted according to the daily evapotranspiration (Reddy et al., 2001).

2.1.1.2 Treatments

At the time of flowering (40 days after sowing), the temperature treatments were imposed in each SPAR unit. Three day/night temperatures of 22/14°C (low), 30/22°C (optimum), and 38/30°C (high) were maintained in each SPAR unit at two CO_2 concentrations of 420 ppm (aCO_2) and 720 ppm (eCO_2). The experiment was carried out in a three-factorial, completely randomized design, considering CO_2, temperature, and cultivar as the main source of variation. The selection of high and low temperatures was based on the previous reports of the optimum temperature of soybean (Alsajri et al., 2020). The daytime temperatures were maintained from sunrise to sunset, with night-time temperatures transitioning over 30 minutes after sunset. Black netted shade cloths were positioned around the edges of the plexiglass chambers to simulate the impact of border plants. The shade net was regularly raised depending on the plant growth.

2.1.1.3 Observations

All the plants were harvested 120 days after planting, corresponding to 80 days after the initiation of treatments. The seed yield attributes were recorded at the time of harvest. The number of pods (no. plant^{-1}) was recorded by counting fully matured pods containing one or more seeds. The pods were hand-threshed after oven-drying at 35°C for 24 hours to maintain a seed moisture content of 14% uniformly. The seeds (no. plant^{-1}) were counted using an Old Mill seed counter (NP5056-Model 850-2, LICOR Inc., Lincoln, NE, USA). The 100 seed weight (g) and seed yield (g plant^{-1}) were recorded for all the treatments. Following the measurements, the total biomass was recorded by subjecting the plant parts (leaf, stem, pod, and root) to oven drying at 80°C for 72 hours. The resulting weights were expressed in grams. The harvest index was calculated by dividing the seed yield by total biomass.

The harvested seeds from each treatment were analyzed for quality. Five grams of seeds from each of the six treatment combinations were analyzed for protein, oil, fatty acids, and sugars using NIRS spectroscopy (Perten DA7520 spectrometer, Perten Instruments, IL, USA), and the content was expressed in percentage.

2.1.2 Experiment II: transgenerational effect of temperature and CO_2 in soybean

2.1.2.1 Experimental setup

This experiment was conducted during May 2023, using the seeds harvested from experiment I, hereafter termed progeny, which underwent temperature and CO_2 alterations during its developmental and maturation stage. The seeds were randomly selected from each treatment and were sown in PVC pots (15 × 46 cm) filled with a 3:1 ratio of fine sand and topsoil mixture. Four seeds were sown in each treatment and were thinned to one plant per pot after the first leaf stage. The pots were arranged in a completely randomized design with four replications per treatment on a concrete platform. The modified Hoagland's nutrient solution was supplied via an automated drip irrigation system. The plants were grown under ambient conditions of temperature and CO_2.

2.1.2.2 Observations

The transgenerational effects of temperature and CO_2 were estimated through progeny performance. The seedling emergence was recorded twice a day at 8.00 and 16.00 hours, considering the seedlings with widely opened cotyledons emerged. After 20 days of sowing, the seedlings were cut at the soil level, and the plant height and leaf area were taken. The plant height was recorded from the base of the stem to the tip of the apical bud. The total leaf area was measured using a LI-3100 leaf area meter (LI-COR, Inc., Lincoln, NE). Plant parts were separated into leaves, stems, and roots, and the biomass was dried at 80°C for 72 hours. The total biomass was calculated by summing the individual biomass values of leaves, stems, and roots and expressed in grams.

2.2 Data analysis

Analysis of variance was performed to ascertain the effect of temperature, CO_2, and cultivars on various growth and yield parameters using three factorial completely randomized design for experiment I and experiment II. The analysis was performed in R studio using 'doebioresearch' package (Popat and Banakara, 2022). Multiple comparison tests were carried out to identify cultivar-specific responses to treatment effects at a 0.05 level of significance using a t-test. To determine the impact of temperature and cultivar or CO_2 and cultivar, a two-way factorial, completely randomized analysis of variance was performed. Graphical representations of the outcomes were generated using Sigmaplot 13.0 (Systat Software Inc., San Jose, CA, USA).

2.2.1 Seedling emergence curve fitting

The germination time course of seeds was fitted in a three-parameter sigmoidal function (Equation 1) using Sigmaplot 13.0 (Singh et al., 2019).

$$Y = \frac{MSG}{\left\{1 + e^{\left[-\frac{t-t_{50}}{G_{rate}}\right]}\right\}} \quad (1)$$

Where 'Y' denotes the cumulative seed germination percentage, 'MSG' is the maximum seed germination percentage, t_{50} is time to 50% emergence, and G_{rate} is the slope of the curve. Using these parameters, the difference in seedling establishment was estimated. The analysis of variance of maximum seed germination (MSG), seed germination rate (SGR), and t_{50} was performed in R studio using three factorial completely randomized design considering parental treatments such as temperature, CO_2, and cultivar as the main source of variation.

2.2.2 Seedling vigor response index

The measured and computed parameters of seedling establishment and growth were utilized to calculate the seedling vigor response index. The individual seedling vigor response index (IVRI) of each parameter was computed by dividing the observed value in each treatment (P_i) by the maximum value from all the treatments (P_m; Equation 2). However, IVRI for t_{50} was calculated by dividing least value (P_l) with the individual observed value (Equation 3). The average values were used for the computation. The cumulative vigor response index (CVRI) was computed by summing the IVRI of all the parameters for each treatment combination.

$$IVRI = \frac{P_i}{P_m} \quad (2)$$

$$IVRI \ (t_{50}) = \frac{P_l}{P_i} \quad (3)$$

2.2.3 Seed constitution to seedling performance

To understand the relationship between per-seed chemical composition and the seedling performance, percentage seed quality parameters estimated during experiment I were converted into per-seed basis using the seed weight and were expressed in milligrams per seed (mg seed^{-1}). A linear regression analysis (Equation 4) was conducted using these individually calculated per-seed quality components against the CVRI, and the regression correlation coefficient (R^2) was monitored to determine the model fitness. We also noticed the relationship between seed emergence and seedling vigor to understand the relationship between metrics of seed germination and seedling vigor.

$$Y = mx + b \quad (4)$$

Where Y is the dependent variable (CVRI), x is the independent variable (individual seed quality parameters), m is the slope of the line, and b is the y-intercept.

3 Results

3.1 Temperature and CO_2 effect on seed yield

The growing temperature during flowering and seed developmental stages significantly impacted ($p<0.5$ to $p<0.001$)

TABLE 1 Analysis of variance across temperature (T), CO_2 and cultivars (V) for seed yield parameters (*, **, *** represent significance level $p \leq 0.05$, 0.01, and 0.001, respectively, and NS-non-significant).

Parameters	T	CO_2	V	T*CO_2	T*V	CO_2*V	T*CO_2*V
Pod (no. plant^{-1})	*	*	*	NS	NS	NS	NS
Seed (no. plant^{-1})	**	*	NS	NS	NS	NS	NS
100 Seed weight (g)	***	NS	***	*	*	NS	NS
Seed yield (g plant^{-1})	***	NS	*	NS	NS	NS	NS
Harvest index	***	NS	NS	NS	NS	NS	NS

the seed yield traits (Table 1). The effect of eCO_2 was non-significant for 100-seed weight, seed yield, and harvest index, while there was a detectable difference in pod number and seed number at $p<0.05$. The two cultivars differed in pod number, 100-seed weight, and seed yield. Among the seed yield traits, only 100-seed weights exhibited notable differences due to the interaction of temperature and CO_2, as well as temperature and cultivar. All other interactions were deemed non-significant across all recorded yield traits.

The high temperature reduced the seed yield and 100-seed weight in both cultivars (Figures 1, 2). The maximum seed yield was observed at optimum temperature. The eCO_2 did not increase the

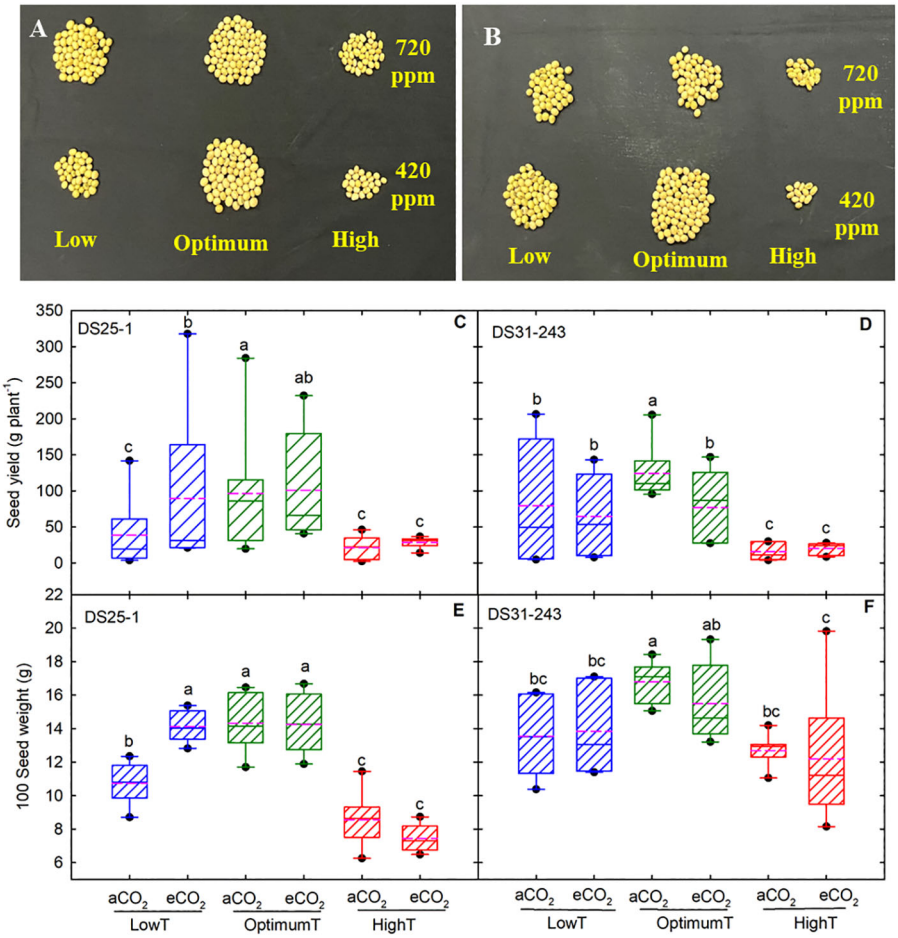

FIGURE 1
Temperature (LowT: 22/14°C; optimumT: 30/22°C; highT: 38/30°C) and CO_2 (aCO_2: 420 ppm and eCO_2: 720 ppm) effects on seed yield, **(A)** DS25-1, **(B)** DS31-243 (Picture shows 10% of total seed yield), **(C, D)** box plot of seed yield (g plant^{-1}), and **(E, F)** 100 seed weight **(G)** of DS25-1 and DS31-243. The pink dotted line indicates the average values. The letters above the boxes are Duncan's multiple range test (DMRT) between six treatments. The treatment boxes with similar letters are statistically non-significant.

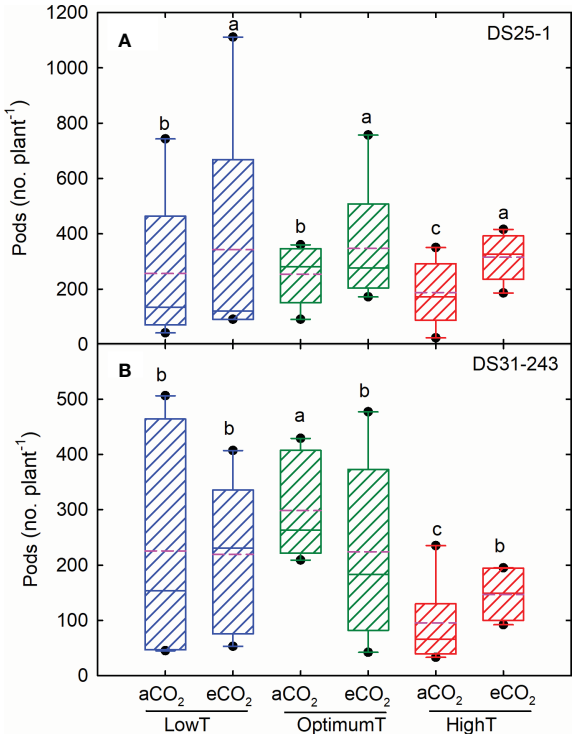

FIGURE 2
Temperature (LowT: 22/14°C; optimumT: 30/22°C; highT: 38/30°C) and CO_2 (aCO_2: 420 ppm and eCO_2: 720 ppm) effects on pod number of **(A)** DS25-1 and **(B)** DS31-243. The pink dotted line indicates the average values. The letters above the boxes are Duncan's multiple range test (DMRT) between six treatments. The treatment boxes with similar letters are statistically non-significant.

yield in both cultivars at optimum temperature. The decline in seed yield at high temperatures was highest in DS31-243 (88% at aCO_2 and 84% at eCO_2) than DS25-1 (78% aCO_2 and 70% at eCO_2) compared to optimum temperature and aCO_2. The low temperature did not have any significant effect on seed yield in DS25-1 and DS31-243 at eCO_2. High growing temperature reduced the 100-seed weight of both cultivars without being potentially affected by eCO_2 (Figures 1E, F). The decline in 100-seed weight at high temperatures was highest in DS25-1 (40% at aCO_2 and 47% at eCO_2) than in DS31-243 (24% at aCO_2 and 23% at eCO_2).

In DS25-1, the maximum number of pods was observed under optimum temperature at eCO_2 (347), followed by the low temperature at eCO_2 (342) (Figures 2A, B). The eCO_2 had a positive effect on the number of pods in both cultivars under high-temperature treatment, resulting in a pod number that was on par with the optimum and low-temperature conditions. The least number of pods was observed at high-temperature treatment and aCO_2 in both cultivars. Comparatively, DS25-1 had a higher pod number in all the treatment conditions. Maximum seed number was observed at optimum temperature (606), and high temperature retarded the production of seeds (Figure 3A). A reduction of 68% and 54% in seed number was observed due to high temperature at aCO_2 and eCO_2, respectively, compared to optimum temperature and aCO_2. The eCO_2 did not result in any significant change in seed number. Under high temperatures, the eCO_2 yielded a 30% but non-significant increase in seed numbers compared to aCO_2. The harvest index of the cultivars declined with extreme temperature conditions exhibiting maximum harvest index at optimum temperature and aCO_2 (0.34) followed by eCO_2 (0.32) (Figure 3B). The high temperature resulted in a reduction of 70% harvest index under both aCO_2 and eCO_2, compared to the optimum temperature at aCO_2. Additionally, even low temperatures declined the harvest index of the plant, which reflects the reduction in seed yield.

3.2 Temperature and CO_2 effect on seed quality

The growing temperature had a remarkable effect on the seed chemical composition (Table 2), while the eCO_2 only affected the accumulation of protein ($p<0.001$) and stachyose ($p<0.05$). The cultivars differed for protein, starch, stachyose, and oleic acids at $p<0.05$ to $p<0.001$. The interactions of these three main factors also resulted in significant changes in starch, stachyose, and linolenic acids (Table 2). In both cultivars, the increase in growing temperature during the flowering and seed development stages increased the seed protein content (Figures 4A, B). At low temperatures, eCO_2 did not result in any detectable change in the protein, while at high temperatures, a 3% and 2% reduction in protein content was recorded for DS25-1 and DS31-243, respectively, compared to aCO_2. In contrast, the maximum oil content was observed at optimum temperature and aCO_2 in DS31-243 (19.5%) (Figure 4D). In the case of DS25-1, the oil

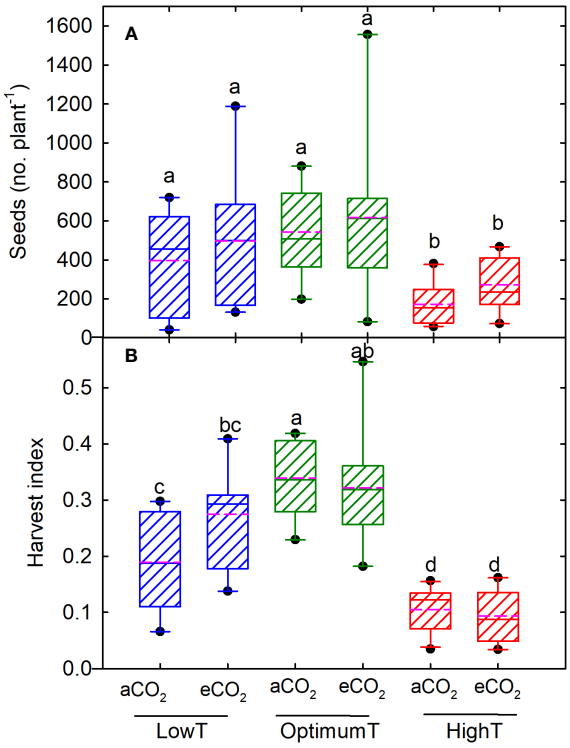

FIGURE 3
Temperature (LowT: 22/14°C; optimumT: 30/22°C; highT: 38/30°C) and CO_2 (aCO_2: 420 ppm and eCO_2: 720 ppm) effects on **(A)** seed number, and **(B)** harvest index across DS25-1 DS31-243. The pink dotted line indicates the average values. The letters above the boxes are Duncan's multiple range test (DMRT) between six treatments. The treatment boxes with similar letters are statistically non-significant.

content at optimum and high temperatures did not significantly differ at their respective CO_2 environment (Figure 4C). On the other hand, the lowest oil content was recorded at low temperature and aCO_2 (17.4%). In comparison, in DS31-243, it was recorded at high temperature and aCO_2 (17.7%). The eCO_2 did not significantly affect the oil content at low and high temperatures in DS31-243.

Sucrose content decreased with an increase in temperature in both cultivars (Figures 5A, B), but eCO_2 did not significantly affect the sucrose accumulation. A reduction of 43% and 15% in sucrose content was recorded in DS25-1 and DS31-243, respectively, due to an increase in temperature from low to high at aCO_2. On the other hand, the maximum starch content was observed at optimum temperature and aCO_2 (Figures 5C, D) for both cultivars. Under extreme temperatures, eCO_2 increased the starch content, except for DS31-243, at low-temperature treatment. However, at optimum temperature, eCO_2 resulted in reduced starch accumulation compared to aCO_2. Unlike starch accumulation, maximum accumulation of stachyose content was observed in low temperatures at eCO_2 (Figures 5E, F). Like sucrose accumulation, the increase in temperature reduced the production of stachyose in seeds.

Among the fatty acids, oleic acid content increased with an increase in growing temperature without being affected by the eCO_2

TABLE 2 Analysis of variance across temperature (T), CO_2, and cultivars (V) for seed quality parameters (*, **, *** represent significance level $p \leq 0.05$, 0.01, and 0.001, respectively, and NS - non-significant).

Parameters	Protein	Oil	Sucrose	Starch	Stachyose	Oleic acid	Linoleic acid	Linolenic acid
T	***	***	***	***	***	***	***	***
CO_2	***	NS	NS	NS	*	NS	NS	NS
V	*	NS	NS	***	*	***	NS	NS
T*CO_2	**	NS	NS	***	***	**	**	NS
T*V	***	***	***	NS	NS	*	**	***
CO_2*V	NS	NS	*	NS	NS	NS	NS	*
T*CO_2*V	NS	NS	NS	*	**	NS	NS	*

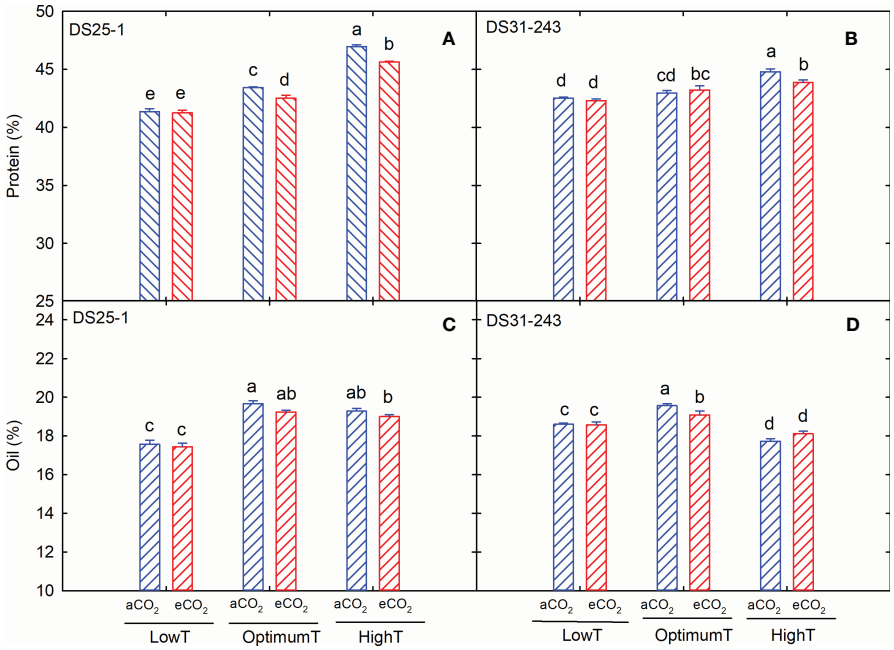

FIGURE 4
Temperature (LowT: 22/14°C; optimumT: 30/22°C; highT: 38/30°C) and CO_2 (aCO_2: 420 ppm and eCO_2: 720 ppm) effects on **(A)** protein (%) of DS25-1 and **(B)** DS31-243, and **(C)** oil (%) of DS25-1 and **(D)** DS31-243. Bars represent the mean ± SE. The letters above the boxes are Duncan's multiple range test (DMRT) between six treatments. The treatment boxes with similar letters are statistically non-significant.

concentration, except for DS25-1 at high temperatures (Figures 6A, B). The highest oleic acid content of 50% (DS25-1) and 46% (DS31-243) was observed in seeds grown under high temperatures and eCO_2. Unlike oleic acid, linoleic and linolenic acid content decreased with an increase in temperature (Figures 6C–F). The maximum linoleic acid production was observed in seeds developed under low-temperature treatment, while eCO_2 did not significantly influence the linoleic acid content in both cultivars. The increase in temperature from low to high at aCO_2 resulted in a 30% and 35% decrease in linoleic acid content in DS25-1 and DS31-243, respectively. Similarly, linolenic acid content declined by 54% and 34%, respectively, in DS25-1 and DS31-243 under aCO_2.

3.3 Temperature and CO_2-induced transgenerational changes in seedling emergence and performance

The seedling emergence and biomass of progenies were significantly affected ($p<0.001$ to 0.5) by parental growing conditions (Figure 7; Table 3). The three-way interaction of temperature, CO_2, and cultivar was non-significant for all the measured progeny parameters except for MSG ($p<0.05$) (Table 3). The time to 50% emergence was only affected by the parental temperature ($p<0.01$). The genetic difference in cultivar ($p<0.01$) contributed to the change in root-to-shoot ratio, and it was neither influenced by parental temperature nor CO_2.

Soybean seeds developed under high-temperature conditions had lower MSG of 49.6% at aCO_2 and 56% at eCO_2 for DS25-1. In comparison, it was 17% and 8.4%, respectively, for DS31-243 (Figures 7, 8A). Highest MSG was recorded at parental low temperature for DS25-1 (79.1%) and DS31-243 (88.25%) at eCO_2 and aCO_2, respectively. The seeds produced at high temperatures took more time to reach 50% emergence of their MSG in DS25-1 (Figure 8B). Seeds grown under low parental temperature had quicker seed emergence than optimum parental temperature. DS25-1 seeds grown under high parental temperature took 7.7 and 8.1 days to reach 50% emergence in comparison with 6.34 and 5.86 days at low parental temperatures under aCO_2 and eCO_2, respectively. At high parental temperatures, DS31-243 took 5.21 and 5.72 days to reach 50% emergence of 17.14% and 8.35% MSG, respectively, at aCO_2 and eCO_2.

The parental eCO_2 treatment increased the plant height of the seedlings in DS25-1 compared to seeds developed under aCO_2 (Figure 8C). At the same time, the plant height in DS31-243 seedlings was not affected by the parental growing condition. A greater reduction in leaf area was noticed in seeds grown under parental high temperature, with a decrease of 61% and 64% under parental aCO_2 and eCO_2 in DS25-1, respectively, compared to the seeds grown under parental optimal temperature at aCO_2 and eCO_2 (Figure 8D). The maximum leaf area in DS25-1 was observed under parental low temperature and eCO_2, while in DS31-243, it was observed in seeds grown under parental optimum temperature and aCO_2. The eCO_2 during the pod-filling stage at low and optimum temperatures increased the seedling biomass in DS25-1 (Figure 9). While seeds grown under eCO_2 and high temperature did not influence the seedling biomass. Conversely, seeds harvested from plants exposed to eCO_2 at optimum and high temperatures did not

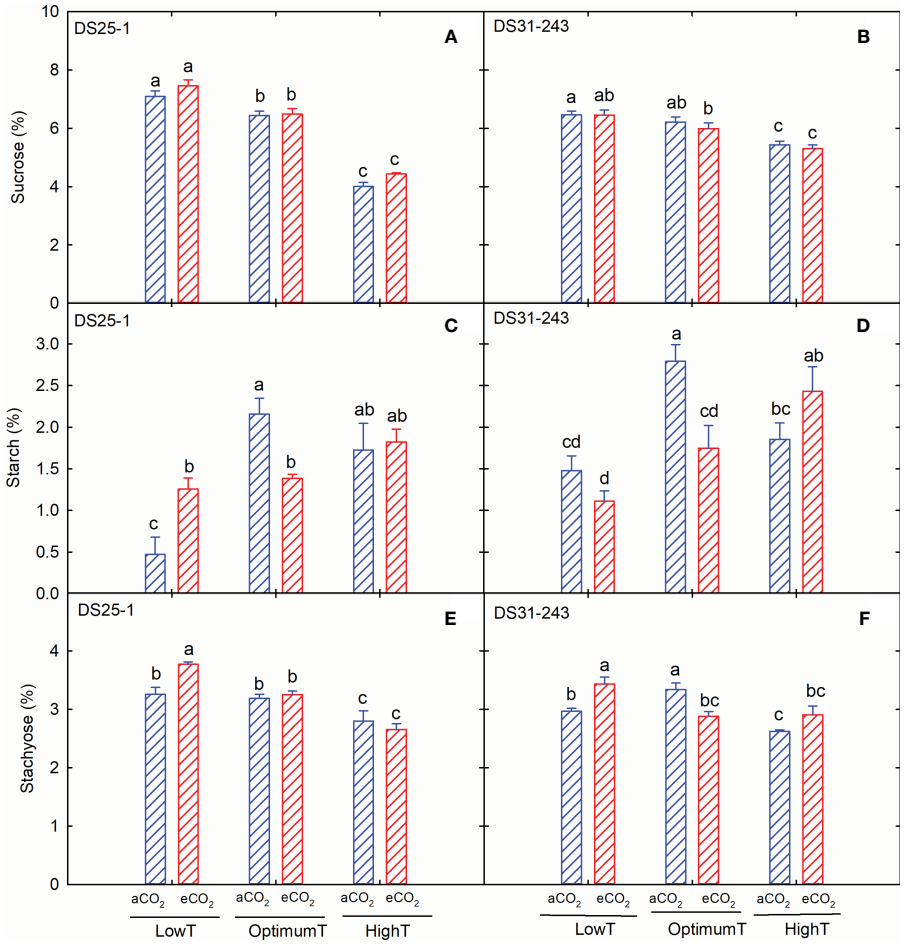

FIGURE 5
Temperature (LowT: 22/14°C; optimumT: 30/22°C; highT: 38/30°C) and CO_2 (aCO_2: 420 ppm and eCO_2: 720 ppm) effects on **(A)** sucrose (%) of DS25-1 and **(B)** DS31-243, **(C)** starch (%) of DS25-1 and **(D)** DS31-243, and **(E)** stachyose (%) of DS25-1 and **(F)** DS31-243. Bars represent the mean ± SE. The letters above the boxes are Duncan's multiple range test (DMRT) between six treatments. The treatment boxes with similar letters are statistically non-significant.

result in higher biomass accumulation in DS31-243. In DS25-1, the highest shoot biomass (2.2 g) was recorded from seeds produced under low temperature and eCO_2 (Figure 9A). Similarly, the root (0.9 g) and total (3.1 g) biomass accumulation was higher in seeds developed under low temperature and eCO_2 (Figures 9B, C). On the contrary, DS31-243 recorded the highest biomass accumulation (shoot: 1.1g; root: 0.6g; total: 1.7g) from seeds grown under parental optimum temperature and aCO_2. The results suggest that the progeny performance is not only influenced by the growing environmental conditions of the parents but also governed by the genetic constitution of the cultivar.

To ascertain the role of seed chemical composition towards the seedling performance, we converted the measured seed quality components from percentage to milligrams per seed (mg $seed^{-1}$). We observed a significant positive linear relationship between maximum seed germination and CVRI (R=0.57; $p<0.05$) (Figure 10A). While the time to 50% emergence had a negative slope and non-significant interaction with CVRI (Figure 10B). The relationship of both protein and oil content per-seed with CVRI was non-significant (Figures 10C, D). Among the carbohydrates measured in the study, stachyose content was highly positively correlated with CVRI (R= 0.72; $p<0.01$), followed by sucrose (R= 0.71; $p<0.01$) (Figures 10E, F). Among the fatty acids, both linoleic and linolenic acids had a positive linear relationship with CVRI having regression coefficient of R= 0.67 ($p<0.01$) and R= 0.65 ($p<0.05$), respectively (Figures 10G, H).

4 Discussion

The investigation shows a discernible shift in seed yield and quality attributed to the fluctuations in growing temperature during the flowering and seed development stages. The day/night temperatures above 30/22°C were observed to be detrimental to soybean seed production, hindering yield. The atmospheric CO_2 concentration played a minimal role in influencing these traits, garnering attention from soybean growers and policymakers alike. The experiment also validated the transgenerational impact of temperature and CO_2 on seed emergence and seedling vigor. We also observed that the degree of influence is intricately tied to the

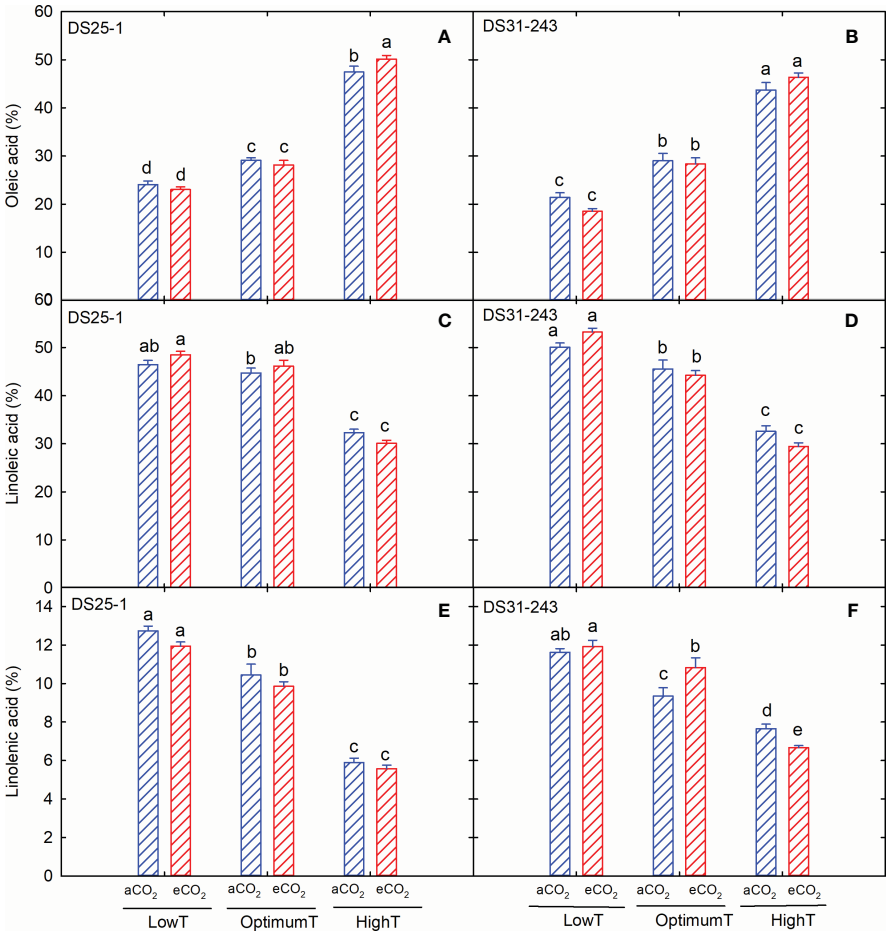

FIGURE 6
Temperature (LowT: 22/14°C; optimumT: 30/22°C; highT: 38/30°C) and CO_2 (aCO_2: 420 ppm and eCO_2: 720 ppm) effects on **(A)** oleic acid (%) of DS25-1 and **(B)** DS31-243, **(C)** linoleic acid (%) of DS25-1 and **(D)** DS31-243, and **(E)** linolenic acid (%) of DS25-1 and **(F)** DS31-243. Bars represent the mean ± SE. The letters above the boxes are Duncan's multiple range test (DMRT) between six treatments. The treatment boxes with similar letters are statistically non-significant.

genetic composition of the seed. The following are the major findings of our study.

4.1 eCO_2 did not compensate for the yield loss under high temperature

The high temperature during the flowering and seed-filling stage decreased the seed yield by 83% over the optimum temperature. The flowering stage is one of the most critical stages in the life cycle of soybean, and the temperature variation could instead lead to altered plant performance, affecting final yield (No et al., 2021; Poudel et al., 2023). It is also important to note that stress at the reproductive stage often has no chance of recovery, resulting in severe yield loss, unlike the vegetative stage (Jumrani and Bhatia, 2018). It has been reported that the optimum temperature for soybean vegetative growth is 30°C (Hesketh et al., 1973), while for anthesis, it is 26°C (Hatfield et al., 2011). The temperature stress at the reproductive stage can lead to flower abortion, primarily attributed to poor pollen germination and stigma receptivity, which impairs fertilization, leading to a lower number of fruit sets and pod filling (Siebers et al., 2015; Iovane and Aronne, 2022). Salem et al. (2007) reported a reduction of 34%, 56%, and 33% in pollen production, pollen germination, and pollen tube elongation, respectively, in soybean when grown under 38/30°C temperature compared to 30/22°C. These outcomes provide a clear explanation for our observation on the reduction in seed number by 68% and 58% under high temperatures of 38/30°C for both aCO_2 and eCO_2, respectively.

Plants accumulate dry matter through photosynthesis, which is an intricate process that is highly plastic to the surrounding environment. The lowered rate of photosynthesis and associated physiological activities of soybean under high temperatures above 30/22°C has resulted in a reduction in seed number and seed yield (Jumrani and Bhatia, 2018). Higher temperatures cause early leaf senescence (Hatfield and Prueger, 2015), leading to poor partitioning of photosynthate to the seed, especially when the plant is stressed during the seed developmental stage. The lower dry matter accumulation and imbalance in a source-sink relationship at high temperatures could result in a decreased harvest index (Rivelli et al., 2024). Since the cultivars under study were indeterminate growth types and the increase in canopy temperature accelerated the

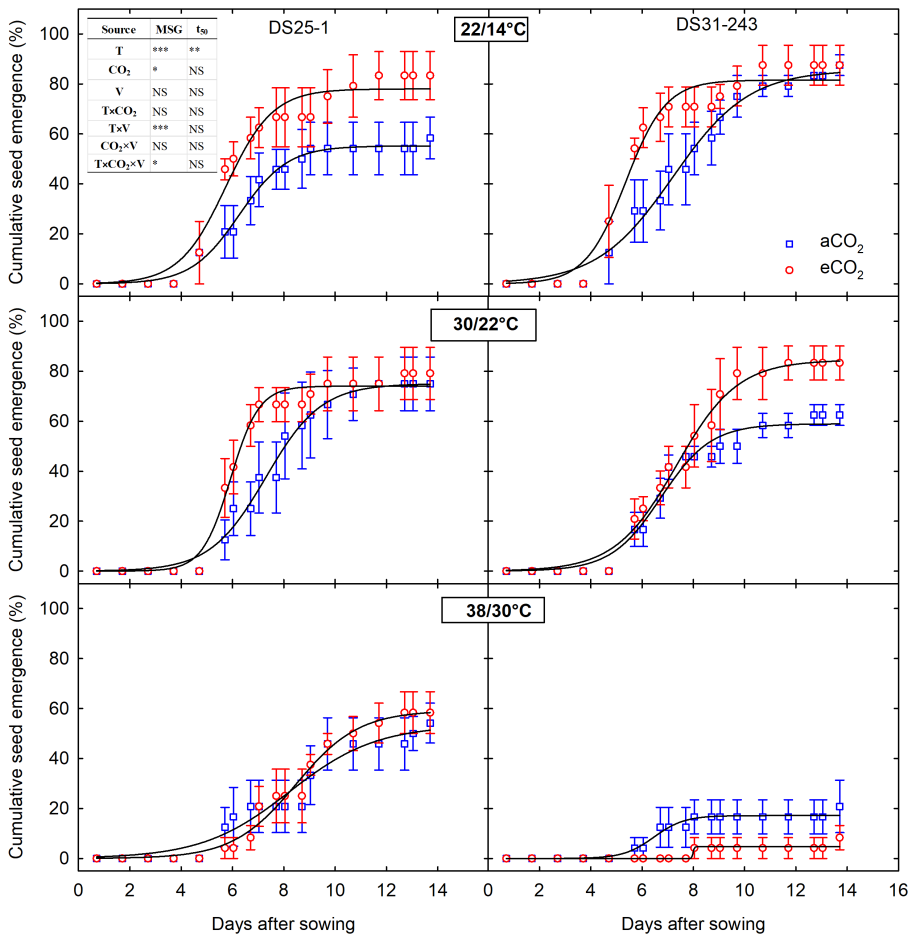

FIGURE 7
Temperature (LowT: 22/14°C; optimumT: 30/22°C; highT: 38/30°C) and CO_2 (aCO_2: 420 ppm and eCO_2: 720 ppm) effects on cumulative seed emergence of progenies of two soybean cultivars (V; DS25-1 and DS31-243). The effect of temperature, CO_2, cultivar, and their interactions are given in the table (*, **, *** represent significance level $p \leq 0.05$, 0.01, and 0.001, respectively, and NS - non-significant).

vegetative development, the plants put more energy into the number of nodes, compromising seed yield. The result was in agreement with the findings of Burroughs et al. (2023).

Like high temperature, low temperature also influences key physiological factors in plants. Under temperatures of 22/14°C and aCO_2, the seed yield, 100 seed weight, pod number, and harvest index were reduced compared to plants grown under 30/22°C. However, the negative impact of high temperature was more severe than low temperature. It has been reported that temperatures below 25°C reduce growth and photosynthetic rate and further lowering disturbed the electron transport system in soybean (Szczerba et al., 2021). Our finding is also supported by Alsajri et al. (2022), displaying reduced stomatal conductance and photosynthesis at 17.3°C, which led to a 6% reduction in 100 seed weight and subsequent decrease in seed yield. Staniak et al. (2021) reported that the day/night temperature of 17/13°C during flowering

TABLE 3 Analysis of variance across temperature (T), CO_2, and varieties (V) for various parameters measured (*, **, *** represent significance level $P \leq 0.05$, 0.01, and 0.001, respectively, and NS - nonsignificant).

Parameters	T	CO_2	V	T*CO_2	T*V	CO2*V	T*CO_2*V
Plant height	NS	*	**	*	NS	*	NS
Leaf area	***	**	*	*	NS	***	NS
Shoot biomass	***	**	NS	*	NS	***	NS
Root biomass	**	NS	NS	NS	NS	*	NS
Total biomass	***	*	NS	*	NS	**	NS
Root-to-shoot ratio	NS	NS	**	NS	NS	NS	NS

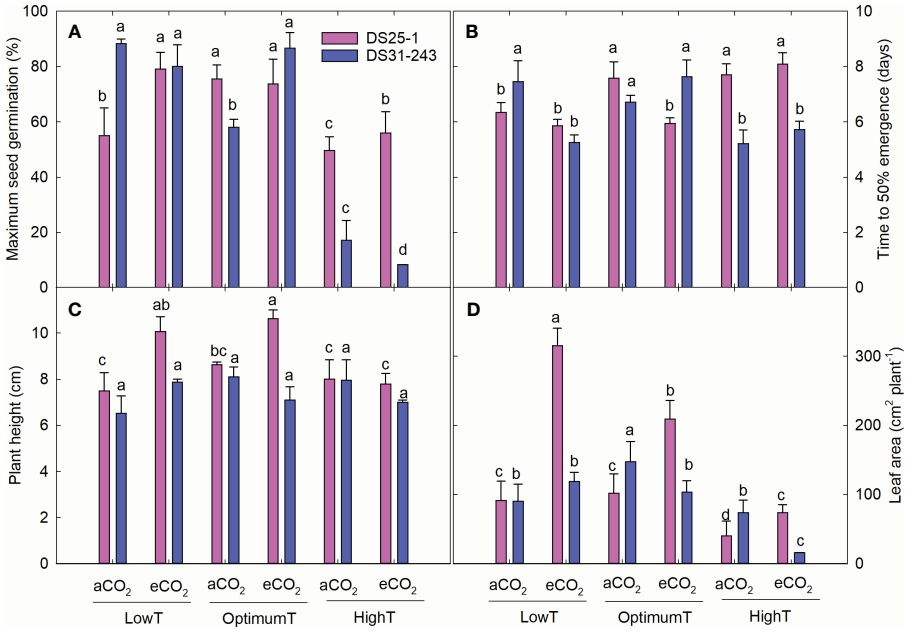

FIGURE 8
Transgenerational effect of temperature (LowT: 22/14°C; optimumT: 30/22°C; highT: 38/30°C) and CO2 (aCO$_2$: 420 ppm and eCO$_2$: 720 ppm) on **(A)** maximum seed germination, **(B)** time to 50% emergence, **(C)** plant height, and **(D)** leaf area of two cultivars of soybean. Bars represent the mean ± SE. The letters above the boxes are Duncan's multiple range test (DMRT) between six treatments in each variety. The treatment boxes with similar letters are statistically non-significant.

negatively influenced the plant structure and reduced pod number and seed yield in soybean.

The eCO$_2$ did not significantly influence most of the seed yield components. There are disparities in the response of C$_3$ plants to eCO$_2$. Soares et al. (2019) reported a considerable cultivar difference in seed yield (ranging from -23.8 to 39.6%) in response to eCO$_2$ in soybean. It has been reported that eCO$_2$ either increases the photosynthesis in non-nodulating soybean cultivars (Ainsworth et al., 2002) or the response to seed yield is less than the response of total biomass (Soares et al., 2019). At optimum temperature, the non-significant but slight decrease in harvest index under eCO$_2$ compared to aCO$_2$ could explain the increased total biomass and reduced seed yield in our study.

4.2 eCO$_2$ did not alter the high temperature-induced changes in seed quality

The growing temperature at flowering and seed developmental stages altered the soybean seed quality. The accumulation of seed protein and oil gradually increases two weeks after fertilization (Sale and Campbell, 1980). Thus, an increase in temperature from 22/14°C to 38/30°C during this period impacted the concentration of seed protein and oil. The heat stress-induced production of enzymes and proteins as part of soybean heat stress tolerance (Kidokoro et al., 2015) has resulted in increased protein content in the cultivars. Being a heat-tolerant cultivar, DS25-1 had higher protein accumulation under high temperatures compared to DS31-243. However, the eCO$_2$ resulted in a reduction of protein and oil content in seeds, attributed to the dilution effect as eCO$_2$ slightly increases the carbohydrate content in seeds (Li et al., 2018). Across the cultivars and temperatures, the studied total carbohydrate content was slightly higher at eCO$_2$ (2.7%) than at aCO$_2$ (2.5%). Hampton et al. (2013) reported that the increase in seed carbon to nitrogen ratio under eCO$_2$ resulted in a decrease in protein content compared to aCO$_2$. Apart from temperature and eCO$_2$, other growth factors such as water, nitrogen uptake, and photoperiod influence protein and oil accumulation in seeds. In this study, the plants were grown under optimum water and nutrient conditions in sunlit chambers without limiting protein accumulation. This resulted in an increased concentration of seed protein with an increase in temperature in both cultivars, which is in line with the outcomes of Alsajri et al. (2020) under similar experimental conditions. Unlike protein, the oil content decreased under high temperatures. Maximum oil content of 19% in both DS31-243 and DS25-1 was recorded at the optimum growth temperature. In contrast, low and high temperature reduced the oil accumulation, supporting the quadratic relationship reported by Alsajri et al. (2020) in soybean.

Sucrose is the major energy source for fermentation (Arendt and Zannini, 2013). High temperature reduced the sucrose content in DS31-243 and DS25-1 without being significantly affected by eCO$_2$. This negative relationship between sucrose content and temperature was reported by Kumar et al. (2010), who reported higher sucrose content at 18/13°C. Decreased photosynthate allocation to seeds during the seed-filling stage at elevated temperatures resulted in reduced carbohydrate content. Given the heightened respiratory demand in elevated temperatures, the availability of oxygen becomes constrained, leading to anaerobic conditions. This limitation impedes phloem unloading from seed

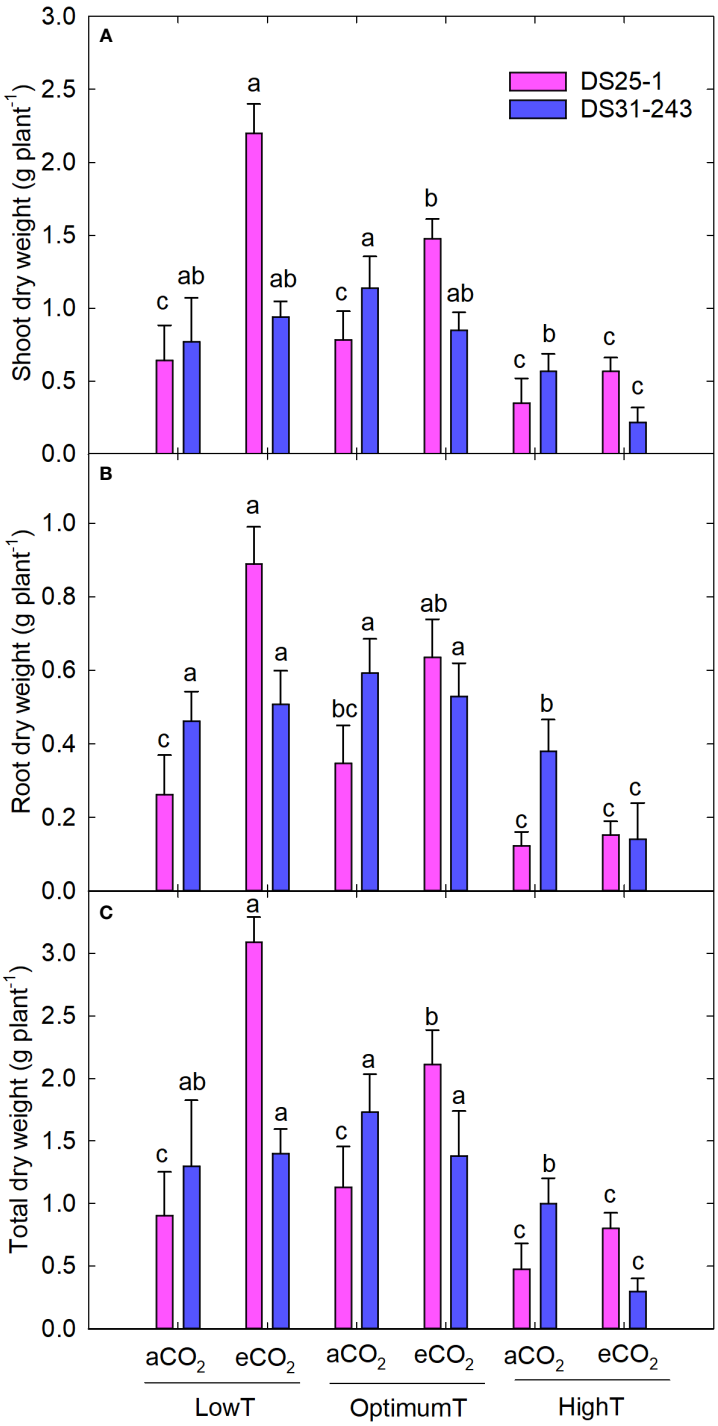

FIGURE 9
Transgenerational effect of temperature (LowT: 22/14°C; optimumT: 30/22°C; highT: 38/30°C) and CO2 (aCO_2: 420 ppm and eCO_2: 720 ppm) on **(A)** shoot dry weight, **(B)** root dry weight, and **(C)** total dry weight of two cultivars of soybean. Bars represent the mean ± SE. The letters above the boxes are Duncan's multiple range test (DMRT) between six treatments in each variety. The treatment boxes with similar letters are statistically non-significant.

coat vascular bundles to the apoplast surrounding the cotyledon cells (Thorne, 1982). The greater accumulation of stachyose content at low temperatures aligns with the findings of Alsajri et al. (2020), reporting 55 mg g^{-1} of stachyose content at 21/13°C.

The linoleic and linolenic acids (omega-6 and omega-3 polyunsaturated fatty acids, respectively) decreased with an increase in growing temperature, while oleic acids increased. The results of the study align with the findings of Alsajri et al. (2020) and Bukowski and Goslee (2024). Notably, as the temperature increased from 15°C to 40°C, there was a reduction in linoleic and linolenic concentrations from 55% and 13% to 30% and 3.5%, respectively (Bukowski and Goslee, 2024). The alteration in nitrogen and carbon

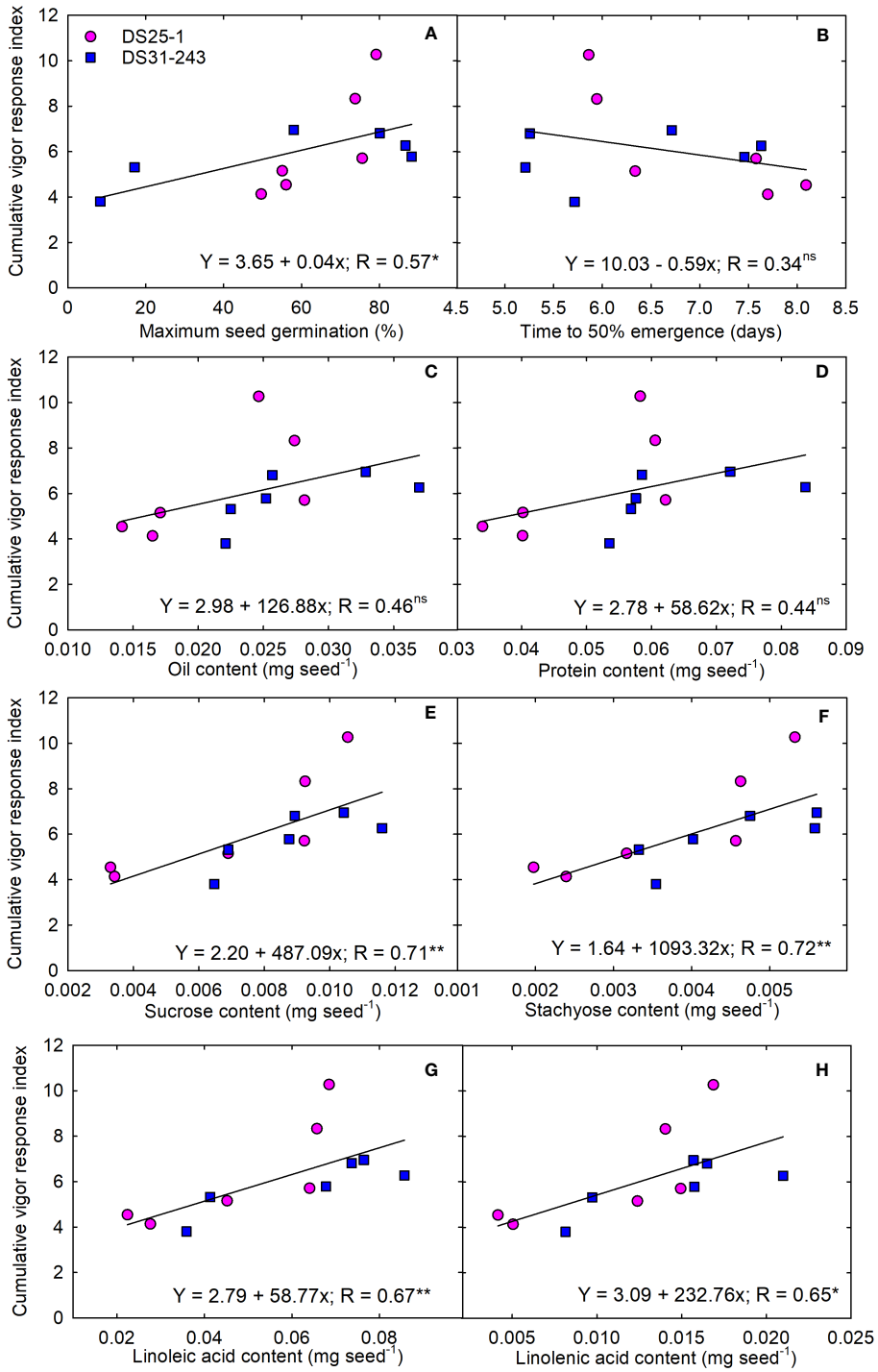

FIGURE 10
Linear regression between quality content per seed and cumulative vigor response index of progenies; **(A)** maximum seed germination (%), **(B)** time to 50% emergence (days), mg seed^{-1} content of **(C)** oil, **(D)** protein, **(E)** sucrose, **(F)** stachyose, **(G)** linoleic acid, and **(H)** linolenic acids. The * and ** indicate the statistical significance at p< 0.05 and 0.01. the 'ns' reference to nonsignificance.

fixation and metabolic pathways led to modification in the polyunsaturated fatty acids (PUFA) in soybeans (Bellaloui et al., 2013). It has been reported that high temperatures above 30-35°C decrease linoleate desaturase activity and degrade the omega-6 desaturase enzyme encoded by the FAD2-1A gene (Cheesbrough, 1989). The high levels of FAD2-2C isoforms of GmFAD2 at 18/12°C (Schlueter et al., 2007) explain the high levels of linoleic acid observed under low temperatures in this study. In addition, the FAD3 enzyme, involved in the production of PUFA, was observed to degrade under temperatures above 30°C (O'Quin et al., 2010). Interestingly, the decreased PUFA (linoleic and linolenic acids) and increased monounsaturated fatty acids, in other words, decreased

unsaturation, under high temperature during early seed developmental stages is a heat tolerance mechanism to ensure membrane stability to protect cell function and embryo development and prevent fatty acid oxidation (Nadakuduti et al., 2023). The eCO_2 did not affect the accumulation of fatty acid except for linolenic acid in DS31-243. The reduced sucrose content at high temperature decreased the production of pyruvate and adenosine triphosphate (ATP), which is involved in the production of fatty acids (Andre and Benning, 2007). Additionally, the high energy requirement for the production of polyunsaturated fatty acids (linoleic and linolenic acids) than monounsaturated fatty acids (oleic acid) resulted in higher accumulation of oleic acid during seed filling stage at higher temperature.

4.3 Temperature and eCO_2 exhibit a transgenerational effect on progenies

The performance of progenies was significantly affected by the parental growing conditions. The higher MSG of DS25-1 compared to DS31-243 at high parental temperature confirms the heat-tolerance characteristics of the cultivar. High-temperature stress prior to the physiological maturity of developing seeds has the potential to reduce germination (Alsajri et al., 2022). This is attributed to the inhibition of the plant's ability to supply necessary assimilates crucial for synthesizing storage compounds essential for successful germination (Hampton et al., 2013). Sparse evidence indicates that only brief episodes of high-temperature stress during critical seed development stages may be adequate to diminish seed vigor (Begcy et al., 2018). A deficient resource supply to the seeds, combined with premature senescence, has adverse effects on seed weight and the composition of seed quality (Alsajri et al., 2022). This leads to a constrained supply of resources from cotyledon to the developing seedlings, resulting in a reduced accumulation of biomass, as evident in the study.

Genotype-by-environment interactions create intraspecific variation in plant responses to environmental treatments. Natural selection acts on this evolving trait plasticity adapted to local conditions influenced by past environments (Groot et al., 2017). The transgenerational plasticity can be either physiologically controlled or epigenetic or by the mother plant through progeny seed coat or endosperm modifications (Suter and Widmer, 2013; Deng et al., 2021). The transgenerational effect will be more pronounced when the progenies are subjected to parental environmental conditions (Uller, 2008). Despite assessing the progenies under standard growth conditions, our study unveiled the transgenerational memory of high parental temperatures, evidenced by the progenies exhibiting reduced MSG and seedling vigor. Transgenerational memory is retained through chromatin modifications, small RNA, and metabolite changes in the reproductive structures (Bilichak and Kovalchuk, 2016). The heat-induced regulated cell death, such as necrosis, apoptosis, and ferroptosis pathways, selectively eliminate specific cells in tissues to uphold homeostasis (Distéfano et al., 2021). This might lead to detectable changes in subsequent generations. Many heat stress-induced DNA methylation and histone changes are reported by several studies (Ramakrishnan et al., 2022; Cao and Chen, 2024). The environment-induced alteration in non-coding RNAs like micro RNAs (miRNA) and small-interfering RNAs (siRNAs) has been reported to play a regulatory role in epigenetic phenomena (Liu et al., 2016). Heat stress-induced modification in miRNA was reported to affect seed storage reserves by altering enzymes such as sucrose synthase, beta-glucosidase, and starch synthase in wheat (Liu et al., 2020). The heat stress-induced expression of Lysine-specific histone demethylase-1 (LSD1), which is involved in the demethylation of histone H3 lysine 4 has been reported in heat-stressed progenies in wheat (Wang et al., 2016). In addition, environmental changes can destabilize the genome either by mobilizing transposable elements or by increasing homologous recombination (Migicovsky and Kovalchuk, 2013). The disruption of the *MutS HOMOLOG 1* (*MSH1*) gene, which encodes a homolog of bacterial mismatch repair protein involved in organelle genome stability, is reported to have increased recombination of repeated sequences, induces male sterility, dwarfed growth, and delayed flowering under stressful environmental conditions in several plants (Ou et al., 2012; Bilichak and Kovalchuk, 2016). The impact of eCO_2 was notably significant across various seedling vigor traits, indicating that even a slight gain in seed composition per seed could lead to discernible changes in seedling characteristics. Panda et al. (2023) reported the transgenerational effect of eCO_2 on *A. thaliana* and *Physcomitrium patens* and demonstrated heritable DNA methylation changes due to eCO_2. Shi et al. (2016) and Begcy et al. (2018) reported that high temperature modifies the quantity and sensitivity of phytohormones and enzymes in seeds, influencing the subsequent generation of seed germination. However, the exact genetic and epigenetic mechanism underlying the transgenerational effect of environmental factors is not yet detailed in soybeans. Our study was only confined to studying the visible changes brought by the parental growing conditions.

4.4 Single-seed chemical composition determines the seedling performance

Post-germinative growth preceding the plant's attainment of photosynthetic self-sufficiency is mainly propelled by the utilization of seed reserves initially stored in the cotyledons of the dormant embryo (Bradow and Bauer, 2010). These dynamics significantly shape the plant's initial stages of development (Snider et al., 2020). The CVRI was positively associated with MSG, sucrose, stachyose, and polyunsaturated fatty acids. Sugars are an essential source of energy, acting as osmotic solutes, building blocks, and signaling molecules (Ruan, 2014). During seed germination and early seedling growth, sucrose acts as an energy source for seed germination upon imbibition. Studies by Snider et al. (2014, 2016) revealed that oil content (mg $seed^{-1}$) and total oil + protein (kcal $seed^{-1}$) strongly and positively influenced the seedling vigor in cotton. However, our study resulted in a significant relationship between seedling vigor with carbohydrates and polyunsaturated fatty acids. It has been reported that the mobilization of lipids and

the initiation of gluconeogenesis from lipid precursors contribute to carbohydrates that can be assimilated into the body of a developing seedling or employed in respiratory processes (Snider et al., 2020). Thus, increased carbohydrates and fatty acids improve the seedling growth and performance.

5 Conclusion

The study delineated the optimal temperature requirements (30/22°C) of soybean during its flowering and seed-filling stages to achieve maximum yield. Exposure of plants to a high temperature of 38/30°C significantly reduced all the seed yield components in both cultivars and the eCO_2 did not consistently compensate for the yield loss. The seed yield was also affected by low temperatures, while the severity increased with an increase in temperature from optimum, resulting in an average reduction of 83%. The deviations in temperature from the optimum levels during flowering and seed-filling stages significantly altered the seed′s chemical composition. Notably, the protein content increased with rising temperatures while the oil content dropped.

Conversely, high temperatures hindered the accumulation of sucrose and stachyose in seeds without being significantly affected by the eCO_2. Similarly, the polyunsaturated fatty acids decreased while oleic acid content rose under high temperatures. The cultivars exhibited a promising difference in their response to temperature and eCO_2 treatments, explaining the genetic variation at play. A considerable transgenerational effect of parental exposure to high temperatures and eCO_2 was observed on the emergence and growth of progenies, emphasizing the long-term implications of climate change on soybean. Seeds developed under 38/30°C temperature had lower MSG, prolonged t_{50}, and reduced biomass accumulation. However, the extent of the effect was determined by the genetics of the cultivar. The eCO_2 increased the seedling performance across the parental temperatures in DS25-1, while the DS31-243 did not exhibit this trend. In addition, a notable positive association was found between the per-seed chemical composition of carbohydrates and fatty acids with seedling vigor. Nonetheless, further research needs to be conducted to validate the association of seed composition with seedling vigor transition.

Data availability statement

The original contributions presented in the study are included in the article/Supplementary Material. Further inquiries can be directed to the corresponding author.

Author contributions

NT: Writing – review & editing, Writing – original draft, Visualization, Software, Formal analysis. RB: Writing – review & editing, Conceptualization. KNR: Writing – review & editing, Funding acquisition. WG: Writing – review & editing. KRR: Writing – review & editing, Writing – original draft, Visualization, Validation, Supervision, Software, Resources, Project administration, Methodology, Investigation, Funding acquisition, Formal analysis, Data curation, Conceptualization.

Funding

The author(s) declare financial support was received for the research, authorship, and/or publication of this article. This research was partly supported by the National Institute for Food and Agriculture, USDA NIFA 2022-34263-38472, and MIS 043050.

Acknowledgments

We thank David Brand for his technical support and other graduate students for their help during the experiment.

Conflict of interest

The authors declare that the research was conducted in the absence of any commercial or financial relationships that could be construed as a potential conflict of interest.

Publisher's note

All claims expressed in this article are solely those of the authors and do not necessarily represent those of their affiliated organizations, or those of the publisher, the editors and the reviewers. Any product that may be evaluated in this article, or claim that may be made by its manufacturer, is not guaranteed or endorsed by the publisher.

Supplementary material

The Supplementary Material for this article can be found online at: https://www.frontiersin.org/articles/10.3389/fpls.2024.1427086/full#supplementary-material

References

Ainsworth, E. A., Davey, P. A., Bernacchi, C. J., Dermody, O. C., Heaton, E. A., Moore, D. J., et al. (2002). A meta-analysis of elevated [CO_2] effects on soybean (*Glycine max*) physiology, growth and yield. *Global Change Biol.* 8, 695–709. doi: 10.1046/j.1365-2486.2002.00498.x

Alsajri, F. A., Wijewardana, C., Bheemanahalli, R., Irby, J. T., Krutz, Y., Golden, B., et al. (2022). Morpho-physiological, yield, and transgenerational seed germination responses of soybean to temperature. *Front. Plant Sci.* 13. doi: 10.3389/fpls.2022.839270

Alsajri, F. A., Wijewardana, C., Irby, J. T., Bellaloui, N., Krutz, L. J., Golden, B., et al. (2020). Developing functional relationships between temperature and soybean yield and seed quality. *Agron. J.* 112, 194–204. doi: 10.1002/agj2.20034

Altieri, M. A., and Nicholls, C. I. (2017). The adaptation and mitigation potential of traditional agriculture in a changing climate. *Clim. Change* 140, 33–45. doi: 10.1007/s10584-013-0909-y

Andre, C., and Benning, C. (2007). Arabidopsis seedlings deficient in a plastidic pyruvate kinase are unable to utilize seed storage compounds for germination and establishment. *Plant Physiol.* 145, 1670–1680. doi: 10.1104/pp.107.108340

Arendt, E. K., and Zannini, E. (2013). *Cereal grains for the food and beverage industries* (Sawston, United Kingdom: Food science, Technology and Nutrition, Woodhead Publishing Limited). doi: 10.1533/9780857098924

Begcy, K., Sandhu, J., and Walia, H. (2018). Transient heat stress during early seed development primes germination and seedling establishment in rice. *Front. Plant Sci.* 9. doi: 10.3389/fpls.2018.01768

Bellaloui, N., Meggistu, A., and Kassem, M. A. (2013). Effect of genetic and environment on fatty acid stability in soybean seed. *Food Nutr. Sci.* (San Diego: Academic Press) 4, 37069. doi: 10.4236/fns.2013.49A1024

Bellaloui, N., Reddy, K. N., and Mengistu, A. (2015). Drought and heat stress effects on soybean fatty acid composition and oil stability. *Processing and Impact on Active Components in Food*. San Diego: Academic Press, 377–384. doi: 10.1016/B978-0-12-404699-3.00045-7

Bilichak, A., and Kovalchuk, I. (2016). Transgenerational response to stress in plants and its application for breeding. *J. Exp. Bot.* 67 (7), 2081–2092. doi: 10.1093/jxb/erw066

Bradow, J. M., and Bauer, P. J. (2010). *Germination and seedling development. Physiol. of Cotton* (Dordrecht: Springer Netherlands), 48–56.

Buis, A. (2019). *Sizing up humanity's impacts on earth's changing atmosphere: a five-part series. the atmosphere: getting a handle on carbon dioxide. climate change: vital signs of the planet* (NASA's Jet Propulsion Laboratory). Available online at: https://climate.nasa.gov/news/2915/the-atmosphere-getting-a-handle-on-carbon-dioxide/ (Accessed on December 25, 2023).

Bukowski, M. R., and Goslee, S. (2024). Climate-based variability in the essential fatty acid composition of soybean oil. *Am. J. Clin. Nutr.* 119, 58–68. doi: 10.1016/j.ajcnut.2023.08.024

Burroughs, C. H., Montes, C. M., Moller, C. A., Mitchell, N. G., Michael, A. M., Peng, B., et al. (2023). Reductions in leaf area index, pod production, seed size, and harvest index drive yield loss to high temperatures in soybean. *J. Exp. Bot.* 74, 1629–1641. doi: 10.1093/jxb/erac503

Calvin, K., Dasgupta, D., Krinner, G., Mukherji, A., Thorne, P. W., Trisos, C., et al. (2023). *IPCC 2023: Climate Change 2023: Synthesis Report. Contribution of Working Groups I, II and III to the Sixth Assessment Report of the Intergovernmental Panel on Climate Change [Core Writing Team, H. Lee and J. Romero (Eds.)]*. Eds. P. Arias, M. Bustamante, I. Elgizouli, G. Flato, M. Howden, C. Méndez-Vallejo, J. J. Pereira, et al (IPCC, Geneva, Switzerland: Intergovernmental Panel on Climate Change (IPCC). doi: 10.59327/ipcc/ar6-9789291691647.001

Cao, S., and Chen, J. (2024). Transgenerational epigenetic inheritance during plant evolution and breeding. *Trends Plant Sci*. doi: 10.1016/j.tplants.2024.04.007

Cendán, C., Sampedro, L., and Zas, R. (2013). The maternal environment determines the timing of germination in *Pinus Pinaster*. *Environ. Exp. Bot.* 94, 66–72. doi: 10.1016/j.envexpbot.2011.11.022

Cheesbrough, T. M. (1989). Changes in the enzymes for fatty acid synthesis and desaturation during acclimation of developing soybean seeds to altered growth temperature. *Plant Physiol.* 90, 760–764. doi: 10.1104/pp.90.2.760

Copernicus Climate Change Service (2023). Available online at: https://climate.copernicus.eu (Accessed March 13, 2024).

CRED (2023). *EM-DAT - The international disaster database*. Available online at: https://www.emdat.be/ (Accessed December 27, 2023).

Deng, Y., Bossdorf, O., and Scheepens, J. F. (2021). Transgenerational effects of temperature fluctuations in *Arabidopsis thaliana*. *AoB Plants* 13, plab064. doi: 10.1093/aobpla/plab064

Distéfano, M. A., López, G. A., Setzes, N., Marchetti, F., Cainzos, M., Cascallares, M., et al. (2021). Ferroptosis in plants: triggers, proposed mechanisms, and the role of iron in modulating cell death. *J. Exp.Bot.* 72, 2125–2135. doi: 10.1093/jxb/eraa425

Groot, M. P., Kubisch, A., Ouborg, N. P., Pagel, J., Schmid, K. J., Vergeer, P., et al. (2017). Transgenerational effects of mild heat in *Arabidopsis thaliana* show strong genotype specificity that is explained by climate at origin. *New Phytol.* 215, 1221–1234. doi: 10.1111/nph.14642

Hampton, J. G., Boelt, B., Rolston, M. P., and Chastain, T. G. (2013). Effects of elevated CO_2 and temperature on seed quality. *J. Agric. Sci.* 151, 154–162. doi: 10.1017/S0021859612000263

Hatfield, J. L., Boote, K. J., Kimball, B. A., Ziska, L. H., Izaurralde, R. C., Ort, D., et al. (2011). Climate impacts on agriculture: implications for crop production. *Agron. J.* 103, 351–370. doi: 10.2134/agronj2010.0303

Hatfield, J. L., and Prueger, J. H. (2015). Temperature extremes: effect on plant growth and development. *Weather Clim. Extremes* 10, 4–10. doi: 10.1016/j.wace.2015.08.001

Hesketh, J. D., Myhre, D. L., and Willey, C. R. (1973). Temperature control of time intervals between vegetative and reproductive events in soybeans. *Crop Sci.* 13, 250–254. doi: 10.2135/cropsci1973.0011183X001300020030x

Hewitt, E. J. (1953). *Sand and water culture methods used in the study of plant nutrition. Technical communication No. 22* (Farnham Royal, Buckinghamshire: Commonwealth Bureau of Horticulture and Plantation Crops, Commonwealth Agricultural Bureaux).

Iovane, M., and Aronne, G. (2022). High temperatures during microsporogenesis fatally shorten pollen lifespan. *Plant Reprod.* 35, 9–17. doi: 10.1007/s00497-021-00425-0

IPCC (2018).Summary for policymakers. In: *Global Warming of 1.5°C. 2018. Intergovernmental Panel on Climate Change* (Cambridge, UK and New York, NY, USA: Cambridge University Press) (Accessed December 27, 2023).

Jumrani, K., and Bhatia, V. S. (2018). Impact of combined stress of high temperature and water deficit on growth and seed yield of soybean. *Physiol. Mol. Biol. Plants: Int. J. Funct. Plant Biol.* 24, 37–50. doi: 10.1007/s12298-017-0480-5

Kidokoro, S., Watanabe, K., Ohori, T., Moriwaki, T., Maruyama, K., Mizoi, J., et al. (2015). Soybean DREB 1/CBF-type transcription factors function in heat and drought as well as cold stress-responsive gene expression. *Plant J.* 81, 505–518. doi: 10.1111/tpj.12746

Kumar, V., Rani, A., Goyal, L., Dixit, A. K., Manjaya, J. G., and Dev, J. (2010). Sucrose and raffinose family oligosaccharides (RFOs) in soybean seeds as influenced by genotype and growing location. *J. Agric. Food Chem.* 58, 5081–5085. doi: 10.1021/jf903141s

Lesk, C., Rowhani, P., and Ramankutty, N. (2016). Influence of extreme weather disasters on global crop production. *Nat* 529, 84–87. doi: 10.1038/nature16467

Li, Y., Yu, Z., Jin, J., Zhang, Q., Wang, G., Liu, C., et al. (2018). Impact of elevated CO_2 on seed quality of soybean at the fresh edible and mature stages. *Front. Plant Sci.* 9. doi: 10.3389/fpls.2018.01413

Liu, H., Able, A. J., and Able, J. A. (2016). SMARTER de-stressed cereal breeding. *Trends Plant Sci.* 21, 909–925. doi: 10.1016/j.tplants.2016.07.006

Liu, H., Able, A. J., and Able, J. A. (2020). Transgenerational effects of water-deficit and heat stress on germination and seedling vigour—new insights from durum wheat microRNAs. *Plants* 9, 189. doi: 10.3390/plants9020189

Migicovsky, Z., and Kovalchuk, I. (2013). Changes to DNA methylation and homologous recombination frequency in the progeny of stressed plants. *Biochem. Cell Bio.* 91, 1–5. doi: 10.1139/bcb-2012-0046

Mourtzinis, S., Gaspar, A. P., Naeve, S. L., and Conley, S. P. (2017). Planting date, maturity, and temperature effects on soybean seed yield and composition. *Agron. J.* 109, 2040–2049. doi: 10.2134/agronj2017.05.0247

MSPB (2023). *Mississippi soybean. Mississippi Soybean Promotion Board*. Available online at: https://mssoy.org/article/us-and-midsouth-soybean-production-trends (Accessed December 27, 2023).

Nadakuduti, S. S., Laforest, L. C., Tachev, M., Decker, A. N., Egesa, A. O., Shirazi,, et al. (2023). Heat stress during seed development leads to impaired physiological function and plasticity in seed oil accumulation in *Camelina sativa*. *Front. Plant Sci.* 14. doi: 10.3389/fpls.2023.1284573

No, D. H., Baek, D., Lee, S. H., Cheong, M. S., Chun, H. J., Park, M. S., et al. (2021). High-temperature conditions promote soybean flowering through the transcriptional reprograming of flowering genes in the photoperiod pathway. *Int. J. Mol. Sci.* 22, 1314. doi: 10.3390/ijms22031314

NOAA (2021). *Climate change impacts* (National Oceanic Atmospheric Administration). Available online at: https://www.noaa.gov/education/resource-collections/climate/climate-change-impacts (Accessed December 27, 2023).

O'Quin, J. B., Bourassa, L., Zhang, D., Shockey, J. M., Gidda, S. K., Fosnot, S., et al. (2010). Temperature-sensitive post-translational regulation of plant omega-3 fatty-acid desaturases is mediated by the endoplasmic reticulum-associated degradation pathway. *J. Biol. Chem.* 285, 21781–21796. doi: 10.1074/jbc.M110.135236

Ohnishi, S., Miyoshi, T., and Shirai, S. (2010). Low temperature stress at different flower developmental stages affects pollen development, pollination, and pod set in soybean. *Environ. Exp. Bot.* 69, 56–62. doi: 10.1016/j.envexpbot.2010.02.007

Ou, X., Zhang, Y., Xu, C., Lin, X., Zhang, Q., Zhuang, T., et al. (2012). Transgenerational inheritance of modified DNA methylation patterns and enhanced tolerance induced by heavy metal stress in rice (*Oryza sativa* L.). *Plos One* 7 (9), e41143. doi: 10.1371/journal.pone.0041143

Pachauri, R. K., Allen, M. R., Barros, V. R., Broome, J., Cramer, W., Christ, R., et al. (2014). *Contribution of working groups I, II and III to the Fifth Assessment Report of the Intergovernmental Panel on Climate Change. Synthesis Report* (Geneva, Switzerland: IPCC), 151.

Panda, K., Mohanasundaram, B., Gutierrez, J., McLain, L., Castillo, S. E., Sheng, H., et al. (2023). The plant response to high CO_2 levels is heritable and orchestrated by dna methylation. *New Phytol.* 238, 2427–2439. doi: 10.1111/nph.18876

Popat, R., and Banakara, K. (2022). *Package Doebioresearch*. Available online at: https://cran.r-project.org/web/packages/doebioresearch/doebioresearch.pdf (Accessed January 24, 2024).

Poudel, S., Adhikari, B., Dhillon, J., Reddy, K. R., Stetina, S. R., and Bheemanahalli, R. (2023). Quantifying the physiological, yield, and quality plasticity of Southern USA soybeans under heat stress. *Plant Stress* 9, 100195. doi: 10.1016/j.stress.2023.100195

Ramakrishnan, M., Zhang, Z., Mullasseri, S., Kalendar, R., Ahmad, Z., Sharma, A., et al. (2022). Epigenetic stress memory: a new approach to study cold and heat stress responses in plants. *Front. Plant Sci.* 13. doi: 10.3389/fpls.2022.1075279

Raza, A., Razzaq, A., Mehmood, S., Zou, X., Zhang, X., and Lv, Y. (2019). Impact of climate change on crops adaptation and strategies to tackle its outcome: a review. *Plants (Basel)* 8, 34. doi: 10.3390/plants8020034

Reddy, K. R., Hodges, H. F., Read, J. J., Mckinion, J. M., Baker, J. T., Tarpley, L., et al. (2001). Soil-plant-atmosphere-research (SPAR) facility: a tool for plant research and modeling. *Biotronics* 30, 27–50.

Rivelli, G. M., Calderini, D. F., Abeledo, L. G., Miralles, D. J., and Rondanini, D. P. (2024). Yield and quality traits of wheat and rapeseed in response to source-sink ratio and heat stress in post-flowering. *Eur. J. Agron.: J. Eur. Soc Agron.* 152, 127028. doi: 10.2139/ssrn.4525646

Ruan, Y. L. (2014). Sucrose metabolism: gateway to diverse carbon use and sugar signaling. *Annu. Rev. Plant Biol.* 65, 33–67. doi: 10.1146/annurev-arplant-050213-040251

Sale, P. W. G., and Campbell, L. C. (1980). Changes in physical characteristics and composition of soybean seed during crop development. *Field Crops Res.* 3, 147–155. doi: 10.1016/0378-4290(80)90020-9

Salem, M. A., Kakani, V. G., Koti, S., and Reddy., K. R. (2007). Pollen-based screening of soybean genotypes for high temperatures. *Crop Sci.* 47, 219–231. doi: 10.2135/cropsci2006.07.0443

Schlueter, J. A., Sander, F. V., Deshpande, S., Yi, J., Siegfried, M., Roe, B. A., et al. (2007). The FAD2 gene family of soybean: insights into the structural and functional divergence of a paleopolyploid genome. *Crop Sci.* 47, S14–S26. doi: 10.2135/cropsci2006.06.0382tpg

Sharma, R. K., Kumar, S., Vatta, K., Dhillon, J., and Reddy, K. N. (2022). Impact of recent climate change on cotton and soybean yields in the southeastern United States. *J. Agric. Food Res.* 9, 100348. doi: 10.1016/j.jafr.2022.100348

Shi, W., Lawas, L. M. F., Raju, B. R., and Jagadish, S. V. K. (2016). Acquired thermotolerance and trans-generational heat stress response at flowering in rice. *J. Agron. Crop Sci.* 202, 309–319. doi: 10.1111/jac.12157

Siebers, M. H., Yendrek, C. R., Drag, D., Locke, A. M., Rios Acosta, L., Leakey, A. D. B., et al. (2015). Heat waves imposed during early pod development in soybean (*Glycine* max) cause significant yield loss despite a rapid recovery from oxidative stress. *Glob. Chang Biol.* 21, 3114–3125. doi: 10.1111/gcb.12935

Singh, B., Singh, S. K., Matcha, S. K., Kakani, V. G., Wijewardana, C., Chastain, D., et al. (2019). Parental environmental effects on seed quality and germination response to temperature of *Andropogon gerardii*. *Argon.* 9, 304. doi: 10.3390/agronomy9060304

Snider, J. L., Collins, G. D., Whitaker, J., Chapman, K. D., and Horn, P. (2016). The impact of seed size and chemical composition on seedling vigor, yield, and fiber quality of cotton in five production environments. *Field Crops Res.* 193, 186–195. doi: 10.1016/j.fcr.2016.05.002

Snider, J. L., Collins, G. D., Whitaker, J., Chapman, K. D., Horn, P., and Grey, T. L. (2014). Seed size and oil content are key determinants of seedling vigor in *Gossypium hirsutum*. *J. Cotton Sci.* 18, 1–9. doi: 10.56454/VBZR9427

Snider, J. L., Pilon, C., and Virk, G. (2020). *Seed characteristics and seedling vigor*. Available online at: https://www.cotton.org/foundation/upload/C-Seed-CH2.pdf (Accessed January 25, 2024).

Soares, J., Deuchande, T., Valente, L. M. P., Pintado, M., and Vasconcelos, M. W. (2019). Growth and nutritional responses of bean and soybean genotypes to elevated CO_2 in a controlled environment. *Plants* 8, 465. doi: 10.3390/plants8110465

Staniak, M., Czopek, K., Stępień-Warda, A., Kocira, A., and Przybyś, M. (2021). Cold stress during flowering alters plant structure, yield and seed quality of different soybean genotypes. *Agron. (Basel Switzerland)* 11, 2059. doi: 10.3390/agronomy11102059

Suter, L., and Widmer, A. (2013). Environmental heat and salt stress induce transgenerational phenotypic changes in *Arabidopsis thaliana*. *PloS One* 8, e60364. doi: 10.1371/journal.pone.0060364

Szczerba, A., Płażek, A., Pastuszak, J., Kopeć, P., Hornyák, M., and Dubert, F. (2021). Effect of low temperature on germination, growth, and seed yield of four soybean (*Glycine max* L.) Cultivars. *Agron. (Basel Switzerland)* 11, 800. doi: 10.3390/agronomy11040800

Tacarindua, C. R. P., Shiraiwa, T., Homma, K., Kumagai, E., and Sameshima, R. (2013). The effects of increased temperature on crop growth and yield of soybean grown in a temperature gradient chamber. *Field Crops Res.* 154, 74–81. doi: 10.1016/j.fcr.2013.07.021

Taub, D. (2010). Effects of rising atmospheric concentrations of carbon dioxide on plants. *Nat. Educ. Knowledge* 3 (10), 21.

Thorne, J. H. (1982). Temperature and oxygen effects on 14C-photosynthate unloading and accumulation in developing soybean seeds. *Plant Physiol.* 69, 48–53. doi: 10.1104/pp.69.1.48

Tielborger, K., and Petru, M. (2010). An experiment test for effects of the maternal environment on delayed germination. *J. Ecol.* 98, 1216–1223. doi: 10.1111/j.1365-2745.2010.01682.x

Uller, T. (2008). Developmental plasticity and the evolution of parental effects. *Trends Ecol. Evol.* 23, 432–438. doi: 10.1016/j.tree.2008.04.005

USDA-FAS (2023). *Soybeans* (USDA- Foreign Agricultural Service). Available online at: https://fas.usda.gov/data/commodities/soybeans (Accessed December 27, 2023).

Wang, X., Xin, C., Cai, J., Zhou, Q., Dai, T., Cao, W., et al. (2016). Heat priming induces trans-generational tolerance to high temperature stress in wheat. *Front. Plant Sci.* 7. doi: 10.3389/fpls.2016.00501

Wijewardana, C., Reddy, K. R., Krutz, L. J., Gao, W., and Bellaloui, N. (2019). Drought stress has transgenerational effects on soybean seed germination and seedling vigor. *PloS One* 14, e0214977. doi: 10.1371/journal.pone.0214977

Zas, R., Cendán, C., and Sampedro, L. (2013). Mediation of seed provisioning in the transmission of environmental maternal effects in *Pinus pinaster*. *Heredity* 111, 248–255. doi: 10.1038/hdy.2013.44

Zhao, C., Bing, L., Shilong, P., Xuhui, W., David, B. L., Yao, H., et al. (2017). Temperature increase reduces global yields of major crops in four independent estimates. *Proc. Natl. Acad. Sci. U. S. A.* 114, 9326–9331. doi: 10.1073/pnas.1701762114

Frontiers in Plant Science

Cultivates the science of plant biology and its applications

The most cited plant science journal, which advances our understanding of plant biology for sustainable food security, functional ecosystems and human health.

Discover the latest Research Topics

See more →

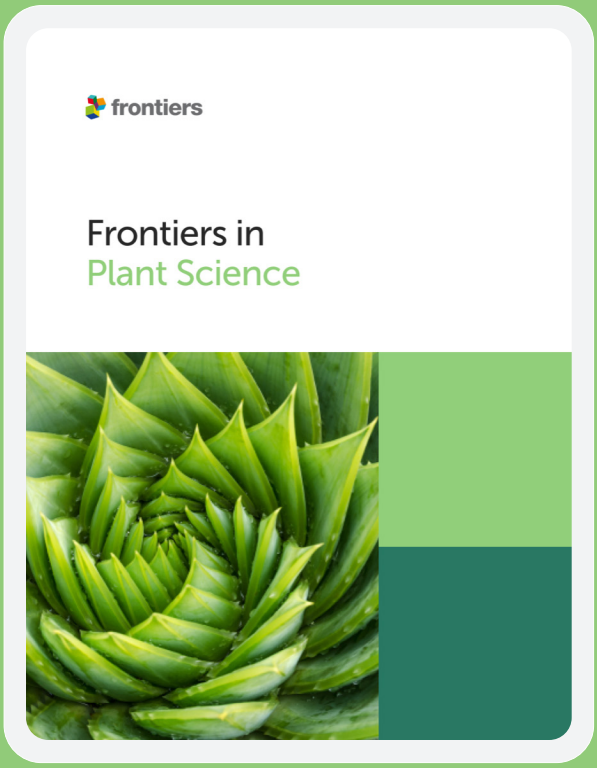

Frontiers

Avenue du Tribunal-Fédéral 34
1005 Lausanne, Switzerland
frontiersin.org

Contact us

+41 (0)21 510 17 00
frontiersin.org/about/contact